Identification and characterization of novel proteolytic interactions of prostate cancer-expressed kallikrein-related peptidases, type II transmembrane serine proteases and matrix metalloproteinases

Janet C. Reid

Bachelor of Science, Master of Science Qualifying, Graduate Diploma of Biotechnology

Institute of Health and Biomedical Innovation

Mater Medical Research Institute

Translational Research Institute

School of Biomedical Sciences, Queensland University of Technology

A thesis submitted to the Queensland University of Technology in fulfillment of the requirements of a Doctor of Philosophy

Jan 2015

Key Words

Activity Based Probe (ABP), Calcium Signalling, Cell Surface, Hepatocyte Growth Factor (HGF), Hepatocyte Growth Factor Activator Inhibitor-1 (HAI-1), Kallikrein-Related Peptidase (KLK), Kidney Proximal Tubule Cells, Matrix Metalloproteinase (MMP), Prostate Cancer, Protease-Activated Receptor (PAR), Proteolytic Cascade, Recombinant Proteins, Serine Protease Inhibitor, Type II Transmembrane Serine Protease (TTSP).

Abstract

In the tumour microenvironment pericellular proteolytic activity affects cells by cleavage of extracellular matrix proteins, activation of cell-surface receptors such as the protease activated receptors (PAR), and processing of mitogenic growth factors such as hepatocyte growth factor (HGF). As proteolysis is irreversible in physiological settings, protease activity is tightly regulated by a number of factors including localization, zymogen activation and protease inhibitors. However, overexpression of proteases in the dysregulated prostate cancer microenvironment has the potential to facilitate disease progression.

The secreted serine proteases kallikrein-related peptidase (KLK)14 and KLK4 as well as the type II transmembrane serine proteases (TTSPs) hepsin and transmembrane protease serine 2 (TMPRSS2) have been implicated in the progression of prostate cancer as all four are upregulated this malignancy. For instance, increased KLK14 expression has been correlated with aggressive, late stage prostate cancer and decreased progression-free survival. KLK4 also has increased expression; however, this is seen in early stages of prostate cancer, with diminished KLK4 levels in late stages. Hepsin has also been implicated as expression increase through all prostate cancer stages to bone metastasis. Further, in a non-metastasising mouse model, hepsin overexpression has been implicated in invasion/extravasion and metastasis of primary prostate tumour cells through disorganisation of the basement membrane. TMPRSS2 also has increased expression in localized prostate cancer. Further, TMPRSS2 has dysregulated cellular localization in prostate cancer, moving from the apical cellular localization of normal epithelial prostate cells to the entire cell surface with intracellular accumulation in prostate cancer cells. Critically, KLK14, KLK4 and TMPRSS2 induce intracellular signalling pathways via proteolytic activation of PARs, and modulation of PAR-mediated signalling has been associated with cells acquiring a more cancerous phenotype.

While hepsin and TMPRSS2 auto-activate, the endogenous activators of KLK14 and KLK4 are unknown. It was recently determined that matrix metalloproteinase MMP3 activates KLK4 *in vitro* and so may be an endogenous activator. Moreover, it is prostate expressed and has also been implication in the progression of several cancer types including prostate. In turn, MMP3 is activated by auto-activating TTSP family member

matriptase, thereby potentially forming an activation cascade from matriptase to MMP3 to KLK4. As auto-activating proteases, hepsin and TMPRSS2 also have the potential to function in proteolytic activation cascades, activating either the KLKs or MMP3. In turn, the activated KLKs may induce PAR-mediated intracellular signalling or activate HGF, the MET receptor ligand.

The goal of this study was to examine pericellular proteolytic activity. In particular, it focussed on proteolytic interactions of KLK14 and KLK4 with hepsin and TMPRSS2. To a lesser extent, interactions of hepsin and TMPRSS2 with MMPs, MMP3 and MMP9 were also examined. This study also examined HGF activation by KLK14 and KLK4, and inhibition of KLK14 by hepatocyte growth factor activator inhibitor-1 (HAI-1). Further, activation of PAR family members PAR1, PAR2 and PAR4 by KLK14, hepsin and matriptase, and PAR2 by KLK4, was examined.

For the first part of this study recombinant pro-KLK14 was generated in insect cells and characterized. It was determined that while pro-KLK14 from this system is N-glycosylated, the protease produced by Cos-7 cells lack this modification. This indicates the potential for cell-type differential N-glycosylation of KLK14. Active recombinant KLK14 was also shown to activate pro-HGF, while KLK4 primarily degrades it. Examination of KLK14 inhibition by HAI-1A and HAI-1B isoforms indicated that this inhibitor is a KLK14 substrate rather than inhibitor as both isoforms were degraded by KLK14. In comparison, hepsin and HAI-1A formed the stable complexes characteristic of inhibition.

The second part of this study examined the interactions between KLK4 and KLK14, the hepsin and TMPRSS2, and to a lesser extent matriptase, MMP3 and MMP9. The data from these studies suggest complex pericellular interactions between these proteases and can be summarized as follows:

- KLK4 and, to a lesser extent, KLK14 are proteolysed by hepsin and TMPRSS2, and the shortened forms of these KLKs were mainly detected in association with the cell
- Proteolysis of KLK4 by hepsin and TMPRSS2 does not appear to lead to activation; however, it is not known if cell-associated forms of KLK14 are activated by these TTSPs

- KLK4 cleaves the stem region of hepsin and TMPRSS2; however, these cleaved forms remain cell membrane-bound through disulphide links in the stem
- While KLK4 and KLK14 co-immunoprecipitate with hepsin and TMPRSS2, KLK14 and active KLK4 are located on the cell surface independently of these TTSPs
- MMP3 and MMP9 are activated by hepsin and TMPRSS2 (and matriptase)
- MMP3 and MMP9 co-immunoprecipitate with hepsin and TMPRSS2.

The third and final part of the study focussed on PAR1, PAR2 and PAR4 activation by KLK14, matriptase and hepsin, as well as inhibition of KLK4 activation of PAR2 using the KLK4-specific inhibitor SFTI-FCQR. PAR2 activation by KLK4 was investigated further using human primary kidney proximal tubule cells (PTC), which have previously been described as co-expressing PAR2 and KLK4. It was determined that while KLK14 activated PAR1, PAR2 and PAR4, and matriptase activated PAR2-mediated signalling, in the form of intracellular Ca^{2+} mobilization, there was negligible activation of PAR1, PAR2 or PAR4 by hepsin. Further, KLK4 activation of PAR2 could be abrogated by the KLK4-specific inhibitor SFTI-FCQR. Interestingly, further examination of KLK4 activation of PAR2 showed that while it activates PAR2 in a number of cell types, it elicited minimal PAR2 activation and Ca^{2+} mobilization in human kidney PTCs. This data suggests cell-type biased agonism of PAR2 by KLK4 potentially initiating alternative intracellular signalling pathways, or alternatively, a KLK4 competitive substrate on the surface of these cells.

In this final section LNCaP cells overexpressing hepsin or active site mutated hepsin were also generated as a tool to examine the participation of hepsin with other serine proteases in proteolytic cascades resulting in PAR activation. However, overexpression of hepsin in these cells resulted in minimal plasma membrane localization in contrast to catalytically inactive hepsin which readily localized to the plasma membrane.

Importantly, this is the first report of KLK14 activation of pro-HGF. Further, this is the first time KLK14 degradation of HAI-1, and formation of hepsin-HAI-1 complexes, have been reported. It is also the first time cell-surface localization of KLK4 and KLK14 has been demonstrated. In addition, this is the first time active KLK4 has been isolated from the cell surface.

The data in this study suggest that KLK14 may have a role in regulation of MET receptor/HGF signalling axis through HGF activation and degradation of key protease inhibitors, HAI-1A and HAI-1B. Further, the data set up the premise for a proteolytic cascade at the plasma membrane involving TMPRSS2 and hepsin activation of MMP3 and MMP9, with MMP3 then activating KLK4. Finally, the cell surface localization of KLK14 and KLK4 may facilitate activation of PARs, degradation of HAI-1 isoforms and pericellular activation of HGF. Based on the results of this study a number of exciting and interesting avenues have been proposed to further explore the role of KLK14, and these other prostate-expressed proteases, in modulation of the pericellular environment.

Table of Contents

List of Figures

List of Tables

List of Abbreviations

2°	secondary antibody
4-MU	4-methylumbelliferone
×	times (multiplication)
α-	Anti-
ABP	activity based probe
ACT	α-1-antichymotrypsin
AGRF	Australian Genomic Research Facility
AM	acetoxymethyl ester
AMC	7-amino-4-methylcoumarin
AP	agonist peptide
APAF	Australian Proteome Analysis Facility
APC	activated protein C
APS	ammonium persulphate
AR	androgen receptor
ATCC	American Type Culture Collection
ATP	adenosine triphosphate
BCA	bicinchoninic acid
Biotin-EGR-CMK	biotinylated Glu-Gly-Arg-chloromethylketone
Biotin-FPR-CMK	biotinylated Phe-Pro-Arg-chloromethylketone
BLAST	basic local alignment search tool
βME	beta-mercaptoethanol
BPE	Bovine Pituitary Extract
BPH	benign prostatic hyperplasia
BSA	bovine serum albumin
C-	carboxyl-
Ca^{2+}	calcium
Ca^{2+}_i	intracellular calcium
CaFA	Ca^{2+} flux assay
CaFL	Ca^{2+} flux load (Buffer)
CAPS	N-cyclohexyl-3-aminopropanesulfonic acid
CDCP1	CUB domain-containing protein 1
cfu	colony forming units
CM	conditioned media
CUB	Cls/Clr, urchin embryonic growth factor and bone morphogenetic protein 1
DAG	diacylglycerol
dATP	deoxyadenosine-triphosphate
DMEM	Dulbecco's Modified Eagle Medium
DMSO	dimethyl sulphoxide
DNA	deoxyribonucleic acid
dNTP	deoxyribonucleotide-triphosphate
DPBS	phosphate-buffered saline (Dulbecco A)
E. coli	*Escherichia coli*
EC_{50}	half-maximal effective concentration
ECM	extracellular matrix
EDTA	ethylene diamine tetra acetate
EGF	epidermal growth factor
EMT	epithelial to mesenchymal transition
ERK	extracellular signal-regulated kinase *or* 44/42 MAPK
FACS	fluorescence-activated cell sorting
FBS	fetal bovine serum
FCM	flow cytometry

FT	flow-through
FVII	factor VII
FVIIa	factor VIIa
FXa	factor Xa
g	relative centrifugal force (RCF)
g	gram
GAS6	growth arrest-specific 6
GDP	guanosine diphosphate
GEF	guanine nucleotide exchange factor
GFP	green fluorescent protein
GPCR	G-protein-coupled receptor
GR	glucocorticoid receptor
GTP	guanosine triphosphate
HAI-1A	hepatocyte growth factor activator inhibitor-1 isoform 2
HAI-1B	hepatocyte growth factor activator inhibitor-1 isoform 1
HAI-1KD1	hepatocyte growth factor activator inhibitor-1 Kunitz domain 1
HAT	human airway trypsin-like protease
HEPES	4-(2-hydroxyethyl)-1-piperazineethanesulfonic acid
HGF	hepatocyte growth factor
HGFA	hepatocyte growth factor activator
HGFR	hepatocyte growth factor receptor (MET receptor)
HRP	horseradish peroxidase
IGF	insulin-like growth factor
IGFBP	insulin-like growth factor binding proteins
IgG	immunoglobulin G
IHC	immunohistochemistry
IL	interleukin
IP	immunoprecipitation
IP_3	inositol-1,4,5-trisphosphate
IP_3R	inositol-1,4,5-trisphosphate receptor
IPTG	isopropyl-β-D-thio-galactoside
K	1000 or kilo
kb	kilobase pair(s)
KD1	Kunitz domain 1
KD2	Kunitz domain 2
kDa	kilodalton
KLK	kallikrein or kallikrein-related peptidase
L	litre
LB	Luria-Bertani
LDLA	low-density lipoprotein receptor class A
LkB1	liver kinase B1
LMF	lung myofibroblast
LN_2	liquid nitrogen
LRP	low density lipoprotein-related protein
µg	microgram
µL	microlitre
µM	micromole per litre
M	mole per litre
mAb	monoclonal antibody
MANEC	motif at N-terminus containing eight cysteines
MAPK	mitogen-activated protein kinase
MFI	mean fluorescence intensity
Milli-Q® water	Milli-Q®(Millipore Ltd, Kilsyth, Vic, Australia) purified ultrapure water
miniprep	minipreparation (of plasmid DNA from bacteria)
mL	millilitre

mM	millimole per litre
MMP	matrix metalloproteinase
MS/MS	tandem mass spectrometry
MT1-MMP	membrane-type-1 matrix metalloproteinase
mRNA	messenger ribonucleic acid
mTOR	phosphoinositide 3-kinase (PI3K)/protein kinase B/mammalian target of rapamycin
MUGB	4-methylumbelliferyl 4-guanidinobenzoate
MW	molecular weight
MWCO	molecular weight cut-off
N-	amino-
N/A	not applicable
NaCl	sodium chloride
NaOH	sodium hydroxide
ND	not determined
NF-κB	nuclear factor kappa-light-chain-enhancer of activated B cells
ng	nanogram
Ni-NTA	nickel-nitrilotriacetic acid
nm	nanometre
nM	nanomole per litre
NR	non-reduced
OD	optical density
PAI-1	plasminogen activator inhibitor-1
PAR	protease-activated receptor
PBS	phosphate-buffered saline
PBS-T	phosphate-buffered saline plus Tween®20
PCR	polymerase chain reaction
pERK	phosphorylated extracellular regulated kinase *or* phosphorylated p44/42 MAPK
PES	polyethersulfone
PI3K	phosphatidylinositide 3-kinase
PIN	prostatic intraepithelial neoplasia
PIP_2	phosphatidylinositol 4,5-bisphosphate
PKC	protein kinase C
PLCβ	phospholipase Cβ
PNGase F	peptide-N4-(N-acetyl-beta-glucosaminyl)asparagine amidase
PSA	prostate-specific antigen
PTC	proximal tubule cells (kidney)
PVDF	polyvinylidene fluoride
QAR-AMC	Boc-Gln-Ala-Arg-7-amido-4-methylcoumarin hydrochloride
R	reduced
RCF	relative centrifugal force (*g*)
RNA	ribonucleic acid
RNase A	ribonuclease A
RO water	reverse osmosis purified water
rpm	revolutions per minute
RmT	room temperature
RTK	receptor tyrosine kinase
s	seconds
SA	serine to alanine serine protease active site residue mutation
SEA	sea urchin sperm protein, enterokinase, agrin
SDS	sodium dodecyl sulphate
SDS-PAGE	sodium dodecyl sulphate-polyacrylamide gel electrophoresis
SFM	serum free media
siRNA	short interfering ribonucleic acid
SPD	serine protease domain

SPINK	serine protease inhibitor, Kazal-type
SRCR	scavenger receptor cysteine-rich
TAE	Tris-acetate-EDTA
TBS-T	Tris-buffered saline plus Tween®20
TEMED	N,N,N',N'-Tetramethylethylenediamine
TF	tissue factor
TMPRSS2	transmembrane protease serine 2
tPA	tissue plasminogen activator
TTSP	type II transmembrane serine protease
Tris	tris(hydroxymethyl)aminomethane
U	units
uPA	urokinase-type plasminogen activator
UQ	University of Queensland
UT	Untransfected
UV	ultraviolet
V	volts
v/v	volume per volume
VEGF	vascular endothelial growth factor
w/v	weight per volume
WB	Western blot
WCL	whole cell lysate
X-gal	5-bromo-4-chloro-indolyl-β-D-galactopyranoside
YFP	yellow fluorescent protein
Zn^{2+}	zinc

Publications contributed to during PhD

He, Y., Wortmann, A., Burke, L.J., **Reid, J.C.**, Adams, M.N., Abdul-Jabbar, I., Quigley, J.P., Leduc, R., Kirchhofer, D., and Hooper, J.D. (2010). Proteolysis-induced N-terminal ectodomain shedding of the integral membrane glycoprotein CUB domain-containing protein 1 (CDCP1) is accompanied by tyrosine phosphorylation of its C-terminal domain and recruitment of Src and PKCdelta. J Biol Chem 285, 26162-26173. PMID: 20551327

Ramsay, A.J., **Reid, J.C.**, Adams, M.N., Samaratunga, H., Dong, Y., Clements, J.A., and Hooper, J.D. (2008a). Prostatic trypsin-like kallikrein-related peptidases (KLKs) and other prostate-expressed tryptic proteinases as regulators of signalling via proteinase-activated receptors (PARs). Biological chemistry 389, 653-668. PMID: 18627286

Ramsay, A.J., **Reid, J.C.**, Velasco, G., Quigley, J.P., and Hooper, J.D. (2008b). The type II transmembrane serine protease matriptase-2--identification, structural features, enzymology, expression pattern and potential roles. Front Biosci 13, 569-579. PMID: 17981570

Sanchez, W.Y., de Veer, S.J., Swedberg, J.E., Hong, E.J., **Reid, J.C.**, Walsh, T.P., Hooper, J.D., Hammond, G.L., Clements, J.A., and Harris, J.M. (2012). Selective cleavage of human sex hormone-binding globulin by kallikrein-related peptidases and effects on androgen action in LNCaP prostate cancer cells. Endocrinology 153, 3179-3189. PMID: 22547569

Swedberg, J.E., Nigon, L.V., **Reid, J.C.**, de Veer, S.J., Walpole, C.M., Stephens, C.R., Walsh, T.P., Takayama, T.K., Hooper, J.D., Clements, J.A., et al. (2009). Substrate-guided design of a potent and selective kallikrein-related peptidase inhibitor for kallikrein 4. Chemistry & biology 16, 633-643. PMID: 19549601

Statement of Original Authorship

The work contained in this thesis contains no material previously submitted at this or any other higher education institution. To the best of my knowledge and belief, this thesis contains no material previously published or written by another person except were due reference has been made in the text.

Signed:

QUT Verified Signature

Janet C. Reid, B.Sc., Grad. Dip. Biotech.

Date: 9th January 2015

Acknowledgments

This work was supported by a Queensland Government Growing the Smart State PhD funding program, an Australian Postgraduate award, and a Queensland University of Technology (QUT) Faculty of Science Top-Up Award. Travel to the Cancer Degradome Symposium, London 2008, and the laboratories of Prof Vincent Ellis (University of East Anglia, UK) and Prof Carlos Lopez-Otin, (Universidad de Oviedo, Spain) were supported by a Queensland Cancer Fund Travel Award, a School of Life Sciences Travel Award, and a QUT Faculty of Science Grants-in-Aid grant.

I would like to sincerely thank my supervisors Associate Professor John Hooper and Professor Judith Clements for their unwavering support, encouragement and constructive criticism. John in particular has gone above and beyond to facilitate the completion of my thesis. I very much appreciate the continued support throughout.

Thank you to the members of the Hooper group and the Hormone-Dependent Cancer Program, past and present. In particular, Melanie Carroll (nee Hunt) for her guidance in the early days of my laboratory work., Dr Nigel Bennett and Carson Stephens for generating specific reagents, to Dr MayLa Linn and Dr Ibtissam Abdul-Jabbar for technical assistance, and to Dr Daniel Kirchhofer, Dr Qingyu Wu and Dr David Vesey for reagents. I would also like to thank Dr Andrew Ramsay, Dr Yaowu He, Dr Lez Burke, Dr Scott Stansfield, Dr Mitchell Lawrence, Dr Ying Dong and Dr Lisa Crowley for invaluable advice, and Grace Eng for her continual encouragement and friendship.

To my family and friends, thanks for you encouragement, patience and support. This truly became a family affair. I will be forever grateful for the magnificent babysitting skills of my Mother, Edna, and Parents-in-law, Jan and Tony. Those extra hours you gave me for working on this project were accompanied by unending encouragement. I am also grateful for the keen editing skills, encouragement and support of my aunts, Barbara and Lyndal. To my Dad, Ian, thanks for the ongoing support and belief in me, and I hope this helps.

It's taken a while to get here. The journey encompassed a transition from the Masters to the PhD program, a whole lot of part-time study, maternity leave, and raising a child. My husband, Neil, you supported me throughout, without your patience this would not have been possible, thankyou. I dedicate this work to you and our wonderful son James.

Chapter 1 Introduction and Literature Review

1.1 Prostate cancer

Prostate cancer has the highest rate of incidence of any cancer in Australian men, excluding non-melanoma skin cancers, and is the second highest cause of cancer-related death after lung cancer (AIHW&AACR, 2012). A feature of prostate cancer that complicates prediction of patient prognosis and treatment is the high levels of heterogeneity, in patient and between patient, in tumour pathology and clinical presentation (Mackinnon et al., 2009; Boyd et al., 2012). Further to this, the molecular mechanisms underlying the development and progression of prostate cancer remain poorly understood (Boyd et al., 2012).

The prostate is an exocrine gland that surrounds the urethra just below the bladder. It is comprised of secretory epithelia containing luminal, basal and neuroendocrine cells, encased by a supportive, fibrous stroma containing smooth muscle cells as well as blood vessels (Aumuller, 1989; Jequier, 2008) (Figure 1.1). The prostate epithelium is separated from the stroma by a basement membrane (or basal lamina) (Aumuller, 1989). The prostate generates a portion of the seminal fluid produced by the male reproductive tract, secreted apically by the luminal epithelial cells (Aumuller, 1989; Jequier, 2008). The prostatic fluid includes high concentrations of citrate and zinc (Zn^{2+}) ions from stores accumulated by the prostate epithelium (Kavanagh, 1985; Costello and Franklin, 1998). Prostatic fluid also contains many proteases, several of which are involved in dissolution of the seminal clot and sperm motility (Aumuller, 1989; Veveris-Lowe et al., 2007; Emami et al., 2009).

A crucial aspect of prostate cancer is the progressive disruption of normal glandular architecture through loss of the basal cell layer, ductal lumen architecture and epithelial cell polarity, and disordering of the basement membrane (Abate-Shen and Shen, 2000; Vasioukhin, 2004; Geiger and Peeper, 2009) (Figure 1.1). It is thought that loss of secretory cell polarity may allow indiscriminate secretion of proteases normally secreted into the luminal space (Djakiew et al., 1992; Webber et al., 1995; Kulasingam and Diamandis, 2008; Pinzani et al., 2008). This in turn facilities further disruption to prostate architecture through numerous mechanisms including degradation of the extracellular matrix (ECM) and basement membrane components, activation of stromal proteases, and other off-target activity (Djakiew et al., 1992; Webber et al., 1995). Ultimately, the breakdown of tissue architecture may become a self-perpetuating cycle mediated by spatially dysregulated proteolytic activity. Importantly, due to the

breakdown of normal tissue architecture and overexpression of particular proteases, there is significant opportunity for proteases to interact in new or altered proteolytic pathways. Therefore, identification of interacting partners is essential to understand the roles of proteases in this pathology.

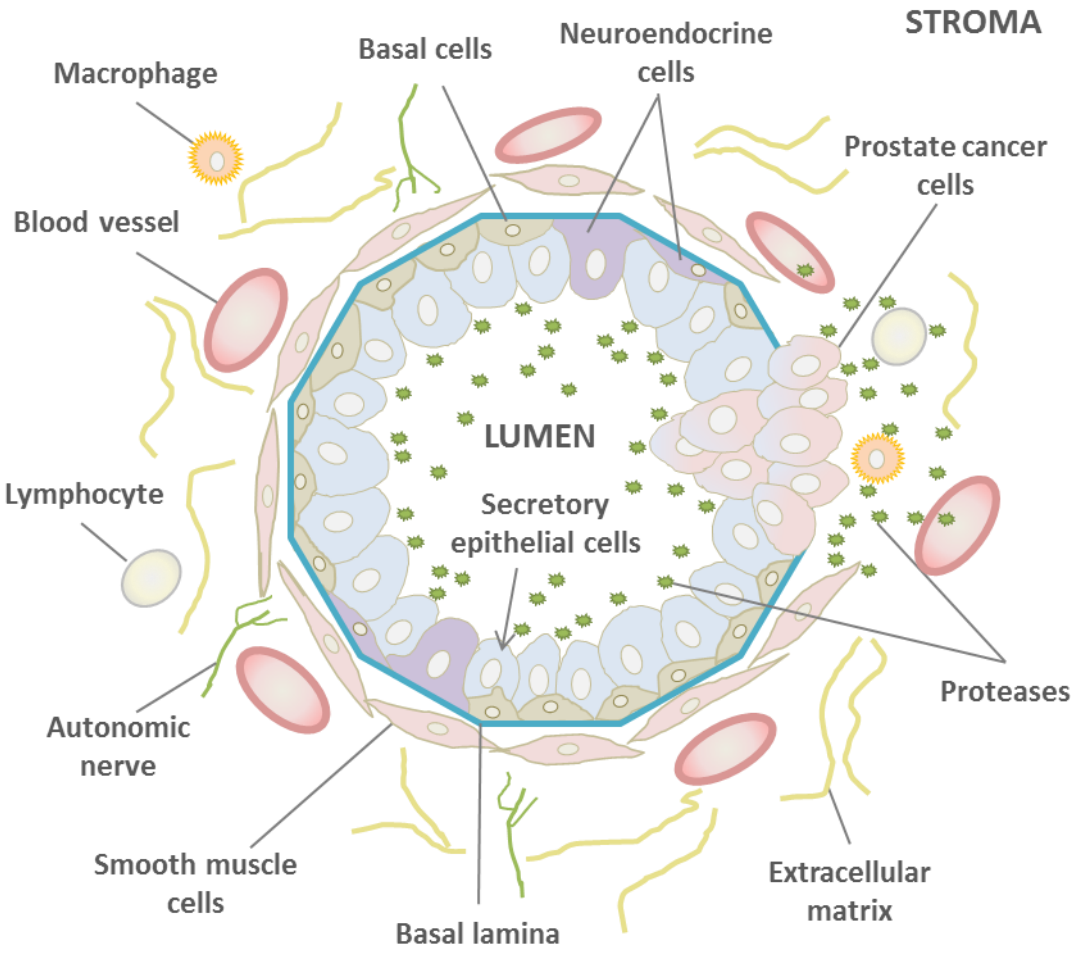

Figure 1.1 Dissemination of prostate lumen proteases into the stroma in prostate cancer. The secretory epithelial cells secrete proteases into the luminal space. As cancer develops and progresses there is loss of epithelial cell polarity and luminal secretion, loss of basal cells and degradation of the basal lamina. These changes facilitate extravasion of the cancer cells and secretion of proteases into the stroma. *Adapted from:* Barron and Rowley, 2012 and Kulasingam and Diamandis, 2008.

1.2 Proteases

Proteases are enzymes that hydrolyse peptide bonds (Rawlings and Salvesen, 2013). Based on mechanistic, sequence and structural similarities and evolutionary relationship they are classified into distinct classes, with further grouping into clans and families

(Rawlings and Salvesen, 2013). The classes of aspartic, cysteine, serine, threonine and metallo- proteases have all been found in mammals (Lopez-Otin and Bond, 2008). They have numerous roles in cellular process regulation through proteolytic processing of bioactive molecules. These include processes such as growth, differentiation, apoptosis, migration, angiogenesis and immune surveillance (Egeblad and Werb, 2002; Lopez-Otin and Bond, 2008). Aberrant protease expression and activity has also been implicated in several disease states including neurodegenerative, inflammatory and vascular disease, and cancer (Egeblad and Werb, 2002; Lopez-Otin and Bond, 2008).

Gene expression studies as well as *in vitro* and *in vivo* assays, have implicated many members of the serine and metallo- protease classes in progression or suppression of multiple cancer types (Lopez-Otin and Matrisian, 2007; Affara et al., 2009). For instance, chymotrypsin- and trypsin-like serine proteases and matrix metalloproteinases (MMPs) have been associated with cancers including breast, ovarian, colorectal, lung and prostate (as reviewed in (Egeblad and Werb, 2002; Rickles et al., 2003; Borgono and Diamandis, 2004; Deryugina and Quigley, 2006; Li and Cozzi, 2007; Lopez-Otin and Matrisian, 2007; List, 2009; Deryugina and Quigley, 2010; Antalis et al., 2011)).

Proteases do not function in isolation, rather as part of dynamic interconnected networks of proteases, substrates, inhibitors, receptors, cofactors and cleavage products (Lopez-Otin and Bond, 2008). In normal tissue, proteases are tightly regulated by several spatial and temporal mechanisms such as gene expression and translation regulation, protein targeting, endogenous inhibitors and protease degradation (Lopez-Otin and Bond, 2008). As another regulatory mechanism, many proteases are generated as inactive precursors or zymogens. For instance, all trypsin-like serine proteases and MMPs are generated as inactive pre-pro-enzymes (Rawlings and Barrett, 2013b, 2013a). The amino (N)-terminal pre- region can confer the signal for secretion and is removed in the process, or, the N-terminal may contain a transmembrane region for cell-surface localization of the protease. Then before the pro-enzyme (zymogen) can catalyse proteolysis, the pro- region requires cleavage by limited proteolysis (Rawlings and Barrett, 2013b, 2013a).

As many proteases are generated as inactive zymogens, several families of proteases participate in highly regulated intracellular and extracellular activation cascades, often initiated by external stimuli (Amour et al., 2004). Protease cascades have been well characterized in a number of essential physiological processes including the complement

(Duncan et al., 2008; Forneris et al., 2012), plasminogen activation (Castellino and Ploplis, 2005; Deryugina and Quigley, 2012), blood coagulation (Spronk et al., 2003) and digestive cascades (Zheng et al., 2009).

There are considered to be three general phases to proteolytic cascades (Figure 1.2) (Amour et al., 2004). In the initiation phase, the proteases are in an inactive zymogen state. The initiating protease self-activates (autoactivates) in response to stimuli and then activates down-stream proteases in a propagation phase. The propagator protease activates executioner proteases in the execution phase but also activates more initiating proteases in a positive-feedback mechanism. This results in amplification of the cascade and downstream proteolytic activity with very little initial activation (Amour et al., 2004). The cascades are governed by specificity of the activating proteases for the zymogens as well as negative-feedback through deactivating proteolysis.

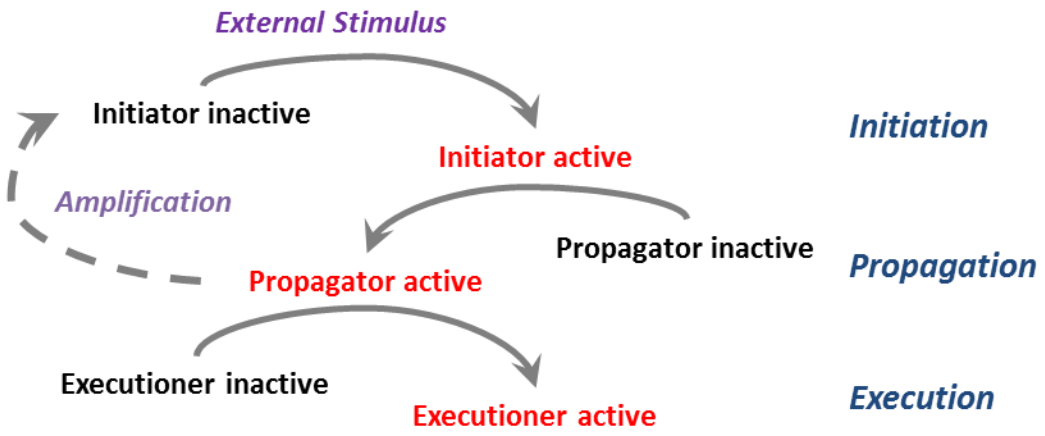

Figure 1.2 Schematic representation of a proteolytic cascade. Classical proteolytic activation cascade with initiation, propagation and execution phases illustrated. Note the cascade amplification provided by the active propagator. *Adapted from:* Amour et al., 2004.

1.3 Serine proteases

There are over 80 families of serine proteases. The trypsin-like, as well as chymotrypsin-like and elastase-like, serine proteases are in the S1 family of serine proteases (Rawlings and Barrett, 2013b). For the remainder of this chapter, trypsin-like and, to lesser extent, chymotrypsin-like proteases will be the focus of discussion about serine proteases. In their active site they possess a catalytic triad of histidine (His)57, aspartic acid (Asp)102

and serine (Ser)195 (chymotrypsin numbering) located at the interface of a fold in the protein known as the chymotrypsin fold (Perona and Craik, 1995, 1997; Page and Di Cera, 2008).

Nomenclature developed by Schechter and Berger (Schechter and Berger, 1967) provides a common terminology describing substrate cleavage and substrate/protease interactions. The substrate cleavage point is between residues P1-P1', with residues on either side numbered outwards P2, P3...Pn to the N-terminus and P2', P3'…Pn to the carboxyl (C-)terminus (Figure 1.3). Correspondingly, there are subsites in the protease that bind the substrate residues. These are numbered Sn...S3, S2, S1, S1', S2', S3'…Sn' (Schechter and Berger, 1967).

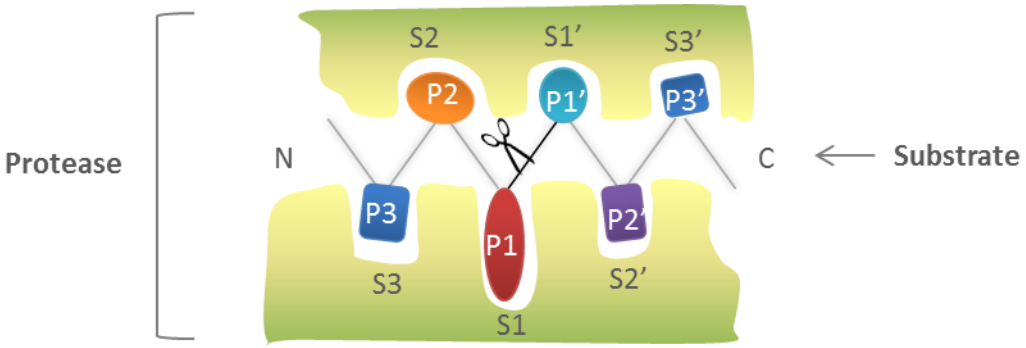

Figure 1.3 Schematic representation of protease-substrate subsite interactions. The active-site of the protease contains subsites that bind substrate residues. The nomenclature devised by Schechter and Berger numbers the substrate residues outwards from the scissile bond between P1 and P1' (indicated with scissors). P1, P2, P3…Pn are increasing towards the N-terminal, and P1', P2', P3'…Pn' are increasing towards the C-terminal. The corresponding protease subsites are likewise numbered S1, S2, S3,…Sn and S1', S2', S3',…Sn'. *Adapted from :* Schechter and Berger, 1967 and Drag and Salvesen, 2010.

Using this terminology, serine protease substrate specificity is governed by P1/S1 complementarity. The S1 residue of the protease is six amino acids N-terminal to the catalytic Ser residue, and it resides in a pocket that is highly complementary to the P1 residue of the substrate (Perona and Craik, 1997; Page and Di Cera, 2008). Trypsin-like serine proteases cleave on the C-terminal side of positively charged residues, arginine (Arg) or lysine (Lys). Correspondingly, the S1 pocket is deep, to accommodate the P1 side-chain, and has a negatively charged S1 residue at the base, Asp189 (Perona and Craik, 1997; Page and Di Cera, 2008). Chymotrypsin-like protease substrates have large

hydrophobic P1 residues. Correspondingly, the S1 pocket is deep and has an S1 residue without a negative charge (Perona and Craik, 1997; Page and Di Cera, 2008).

Other aspects of substrate/protease interactions influencing specificity include, residues that line the sides of the S1 pocket, complementarity at subsites other that S1, and interactions with surface loops on the protease (Brillard-Bourdet et al., 1995; Perona and Craik, 1997; Page and Di Cera, 2008). In addition, binding of a substrate residue at a particular protease subsite can negatively or positively regulate binding of residues at other subsites, a property known as subsite cooperatively (Ng et al., 2009). Together these factors regulate which substrates are hydrolysed by a protease, and the efficiency of the process.

While in zymogen form, the S1 site and active site of the serine protease are deformed which means they have very low activity. Once the pro- region is cleaved, the nascent N-terminal residue (P1'), a hydrophobic residue such as isoleucine (Ile) or valine (Val), forms a salt bridge with the conserved Asp residue located immediately prior to the catalytic Ser. This induces a conformation change that opens up the active site and S1 pocket (Hedstrom, 2002; Rawlings and Barrett, 2013b). When the active serine protease binds a substrate, five enzyme-substrate hydrogen bond points, at positions P1 and P3, position the scissile peptide bond in the active site for nucleophilic attack by catalytic Ser195 (Perona and Craik, 1997). Briefly, nucleophilic Ser operates together with His and Asp in a charge relay system to catalyse hydrolysis (proteolysis) of the scissile peptide bond between P1 and P1' of the substrate (Banacky and Linder, 1981; Page and Di Cera, 2008). When the bond is cleaved, the C-terminus part of the substrate is released as an amine. The N-terminus portion remains bound to the protease as a covalent (acyl-enzyme) intermediate. The sequence then repeats as water attacks and binds the acyl-enzyme. As a result the N-terminus of the substrate is released and the protease active site is regenerated (Perona and Craik, 1995; Hedstrom, 2002).

1.4 Kallikrein-related peptidases (KLKs)

The KLKs are secreted serine proteases comprising 15 highly homologous family members encoded by genes (*KLK*) clustered on chromosome 19q13.3-13.4 (Clements et al., 2001), and include tissue kallikrein, designated KLK1, and 14 kallikrein-related peptidases designated KLK2 to KLK15 (Lundwall et al., 2006) (Figure 1.4).

A

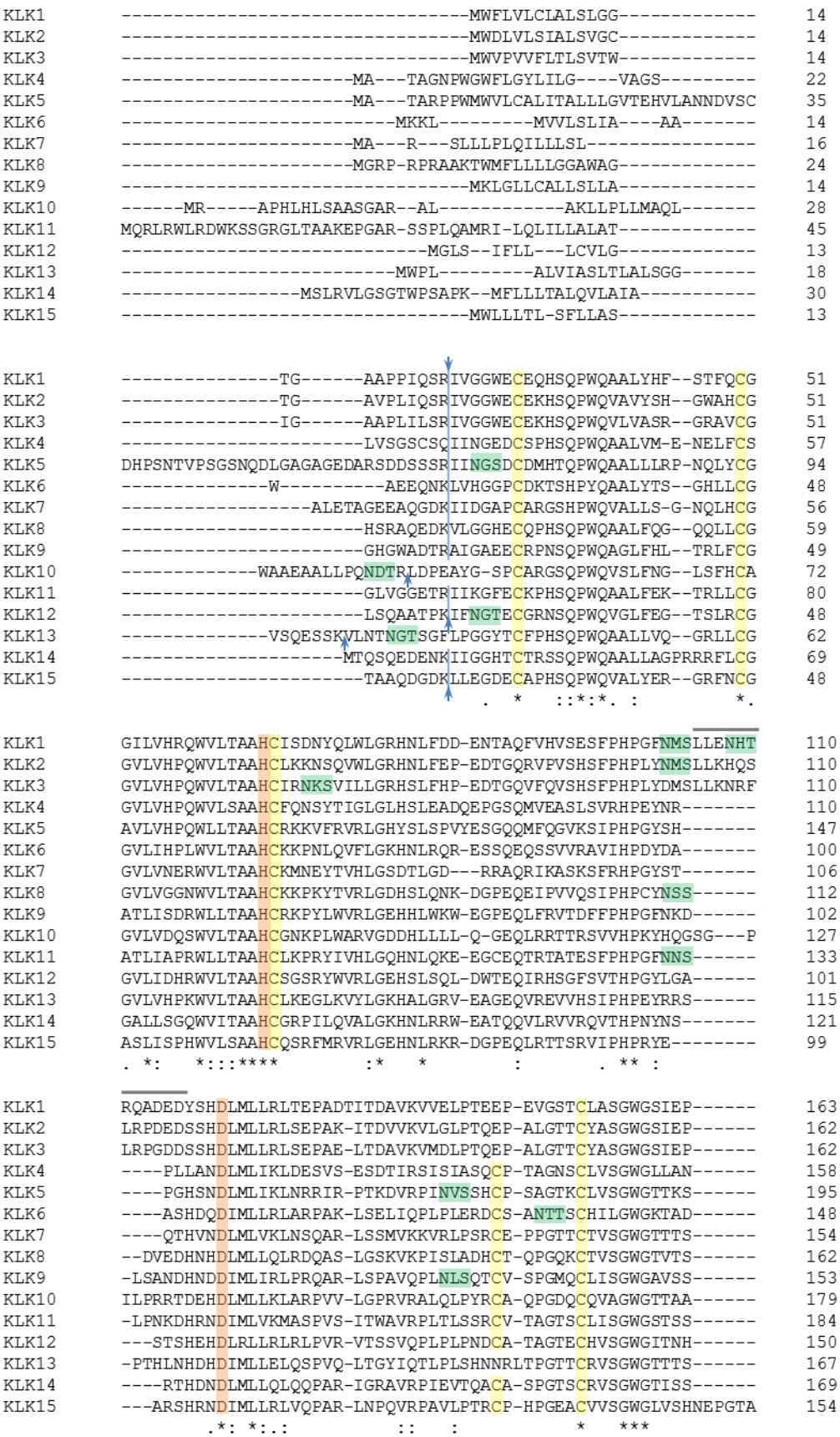
KLK1 ----------MWFLVLCLALSLGG---------- 14
KLK2 ----------MWDLVLSIALSVGC---------- 14
KLK3 ----------MWVPVVFLTLSVTW---------- 14
KLK4 ----------MA---TAGNPWGWFLGYLILG----VAGS--------- 22
KLK5 ----------MA---TARPPWMWVLCALITALLLGVTEHVLANNDVSC 35
KLK6 ----------MKKL---------MVVLSLIA----AA------- 14
KLK7 ----------MA---R---SLLLPLQILLLSL---------- 16
KLK8 ----------MGRP-RPRAAKTWMFLLLLGGAWAG---------- 24
KLK9 ----------MKLGLLCALLSLLA---------- 14
KLK10 ------MR-----APHLHLSAASGAR--AL----------AKLLPLLMAQL------- 28
KLK11 MQRLRWLRDWKSSGRGLTAAKEPGAR-SSPLQAMRI-LQLILLALAT---------- 45
KLK12 ----------MGLS--IFLL---LCVLG---------- 13
KLK13 ----------MWPL---------ALVIASLTLALSGG------- 18
KLK14 ----------MSLRVLGSGTWPSAPK--MFLLLTALQVLAIA---------- 30
KLK15 ----------MWLLLTL-SFLLAS---------- 13
KLK1 ----------TG------AAPPIQSRIVGGWECEQHSQPWQAALYHF--STFQCG 51
KLK2 ----------TG------AVPLIQSRIVGGWECEKHSQPWQVAVYSH--GWAHCG 51
KLK3 ----------IG------AAPLILSRIVGGWECEKHSQPWQVLVASR--GRAVCG 51
KLK4 ----------LVSGSCSQIINGEDCSPHSQPWQAALVM-E-NELFCS 57
KLK5 DHPSNTVPSGSNQDLGAGAGEDARSDDSSSRIINGSDCDMHTQPWQAALLLRP-NQLYCG 94
KLK6 ----------W----------AEEQNKLVHGGPCDKTSHPYQAALYTS--GHLLCG 48
KLK7 ----------ALETAGEEAQGDKIIDGAPCARGSHPWQVALLS-G-NQLHCG 56
KLK8 ----------HSRAQEDKVLGGHECQPHSQPWQAALFQG--QQLLCG 59
KLK9 ----------GHGWADTRAIGAEECRPNSQPWQAGLFHL--TRLFCG 49
KLK10 ----------WAAEAALLPQNDTRLDPEAYG-SPCARGSQPWQVSLFNG--LSFHCA 72
KLK11 ----------GLVGGETRIIKGFECKPHSQPWQAALFEK--TRLLCG 80
KLK12 ----------LSQAATPKIFNGTECGRNSQPWQVGLFEG--TSLRCG 48
KLK13 ----------VSQESSKVLNTNGTSGFLPGGYTCFPHSQPWQAALLVQ--GRLLCG 62
KLK14 ----------MTQSQEDENKIIGGHTCTRSSQPWQAALLAGPRRRFLCG 69
KLK15 ----------TAAQDGDKLLEGDECAPHSQPWQVALYER--GRFNCG 48
KLK1 GILVHRQWVLTAAHCISDNYQLWLGRHNLFDD-ENTAQFVHVSESFPHPGFNMSLLENHT 110
KLK2 GVLVHPQWVLTAAHCLKKNSQVWLGRHNLFEP-EDTGQRVPVSHSFPHPLYNMSLLKHQS 110
KLK3 GVLVHPQWVLTAAHCIRNKSVILLGRHSLFHP-EDTGQVFQVSHSFPHPLYDMSLLKNRF 110
KLK4 GVLVHPQWVLSAAHCFQNSYTIGLGLHSLEADQEPGSQMVEASLSVRHPEYNR------- 110
KLK5 AVLVHPQWLLTAAHCRKKVFRVRLGHYSLSPVYESGQQMFQGVKSIPHPGYSH------- 147
KLK6 GVLIHPLWVLTAAHCKKPNLQVFLGKHNLRQR-ESSQEQSSVVRAVIHPDYDA------- 100
KLK7 GVLVNERWVLTAAHCKMNEYTVHLGSDTLGD---RRAQRIKASKSFRHPGYST------- 106
KLK8 GVLVGGNWVLTAAHCKKPKYTVRLGDHSLQNK-DGPEQEIPVVQSIPHPCYNSS------ 112
KLK9 ATLISDRWLLTAAHCRKPYLWVRLGEHHLWKW-EGPEQLFRVTDFFPHPGFNKD------ 102
KLK10 GVLVDQSWVLTAAHCGNKPLWARVGDDHLLLL-Q-GEQLRRTTRSVVHPKYHQGSG---P 127
KLK11 ATLIAPRWLLTAAHCLKPRYIVHLGQHNLQKE-EGCEQTRTATESFPHPGFNNS------ 133
KLK12 GVLIDHRWVLTAAHCSGSRYWVRLGEHSLSQL-DWTEQIRHSGFSVTHPGYLGA------ 101
KLK13 GVLVHPKWVLTAAHCLKEGLKVYLGKHALGRV-EAGEQVREVVHSIPHPEYRRS------ 115
KLK14 GALLSGQWVITAAHCGRPILQVALGKHNLRRW-EATQQVLRVVRQVTHPNYNS------- 121
KLK15 ASLISPHWVLSAAHCQSRFMRVRLGEHNLRKR-DGPEQLRTTSRVIPHPRYE-------- 99
KLK1 RQADEDYSHDLMLLRLTEPADTITDAVKVVELPTEEP-EVGSTCLASGWGSIEP------ 163
KLK2 LRPDEDSSHDLMLLRLSEPAK-ITDVVKVLGLPTQEP-ALGTTCYASGWGSIEP------ 162
KLK3 LRPGDDSSHDLMLLRLSEPAE-LTDAVKVMDLPTQEP-ALGTTCYASGWGSIEP------ 162
KLK4 ----PLLANDLMLIKLDESVS-ESDTIRSISIASQCP-TAGNSCLVSGWGLLAN------ 158
KLK5 ----PGHSNDLMLIKLNRRIR-PTKDVRPINVSSHCP-SAGTKCLVSGWGTTKS------ 195
KLK6 ----ASHDQDIMLLRLARPAK-LSELIQPLPLERDCS-ANTTSCHILGWGKTAD------ 148
KLK7 ----QTHVNDLMLVKLNSQAR-LSSMVKKVRLPSRCE-PPGTTCTVSGWGTTTS------ 154
KLK8 --DVEDHNHDLMLLQLRDQAS-LGSKVKPISLADHCT-QPGQKCTVSGWGTVTS------ 162
KLK9 -LSANDHNDDIMLIRLPRQAR-LSPAVQPLNLSQTCV-SPGMQCLISGWGAVSS------ 153
KLK10 ILPRRTDEHDLMLLKLARPVV-LGPRVRALQLPYRCA-QPGDQCQVAGWGTTAA------ 179
KLK11 -LPNKDHRNDIMLVKMASPVS-ITWAVRPLTLSSRCV-TAGTSCLISGWGSTSS------ 184
KLK12 ---STSHEHDLRLLRLRLPVR-VTSSVQPLPLPNDCA-TAGTECHVSGWGITNH------ 150
KLK13 -PTHLNHDHDIMLLELQSPVQ-LTGYIQTLPLSHNNRLTPGTTCRVSGWGTTTS------ 167
KLK14 ----RTHDNDLMLLQLQQPAR-IGRAVRPIEVTQACA-SPGTSCRVSGWGTISS------ 169
KLK15 ---ARSHRNDIMLLRLVQPAR-LNPQVRPAVLPTRCP-HPGEACVVSGWGLVSHNEPGTA 154

Figure 1.4

```
KLK1       ----ENFSFPDDLQCVDLKILPNDECKKAHVQKVTDFMLCVGHLEGGKDTCVGDSGGPLM     219
KLK2       ----EEFLRPRSLQCVSLHLLSNDMCARAYSEKVTEFMLCAGLWTGGKDTCGGDSGGPLV     218
KLK3       ----EEFLTPKKLQCVDLHVISNDVCAQVHPQKVTKFMLCAGRWTGGKSTCSGDSGGPLV     218
KLK4       ------GRMPTVLQCVNVSVVSEEVCSKLYDPLYHPSMFCAGGGHDQKDSCNGDSGGPLI     212
KLK5       ----PQVHFPKVLQCLNISVLSQKRCEDAYPRQIDDTMFCAGDK-AGRDSCQGDSGGPVV     250
KLK6       ------GDFPDTIQCAYIHLVSREECEHAYPGQITQNMLCAGDEKYGKDSCQGDSGGPLV     202
KLK7       ----PDVTFPSDLMCVDVKLISPQDCTKVYKDLLENSMLCAGIPDSKKNACNGDSGGPLV     210
KLK8       ----PRENFPDTLNCAEVKIFPQKKCEDAYPGQITDGMVCAGSS-KGADTCQGDSGGPLV     217
KLK9       ----PKALFPVTLQCANISILENKLCHWAYPGHISDSMLCAGLWEGGRGSCQGDSGGPLV     209
KLK10      ----RRVKYNKGLTCSSITILSPKECEVFYPGVVTNNMICAGLD-RGQDPCQSDSGGPLV     234
KLK11      ----PQLRLPHTLRCANITIIEHQKCENAYPGNITDTMVCASVQEGGKDSCQGDSGGPLV     240
KLK12      ----PRNPFPDLLQCLNLSIVSHATCHGVYPGRITSNMVCAGGV-PGQDACQGDSGGPLV     205
KLK13      ----PQVNYPKTLQCANIQLRSDEECRQVYPGKITDNMLCAGTKEGGKDSCEGDSGGPLV     223
KLK14      ----PIARYPASLQCVNINISPDEVCQKAYPRTITPGMVCAGVPQGGKDSCQGDSGGPLV     225
KLK15      GSPRSQVSLPDTLHCANISIISDTSCDKSYPGRLTNTMVCAGAEGRGAESCEGDSGGPLV     214
                         : *  : :    *   :      *.*..       * .*****::

KLK1       CDGVLQGVTSWGY-VPCGTPNKPSVAVRVLSYVKWIEDTIAENS----------          262
KLK2       CNGVLQGITSWGP-EPCALPEKPAVYTKVVHYRKWIKDTIAANP----------          261
KLK3       CNGVLQGITSWGS-EPCALPERPSLYTKVVHYRKWIKDTIVANP----------          261
KLK4       CNGYLQGLVSFGK-APCGQVGVPGVYTNLCKFTEWIEKTVQAS----------           254
KLK5       CNGSLQGLVSWGD-YPCARPNRPGVYTNLCKFTKWIQETIQANS----------          293
KLK6       CGDHLRGLVSWGN-IPCGSKEKPGVYTNVCRYTNWIQKTIQAK----------           244
KLK7       CRGTLQGLVSWGT-FPCGQPNDPGVYTQVCKFTKWINDTMKKHR----------          253
KLK8       CDGALQGITSWGS-DPCGRSDKPGVYTNICRYLDWIKKIIGSKG----------          260
KLK9       CNGTLAGVVSGGA-EPCSRPRRPAVYTSVCHYLDWIQEIMEN-----------           250
KLK10      CDETLQGILSWGV-YPCGSAQHPAVYTQICKYMSWINKVIRSN----------           276
KLK11      CNQSLQGIISWGQ-DPCAITRKPGVYTKVCKYVDWIQETMKNN----------           282
KLK12      CGGVLQGLVSWGSVGPCGQDGIPGVYTYICKYVDWIRMIMRNN----------           248
KLK13      CNRTLYGIVSWGD-FPCGQPDRPGVYTRVSRYVLWIRETIRKYETQQQKWLKGPQ         277
KLK14      CRGQLQGLVSWGM-ERCALPGYPGVYTNLCKYRSWIEETMRDK----------           267
KLK15      CGGILQGIVSWGD-VPCDNTTKPGVYTKVCHYLEWIRETMKRN----------           256
           *   * *: * *    *     *.: . :  :  **.  :
```

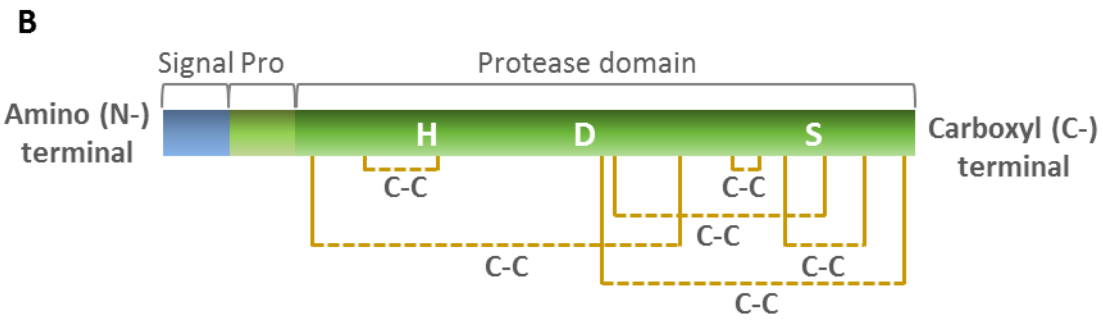

Figure 1.4 Sequence alignment and structure of kallikrein-related peptidases. **A.** Gapped residues are marked by dashes and the pro- region cleavage point for zymogen activation is marked with arrows. The residues of the catalytic triad are shaded in orange, residues at the base of the catalytic pocket are shaded in blue, and the cysteine residues are shaded in yellow. The consensus (N-X-S/T) N-glycosylation sites are shaded green and a conserved atypical (N-X-C) N-glycosylation site in KLK4, KLK5, KLK6, KLK8 and KLK14 is shaded purple. The kallikrein loop area is marked with a overhead line. Symbols below the aligned sequences denote conserved residues: an asterisk indicates positions which have a single, fully conserved residue; a colon indicates conservation between groups of strongly similar properties; a period indicates conservation between groups of weakly similar properties. **B**. KLKs consist of a single serine protease domain with short pre- and pro- regions removed during processing to mature protease. The protease domain contains the catalytic triad residues histidine (H), aspartate (D) and serine (S) and 10-12 cysteine (C) residues that for 5-6 disulphide bonds.

The KLKs have widespread tissue expression (Harvey et al., 2000; Shaw and Diamandis, 2007), with immunohistochemistry studies showing that they are largely expressed by glandular epithelial cells and are secreted (Petraki et al., 2006). They also cleave or degrade several ECM proteins and growth factors, as well as activate a number of proteases (Lawrence et al., 2010). For these reasons KLKs have been associated with a wide range of normal physiological functions as well as pathological processes.

Importantly, deregulated KLK expression has been noted in several cancers, most notably, reproductive organ cancers (Borgono and Diamandis, 2004; Schmitt et al., 2013). Moreover, a singular feature of KLKs is the co-ordinated gene expression regulation and de-regulation of groups of KLKs by steroid hormones in hormone-related cancers such as breast, ovarian, prostate and testicular (Lawrence et al., 2010).

The KLKs are synthesized as pre-pro-enzymes, with the 16-34 amino acid signal peptide pre- region cleaved prior to zymogen secretion (Lundwall and Brattsand, 2008; Clements et al., 2013). The KLK zymogens range from 228 to 264 residues with molecular masses of 24-29 kDa which increase to 30-40 kDa with glycosylation (Lundwall and Brattsand, 2008). Specific N-glycosylation sites have been identified *in vitro* for KLK1 (Kellermann et al., 1988), KLK5 (Debela et al., 2007a) and KLK12 (Picariello et al., 2008), while the remainder have been identified *in silico*.

The cleavage site for removal of the pro- region from the zymogen is evenly split across the KLKs as either an Arg or a Lys P1 residue, except for KLK4, which has a glutamine (Gln) P1 (Yousef and Diamandis, 2001) (Figure 1.4). All the KLKs, except KLK3, KLK7, KLK9 and KLK15, have an Asp S1 residue (Yousef and Diamandis, 2001)(Figure 1.4) and *in vitro* analyses confirmed that most of the Asp S1 KLKs have trypsin-like substrate specificity with a preference for Arg at P1 (Lundwall and Brattsand, 2008; Goettig et al., 2010). Similarly, the cysteine residues are highly conserved in the KLKs with all having 12, except for KLK1-KLK3 and KLK13 which have 10 cysteine residues (Yousef and Diamandis, 2001) (Figure 1.4). Crystal structure analyses have confirmed that in KLK4-KLK7 the 12 cysteine residues form 6 disulphide bridges (Gomis-Ruth et al., 2002; Debela et al., 2006a; Debela et al., 2007a; Debela et al., 2007b) and in KLK1 and KLK3 the 10 residues form 5 bridges(Laxmikanthan et al., 2005; Menez et al., 2008).The KLKs also have a conserved "kallikrein loop" prior to the catalytic Asp, consisting of eleven or fewer amino acids,

and it has been speculated that the loop influences substrate specificity for the KLKs (Clements et al., 2001).

To identify potential KLK substrates and design specific inhibitors, the substrate preferences beyond P1, extended substrate specificity, has been examined for a number of KLKs using methods such as phage display, systematic positional scanning approaches or peptide libraries (Brillard-Bourdet et al., 1995; Felber et al., 2005; Debela et al., 2006b; Borgono et al., 2007a; Debela et al., 2008; Li et al., 2008; Swedberg et al., 2009; Goettig et al., 2010). *In vitro* studies have also identified potential mechanisms of KLK inhibition including a variety of serine protease inhibitors, Zn^{2+} and pH (Goettig et al., 2010). For instance, KLK4 and KLK14 are inhibited by several serpins (Luo and Jiang, 2006; Obiezu et al., 2006; Stefansson et al., 2006; Borgono et al., 2007c). KLK14 is also inhibited by the Kazal-type inhibitors SPINK5 and SPINK6 (Borgono et al., 2007b; Deraison et al., 2007; Meyer-Hoffert et al., 2010; Fortugno et al., 2011). Furthermore, work done in our laboratory exploited the Bowman-Birk serine protease inhibitor sunflower trypsin inhibitor (SFTI) (Luckett et al., 1999) to develop a highly selective, potent KLK4 inhibitor (SFTI-FCQR) for potential therapeutic use (Swedberg et al., 2009).

Another mode of KLK regulation is deactivating proteolysis, enacted by other proteases, or autolysis in the case of KLK14 and several other KLKs (Goettig et al., 2010). Indeed, active KLK14 efficiently autolyses, with several Arg residue cleavage points identified in the body of the protein (Borgono et al., 2007c).

1.4.1 KLK4

The protein sequence of KLK4 was first determined from isolates from enamel of developing pig teeth (Simmer et al., 1998a). Human *KLK4* coding sequence was subsequently identified by several groups (Simmer et al., 1998b; DuPont et al., 1999; Nelson et al., 1999; Stephenson et al., 1999; Yousef et al., 1999). Human KLK4 mRNA and protein is expressed in tissues including kidney, liver, pituitary and cervix (Shaw and Diamandis, 2007). The protein is also normally expressed by prostatic epithelial cells, is secreted into the prostate gland lumen, and has been detected in seminal fluid and urine (Obiezu et al., 2002; Dong et al., 2005; Obiezu et al., 2005; Veveris-Lowe et al., 2005; Shaw and Diamandis, 2007; Veveris-Lowe et al., 2007). It has been detected in the

cytoplasm of cells from normal and cancerous prostatic tissue (Day et al., 2002; Obiezu et al., 2002; Veveris-Lowe et al., 2005) as well as the nuclei of LNCaP cells, and normal epithelial and malignant prostate cells (Dong et al., 2005; Klokk et al., 2007). Moreover, there are several reports of increased KLK4 mRNA expression in prostate cancer (Obiezu et al., 2002; Xi et al., 2004; Avgeris et al., 2012). However, there are conflicting reports on the expression of KLK4 at the protein level when compared to benign or normal prostate. For instance, work done by Veveris-Lowe and colleagues (2005) and by Klokk and colleagues (2007) have shown increased KLK4 expression in prostate cancer. In contrast, Obiezu and colleagues (2002; 2005) reported lower expression or no difference to KLK4 in prostate cancer. Most recently, Seiz and colleagues (2010) reported increased KLK4 in early stages of prostate cancer followed by decreased levels in later stages.

While KLK4 is expressed in the prostate, its role in this tissue is unclear. Recent studies of KLK4 (-/-) mice (Simmer et al., 2009; Smith et al., 2011), and analysis of *KLK4* mutations in humans with the hereditary tooth disorder, amelogenesis imperfecta (Hart et al., 2004), it has been shown that KLK4 is crucial to the development and mineralization of tooth enamel. This role is likely achieved through degradation of ECM proteins amelogenin and enamelin (Ryu et al., 2002; Yamakoshi et al., 2006). However, no other alteration to phenotype was detected in the KLK4 (-/-) mice (Simmer et al., 2009; Smith et al., 2011).

KLK4 is a 254 amino acid pre-pro-protease with one consensus N-glycosylation sequence (Marshall, 1967; Neuberger and Marshall, 1968) at Asn169-Val-Ser (Nelson et al., 1999). It also has an atypical N-glycosylation sequence (Bause and Legler, 1981) at Asn239-Leu-Cys. Moreover, the increased MW of recombinant KLK4 over the calculated MW of 28 kilodaltons (kDa) (Nelson et al., 1999) has been attributed to N-glycosylation (Day et al., 2002; Dong et al., 2005; Obiezu et al., 2006; Ramsay, 2008); however, the sites that are N-glycosylated have not been confirmed. It has also been demonstrated *in vitro* to be a trypsin-like protease with a preference for Arg P1 residues in substrates (Takayama et al., 2001b; Matsumura et al., 2005; Debela et al., 2006a; Debela et al., 2006b; Obiezu et al., 2006; Borgono et al., 2007a; Swedberg et al., 2009).

As KLK4 is unique in the KLK family with a Gln(30) P1 residue for zymogen activation (Nelson et al., 1999; Yousef and Diamandis, 2001), it has been proposed that the endogenous KLK4 activator is not a trypsin-like serine protease. Indeed, KLK inter-

activation studies have shown that none of the KLKs activate KLK4 *in vitro* (Yoon et al., 2007; Yoon et al., 2008; Beaufort et al., 2010). Nor is it activated by serine proteases plasmin, urokinase-type plasminogen activator (uPA), tissue plasminogen activator (tPA), thrombin, factor Xa (FXa) or plasma kallikrein (Yoon et al., 2009). So far, only cysteine exopeptidase cathepsin C, and MMP3 and MMP20 have been shown to activate KLK4 *in vitro* (Tye et al., 2009; Beaufort et al., 2010; Yamakoshi et al., 2013; Yoon et al., 2013). However, as yet, the KLK4 *in vivo* activator has not been identified. Certainly, MMP20 is a possible *in vivo* KLK4 activator as they are co-expressed in developing enamel (Lu et al., 2008). However, while KLK4 has low level protein expression across multiple tissues (Obiezu et al., 2005; Shaw and Diamandis, 2007), MMP20 has very restricted expression, so far detected only in teeth and some oral carcinomas (Fukae et al., 1998; Takata et al., 2000; Vaananen et al., 2004). In contrast, MMP3 has fairly widespread expression in connective tissues (Nagase, 1998), and cathepsin C is ubiquitously expressed (Rawlings and Salvesen, 2013), and therefore they may be candidates for activation of KLK4 in other tissues.

1.4.2 KLK14

KLK14 was one of the last genes to be identified in the *KLK* locus. It was identified and initially characterized by Yousef and colleagues (2001) and by our laboratory (Hooper et al., 2001a). KLK14 has widespread, low level protein expression across many tissues (Shaw and Diamandis, 2007). The prostate is one site of higher level expression. It has been detected in normal prostate epithelial cells, and secreted into seminal fluid (Borgono et al., 2003; Petraki et al., 2006; Borgono et al., 2007c; Shaw and Diamandis, 2007; Rabien et al., 2008). Importantly, in prostate cancer KLK14 expression is increased at both the mRNA and protein level, with a correlation between increased expression level and disease progression (Yousef et al., 2003b; Borgono et al., 2007c; Rabien et al., 2008).

KLK14 is a 267 amino acid pre-pro-protease with a Lys(40) P1 residue for zymogen activation (Hooper et al., 2001a; Yousef et al., 2001). While KLK14 has a consensus N-glycosylation sequence at Asn184-Ile-Ser and an atypical N-glycosylation sequence, Asn252-Leu-Cys, glycosylation of recombinant or endogenous KLK14 has not been reported (Borgono et al., 2003; Borgono et al., 2007c). Also like KLK4, KLK14 has a strong preference for an Arg P1 residue in substrates (Brattsand et al., 2005; Felber et

al., 2005; Oikonomopoulou et al., 2006a; Borgono et al., 2007a; Borgono et al., 2007c; Rajapakse and Takahashi, 2007; Stefansson et al., 2008; de Veer et al., 2011). However, low level chymotrypsin-like activity has also been reported for KLK14 (Brattsand et al., 2005; Felber et al., 2005).

The KLK14 zymogen is not able to autoactivate (Brattsand et al., 2005; Borgono et al., 2007c). However, despite having a strong Arg P1 substrate preference, active KLK14 has a low level ability to activate zymogen KLK14 *in vitro* (Yoon et al., 2007). Similarly, while most of the KLK family members also have a preference for Arg P1 residues (Ramsay et al., 2008b), a few have been identified as *in vitro* KLK14 activators of varying efficiency. These include KLK5 (Brattsand et al., 2005), KLK11 (Yoon et al., 2007) and KLK15 (Yoon et al., 2009) as well as potentially KLK4 and KLK12 (Yoon et al., 2007). Outside of the KLK family only the transmembrane serine protease enteropeptidase (Brattsand et al., 2005) and secreted serine protease plasmin (Yoon et al., 2008) have been identified as KLK14 activators.

Interestingly, due to overlapping tissue/gland localization the KLK14 activators identified *in vitro* may be physiologically relevant. For instance, the epidermis is a site of high levels of KLK14 expression, in particular the epithelial cells of eccrine sweat glands where KLK14 is secreted into sweat (Borgono et al., 2003; Komatsu et al., 2005; Komatsu et al., 2006; Stefansson et al., 2006; Borgono et al., 2007c; Shaw and Diamandis, 2007). The epidermis is also a site of KLK5, KLK11 and enteropeptidase expression (Brattsand and Egelrud, 1999; Ekholm et al., 2000; Komatsu et al., 2005; Komatsu et al., 2006; Shaw and Diamandis, 2007; Nakanishi et al., 2010). Plasma-derived plasmin is also located in the skin as it has a tightly regulated role in ECM degradation and MMP activation in dermal/epidermal wound healing (Toriseva and Kahari, 2009). Similarly in the prostate, KLK14, KLK5 and KLK11 are co-expressed and secreted into the seminal plasma (Luo et al., 2006; Michael et al., 2006; Shaw and Diamandis, 2007). Moreover, plasmin is also a seminal fluid protein (Lwaleed et al., 2004; Stief, 2007).

1.4.3 KLKs in proteolytic cascades

KLK substrate specificity, pro-peptide cleavage sites, as well as the coordinated expression of the *KLK* genes, has led to speculation about tissue-specific KLK

activation cascades. This has been borne out by studies showing *in vitro* KLK cross-activation and deactivation (Yoon et al., 2007; Emami and Diamandis, 2008; Yoon et al., 2009; Beaufort et al., 2010). In addition, a number of KLKs autoactivate, and in so doing potentially serve as cascade initiators (Pampalakis and Sotiropoulou, 2007).

In a physiological context, KLK14 along with KLK5, KLK7 and KLK8 have been associated with proteolytic cascades culminating in epidermal desquamation through degradation of corneodesmosome proteins (Lundstrom and Egelrud, 1991; Egelrud, 1993; Brattsand and Egelrud, 1999; Caubet et al., 2004; Brattsand et al., 2005; Borgono et al., 2007b; Kishibe et al., 2007; Ishikawa et al., 2008; Eissa et al., 2011). In this scenario, KLK14 is activated by autoactivating KLK5 which also activates KLK7 and KLK8 (Brattsand et al., 2005; Eissa et al., 2011). Furthermore, cascade amplification may occur through KLK14 activating KLK5 (Brattsand et al., 2005).

Similarly, KLK4 and KLK14 may be involved in proteolytic cascades essential to sperm motility. While seminal fluid liquefaction through degradation of seminogelins and fibronectin is largely mediated by KLK3 (Sotiropoulou et al., 2009; Lawrence et al., 2010), the KLK3 zymogen does not autoactivate (Denmeade et al., 2001; Yoon et al., 2007). *In vitro* studies of prostate-expressed proteases have shown that it is activated by KLK4 and KLK14 as well as KLK2, KLK5, and KLK15 (Kumar et al., 1997; Lovgren et al., 1997; Takayama et al., 1997; Vaisanen et al., 1999; Malm et al., 2000; Takayama et al., 2001a; Takayama et al., 2001b; Michael et al., 2006; Emami et al., 2008; Emami and Diamandis, 2008; Emami et al., 2009). The cascades are potentially initiated by the autoactivating KLK2, KLK5, KLK6, KLK11 and KLK13 (Mikolajczyk et al., 1998; Lovgren et al., 1999; Denmeade et al., 2001; Magklara et al., 2003; Sotiropoulou et al., 2003; Brattsand et al., 2005; Yoon et al., 2007). When all prostate-expressed KLKs are considered, the inter-activation web is fairly complex (Figure 1.5). For example, KLK5 activates KLK2 (Michael et al., 2006) and, as mentioned earlier, it also activates KLK7, and KLK5 and KLK14 activate each other (Brattsand et al., 2005). Furthermore, KLK2 and KLK14 (Yoon et al., 2007; Emami and Diamandis, 2008) activate KLK1; KLK11 is activated by KLK4, KLK5 (Beaufort et al., 2010) and KLK14 (Yoon et al., 2007); and KLK14 is activated by KLK11 (Yoon et al., 2007) and KLK15 (Yoon et al., 2009).

KLK4 and KLK14 also potentially participate in cascades with other proteases. For instance, KLK4, KLK14 and other KLKs may participate in the plasminogen activation

system. In this cascade uPA and tPA require proteolytic activation and they in turn activate plasminogen to plasmin which is involved in degradation of ECM components,

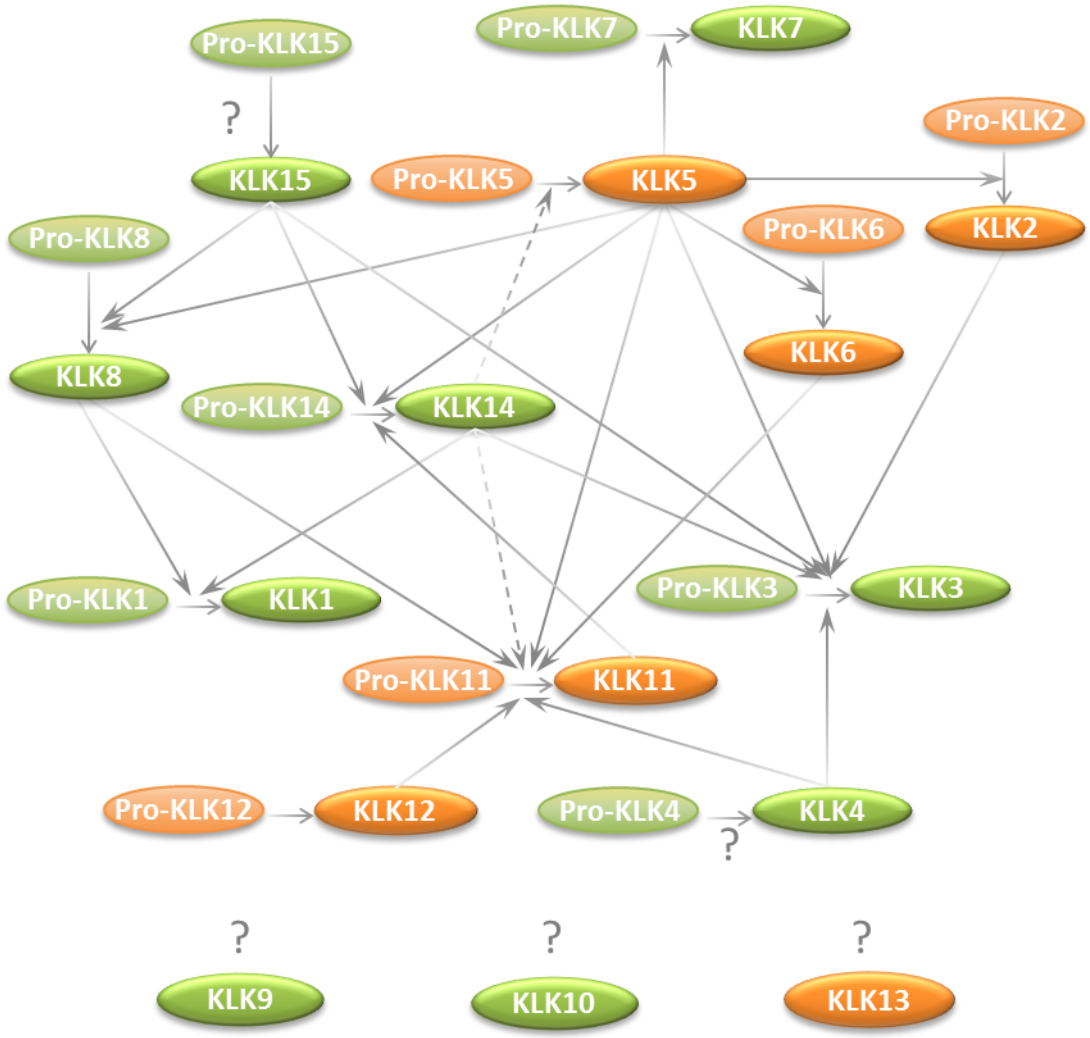

Figure 1.5 Inter-activation web of prostate-expressed kallikrein-related peptidases. KLK2, KLK5, KLK6, KLK11, KLK12 and KLK13 autoactivate (orange). KLK5 activates KLK2, KLK3, KLK6-8, KLK11 and KLK14 and may be a cascade initiator. KLK14 may participate in cascade amplification through positive feedback activation (dotted lines) of KLK5 and KLK11. KLK3 and KLK11 are activated by several KLKs each, possibly indicating their roles as execution proteases. Activators of KLK4 and KLK15 from within the KLK family have not been established. Participation in the KLK inter-activation web has not been determined for KLK9, KLK10 and KLK13.

activation of growth factors, cytokines, and MMPs (Deryugina and Quigley, 2012), as well as cleavage of cell-surface signal transduction protein Cub domain-containing protein 1 (CDCP1) (Brown et al., 2004; Casar et al., 2012a; Casar et al., 2012b). The plasminogen system is regulated by plasminogen activator inhibitors (PAI)-1 and PAI-2,

as well as by cell-surface receptors that bind uPA and plasminogen to the cell surface (Deryugina and Quigley, 2012). KLK4 may positively regulate the plasminogen system through activation uPA (Takayama et al., 2001b). On the other hand, KLK4 may negatively regulate the plasminogen system through fragmentation of the urokinase plasminogen activator receptor (uPAR) (Beaufort et al., 2006). In addition, KLK14 may also negatively regulate the system through degradation of plasminogen to generate anti-angiogenic angiostatin and angiostatin-like fragments (Borgono et al., 2007c). In so doing, the KLK14 may reduce ECM turnover as well as reducing angiogenic capability of the cells.

Interestingly, it was also shown that KLK14 proteolysed complement C3 *in vitro* to generate complement C3a, and also induced complement C3a receptor-mediated cell signalling *in vivo* (Oikonomopoulou et al., 2013). The C3a receptor is expressed by many cell types including cells of myeloid origin as well as epithelial and smooth muscle cells (Klos et al., 2009). Moreover, C3a-induced signalling has been associated with a range of cellular effects that facilitate cancer progression including inflammation, increased activity of mitogenic pathways, up regulation of cytokines, anti-apoptotic effects, angiogenesis and migration (Rutkowski et al., 2010). This represents a novel pathway for KLK14 interaction in the complement cascade and may have particular relevance to the inflammatory aspects of prostate cancer development.

1.4.4 KLKs in prostate cancer

As disruption of normal prostate architecture, in particular the loss of epithelial cell polarity, alters the secretory characteristics of the epithelial cells (Djakiew et al., 1992; Webber et al., 1995; Pinzani et al., 2008), this results in increased release of KLK3 (also known as prostate-specific antigen or PSA) into the surrounding tissue and the blood, instead of the luminal space (Webber et al., 1995; Ishida et al., 2003; Lilja et al., 2008; Pinzani et al., 2008). So, despite an overall decrease in KLK3 expression at the mRNA and protein levels in prostate cancer (Qiu et al., 1990; Magklara et al., 2000; Herrala et al., 2001), increased serum PSA is the basis for clinical diagnostic tests of prostatic disease (Kuriyama et al., 1981; Wang et al., 1981; Lilja et al., 2008).

Indeed, a similar scenario is likely for other prostate expressed KLKs. For example, in prostate cancer patients, serum KLK14 (Borgono et al., 2007c) is elevated compared to

normal. Another example is that the level of KLK4 in sera of healthy subjects or prostate cancer patients is not significant (Obiezu et al., 2002; Obiezu et al., 2005), however, serum antibodies to KLK4 have been detected in prostate cancer patients (Day et al., 2002) possibly indicating increased access to the immune system afforded by prostate architecture disorganization.

Moreover, spatial dysregulation of KLKs combined with the dysregulated expression of several KLKs in prostate cancer, has the potential to alter KLK interactions with proteins in the prostate environment. As a consequence, the dysregulated proteases may initiate or participate in proteolytic cascades normally compartmentalized by tissue architecture. Furthermore, pre-malignant prostate cells have significantly reduced ability to accumulate Zn^{2+} (Costello et al., 2004). Therefore, as many KLKs including KLK4 and KLK14 are inhibited by Zn^{2+} *in vitro* (Debela et al., 2006a; Borgono et al., 2007c), regulation of KLK activity may be compromised in prostate cancer due to the reduced concentration of Zn^{2+} in the tissue.

Importantly for prostate cancer, stable overexpression of KLK4 leads to increased *in vitro* migration of PC-3 cells, and this was associated with the loss of E-cadherin and epithelial to mesenchymal transition (EMT) (Veveris-Lowe et al., 2005). EMT is a trait of cancer progression marked by loss of cell polarity, down regulation of cell-cell adhesive proteins, such as E-cadherin, and, occasionally, morphological changes to a spindle shape cell (Thiery, 2002; Christofori, 2006). The mechanism by which KLK4 effects this functional change is not yet known.

As well as inducing increased migratory ability, overexpression of KLK4 also results in increased LNCaP cell proliferation (Klokk et al., 2007). Consistent with this, knockdown of *KLK4* inhibited cell growth (Klokk et al., 2007). Recent work by Jin and colleagues (2013) showed that the KLK4 contribution to increased proliferation may be due to alteration of two proliferative pathways – phosphatidylinositol 3-kinase (PI3K)/protein kinase B/mammalian target of rapamycin (mTOR) and androgen receptor (AR) signalling. Further work by this group showed knockdown of *KLK4* in LNCaP cells inhibited *in vitro* and *in vivo* growth, as well as reducing anchorage independent growth, inducing apoptosis and increasing cell susceptibility to apoptosis-inducing agents (Jin et al., 2013).

Of the KLK proteolytic targets identified *in vitro*, several have potential to contribute to prostate cancer progression. For example, KLK14 cleaves insulin-like growth factor binding proteins (IGFBP) thus potentially increasing the availability of insulin-like growth factor (IGF) and thereby contributing to increased cell proliferation (Borgono et al., 2007c). In addition, KLK14 cleaves cell-cell adhesion protein desmogelin (Borgono et al., 2007b) and degrades ECM proteins like the collagens, laminin, fibronectin and vitronectin (Borgono et al., 2007c; Rajapakse and Takahashi, 2007). KLK4 also cleaves without degrading sex hormone-binding globulin (SHBG), a protein involved in the stabilization and delivery of steroid hormones such as androgens to target tissues including the prostate (Sanchez et al., 2012). However, as SHBG retains function after KLK4 cleavage, the relevance of this to cell homeostasis is as yet unknown (Sanchez et al., 2012). In contrast, KLK14 degrades unbound SHBG, thereby potentially participating in negative regulation of androgen delivery through decreasing the availability of SHBG (Sanchez et al., 2012).

The *in vivo* function of KLK4 and KLK14 in normal prostate and seminal fluid is speculative, as is the role of dysregulated KLKs in prostate cancer progression. However, taken together, there is potential enhancement in the invasive capability of tumour cells through increased KLK protease activity, breakdown of tissue structure and release of cells.

1.5 Type II transmembrane serine proteases (TTSPs)

Similar to the KLKs, the TTSPs are a large family of serine proteases with 17 human TTSPs identified (Bugge et al., 2009). They are synthesized as single chain pre-pro-enzymes characterized by an N-terminal signal peptide that is not removed but is retained as a short intracellular domain and transmembrane anchor domain. They also have a highly homologous extracellular serine protease domain at the C-terminal. In between the transmembrane domain and the serine protease domain, TTSPs have an extracellular stem region of varying lengths (Hooper et al., 2001b) (Figure 1.6).

TTSP activation by proteolysis generates a heterodimer as the serine protease domain remains tethered to the stem region by an intramolecular disulphide bond conserved in other two-chain proteases such as plasminogen and plasma kallikrein (Lin et al., 1999c; Hooper et al., 2001b). In addition, the TTSP hepsin has a further eight conserved

cysteine residues in the serine protease domain that form four intra-domain disulphide bonds confirmed by crystal structure analysis (Somoza et al., 2003). Similarly, six conserved cysteine residues in the matriptase serine protease domain form three intra-domain disulphide bonds (Friedrich et al., 2002). Transmembrane protease serine 2 (TMPRSS2) is also predicted to have three intra-domain disulphide bonds; however, this has not been confirmed experimentally. There is also one unpaired cysteine residue in the serine protease domain of TMPRSS2. It is semi-conserved in several other serine proteases including hepsin as one of a pair of cysteine residues found forming a fourth disulphide bond (Paoloni-Giacobino et al., 1997; Jacquinet et al., 2001). However, the second cysteine of the pair is not conserved in TMPRSS2 (Paoloni-Giacobino et al., 1997; Jacquinet et al., 2001). Hepsin also has one unpaired cysteine residue in its serine protease domain, however, it is not conserved in other serine proteases (Leytus et al., 1988; Kurachi et al., 1994). The significance of these unpaired cysteines is unknown. However, Kurachi and colleagues (Kurachi et al., 1994) suggest that in the case of hepsin, the unpaired cysteine may assist with protein or ligand interactions.

TTSP stem regions contain up to 11 modular structural domains that are also potentially involved in protein or ligand interactions (Antalis et al., 2011). Hepsin and TMPRSS2 have a single scavenger receptor cysteine-rich (SRCR) domain, while TMPRSS2 has an additional low density lipoprotein receptor class A (LDLA) domain (Szabo and Bugge, 2008) (Figure 1.6). In contrast, matriptase has multiple domains in the stem (Szabo and Bugge, 2008) (Figure 1.6). Studies have shown that these domains may be involved in cellular localization, as well as matriptase activation and inhibition (Oberst et al., 2003b; List et al., 2006a; Kojima et al., 2009). Furthermore, crystal structure analysis of hepsin has shown the stem region may have a role in orienting the serine protease domain on the cell surface (Somoza et al., 2003).

Localization to the cell surface suggests these proteases have an important role in modulating the pericellular environment. However, several TTSPs such as enteropeptidase, matriptase, hepsin and TMPRSS2 do not require membrane anchoring for *in vitro* activity (Bugge et al., 2009). Indeed, *in vivo* shed forms have been found for enteropeptidase (Louvard et al., 1973; Fonseca and Light, 1983), TMPRSS2 (Afar et al., 2001; Lucas et al., 2008) and matriptase (Lin et al., 1999b; Benaud et al., 2001; Jin et al., 2005; Wang et al., 2009) which suggests some may have roles in addition to in the immediate pericellular environment.

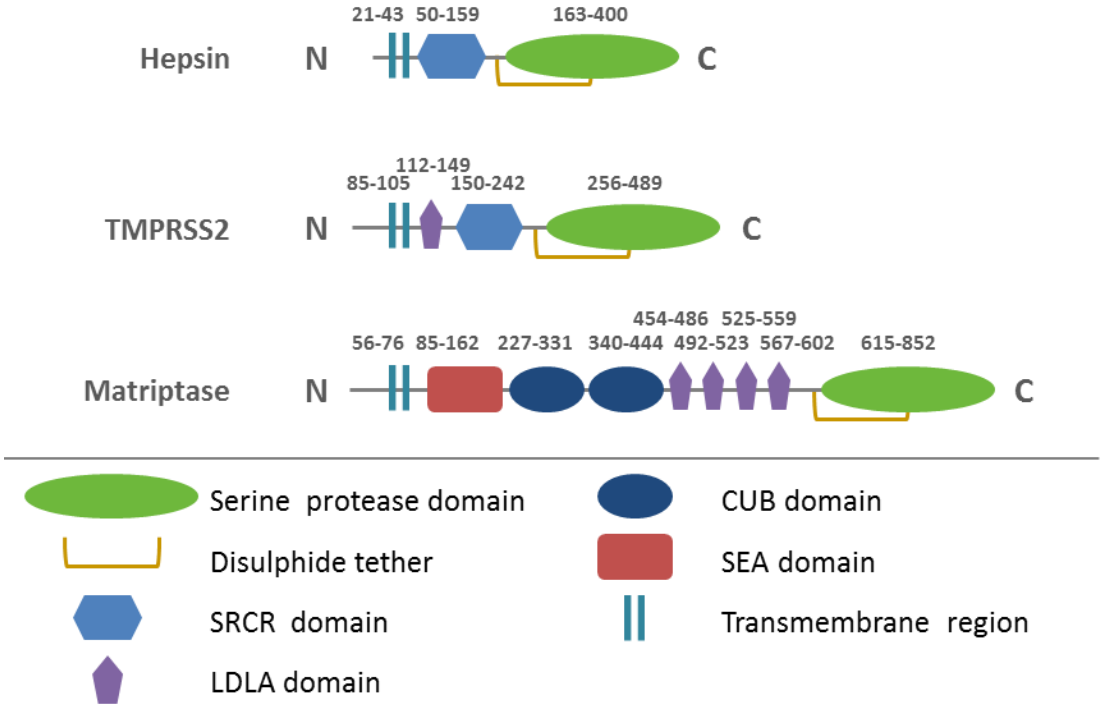

Figure 1.6 Domain structures of hepsin, TMPRSS2 and matriptase. Hepsin, TMPRSS2 and matriptase are Type II transmembrane serine proteases (TTSP) characterized by an N-terminal transmembrane/signal-anchor region, an extracellular modular stem region and C-terminal trypsin-like serine protease domain. They are synthesized as a single chain and are then activated by limited proteolysis between the stem and the serine protease domain. After activation the serine protease domain remains tethered to the stem region by a disulphide bond. Abbreviations: SRCR, Scavenger receptor cysteine-rich; LDLA, lipoprotein receptor class A; CUB, C1s/C1r, urchin embryonic growth factor and bone morphogenic protein 1; SEA, sea urchin sperm protein, enterokinase, agrin. The amino acid numbers indicated above each domain delineate the location of each domain. *Adapted from* Bugge et al., 2009.

1.5.1 Hepsin

The gene encoding hepsin was first cloned from human liver cDNA libraries (Leytus et al., 1988), and it encodes a 417 residue protein (Leytus et al., 1988; Tsuji et al., 1991) (Figure 1.6). Peptide substrate assays using recombinant extracellular region (soluble) hepsin have shown it has a strong preference for Arg P1 residues (Herter et al., 2005). The P1 activation residue for hepsin zymogen is also an Arg (Leytus et al., 1988). Furthermore, hepsin is regarded as capable of autoactivation (Bugge et al., 2009), as demonstrated for mouse hepsin (Vu et al., 1997) and proposed for human hepsin by

Qiu and colleagues (2007). Certainly, mutation of active site residues prevents autoactivation of mouse hepsin (Vu et al., 1997).

Hepsin is highly expressed at the mRNA and protein level in the liver, with lower level expression in most tissues including prostate (Leytus et al., 1988; Tsuji et al., 1991; Li et al., 2005). Interestingly, hepsin has been associated with hearing and inner ear development, as deletion of hepsin in mice leads to profound hearing loss (Guipponi et al., 2007; Guipponi et al., 2008).

Importantly, hepsin mRNA and protein are highly overexpressed in primary prostate carcinoma compared to benign prostatic tissue (Dhanasekaran et al., 2001; Luo et al., 2001; Magee et al., 2001; Stamey et al., 2001; Welsh et al., 2001; Ernst et al., 2002; Chen et al., 2003; Stephan et al., 2004; Halvorsen et al., 2005; Landers et al., 2005; Riddick et al., 2005; Xuan et al., 2006; Kube et al., 2007; Goel et al., 2011), and is considered a significant biomarker for diagnosis and prognosis of prostate cancer (Dhanasekaran et al., 2001; Stephan et al., 2004; Landers et al., 2005). Hepsin protein expression has been shown to increase as early as the transition from normal epithelium to prostatic intraepithelial neoplasia (PIN) (Dhanasekaran et al., 2001) with continued increase as prostate cancer progresses to high grade carcinoma (Dhanasekaran et al., 2001; Xuan et al., 2006; Goel et al., 2011). As prostate cancer metastasizes, higher hepsin protein expression has been found in bone metastasis than lymph node or liver metastasis (Morrissey et al., 2008). Another study found the hepsin protein expression increase continues from low grade carcinoma through to bone metastasis (Xuan et al., 2006). However, in two studies, a decrease in hepsin mRNA and/or protein has been found in hormone refractory metastatic prostate cancer, when compared to primary prostate cancer (Dhanasekaran et al., 2001; Fromont et al., 2005).

1.5.2 TMPRSS2

TMPRSS2 cDNA was first cloned in the development of a transcription map of chromosome 21 (Paoloni-Giacobino et al., 1997). The *TMPRSS2* gene was mapped to chromosome 21q22.3 (Paoloni-Giacobino et al., 1997; Hattori et al., 2000; Jacquinet et al., 2001) and described as encoding a protein of 492 residues (Paoloni-Giacobino et al., 1997) (Figure 1.6). Since the cloning of *TMPRSS2*, several studies have focussed on the role of the 5'-untranslated region of *TMPRSS2* in gene fusions with members of the

erythroblast transformation specific (ETS) transcription factor family genes (Tomlins et al., 2005). However, fusion of *TMPRSS2* with ETS genes is unlikely to result in proteolytic function as the product does not encode the TMPRSS2 serine protease domain (Kumar-Sinha et al., 2008). For this reason, *TMPRSS2* fusion with ETS will not be discussed further. Few studies have been made of the structure or serine protease activities of the TMPRSS2 protein. As a result many of the features have been inferred from sequence and domain structure conservation between TMPRSS2 and other TTSPs and serine proteases.

TMPRSS2 cleaves after arginine residues in synthetic substrate assays (Wilson et al., 2005; Bottcher-Friebertshauser et al., 2010; Meyer et al., 2013). The TMPRSS2 zymogen activation also occurs at an Arg P1 (Afar et al., 2001). In this same study it was shown that mutation of the active site serine to an alanine residue prevented activation and also prevented cleavage of TMPRSS2 at other sites, demonstrating TMPRSS2 autoactivation and self-cleavage (Afar et al., 2001).

The prostate has the highest TMPRSS2 mRNA and protein expression levels with lower levels in several other tissues (Lin et al., 1999a; Afar et al., 2001; Jacquinet et al., 2001; Vaarala et al., 2001b; Donaldson et al., 2002; Lucas et al., 2008; Bertram et al., 2012). Immunohistochemistry studies have shown TMPRSS2 protein is localized to epithelial cells (Afar et al., 2001; Lucas et al., 2008; Chen et al., 2010b). In the prostate the protein is localized to the apical plasma membrane of the luminal cells (Afar et al., 2001; Lucas et al., 2008; Chen et al., 2010b). As mentioned earlier, TMPRSS2 is shed into the prostate luminal space and has been detected in seminal fluid (Afar et al., 2001; Lucas et al., 2008). It has also been detected as a component of prostasomes (Utleg et al., 2003; Chen et al., 2010b) along with a number of other proteases including KLK3, and protease inhibitors including hepatocyte growth factor activator inhibitor (HAI)-1 (Utleg et al., 2003; Poliakov et al., 2009). These organelle-like membrane vesicles are secreted from the prostate luminal cells into seminal fluid and are thought to facilitate sperm function (Kravets et al., 2000). Therefore, TMPRSS2 may play a key role in the cascade of KLKs in the prostate microenvironment.

Importantly, TMPRSS2 mRNA and protein expression is increased in prostate cancer (Lin et al., 1999a; Afar et al., 2001; Vaarala et al., 2001a; Vaarala et al., 2001b; Lucas et al., 2008; Chen et al., 2010b). Moreover, cellular localization of TMPRSS2 is dysregulated, moving from the apical to the entire plasma membrane surface and

increased intracellular accumulation as the acinar macrostructure is lost during prostate cancer progression (Lucas et al., 2008; Chen et al., 2010b). A significant aspect of TMPRSS2 is that similar to members of the KLK family, expression is androgen-regulated in prostate cancer-derived cell lines expressing androgen receptor (Lin et al., 1999a; Afar et al., 2001; Jacquinet et al., 2001). Furthermore, TMPRSS2 expression is down-regulated in bone metastasis-derived androgen-independent prostate cancer xenograft tissue (Afar et al., 2001).

Interestingly, the physiological role of TMPRSS2 remains undetermined from *TMPRSS2* (-/-) mice studies as the mice were viable and fertile and exhibited no detectable abnormalities (Kim et al., 2006). Moreover, there were no differences in prostate secretions, development of prostate cancer or regeneration of the prostate epithelium after castration in the *TMPRSS2* (-/-) mice. This lack of phenotype suggests either functional redundancy involving one or more serine proteases or that TMPRSS2 has a function in circumstances of disease or stress (Kim et al., 2006).

1.5.3 Matriptase

Matriptase was first identified from the media of cultured breast cancer cells as a gelatin-degrading protease (Shi et al., 1993). Matriptase is an 855 residue protein encoded by a gene located on chromosome 11q24-25 (Lin et al., 1999c; Takeuchi et al., 1999) (Figure 1.6). It has a preference for Arg P1 residues in substrates (Takeuchi et al., 2000; Bhatt et al., 2007), and a two-step process involving cleavage in the sea urchin sperm protein, enterokinase, agrin (SEA) domain followed by cleavage at the conserved activation site is required for matriptase activation. Matriptase autoactivates, however, the mechanisms of the process are complex involving domains in the stem region, N-glycosylation (Oberst et al., 2003b; Inouye et al., 2013), homodimer formation (Xu et al., 2011) and cell-surface localization (Benaud et al., 2002), and can also be induced in LNCaP cells by androgen treatment (Kiyomiya et al., 2006). Furthermore, activated matriptase cell-surface localization depends on specific interactions with its cognate inhibitor HAI-1 (Oberst et al., 2003b; Oberst et al., 2005).

Matriptase mRNA and protein are widely expressed in epithelial cells of most tissues (Takeuchi et al., 1999; Oberst et al., 2003a; List et al., 2006b; Netzel-Arnett et al., 2006; Szabo et al., 2007). Studies in matriptase-null mice have identified it as crucial for

terminal epidermal differentiation, epidermal barrier formation and hair follicle development (List et al., 2002; List et al., 2003; List et al., 2009). Moreover, tissue-dependent effects of matriptase deficiency have been determined demonstrating its role in loss of secretory and epidermal barrier function, and, in some tissues, loss of anatomical integrity (List et al., 2007; List et al., 2009; Buzza et al., 2010).

In vitro studies have shown this protease is expressed in the basolateral surface of prostate epithelial cells and when activated, translocates to the apical surface in complex with HAI-1 (Wang et al., 2009). Significantly, there is increased matriptase expression in prostate cancer with a positive correlation to increased tumour grade (Riddick et al., 2005; Saleem et al., 2006). However, while matriptase expression increases in localized prostate cancer compared to benign tissue, it decreases in metastatic disease (Warren et al., 2009).

1.5.4 TTSPs in proteolytic cascades

Similarly to the KLK family, studies have addressed the potential for other proteolytic cascades featuring TTSPs. Indeed, as matriptase (Takeuchi et al., 2000; Oberst et al., 2003b; Desilets et al., 2008), hepsin (Qiu et al., 2007) and TMPRSS2 (Afar et al., 2001) autoactivate they have the potential to function as cascade initiators.

Matriptase is one of the most comprehensively studied TTSPs. It has been implicated in proteolytic cascades in the skin through activation of the serine protease prostasin (Netzel-Arnett et al., 2006). As determined from the phenotypes of matriptase- and prostasin-deficient mice, matriptase-activated prostasin is required for epidermal differentiation and epithelial barrier function (List et al., 2002; List et al., 2003; Leyvraz et al., 2005; List et al., 2009).

Hepsin also activates transmembrane serine protease prostasin (Chen et al., 2010a), as a result providing an avenue for participation in the matriptase/prostasin cascade and epithelial barrier function (List et al., 2002; Leyvraz et al., 2005). Indeed, recent subcellular localization studies showing hepsin localized to desmosomal junctions in ovarian cancer cell lines (Miao et al., 2008) and primary mouse mammary epithelial cells (Partanen et al., 2012) also suggest a possible role in epithelial integrity. Co-localization studies have also implicated matriptase in cascades with prostasin or hepsin in embryonic development (Camerer et al., 2010). Prostasin and hepsin activate matriptase

(Camerer et al., 2010), though the mechanism by which prostasin achieves this is indirect, in the manner of a co-factor (Buzza et al., 2013). However, while a number of tissues and organs in matriptase- and prostasin-null mice have similarities in epithelial defects (List et al., 2002; List et al., 2003; Leyvraz et al., 2005; List et al., 2009), no epithelial phenotypic changes were detected in hepsin-null mice (Wu et al., 1998; Yu et al., 2000; Guipponi et al., 2007).

1.5.5 TTSPs in prostate cancer

In vitro and *in vivo* studies have been used to examine the roles of TTSPs in prostate and other cancers. For instance, matriptase is considered an oncogenic protein as increases in expression have been associated with progression of several cancers of epithelial origin including prostate cancer (List et al., 2005; Saleem et al., 2006; List, 2009). In accord, *in vivo* inhibition of matriptase reduced the growth of androgen-independent prostate cancer xenografts in mice (Galkin et al., 2004). Furthermore, *in vitro* matriptase inhibition or expression knockdown, by using siRNA or hammerhead ribozyme transgenes, reduced invasion of PC-3 and prostate cancer brain metastasis-derived DU145 cells (Forbs et al., 2005; Sanders et al., 2006). It has also been found that reduction in matriptase inhibitor HAI-1 led to increased motility and invasion of PC-3 and DU145 cells *in vitro* (Sanders et al., 2007). Similarly, decreased HAI-2 in a prostate cancer xenograft model led to increased matriptase activation and increased tumour cell migration invasion and metastasis (Tsai et al., 2013).

Other *in vitro* and *in vivo* overexpression models have also demonstrated possible influences of hepsin on progression of prostate cancer (Klezovitch et al., 2004; Moran et al., 2006; Xuan et al., 2006; Yemelyanov et al., 2007; Tripathi et al., 2008; Li et al., 2009; Ganesan et al., 2011; Wittig-Blaich et al., 2011). For instance, a study has shown that blocking hepsin activity using hepsin-neutralising antibodies inhibited *in vitro* Matrigel invasion of DU145 cells and ovarian cancer CAOV-3 cells while not altering cell growth (Xuan et al., 2006). Furthermore, in an *in vivo* study using hepsin-overexpressing ovarian cancer SKOV-3 cells, blocking hepsin activity by mutating the catalytic residues of hepsin reduced the size of subcutaneous tumours grown in mice (Miao et al., 2008). One of the tools developed for studying hepsin in prostate cancer is a hepsin-overexpressing LNCaP cell line, designated LNCaP-34. Generated by Moran and colleagues (2006), these cells have been used to demonstrate the *in vitro* ability of cell-

surface hepsin to activate uPA (Moran et al., 2006) and macrophage-stimulating protein (Ganesan et al., 2011), and degrade laminin-332 (Tripathi et al., 2008). The LNCaP-34 cells, implanted into mouse prostate to model prostate cancer, were also used to demonstrate the increased growth rate, invasive and metastatic potential of the hepsin-overexpressing cells (Li et al., 2009).

Interestingly, studies have also demonstrated a growth suppressive effect of hepsin overexpression *in vitro*. For instance, overexpression of hepsin in metastatic prostate cancer-derived PC-3, LNCaP and DU145 cells reduced cell growth, invasion and colony formation in soft agar assays (Srikantan et al., 2002). As such, it was proposed that the hepsin down-regulation observed in hormone-refractory prostate cancer may contribute to the growth and invasive capability of the metastatic cells (Fromont et al., 2005). Certainly studies in cell lines derived from ovarian and endometrial cancers have also shown hepsin overexpression reduced cell growth and anchorage-independent growth, increased apoptosis, *in vitro,* and decreased *in vivo* tumourigenicity (Nakamura et al., 2006; Nakamura et al., 2008). Furthermore, in a study by Klezovitch and colleagues (2004) using mice with SV40 large T antigen in the prostate epithelium, a mouse model of non-metastasizing prostate cancer, while hepsin overexpression caused disruption to the basement membrane and metastasis of prostate tumour cells to lung, liver and bone in the prostate epithelium, it had no observed impact on tumour cell proliferation (Klezovitch et al., 2004).

The study by Klezovitch and colleagues (2004) highlighted an interesting aspect of hepsin overexpression as they observed a weakening of epithelial-stromal adhesion in the prostate. Changes to epithelial integrity were also observed in a study by Partanen and colleagues (2012) of mouse mammary epithelium, tumourigenesis promoted by a loss of expression of the tumour suppressor liver kinase B1 (LkB1) combined with overexpression of the oncogene c-Myc resulted in loss of epithelial integrity marked by loss of cell polarity, desmosomal junction and basement membrane deterioration. Hepsin was identified as a key factor in the structural alterations as it was no longer seen to be confined to desmosomal complexes. Moreover, silencing hepsin restored basement membrane integrity in this tumourigenesis model. Interestingly, this model demonstrated the delocalization of hepsin from the desmosomal junctions at the cell surface to the cytosol in response to either LkB1 loss and c-Myc expression, or the deterioration of cell-cell junctions induced by calcium depletion. This study is

complemented by a study in which an overexpression of hepsin and c-Myc in a prostate cancer mouse model demonstrated rapid progression of prostate cancer (Nandana et al., 2010). Interestingly, unlike the hepsin overexpressing prostate cancer mouse model studied by Klezovitch and colleagues (2004), in the hepsin/c-Myc model, the cancer did not progress to metastasis, further highlighting the vagaries of hepsin (Nandana et al., 2010).

Taken together, these studies suggest that the serine protease activity exerted by hepsin is one mechanism by which hepsin contributes to prostate cancer progression. Furthermore, hepsin may have a complex role in maintenance of epithelial integrity. Deregulation of hepsin may contribute to prostate cancer progression through disruption of the basement membrane and altered interactions with proteins involved in cell-to-cell contact and cell-to-substratum adhesion (Vasioukhin, 2004).

1.6 Hepatocyte growth factor

Activated HGF (also known as scatter factor) (Figure 1.7) is the ligand of a tyrosine kinase receptor, hepatocyte growth factor receptor (HGFR) (also known as the MET receptor) (Bottaro et al., 1991). Primarily produced by stromal cells, HGF induces epithelial cell proliferation, motility and morphogenesis through activation of HGFR (Nakamura and Mizuno, 2010). Irregular receptor signalling due to HGFR and HGF overexpression has an established role in tumourigenesis (Trusolino et al., 2010; Gherardi et al., 2012) and, in particular, has been associated with the progression of prostate cancer (Humphrey et al., 1995; Nakashiro et al., 2000; Knudsen et al., 2002; Nakashiro et al., 2003; Knudsen and Edlund, 2004; Hashem and Essam, 2005; Yasuda et al., 2009).

HGF has a domain structure similar to the serine protease plasminogen (Figure 1.7) (Miyazawa et al., 1989; Nakamura et al., 1989; Donate et al., 1994), however, the serine protease domain of HGF is catalytically inactive (Lokker et al., 1992). Activation of the HGF single chain precursor (pro-HGF) to produce a heterodimer linked by a disulphide bond occurs by proteolysis at an arginine residue immediately prior to the serine protease homology domain (Gak et al., 1992; Naka et al., 1992; Naldini et al., 1992). Several serine proteases with a preference for Arg P1 residues activate HGF including the serum protease hepatocyte growth factor activator (HGFA) (Shimomura et al., 1995;

Itoh et al., 2004), and the transmembrane proteases matriptase (Lee et al., 2000; Owen et al., 2010) and hepsin (Herter et al., 2005; Kirchhofer et al., 2005; Owen et al., 2010). In contrast, two prostate-expressed members of the KLK family, KLK4 and KLK5, both with Arg P1 specificity, degrade rather than activate HGF (Mukai et al., 2008). In this same study it was determined that these KLKs activate HGFA, thereby potentially positively regulating the HGF-HGFR signalling cascade. However, a role for KLK14 in HGF activation and the HGF-HGFR signalling cascade has not been reported.

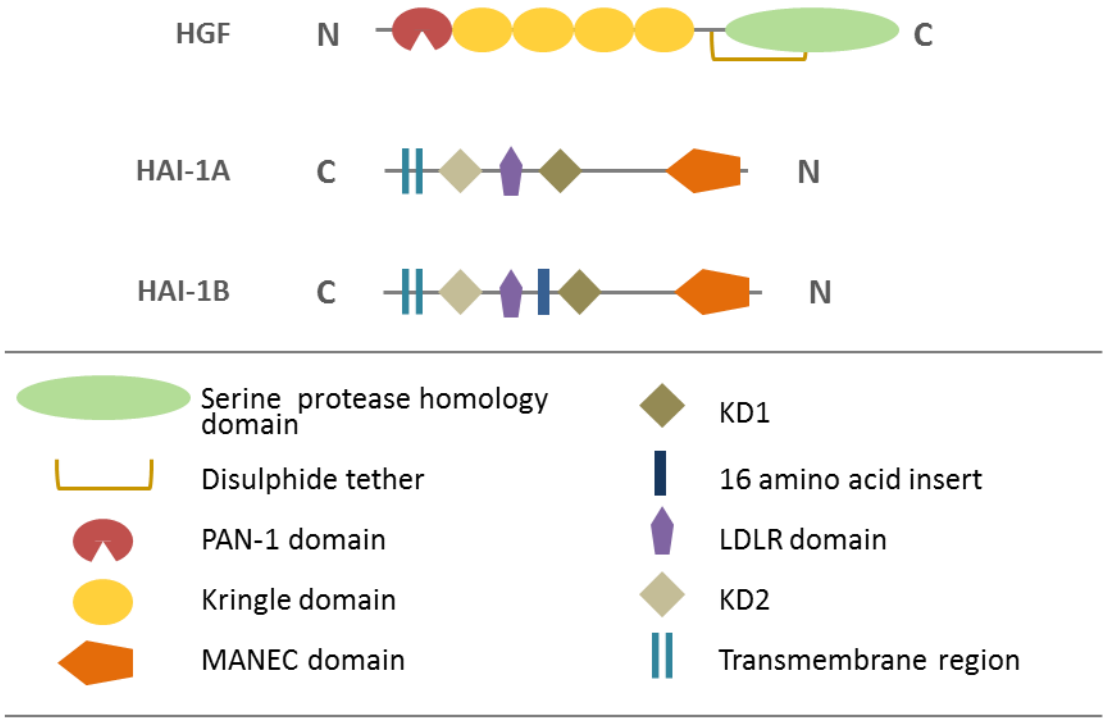

Figure 1.7 Domain structures of HGF, HAI-1A and HAI-1B. HGF is a secreted cell growth, motility and morphogenesis factor. It is characterized by a PAN-1 domain at the N-terminal and four kringle domains, with a C-terminal serine protease homology domain lacking proteolytic activity. When activated by limited proteolysis between the last kringle domain and the serine protease domain, the serine protease domain remains tethered to the stem by a disulphide bond. **HAI-1A** and **HAI-1B** are transmembrane serine protease inhibitors with near identical sequences. They consist of an extracellular motif at N-terminus with eight cysteines (MANEC) domain with two Kunitz domains (KD1 and KD2) separated by a Low-Density Lipoprotein Receptor (LDLR) domain. HAI-1B also has an extra 16 amino acid insert between KD1 and the LDLR domain.

1.7 Hepatocyte growth factor activator inhibitor-1

A crucial aspect of HGF activation and induced HGFR signalling, is regulation of the activating proteases by inhibitors (Gherardi et al., 2012). HAI-1 is a Kunitz-type, type-1 transmembrane serine protease inhibitor with two isoforms, HAI-1A and splice variant HAI-1B (Shimomura et al., 1997; Kirchhofer et al., 2003). HAI-1 is an endogenous inhibitor of HGF activators HGFA and matriptase (Shimomura et al., 1997; Lin et al., 1999b; Benaud et al., 2001; Wang et al., 2009). Moreover, a role for HAI-1 in tight regulation of matriptase pericellular activity has been proposed (Oberst et al., 2003b; Oberst et al., 2005; Fan et al., 2007; Lee et al., 2007; Szabo et al., 2007; Tseng et al., 2010; Friis et al., 2011). It has also been shown to inhibit other HGF activators *in vitro* including hepsin (Herter et al., 2005; Kirchhofer et al., 2005).

The HAI-1 isoforms are expressed on the surface of epithelial cells with high expression of mRNA and protein in tissues such as prostate, kidney, intestine and placenta (Kataoka et al., 1999; Itoh et al., 2000; Tanaka et al., 2009; Wang et al., 2009). While one study determined that compared to normal prostate tissue HAI-1 protein expression decreased in prostate cancer with increasing cancer grade (Saleem et al., 2006), several other studies have demonstrated contrary results. For instance, Knudsen and colleagues (2005) found that HAI-1 increased in localized and metastasized prostate cancer compared to normal tissue. Similarly, in another study HAI-1 was found to increase in all proliferative prostate diseases, from benign prostatic hyperplasia (BPH) to aggressive and metastatic prostate cancer, with no distinction between diseased tissue type (Warren et al., 2009). Recently, Yasuda and colleagues (2013) also found that HAI-1 had higher expression in prostate tissue from patients with prostate cancer compared to patients with benign disease. However, they also found that HAI-1 decreased in patients with castration-resistant prostate cancer compared to those with untreated metastasized prostate cancer. HAI-1 has also been detected in the serum from patients with prostate cancer and found to be significantly elevated compared to patients with BPH (Nagakawa et al., 2006). This study also showed that serum HAI-1 was higher in patients with metastasized and hormone-resistant prostate cancer compared to those with localized disease.

The HAI-1 isoforms are very similar (Figure 1.7), consisting of a region at the N-terminus with eight cysteines called the MANEC domain (Guo et al., 2004), a Kunitz domain (KD1), a LDLR domain, a second Kunitz domain (KD2), a transmembrane

region, and a cytoplasmic domain (Shimomura et al., 1997). However, HAI-1B has an extra 16 amino acid insert between KD1 and LDLR of unknown significance (Kirchhofer et al., 2003).

HAI-1 inhibitory activity likely occurs via standard mechanism inhibition (Laskowski and Qasim, 2000; Krowarsch et al., 2003), mediated by the Kunitz domains (Shimomura et al., 1997). These domains in effect act like substrates, binding to a protease active site through a P1 residue in a substrate-like binding loop on the surface of the domain (Laskowski and Qasim, 2000; Krowarsch et al., 2003). It binds the serine protease in a very stable, but also reversible complex, resembling a Michaelis complex. Dissociation of the complex can either result in release of the protease and intact inhibitor or can result in release of protease and inhibitor hydrolysed at the reactive site. The inhibitor hydrolysed at the active site is still able to form the same complex with the protease as the intact inhibitor. As the protease-inhibitor complex formed is very stable, the progression to dissociation is very slow, which results in the inhibition of the protease by holding it in complex for extended periods (Laskowski and Qasim, 2000; Krowarsch et al., 2003).

A recent study, using LNCaP cells overexpressing hepsin implanted into mouse prostate to model prostate cancer, found that a truncated form of HAI-1 containing KD1 inhibits hepsin-mediated tumour growth and invasion (Li et al., 2009). Mukai and colleagues (2008) also showed that this same form of truncated HAI inhibits KLK4. However, the inhibition of KLK14 by HAI-1 has not been reported.

1.8 Matrix metalloproteinases (MMPs)

Metalloproteinases are proteases that contain a Zn^{2+} ion in the active site (Bode et al., 1993). They are grouped into several clans and families of which the MMPs are a part (Rawlings et al., 2012). There are 23 MMPs found in humans (Quesada et al., 2009) and the structure, function and activation of these have been well reviewed recently by several authors (Nagase et al., 2006; Ra and Parks, 2007; Gomis-Ruth, 2009; Tallant et al., 2010; Klein and Bischoff, 2011).

In MMPs, the Zn^{2+} ion in the catalytic domain is coordinated by three histidine residues in a conserved zinc binding motif, HEXXHXXGXXH, followed by a strictly conserved methionine-containing turn. Based on studies of other members of the

metalloproteinase superfamily, catalysis of a peptide substrate probably follows a mechanism in which the glutamate reside in the catalytic motif, as a general base, polarizes a zinc bound water molecule to provide a nucleophile that attacks the carbonyl group of the substrate scissile bond (Ra and Parks, 2007; Tallant et al., 2010). In general MMPs cleave substrates before a P1' residue with a hydrophobic side chain, such as Ile, Leu, Phe, Met and Tyr (Murphy and Nagase, 2008). Substrate specificity is governed by several factors including the shape of the MMP S1' pocket which accommodates the P1' residue, and other substrate contact points (Murphy and Nagase, 2008).

Similar to the serine proteases, the MMPs are produced as a zymogen with a signal peptide sequence targeting them to secretory vesicles from which they are secreted or anchored to the cell surface (Ra and Parks, 2007). In addition, all the MMPs, except MMP23, contain a cysteine switch motif, PRCGXPD, in the pro-region of the zymogen. The thiol of the cysteine residue in the motif interacts with the catalytic site Zn^{2+} to keep the MMP inactive (Ra and Parks, 2007). This thiol-Zn^{2+} interaction can be broken by alkylating agents, heavy metal ions and reducing agents, rendering the zymogen MMP active. However, it is generally considered that zymogen MMPs are activated by proteolytic cleavage to remove the pro-region, similar to other zymogen proteases (Ra and Parks, 2007).

All the MMPs, except MMP7, MMP23 and MMP26, also have a flexible proline-rich hinge region after the catalytic domain which connects to a C-terminal hemopexin-like domain (Ra and Parks, 2007). This domain functions particularly in substrate recognition, for example, it is essential for the cleavage of triple helical collagen chains (Murphy and Nagase, 2008). The hemopexin domains of proMMP2 and proMMP9 also bind tissue inhibitors of metalloproteinases (TIMPs) forming complexes that, in some instances, are known to inhibit other MMPs (Murphy and Nagase, 2008). Figure 1.8 shows schematic diagrams of the domain structures of MMP3 and MMP9.

1.8.1 MMP3

MMP3 is found in the stroma of tumours, expressed by fibroblasts and endothelial cells (Deryugina and Quigley, 2010) and is induced by inflammatory cytokines and a number of growth factors (Nagase, 2013). However, the role of MMP3 in cancer is uncertain with early studies pointing to pro-carcinogenic effects of MMP3 in breast cancer

(Sternlicht et al., 1999; Sternlicht et al., 2000) while more recent studies have suggested a protective role in some cancers such as squamous cell carcinoma (McCawley et al., 2004). The role of MMP3 in prostate cancer has not yet been determined. However, there are higher levels of MMP3 in the serum of prostate cancer patients with metastases (Jung et al., 1997) and it has been detected in the ECM surrounding neoplastically transformed cells in prostate cancer (Bodey et al., 2001). Furthermore, in a prostate cancer mouse model, MMP3 mRNA expression was 6-fold higher in the stromal cells of invasive prostate cancer compared to prostate intraepithelial neoplasms (Bacac et al., 2006). Together these results suggest a role for MMP3 in tumour progression.

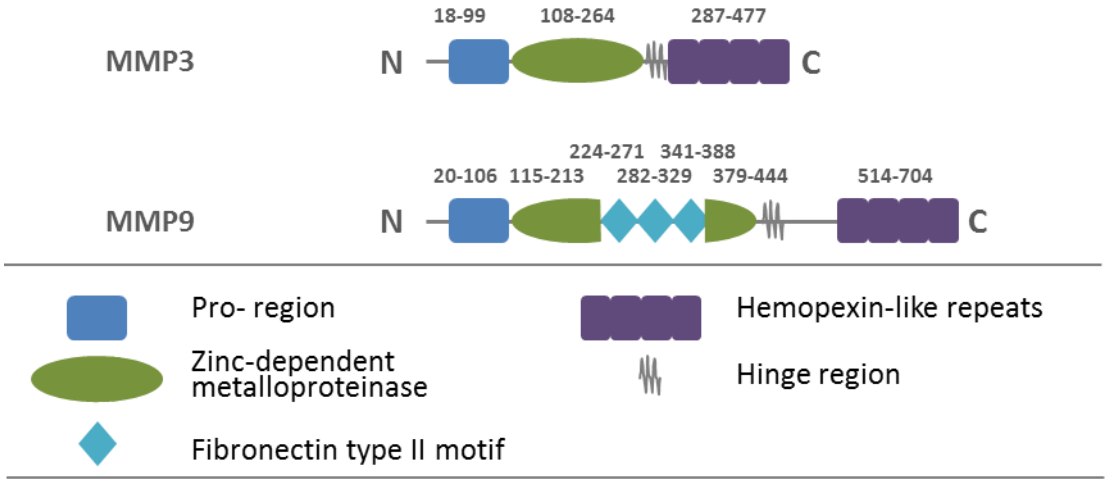

Figure 1.8 Domain structures of the metalloproteinases MMP3 and MMP9. MMP3 and MMP9 are directed to the secretory pathway by an N-terminal signal peptide. Each consists of a pro-region; a catalytic metalloproteinase domain containing a zinc binding motif; a linker region also known as the hinge region; and a hemopexin domain. MMP9 also has three repeats of a fibronectin type II motif in the metalloproteinase domain. A cysteine in the pro-region coordinates with the zinc in the metalloproteinase domain to keep the protease inactive. Activation requires proteolytic removal of the pro-region or physical removal of the cysteine from coordination with the zinc. The amino acid numbers indicated above each domain delineate the location of each domain.

MMP3 cleaves a variety of ECM and non-matrix proteins, generating several bioactive molecules including anti-angiogenic factors endostatin and tumstatin (Ferreras et al., 2000; Noe et al., 2001; Hamano et al., 2003; Heljasvaara et al., 2005). It shows a strong preference for hydrophobic P1' residues with no particular preference for the P1 (Nagase, 2013). For this reason, it has the potential to activate a wide range of serine proteases possessing a hydrophobic P1' (Hedstrom, 2002; Rawlings and Barrett, 2013b).

Indeed, as mentioned earlier, MMP3 activates KLK4 (Beaufort et al., 2010; Yoon et al., 2013). Moreover, MMP3 activates other MMPs including MMP9 (Ogata et al., 1992; Nagase, 2013). In turn, MMP3 can be activated by trypsin-2 (Moilanen et al., 2003), plasmin (Nagase et al., 1990) and matriptase (Jin et al., 2006), thereby potentially participating in activation cascades with a range of serine proteases.

1.8.2 MMP9

MMP9 is a gelatinase capable of degrading ECM proteins as well as releasing pro-angiogenic vascular endothelial growth factor (VEGF) and anti-angiogenic factors such as tumstatin (Egeblad and Werb, 2002; Deryugina and Quigley, 2006; Klein and Bischoff, 2011). Similar to MMP3, it is expressed by stromal cells such as fibroblasts, inflammatory and endothelial cells (Egeblad and Werb, 2002). MMP9 has also been well documented in diverse malignant processes. Certainly, a number of studies have implicated MMP9 in pro-/anti-angiogenesis, invasion, metastasis and regulation of inflammatory cells in cancer (Egeblad and Werb, 2002; Deryugina and Quigley, 2006; Klein and Bischoff, 2011). Moreover, upregulation of MMP9 expression is well correlated with diagnosis or prognosis in several cancer types including prostate cancer (Stearns and Wang, 1993; Escaff et al., 2011a; Klein and Bischoff, 2011). Immunohistochemical analysis has shown that MMP9 has very low expression in normal or benign prostate tissue and it remained confined to the epithelial cells and was not detected in the stroma to any significant degree (Stearns and Wang, 1993; Escaff et al., 2010, 2011b). However, in prostate cancer MMP9 expression increased in epithelial cells with increasing grade and was also detected in stromal cells (Stearns and Wang, 1993; Escaff et al., 2010, 2011b). Furthermore, similar to MMP3, MMP9 plasma concentrations were higher in patients with metastasis (Morgia et al., 2005).

Several studies have shown a clear link between MMP9 and degradation of bone matrix (Edlund et al., 2004) as well as it being a key protease in prostate cancer development (Deryugina and Quigley, 2006; Littlepage et al., 2010). *In vitro* studies have also demonstrated that MMP9 overexpression promoted the invasive capability of LNCaP cells (Aalinkeel et al., 2011). Moreover, MMP9 expression knockdown reduced DU145 *in vitro* cell proliferation and *in vivo* tumour growth, invasion and angiogenesis (London et al., 2003). However, in a prostate cancer mouse model MMP9 knockdown had no effect on tumour growth or survival, though it was associated with decreased blood

vessel size (Littlepage et al., 2010). Similarly, MMP9 positively affected angiogenesis in a prostate cancer bone metastasis mouse model (Bruni-Cardoso et al., 2010).

In addition to *in vitro* activation by MMP3, MMP9 is activated by several serine proteases including KLK1 (Tschesche et al., 1989; Desrivieres et al., 1993; Menashi et al., 1994), trypsin (Okada et al., 1992), trypsin-2 (Sorsa et al., 1997) and plasmin (Mazzieri et al., 1997). While MMP9 has a preference for small P1 residues and hydrophobic, aliphatic P1' residues, it is unlikely to activate trypsin-like serine proteases with Arg/Lys P1 residues (Eisen et al., 2013). So, MMP9 is more likely to be activated by, than activate, serine proteases in a proteolytic cascade. This possibly relegates MMP9 to the role of executor at the end of a cascade. This is consistent with the substrates identified as favoured by MMP9 which include mostly ECM proteins, as well as processing of a few growth factors and cytokines, a serine protease inhibitor, and plasmin into angiostatin (Eisen et al., 2013).

1.9 Protease-activated receptors (PARs)

The four PAR family members, designated PAR1-PAR4, are members of the GPCR superfamily (Macfarlane et al., 2001) of transmembrane proteins that transduce extracellular stimuli into intracellular signals. While the general mechanism of GPCR activation is by interaction or binding with soluble ligands (Metaye et al., 2005), the PARs are a unique group in which specific proteolytic cleavage of the PAR extracellular N-terminal creates a new N-terminal which functions as a tethered ligand (Vu et al., 1991a; Macfarlane et al., 2001) (Table 1.1). However, PAR1, PAR2 and PAR4 can also be activated *in vitro* by short peptides, known as agonist peptides (AP), which mimic the tethered ligand sequence (Ramachandran et al., 2012b 1443). PAR signalling is thought to occur when a protease-exposed tethered ligand or AP binds intramolecularly to conserved regions of the PAR including the second extracellular loop (Vu et al., 1991a; Lerner et al., 1996; Adams et al., 2011).

The range of cellular effects resulting from PAR activation is extensive. They include inflammation, immune response, differentiation, proliferation, migration, angiogenesis, apoptosis evasion and metastasis (Steinhoff et al., 2005; Adams et al., 2011; Kaufmann and Hollenberg, 2012), and they are all functional capabilities acquired by cancer cells (Hanahan and Weinberg, 2011). Importantly for this project, increased mRNA and

protein expression of PAR1, PAR2 and PAR4, but not PAR3, have been detected in prostate adenocarcinoma compared to normal prostate tissue (Tantivejkul et al., 2005; Kaushal et al., 2006; Black et al., 2007). Moreover, PARs are activated by proteases from well-established proteolytic cascades such as the coagulation, plasminogen activation and digestive enzyme cascades (Ossovskaya and Bunnett, 2004; Adams et al., 2011). Likewise, PARs may be activated by other proteolytic cascades or as a result of aberrant cascades in a tumour microenvironment.

1.9.1 PARs structure and activation

The structural features for each of the four PARs are detailed in Figure 1.9. The general features of this receptor family include: length of between 374 and 425 amino acids; an extracellular N-terminal, seven-transmembrane domains, a conserved second extracellular loop, and an intracellular C-terminal (Macfarlane et al., 2001; Luttrell, 2008). The PAR1 and PAR3 N-termini also contain thrombin-binding hirudin-like domains (Macfarlane et al., 2001).

PAR1 was the first of the PARs identified and characterized as the thrombin receptor (Vu et al., 1991a; Vu et al., 1991b) and it is the most extensively studied of the PAR family. Identification of PAR1 was followed by identification of PAR2 as a trypsin- and tryptase-activated receptor (Nystedt et al., 1994; Nystedt et al., 1995a; Nystedt et al., 1995b), and PAR3 (Ishihara et al., 1997) and PAR4 (Kahn et al., 1998; Xu et al., 1998) as thrombin-activated receptors.

A number of other serine proteases were found capable of PAR activation including members of the KLK and TTSP families including KLK4, KLK14, TMPRSS2 and matriptase (Ramsay et al., 2008b; Adams et al., 2011). Proteases from other classes are also capable of PAR activation including PAR1 activation by MMP1 (Boire et al., 2005), MMP2 (Malaquin et al., 2013) and MMP13 (Jaffre et al., 2012), and PAR2 and PAR4 activation by cysteine protease cathepsin S (Reddy et al., 2010).

In addition to using proteases to cleave the PAR tethered ligand in *in vitro* studies, APs have proved to be useful tools for investigating PAR activation. However, the AP modelled directly on the six residue sequence of the PAR1 tethered ligand, SFLLRN-NH_2 (also known as TRAP), also activates PAR2 (Nystedt et al., 1995b; Blackhart et al., 1996; Lerner et al., 1996). So a PAR1-specific AP was developed in which the S is

substituted for T in the first position of SFLLRN-NH_2, this modification abrogated the ability of the peptide to cross-activate PAR2 while retaining PAR1 activation ability (Hollenberg et al., 1997). Furthermore, the final residue, N, was found to have little effect on the potency of the activating peptide as so was eliminated to yield the agonist peptide TFLLR-NH_2 (Hollenberg et al., 1997).

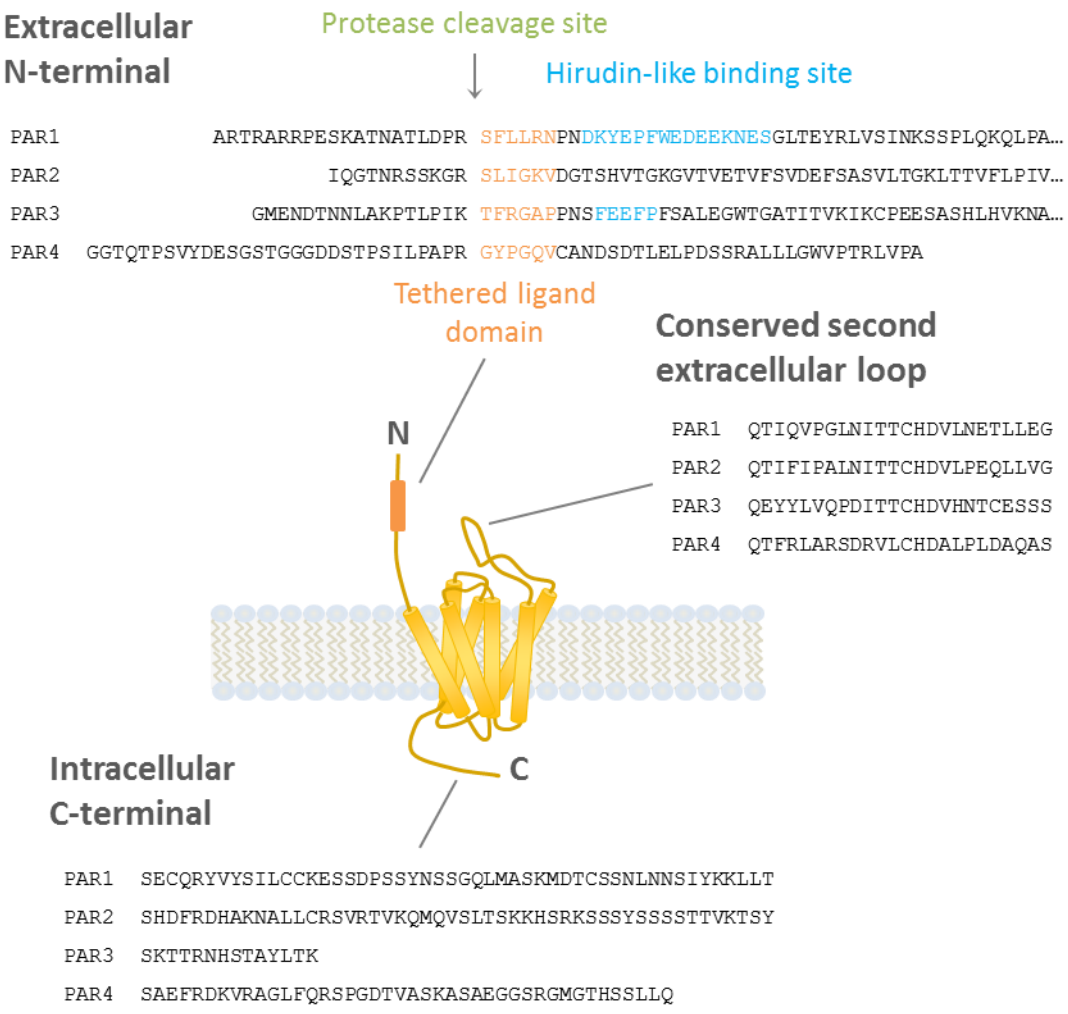

Figure 1.9 PAR structural features. The regions highlighted include the extracellular N-terminal showing the protease cleavage sites to reveal the tethered ligand domain; the Hirudin-like binding domains of PAR1 and PAR3; the conserved second extracellualar loop which contains the regions involved in tethered ligand interaction; and the intracellular C-terminal which is involved in signal transduction. *Adapted from* Zhang et al., 2013; Steinhoff et al., 2005; and MacFarlane et al., 2001.

In analysis of PAR APs, Hollenberg and colleagues (1997) also demonstrated that a PAR2-activating peptide modelled on the sequence of mouse PAR2, SLIGRL-NH_2 has

higher potency in human PAR2 activation than the human sequence SLIGKV-NH_2. Similarly, structure-activity analysis revealed that the low potency PAR4 AP based on the tethered ligand, GYPGFK-NH2, was 10 times more potent if modified to AYPGFK-NH_2 (Faruqi et al., 2000). On the other hand, PAR3 is not activated by its thrombin-revealed tethered ligand sequence (Ishihara et al., 1997) and so far a PAR3 AP has not been developed. Indeed, peptide sequences modelled on the PAR3 tethered ligand activate PAR1 and PAR2 but not PAR3 (Hansen et al., 2004; Kaufmann et al., 2005). As there is no PAR3 AP or conclusive method to activate PAR3 singly, it was not included in this PhD project.

1.9.2 PAR signal transduction

Similar to other GPCRs, it is likely that ligand binding causes conformational changes in the PAR. It then functions as a guanine nucleotide exchange factor (GEF) facilitating the exchange of guanosine diphosphate (GDP) for guanosine triphosphate (GTP) on the Gα subunit of heterotrimeric G proteins that associate with GPCRs (Figure 1.10) (Oldham and Hamm, 2008; Soh et al., 2010). The PARs associate with a number of different heterotrimeric G protein subtypes including, $G_{12/13}$, $G_{q/11}$ and $G_{i/o}$ (Russo et al., 2009b; McCoy et al., 2010). The GTP-bound Gα subunit of the heterotrimeric G protein is able to dissociate from tight-binding with the Gβγ heterodimer subunit (Oldham and Hamm, 2008). GTP-Gα and Gβγ then independently activate effector proteins, such as ionic channels, phospholipase Cβ (PLCβ), Rho GEFs, and PI3K, depending on the G protein subtype activated (Oldham and Hamm, 2008; Russo et al., 2009b). The effector proteins in turn modulate cellular levels of second messenger molecules such as diacylglycerol (DAG), inositol 1,4,5-trisphosphate (IP_3) and Ca^{2+}, as well as regulating down-stream effector pathways such as the mitogen-activated protein kinase (MAPK) and RhoA pathways (Metaye et al., 2005; Luttrell, 2008; Soh et al., 2010). Ultimately, the second messenger levels and down-stream effector pathways modify cellular metabolism and biological responses (Metaye et al., 2005; Soh et al., 2010).

In addition to the heterotrimeric G proteins, PARs recruit other interacting proteins to regulate receptor signalling, ligand specificity, cell-surface localization, endocytosis and recycling or degradation (Soh et al., 2010). This includes termination of PAR1 and PAR2 signalling by phosphorylation of PAR C-terminal regions, thereby, desensitizing

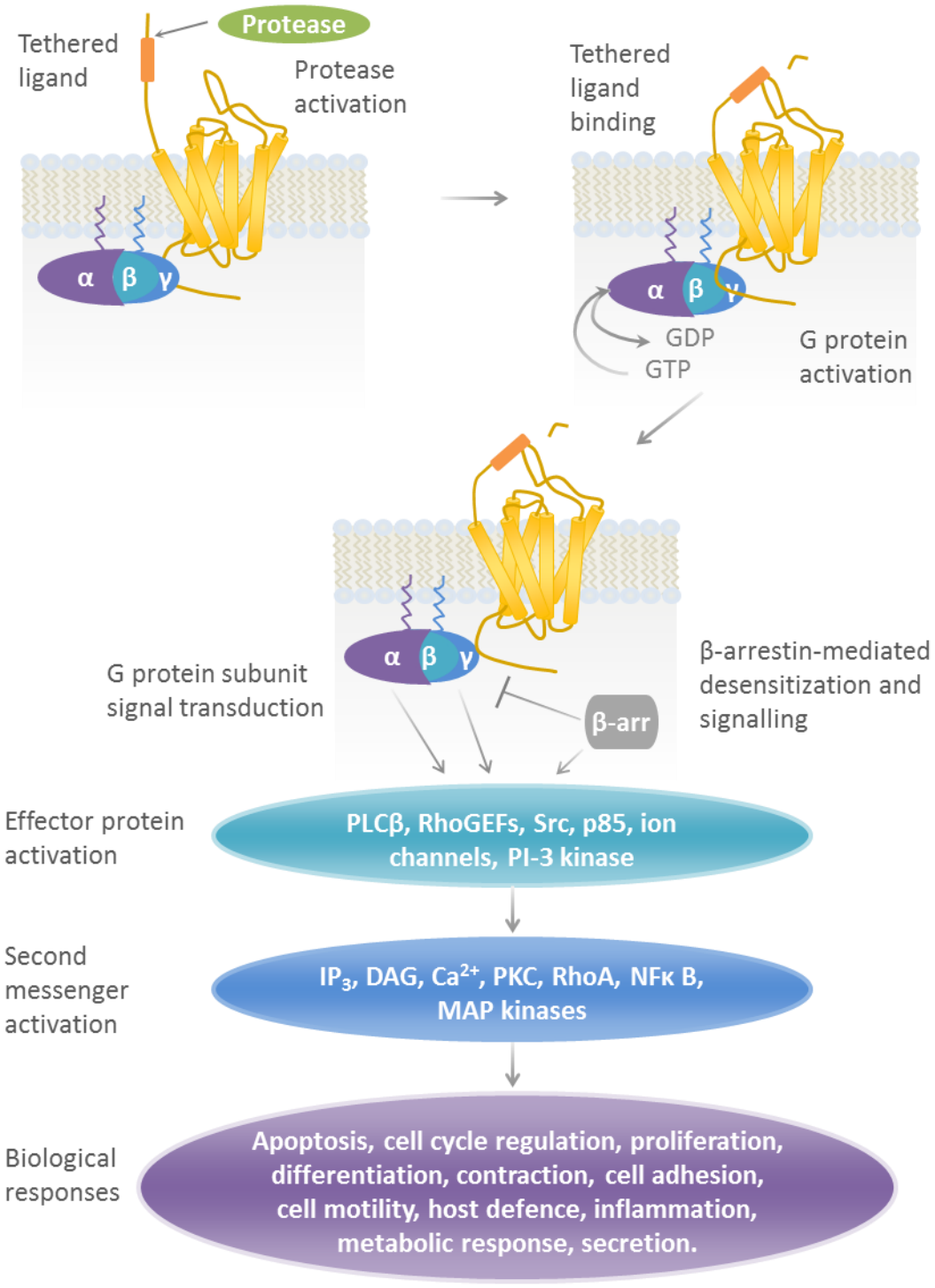

Figure 1.10 Protease-activated receptor (PAR) signalling. The protease revealed tethered ligand of activated PAR binds intra-molecularly. This causes a conformation shift in PAR that facilitates activation of associated heterotrimeric G protein through exchange of guanosine diphosphate (GDP) for guanosine triphosphate (GTP). Gα and heterodimer Gβγ subunits activate effector proteins which in turn activate second messenger molecules that induce biological responses. β-arrestin couples to PAR2 regulating desensitization, internalization and G protein-independent signalling. *Adapted from* Soh, 2010; and Steinhoff, 2005.

the receptor (Ishii et al., 1994; Bohm et al., 1996a; Tiruppathi et al., 2000; Ricks and Trejo, 2009). PAR1 and PAR2 receptor desensitization and G protein-independent signalling are also mediated by β-arrestins (DeFea et al., 2000; Paing et al., 2002; Chen et al., 2004; Defea, 2008; Soh and Trejo, 2011), as is the internalization by endocytosis of PAR2 (Dery et al., 1999; DeFea et al., 2000). Furthermore, while β-arrestins also promote PAR4 G protein-independent signalling (Li et al., 2011), the mechanisms of PAR3 and PAR4 desensitization and internalization are largely unknown (Ramachandran et al., 2012b).

Proteolytic activation of PARs is irreversible therefore receptor desensitization and internalization are crucial aspects of PAR regulation to prevent continuous signal transduction by activated PAR (Ossovskaya and Bunnett, 2004). For instance, PAR1 signalling via G_q is active for a finite period in which it initiates production of a specific quantity of second messenger (Ca^{2+}) before signal termination (Ishii et al., 1993). Following desensitization, renewed PAR1 and PAR2 signalling requires mobilization of intracellular stores or synthesis of new receptors (Hein et al., 1994; Bohm et al., 1996a; Roosterman et al., 2003; Paing et al., 2006; Luo et al., 2007), a process known as resensitization. The mechanism of PAR3 and PAR4 resensitization is unknown. However, recent work has shown that heterodimerization with PAR2 facilitates PAR4 translocation from the endoplasmic reticulum (ER) to the plasma membrane and also PAR4 signalling (Cunningham et al., 2012).

1.9.3 PAR disarming proteases and biased agonism

Proteases can also disarm PARs through cleavage at sites to remove the N-terminal tethered ligand sequence (Hollenberg and Compton, 2002; Ramachandran et al., 2012b). This disarming event may prevent PAR activation by other proteases, but not by AP (Hollenberg and Compton, 2002). For instance, neutrophil elastase, cathepsin G and proteinase 3 have distinct PAR1 N-terminal cleavage sites that disarm PAR1 preventing subsequent activation by thrombin (Renesto et al., 1997). Similarly, PAR2 is disarmed by N-terminal cleavage downstream of the tethered ligand by neutrophil elastase, cathepsin G and proteinase 3, preventing subsequent trypsin activation (Dulon et al., 2003; Ramachandran et al., 2011).

Interestingly, however, Ramachandran and colleagues (2011) demonstrated that while neutrophil elastase treatment of rat kidney-derived cell line KNRK transfected with human PAR2 (KNRK-PAR2) did not exhibit a G_q-mediated intracellular calcium signalling response (Ca^{2+} mobilization), neutrophil elastase elicited PAR2 signalling via the extracellular signal-regulated kinase (ERK)1/2 MAPK signalling pathway. This induction of distinct signalling pathways by different GPCR agonists/antagonists is the result of association with multiple signalling effectors and is known as functional selectivity or biased agonism (Kenakin, 2007; Urban et al., 2007; Kenakin, 2011). Another example of biased agonism in PARs is that AP-induced PAR1 signalling favours $G\alpha_q$ over $G\alpha_{12/13}$-mediated pathways while the opposite was observed for PAR1 thrombin-activation (McLaughlin et al., 2005). As reviewed by Russo and colleagues (2009b), plasma membrane localization of PAR1 and PAR2 also facilitates biased agonism through recruitment of different signalling effectors. These observations of biased agonism increase the complexity of PAR-induced signalling and necessitate examination of what constitutes a PAR-activating or -inactivating protease.

1.9.4 PARs in prostate cancer

Prostate expression of PARs at the mRNA and protein level has been assessed in a number of studies comparing normal prostate with BPH and prostate cancer. Immunohistochemical analysis of tissue microarrays of prostate biopsies demonstrated that PAR1 expression was significantly increased in prostate cancer compared to normal and BPH prostatic tissue (Tantivejkul et al., 2005). Similarly, Kausal and colleagues (2006) demonstrated PAR1 protein expression in advanced prostate cancer was 2.75-fold higher than in early-stage prostate cancer. This group also showed that PAR1 expression was predominantly localized to the vascular endothelial cells in the prostate tumour. Significantly, PAR1 expression was also correlated with advanced disease.

In an examination of all four PARs, Black and colleagues (2007) determined PAR1 expression was mostly negative in normal prostate tissue, while, PAR2 was detected occasionally. In contrast, PAR4 was detected in over 50% of normal tissue. However, in prostate cancer PAR1, PAR2 and PAR4 all demonstrated increased expression levels. PAR3 levels on the other hand were consistently low in all normal and diseased prostate tissue. Interestingly, PAR1, PAR2 and PAR4 were detected mostly in the epithelial cells. However, increased PAR1 expression was also detected in periglandular stroma of

higher grade cancer compared to lower grades and was associated with prostate cancer recurrence.

A further study by this group determined that over 80% of primary prostate cancer tissues expressed PAR1 in the peritumoural stroma (Zhang et al., 2009). PAR1 was localized predominantly to stromal myofibroblast cells while PAR2 was predominantly localized to the primary tumour cells and, to a lesser extent, the smooth muscle cells of the stroma. Similarly, in a study of BPH, this group also detected increased PAR1 stromal expression in BPH compared to normal prostate stroma (Wang et al., 2008). Mannowetz and colleagues (2010) also demonstrated the differential localization of PAR2 in normal, prostate cancer and BPH tissues. In normal tissue PAR2 was located in the apical membrane of epithelial cells. However, in prostate cancer tissue PAR2 was located on both the apical and basal membrane as well as a small amount in the stroma. On the other hand, in BPH, PAR2 was absent from the epithelial cells and localized to the stroma.

Examination of bone metastasis also demonstrated PAR1 expression in the bone reactive stroma, in endothelial and fibroblast cells predominantly, and in the carcinoma cells to a lesser extent while PAR2 remained primarily expressed by the carcinoma cells (Zhang et al., 2009). However, both PAR1 and PAR2 were expressed by osteoclasts and osteoblasts in the bone reactive stroma. An earlier study comparing cells derived from prostate cancer bone metastasis with soft tissue metastasis-derived cells identified increased PAR1 gene expression as relevant to prostate cancer metastasis to bone (Chay et al., 2002). Interestingly, in a study by our laboratory, it was also shown that in addition to elevated PAR2 and KLK4 co-expression in primary prostate cancer, there was elevated co-expression of these proteins in prostate cancer bone metastases (Ramsay et al., 2008a).

In vitro studies have indicated PAR activation has a range of cellular effects in prostate cancer-derived cells. For instance, in DU145 and LNCaP cells, thrombin induces concentration-dependent effects on cell cycle and proliferation (Zain et al., 2000; Liu et al., 2003). Low levels of thrombin induced cell proliferation of DU145 and LNCaP cells, however, higher concentrations of thrombin resulted in cell cycle arrest and apoptosis for the DU145 cells (Zain et al., 2000) and initial growth stimulation followed by growth inhibition for the LNCaP cells (Liu et al., 2003), indicating concentration- and cell-type-dependent biased agonism of PAR1 by thrombin. In addition, Greenberg and colleagues

(2003) demonstrated the role of PARs in morphology, adhesion and migration as thrombin and trypsin, as well as PAR1 and PAR2 APs, induced RhoA activation in LNCaP cells. Thrombin and trypsin also induced morphological changes in the LNCaP cells through cytoskeletal rearrangement and formation of stress fibres and focal adhesions. Recent work in the same laboratory has shown that in addition to RhoA, migration signalling proteins Rac1 and Cdc42 were recruited and migration was induced in LNCaP cells by thrombin and trypsin activation of PAR1 and PAR2, respectively (Black et al., 2007).

1.9.5 PARs, KLKs and TTSPs

As mentioned before, KLK4, KLK14, TMPRSS2 and matriptase activate PAR family members. For instance, PAR1, PAR2 and PAR4 are activated by KLK14 (Oikonomopoulou et al., 2006b; Stefansson et al., 2008; Gratio et al., 2011; Chung et al., 2012). However, KLK14 also disarms and desensitizes PAR1 to activation by other proteases in a concentration-dependent manner (Oikonomopoulou et al., 2006a). Furthermore, in HT-29 colon cancer-derived cells and platelets, KLK14 preferentially activates PAR2 and PAR4, respectively, over PAR1 (Oikonomopoulou et al., 2006a; Gratio et al., 2011; Chung et al., 2012). PAR2 activation by KLK14 in HT29 cells results in intracellular signalling via ERK1/2 as well as cell proliferation. As KLK14 expression is up-regulated in colon adenocarcinoma compared to normal colon cells, it is possible that KLK14 acts in an autocrine/paracrine fashion to effect cell signalling and growth of colon cancer cells (Gratio et al., 2011; Chung et al., 2012). Similarly, Stefansson and colleagues (2008) showed that while KLK14 expression is usually restricted to epithelial cells of sweat glands in normal skin, in inflammatory skin conditions such as atopic dermatitis and rosacea, KLK14 is also highly expressed in the upper squamous and granular layers of the epidermis and is co-localized with PAR2. This suggests PAR2-mediated inflammatory responses in the skin (Steinhoff et al., 2005) may involve KLK14 (Stefansson et al., 2008). It is possible that KLK14 participates in similar inflammatory or proliferative processes in the prostate.

Studies in this laboratory demonstrated KLK4 activates PAR1 and PAR2, but not PAR4 (Ramsay et al., 2008a). Moreover, KLK4 activated PAR2-induced intracellular signalling via ERK1/2 in PC-3 cells (Ramsay et al., 2008a). KLK4 activation of PAR1 and PAR2 was also demonstrated in DU145 cells by Mize and colleagues (2008) who also showed

KLK4-induced proliferation via PAR activation. On the other hand, Gratio and colleagues (2010) showed that in colon cancer-derived cell lines, KLK4 activated PAR1 but not PAR2. Together these results suggest there may be cell line/type-specific KLK4 activation of PAR2.

The paracrine effects of stromal PAR activation were also examined by Wang and colleagues (2010). In this study PAR1 AP or thrombin treatment induced ERK1/2 signalling and mitogenic cytokine interleukin (IL)-6 release from WPMY-1 prostate stromal myofibroblast cells. Subsequent treatment of LNCaP cells with the conditioned media from the AP-treated WPMY-1 cells induced LNCaP cell proliferation and ERK1/2 signalling. KLK3 and KLK4 expression were also induced in the LNCaP cells via the IL-6 pathway. Furthermore, KLK4 activated PAR1 on WPMY-1 cells inducing ERK1/2 signalling and up-regulation of IL-6. This suggests prostate epithelium/stromal cell interaction via a double-paracrine mechanism involving KLK4 (Wang et al., 2010). PAR1 siRNA mitigated the thrombin- and KLK4-induced IL-6 upregulation by 80% and 60%, respectively. From this the authors concluded the lower reduction in KLK4-induced IL-6 may be due to the ability of KLK4 to activate both PAR1 and PAR2 (Wang et al., 2010).

TMPRSS2 also activates PAR2 in LNCaP cells, inducing intracellular Ca^{2+} mobilization (Wilson et al., 2005). It is unknown whether it also activates PAR4, however, PAR1 activation was deemed unlikely as pre-treatment of the LNCaP cells with PAR1 AP failed to abrogate TMPRSS2-induced Ca^{2+} mobilization. Similarly matriptase is a potent PAR2 activator, but it does not activate PAR1 or PAR4 (Takeuchi et al., 2000; Seitz et al., 2007; Camerer et al., 2010). PAR2 activation by matriptase has also been shown to induce release of cytokines IL-6 and IL-8 by human umbilical vein endothelial (HUVEC) cells, implicating matriptase in inflammatory, mitogenic and pro-angiogenic processes (Seitz et al., 2007).

In contrast, Camerer and colleagues (2010) demonstrated that hepsin does not activate PAR1 or PAR2. However, in this study they demonstrated a possible proteolytic cascade in keratinocyte-derived HaCaT cells in which hepsin activated matriptase which subsequently activated PAR2. Furthermore, this cascade was blocked by a matriptase-activity blocking antibody.

1.10 Study aims

1.10.1 Rationale

The role of KLK14 in both normal and cancerous prostate is likely to involve participation in proteolytic cascades. In the normal prostate, this role may be highly regulated to prevent inappropriate activation/degradation cascades. However, in the cancerous prostate, up-regulation of KLK14 protein expression in combination with dysregulation of other proteases and/or inhibitors and the breakdown of tissue architecture may result in a significant role for KLK14 in the progression of prostate cancer.

KLK14, HGF and HAI-1 are all prostate-expressed, with KLK14 and HGF over expressed in prostate cancer. HGF-induced HGFR signalling has been implicated in prostate cancer progression. Furthermore, HGFR signalling is reliant on proteolytic processing of HGF. In turn, several HGF activating proteases such as hepsin and matriptase are regulated by HAI-1 inhibition.

KLK14 is also co-expressed with KLK4, hepsin, TMPRSS2 and matriptase in the prostate epithelium and overexpressed in prostate cancer. Similarly, MMP3 and MMP9 are overexpressed in prostate cancer, in the stromal and epithelial cells, respectively. PAR1, PAR2, and PAR4 are also overexpressed in prostate cancer stromal and/or epithelial cells. By virtue of this, these proteins have been implicated in the progression of prostate cancer.

While hepsin, matriptase and TMPRSS2 autoactivate, proteolytic cleavage by alternative proteases is required for KLK4, KLK14, MMP3 and MMP9 activation. It has already been determined that matriptase activates MMP3, MMP3 activates KLK4, and KLK4 activates PAR1 and PAR2. It has also been determined that hepsin activates matriptase which in turn activates PAR2. Further identification of interacting partners for these proteases overexpressed in prostate cancer is essential to understand their roles in this pathology.

1.10.2 Hypothesis

Based upon the above summary the hypotheses of this PhD project are:

- KLK14 activates pro-HGF and is inhibited by HAI-1 isoforms

- KLK4 and/or KLK14 may proteolyse hepsin and/or TMPRSS2, or vice versa, in the prostate or prostate cancer.
- Hepsin and TMPRSS2 activate MMP3 and MMP9
- The proteolytic cascade of serine proteases and MMPs regulates PAR signalling.

1.10.3 Objectives

Aim 1 To generate and enzymatically characterize recombinant KLK14 and to examine its activation of HGF and inhibition by HAI-1. [Chapter 3]

Aim 2 To analyse KLK14 in an enzymatic cascade involving the prostate cancer-associated serine proteases KLK4, hepsin and TMPRSS2. [Chapter 4]

Aim 3 To analyse an enzymatic cascade involving hepsin, TMPRSS2, matriptase, MMP3 and MMP9. [Chapter 4]

Aim 4 To examine whether these enzymatic cascades facilitate activation of the protease activated receptors PAR1, PAR2 and PAR4. [Chapter 5]

Chapter 2 Materials and Methods

2.1 Materials

Table 2.1 General materials

MATERIAL	SUPPLIER
Amicon® Ultra-15 Ultracel-10	Millipore Ltd, Kilsyth, Vic, Australia
BioTrace™ polyvinylidene fluoride (PVDF)	Pall Australia, Cheltenham, Vic, Australia
Cell Scraper, 25cm (1.7cm blade)	Sarstedt, Mawson Lakes, SA, Australia
Cell Strainer, 70 µm	BD Biosciences, San Jose, Ca, USA
Corning® bottle-top vacuum filter system cellulose acetate membrane, pore size 0.22 µm, membrane area 33.2 cm^2, filter capacity 500 mL	Sigma-Aldrich Pty Ltd, Castle Hill, NSW, Australia
Dialysis Tubing Cellulose Membrane	Sigma-Aldrich Pty Ltd, Castle Hill, NSW, Australia
Glass Econo-Column®	Bio-Rad Laboratories Pty, Ltd, Gladesville, NSW, Australia
NucleoCassettes™	ChemoMetec A/S, Allerød, Denmark
Nitrocellulose	Pall Australia, Cheltenham, Vic, Australia
Pierce Spin Columns - Snap Cap	Pierce, Thermo Fisher Scientific, Scoresby, Vic, Australia
Poly-Prep® Column	Bio-Rad Laboratories Pty, Ltd, Gladesville, NSW, Australia
Slide-A-Lyzer™ Dialysis Cassettes 10K molecular weight cut-off (MWCO) 3 mL, 10 mL	Pierce, Thermo Fisher Scientific, Scoresby, Vic, Australia
Vivaflow 200 10,000 MWCO polyethersulfone (PES)	Sartorius Stedim Australia Pty Ltd, Dandenong South, Vic, Australia
X-ray film	Imaging Solutions Pty, Underwood, Australia

Table 2.2 Chemicals and reagents

Common chemicals and reagents for solution preparation were obtained from either Sigma-Aldrich Pty Ltd or Ajax FineChem Pty Ltd (now Thermo Fisher Scientific). Specialized reagents and suppliers are listed below. All reagents were analytical grade or highest purity possible.

REAGENTS	SUPPLIER
4-methylumbelliferone (4-MU)	Sigma-Aldrich Pty Ltd, Castle Hill, NSW, Australia
4-methylumbelliferyl 4-guanidinobenzoate (MUGB)	Sigma-Aldrich Pty Ltd, Castle Hill, NSW, Australia

REAGENTS	SUPPLIER
5-bromo-4-chloro-indolyl-β-D-galactopyranoside (X-gal)	Sigma-Aldrich Pty Ltd, Castle Hill, NSW, Australia
7-amino-4-methylcoumarin (AMC)	Sigma-Aldrich Pty Ltd, Castle Hill, NSW, Australia
40% Acrylamide/Bis Solution, 29:1	Bio-Rad Laboratories Pty, Ltd, Gladesville, NSW, Australia
Ammonium persulfate (APS)	Sigma-Aldrich Pty Ltd, Castle Hill, NSW, Australia
Ampicillin	Roche Diagnostics Australia Pty Ltd, Castle Hill, NSW, Australia
Beta-mercaptoethanol (βME)	Sigma-Aldrich Pty Ltd, Castle Hill, NSW, Australia
Biotinylated Glu-Gly-Arg-chloromethylketone (Biotin-EGR-CMK)	Haematologic Technologies, Inc., Essex Junction, VT, USA
Biotinylated Phe-Pro-Arg-chloromethylketone (Biotin-FPR-CMK)	Haematologic Technologies, Inc., Essex Junction, VT, USA
Boc-Gln-Ala-Arg-7-amido-4-methylcoumarin hydrochloride (QAR-AMC)	Sigma-Aldrich Pty Ltd, Castle Hill, NSW, Australia
Cellfectin® Reagent	Invitrogen, Life Technologies Australia Pty Ltd, Mulgrave, Vic, Australia
cOmplete™, Mini, EDTA-free Protease Inhibitor Cocktail Tablets	Roche Diagnostics Australia Pty Ltd, Castle Hill, NSW, Australia
Coomassie Brilliant Blue R250 (Fluka)	Sigma-Aldrich Pty Ltd, Castle Hill, NSW, Australia
deoxyadenosine-triphosphate (dATP)	Roche Diagnostics Australia Pty Ltd, Castle Hill, NSW, Australia
Dimethyl sulphoxide (DMSO) anhydrous ≥99.9%	Sigma-Aldrich Pty Ltd, Castle Hill, NSW, Australia
Deoxyribonucleic acid (DNA) Molecular Weight Marker VII	Roche Diagnostics Australia Pty Ltd, Castle Hill, NSW, Australia
DNA Molecular Weight Marker XIV (100 base pair ladder)	Roche Diagnostics Australia Pty Ltd, Castle Hill, NSW, Australia
Deoxyribonucleotide-triphosphate (dNTPs)	Roche Diagnostics Australia Pty Ltd, Castle Hill, NSW, Australia
Ethidium bromide	Sigma-Aldrich Pty Ltd, Castle Hill, NSW, Australia
EZ-Link™ Sulfo-NHS-SS-Biotin	Pierce, Thermo Fisher Scientific, Scoresby, Vic, Australia
Fura-2 acetoxymethyl ester (AM)	Invitrogen, Life Technologies Australia Pty Ltd, Mulgrave, Vic, Australia
Gelatin from porcine skin	Sigma-Aldrich Pty Ltd, Castle Hill, NSW, Australia

REAGENTS	SUPPLIER
Hepsin (recombinant - generated minus the transmembrane and intracellular regions)	Dr D. Kirchhofer, Genentech, Inc., South San Francisco, CA, USA (Kirchhofer et al., 2005)
Hepatocyte growth factor activator inhibitor-1 isoform 1 (HAI-1B) (recombinant - generated minus the transmembrane and intracellular regions)	Dr D. Kirchhofer, Genentech, Inc., South San Francisco, CA, USA (Kirchhofer et al., 2003)
Hepatocyte growth factor activator inhibitor-1 isoform 2 (HAI-1A) (recombinant - generated minus the transmembrane and intracellular regions)	Dr D. Kirchhofer, Genentech, Inc., South San Francisco, CA, USA
Isopropyl-β-D-thiogalactophyranoside (IPTG)	Sigma-Aldrich Pty Ltd, Castle Hill, NSW, Australia
Lipofectamine™ 2000	Invitrogen, Life Technologies Australia Pty Ltd, Mulgrave, Vic, Australia
Lipofectamine™ LTX	Invitrogen, Life Technologies Australia Pty Ltd, Mulgrave, Vic, Australia
Matriptase (recombinant - generated minus the transmembrane and intracellular regions)	Dr D. Kirchhofer, Genentech, Inc., South San Francisco, CA, USA (Kirchhofer et al., 2003)
N,N,N′,N′-tetramethylethylenediamine (TEMED)	Sigma-Aldrich Pty Ltd, Castle Hill, NSW, Australia
Nickel-nitrilotriacetic acid (Ni-NTA) Superflow Resin	QIAGEN Pty Ltd, Doncaster, Vic, Australia
NucleoCounter® Reagent A	ChemoMetec A/S, Allerød, Denmark
NucleoCounter® Reagent B	ChemoMetec A/S, Allerød, Denmark
PageRuler™ Prestained Protein Ladder #0671	Fermentas, Thermo Fisher Scientific, Scoresby, Vic, Australia
Phosphoramidon	Sigma-Aldrich Pty Ltd, Castle Hill, NSW, Australia
Pluronic® F-127	Sigma-Aldrich Pty Ltd, Castle Hill, NSW, Australia
Precision Plus Protein™ Dual Color Standards	Bio-Rad Laboratories Pty, Ltd, Gladesville, NSW, Australia
Prestained sodium dodecyl sulphate-polyacrylamide gel electrophoresis (SDS-PAGE) Standards, low range	Bio-Rad Laboratories Pty, Ltd, Gladesville, NSW, Australia
Pro-hepatocyte growth factor (pro-HGF)	Dr D. Kirchhofer, Genentech, Inc., South San Francisco, CA, USA (Kirchhofer et al., 2005)
Probenecid	Fairlie Research Group, Chemistry and Human Therapeutics, Institute for Molecular Bioscience, University of Queensland, St Lucia, Qld, Australia

REAGENTS	SUPPLIER
Protease-activated receptor 1 agonist peptide (PAR1AP) H-Thr-Phe-Leu-Leu-Arg-NH_2 (TFLLR)	Auspep Pty Ltd, Tullamarine, Vic, Australia
Protease-activated receptor 2 agonist peptide (PAR2AP) H-Ser-Leu-Ile-Gly-Lys-Val-NH_2 (SLIGKV)	Auspep Pty Ltd, Tullamarine, Vic, Australia
Protease-activated receptor 2 agonist peptide (PAR2AP) H-Ser-Leu-Ile-Gly-Arg-Leu-NH_2 (SLIGRL)	Auspep Pty Ltd, Tullamarine, Vic, Australia
Protease-activated receptor 4 agonist peptide (PAR4AP) H-Ala-Tyr-Pro-Gly-Lys-Phe-NH_2 (AYPGKF)	Auspep Pty Ltd, Tullamarine, Vic, Australia
Protein A Agarose	Roche Diagnostics Australia Pty Ltd, Castle Hill, NSW, Australia
Protein G Agarose	Roche Diagnostics Australia Pty Ltd, Castle Hill, NSW, Australia
Ribonuclease A (RNase A) (20 mg/mL)	Invitrogen, Life Technologies Australia Pty Ltd, Mulgrave, Vic, Australia
Skim milk powder	Fonterra Foodservices, Hendra, Qld, Australia
Slide-A-Lyzer™ Concentrating Solution	Pierce, Thermo Fisher Scientific, Scoresby, Vic, Australia
Sodium dodecyl sulphate (SDS)	Amresco LLC, Solon, OH, USA
Streptavidin Agarose Resin	Pierce, Thermo Fisher Scientific, Scoresby, Vic, Australia
Streptavidin, Alexa Fluor® 680 conjugate	Invitrogen, Life Technologies Australia Pty Ltd, Mulgrave, Vic, Australia
SuperSignal™ West Femto Chemiluminescent Substrate	Pierce, Thermo Fisher Scientific, Scoresby, Vic, Australia
SYBR® Safe DNA Gel Stain	Invitrogen, Life Technologies Australia Pty Ltd, Mulgrave, Vic, Australia
Thermolysin	Calbiochem, San Diego, CA, USA
Thioglycolic acid $\geq$ 98%	Sigma-Aldrich Pty Ltd, Castle Hill, NSW, Australia
Triton X-100	Amresco LLC, Solon, OH, USA
Trypan blue solution , 0.4%	Sigma-Aldrich Pty Ltd, Castle Hill, NSW, Australia
Trypsin	Worthington Biochemical, Lakewood, NJ, USA
Tween® 20	Amresco LLC, Solon, OH, USA

Table 2.3 DNA vectors

VECTOR	SUPPLIER
pcDNA™3.1/hygro©(+)	Invitrogen, Life Technologies Australia Pty Ltd, Mulgrave, Vic, Australia
pIB/V5-His	Invitrogen, Life Technologies Australia Pty Ltd, Mulgrave, Vic, Australia
pEFIRES-P	Dr Steve Hobbs, Institute of Cancer Research, Sutton, UK (Hobbs et al., 1998)
pReceiver-M02	GeneCopoeia, Rockville, MD, USA

Table 2.4 DNA expression constructs

EXPRESSION CONSTRUCT	SOURCE
pIB-KLK14-V5-His	Dr N. Bennett
pcDNA3.1-KLK4-V5-His	Dr N. Bennett
pcDNA3.1-KLK4SA-V5-His	Dr N. Bennett
pcDNA3.1-Hepsin-Flag	Assoc. Prof. J. Hooper
pcDNA3.1-Hepsin-Myc	Assoc. Prof. J. Hooper
pcDNA3-TMPRSS2-Myc	Assoc. Prof. J. Hooper
pcDNA3.1-Matriptase	Assoc. Prof. C-Y. Lin, Greenborne Cancer Centre, Baltimore, MD, USA (Lin et al., 1999b)
pEZ-M02-MMP3	GeneCopoeia, Rockville, MD, USA
pEZ-M02-MMP9	GeneCopoeia, Rockville, MD, USA
pBluescript-Enteropeptidase*	Dr J. Evan Sadler, School of Medicine, Washington University, St Louis, MO, USA (Kitamoto et al., 1995)

* pBluescript is a phagemid cloning vector

Table 2.5 Restriction endonuclease

Enzymes were supplied with appropriate buffer concentrates.

RESTRICTION ENDONUCLEASE	SUPPLIER
BamHI	Fermentas, Thermo Fisher Scientific, Scoresby, Vic, Australia
DpnI	Roche Diagnostics Australia Pty Ltd, Castle Hill, NSW, Australia
EcoRI	Fermentas, Thermo Fisher Scientific, Scoresby, Vic, Australia
KpnI	Roche Diagnostics Australia Pty Ltd, Castle Hill, NSW, Australia
NotI	Fermentas, Thermo Fisher Scientific, Scoresby, Vic, Australia
XhoI	Fermentas, Thermo Fisher Scientific, Scoresby, Vic, Australia

Table 2.6 Other DNA manipulation enzymes

Enzymes were supplied with appropriate buffer concentrates.

OTHER ENZYMES	SUPPLIER
Platinum® *Pfx* DNA Polymerase	Invitrogen, Life Technologies Australia Pty Ltd, Mulgrave, Vic, Australia
Shrimp Alkaline Phosphatase (SAP)	Fermentas, Thermo Fisher Scientific, Scoresby, Vic, Australia
T4 DNA Ligase	Promega Australia, Alexandria, NSW, Australia
Taq DNA Polymerase	Roche Diagnostics Australia Pty Ltd, Castle Hill, NSW, Australia

Table 2.7 Primers

All oligonucleotide primers for DNA amplification, modification and sequencing were purchased from Proligo, now Sigma-Aldrich Pty Ltd, Castle Hill, NSW, Australia.

PRIMER NAME	SEQUENCE 5' to 3'	USE
K14-F7	GGACTCTTGTCAGGGTGACGC TGGGGGACCCCTGG	*KLK14* site-directed mutation (KLK14 S^{220}→A) (underline), forward
K14-R5	CCAGGGGTCCCCCAGCGTCAC CCTGACAAGAGTCC	*KLK14* site-directed mutation (KLK14 S^{220}→A) (underline), reverse
K14-F10	ggatccTGCTGTGTCTTCATGTC CC	*KLK14* with BamHI site (lower case), forward
K14-R7	ctcgagTTA**AGCGTAATCTGGA ACATCGTATGGGTA**TTTGTCC CGCATCGTTTCC	*KLK14* with HA tag (bold), stop codon and XhoI site (lower case), reverse
K14-R9	ctcgagTTA**CAGGTCCTCCTCCG AGATAAGCTTCTGCTC**TTTGTC CCGCATCGTTTCC	*KLK14* with Myc tag (bold), stop codon and XhoI site (lower case), reverse
Hep-F S-A	GCCTGCCAGGGCGACGCCGGT GGTCCCTTTGTG	*Hepsin* site-directed mutation (hepsin S^{353}→A) (underline), forward
Hep-R S-A	CACAAAGGGACCACCGGCGTC GCCCTGGCAGGC	*Hepsin* site-directed mutation (hepsin S^{353}→A) (underline), reverse
tmprss2-F S-A	GCCAGGGTGACGCTGGAGGG CCTCTGG	*Tmprss2* site-directed mutation (TMPRSS2 S^{478}→A) (underline), forward

PRIMER NAME	SEQUENCE 5' to 3'	USE
tmprss2-R S-A	CCAGAGGCCCTCCAGCGTCAC CCTGGC	*Tmprss2* site-directed mutation (TMPRSS2 S^{478}→A) (underline), reverse
K14-F2	CTGGGCAAGCACAACCTGAG	forward KLK14 internal sequencing
K14-R3	CAAGACACGAGGCCCTGGAG	reverse KLK14 internal sequencing
M13F-mod	GCCAGGGTTTTCCCAGTCACG	pGEM forward sequencing primer
pGEM-rev	GACCATGATTACGCCAAGC	pGEM reverse sequencing primer
T7	TAATACGACTCACTATAGGG	pcDNA3 series forward sequencing primer
BGH-rev	TAGAAGGCACAGTCGAGG	pcDNA3 series reverse sequencing primer
pIB-F (OplE2 forward)	CGCAACGATCTGGTAAACAC	pIB forward sequencing primer
pIB-R	CTCAATGGTGATGGTGATGAT GACC	pIB reverse sequencing primer
pEFIRES-for	ACTCCCAGTTCAATTACAGC	pEFIRES forward sequencing primer
pEFIRES-rev	ATAGACAAACGCACACCG	pEFIRES reverse sequencing primer

Table 2.8 ***Escherichia coli* (*E. coli*) strains**

BACTERIAL STRAIN NAME	SUPPLIER
JM109 Competent Cells, High Efficiency (>10^8 cfu/µg of pUC19 DNA)	Promega Australia, Alexandria, NSW, Australia
JM109 Competent Cells (>10^8 cfu/µg of pUC19 DNA)	Stratagene, Agilent Technologies, Inc., Life Sciences and Chemical Analysis Group, Santa Clara, CA, USA
XL10-Gold Ultracompetent cells (5 ×10^9 cfu/µg of pUC19 DNA)	Stratagene, Agilent Technologies, Inc., Life Sciences and Chemical Analysis Group, Santa Clara, CA, USA
XL10-Gold cells	Stratagene, Agilent Technologies, Inc., Life Sciences and Chemical Analysis Group, Santa Clara, CA, USA

Table 2.9 Bacterial culture media

CULTURE MEDIUM NAME	COMPOSITION
Luria-Bertani (LB) broth	1% (w/v) tryptone, 0.5% (w/v) yeast extract , 1% (w/v) NaCl, autoclaved
Luria-Bertani (LB) agar	1% (w/v) tryptone, 0.5% (w/v) yeast extract , 1% (w/v) NaCl, 1.5% (w/v) bactoagar, autoclaved

When required for antibiotic selection, ampicillin (100 µg/mL) (Table 2.2) was added to LB broth and to melted, cooled (≤ 55°C) LB agar prior to pouring plates.

Table 2.10 Cell culture lines

CELL LINE	ORIGIN	SOURCE
22Rv1	*Homo sapiens*, prostate carcinoma	American Type Culture Collection, Manassas, VA, USA
Cos-7	Chlorocebus aethiops, kidney fibroblast	American Type Culture Collection, Manassas, VA, USA
DU145	*Homo sapiens*, prostate carcinoma, brain metastasis	American Type Culture Collection, Manassas, VA, USA
HeLa	*Homo sapiens*, cervical carcinoma	American Type Culture Collection, Manassas, VA, USA
Kidney proximal tubule cells (PTC)	*Homo sapiens*, primary kidney proximal tubule cells	Dr David Vesey, Princess Alexandra Hospital, Woolloongabba, Qld, Australia
LNCaP	*Homo sapiens*, prostate carcinoma, lymph node metastasis	American Type Culture Collection, Manassas, VA, USA
PAR1-LMF	*Mus musculus*, PAR1-/- lung myofibroblasts reconstituted with human PAR1	Johnson & Johnson Pharmaceutical Research and Development, Spring House, PA, USA (Darrow et al., 1996; Andrade-Gordon et al., 1999)
PAR2-LMF	*Mus musculus*, PAR1-/- lung myofibroblasts reconstituted with human PAR2	Johnson & Johnson Pharmaceutical Research and Development, Spring House, PA, USA (Darrow et al., 1996; Andrade-Gordon et al., 1999)
PAR4-LMF	*Mus musculus*, PAR1- lung myofibroblasts reconstituted with human PAR4	Johnson & Johnson Pharmaceutical Research and Development, Spring House, PA, USA (Darrow et al., 1996; Andrade-Gordon et al., 1999)
PC-3	*Homo sapiens*, prostate adenocarcinoma, bone metastasis	American Type Culture Collection, Manassas, VA, USA

CELL LINE	ORIGIN	SOURCE
RWPE-1	*Homo sapiens*, prostate normal	American Type Culture Collection, Manassas, VA, USA
RWPE-2	*Homo sapiens,* prostate normal	American Type Culture Collection, Manassas, VA, USA
Sf9 (SFM Adapted)	*Spodoptera frugiperda*, ovary	Gibco®, Life Technologies Australia Pty Ltd, Mulgrave, Vic, Australia

Table 2.11 Cell culture media and supplements

MEDIUM	SUPPLIER
Blasticidin	InvivoGen, San Diego, CA, USA; Invitrogen, Life Technologies Australia Pty Ltd, Mulgrave, Vic, Australia
DMEM (Dulbecco's Modified Eagle Medium), High Glucose – L-Glutamine	Gibco®, Life Technologies Australia Pty Ltd, Mulgrave, Vic, Australia
DMEM-F-12	Thermo Fisher Scientific, Scoresby, Vic, Australia
Fetal Bovine Serum (FBS)	Gibco®, Life Technologies Australia Pty Ltd, Mulgrave, Vic, Australia
G418	InvivoGen, San Diego, CA, USA; Invitrogen, Life Technologies Australia Pty Ltd, Mulgrave, Vic, Australia
Hygromycin B	Invitrogen, Life Technologies Australia Pty Ltd, Mulgrave, Vic, Australia
Keratinocyte-SFM (Serum-Free Medium) with Epidermal Growth Factor 1-53 (EGF 1-53) and Bovine Pituitary Extract (BPE)	Gibco®, Life Technologies Australia Pty Ltd, Mulgrave, Vic, Australia
Opti-MEM®I Reduced Serum Medium	Gibco®, Life Technologies Australia Pty Ltd, Mulgrave, Vic, Australia
Penicillin and Streptomycin	Invitrogen, Life Technologies Australia Pty Ltd, Mulgrave, Vic, Australia
Puromycin	InvivoGen, San Diego, CA, USA
RPMI-1640 - L-Glutamine	Gibco®, Life Technologies Australia Pty Ltd, Mulgrave, Vic, Australia
Sf-900 II SFM (Serum-Free Medium)	Gibco®, Life Technologies Australia Pty Ltd, Mulgrave, Vic, Australia

Table 2.12 Primary antibodies

All antibodies were reconstituted and stored according to manufacturer's recommendations.

PRIMARY ANTIBODIES	DILUTIONS USED	SUPPLIER
Anti-Enterokinase LC antibody (sc-51283)	1:1000 (WB)	Santa Cruz Biotechnology, Inc. Dallas, TX, USA
Anti-Flag® M2 (F1804) Mouse	1:1000 (FCM)	Sigma-Aldrich Pty Ltd, Castle Hill, NSW, Australia
Anti-Flag® (F7425) Rabbit	1:3000-5000 (WB), 8 ng/µg lysate (IP)	Sigma-Aldrich Pty Ltd, Castle Hill, NSW, Australia
Anti-GAPDH Mouse	1:5000-10,000 (WB)	Chemicon (now Millipore Ltd, Kilsyth, Vic, Australia)
Anti-GAPDH (G9545) Rabbit	1:10,000 (WB)	Sigma-Aldrich Pty Ltd, Castle Hill, NSW, Australia
Anti-HA (H6908) Rabbit	1:1250-2500 (WB)	Sigma-Aldrich Pty Ltd, Castle Hill, NSW, Australia
Anti-Hepsin A15 Mouse	1:1000-5000 (WB)	Dr Q. Wu, Cleveland Clinic, Cleveland, OH, USA (Xuan et al., 2006)
Anti-Kallikrein 14 (ab28841) Rabbit	1:1000 (WB)	Abcam, Cambridge, MA, USA(Brattsand et al., 2005)
Anti-Kallikrein 4 mid Rabbit	1:1000	Hormone Dependent Cancer Program, IHBI, Kelvin Grove, Qld, Australia (Harvey et al., 2003)
Anti-Kallikrein 4 C-term Rabbit	1:1000	Hormone Dependent Cancer Program, IHBI, Kelvin Grove, Qld, Australia (Harvey et al., 2003)
Anti-Matriptase M69 Mouse	1:1000	Assoc. Prof. C-Y. Lin, Greenborne Cancer Centre, Baltimore, MD, USA (Lin et al., 1999b; Benaud et al., 2001)
Anti-MMP3 antibody (ab18898) Goat	1:500 (WB), 1:200 (IP)	Abcam, Cambridge, MA, USA
Anti-MMP9 antibody - Whole molecule (ab38898) Rabbit	1:5000 (WB), 1:1000 (IP)	Abcam, Cambridge, MA, USA
Anti-Myc-Tag (9B11) Mouse mAb	1:5000 (WB), 1:1000 (IP)	Cell Signaling Technology Inc., Danvers, MA, USA
Anti-V5 (R96025) Mouse	1:5000-10,000 (WB), 1:1000 (IP)	Invitrogen , Life Technologies Australia Pty Ltd, Mulgrave, Vic, Australia

Table 2.13 Secondary antibodies

SECONDARY ANTIBODIES	DILUTIONS USED	SUPPLIER
Alexa Fluor® 488 goat anti-mouse IgG	1:750 (FCM)	Invitrogen, Life Technologies Australia Pty Ltd, Mulgrave, Vic, Australia
Alexa Fluor® 680 goat anti-rabbit IgG	1:10,000 (WB)	Invitrogen, Life Technologies Australia Pty Ltd, Mulgrave, Vic, Australia
Anti-Goat IgG (H&L) (Donkey) Antibody IRDye®700-Conjugated	1:10,000 (WB)	Rockland Immunochemicals Inc., Gilbertsville, PA, USA
Anti-Goat IgG (H&L) (Donkey) Antibody IRDye®800CW-Conjugated	1:10,000 (WB)	Rockland Immunochemicals Inc., Gilbertsville, PA, USA
Anti-Mouse IgG (H&L) (Donkey) Antibody IRDye®800-Conjugated	1:10,000 (WB)	Rockland Immunochemicals Inc., Gilbertsville, PA, USA
Anti-Mouse IgG (H&L) (Donkey) Antibody IRDye®800CW-Conjugated	1:10,000 (WB)	Rockland Immunochemicals Inc., Gilbertsville, PA, USA
Anti-Rabbit IgG (H&L) (Donkey) Antibody IRDye®700CW-Conjugated	1:10,000 (WB)	Rockland Immunochemicals Inc., Gilbertsville, PA, USA
Anti-Rabbit IgG (H&L) (Donkey) Antibody IRDye®800CW-Conjugated	1:10,000 (WB)	Rockland Immunochemicals Inc., Gilbertsville, PA, USA
Anti-Rabbit IgG (H&L) (Donkey) Antibody IRDye®800-Conjugated	1:10,000 (WB)	Rockland Immunochemicals Inc., Gilbertsville, PA, USA
Goat Anti-Mouse IgG (H&L) horseradish peroxidase (HRP)	1:2000-4000 (WB)	Pierce, Thermo Fisher Scientific, Scoresby, Vic, Australia
Goat Anti-Rabbit IgG (H&L) HRP	1:2000-4000 (WB)	Pierce, Thermo Fisher Scientific, Scoresby, Vic, Australia
Anti-Mouse IgG +A+M (Goat)	1:4000 (ELISA)	Zymed, Life Technologies Australia Pty Ltd, Mulgrave, Vic, Australia

Table 2.14 Isotype antibodies

ISOTYPE ANTIBODY CONTROLS	SUPPLIER
Mouse IgG 2a	Sigma-Aldrich Pty Ltd, Castle Hill, NSW, Australia
Rabbit IgG	Invitrogen , Life Technologies Australia Pty Ltd, Mulgrave, Vic, Australia

Abbreviations: FCM, Flow cytometry; IP, immunoprecipitation; WB, Western blot.

Table 2.15 Commercial kits

KIT	SUPPLIER
BCA™ Protein Assay Kit	Pierce, Thermo Fisher Scientific, Scoresby, Vic, Australia
High Pure™ PCR Product Purification Kit	Roche Diagnostics Australia Pty Ltd, Castle Hill, NSW, Australia
pGEM®-T Easy Vector System I Kit	Promega Australia, Alexandria, NSW, Australia
PNGase F De-N-glycosylation kit	New England BioLabs Inc., Ipswich, MA, USA
PureLink® HiPure Plasmid Midiprep Kit	Invitrogen, Life Technologies Australia Pty Ltd, Mulgrave, Vic, Australia
PureLink™ Quick Plasmid Miniprep Kit	Invitrogen, Life Technologies Australia Pty Ltd, Mulgrave, Vic, Australia
QIAGEN Plasmid Maxi Kit	QIAGEN Pty Ltd, Doncaster, Vic, Australia
QIAprep Miniprep Kit	QIAGEN Pty Ltd, Doncaster, Vic, Australia

Table 2.16 Buffers and solutions

BUFFER OR SOLUTION NAME	COMPOSITION or SUPPLIER
Binding Buffer	28 mM NaH_2PO_4, 72 mM Na_2HPO_4, 0.15 M NaCl, pH 7.2
Ca^{2+} Flux Assay (CaFA) Buffer	1.26 mM $CaCl_2$, 5.37 mM KCl, 0.44 mM KH_2PO_4, 8.12 mM $MgSO_4$, 136.9 mM NaCl, 0.336 mM Na_2HPO_4, 4.17 mM $NaHCO_3$, 5.55 mM D-glucose, 20 mM HEPES, pH 7.4, filtered, 2.5 mM probenecid added immediately prior to use (from a stock solution of 0.5 M probenecid suspended in 1N NaOH)

BUFFER OR SOLUTION NAME	COMPOSITION or SUPPLIER
CAPS Buffer	N-cyclohexyl-3-aminopropanesulfonic acid (CAPS), 10 mM, adjusted to pH 11.0 with NaOH
Coomassie Blue R250 Stain	0.25% (w/v) Coomassie Brilliant Blue R250 (Fluka), 45% (v/v) methanol, 10% (v/v) acetic acid
Coomassie Destain	45% (v/v) methanol, 10% (v/v) acetic acid
DNA Loading Buffer, 6× (diluted to 1× in use)	0.25% Bromophenol blue, 30% (v/v) glycerol
HEPES Buffer Solution	Gibco®, Life Technologies Australia Pty Ltd, Mulgrave, Vic, Australia
KLK14 Buffer	5 mM NaH_2PO_4, 95 mM Na_2HPO_4, 0.01% (v/v) Tween®20, pH 8.0
Lysis Buffer	10 mM Tris pH 8.0, 150 mM NaCl, 1% (v/v) Triton X-100, 5 mM EDTA.
MUGB Assay Buffer	50mM Tris, 50mM NaCl, pH8.8, 0.01% (v/v) Tween®20
Ni-NTA Dialysis Buffer	50 mM NaH_2PO_4, 500 mM NaCl, pH 8.0
Ni-NTA Elution Buffer 250	250 mM imidazole, 50 mM NaH_2PO_4, 300 mM NaCl, pH 8.0
Ni-NTA PE Buffer 300	300 mM imidazole, 50 mM NaH_2PO_4, 300 mM NaCl, pH 8.0
Ni-NTA Wash Buffer 10	10 mM imidazole, 50 mM NaH_2PO_4, 300 mM NaCl, pH 8.0
Ni-NTA Wash Buffer 30	30 mM imidazole, 50 mM NaH_2PO_4, 300 mM NaCl, pH 8.0
Odyssey® Blocking Buffer	LI-COR Biosciences, Lincoln, NE, USA
Phosphate-buffered saline (PBS)	137 mM NaCl, 2.7 mM KCl, 4.3 mM Na_2HPO_4, 1.47 mM KH_2PO_4, pH 7.4
Phosphate-buffered saline (Dulbecco A) –(DPBS)	Oxoid, Thermo Fisher Scientific, Scoresby, Vic, Australia
Phosphate-buffered saline plus Tween®20 (PBS-T)	137 mM NaCl, 2.7 mM KCl, 4.3 mM Na_2HPO_4, 1.47 mM KH_2PO_4, pH 7.4, 0.1% (v/v) Tween®20
SDS-PAGE Loading Buffer, 6× (diluted to 1× in use)	0.35 M Tris pH 6.8, 30% (v/v) glycerol, 12% (w/v) SDS, 0.012% (w/v) Bromophenol Blue plus 10% (v/v) beta-mercaptoethanol for reducing conditions
SDS-PAGE, Resolving Gel 12%	12% (v/v) Acrylamide/Bis (29:1), 0.37 M Tris pH 8.8, 0.1% (w/v) SDS, 0.05% (w/v) APS, 0.05% (v/v) TEMED
SDS-PAGE, Resolving Gel 10%	10% (v/v) Acrylamide/Bis (29:1), 0.37 M Tris pH 8.8, 0.1% (w/v) SDS, 0.05% (w/v) APS, 0.05% (v/v) TEMED
SDS-PAGE, Stacking Gel 4%	4% (v/v) Acrylamide/Bis (29:1), 0.125 M Tris pH 6.8, 0.1% (w/v) SDS, 0.05% (w/v) APS, 0.1% (v/v) TEMED

BUFFER OR SOLUTION NAME	COMPOSITION or SUPPLIER
Skim milk blocking buffer	50 mM Tris, 150 mM NaCl, pH 7.4, 5% (w/v) skim milk powder
Tris-acetate-EDTA (TAE)	40 mM Tris, 20 mM acetic acid, pH 8.0, 1 mM EDTA
Tris-buffered saline plus Tween®20 (TBS-T)	50 mM Tris, 150 mM NaCl, pH 7.4, 0.1% (v/v) Tween®20
Tris-Glycine Running Buffer	25 mM Tris, 192 mM glycine, 0.1% (w/v) SDS
Tris-Glycine Transfer Buffer	25 mM Tris, 192 mM glycine, 0.1% (w/v) SDS, 20% (v/v) methanol
Tris-NaCl Buffer	50 mM Tris, 50 mM NaCl, pH 7.4
Versene	0.53 mM EDTA in DPBS, autoclaved
Zymography Developing Buffer	50 mM Tris, 5 mM $CaCl_2$, 1 µM $ZnCl_2$, pH 7.4
Zymography Renaturation Buffer	50 mM Tris, 5 mM $CaCl_2$, 1 µM $ZnCl_2$, pH 7.4, 2.5% Triton X-100
Zymography Stain	0.5% (w/v) Coomassie Brilliant Blue R250 (Fluka), 30% (v/v) ethanol, 10% (v/v) acetic acid
Zymography Destain	30% (v/v) ethanol, 10% (v/v) acetic acid

2.2 Computer software

Chromatograms from DNA sequencing were viewed using DNASTAR® SeqMan®.

MARS Data Analysis Software (BMG LABTECH, Mornington, Vic., Australia), GraphPad Prism 5, Microsoft® Excel 2003 and Microsoft® Excel 2010 were used for data analysis for BCA, enzyme activity, kinetic and Ca^{2+} flux assays.

LI-COR Odyssey® 2.0 and 3.0 (LI-COR, Lincoln, NE, USA) and Microsoft® PowerPoint 2010 were used for image analysis.

Flow cytometry data were analysed and manipulated using Flowing Software (Terho, 2010) (http://www.flowingsoftware.com).

2.3 Web resources

Australian National Genomic Information Service (ANGIS) BioManager (Cattley and Arthur, 2007) (http://www.angis.org.au/) (now closed) for DNA sequence manipulation.

Center for Biological Sequence Analysis (CBS) Prediction Servers (http://www.cbs.dtu.dk/services/) to access signal peptide prediction program SignalP-4.0 Server (Petersen et al., 2011), N-linked glycosylation prediction program NetNGlyc-1.0 Server (Gupta et al., 2004) and NetSurfP-1.0, protein surface accessibility and secondary structure prediction program.

The European Bioinformatics Institute (EMBL-EBI) (http://www.ebi.ac.uk/) to access ClustalW(Larkin et al., 2007) and ClustalO(Sievers et al., 2011) for multiple sequence alignment.

ExPASy Bioinformatics Resource Portal (http://expasy.org/) to access SWISS-MODEL and DeepView PDB Viewer (Guex and Peitsch, 1997; Schwede et al., 2003; Arnold et al., 2006).

GeneCards human gene database (http://www.genecards.org/).

National Center for Biotechnology Information (NCBI) (http://www.ncbi.nlm.nih.gov/guide/) to access PubMed, nucleotide, protein sequence databases and also Basic Local Alignment Search Tool (BLAST).

New England BioLabs (NEB) NEBcutter V2.0 (http://tools.neb.com/NEBcutter2/) to locate restriction endonuclease sites in DNA sequences.

The Sequence Manipulation Suite (http://www.bioinformatics.org/sms/index.html) for access to open reading frame finder and DNA → protein translation programs.

Stockholm Bioinformatics Centre (http://phobius.sbc.su.se/) to access signal peptide prediction program Phobius (Kall et al., 2004).

UniProt (http://www.uniprot.org/) for sequence and function information.

2.4 Methods

2.4.1 Characterization of the KLK14 amino acid sequence

The complete KLK14 amino acid sequence (NCBI Reference Sequence NP_071329.2) was examined using online protein prediction tools.

The KLK14 signal peptide was examined using SignalP-4.0 Server (Petersen et al., 2011), hosted by the Centre for Biological Sequence Analysis (CBS) (http://www.cbs.dtu.dk/services/), and Phobius (Kall et al., 2004), hosted by the Stockholm Bioinformatics Centre (http://phobius.sbc.su.se/). Predictions about KLK14 N-glycosylation as well as secondary structure and surface solvent accessibility were explored using NetNGlyc-1.0 Server (Gupta and Brunak, 2002; Gupta et al., 2004) and NetSurfP-1.0 (Petersen et al., 2009) (CBS). SWISS-MODEL hosted by ExPASy (http://expasy.org/) and DeepView-4.1 Swiss PDB-Viewer (Guex and Peitsch, 1997; Schwede et al., 2003; Arnold et al., 2006) were used to generate and analyse a KLK14 homology model using the crystal structure of KLK5 (Protein Data Bank (PDB) identification (ID) 2PSX) (Debela et al., 2007a) as a template. KLK14 and KLK5 protein sequence alignment was performed using ClustalO (Sievers et al., 2011).

2.4.2 General molecular biology techniques

The general techniques outlined in this section were used in the generation, manipulation and isolation of DNA expression constructs.

2.4.2.1 Plasmid DNA isolation

To extract and purify high quality plasmid DNA from bacterial cultures for sequencing, gene cloning and transfection, one of four kits was used depending on the quantity of DNA required. The QIAprep Miniprep Kit and the PureLink™ Quick Plasmid Miniprep Kit (Table 2.15) were used for isolation of <30 μg DNA. The PureLink®HiPure Plasmid Midiprep Kit and the QIAGEN Plasmid Maxi Kit (Table 2.15) were used for isolation of quantities of up to 350 and 500 μg DNA, respectively. The manufacturer's instructions were followed for the growth and preparation of the bacterial cultures and purification of the plasmid DNA.

DNA concentration and purity was assessed using a Pharmacia GeneQuantII RNA/DNA Spectrophotometer (now GE Healthcare Australia Pty Ltd, Rydalmere, NSW, Australia) or a Nanodrop 1000 spectrophotometer (Thermo Fisher Scientific, Scoresby, Vic, Australia). An absorbance at 260 nm (A_{260}) of 1 represents 50 μg/mL DNA and an A_{260}/A_{280} ratio of ≥1.8 was regarded as a pure sample.

2.4.2.2 DNA sequencing

An 8 μL sequencing mix was prepared containing ~600 ng of plasmid DNA and 6.4 pmol of a primer. The primers (Table 2.7) were either vector specific or internal sequencing specific. DNA sequencing was performed using ABI BigDye Terminator sequencing by the Australian Genomic Research Facility (AGRF), St Lucia, Qld, Australia.

2.4.2.3 Agarose gel electrophoresis

DNA was separated and analysed on gels of 0.8-2.0% (w/v) agarose in Tris-acetate-EDTA (TAE) buffer (40 mM Tris, 20 mM acetic acid, pH 8.0, 1 mM EDTA, Table 2.16). Ethidium bromide (0.1 μg/mL) (Table 2.2) or SYBR® Safe DNA Gel Stain (0.1 μL/mL) (Table 2.2) was added to the gel solution prior to casting. Samples were diluted 5:1 in 6× DNA loading buffer (for final concentration 0.25% Bromophenol blue, 30% (v/v) glycerol, Table 2.16) prior to loading into gel wells. DNA Molecular Weight Markers VII or XIV (Table 2.2) were also loaded onto the gel for DNA size comparison. Electrophoresis was conducted in TAE buffer at 100-120V for up to 1 hour (h), depending on fragment size. For ethidium bromide cast gels, DNA was visualized and photographed using ultraviolet (UV) illumination (Syngene UV System, Geneworks, Adelaide, SA, Australia). For SYBR® Safe cast gels, a Safe Imager™ 2.0 Blue-Light Transilluminator (Invitrogen, Life Technologies Australia Pty Ltd, Mulgrave, Vic, Australia) was used for DNA visualization and images were captured using a Fujifilm FLA-5000 laser scanner (Fuji Photo Film Co., Stafford, Qld, Australia).

2.4.2.4 Polymerase chain reaction (PCR) protocols

A PTC-200 Peltier thermal cycler DNA Engine (Bresatec, Adelaide, SA, Australia) or a Bio-Rad C1000™ Thermal Cycler (Bio-Rad Laboratories Pty, Ltd, Gladesville, NSW, Australia) were used for PCR reactions and also linear amplifications.

PCR reactions for overlap extension polymerase chain reaction (OE-PCR) routinely consisted of a 25 or 50 μL reaction volume with 0.5 ng/μL template DNA, 200-300 nM of primers (Table 2.7), 0.3 mM of deoxyribonucleotide triphosphates (dNTPs) (Table 2.2), 1 mM $MgSO_4$ and 1-1.25 units (U) of Platinum® *Pfx* DNA polymerase (Table 2.6). The cycling conditions consisted of an initial denaturation at 94-95°C for 2-3 minutes followed by 30-32 cycles of three steps: denaturation at 94-95°C for 15-30 seconds, annealing at 53°C for 30 seconds and extension at 68°C for 1 minute per kilobase (kb) of the amplicon. To isolate PCR products, the reaction products were electrophoresed on agarose gel. Bands were visualized, and then bands of appropriate size were excised in gel slices and purified using the High Pure™ PCR Product Purification Kit (Table 2.15).

2.4.2.5 Site-directed mutagenesis

For site-directed mutagenesis, linear amplification reactions of whole plasmid consisted of a 25 μL reaction with 1 ng/μL template DNA, 440-600 nM of mutagenic primers (Table 2.7), 0.4 mM of dNTPs, 1.5 mM $MgSO_4$ and 2.5 U of Platinum® *Pfx* DNA polymerase. The thermal cycling conditions consisted of an initial denaturation at 95°C for 30 seconds followed by 18 cycles of three steps: denaturation at 95°C for 30 seconds, annealing at 55°C for 1 minute and extension at 68°C for 1 minute per kilobase (kb) of the plasmid. Following amplification, the template DNA was eliminated by selective digestion of methylated DNA using the enzyme DpnI (5 U) (Table 2.5) for 1 hour at 37 °C. The digestion reaction product was then used directly for transformation of competent *Escherichia coli* (*E. coli*) cells (Section 2.4.2.8).

2.4.2.6 Ligation of DNA

Ligation of DNA into expression vectors or pGEM™T-Easy (Table 2.15) typically consisted of a 10 μL reaction containing T4 DNA ligase buffer, 3 U of T4 DNA ligase

(Table 2.6), 50 ng vector DNA and insert DNA added to achieve a 3:1 insert:vector molar ratio. After incubation overnight at 4°C, ligation reactions (1-10 μL) were used directly for transformation of competent *E.coli* cells (Section 2.4.2.8).

As Platinum® *Pfx* has extensive 3' to 5' exonuclease activity it does not leave 3' poly A-overhangs. Therefore, before ligation into the pGEM™T-Easy vector, insert DNA generated by PCR was always subjected to an A-tailing reaction. The A-tailing reaction typically consisted of a 10 μL mixture containing 6 μL of the PCR product, 2 mM deoxyadenosine triphosphate (dATP) (Table 2.2), 1 U *Taq* DNA polymerase (Table 2.6) and PCR buffer with $MgCl_2$ (1.5 mM). The mixtures were incubated at 90°C for 10 minutes then 70°C for 30 minutes. The A-tailed product was used directly in pGEM™T-Easy ligation reactions.

2.4.2.7 Restriction digest of DNA

Routinely, purified DNA (0.5-9 μg) was digested with restriction endonuclease/s (1-10 U) of choice (Table 2.5) in an appropriate buffer for 1.5-2 hours at 37°C. The digestion reaction products were electrophoresed on agarose gel and the bands visualized. To isolate DNA fragments for ligation reactions, bands were excised in gel slices and purified using the High Pure™ PCR Product Purification Kit.

When preparing vector DNA for cloning using a single restriction endonuclease, shrimp alkaline phosphatase (SAP) (1 U) (Table 2.6) was included in the digestion reaction to prevent vector re-circularization. The SAP was then deactivated by heating at 65°C for 15 minutes. DNA clean-up for SAP-treated vector digests was performed by adding 900 μL of 95% (v/v) ethanol and 0.16 M sodium acetate (pH 4.7) and incubating overnight at -80°C. The sample was then centrifuged at 18,000 relative centrifugal force (RCF or *g*) for 30 minutes at 4°C. Supernatant was aspirated and the pellet was washed in ice-cold 75% (v/v) ethanol. After centrifugation at 18,000 *g* for 30 minutes the supernatant was aspirated and the pellet was allowed to air dry for 5 minutes before resuspension in 10 μL of 10 mM Tris, pH 8.5.

2.4.2.8 Preparation and transformation of competent E.coli *cells*

All *E. coli* strains used for transformation with plasmid DNA in this study were chemically-induced competent cells. For transformation of commercial preparations of competent cells JM109 and XL10-Gold Ultracompetent (Table 2.8), the manufacturer's instructions were followed except that in all instances LB broth was used as the post-recovery incubation medium.

XL10-Gold competent cells were also prepared in-house using a calcium chloride method (Sambrook et al., 1989) described as follows. A single colony of XL10-Gold (Table 2.8) picked from a Luria Bertani (LB) agar plate (Table 2.9) was used to inoculate 2 mL LB broth (Table 2.9). After overnight incubation with shaking at 37°C, the culture was used to inoculate 200 mL LB broth and was further incubated until log phase growth was reached, as indicated by an optical density (OD) at 600 nm of 0.4-0.5. After transfer to sterile falcon tubes, the culture was placed on ice for 20 min. All further manipulations were performed on ice or at 4°C. Cells were pelleted by centrifugation at 4,000 *g* for 10 minutes. The cells were then resuspended in 24 mL of ice-cold 100 mM $CaCl_2$ (autoclaved) then incubated for 40 minutes. Cells were pelleted by centrifugation at 4,000 *g* for 10 minutes and resuspended in ice-cold 100 mM $CaCl_2$, 14% (v/v) glycerol (autoclaved). Cells were aliquoted at 100 μL per 2 mL sterile tube and frozen in liquid nitrogen before transfer to -80°C until required.

For transformation of in-house preparations of XL10-Gold competent cells, cells (100 μL) thawed on ice were then incubated on ice with DNA (~1 ng of plasmid DNA or 1-10 μL of a ligation mixture, or 10-25 μL of site-directed mutagenesis mixture) for 30 minutes. Cells were then heat shocked in a water bath at 42°C for 45 seconds and then allowed to recover on ice for 15 minutes. LB broth (900 μL) was then added to the tube and cells were incubated for 1 hour at 37°C.

After incubation, for all transformations, cells were pelleted by centrifugation at 4,000 *g* for 10 minutes and then resuspended in warmed LB broth (100-200 μL). As all plasmids used in this study contained genes to confer ampicillin resistance, cells (50-200 μL) were then plated onto warmed LB-ampicillin (100 μg/mL) agar plates (Table 2.9). Plates were then incubated overnight at 37°C. For all pGEM®-T Easy transformations, plates were impregnated with 100 μL of 100 mM isopropyl-β-D-thio-galactoside (IPTG) (Table 2.2) and 20 μL of 50 mg/mL 5-bromo-4-chloro-indolyl-β-D-galactopyranoside (X-gal) (Table 2.2) before use.

2.4.2.9 Screening transformed clones

Individual *E.coli* colonies selected from overnight culture plates of transformed cells were propagated in LB-ampicillin (100 μg/mL) broth (5 mL), overnight, shaking at 37°C. For transformants with pGEM®-T Easy vector, colony selection was assisted by the pGEM®-T Easy cloning site located within the coding region of a β-galactosidase enzyme. This allowed for screening by insertional inactivation and blue-white colony selection on LB-ampicillin plus IPTG and X-gal agar plates. For transformation with other vectors, colonies were selected at random.

After overnight culture, plasmid DNA was isolated using a miniprep kit and the DNA yield determined (Section 2.4.2.1). For all transformants resulting from ligation reactions the purified plasmid DNA was subjected to diagnostic restriction digestion using restriction endonuclease EcoRI or KpnI (Section 2.4.2.7) and agarose gel electrophoresis (Section 2.4.2.3) to confirm the presence of the insert in the vector. When a single restriction endonuclease was used for preparing the vector and insert DNA for ligation, an alkaline lysis protocol to extract plasmid DNA was performed to economically screen multiple clones before proceeding to isolation of high quality plasmid DNA using a commercial miniprep kit.

For the alkaline lysis protocol a 200 μL sample of overnight culture of transformed bacteria was combined with 200 μL 0.2 M NaOH, 1% (w/v) SDS and the tube was inverted 4-5 times. To neutralize the solution, 200 μL 3 M potassium acetate, pH 4.7 was added and the tube was inverted again 4-5 times. After centrifugation at 18,000 *g* for 5 minutes, the supernatant was removed to a new tube and the DNA was precipitated by adding 500 μL 100% isopropanol and inverting the tube 4-5 times. The sample was then centrifuged for 5 minutes at 18,000 *g*. After discarding the supernatant, the pellet was centrifuged again, as above, and the remaining isopropanol was removed. A diagnostic restriction digest of the isolated DNA was then performed by resuspending the pellet in a digestion mix comprising restriction endonuclease/s (0.5 U/ μL) plus Ribonuclease A (RNase A) (200 ng/μL) (Table 2.2) in a total volume of 10 μL. After 1.5 hours incubation at 37°C, agarose gel electrophoresis was performed. Those transformants found to have plasmid DNA fragments of the expected size were selected for plasmid DNA isolation by miniprep kit.

In all instances DNA sequencing (Section 2.4.2.2) was performed on purified plasmid DNA to check for the desired sequence. Transformed *E. coli* clones containing plasmid

with the correct sequence were prepared for long term storage by combining 800 µL overnight culture with 200 µL autoclaved 80% (v/v) glycerol and then stored at -80°C.

2.4.3 Generation of expression constructs

2.4.3.1 Construct for expression in insect cells

To generate a construct for the expression of KLK14 in insect cells, full-length *KLK14* (NCBI Reference Sequence NM_022046.4) coding sequence was amplified from the construct pGEM®-T Easy KLK-L6 (KLK14) using primers (forward) 5'GAC ggatccTGCTGTGTCTTCATGTCCCT3' and (reverse) 5'CGctcgagACTTTGTCCCGC ATCGTTTCC3' to engineer BamHI and XhoI restriction sites (lower case, respectively) at either end of the coding sequence of KLK14. Following amplification and gel purification, the product was ligated into the shuttle vector pGEM®-T Easy, transformed into *E. coli*, propagated and isolated. Clones were screened for correct sequence by sequencing using vector-specific primers, M13F-mod and pGEM-rev. KLK14 was then excised from the shuttle vector using BamHI and XhoI and ligated into BamHI/XhoI digested insect expression vector pIB/V5-His, in frame with the V5-His tag and stop codon. Following transformation into JM109 *E. coli*, pIB-KLK14-V5-His was propagated and isolated. Clones were then selected based on screening by restriction digest followed by sequencing using vector-specific primers, pIB-F and pIB-R, and internal sequencing primers, K14-F2 and K14-R3. (Sub-cloning was performed by Dr Nigel Bennett, Table 2.4).

2.4.3.2 Constructs for expression in mammalian cells

Table 2.17 contains a summary of the constructs generated including the primers and templates used for each construct. Three main methods of construct generation were used: OE-PCR to generate new DNA restriction sites and/or protein C-terminal epitope tags; site-directed mutagenesis to generate constructs with specific mutations in the coding sequence of the protein; and excision and ligation to shuttle coding sequence from one vector to another.

For the expression of KLK14 in mammalian cells, DNA sequence encoding full-length KLK14 (NCBI Reference Sequence NM_022046.4) was amplified by OE-PCR using

the pIB-KLK14-V5-His construct (Table 2.4) as a template. The primers used, K14-F10, K14-R7 and K14-R9 (primer sequences, Table 2.7), were designed to engineer KLK14 coding sequence with either a HA (K14-R7) or Myc (K14-R9) C-terminus epitope tag and a stop codon as well as BamHI and XhoI restriction sites at either end. Following amplification and gel purification, the products were ligated into the shuttle vector pGEM®-T Easy, transformed into JM109 *E. coli*, propagated and isolated. Clones were screened for correct sequence by sequencing using vector-specific primers, M13F-mod and pGEM-rev. Sequence encoding KLK14-HA and KLK14-Myc were then excised from the shuttle vector using BamHI and XhoI (Table 2.5) and ligated into BamHI/XhoI digested mammalian expression vector pcDNA™3.1/hygro©(+) (Table 2.3). Following transformation into JM109 *E. coli*, pcDNA3.1-KLK14-HA and pcDNA3.1-KLK14-Myc clones were propagated and isolated. Clones with correct sequence were then selected based on screening by restriction digestion followed by sequencing using vector specific primers, T7 and BGH-rev, and internal sequencing primers, K14-F2 and K14-R3.

Site-directed mutagenesis was used to generate constructs containing a mutation in the coding sequence of KLK14, Hepsin and TMPRSS2 to alter the coded protease active site serine residue to an alanine residue, $S^{220}\rightarrow A$, $S^{353}\rightarrow A$ and $S^{478}\rightarrow A$, respectively. The templates used encoded KLK14-HA, KLK14-Myc, Hepsin-Flag, Hepsin-Myc and TMPRSS2-Myc, all with C-terminus epitope tags (Table 2.17). Following whole plasmid amplification using mutagenic primers (primer sequences, Table 2.7), the template DNA was digested with DpnI and the reaction mix was used to transform XL10-Gold *E. coli*. Clones were propagated, isolated and screened by sequencing using vector specific primers, T7 and BGH-rev. Clones with the correct mutation and sequence integrity were selected.

For stable expression of hepsin-Flag and hepsinSA-Flag in the PAR2-LMF cell line, pEFIRES-P (Hobbs et al., 1998), a bicistronic vector encoding puromycin resistance, was used in the generation of the constructs. DNA sequence encoding hepsin-Flag and hepsinSA-Flag were excised using the restriction endonuclease NotI (Table 2.5) from the pcDNA3.1 construct and ligated into the NotI digested pEFIRES-P vector (Table 2.3). Following transformation of *E. coli* XL10-Gold and propagation, the pEFIRES-P-Hepsin-Flag and pEFIRES-P-HepsinSA-Flag (pEF-Hepsin-Flag and pEF-HepsinSA-Flag) clones were screened using restriction digest analysis of alkaline lysis preparations.

Constructs found to have the insert in the correct orientation were then isolated and screened by sequencing using vector-specific primers.

For the expression of enteropeptidase in mammalian cells DNA sequence encoding full-length enteropeptidase was excised using the *HindIII* and *XbaI* from the pBluescript-enteropeptidase phagemid construct (Kitamoto et al., 1995)and then ligated into the *HindIII*/*XbaI* digested pcDNA™3.1/hygro©(+). Following transformation of *E. coli* XL10-Gold and propagation, the pcDNA3.1-enteropeptidase clones were screened using restriction digest analysis of alkaline lysis preparations followed by sequencing using vector specific primers, T7 and BGH-rev.

Table 2.17 Summary of mammalian expression constructs generated.

Method Construct generated	Primers† Forward	Reverse	Template
OE-PCR			
pcDNA3.1-KLK14-HA	K14-F10	K14-R7	pIB-KLK14-V5-His
pcDNA3.1-KLK14-Myc	K14-F10	K14-R9	pIB-KLK14-V5-His
Site-directed mutagenesis			
pcDNA3.1-KLK14SA-HA	K14-F7	K14-R5	pcDNA3.1-KLK14-HA
pcDNA3.1-KLK14SA-Myc	K14-F7	K14-R5	pcDNA3.1-KLK14-Myc
pcDNA3.1-HepsinSA-Flag	Hep-F S-A	Hep-R S-A	pcDNA3.1-Hepsin-Flag
pcDNA3.1-HepsinSA-Myc	Hep-F S-A	Hep-R S-A	pcDNA.3.1-Hepsin-Myc
pcDNA3-TMPRSS2SA-Myc	tmprss2-F S-A	tmprss2-R S-A	pcDNA3-TMPRSS2-Myc
Other			
pEF-Hepsin-Flag	N/A*	N/A*	pcDNA3.1-Hepsin-Flag
pEF-HepsinSA-Flag	N/A*	N/A*	pcDNA3.1-HepsinSA-Flag
pcDNA3.1-Enteropeptidase	N/A*	N/A*	pBluescript-Enteropeptidase

†, see Table 2.7 for primer sequences; OE-PCR, overlap extension polymerase chain reaction; *N/A - not applicable, sub-cloning was performed without *in vitro* PCR amplification of target DNA.

2.4.4 General cell culture

2.4.4.1 Insect cell culture

Sf9 (SFM Adapted) insect cells (from now on referred to as Sf9) were kept at 28°C in a non-humidified ambient air-regulated incubator. The cells were cultured in Sf-900 II SFM (Table 2.11) supplemented with penicillin (50 U/mL) and streptomycin (50 μg/mL) (Table 2.11). For adherent cell culture, the medium was replaced every 3-4 days and cells were grown until a confluent monolayer was formed. To passage the cells the culture medium was then discarded and replaced with fresh medium and cells were dislodged by sharply rapping the culture flask. Detached cells were re-seeded at 10-20% confluence in pre-warmed medium.

For cryopreservation, pre-confluent cells were resuspended in a medium consisting of 50% conditioned culture medium and 50% fresh medium with dimethyl sulphoxide (DMSO) (Table 2.2) added to a final concentration of 7.5% (v/v). Aliquoted into cryovials, the cells were frozen at a rate of -1°C/minute to -80°C in an isopropanol cryovessel and were then transferred to liquid nitrogen for long-term storage. To resuscitate, the cells were thawed rapidly in a 37°C water bath. The entire aliquot of cells was transferred to a culture flask containing pre-warmed medium. After allowing cells to attach, the medium was replaced with fresh culture medium.

When grown as a suspension for the purpose of recombinant protein production, cells in conical flasks were placed on an orbital shaker platform rotating at ~150 revolutions per minute (rpm). Medium volume for suspension culture did not exceed 35% of flask total volume. Cells were seeded at 2-3 × 10^5 cells/mL and conditioned medium harvested when cell density reached 1-2 × 10^7 cells/mL.

One of two methods was used to determine cell numbers. The first method, used predominantly, used NucleoCassettes™ (Table 2.1) containing immobilized propidium iodide and a NucleoCounter®N-100™ (ChemoMetec A/S, Allerød, Denmark) to detect the fluorescent signals of DNA intercalation by PI. Cell suspensions were lysed with Reagent A100 (Table 2.2) and stabilized with Reagent B (Table 2.2) then drawn up into NucleoCassettes™ to determine total cell count. A non-viable cell count, based on PI exclusion from viable cells, was determined using a non-lysed cell suspension. The second method to determine cell numbers used cell suspensions mixed with 0.4% trypan blue solution (Table 2.2). Based on trypan blue exclusion from viable cells, viable (white) cells were manually counted using a haemocytometer and a microscope.

2.4.4.2 Mammalian cell culture

All cells were kept in a humidified incubator at 37°C, under 5% CO_2. Cos-7, HeLa and PAR-LMF cells (Table 2.10) were cultured in DMEM (Table 2.11). Culture medium of PAR-LMF cells was supplemented with 200 μg/mL hygromycin B (Table 2.11). 22Rv1, DU145, LNCaP and PC-3 cells (Table 2.10) were cultured in RPMI-1640-L-Glutamine (Table 2.11). Kidney tubule cells (Table 2.10) were cultured in serum-free, hormonally defined culture medium, supplied by D. Vesey, consisting of DMEM-F-12 (Thermo Fisher Scientific, Scoresby, Vic, Australia) supplemented with 10 ng/ml epidermal growth factor, 5 g/ml insulin, 5 g/ml transferrin, 50 nM hydrocortisone, 50 μM prostaglandin E1, 50 nM selenium, and 5 pM triiodothyronine (all from Sigma-Aldrich Pty Ltd, Castle Hill, NSW, Australia). RWPE-1 and RWPE-2 cells (Table 2.10) were grown in Keratinocyte serum-free medium (SFM) supplemented with 5 ng/mL epidermal growth factor 1-53 (EGF 1-53) and 50 μg/mL bovine pituitary extract (BPE) (Table 2.11). The culture medium for all cell lines, except for RWPE-1, RPWE-2 and kidney proximal tubule cells (PTC), was supplemented with 10% (v/v) fetal bovine serum (FBS) (Table 2.11) unless otherwise specified. The culture medium was replaced every 2-4 days.

To passage cell monolayers, after discarding culture medium, cells were washed with phosphate-buffered saline (Dulbecco A) (DPBS) (Table 2.16) then incubated in 1-2 mL Versene (0.53 mM EDTA in DPBS, autoclaved, Table 2.16) at 37°C until cells detached. PAR-LMF and NILF cells were seeded at 10-20% and passaged at 60-70% confluence. All other cell lines were seeded at 10-20% and passaged at >80% confluence.

Cryopreservation, resuscitation and cell number determination methods used for mammalian cells are as described in Section 2.4.4.1, Insect Cell Culture, with the exception that mammalian cell cryopreservation medium consisted of fresh culture medium plus 10% (v/v) DMSO.

2.4.5 General protein techniques

2.4.5.1 Protein quantification

Protein concentrations were assayed by bicinchoninic acid protein assay using a BCA™ Protein Assay kit (Table 2.15) according to the manufacturer's instructions. A standard curve of bovine serum albumin (BSA) ranging from 0-1.5 mg/mL was generated. Ten

μL replicates of each standard, unknown sample and blank (diluent) were pipetted into a microplate. Two hundred μL BCA™ Working Reagent was added to each well, mixed gently by rocking, covered and incubated at 37°C for 30 minutes. After cooling the plate to room temperature, the absorbance at 560 nm was read using either a Benchmark™ Plus (Bio-Rad Laboratories Pty, Ltd, Gladesville, NSW, Australia) or POLARstar Omega fluorescence polarization (BMG LABTECH, Mornington, Vic., Australia) microplate reader. A standard curve was generated and unknown protein concentrations calculated using linear regression using either Microsoft® Excel 2003 or MARS Data Analysis software (BMG LABTECH, Mornington, Vic., Australia).

2.4.5.2 Conditioned medium and whole-cell lysate preparation

Conditioned medium was collected and centrifuged at 370 *g* for 5 minutes to remove whole cells. Supernatant was then collected and centrifuged at 16,000 *g* for 5 minutes. Supernatant was collected and pellets discarded.

Whole-cell lysate was prepared by removing the medium from cell monolayers, then washing the monolayer with DPBS. Ice-cold Lysis Buffer (10 mM Tris pH 8.0, 150 mM NaCl, 1% (v/v) Triton X-100, 5 mM EDTA, Table 2.16) was prepared with 1× cOmplete™ EDTA-free Protease Inhibitor Cocktail (Table 2.2) and added to the cells (100 μL/well for a 6-well plate, 1 mL/flask for a T-75 flask, 2 mL/flask for a T-175 flask). Cells were incubated by rocking on ice for 15 minutes and then detached using a cell scraper and lysed cells were then collected into a microcentrifuge tube. Lysed cells were passed through a syringe with 26 gauge needle 5-6 times, vortexed briefly, placed on ice for 10 minutes and then vortexed again. After centrifuging the cells at 16,000 *g* for 10 minutes at 4°C, the supernatant was collected and the protein concentration was determined using the BCA assay (Section 2.4.5.1).

2.4.5.3 Sodium dodecyl sulphate-polyacrylamide gel electrophoresis (SDS-PAGE)

Routinely proteins were separated by SDS-PAGE conducted using hand-cast gels comprised of 4% acrylamide stacking gel with a 10% or 12% acrylamide resolving gel (Table 2.16). For routine sample preparation, proteins (20-40 μg lysate or 5-40 μL medium) were combined with 6× SDS-PAGE Loading Buffer (0.35 M Tris pH 6.8,

30% (v/v) glycerol, 12% (w/v) SDS, 0.012% (w/v) Bromophenol Blue, ± 10% (v/v) beta-mercaptoethanol (βME), Table 2.16) to dilute the loading buffer to 1× in the sample. Addition or omission of 10% βME allows for samples to be separated by SDS-PAGE under reducing or non-reducing conditions, respectively. Incubation in loading buffer was carried out at either room temperature for a minimum of 20 minutes or at 100°C for 5 minutes. Samples were then loaded into the gel well alongside a pre-stained molecular weight marker, one of Precision Plus Protein™ Dual Color Standards, Prestained SDS-PAGE Standards low range or PageRuler™ Prestained Protein Ladder #0671 (Table 2.2). Samples were then electrophoresed at 90-110 V in Tris-Glycine Running Buffer (25 mM Tris, 192 mM glycine, 0.1% (w/v) SDS, Table 2.16) on a Mini-Protean® 3 apparatus (Bio-Rad Laboratories Pty, Ltd, Gladesville, NSW, Australia).

2.4.5.4 Electrophoretic transfer of protein from SDS-PAGE gel to membrane

Proteins separated by SDS-PAGE were transferred onto either nitrocellulose (Table 2.1) or BioTrace™ polyvinylidene fluoride (PVDF) (Table 2.1) membrane using a Mini Trans-Blot® Electrophoretic Transfer Cell (Bio-Rad Laboratories Pty, Ltd, Gladesville, NSW, Australia) with Tris-Glycine Transfer Buffer (25 mM Tris, 192 mM glycine, 0.1% (w/v) SDS, 20% (v/v) methanol, Table 2.16). Prior to assembly of the apparatus for transfer, the gel was equilibrated for 15 minutes in Tris-Glycine Transfer Buffer and the filter paper, fibre pads and nitrocellulose membrane were soaked in the same. If PVDF was used, the membrane was pre-wet in 100% methanol before equilibration in Transfer Buffer. Proteins were then transferred to the membrane at 100-110 V for 1-1.5 hours or 25 V overnight.

2.4.5.5 Western blot analysis

To prevent non-specific antibody binding, Western blot analysis consisted first of blocking the nitrocellulose membrane for 10-15 minutes using primarily Odyssey® Blocking Buffer (Table 2.16) or, less often, skim milk blocking buffer (50 mM Tris, 150 mM NaCl, pH 7.4, 5% (w/v) skim milk powder, Table 2.16). After blocking, the membranes were then incubated in primary antibody diluted in blocking buffer for a minimum of 1 hour at room temperature or, alternatively, at 4°C overnight.

Membranes were then washed 3 times for 5 minutes each in either tris-buffered saline plus Tween®20 (TBS-T) (50 mM Tris, 150 mM NaCl, pH 7.4, 0.1% (v/v) Tween®20, Table 2.16) or phosphate-buffered saline plus Tween®20 (PBS-T) (137 mM NaCl, 2.7 mM KCl, 4.3 mM Na_2HPO_4, 1.47 mM KH_2PO_4, pH 7.4, 0.1% (v/v) Tween®20, Table 2.16). A species-appropriate secondary antibody diluted in blocking buffer was then applied to the membranes and was incubated in the dark for 45-60 minutes at room temperature. Membranes were then washed as above. Routinely the secondary antibodies used were fluorescent dye conjugates with excitation at 680, 700 or 800 nm to allow detection using a LI-COR Odyssey® Infrared Imaging System (LI-COR, Lincoln, NE, USA). On rare occasions, a species-appropriate horseradish peroxidase (HRP)-conjugated secondary antibody was used in place of fluorescent dye conjugates. In this case, chemiluminescent detection was carried out using SuperSignal™ West Femto Chemiluminescent Substrate (Table 2.2) according to the manufacturer's instructions and then exposing the membranes to X-ray film (Table 2.1). The film was then developed using an AGFA CP 1000 automated X-ray film processor (Agfa-Gevaert Ltd, Scorsby, Australia). See Table 2.12 and Table 2.13 for complete lists of primary and secondary antibodies as well as dilutions routinely used.

2.4.5.6 Protein staining

To stain proteins in SDS-PAGE gels, the proteins were fixed in the gels by soaking in the Coomassie Destain (45% (v/v) methanol, 10% (v/v) acetic acid, Table 2.16) for 30 minutes and then were stained using Coomassie Blue R250 stain (0.25% (w/v) Coomassie Brilliant Blue R250, 45% (v/v) methanol, 10% (v/v) acetic acid, Table 2.16) with gentle rocking overnight at room temperature. Gels were destained by washing the gels first with Milli-Q® water, then with multiple changes of Coomassie Destain with gentle rotation until there was sufficient contrast between the protein bands and the background.

To stain proteins transferred onto nitrocellulose or PVDF membranes, the membranes were first washed in Milli-Q® water, 3 times for 5 minutes each and then stained with fresh Coomassie Blue R250 stain for 5 minutes. Membranes were destained by washing first with Milli-Q® water, then with multiple changes of Coomassie Destain with gentle rotation until there was sufficient contrast between the protein bands and the

background. For N-terminal sequencing samples Coomassie Blue R250 stain and Coomassie Destain were prepared without acetic acid.

2.4.5.7 Active-site titration of serine proteases using 4-methylumbelliferyl 4-guanidinobenzoate (MUGB)

To determine the quantity of active protease to use in assays, active-site titration was performed immediately prior to use of preparations of recombinant KLK14 and KLK4, as well as spontaneously active recombinant hepsin and matriptase (supplied by Dr D. Kirchhofer, Genentech (Kirchhofer et al., 2005)), and natural bovine trypsin (Table 2.2). Active-site titration was performed using suicide pseudo-substrate MUGB to determine the number of active sites available in activated or spontaneously active protease preparations and was performed as follows. Serine protease (300 nM) was incubated with MUGB (1 μM) (Table 2.2) in MUGB Assay Buffer (50mM Tris, 50mM NaCl, pH8.8, 0.01% (v/v) Tween®20, Table 2.16) for 10 minutes at 37°C. Stoichiometric 1:1 release of fluorescent 4-methylumbelliferone (4-MU) from the MUGB for every active protease molecule was measured over a further 10 minutes at 37°C using a POLARstar Optima or Omega fluorescent plate reader (BMG LABTECH, Mornington, Vic., Australia) by excitation at 355 nm and reading emission at 460 nm. Concentration of active protease was calculated using the relative fluorescence against a standard curve generated from known concentrations of 4-MU (0-1 μM) (Table 2.2).

2.4.6 Generation of recombinant KLK14 and KLK4 in Sf9 cells and purification from conditioned medium

2.4.6.1 Generation and purification of recombinant KLK14

The expression construct used here, pIB-KLK14-V5-His, was generated by Dr N. Bennett, a former student in the School of Biomedical Sciences, QUT.

Sf9 cells were seeded to approximately 60% confluency in a well of a six well plate and allowed to attach for 15 minutes in Sf-900 II SFM without antibiotics then the medium was removed. Cellfectin® Reagent (Table 2.2) (6 μL) and pIB-KLK14-V5-His (2 μg) were diluted in Sf-900 II SFM and added to the cells. The cells plus transfection mix (1 mL) were incubated at 27°C on a rocker for 3 hours whereupon extra medium (1 mL)

was added and incubation without rocking continued for a further 2 days. Selection pressure for stable transfection was applied using Blasticidin (50 μg/mL) (Table 2.11) in Sf-900 II SFM with medium changes and/or passaging every 2-3 days. Expression of pro-KLK14-V5-His was confirmed using Western blot analysis of conditioned medium probed with mouse anti-V5 antibody and with rabbit anti-kallikrein 14 antibody ab28841. At 3 weeks post-transfection, Blasticidin maintenance concentration for the stable transfectants was established at 10 μg/mL.

For recombinant protein production cells stably expressing KLK14-V5-His were cultured as described in Section 2.4.4.1. As the pIB-KLK14-V5-His construct contains the endogenous coding sequence for the KLK14 secretion signal peptide, conditioned medium was harvested for recombinant KLK14 purification. This was done by pelleting the Sf9-KLK14-V5-His cells with centrifugation at 370 *g* for 5 minutes and then decanting the medium. After harvest all manipulations of the conditioned medium and downstream products were performed at 4°C or on ice, unless otherwise stated. The conditioned medium was then centrifuged at 20,000 *g* for 15 minutes or filtered using a bottle-top vacuum filter set (Corning) to remove small particulate matter. The conditioned medium was then prepared for recombinant protein purification by one of three different methods using concentration and dialysis or dialysis alone. The dialysis tubing cellulose membrane (Table 2.1) was prepared for use by boiling for 10 minutes in 100 mM Na_2CO_3, 10 mM EDTA then boiling for a further 10 minutes in reverse osmosis-purified (RO) water followed by extensive rinsing in RO water. All dialysis was performed on a magnetic stirrer with at least two changes of buffer.

The three different methods for preparation of the conditioned medium were:

1/ Concentration using ammonium sulphate precipitation at 4°C; ammonium sulphate was added slowly with continuous stirring to 50% saturation (262 g/L) and allowed to equilibrate overnight. Equilibrated conditioned medium was centrifuged at 20,300 *g* for 15 minutes and supernatant was decanted and discarded. The pellet was resuspended in nickel-nitrilotriacetic acid (Ni-NTA) Dialysis Buffer (Table 2.16) and dialysed into same overnight.

2/ Concentration by diafiltration; a VivaFlow 200 diafiltration cassette with a 10,000 MWCO polyethersulfone (PES) membrane (Table 2.1) connected to a peristaltic pump (Masterflex L/S economy, John Morris Scientific, Murarrie, Qld, Australia) was used to

concentrate conditioned medium by a factor of 10 to 20. The concentrated medium was then dialysed against Ni-NTA Dialysis Buffer (50 mM NaH_2PO_4, 500 mM NaCl, pH 8.0, Table 2.16) overnight.

3/ Unconcentrated conditioned medium was dialysed against Ni-NTA Dialysis Buffer overnight.

For efficiency, the first method was favoured. However, recombinant KLK14 purified by all three methods was used in later assays and all methods generated similar end results.

Following dialysis, 1 mL Ni-NTA Superflow resin (Table 2.2) slurry per 1 L of original conditioned medium volume, was washed 3 times in Ni-NTA Dialysis Buffer, loaded onto a column (1 × 10 cm glass Econo-column® or Poly-Prep® column, Table 2.1) and the dialysed medium was applied by gravity flow. After 3 washes of 10 column volumes of each of Ni-NTA Wash Buffer 10 (10 mM imidazole, 50 mM NaH_2PO_4, 300 mM NaCl, pH 8.0, Table 2.16) and Ni-NTA Wash Buffer 30 (30 mM imidazole, 50 mM NaH_2PO_4, 300 mM NaCl, pH 8.0, Table 2.16), pro-KLK14-V5-His was eluted from the Ni-NTA resin by competition affinity using Ni-NTA Elution Buffer 250 (250 mM imidazole, 50 mM NaH_2PO_4, 300 mM NaCl, pH 8.0, Table 2.16) 10 fraction series of 1 column volume each. Post-elution, a final wash of the resin with 1 × 5 column volumes of Ni-NTA PE Buffer 300 (300 mM imidazole, 50 mM NaH_2PO_4, 300 mM NaCl, pH 8.0, Table 2.16) was used to remove remaining proteins.

Aliquots of 30 µL conditioned medium, concentrated conditioned medium and flow through from the Ni-NTA resin as well as wash fractions and elution fractions were subjected to reducing SDS-PAGE. Known quantities of BSA were also run on each gel to allow for quantification of pro-KLK14-V5-His in each elution. Gels were stained with Coomassie Blue R-250 stain and elutions showing a high level of purity were pooled, further concentrated using Slide-A-Lyzer™ 10K dialysis cassettes (Table 2.1) and Slide-A-Lyzer™ Concentrating Solution (Table 2.2) and then dialysed in the cassettes against two changes of KLK14 Buffer (5 mM NaH_2PO_4, 95 mM Na_2HPO_4, 0.01% (v/v) Tween®20, pH 8.0, Table 2.16) (Borgono et al., 2007b). After dialysis, the protein concentration was determined using the BCA assay. Aliquots of purified pro-KLK14-V5-His were stored at -80°C.

2.4.6.2 Generation and purification of recombinant KLK4

Initial batches of pro-KLK4-V5-His were purified from the conditioned medium of stably expressing Sf9 cells as described in Ramsay (2008) by Ms Melanie Carroll (née Hunt) and Mr Carson Stephens. Later batches of pro-KLK4-V5-His were produced using the procedures for the cell culture and purification for pro-KLK14-V5-His described in Section 2.4.6.1, with the exception that final dialysis of pro-KLK4-V5-His was into phosphate-buffered saline (PBS) (137 mM NaCl, 2.7 mM KCl, 4.3 mM Na_2HPO_4, 1.47 mM KH_2PO_4, pH 7.4, Table 2.16) not KLK14 Buffer. Aliquots of purified pro-KLK4-V5-His were stored at -80°C.

2.4.7 N-glycosylation status of KLK14

Recombinant pro-KLK14-V5-His and pro-KLK4-V5-His (100 ng) from stable Sf9 cells as well as medium (40 µL) harvested from Cos-7 cells transiently transfected with pcDNA3.1-KLK14-Myc (Table 2.17) or pcDNA3.1-KLK4-V5-His (generated by Dr N. Bennett, Table 2.4) were heated for 5 minutes at 100°C in 0.5× SDS-PAGE Loading Buffer plus βME. Samples were cooled and 250 U peptide-N4-(N-acetyl-beta-glucosaminyl)asparagine amidase (PNGase F) and 1% Nonidet P-40 (Table 2.15) were added and samples were incubated overnight at 37°C in buffer containing 50 mM sodium phosphate pH 7.5. After incubation, 6× SDS-PAGE Loading Buffer was added to 1× final concentration and samples were subjected to SDS-PAGE and Western blot analysis. Blots were probed using mouse anti-Myc and mouse anti-V5 antibodies.

2.4.8 Activation of recombinant KLK14 and KLK4 with thermolysin

First, the optimal incubation time and ratio of KLK14 zymogen to thermolysin for KLK14 activation was determined by incubating pro-KLK14-V5-His with thermolysin (Table 2.2) at ratios of 10:0, 10:0.125, 10:0.25, 10:1, 10: 2 µg/mL (molar ratios: 13.8:0, 13.8:0.125, 13.8:0.25, 13.8:1, 13.8:2) for 1, 1.5 and 2 hours at 37°C in KLK14 Buffer. After terminating thermolysin activity with phosphoramidon (33 µM) (Table 2.2), activated KLK14 was then subjected to active-site titration with MUGB and the proportion of active KLK14 calculated as detailed in Section 2.4.5.7.

Subsequently, immediately prior to use in assays pro-KLK14-V5-His was incubated with thermolysin at 37°C for 1.5 hours at a ratio of 10 μg/mL KLK14 to 1 μg/mL thermolysin (13.8:1 molar ratio) in KLK14 Buffer. Further thermolysin activity was inhibited using phosphoramidon (33 μM) or EDTA (50 mM) followed by MUGB active-site titration of activated KLK14.

Likewise, pro-KLK4-V5-His was incubated with thermolysin at 37°C for 1 hour at a molar ratio of 80:1 (pro-KLK4:thermolysin) in PBS, pH 7.4 (Ramsay et al., 2008a). Further thermolysin activity was inhibited using phosphoramidon (10 μM) followed by MUGB active-site titration of activated KLK4.

2.4.9 N-terminal sequencing of zymogen KLK14 and thermolysin activated KLK14

For each sequencing submission, 10 μg (~330 picomoles) of pro-KLK14-V5-His was activated as above in Section 2.4.8. Activated KLK14 (10 μg) and pro-KLK14-V5-His (1.5 μg, ~50 picomoles) were subjected to reducing SDS-PAGE. Prior to loading the sample the gel was pre-run for 15 minutes at 100 V with 139 μL/L of ≥ 98% thioglycolic acid (Table 2.2) included in the running buffer of the inner well of the electrophoresis tank to prevent oxidative changes to the protein during electrophoresis. Proteins separated by SDS-PAGE were then transferred exclusively onto PVDF membrane using 10 mM CAPS Buffer, pH 11 (Table 2.16), instead of Tris-Glycine Transfer Buffer, to avoid the presence of primary amines which can cause high background readings. Prior to assembly of the transfer apparatus, the gel was washed in Milli-Q® (Millipore Ltd, Kilsyth, Vic, Australia) purified ultrapure water for 15 minutes before equilibration in CAPS Buffer. Filter paper, fibre pads and methanol soaked PVDF membrane were all soaked in CAPS Buffer. Proteins were transferred at 25 V overnight and then the blot was stained with Coomassie Blue R-250 staining solution with or without acetic acid. Bands of 30 kDa for the pro- and 25 kDa for the active KLK14 were excised and sent for Edman degradation N-terminal sequencing to the University of Queensland (UQ), School of Chemistry and Molecular Biosciences (SCMB) sequencing facility, or to the Australian Proteome Analysis Facility (APAF Ltd).

2.4.10 Kinetic measurements of thermolysin activated KLK14

To determine the activity of KLK14 toward the tri-peptide substrate Boc-Gln-Ala-Arg-7-amido-4-methylcoumarin hydrochloride (QAR-AMC) (Table 2.2), active KLK14 (12 nM), KLK4 (12 nM) and trypsin (0.4 nM) (concentration determined by MUGB active-site titration assay) were incubated with substrate at concentrations of 1, 0.5, 0.1, 0.05, 0.01, 0.005, 0.001 and 0 mM in KLK14 Buffer. Fluorescence of released 7-amido-4-methylcoumarin hydrochloride (AMC) (Table 2.2) was measured over 20 minutes at 37°C using a POLARstar Omega fluorescent plate reader by excitation at 380 nm and reading emission at 460 nm. Concentration of released AMC was calculated using the relative fluorescence against a standard curve generated from known concentrations of AMC. The Michaelis-Menten enzyme kinetics model was used to calculate the k_{cat}/K_M constants using non-linear regression and GraphPad Prism 5 software.

2.4.11 KLK14 activation of pro-HGF

To examine whether KLK14 activates recombinant pro-HGF (supplied by Dr D.Kirchhofer, Genentech (Kirchhofer et al., 2005)), active recombinant KLK14 with concentrations ranging 0 nM to 100 nM was incubated with recombinant pro-HGF (1 μM) in KLK14 Buffer for 4 hours at 37°C. As negative and positive controls, respectively, active recombinant KLK4 and active recombinant hepsin, that was generated minus the transmembrane and intracellular regions (Kirchhofer et al., 2005), were also incubated with pro-HGF under the same conditions. The reactions, stopped with 6× SDS-PAGE Loading Buffer plus βME added to 1× final concentration, were subjected to SDS-PAGE then electrophoretic transfer onto nitrocellulose membrane. Blots were then stained with Coomassie Blue R250.

2.4.12 Examination of KLK14 inhibition by HAI-1A and 1B

To assess HAI-1 inhibition of KLK14 hydrolysis of QAR-AMC, recombinant HAI-1A and HAI-1B generated minus the transmembrane and intracellular regions (supplied by Dr D. Kirchhofer, Genentech) (Kirchhofer et al., 2003; Fan et al., 2005) at concentrations of 0 to 50 nM were incubated with 5 nM active KLK14 in KLK14 Buffer for 30 minutes at 37°C. Substrate QAR-AMC (200 μM) was added and then the fluorescence of released AMC was measured over 20 minutes at 37°C using a

POLARstar Omega fluorescent plate reader by excitation at 380 nm and reading emission at 460 nm. Concentration of released AMC was calculated using the relative fluorescence against a standard curve generated from known concentrations of AMC. Rate of hydrolysis of QAR-AMC by uninhibited KLK14 was set as 100 per cent activity, the hydrolysis rate of HAI-1A- and HAI-1B-inhibited KLK14 as a per cent thereof.

2.4.13 KLK14 interaction with HAI-1A and 1B

To assess whether active KLK14 forms stable complexes with HAI-1A and 1B, three assay sets were performed. The interaction of HAI-1A and 1B with hepsin was assessed concurrently:

1) Active KLK14 (1 μM) was incubated with either HAI-1A or 1B, concentrations ranging from 0 μM to 10 μM, for 30 minutes at 37°C. Included were 10 μM HAI-1A or 1B only and 10 μM HAI-1A or 1B plus 50 mM EDTA inhibited thermolysin control incubations.
2) Active KLK14 and hepsin with final concentration of 1 μM were each incubated with HAI-1A and 1B, concentrations ranging from 0 μM to 1 μM, for 30 minutes at 37°C. Included were 1 μM HAI-1A and 1B only incubations.
3) Active KLK14 and hepsin with final concentrations ranging from 0 μM to 1 μM were each incubated with HAI-1A (1 μM) for 30 minutes at 37°C. Included were KLK14 (1 μM) and hepsin (1 μM) only incubations.

Reactions, stopped with 6× SDS-PAGE Loading Buffer plus βME added to 1× final concentration, were then subjected to SDS-PAGE, proteins were transferred onto PVDF membrane and the blots were stained using Coomassie Blue R-250.

2.4.14 Transient transfection of Cos-7 cells

A series of transient transfections and co-transfections into Cos-7 cells were performed as follows. Cells were transfected with DNA expression or vector constructs using Lipofectamine™ 2000 or Lipofectamine™ LTX (Table 2.2) according to the manufacturer's instructions. Table 2.18 lists the expression constructs used as well as the protein encoded by each. Briefly, the DNA and Lipofectamine™ were prepared in Opti-MEM®I Reduced Serum Medium (Table 2.11) with a ratio of

DNA:Lipofectamine™ (μg:μL) of 1:2. The transfection mixture was applied to sub-confluent cells seeded in complete medium in the absence of antibiotics and cells were cultured for 24 hours post-transfection. For co-expression experiments, when co-expressing two or more proteins, equal quantities (μg) of expression construct DNA were co-transfected into the Cos-7 cells. For the single protein controls in the co-expression experiments, the expression construct was co-transfected with an equal quantity (μg) of a vector with a backbone matching the expression construct. The total quantity of DNA used for co-transfection in 6-well plates, 10 cm culture dishes or T-75 flasks, was 4, 16 or 40 μg, respectively.

To analyse the proteolytic interactions between co-expressed proteases, SDS-PAGE of the whole-cell lysate (20 μg) and conditioned medium (40 μL) from transfected Cos-7 cells was performed followed by Western blot analysis using epitope tag-specific or protein-specific primary antibodies (Table 2.18) and species-appropriate secondary antibodies were used for detection (Table 2.13). Table 2.19 contains a summary of the protein co-expression combinations.

2.4.15 Recombinant hepsin incubation with recombinant pro-KLK14 and pro-KLK4

Recombinant pro-KLK14-V5-His and pro-KLK4-V5-His (3 μM) were each incubated with recombinant hepsin (active) with concentrations ranging from 0 to 3 μM. As a control pro-KLK14-V5-His and pro-KLK4-V5-His (3 μM) were also incubated with thermolysin at molar ratios of 1:0.08 and 1:0.008. Incubations were carried out in a Tris-NaCl buffer (50 mM Tris, 50 mM NaCl, pH 7.4) for 1 hour at 37°C. The reactions, stopped with 6× SDS-PAGE Loading Buffer plus 10% βME added to 1× final concentration, were subjected to SDS-PAGE and Western blot analysis using anti-V5, anti-Kallikrein 14 ab28841 and anti-KLK4 mid and C-term (combined) (Hormone Dependent Cancer Program, IHBI, Kelvin Grove, Qld, Australia (Harvey et al., 2003)) antibodies.

Table 2.18 Summary of expression constructs, protein product and primary antibodies used for Western blot analysis.

Construct	Product	Primary antibodies†
pcDNA3.1-Enteropeptidase	Enteropeptidase	Anti-Enterokinase LC antibody (sc-51283)
pcDNA3.1-KLK14-HA	KLK14-HA	Anti-HA (H6908) Rabbit* or anti-Kallikrein 14 (ab28841) Rabbit
pcDNA3.1-KLK14SA-HA	KLK14SA-HA	
pcDNA3.1-KLK14-Myc	KLK14-Myc	Anti-Myc-Tag (9B11) Mouse mAb* or anti-Kallikrein 14 (ab28841) Rabbit
pcDNA3.1-KLK14SA-Myc	KLK14SA-Myc	
pcDNA3.1-KLK4-V5-His	KLK4-V5	Anti-V5 (R96025) Mouse*, anti-Kallikrein 4 mid Rabbit or anti-Kallikrein 4 C-term Rabbit
pcDNA3.1-KLK4SA-V5-His	KLK4SA-V5	
pcDNA3.1-Hepsin-Flag	Hepsin-Flag	Anti-Flag® (F7425) Rabbit* or anti-Hepsin A15 Mouse
pcDNA3.1-HepsinSA-Flag	HepsinSA-Flag	
pcDNA-3.1-Hepsin-Myc	Hepsin-Myc	Anti-Myc-Tag (9B11) Mouse mAb* or anti-Hepsin A15 Mouse
pcDNA3.1-HepsinSA-Myc	Hepsin-SA-Myc	
pcDNA3-TMPRSS2-Myc	TMPRSS2-Myc	Anti-Myc-Tag (9B11) Mouse mAb
pcDNA3-TMPRSS2SA-Myc	TMPRSS2SA-Myc	
pcDNA3.1-Matriptase	Matriptase	Anti-Matriptase M69 Mouse
pEZ-M02-MMP3	MMP3	Anti-MMP3 antibody (ab18898) Goat
pEZ-M02-MMP9	MMP9	Anti-MMP9 antibody (ab38898) Rabbit

† Antibody supplier and dilutions in Table 2.12; * most frequently used antibody.

Table 2.19 Summary of proteins co-expressed in Cos-7 cells for proteolysis and immunoprecipitation analysis.

Expressed protease	Co-expressed protease: KLK4	KLK4SA	Hepsin	HepsinSA	TMPRSS2	TMPRSS2SA	Matriptase	Enteropeptidase
KLK14	+	+	+ IP Biotin ABP*	+ Biotin	+ IP	+		+
KLK14SA	+	+	+ IP ABP*	+	+ IP	+		+
KLK4			+ IP Biotin ABP	+ Biotin	+ IP ABP	+		
KLK4SA			+ IP ABP	+	+ IP ABP	+		
HepsinSA			+	+				
MMP3			+ IP		+ IP		+	
MMP9			+ IP		+ IP		+	

+, Co-transfections; IP, Immunoprecipitations; Biotin, cell-surface biotinylation; ABP, activity based probe; *, ABP of conditioned media only.

2.4.16 Immunoprecipitation of proteases expressed in transiently transfected Cos-7 cells

Cos-7 cells were transiently co-transfected in 10 cm culture dishes as outlined in Section 2.4.14. The co-transfection combinations performed for immunoprecipitation studies are detailed in Table 2.19. Cells were washed twice with ice-cold DPBS and then 400 µL of Lysis Buffer with Protease Inhibitor Cocktail was added. Whole-cell lysate was prepared and then protein concentration determined by BCA assay. Protein A Agarose and/or Protein G Agarose (Table 2.2) was equilibrated in Lysis Buffer and then whole-cell lysate was pre-cleared by adding 10 µL Protein A and/or G Agarose to 200-300 µg

of whole-cell lysate and incubating for 1 hour at 4°C on a rolling platform. The agarose beads were pelleted by centrifugation at 3000 *g* for 2 minutes and the pre-cleared supernatant recovered. Appropriate antibodies (Table 2.18) or isotype immunoglobulin G (IgG)s (control) (2-5 μg) (Table 2.14) were added to the supernatant and incubated overnight at 4°C on a rotating wheel. Fresh aliquots of Protein A and/or G Agarose (10 μL) were added and incubated for 4 hours at 4°C with gentle agitation. The unbound (flow through) protein fraction was then collected by centrifugation of the agarose in Pierce Spin Columns (Table 2.1) for 2 minutes at 3000 *g*. The agarose was then washed three times with 20 column volumes of Lysis Buffer, centrifuging for 1 minute at 3000 *g* after each wash. The bound (immunoprecipitated) fraction was then eluted by adding 40 μL of 3× SDS-PAGE Loading Buffer plus βME, incubating at 100°C for 10 minutes then centrifuging at 3000 *g* for 2 minutes to collect eluate. The immunoprecipitated, column flow through as well as the input whole-cell lysate fractions were then subjected to SDS-PAGE and Western blot analysis. Primary antibodies used in the Western blot analysis were directed at detecting proteins that co-immunoprecipitated with the target protein (Table 2.2).

2.4.17 Cell-surface biotinylation of transiently transfected Cos-7 cells

Cos-7 cells in 10 cm culture dishes were transiently co-transfected as outlined in Section 2.4.14. The co-transfection combinations performed are detailed in Table 2.19. In order to isolate cell surface localized proteins cell-surface biotinylation and streptavidin agarose pull-down was performed, outlined as follows. Cell monolayers were washed twice with ice-cold DPBS then plasma membrane proteins were biotin-labelled by incubation with 1.22 mg/mL EZ-Link™ Sulfo-NHS-SS-Biotin (Table 2.2) for 10 minutes on ice with gentle rocking. Cells were then washed 3 times with ice-cold DPBS and then 0.5-1 mL Lysis Buffer plus Protease Inhibitor Cocktail was added per 10 cm culture dish or T-75 culture flask and whole-cell lysate was prepared. From this a sample of whole-cell lysate (50-100 μL) was taken for later analysis. To pull down the biotinylated proteins in the remaining whole-cell lysate, Streptavidin Agarose Resin (streptavidin agarose) (Table 2.2) 50% slurry (20 μL), equilibrated in Binding Buffer (28 mM NaH_2PO_4, 72 mM Na_2HPO_4, 0.15 M NaCl, pH 7.2, Table 2.16), was added and the mixture incubated on ice for 1 hour rocking gently. The unbound (cytoplasmic) protein fraction was then collected by centrifugation in Pierce Spin Columns for 2 minutes at

1000 *g*. The resin was then washed three times with 10 column volumes of Lysis Buffer, centrifuging for 1 minute at 1000 *g* after each wash. The bound (plasma membrane) fraction was then eluted by adding 40 μL of 3× SDS-PAGE Loading Buffer plus βME, incubating at 100°C for 10 minutes then centrifuging at 1000 *g* for 2 minutes to collect eluate. The cytoplasmic, plasma membrane and whole-cell lysate fractions were then subjected to SDS-PAGE and Western blot analysis using primary antibodies listed in Table 2.2.

2.4.18 Activity-based probe (ABP) labelling of proteases expressed in transiently transfected Cos-7 cells

In order to isolate active serine proteases, biotin tagged ABPs were used in conjunction with streptavidin agarose pull-down, described as follows. Cos-7 cells in T-75 flasks were transiently co-transfected (Section 2.4.14). . The co-transfection combinations performed are detailed in Table 2.3. For ABP of conditioned medium, the medium was collected and then concentrated and buffer exchanged into 50 mM Tris pH 7.4 using an Amicon® Ultra-15 Ultracel-10 spin column (Table 2.1) spun at 3,200 *g*. The protein concentration was then assayed by BCA assay and then to an equivalent of 40 μg of protein, ABP, biotinylated Glu-Gly-Arg-chloromethylketone (biotin-EGR-CMK) or biotinylated Phe-Pro-Arg-chloromethylketone (biotin-FPR-CMK) (Table 2.2) was added to a final concentration of 50 μM. The mixture was incubated alongside an untreated control for 1.5 hours at 37°C.

For ABP of whole cells, after removing the conditioned medium, the cell monolayer was first washed with DPBS then cells were detached with Versene as described in Section 2.4.4.2. The cells were then washed twice in DPBS with centrifugation for 5 minutes at 370 *g* after each wash to remove buffer. The cells were then resuspended in DPBS (300 μL) and divided equally into three microcentrifuge tubes. One hundred μL of ABP, to a final concentration of 50 μM, or 100 μL DPBS (untreated control) was added to each tube and allowed to incubate with gentle rotation for 1.5 hours at 37°C. After incubation, cells were washed twice with ice-cold DPBS, as above, and then 100 μL of ice-cold Lysis Buffer with Protease Inhibitor Cocktail was added to the cell pellet. Whole-cell lysate was then prepared and a sample (5 μL) was taken from each preparation for quantification by BCA assay.

Streptavidin agarose was used to pull down the proteins attached to the biotinylated ABP in the conditioned medium and the whole-cell lysate. The streptavidin agarose was prepared by equilibrating with Binding Buffer and then a 50% slurry of streptavidin agarose (2 μL per μg of ABP) was added to the ABP-treated and also the untreated controls. After incubation for 10 minutes rocking gently at room temperature, the unbound protein fraction was then collected by centrifuging the samples in Pierce Spin Columns for 2 minutes at 1000 *g*. The resin was then washed twice with 20 column volumes of Binding Buffer, centrifuging for 1 minute at 1000 *g* after each wash. The bound fraction was then eluted by adding 8-10 column volumes of SDS-PAGE Loading Buffer plus βME, incubating at 100°C for 10 minutes then centrifuging at 1000 *g* for 2 minutes to collect eluate. The eluted fractions, as well as the input conditioned medium and whole-cell lysate, were then subjected to SDS-PAGE and Western blot analysis using primary antibodies listed in Table 2.2. In addition, the blots were probed with Streptavidin, Alexa Fluor® 680 conjugate (Table 2.2) to detect all proteases pulled down by the ABPs.

2.4.19 Gelatin zymography of conditioned media from transiently transfected cells

Conditioned media were collected from Cos-7 cells transiently transfected for 24 hours with constructs encoding either wild-type hepsin or TMPRSS2 and either MMP3 or MMP9. After concentrating the media ×10, gelatin zymography was carried out under non-reducing conditions (without βME) using hand-cast SDS-PAGE gels comprising 4% acrylamide stacking gel and 10% acrylamide resolving gel including 1 mg/mL gelatin from porcine skin (Table 2.2) in the resolving gel. Following electrophoresis the proteins were renaturated by incubating the gels in Zymography Renaturation Buffer (50 mM Tris, 5 mM $CaCl_2$, 1 μM $ZnCl_2$, pH 7.4, 2.5% Triton X-100, Table 2.16) for 1 hour at room temperature on an orbital shaker platform. The gels were then washed briefly in Milli-Q® water followed by incubation rotating overnight at 37°C in Zymography Developing Buffer (50 mM Tris, 5 mM $CaCl_2$, 1 μM $ZnCl_2$, pH 7.4, Table 2.16). The gels were then stained using Zymography Stain (0.5% (w/v) Coomassie Brilliant Blue R250 (Fluka), 30% (v/v) ethanol, 10% (v/v) acetic acid, Table 2.16) for 60 minutes followed by de-staining with Zymography Destain (30% (v/v) ethanol, 10% (v/v) acetic acid, Table 2.16). When clear bands appeared in the gels the de-staining was stopped using 2% acetic acid followed by rehydration of the gel overnight in the same.

2.4.20 Recombinant hepsin and matriptase and bovine trypsin incubation with MMP3 and MMP9 from transiently transfected Cos-7 cells

Conditioned medium from Cos-7 cells transiently transfected for 24 hours with constructs encoding either MMP3 or MMP9 was incubated at 37°C for 1 or 14 hours with recombinant hepsin (50 nM), recombinant matriptase (50 nM) or bovine trypsin (10 nM). The reactions, stopped with Protease Inhibitor Cocktail and 6× SDS-PAGE loading buffer ± βME added to 1× final concentration, were subjected to SDS-PAGE under reducing and non-reducing conditions (data not shown) and Western blot analysis using anti-MMP3 and anti-MMP9 antibodies.

2.4.21 Intracellular Ca^{2+}flux assays to examine serine protease-initiated PAR activation

For Ca^{2+} flux assays cells grown to 80% confluence were washed with DPBS, then detached using Versene and collected. The cells were washed twice with Ca^{2+} Flux Assay (CaFA) Buffer (Table 2.16) without probenecid and centrifuged at 370 *g* for 5 minutes after each wash to remove Versene. The cells were then loaded with the ratiometric calcium indicator Fura-2 acetoxymethyl ester (Fura-2 AM) by resuspending (4×10^6 cells/mL) in CaFA Buffer with probenecid plus Fura-2 AM (6 μM) (Table 2.2) and 0.021% (w/v) Pluronic® F127 (Table 2.2). After incubation for 1 hour in the dark at 37°C, cells were pelleted by centrifugation at 370 *g* for 5 minutes, load buffer was aspirated and cells resuspended (2×10^6 cells/mL) in CaFA Buffer. For fluorescence measurements, 100 μL cell suspension replicates were pipetted into black 96-well microplates and maintained at 37°C. All agonists, either active serine proteases or agonist peptides (AP), PAR1AP, PAR2AP and PAR4AP (Table 2.2), were diluted in CaFA Buffer and brought to 37°C immediately before use. A continuous measurement of free intracellular Ca^{2+} ion concentration ($[Ca^{2+}_i]$) was established by exciting Fura-2 at alternating 340 and 380 nm, and the emission at 510 nm was measured using a POLARstar Optima or Omega fluorescent plate reader. After recording a baseline $[Ca^{2+}_i]$ for 30 seconds, agonist or buffer was applied to the Fura-2 loaded cells and changes in $[Ca^{2+}_i]$ were measured for 180 seconds. A consecutive agonist treatment could then be applied, if required, and changes in $[Ca^{2+}_i]$ measured for a further 210 seconds. The data are presented as the change in ratio of emission 510 $nm_{(340/380\ nm)}$, proportional to free $[Ca^{2+}_i]$., and are representative of experiments performed in

triplicate and repeated on 3 independent occasions unless limited by the availability of serine proteases.

2.4.21.1 Examination of PAR activation by KLK14, hepsin, matriptase and trypsin using intracellular Ca^{2+} flux assays

PAR1-, PAR2- and PAR4-lung myofibroblast (LMF) cells (Table 2.10) were used to assess serine protease-initiated changes in $[Ca^{2+}_i]$. These cell lines are derived from lung myofibroblasts immortalized from PAR1 -/- mice (Darrow et al., 1996). These cells, also lacking functional endogenous mouse PAR2 and PAR4, have been transfected to stably express human PAR1, PAR2 or PAR4 (Andrade-Gordon et al., 1999). Expressing only one each of PARs, the cells, designated PAR1-LMF, PAR2-LMF and PAR4-LMF, are useful *in vitro* tools for examining PAR activation as Ca^{2+} flux response is elicited from each line by the respective PAR AP.

To assess the ability of the serine proteases to completely activate each PAR, consecutive treatments of a serine protease followed by a PAR AP were made as described in Section 2.4.21. The cells were first treated with one of the following active serine proteases, KLK14 (150 nM), hepsin (50 nM), matriptase (10 nM for PAR1- and PAR2-LMF; 50 nM for PAR4-LMF), or bovine trypsin (10 nM for PAR1- and PAR2-LMF; 50 nM for PAR4-LMF). One of the following APs was then applied: PAR1AP (TFLLR) (50 μM), PAR2AP (SLIGRL) (50 μM) and PAR4AP (AYPGKF) (500 μM; 150 μM for KLK14), to PAR1-, PAR2- and PAR4-LMF cells, respectively.

HAI-1B inhibition of hepsin and matriptase activation of PAR2 was also assessed. Hepsin (50 nM) and matriptase (10 nM) were pre-incubated with 1 μM HAI-1B. Then application of HAI-1B/hepsin and HAI-1B/matriptase to the PAR2-LMF cells was followed by application of PAR2AP (SLIGRL) (50 μM).

Dose response of PAR-LMF cells to hepsin, trypsin and matriptase (for PAR2-LMF only) was also ascertained by Ca^{2+} flux assay. The hepsin concentration range assayed for all PAR-LMF cells was 1 to 100 nM. The trypsin concentration range assayed for PAR1-LMF was 0.1 to 100 nM; for PAR2-LMF, 0.05 to 5 nM; and for PAR4-LMF, 1 to 100 nM. The matriptase concentration range for the PAR2-LMF cells was 0.06 to 30 nM. The concentration to stimulate half-maximal response (EC_{50}) was calculated from a nonlinear regression curve using GraphPad Prism 5. Data is presented as the mean

value, +/- SEM, of experiments performed in triplicate. Due to limited availability of the recombinant proteases, only the trypsin experiments were conducted three times.

2.4.21.2 Inhibition of KLK4 induced activation of PAR2 using the inhibitor peptide SFTI-FCQR

Inhibition of KLK4 activation of PAR2 by KLK4-specific inhibitor SFTI-FCQR (Swedberg et al., 2009) was assessed by Ca^{2+} flux assay. PAR2-LMF cells were challenged with buffer only, PAR2AP (SLIGKV) (50 μM), trypsin (10 nM), trypsin (10 nM) pre-incubated with 1 μM SFTI-FCQ, and KLK4 (200 nM). To assess the status of PAR2 after agonist treatment, PAR2-LMF cells were also challenged with consecutive treatments of KLK4 (200 nM) pre-incubated with 1 μM SFTI-FCQR followed by either PAR2AP (SLIGKV) (50 μM) or trypsin (10 nM).

2.4.21.3 Examination of activation of PAR2 in primary kidney proximal tubule cells (PTC)

Cultures of human primary kidney PTC (passage number 2-3, provided by Dr D. Vesey, Princess Alexandra Hospital, Brisbane) were assessed by Ca^{2+} flux assay for activation of PAR2 by KLK4. The kidney PTC were passaged no more than once in our laboratory before they were challenged with buffer only, trypsin (10 nM), or KLK4 (300 nM, 600 nM and 1.2 μM). To examine the activity of KLK4 post-Ca^{2+} flux assay, the assay mix was collected from the wells of the microplate. Half the assay mix was centrifuged at 370 *g* for 5 minutes to pellet the kidney PTC, and the supernatant was collected. The cell-free supernatant and the cell-containing assay mix were both subjected to MUGB active-site titration to determine KLK4 activity.

To assess how much of the Ca^{2+} flux initiated by trypsin and KLK4 was mediated via PAR2, the cells were also challenged with consecutive treatments of PAR2AP (SLIGKV) (100 μM) to desensitize the PAR2 response, followed by either trypsin (10 nM) or KLK4 (300 μM).

2.4.22 Generation and characterization of prostate cancer LNCaP and PAR2-LMF cells stably expressing the cell-surface serine protease hepsin

2.4.22.1 Generation of LNCaP and PAR2-LMF cells stably expressing hepsin or catalytically inactive hepsin

Prostate cancer LNCaP cells were stably transfected with constructs encoding full-length hepsin or active-site mutated hepsinSA, with a carboxyl-terminus Flag epitope tag (designated hepsin-Flag and hepsinSA-Flag) as follows. The cells were transfected using Lipofectamine™ LTX (4 μL) with 2 μg of pcDNA3.1-Hepsin-Flag, pcDNA3.1-HepsinSA-Flag (Table 2.4 and Table 2.17) or pcDNA3.1 vector. The DNA/Lipofectamine™ mixture was prepared in Opti-MEM®I Reduced Serum Medium and applied to cells seeded in 6-well plates at ~70% confluency in culture medium, RPMI-1640-L-Glutamine containing 10% FBS (v/v). At 48 hours post-transfection the transfection medium was replaced with culture medium. For stable transfection of the LNCaP cells selection pressure was applied using G418 (500 μg/mL) (Table 2.11) in the culture medium. For maintenance of the stable cell lines, the medium was changed and/or cells passaged every 2 to 3 days. G418 concentration was set at 350 μg/mL 2 weeks post-transfection.

PAR2-LMF cells were also transfected with constructs encoding hepsin-Flag and hepsinSA-Flag by the method as follows. The cells were seeded in a 6-well plate to ~60% confluency in DMEM containing 10% FBS (v/v) and then transfected using Lipofectamine™ LTX (5 μL) with 4 μg of pEF-Hepsin-Flag, pEF-HepsinSA-Flag (Table 2.17) or pEFIRES-p vector prepared in Opti-MEM®I Reduced Serum Medium. At 48 hours post-transfection the transfection medium was replaced with culture medium, DMEM containing 10% FBS (v/v), 200 μg/mL hygromycin B. The culture medium contained hygromycin for the maintenance of the PAR2 transfection (Andrade-Gordon et al., 1999). For stable transfection, selection pressure was applied using puromycin (5 μg/mL) (Table 2.11) in the culture medium. The medium was changed and/or cells passaged every 2 to 3 days.

2.4.22.2 Fluorescence-Activated Cell Sorting (FACS) and screening by flow cytometry of stably transfected LNCaP-hepsin and LNCaP-hepsinSA cells

To obtain homogeneous populations of LNCaP cells expressing high levels of hepsin-Flag or active-site mutated hepsinSA-Flag, FACS using an anti-Flag antibody was used to isolate single cells with high plasma membrane expression of hepsin-Flag or hepsinSA-Flag a minimum of two weeks post-transfection and antibiotic selection.

To prepare cells for FACS, conditioned medium was collected from cell monolayers, centrifuged to remove cells at 500 *g* for 5 minutes, filtered with a sterile 0.2 μM filter and reserved for later use. The cell monolayers were washed with DPBS and detached with Versene and cells were then collected in DPBS with 2% (v/v) FBS (DPBS-FBS). Cells were pelleted by centrifugation at 500 *g* for 5 minutes and then resuspended at 1×10^7 cells/mL in DPBS-FBS plus mouse anti-Flag M2 primary antibody (Table 2.12) diluted 1/1000. After incubation at room temperature for 20 minutes, cells were washed in DPBS-FBS and centrifuged to pellet cells. Pelleted cells were then resuspended to 8×10^6 cells/mL in Alexa Fluor® 488 goat anti-mouse IgG secondary antibody (Table 2.13) diluted 1/750 in DPBS-FBS and then incubated at room temperature for 20 min. After being washed in DPBS-FBS, cells were pelleted and then resuspended to at 8×10^6 cells/mL in DPBS-FBS. Before FACS, cells were filtered using a Cell Strainer (70 μm) (Table 2.1) and then cells were sorted using a DAKO MoFlo High Speed FACS (Beckman Coulter, Gladesville, NSW, Australia). Operation of the FACS machine was performed by Dr. Ibtissam Abdul-Jabbar of the Diamantina Institute, University of Queensland, Brisbane.

For monoclonal populations, cells were sorted one cell/well in 96-well plates. For triclonal populations, cells were sorted three cells/well in 96-well plates. For polyclonal populations, 8,000 – 20,000 cells were sorted into medium (3 mL) which was then split across two or three wells of a 24-well plate. In the first round of FACS, cells were sorted into 96-well plates or 5 mL tubes pre-aliquoted with cell-conditioned RMPI-1640, 10% (v/v) FBS and 350 μg/mL G418. In subsequent rounds of FACS, the make-up of the medium was modified to include 50% cell-conditioned medium plus 50% fresh medium with FBS supplemented to 20% (v/v) and G418 (350 μg/mL).

Cell-surface expression of hepsin-Flag and hepsinSA-Flag in the stably transfected cell lines was screened by flow cytometry using an anti-Flag antibody. Cell monolayers were

washed with DPBS, detached with Versene and cells were then collected in DPBS-FBS. Cells were pelleted by centrifugation at 500 *g* for 5 minutes and then resuspended at 0.75 × 10^7 cells/mL in DPBS-FBS containing mouse anti-Flag M2 primary antibody diluted 1/1000. After incubation at room temperature for 20 minutes, cells were washed in DPBS-FBS, then centrifuged to pellet. Pelleted cells were then resuspended at 0.75 × 10^7 cells/mL in Alexa Fluor® 488 goat anti-mouse IgG secondary antibody diluted 1/750 in DPBS-FBS and incubated at room temperature for 20 min. After washing in DPBS, cells were pelleted then resuspended at 0.75 × 10^6 cells/350 μL in DPBS. Cell surface hepsin-Flag and hepsinSA-Flag were then assessed using an FC500 flow cytometer (Beckman Coulter, Gladesville, NSW, Australia).

2.4.22.3 Examination of LNCaP-hepsin and LNCaP-hepsinSA expression by Western blot analysis

To compare relative expression of hepsin and hepsinSA, whole-cell lysates were prepared from several LNCaP-hepsin-Flag and LNCaP-hepsinSA-Flag monoclonal and triclonal populations as well as vector transfected and untransfected LNCaP cells. The whole-cell lysates were subjected to reducing Western blot analysis. The blots were probed using the following antibodies: rabbit anti-Flag, mouse anti-hepsin A15 (Dr Q.Wu, Cleveland Clinic) and mouse anti-GAPDH (Table 2.12).

To examine endogenous expression of hepsin in prostate cancer cell lines, whole cell lysates were prepared from LNCaP 22Rv1, DU145, PC-3 and RWPE2 cells. Whole cell lysate from Cos-7 cells transiently transfected with a construct encoding hepsin-Flag was used as a positive control. The lysates were subjected to Western blot analysis using mouse anti-hepsin A15 antibody.

2.4.22.4 Examination of LNCaP-hepsin and LNCaP-hepsinSA expression by Western blot analysis of cell-surface biotinylated fractions

To examine relative cell surface expression of hepsin and hepsinSA, cell surface biotinylation was performed (as described in Section 2.4.17) for one each of the LNCaP-hepsin-Flag and LNCaP-hepsinSA-Flag clones as well as LNCaP-vector and untransfected LNCaP cells. The biotinylated plasma membrane, unbiotinylated cytoplasmic flow-through, and whole-cell lysate fractions were subjected to reducing

SDS-PGE followed by Western blot analysis. The blots were probed using the following antibodies: rabbit anti-Flag, mouse anti-hepsin A15 and mouse anti-GAPDH.

2.4.22.5 Examination of zymogen KLK14 and KLK4 interactions with cell surface hepsin and hepsinSA

To examine whether KLK14 and KLK4 interact with cell surface expressed hepsin, LNCaP-hepsin-Flag and LNCaP-hepsinSA-Flag cells at 90% confluence in 6-well plates were washed twice with PBS and then incubated with RMPI-1640-L-Glutamine (without FBS) containing 80 μM recombinant pro-KLK14-V5-His or pro-KLK4-V5-His. The cells were then incubated for 1, 5 or 18 hours at 37°C, under 5% CO_2. After incubation, the conditioned media and whole-cell lysate were prepared and then subjected to reducing and non-reducing Western blot analysis using mouse anti-V5 and rabbit anti-Flag antibodies (Table 2.12).

Chapter 3 Generation and characterization of recombinant KLK14

3.1 Introduction

KLK14 is a secreted serine protease with unresolved physiological roles (Hooper et al., 2001a; Yousef et al., 2001). It has widespread tissue expression with higher levels in skin, breast and prostate (Borgono et al., 2003; Brattsand et al., 2005; Komatsu et al., 2006; Stefansson et al., 2006; Borgono et al., 2007c), and suggested roles in seminal clot liquefaction (Emami and Diamandis, 2008), epidermal desquamation (Brattsand et al., 2005; Stefansson et al., 2006; Borgono et al., 2007b; Deraison et al., 2007; Komatsu et al., 2007a; Komatsu et al., 2007b; Emami and Diamandis, 2008) and also PAR activation/inactivation (Oikonomopoulou et al., 2006a; Stefansson et al., 2008). Furthermore, increased KLK14 expression in prostate cancer has been correlated with disease progression.

In recent years several groups have generated recombinant KLK14 for characterization using expression systems including insect cell *Drosophila* Schneider 2 cells (Brattsand et al., 2005), yeast expression in *Pichia pastoris* (Borgono et al., 2003; Brattsand et al., 2005), and mammalian cell expression in HEK293 (Borgono et al., 2007c) and Cos-7 (Rajapakse and Takahashi, 2007) cells. Of these, Borogono and colleagues (2007a) reported that KLK14 generated in *Pichia pastoris* was not N-glycosylated. In addition, they speculated that based on MW KLK14 generated in HEK293 cells was also not N-glycosylated (Borgono et al., 2003). The N-glycosylation status of KLK14 has not been reported for any other expression system. Nonetheless, N-glycosylation is a significant post-translational modification that can have a wide range of effects on function, activity, localization and stability of a protein (Skropeta, 2009).

In contrast to N-glycosylation, the enzymatic properties of recombinant KLK14 generated in various expression systems have been well described. Approaches have included hydrolytic activity of recombinant KLK14 against synthetic tripeptide substrates (Brattsand et al., 2005; Borgono et al., 2007c; Rajapakse and Takahashi, 2007), phage display (Felber et al., 2005), and combinatorial and sparse matrix libraries (Borgono et al., 2007a; de Veer et al., 2011). From these it has been determined that KLK14 has a preference in substrates for Arg P1 residues over Lys>Tyr residues (Brattsand et al., 2005; Felber et al., 2005; Oikonomopoulou et al., 2006a; Borgono et al., 2007a; Borgono et al., 2007c; Rajapakse and Takahashi, 2007; Stefansson et al., 2008; de Veer et al., 2011).

Using *in vitro* approaches a number of KLK14 substrates have also been determined (Lawrence et al., 2010), as have inhibitors including several serpins, and Kazal-type inhibitors SPINK5 and SPINK6 (Goettig et al., 2010). However, to date there has been no report of the growth, motility and morphogenic factor HGF (Bottaro et al., 1991; Nakamura and Mizuno, 2010) as a substrate for KLK14. Furthermore, KLK14 interactions with isoforms of the Kunitz-type inhibitor HAI-1 have not been defined. HGF is expressed in the prostate (Humphrey et al., 1995; Gmyrek et al., 2001), with increased expression, along with its cognate receptor HGFR, in prostate cancer (Kurimoto et al., 1998; Zhu and Humphrey, 2000). Moreover, there is increased activated HGF in the serum of patients with untreated prostate cancer compared to those with benign disease (Hashem and Essam, 2005; Yasuda et al., 2009). In contrast, HAI-1 has been associated with prostate cancer progression through decreased expression (Kataoka et al., 1999; Wang et al., 2009; Warren et al., 2009).

As KLK14 has a preference for Arg P1 residues, it is a potential HGF activator as activation of HGF single chain precursor (pro-HGF) occurs by limited proteolysis after residue Arg494 to produce a heterodimer linked by a disulphide bond (Gak et al., 1992; Naka et al., 1992; Naldini et al., 1992) (Figure 3.1). In so doing, KLK14 potentially joins a list of HGF-activating proteases including the serum protease HGFA (Shimomura et al., 1995; Itoh et al., 2004), and the transmembrane proteases matriptase (Lee et al., 2000; Owen et al., 2010), hepsin (Herter et al., 2005; Kirchhofer et al., 2005; Owen et al., 2010) and TMPRSS13 (Hashimoto et al., 2010).

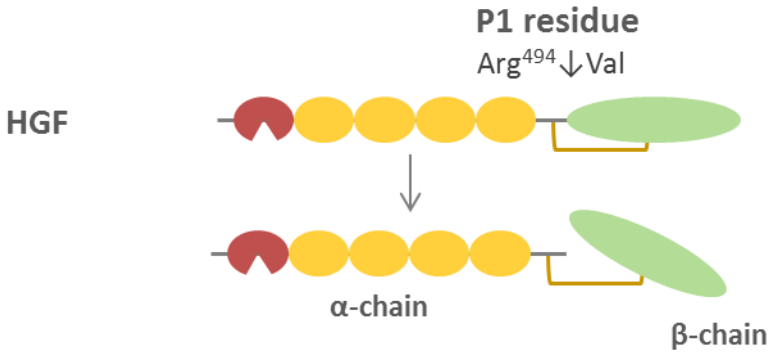

Figure 3.1 Pro-region cleavage site of HGF. Limited proteolysis at Arg494 generates activated HGF, a two chain form tethered by an intramolecular disulphide bond.

Protease inhibitors are a crucial aspect of regulation of HGF activation (Gherardi et al., 2012). Indeed, HAI-1 is an endogenous inhibitor of HGFA and matriptase (Shimomura et al., 1997; Lin et al., 1999b; Benaud et al., 2001; Wang et al., 2009) and a role of tight regulation of matriptase pericellular activity has been proposed (Oberst et al., 2003b; Oberst et al., 2005; Fan et al., 2007; Lee et al., 2007; Szabo et al., 2007; Tseng et al., 2010; Friis et al., 2011). HAI-1A and 1B isoforms are very similar, however, HAI-1B has an extra 16 amino acid insert between KD1 and LDLR domain of unknown significance (Kirchhofer et al., 2003). The inhibitory activity of the HAI-1 isoforms is mediated by Kunitz domains KD1 and KD2 (Denda et al., 2002; Kirchhofer et al., 2003; Fan et al., 2005; Kirchhofer et al., 2005; Kojima et al., 2008). These domains have an Arg and a Lys P1 residue, respectively, in a substrate-like binding loop on the surface of the domain (Denda et al., 2002; Kirchhofer et al., 2003) (Figure 3.2). As KLK14 has a preference for Arg P1 residues, KLK14 is a possible target for HAI-1 inhibition.

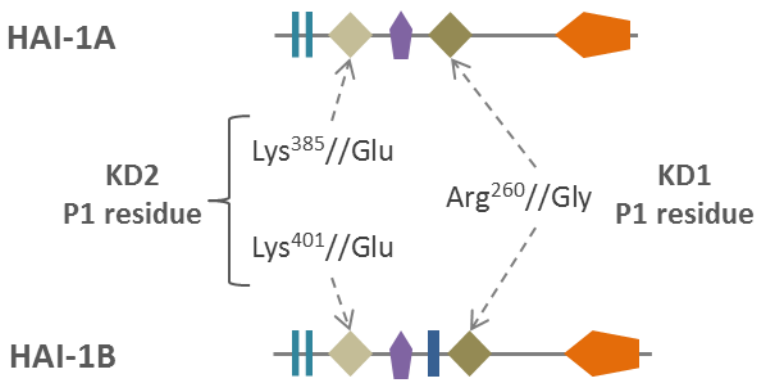

Figure 3.2 P1 residues of HAI-1A and HAI-1B. The P1 residues of HAI-1 isoforms Kunitz domains (KD)1 and KD2 are Arg and Lys, respectively. These P1 residues bind proteases in a substrate-like binding loop.

The aim of this chapter was to generate recombinant human KLK14 for use in *in vitro* assays in this and subsequent chapters. A number of expression systems are used for recombinant protein production including bacterial, yeast, insect and mammalian, each with advantages and disadvantages (Brondyk, 2009). The Sf9 insect cell expression system was chosen for its cost effective high capacity for secreted protein production as well as the ability to provide post-translational modifications including N-glycosylation (Altmann et al., 1999; Brondyk, 2009). This chapter describes the characterization of N-glycosylation status and enzymatic activity of the generated KLK14. It also describes the

examination of HGF as a potential KLK14 substrate and HAI-1 isoforms HAI-1A and 1B as inhibitors. Examination of recombinant KLK4 and hepsin activity were included in this study for comparison. Furthermore, in this chapter, the KLK14 protein sequence, including post-translational modification predictions, is reviewed. To further explore KLK14, a KLK14 structure homology model was also developed in this chapter.

3.2 Results

3.2.1 Characterization and review of the KLK14 amino acid sequence

The *KLK14* gene includes DNA sequence that encodes a protein of 267 amino acids. The complete KLK14 translated sequence is shown in Figure 3.3A and it is annotated with some pertinent features. KLK14 is comprised of an N-terminal signal peptide followed by a short, 6 residue, pro- sequence and then the catalytic domain spanning 227 residues (Hooper et al., 2001a; Yousef et al., 2001). KLK14 is directed to the secretory pathway by the signal peptide whereupon it is secreted into the extracellular space as a zymogen. To activate KLK14, the pro- region is removed by limited proteolysis between the Lys40 and Ile41 (Hooper et al., 2001a; Yousef et al., 2001).

The DNA sequence has three potential ATG translation start codons (Hooper et al., 2001a) that translate as residues Met1, Met17 and Met31 (see schema in Figure 3.3B). It has been considered that KLK14 translation begins from the second start codon (Met17) to yield a 251 amino acid product (Hooper et al., 2001a; Yousef et al., 2001). In this model, KLK14 has a signal peptide sequence of 18 amino acids which falls comfortably within the average range for eukaryotic signal peptides of 23 +/- 6 amino acids (Hiss and Schneider, 2009). However, longer (and shorter) signal peptides are possible (Hiss and Schneider, 2009). So, to analyse which of the three start codons yields a likely signal peptide, the signal peptide prediction software SignalP 4.0 Server (Petersen et al., 2011) and Phobius (Kall et al., 2004) were used to evaluate the KLK14 amino acid sequence starting at each of the three Met residues. SignalP 4.0 and Phobius predicted that the protein encoded by translation from the Met31 codon lacks a signal peptide and would be located intracellularly, however, to date there have been no reports of KLK14 localized intracellularly. In contrast, both analysis programs predicted that peptides beginning at either Met1 or Met17, and terminating at serine (Ser) 34, were

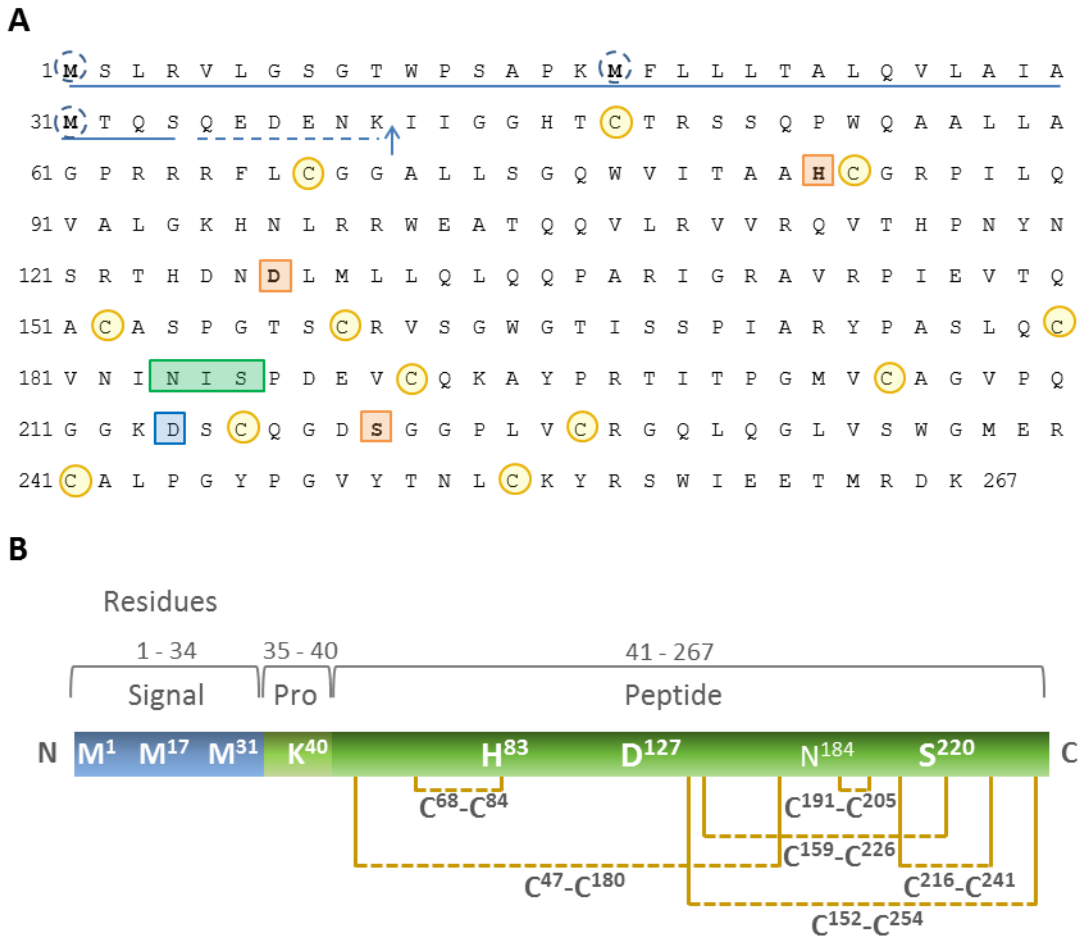

Figure 3.3 Features of the KLK14 protein. A. KLK14 complete protein sequence with residue numbering on left. The putative signal peptide, residues 1-34, is underlined, with the three methionine (M) residues circled (◌). The pro-peptide region, underlined, is residues 35-40 with the protease activation hydrolysis point between lysine (K) and isoleucine (I) indicated (↑). The mature protease is residues 41-267, with catalytic active-site residues histidine (H), aspartate (D) and serine (S) boxed ▢ and the D residue six residues before the catalytic S boxed ▢. Predicted disulphide paired cysteine (C) residues are circled ◯; and a N-glycosylation consensus sequence asparagine (N), isoleucine (I), serine (S) (N-X-S/T) is boxed ▢. **B.** Schematic of key features of full-length KLK14 including: the three M residues in the signal peptide; the pro-peptide activation point residue K; the predicted pairing of disulphide bonded cysteine residues; catalytic residues H, D and S; and potential N-glycosylation residue N.

signal peptides targeting the zymogen for secretion. Met1 and Met17 yield signal peptides of 34 and 18 residues, respectively. Indeed, several groups have used the truncated coding sequence of KLK14, beginning at the second start codon (Met17), to produce secreted recombinant KLK14 in mammalian and insect cell cultures (Brattsand et al., 2005; Borgono et al., 2007c; Rajapakse and Takahashi, 2007). However, as sequences beginning with both Met1 and Met17 produce recognized signal peptides, in

this project, the entire coding sequence beginning at the first ATG start codon (Met1) was used for all sub-cloning and subsequent protein expression of KLK14.

Hooper and colleagues (2001a) and Yousef and colleagues (2001) performed sequence alignments and comparisons of KLK14 with the other 14 members of the KLK family to show highly conserved regions within KLK14 that are potentially linked to functionality. The conserved serine protease catalytic triad residues are histidine (His) 83 (KLK14 numbering from the first Met residue), aspartate (Asp) 127 and serine (Ser) 220 (Figures 3.1).

Using nomenclature established by Schechter and Berger (1967), the active site of an enzyme is described as semi-discrete subsites (residues), designated S3-S2-S1-S1'-S2'-S3', into which the scissile bond of the substrate, P1-P1', is inserted. There is an Asp in position 214 in the S1 binding pocket of KLK14 (Figure 3.3A), six residues N-terminal to catalytic Ser220, which generally indicates a preference for arginine (Arg) or Lys residues in the substrate P1 position (Perona and Craik, 1997). This gives KLK14 an apparent trypsin-like as opposed to chymotrypsin-like specificity. Using recombinant KLK14, P1 specificity of KLK14 has been determined to be a trypsin-like specificity with preference for Arg over Lys over tyrosine (Tyr) (Brattsand et al., 2005; Felber et al., 2005; Oikonomopoulou et al., 2006a; Borgono et al., 2007a; Borgono et al., 2007c; Rajapakse and Takahashi, 2007; Stefansson et al., 2008; de Veer et al., 2011). One synthetic tri-peptide substrate for which KLK14 showed high catalytic efficiency consists of the sequence glutamine-alanine-arginine (Gln-Ala-Arg) (P3-P2-P1) with a fluorogenic leaving group, AMC (7-amino-4-methylcourmarin) (QAR-AMC) (Borgono et al., 2007c; Rajapakse and Takahashi, 2007). This substrate was used exclusively in this project to test the catalytic efficiency of the recombinant KLK14 produced in insect cells.

There are 6 predicted disulphide bonds between cysteine (Cys) residues Cys47-Cys180, Cys68-Cys84, Cys152-Cys254, Cys159-Cys226, Cys191-Cys205 and Cys216-Cys241 (Figure 3.3B) (Hooper et al., 2001a). In KLKs 4-7 the 6 disulphide bonds between these conserved cysteine residues have been confirmed in crystal structure analysis (Gomis-Ruth et al., 2002; Debela et al., 2006a; Debela et al., 2007a; Debela et al., 2007b). Interestingly, there is only one consensus N-glycosylation motif in KLK14. Residues asparagine (Asn) 184-Ile-Ser (Figure 3.3A) comply with the N-glycosylation motif, asparagine-any amino acid-threonine/serine (Asn-Xaa-Thr/Ser) (Marshall, 1967;

Neuberger and Marshall, 1968). However, analysis of the KLK14 sequence with NetNGlyc-1.0 Server (Gupta et al., 2004) predicts no N-glycosylation on KLK14 on Asn184. This analysis software uses sequence context to predict N-glycosylation of Asn-Xaa-Thr/Ser motifs. The N-glycosylation status of recombinant KLK14 produced in Sf9 insect cells and in transiently transfected Cos-7 (monkey kidney) cells was explored further in Section 3.2.3.

3.2.2 Generation and purification of recombinant KLK14

Recombinant KLK14 was required for enzymatic characterization of KLK14 and for *in vitro* assays in this chapter and subsequent chapters. For this purpose, the pIB/V5-His expression construct encoding full-length KLK14 with an in-frame carboxyl- (C-) terminus V5-HisX6 tag, pIB-KLK14-V5-His, was generated and then stably transfected into Sf9 insect cells. In this system, the endogenous KLK14 signal peptide directs the KLK14 zymogen to the secretory pathway. Preliminary experiments determined that highest yields of pro-KLK14-V5-His in the conditioned medium were obtained from Sf9 cells grown in suspension compared with cells grown adherently (data not shown). Consequently, the stably transfected insect cell lines were cultured shaking in suspension culture flasks and the conditioned medium harvested periodically for purification of pro-KLK14-V5-His.

Purification of pro-KLK14-V5-His was performed using Ni-NTA Superflow resin exploiting the affinity of the HisX6 tag for the immobilized nickel ions on the resin. Elution from the resin was achieved using competition affinity of imidazole for the nickel ions. The acidity of the Sf-900 II media (~pH 6) and the presence of electron donating groups in the media can interfere with the affinity binding of the His×6 tag to the Ni-NTA resin (QIAGEN, 2003). In addition, high quantities of amino acids such as glycine, glutamine and histidine can compete for binding sites on the Ni-NTA resin (QIAGEN, 2003). Consequently, the Sf9-conditioned medium was prepared for pro-KLK14-V5-His purification by dialysis to adjust the pH and also to remove low molecular weight binding competitors.

To determine the purity of the eluted fractions, aliquots of conditioned media as well as the flow through from the Ni-NTA resin were run on SDS-PAGE gels with aliquots of the wash steps and elution fractions. Known quantities of BSA were also run on each

gel to allow for approximations of the quantity of pro-KLK14-V5-His in each elution. The images in Figure 3.4 are representative Coomassie stained gels from one batch of purified pro-KLK14-V5-His. The purity of pro-KLK14-V5-His was estimated to be ~85-95%. The expected molecular weight of endogenous pro-KLK14 is ~25.6 kDa. When produced from the pIB/V5-His vector, additional amino acids encoded by the residual nucleotides from the cloning site of the vector, as well as the V5-His tag, add to the molecular weight and ~27-8 kDa would be expected. However, using a recombinant protein molecular weight marker, Precision Plus Protein Dual Color Standard (Bio-Rad), for comparison, the weight of pro-KLK14-V5-His was ~29 kDa.

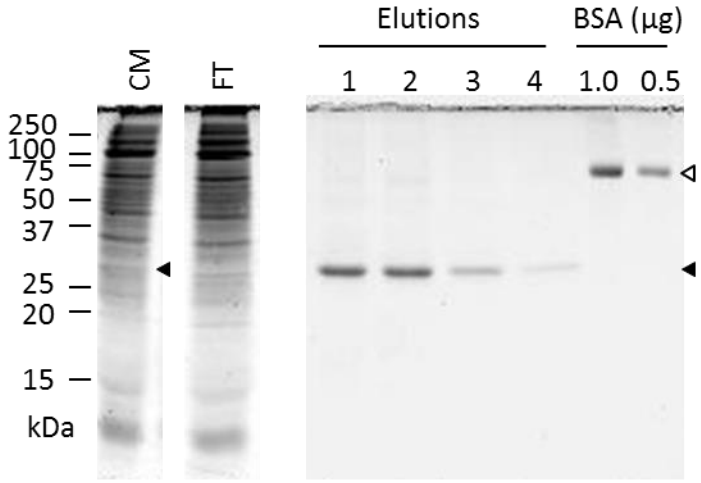

Figure 3.4 Generation and purification of recombinant KLK14 from Sf9 cell conditioned medium. Coomassie stained SDS-PAGE gels of conditioned medium (CM) and flow-through (FT) (30µL) from the Ni-NTA agarose; and pro-KLK14V5-His elutions 1 – 4 (30 µL) from the Ni-NTA agarose with BSA as loading controls. *Solid arrowhead* indicates pro-KLK14-V5-His, *open arrowhead* indicates BSA.

3.2.3 N-glycosylation status of KLK14

It has been reported previously that recombinant KLK14 generated in yeast, *Pichia pastoris,* and mammalian cells, HEK293, is not N-glycosylated (Borgono et al., 2003; Borgono et al., 2007c). Furthermore, as noted in Section 3.2.1, KLK14 has a consensus N-glycosylation sequon, Asn184-Ile-Ser, that is predicted by the NetNGlyc-1.0 Server to not be N-glycosylated on the Asn. To determine if recombinant pro-KLK14-V5-His generated in stably transfected Sf9 insect cells holds with these predictions, purified pro-KLK14-V5-His was treated with the amidase PNGase F which removes N-linked glycans. KLK14 generated in transiently transfected Cos-7 cells was also examined.

KLK4 was chosen as a positive control as it has previously been shown to be glycosylated when produced in Sf9 stable and transiently transfected HeLa (Ramsay, 2008) and PC-3 cells (Dong et al., 2005). Moreover, the predictions made by the NetNGlyc-1.0 Server support the presence of an N-glycosylation on the Asn of the Asn169-Val-Ser sequon in KLK4 (KLK4 numbering).

As shown in Figure 3.5, PNGase F treatment resulted in a decrease in molecular weight of ~2 kDa for pro-KLK14-V5-His from Sf9 cells. Consistent with results obtained previously (Ramsay, 2008), PNGase F treatment of pro-KLK4-V5-His from Sf9 cells also resulted in a ~2 kDa molecular weight decrease in the upper band of the pro-KLK4-V5-His doublet. In contrast, PNGase F treatment had no effect on KLK14-Myc or KLK4-V5-His transiently expressed by monkey kidney Cos-7 cells.

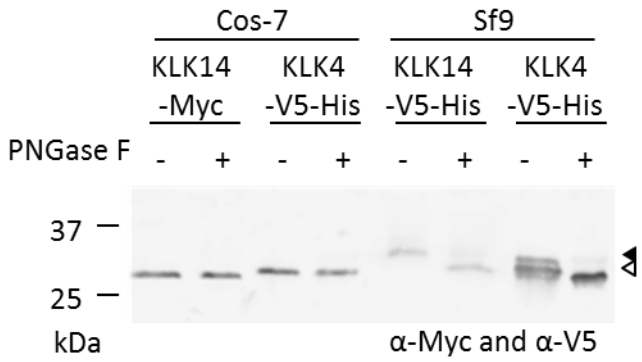

Figure 3.5 Recombinant KLK14 is N-glycosylated when generated in Sf9 cells. Western blot analysis of conditioned media from Cos-7 cells transiently expressing KLK14-Myc or KLK4-V5-His and purified recombinant pro-KLK14-V5-His or pro-KLK4-V5-His either untreated (-) or treated (+) with PNGase F. *Solid arrowhead* indicates glycosylated (~29 kDa) and *open arrowhead* indicates de-N-glycosylated (~27 kDa) pro-KLK14-V5-His from Sf9 cells.

As the result for pro-KLK14-V5-His was inconsistent with the NetNGlyc-1.0 Server predictions and with recombinant KLK14 produced from yeast *Pichia pastoris* and HEK293 cells (Borgono et al., 2003; Borgono et al., 2007c), two approaches were taken to analyse the position of the N-glycosylation consensus sequon, Asn184-Ile-Ser, relative to the protein structure. First, the NetSurfP-1.0 (Petersen et al., 2009) software, which predicts solvent accessibility and secondary structure, was applied to the KLK14 sequence. This analysis indicated that Asn184 has probable exposure on the surface of the protein (data not shown) with the remaining residues of the sequon as well as the

residue immediately prior, Ile183, predicted to be buried beneath the surface of the protein structure.

The second approach was to develop and analyse a homology model of KLK14 using protein homology modelling software SWISS-MODEL and DeepView-4.1 Swiss PDB Viewer (Guex and Peitsch, 1997; Schwede et al., 2003; Arnold et al., 2006). A template for the KLK14 homology model was selected from the KLK family members as they have a high degree of sequence similarity. While KLK14 has high overall homology to KLK6, KLK8 and KLK13 (45, 44 and 43% respectively), across active sites there is greater homology (50%) between KLK14 and KLK5 (Goettig et al., 2010; Swedberg et al., 2010; de Veer et al., 2011). Based on this, a homology model of KLK14 was generated using the crystal structure of KLK5 (PBD ID 2PSX) (Debela et al., 2007a) as a template.

The generated model predicts that the potential N-glycosylation site, Asn184(-Ile-Ser), is located on the opposite side to the active site cleft, His83, Asp127 and Ser220 (Figure 3.6A and B). Furthermore, the Asn184 residue is exposed on the surface, consistent with the NetSurfP-1.0 prediction. Alignment of the KLK14 and KLK5 sequence (Figure 3.6C) shows that the confirmed KLK5 N-glycosylation sequon (Debela et al., 2007a) is located at Asn182-Ile-Ser (KLK14 numbering). This sequon also conserved across KLK4, KLK9, KLK11, KLK12, and KLK15 (Lundwall and Brattsand, 2008), and is predicted to be the N-glycosylation site of KLK4 (Ramsay, 2008). Interestingly, in KLK14 this position is taken by an N-glycosylation acceptor residue, Asn182. However, the sequon at this position (Asn182-Ile-Asn) does not conform with consensus N-glycosylation sequons of Asn-Xaa-Ser/Thr (Marshall, 1967; Neuberger and Marshall, 1968).

3.2.4 Activation of recombinant KLK14 with thermolysin

It has previously been shown that the secreted zymogen pro-KLK14 does not self-activate (Brattsand et al., 2005; Borgono et al., 2007c; Yoon et al., 2007). Therefore, once purified from the Sf9-conditioned medium the pro-KLK14-V5-His requires further processing by proteolytic removal of the pro-region to obtain active or mature KLK14.

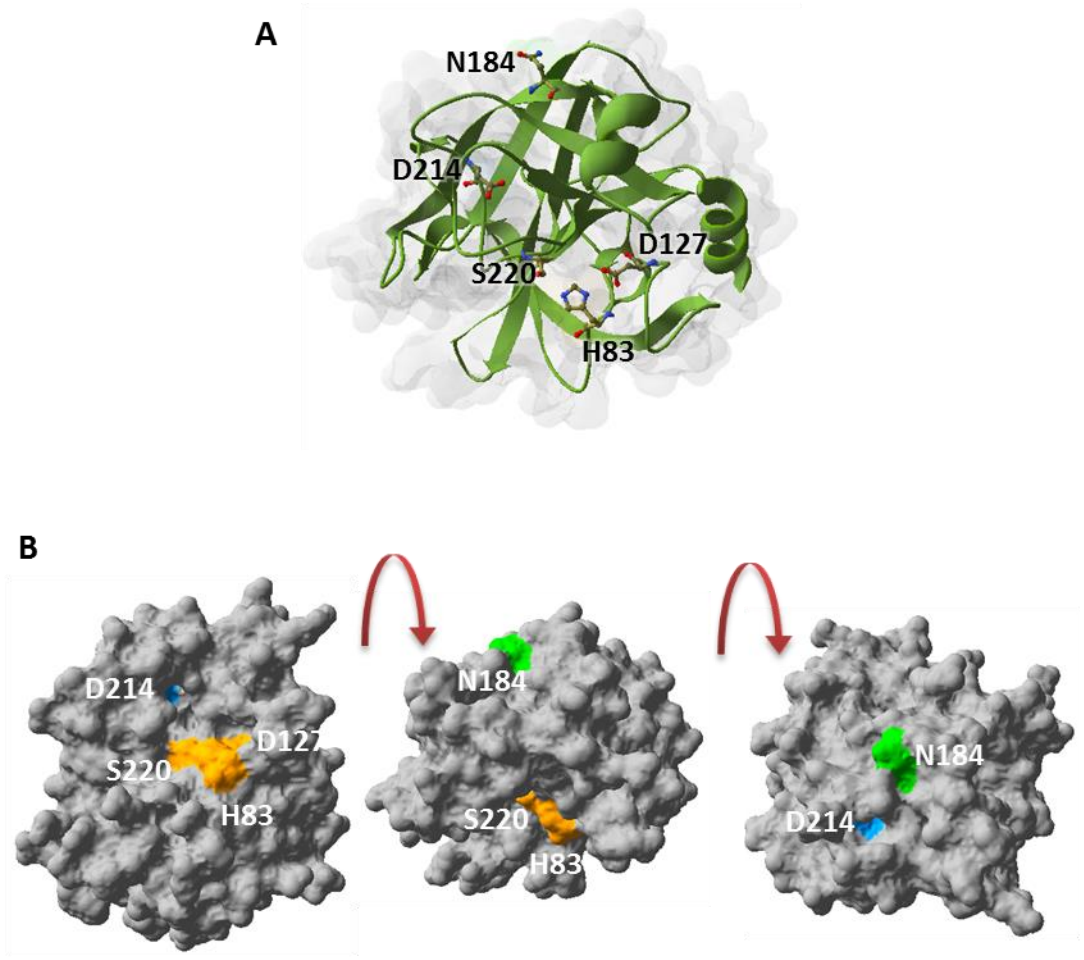

C

```
      41
KLK5   IINGSDCDMHTQPWQAALLLRPN-QLYCGAVLVHPQWLLTAAHCRKKVFRVRLGHYSLSP
KLK14  IIGGHTCTRSSQPWQAALLAGPRRRFLCGGALLSGQWVITAAHCGRPILQVALGKHNLR-
       ** *  *   :******** *. :: **..*:  **::***** : :::* **::.*
     100
KLK5   VYESGQQMFQGVKSIPHPGYSHPGHSNDLMLIKLNRRIRPTKDVRPINVSSHCPSAGTKC
KLK14  RWEATQQVLRVVRQVTHPNYNSRTHDNDLMLLQLQQPARIGRAVRPIEVTQACASPGTSC
        :*: **::: *:.: ** *.   *.*****::*::  *  : ****:*:. * * **.*
     160
KLK5   LVSGWGTTKSPQVHFPKVLQCLNISVLSQKRCEDAYPRQIDDTMFCAGDK-AGRDSCQGD
KLK14  RVSGWGTISSPIARYPASLQCVNINISPDEVCQKAYPRTITPGMVCAGVPQGGKDSCQGD
        ****** .** .::*  ***:**.:  :: *:.**** *   *.***   .*:******
     220
KLK5   SGGPVVCNGSLQGLVSWGDYPCARPNRPGVYTNLCKFTKWIQETIQANS
KLK14  SGGPLVCRGQLQGLVSWGMERCALPGYPGVYTNLCKYRSWIEETMRDK-
       ****:**.*.********   ** *  *********: .**:**:: :
```

Figure 3.6

Other studies have used the protease domain of transmembrane serine protease enteropeptidase (Brattsand et al., 2005) or serine protease lysyl endopeptidase conjugated to Cyanogen Bromide-activated sepharose (CNBr-seph) (Rajapakse and Takahashi, 2007) to activate pro-KLK14. However, after initial experiments (data not shown), metalloproteinase thermolysin was chosen for pro-KLK14-V5-His activation in this laboratory (de Veer et al., 2011; Sanchez et al., 2012) over enteropeptidase and lysyl endopeptidase. This was because enteropeptidase and lysyl endopeptidase are serine proteases, like KLK14, therefore, overlapping substrate specificity could confound downstream assay results. Also, inhibition of residual enteropeptidase or lysyl endopeptidase activity using serine protease inhibitors would inhibit KLK14 as well. To overcome this, conjugating the enteropeptidase or lysyl endopeptidase to CNBr-seph to minimize residual activity was considered. However, conjugating lysyl endopeptidase to CNBr-seph proved to be an expensive and lengthy process. This was because a large excess of the protease was required to achieve optimal coverage of the CNBr-seph. In addition, the conjugation procedure had multiple extended incubations, and the storage temperature of the CNBr-seph was 2-8°C. As these conditions are not optimal for the viability of the lysyl endopeptidase it would need to be prepared anew each time KLK14 required activation. Thermolysin on the other hand is relatively inexpensive; it could be used in small quantities that required little forward preparation, it retained proteolytic activity for long periods of time when stored appropriately; and it could be inhibited by the relatively inexpensive metalloproteinase inhibitors phosphoramidon (Kitagishi and Hiromi, 1984) or EDTA (Morihara and Tsuzuki, 1966).

Figure 3.6 KLK14 homology model. A homology model of KLK14 based on the crystal structure of active KLK5 (PDB ID 2PSX) was generated using SWISS-MODEL. **A.** KLK14 homology model shown as a ribbon plot, features indicated, shown as stick models, include the catalytic active-site residues histadine (H83), aspartate (D127) and serine (S220); the S1 residue aspartate (D214); and potential N-glycosylation residue asparagine (N184). **B**. Incrementally rotated view of the molecular surface of the KLK14 homology models indicating the relative positions of the active site (orange), and the S1 residue pocket (blue), and the N-glycosylation residue (green) on the opposite side to the active site cleft. The structural orientation of the image in (**A**) and the middle image in (**B**) are identical. **C**. Sequence alignment of KLK5 and KLK14 with KLK14 amino acid numbering. The active site residues (orange shading), the S1 residue pocket (blue) and the N-glycosylation sequon (green) are indicated. Identical residues are indicated with an asterisk (*), and conserved substitutions as a colon (:) for strongly similar residues, or a period (.) for weakly similar residues.

It was necessary to determine the optimal ratio of pro-KLK14-V5-His to thermolysin to achieve the highest conversion to active KLK14. This was performed by quantifying at the molar level the conversion of pro- to active KLK14. To begin, various ratios of pro-KLK14-V5-His to thermolysin were incubated for between 1 and 2 hours. Longer incubations were not used because active KLK14 auto-degrades in extended incubations (Borgono et al., 2007c). The concentration of active KLK14 was then determined by active-site titration using the suicide pseudo-substrate MUGB (Jameson et al., 1973). The MUGB ester is non-fluorogenic; however when an active trypsin-like serine protease molecule such as KLK14 hydrolyses MUGB, there is a rapid acylation step and release of 4-MU, which fluoresces at 460 nm when excited at 355 nm (Figure 3.7A). The protease effectively becomes trapped in the acylation step as an acyl-enzyme with p-

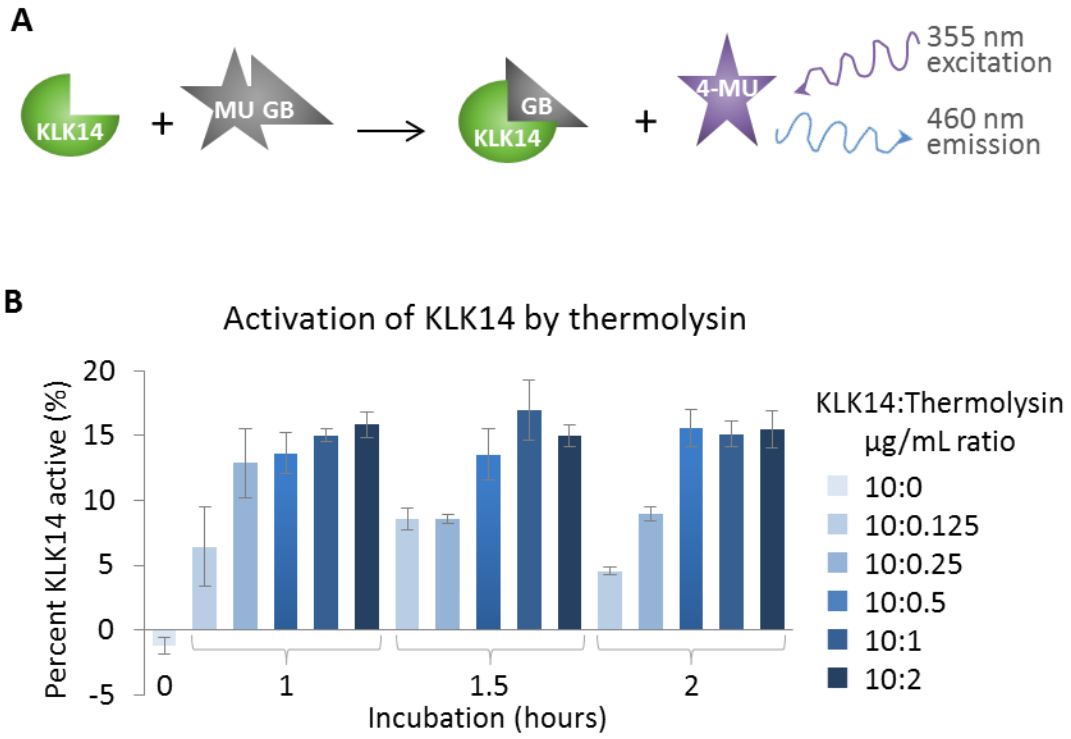

Figure 3.7 Activation of recombinant KLK14 with thermolysin. A. Schematic representing the hydrolysis of 4-methylumbelliferyl 4-guanidinobenzoate (MUGB) by active protease which results in the stoichiometric 1:1 release of the fluorescent 4-methylumbelliferone (4-MU) for every active protease molecule. Release of 4-MU can be measured using a fluorescent plate reader by excitation at 355 nm and emission at 460 nm. **B.** Pro-KLK14-V5-His was incubated with thermolysin at varying ratios (µg/mL) for 1, 1.5 and 2 hours at 37°C. Reactions were stopped with phosphoramidon (400 µM) and then the proportion of active KLK14 was determined by MUGB assay. Data are averages of triplicate experiments ± SEM.

guanidinobenzoyl as deacylation is extremely slow (Jameson et al., 1973; Urano et al., 1988; Payne et al., 1996; Toth et al., 2006). Therefore the release of 4-MU is in a 1:1 stoichiometric ratio to active protease and the concentration of active protease can be determined using a standard curve prepared using known concentrations of 4-MU.

In Figure 3.7B, it can be seen that highest levels of conversion (17%) to active KLK14 were achieved using a 10:1 μg/mL ratio (13.8:1 molar ratio) of pro-KLK14-V5-His to thermolysin, with a 1.5 hour incubation. This was the condition used for future activation of pro-KLK14-V5-His.

Conversion of pro-KLK14-V5-His to active KLK14 was then examined by Coomassie Blue R-250 stained SDS-PAGE gel and Western blot analyses probed with anti-V5 and anti-KLK14 antibodies (Figure 3.8A). Conversion of pro-KLK14-V5-His (29 kDa) to mature KLK14 is apparent as a 4 kDa reduction in molecular weight. Mature KLK14 is represented by a ~25 kDa band that can be seen on the Coomassie stained gel and the anti-KLK14 probed Western blot in the lanes representing thermolysin treatment (+).

The low level of conversion of pro-KLK14-V5-His to active KLK14 seen previously in the MUGB assay (Figure 3.7) is reflected in the Coomassie stained gel. This low level of conversion to mature/active KLK14 may be due to fragmentation and inactivation by cleavage at other points by thermolysin. The potential for thermolysin cleavage at sites other than the pro-site is exemplified in the anti-V5 Western blot analysis. In this it can be seen that treatment of pro-KLK14-V5-His with thermolysin also appears to remove part or all the V5-His tag as no forms of KLK14 were detected with the anti-V5 antibody. It is also interesting to note that KLK14 untreated by thermolysin is detected as a doublet on the Coomassie and also the anti-KLK14 Western blot analysis. The lower band of the KLK14 doublet is not visible on the anti-V5 probed Western blot and is likely pro-KLK14 which has lost the V5-His tag during the generation or purification of the enzyme. Figure 3.8B illustrates the various forms of KLK14.

3.2.5 N-terminal sequencing of zymogen KLK14 and thermolysin activated KLK14

N-terminal sequencing was used to confirm that the activation with thermolysin produced the expected mature KLK14 N-terminal. For sequencing, 2 picomoles or more of protein per sample was required by University of Queensland (UQ), School of

Chemistry and Molecular Biosciences (SCMB) sequencing facility and also the Australian Proteome Analysis Facility (APAF). Figure 3.9 shows an image of a Coomassie stained PVDF membrane blot of 10 µg (~330 picomoles) of thermolysin-activated pro-KLK14-V5-His and 1.5 µg of pro-KLK14-V5-His (~5 picomoles) resolved by SDS-PAGE. Bands of approximately 29 kDa for the pro- and 25 kDa for the active KLK14 were excised and sent for N-terminal sequencing at the UQ SCMB and APAF.

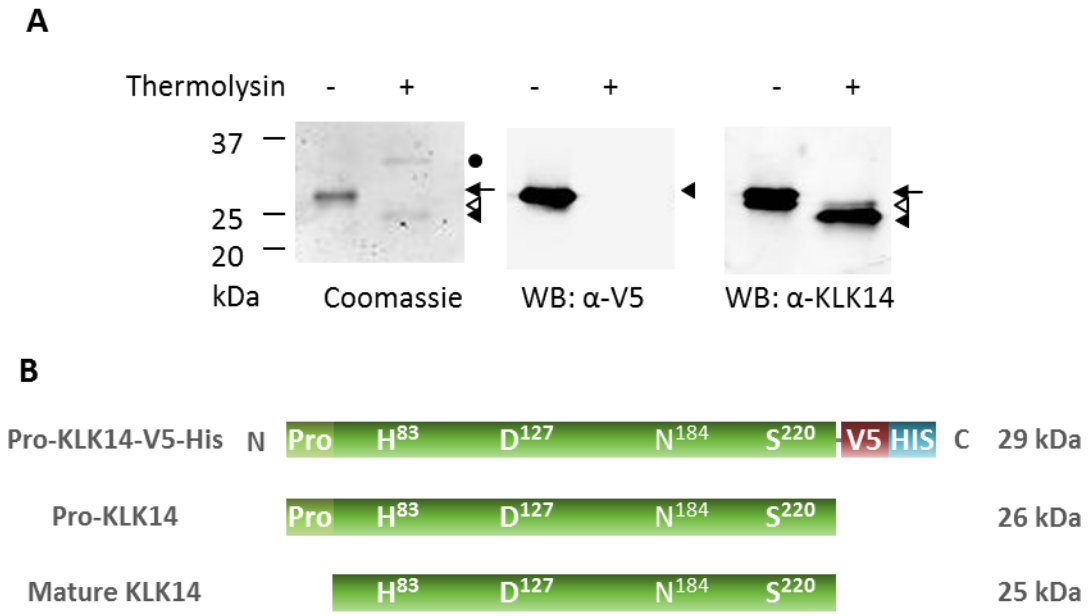

Figure 3.8 Coomassie and Western blot analyses of thermolysin-activated recombinant KLK14. A. Pro-KLK14-V5-His was incubated with thermolysin (10:1 µg/mL) for 1 hour at 37°C and then resolved by SDS-PAGE under reducing conditions. Gels were stained with Coomassie or subjected to Western blot analysis using either an anti-V5 or anti-Kallikrein 14 antibody (Abcam ab28841). Pro-KLK14-V5-His is represented by bands at 29 kDa (*solid arrow*), pro-KLK14 at 26 kDa (*open arrowhead*) and mature KLK14 at 25 kDa (*solid arrowhead*). Thermolysin is visible on the Coomassie stained gel at 36 kDa (*solid circle*). **B.** Schematics of the secreted KLK14 zymogen produced in the pIB vector, pro-KLK14-V5-His, and thermolysin-generated pro-KLK14 and mature KLK14. Key features indicated include the catalytic residues histadine (H^{83}), aspartate (D^{127}) and serine (S^{220}); and potential N-glycosylation residue asparagine (N^{184}).

An initial report from the UQ SCMB sequencing facility suggested that a clear sequencing result could not be obtained due to either insufficient sample material or that the sequences were N-terminally blocked. However, due to the clear Coomassie staining of the bands on the PVDF membrane, the report further concluded that

insufficient protein was unlikely to be the cause of the sequencing failure. Before making further sequencing sample submissions, the techniques used to prepare the samples were refined based on the premise that the protein samples were N-terminally blocked. Using recommendations from the UQ SCMB sequencing facility manager Chris Wood and also publications (Hunkapiller et al., 1983; Walsh et al., 1988; Smith, 1997) on the subject of the N-terminal sequencing technique, refinements included adding thioglycolic acid to the buffer of the inner chamber of the SDS-PAGE running rig; pre-running the gel without sample for 15 minutes; preparing fresh Coomassie Blue R-250 solution for each staining; and preparing the Coomassie solution without acetic acid. Unfortunately, subsequent sequencing submissions to UQ SCMB and APAF sequencing facilities were unable to produce clear sequencing results for either the pro-KLK14-V5-His or thermolysin-activated KLK14. There is potential for trialling alternative sequencing methods in future work.

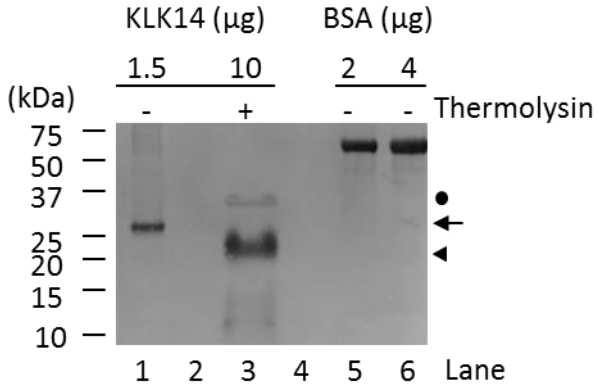

Figure 3.9 Samples used for N-terminal sequencing of zymogen KLK14 and activated KLK14. Coomassie stained PVDF membrane of pro-KLK14-V5-His untreated (-) and treated (+) with thermolysin at a 10:1 µg/mL ratio of pro-KLK14 to thermolysin for 1 hour at 37°C . Samples were subjected to reducing SDS-PAGE before transfer onto PVDF. Bands of ~29 kDa for pro-KLK14-V5-His (lane 1) and ~25 kDa for activated KLK14 (lane 3) were cut out of the PVDF and submitted for 5 residue Edman degradation N-terminal sequencing. BSA was run in lanes 5 and 6 as loading controls. S*olid arrow*, pro-KLK14-V5-His; *solid arrowhead*, mature KLK14; *solid circle*, thermolysin.

3.2.6 Kinetic measurements of thermolysin activated KLK14

The kinetic activity of thermolysin-activated KLK14 was assessed using the synthetic tripeptide substrate QAR-AMC as KLK14 has a high affinity for this substrate

(Borgono et al., 2007c; Rajapakse and Takahashi, 2007). The assay relies on hydrolysis of the bond between the P1 residue and the AMC leaving group of the synthetic substrate, QAR-AMC (Figure 3.10). From this kinetic assay, a measure of the catalytic efficiency, or how well KLK14 hydrolyses its substrate, was determined. For comparison activated KLK4 and bovine trypsin were also assayed alongside KLK14 under the same conditions.

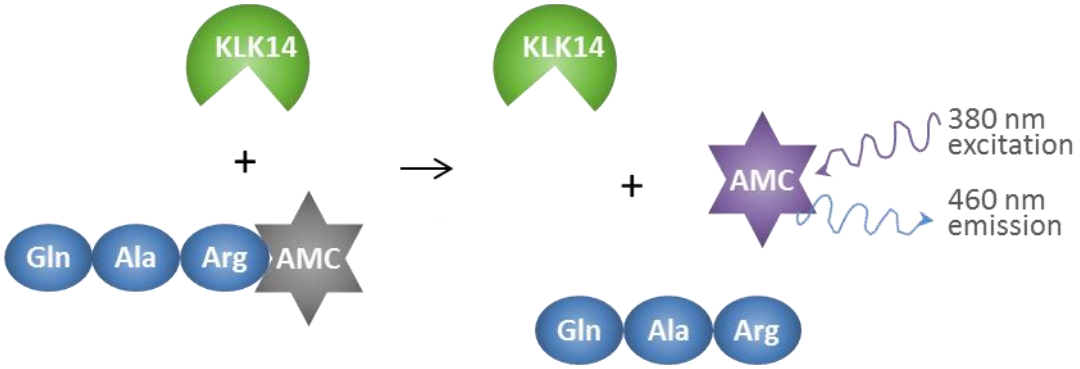

Figure 3.10 Hydrolysis of tripeptide substrate QAR-AMC by KLK14. A. Schematic representing the hydrolysis of the tripeptide substrate Boc-Gln-Ala-Arg-7-amido-4-methylcoumarin hydrochloride (QAR-AMC) by active KLK14 (or other protease) which results in release of the fluorescent 7-amino-4-methylcoumarin (AMC). Release of AMC can be measured using a fluorescent plate reader by excitation at 380 nm and emission at 460 nm.

The rate of hydrolysis was obtained by measuring the increase of AMC over a defined time period. As a single-substrate reaction, by analysing an increasing range of substrate concentrations applied to a fixed protease concentration, the initial rates of hydrolysis were used in a Michaelis-Menten kinetic model of protease–substrate reaction (Mathews et al., 2000). The two main parameters derived from this model were K_M, which is the substrate concentration ([S]) at which reaction velocity is half maximal; and V_{max}, the maximal velocity (Mathews et al., 2000). The K_M is indicative of the substrate concentration required for maximum reaction velocity; a small K_M indicates that a small amount of substrate is required to saturate the protease (Mathews et al., 2000). Using the protease concentration and V_{max}, the substrate per molecule protease turnover rate, k_{cat}, was derived and subsequently, the ratio k_{cat}/ K_M, as a measure of catalytic efficiency (Mathews et al., 2000). Direct comparison of catalytic efficiency between KLK14, KLK4 and trypsin cannot be made as the ratio k_{cat}/ K_M depends on the ratio [S]/ K_M (Eisenthal et al., 2007). This means that unless the K_M of the enzymes is equal the catalytic efficiency cannot be compared (Eisenthal et al., 2007). With this in mind, it can

be seen from the results presented in Table 3.1 that KLK14 has a high K_M of 258 μM suggesting a lower affinity for the substrate than either KLK4 or trypsin. The substrate turnover rate, k_{cat}, for KLK14 is higher than that of KLK4 which ultimately yields a higher catalytic efficiency, a k_{cat}/K_M of 4.66×10^4 $M^{-1}s^{-1}$, for KLK14 under the conditions tested. Trypsin had the lowest K_M and highest k_{cat} and as a result, the highest catalytic efficiency for the substrate QAR-AMC.

Table 3.1 Kinetic parameters for protease hydrolysis of the tri-peptide substrate QAR-AMC. Substrate at concentrations ranging 0.001 to 1 mM were incubated with KLK14, KLK4 and trypsin at 37°C. Initial rates of hydrolysis of QAR-AMC were determined by measuring free AMC at 1 min intervals for 20 min. A standard curve constructed using known concentrations of AMC was used to calculate the rate of release of free AMC. The Michaelis-Menten enzyme kinetics model was used to calculate the *kcat/Km* constants using non-linear regression and GraphPad Prism 5 software. Data are averages of triplicate experiments ± SEM.

Protease	Concentration (nM)	K_M (μM)	V_{max} (μM s^{-1})	k_{cat} (s^{-1})	k_{cat}/K_M (M^{-1} s^{-1})
KLK14	12	258± 11	0.145	12.05	4.66×10^4
KLK4	12	124± 4	0.017	1.4	1.12×10^4
Trypsin	0.4	38± 4	0.045	114.75	3.04×10^6

3.2.7 Concentration-dependent activation of HGF by KLK14

To examine KLK14 activation of pro-HGF, increasing concentrations of active recombinant KLK14 were incubated with recombinant pro-HGF. KLK4 and hepsin were assayed concurrently as KLK4 degrades rather than activates HGF (Mukai et al., 2008), and hepsin is an efficient HGF activator (Herter et al., 2005; Kirchhofer et al., 2005; Owen et al., 2010). Reaction mixtures were resolved by SDS-PAGE under reducing conditions then transferred onto nitrocellulose membrane and stained using Coomassie Blue R-250. As shown in Figure 3.11A, KLK14 converts pro-HGF to the two chain form in a concentration-dependent manner. Pro-HGF (1 μM) is completely converted to the 2 chain form at between 1 and 5 nM KLK14 (molar ratios of 1000:1 and 200:1). However, at concentrations of KLK14 between 10 to 100 nM (molar ratios 100:1 to 10:1), the HGF α-chain is completely degraded while the β-chain remains largely intact. In contrast, KLK4 demonstrates little activity toward pro-HGF (Figure

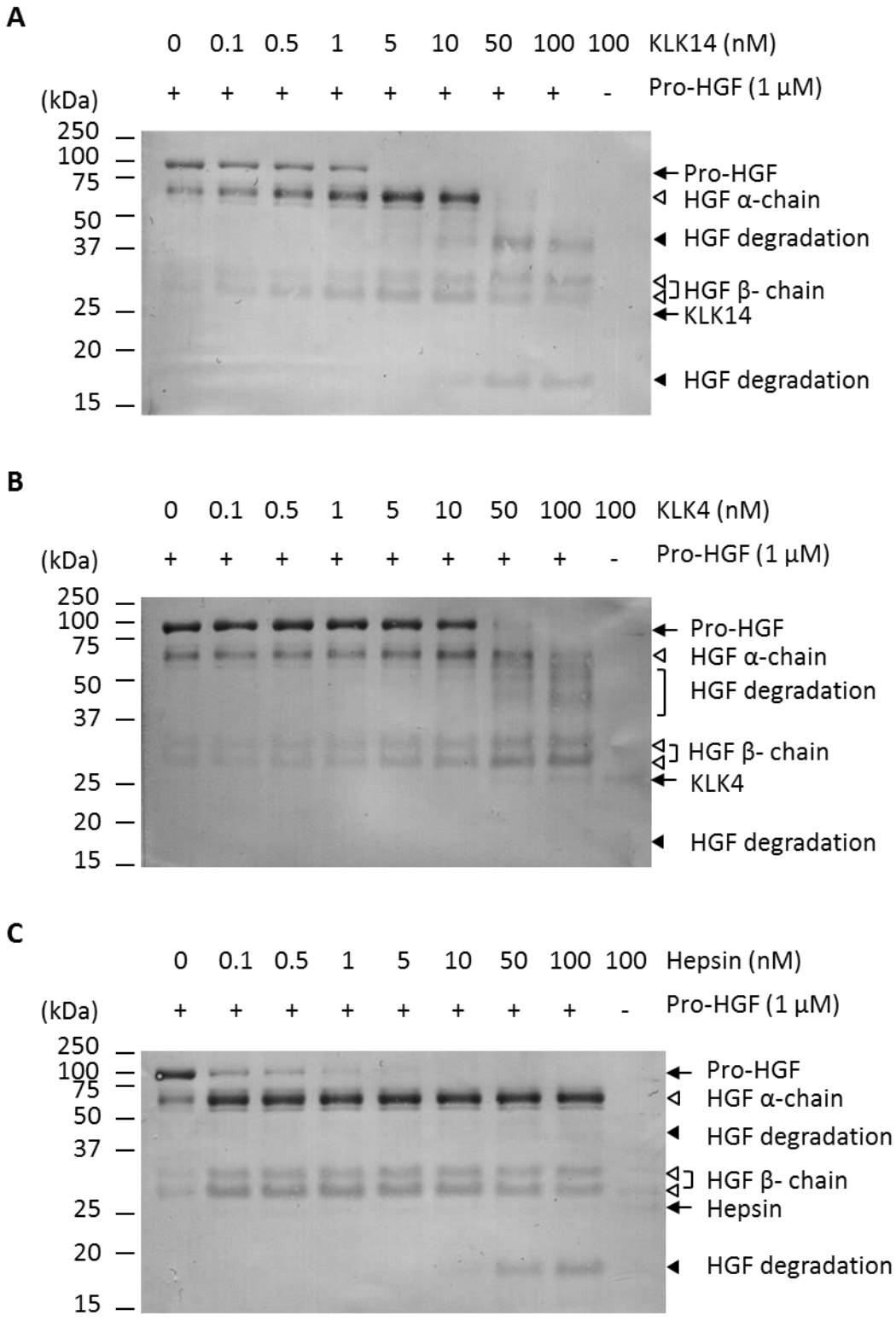

Figure 3.11 Activation of recombinant pro-HGF. Recombinant KLK14 (**A**), KLK4 (**B**) and hepsin (**C**) (0 – 100 nM) were co-incubated with recombinant pro-HGF (1 µM) for 4 hours at 37°C. Reactions stopped with reducing SDS-PAGE loading buffer were subjected to SDS-PAGE and analysis using Coomassie R250.

3.11B) until between 10 to 100 nM KLK4, whereupon it proceeds to degrade the HGF α-chain. As expected, hepsin demonstrates efficient concentration-dependent conversion of pro-HGF to the two chain form (Figure 3.11C). At concentrations of hepsin as low as 0.1 nM (molar ratio of 10,000:1), there is near complete conversion of pro-HGF. Furthermore, at high concentrations of hepsin there is very little degradation of the HGF α-chain. These data show that KLK14 activates HGF in a defined HGF:KLK14 'window' after which HGF degradation becomes evident.

3.2.8 Examination of KLK14 inhibition by HAI-1A and 1B

To examine KLK14 inhibition by HAI-1A and HAI-1B, activated recombinant KLK14 was pre-incubated with recombinant soluble HAI-1A or 1B (HAI-1 isoforms minus the transmembrane region). Synthetic substrate QAR-AMC was added and measurement taken of the hydrolysis of the substrate relative to the hydrolysis by uninhibited protease.

As shown in Figure 3.12, at equimolar concentrations of HAI-1A or 1B and KLK14 (5 nM), there is no inhibition of KLK14. As the ratio shifts to excess HAI-1 (25, 50 nM), KLK14 is mildly inhibited. At 50 nM inhibitor, KLK14 activity is inhibited by 35% and 26% for HAI-1A and 1B treatment, respectively. Due to the small amount of HAI-1 isoforms available to use in these experiments, a full inhibition curve to determine the inhibitor concentration at which KLK14 was inbibited by 50% (IC50) was not performed.

3.2.9 KLK14 interaction with HAI-1A and HAI-1B

To further explore whether KLK14 proteolysis is impacted by HAI-1, the ability of the protease to form stable complexes with the inhibitor was examined. For comparison KLK14 and hepsin interactions with HAI-1 were also examined as HAI-1 isoforms have previously been reported as *in vitro* inhibitors of hepsin (Herter et al., 2005; Kirchhofer et al., 2005); however, it was not shown in these publications whether hepsin and HAI-1 form stable complexes. Recombinant soluble hepsin (hepsin minus the cytoplasmic domain and transmembrane region) was used in the following assays and appears at 30 kDa on Western blot analyses under reducing conditions.

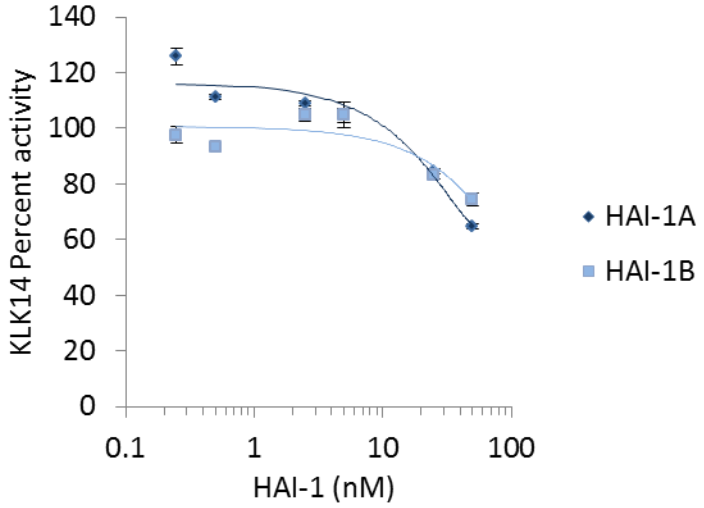

Figure 3.12 HAI-1A and HAI-1B inhibition of KLK14 hydrolysis of tri-peptide substrate QAR-AMC. Inhibitor concentrations ranging from 0 to 50 nM were pre-incubated with 5 nM KLK14 for 30 minutes at 37 °C. Substrate QAR-AMC (200 μM) was added and initial rates of hydrolysis were determined by measuring free AMC (using excitation and emission wavelengths 380 and 460 nM, respectively) at 1 minute intervals for 20 minutes. A standard curve constructed using known concentrations of AMC was used to calculate the rate of release of free AMC. The rate of hydrolysis of QAR-AMC by uninhibited KLK14 is set as 100 % activity and the rate of HAI-1A and HAI-1B inhibited KLK14 as a per cent thereof. Data are averages of triplicate experiments ± SEM.

First, active KLK14 was incubated with decreasing amounts of HAI-1A and 1B starting with HAI-1 isoforms at 10 times the molar concentration of KLK14. The samples were subjected to reducing SDS-PAGE then transferred onto PVDF and stained with Coomassie Blue R-250. HAI-1A and 1B run at approximately 55 kDa as can be seen in Figure 3.13. KLK14 was detected at ~25 kDa as expected for mature KLK14. An SDS and reducing agent-stable complex between HAI-1 isoforms and KLK14 would be expected at around 80 kDa with concomitant reduced signal intensity for HAI-1 isoforms detected at 55 kDa and KLK14 at 25 kDa. Instead, the quantity of KLK14 appears unchanged at 25 kDa and an extra band does not appear around 80 kDa. In addition, HAI-1A and 1B appear to be degraded in the presence of KLK14 with the appearance of several lower MW bands, most notably around 40, 35, 22 and 15 kDa, clearly seen in lanes 3 and 4 of both membranes. In lanes 5 and 6 HAI-1 at 55 kDa is almost undetectable; however, several lower MW degradation bands are still visible.

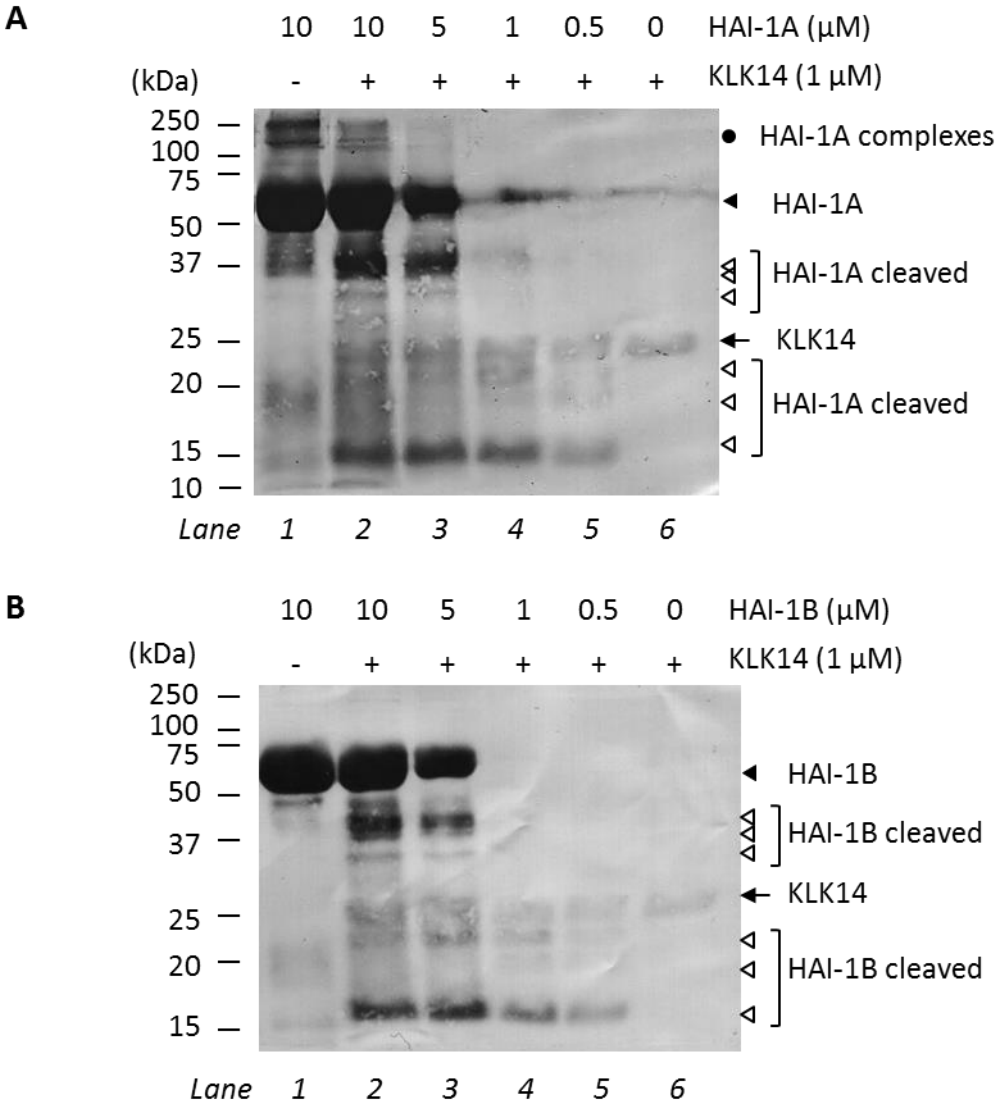

Figure 3.13 KLK14 degrades HAI-1A and 1B. Varying molar ratios of recombinant HAI-1A (**A**) and HAI-1B (**B**) were incubated with active KLK14, as indicated, for 30 minutes at 37 °C. Reactions stopped with reducing SDS-PAGE loading buffer were subjected to electrophoresis, transferred to PVDF membrane and stained with Coomassie R-250. *Solid arrowheads*, full length HAI-1A (**A**) and HAI-1B (**B**); *solid arrows*, KLK14; *open arrowheads*, degradation fragments of HAI-1A (**A**) and 1B (**B**); *solid circle* HAI-1A complexes independent of KLK14 (**A**).

Next, to compare the interactions between KLK14 and hepsin with HAI-1A and HAI-1B, fixed concentrations of active KLK14 and hepsin were incubated with decreasing concentrations of HAI-1A and HAI-1B (Figure 3.14). The starting concentration of HAI-1 (1 μM) was less than in Figure 3.13 (10 μM). This was done to show that this quantity (~2.3 μg) of HAI-1 is still visible on the membrane when unchallenged by KLK14. Consistent with data from the results shown in Figure 3.13, KLK14 degrades

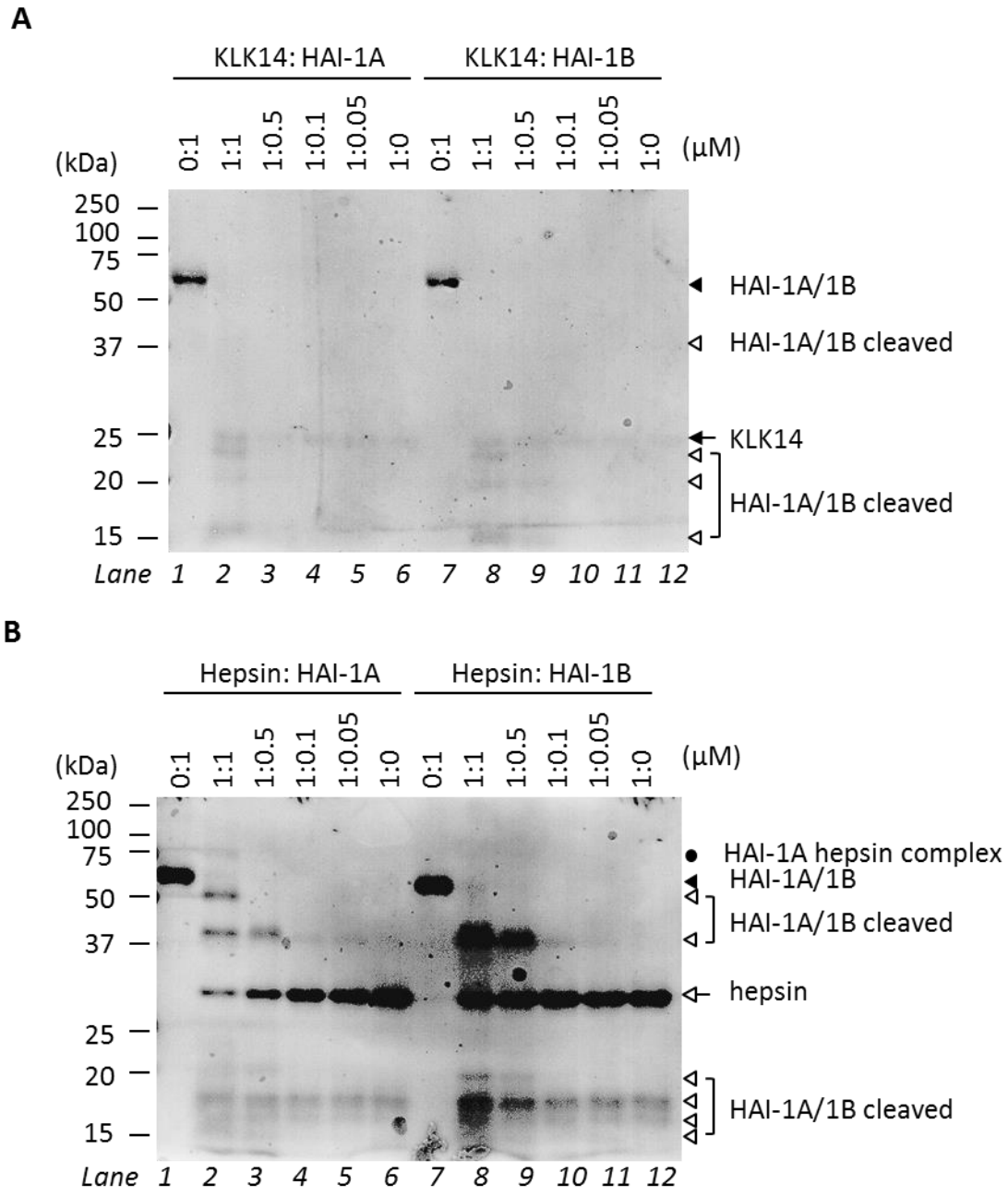

Figure 3.14 KLK14 degrades HAI-1A and HAI-1B while hepsin forms complexes with HAI-1A and degrades HAI-1B. Varying molar ratios of HAI-1A and HAI-1B were co-incubated with active recombinant KLK14 and hepsin, as indicated, for 30 minutes at 37°C. Reactions stopped with reducing SDS-PAGE loading buffer were subjected to electrophoresis, transferred to PVDF membrane and stained with Coomassie R-250. At the concentrations tested, HAI-1A and HAI-1B do not form an SDS and βME stable complex with KLK14 (**A**). When incubated with hepsin, a complex with HAI-1A can be seen (**B**) whereas there is no complex formation with HAI-1B. Hepsin also degrades both HAI-1A and HAI-1B. S*olid arrows*, KLK14; *open arrows*, hepsin; *solid* arrowheads, intact HAI-1A or 1B; *solid circles*, hepsin HAI-1A complexes; *open arrowheads*, hepsin or KLK14 generated HAI-1A or 1B fragments.

both HAI-1 isoforms thoroughly (Figure 3.14A). In contrast, hepsin, when incubated with an equimolar concentration of HAI-1A shows appearance of a band in the vicinity of 85 kDa with the concomitant reduced signal intensity for 30 kDa hepsin (Figure 3.14B). As the concentration of HAI-1A decreases, so does the loss of hepsin from the30 kDa band. There is also a small amount of possible degradation of HAI-1A by

hepsin and possible complex formation between truncated HAI-1A and hepsin with bands appearing at around 50, 40, 20, 15 kDa. Hepsin does not appear to form a complex with HAI-1B as there is no appearance of a band around 85 kDa and there is no loss of hepsin from 30 kDa. HAI-1B, however, is significantly degraded with major bands appearing around 40, 20, 18 and 15 kDa.

In Figure 3.15, using a fixed concentration of HAI-1A (1 μM) and decreasing concentrations of KLK14 and hepsin, the dose response of HAI-1A to the proteases is

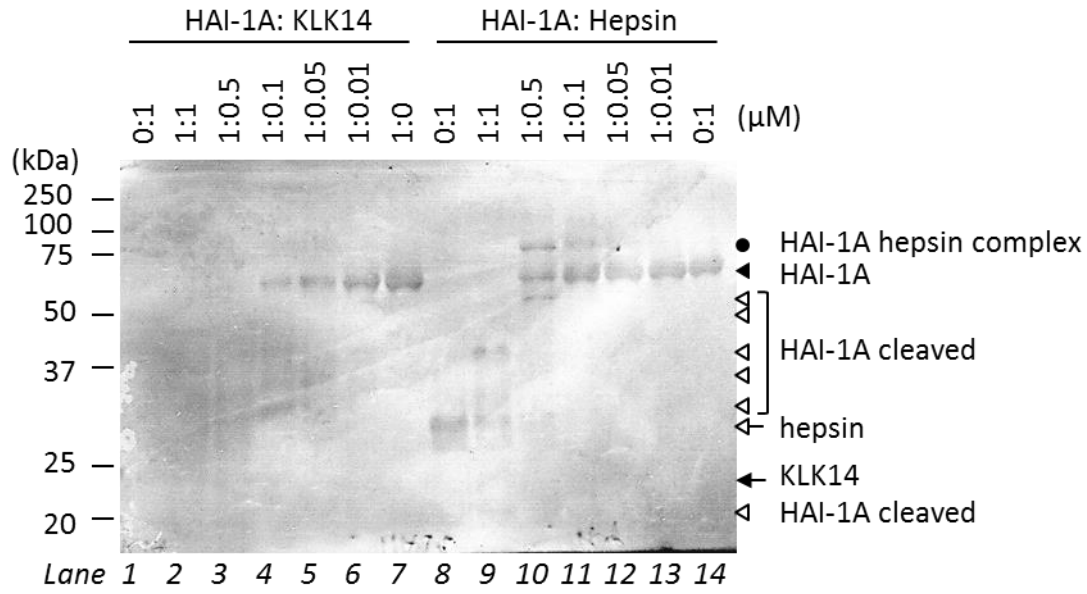

Figure 3.15 KLK14 degrades HAI-1A in a dose dependent manner while hepsin forms complexes with HAI-1A. HAI-1A was co-incubated with varying molar ratios of active recombinant KLK14 and hepsin, as indicated, for 30 minutes at 37°C. Reactions stopped with reducing SDS-PAGE loading buffer were subjected to electrophoresis, transferred to nitrocellulose membrane and stained with Coomassie R-250. At the concentrations tested, HAI-1A does not form an SDS and βME stable complex with KLK14. KLK14 shows dose dependent degradation of HAI-1A. Hepsin forms a complex with and also degrades HAI-1A. S*olid arrows*, KLK14; *open arrows*, hepsin; *solid* arrowheads, intact HAI-1A or 1B; *solid circles*, hepsin HAI-1A complexes; *open arrowheads*, hepsin or KLK14 generated HAI-1A or 1B fragments.

illustrated. The 55 kDa band of HAI-1A appears completely degraded at 1 μM and 0.5 μM KLK14 (lanes 2, 3) with decreasing degradation as KLK14 concentration decreases (lanes 4-6). Equimolar concentration of hepsin (lane 9) has a similar degradative effect on HAI-1A. However, there is also stable complex formation as there is a depletion of 30 kDa hepsin when compared to hepsin alone (lane 8). While there are some degradation bands for HAI-1B at 0.5 μM hepsin (lane 10), there is clear appearance of the 85 kDa band and decrease in the 55 kDa HAI-1A band. As the concentration of hepsin decreases (lanes 11 and 12) so does the 85 kDa band.

These results show that while HAI-1A and 1B mildly inhibit proteolytic activity of KLK14, they do not form the stable complexes with KLK14. KLK14 instead comprehensively degrades the HAI-1 isoforms. Moreover, these results are the first time complexes of hepsin and HAI-1A have been demonstrated.

3.3 Discussion

In this chapter the KLK14 amino acid sequence was reviewed and recombinant pro-KLK14-V5-His was generated in insect Sf9 cells and then characterized. KLK14 zymogen activation was achieved using thermolysin and this was followed by assessment of KLK14 proteolytic activity using the synthetic substrate QAR-AMC. Comparisons of pro-HGF activation by KLK14, KLK4 and hepsin were made. KLK14 inhibition by HAI-1 isoforms was also examined. As was complex formation between KLK14 and HAI-1, and hepsin and HAI-1. It was found that:

- KLK14 zymogen generated in Sf9 cells was a 29 kDa N-glycosylated protein.

And as summarized in Figure 3.16:

- KLK14 and hepsin activate pro-HGF, while KLK4 primarily degrades it
- KLK14 degrades HAI-1A and HAI-1B, while hepsin and HAI-1A form stable complexes.

This is the first time KLK14 activation of pro-HGF has been reported. Moreover, this is the first time KLK14 degradation of HAI-1, and formation of hepsin-HAI-1 complexes, have been reported. The data suggests KLK14 may have a role in regulation of HGF/HGFR signalling axis through activation of pro-HGF and degradation of key protease inhibitors, HAI-1A and HAI-1B.

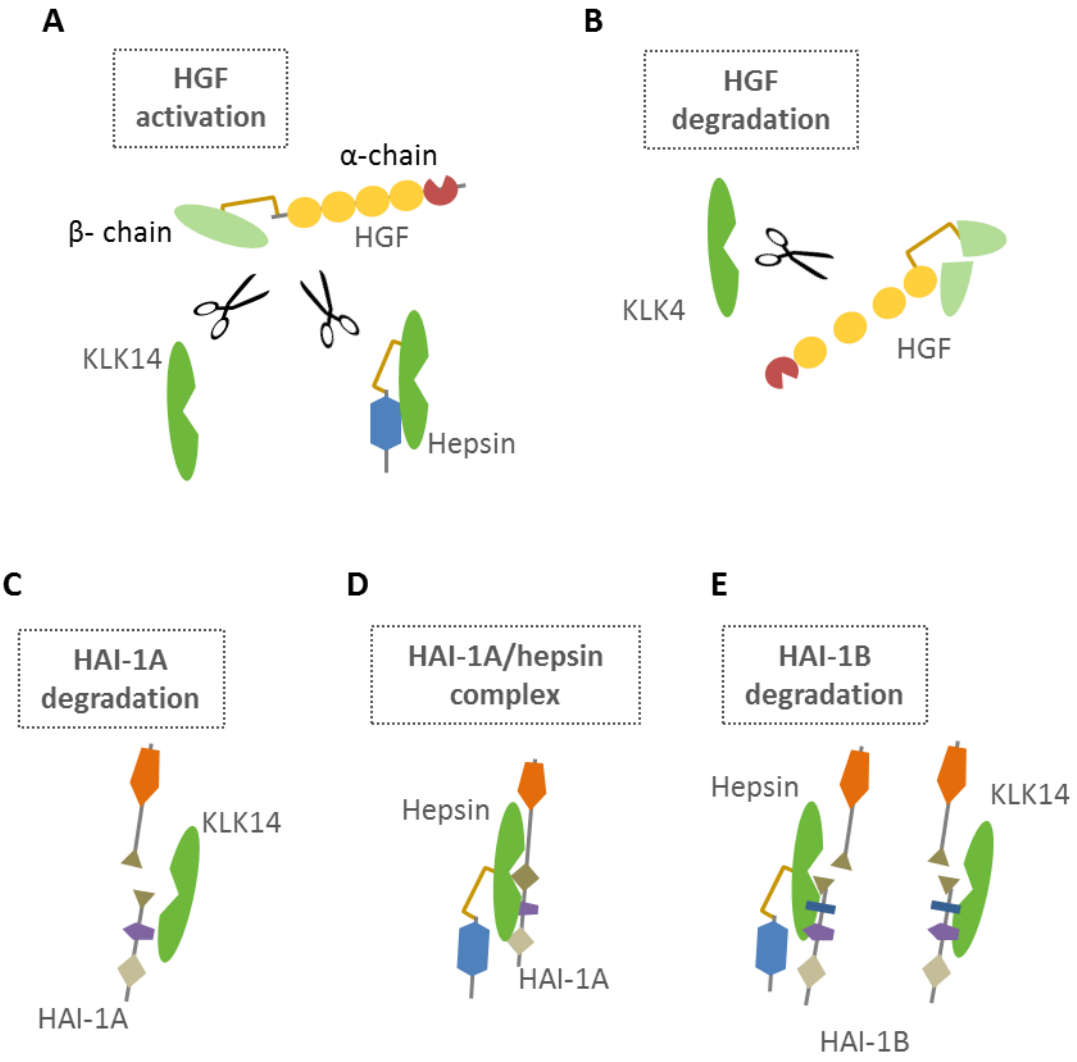

Figure 3.16 HGF activation and HAI-1 degradation by KLK14. A. KLK14 and hepsin activate HGF. **B.** KLK4 degrades HGF. **C.** KLK14 degrades HAI-1A. **D.** Hepsin forms stable complexes with HAI-1A. **E.** KLK14 and hepsin degrade HAI-1B.

3.3.1 KLK14 activation and sequencing

The recombinant KLK14 zymogen generated in Sf9 cells was activated using the metalloproteinase thermolysin. Thermolysin was used in this manner because it has a preference for hydrolysis before accessible hydrophobic residues (van den Burg and Eijsink, 2013), and when trypsin-like serine proteases, such as KLK14, and chymotrypsin-like serine proteases are activated by proteolytic removal of the pro-region, the nascent N-terminal residue is invariably a hydrophobic residue (Page and Di Cera, 2008). This substrate specificity of thermolysin has been exploited extensively for

in vitro activation of KLK family members KLK1 (Takada et al., 1985), KLK4 (Ramsay et al., 2008a) and KLK7 (Ramani and Haun, 2008), and other serine proteases.

To confirm that activation by thermolysin removed the pro-region of KLK14 at the Lys40↓Ile41 activation site, N-terminal sequencing by Edman degradation was used. This method uses labelling of the free amide group of the N-terminal residue followed by cleavage of the residue which is isolated and then identified by comparison with amino acid standards using liquid chromatography. This degradation cycle is repeated 5-10, and up to 30 times to identify sequential N-terminal residues. However, Edman degradation cannot be used on proteins whose N-terminal residue has been blocked through post-translational modification or during sample preparation.

As neither APAF nor UQ SCMB sequencing facility was able to obtain clear sequence it was concluded that zymogen and activated KLK14 forms were N-terminally blocked. While initially it was thought they might be blocked by acetylation of the N-terminal residue, subsequent literature review showed that this modification is an *in vivo* post-translational modification limited to particular residues including methionine, serine, alanine, threonine, valine, glycine and cysteine (Krishna and Wold, 1993; Leone et al., 2011). As the predicted N-terminal residue of zymogen KLK14 is glutamine (Figure 3.1A) it is unlikely to be acetylated. Furthermore, KLK14 activated *in vitro* is separated from the cellular machinery required for acetylation, therefore the nascent N-terminal could not be acetylated in this manner.

Similarly, most other N-terminal modifications that block Edman degradation are the result of *in vivo* processing events (Krishna and Wold, 1993; Leone et al., 2011) and therefore do not influence sequencing of KLK14 activated *in vitro*. In contrast, the N-terminal of pro-KLK14, generated in *in vivo* processing and removal of the signal peptide, is predicted to be a glutamine. This residue may be modified by pyrroidone carboxylation, which is the cyclization of N-termini glutamine (Blomback, 1967) or glutamic acid (Twardzik and Peterkofsky, 1972; Jones, 1974; Beck et al., 2001; Chelius et al., 2006) residues to form pyroglutamic acid. Modification by pyrroidone carboxylation has been speculated to protect these proteins from aminopeptidase degradation and can occur as a post-translational modification (Stott and Munro, 1972; Fischer and Spiess, 1987) or spontaneously in response to storage or incubation conditions (Blomback, 1967; Shih, 1985; Khandke et al., 1989). An N-terminal nitrogen attack on the side chain carbonyl carbon of glutamine forms 2-pyrrolidone-5-carboxylic acid or pyroglutamic

acid (Figure 3.17) and results in the loss of the free amide terminal required for Edman degradation (Abraham and Podell, 1981; Rehder et al., 2006). So while cyclization of glutamine is a possible explanation for the inability to sequence pro-KLK14 by Edman degradation, there is no comparable explanation for the failure to sequence activated KLK14. Furthermore, endogenous active KLK14 has been isolated from human skin, plantar stratum corneum, and sequenced by Edman degradation (Stefansson et al., 2006). Certainly, there may be differences to post-translational modification between endogenous KLK14 and insect cell-generated recombinant KLK14, and this may explain the sequencing failure.

Interestingly, Borgono and colleagues (2007c) used tandem mass spectrometry (MS/MS) to identify recombinant KLK14 generated in *Pichia pastoris*. This method is a viable approach to obtain N-terminal sequence data for the potentially blocked zymogen and activated forms of KLK14. Briefly, sequencing proteins by MS/MS employs the vaporization then ionization of a sample followed by separation/selection of the ions based on their mass-to-charge ratio by applying electromagnetic fields. Ions are subjected to a second fragmentation and second mass-to-charge ratio separation, then detected and quantified based on ion type (Gross, 2011). Significantly, MS/MS is not obstructed by N-terminal modifications. Certainly, scope exists for this to be pursued in the future.

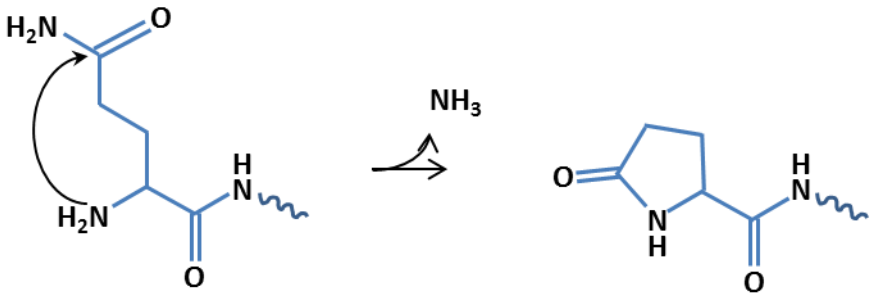

Figure 3.17 Formation of pyroglutamic acid from glutamine. Spontaneous or enzyme catalysed N-terminal nitrogen attack on the side chain carbonyl carbon of glutamine to form pyroglutamic acid (2-pyrrolidone-5-carboxylic acid) and ammonia. (*Adapted from* Wikipedia http://en.wikipedia.org/wiki/File:Pyroglutamate.png and Rehder, 2006)

3.3.2 Examination of the N-glycosylation status of zymogen KLK14

The KLK14 amino acid sequence contains a consensus N-glycosylation sequon at Asn184-Ile-Ser, however, NetNGlyc-1.0 (Gupta et al., 2004) predicts that this site would not be N-glycosylated. Therefore it is interesting that the *in vitro* results in this study indicate that recombinant KLK14-V5-His zymogen produced in stably transfected insect Sf9 cells was N-glycosylated. In contrast, KLK14-Myc zymogen from transiently transfected Cos-7 cells was not. This finding in Cos-7 cells is consistent with that of Borgono and colleagues (2003) who determined that KLK14 was not N-glycosylated when generated in yeast *Pichia pastoris*. Additionally, in another study they speculated that based on the molecular weight observed by Western blot analysis KLK14 produced in HEK293 cells was also not glycosylated (Borgono et al., 2007c).

The distinct pattern of N-glycosylation was also seen for KLK4 as recombinant KLK4-V5-His zymogen was N-glycosylated when produced in stably transfected Sf9 cells and not when generated by transiently transfected Cos-7cells. KLK4 was chosen as a positive control for de-glycosylation as it has previously been shown to be N-glycosylated when produced in stable Sf9 cells, as well as in transiently transfected HeLa (Ramsay, 2008) and PC-3 cells (Dong et al., 2005). Furthermore, in contrast to KLK14, NetNGlyc-1.0 predictions for KLK4 support the presence of N-glycosylation on Asn169(-Val-Ser).

This raises two issues. First, KLK14 generated in Sf9 cells was N-glycosylated despite bioinformatics-based predictions. Second, there was cell-type-dependent differential N-glycosylation for KLK14 and KLK4. Examining the first issue, it has been estimated that only around 60% of the consensus sequon Asn-Xaa-Thr/Ser are glycosylated (Apweiler et al., 1999; Ben-Dor et al., 2004; Petrescu et al., 2004). N-glycosylation is affected by factors including the availability of N-glycans in the endoplasmic reticulum, the enzyme kinetics of glycan attachment, and the sequon availability (as reviewed by Jones and colleagues (2005)), as well as the protein secondary structure and surface hydrophobicity (Petrescu et al., 2004). It is also affected by the identity of Xaa and residues immediately adjacent to the consensus sequon, in particular proline (Pro) residues as Xaa or Xaa+2 are not favoured (Gavel and von Heijne, 1990; Mellquist et al., 1998; Ben-Dor et al., 2004; Petrescu et al., 2004). Furthermore, sequons ending with Thr are more likely to be N-glycosylated that those ending with Ser (Kasturi et al., 1997; Ben-Dor et al., 2004; Petrescu et al., 2004). Therefore it is possible that KLK14 was

predicted to not be N-glycosylated by NetNGlyc-1.0 for reasons including Ser186 as the final residue in the sequon and Pro187 at Xaa+2 (Figure 3.1A).

However, there are limitations to the predictive capability NetNGlyc-1.0. Briefly, as outlined by the authors, Gupta and colleagues (2004), based on validated glycosylation sites, the software predicts 86% of glycosylated sequons and 61% of nonglycosylated. Moreover, the default parameters for NetNGlyc-1.0 predictions do not include analysis of atypical N-glycosylation sites. However, as predicted by Bause and Legler (1981), atypical sequon Asn-Xaa-Cys is an N-glycan acceptor in proteases with examples in protein C (Foster and Davie, 1984; Miletich and Broze, 1990), recombinant tissue plasminogen activator (tPA) (Borisov et al., 2009) and also in the insect protease, Cowpea bruchid cathepsin B-like protein (Chi et al., 2010). Other atypical sequons include, Asn-Gly-Gly-Ser (Gavel and von Heijne, 1990) and Asn-Ser-Gly (Valliere-Douglass et al., 2009) from murine and human antibodies, respectively.

Expansion of the NetNGlyc-1.0 sequence analysis parameters to include all Asn residues in KLK14 results in four of seven residues predicted to be potential N-glycosylation acceptors. In a family KLK sequence alignment (Clements et al., 2001) one of these residues, Asn182, is in a consensus sequon conserved across KLK4, KLK5, KLK9, KLK11, KLK12 and KLK15. It has also been confirmed as an N-glycosylation acceptor in KLK5 (Debela et al., 2007a) and a predicted acceptor in KLK4 (Ramsay, 2008). In KLK14 however, it is the first residue of the nonconsensus sequon Asn182-Ile-Asn. Interestingly, the second Asn of this sequon is in the previously discussed consensus sequon Asn184-Ile-Ser (Figure 3.1A). Furthermore, another, Asn252, is in the atypical sequon Asn-Xaa-Cys, this sequon is also conserved across KLK4-6 and KLK8 (Clements et al., 2001). Taken together, Asn184 in the consensus sequon, as well as one or more of the other Asn residues in atypical sequons, may act as N-glycosylation acceptors in KLK14. This could be examined further using site-directed mutagenesis to alter coding sequence for the individual Asn residues to identify the N-glycosylation residues.

The second issue of cell-type differential N-glycosylation for KLK14 and KLK4 is interesting because as mentioned earlier, N-glycosylation has the potential to affect activity (Skropeta, 2009). Indeed, there are several reported examples of N-glycosylation affecting distinct properties of proteases. For instance, Oka and colleagues (2002) found that abolishing the N-glycosylation site of KLK8 by mutagenesis altered the catalytic

activity, reducing the K_M and k_{cat}. Ramsay (2008) also speculated that N-glycosylation lowered the catalytic efficiency (k_{cat}/K_M) of KLK4. Furthermore, while matriptase N-glycosylation is required for autoactivation (Oberst et al., 2003b; Miyake et al., 2010), aberrant glycosylation by attachment of N-glycan structures associated with malignant or metastatic states results in prolonged stabilization of matriptase and has a pro-metastatic effect (Ihara et al., 2002; Ihara et al., 2004; Ito et al., 2006).

Differential N-glycosylation has also been reported for several proteases including tPA which has four typical N-glycosylation sites, two of which are generally occupied and a third occasionally occupied (Pohl et al., 1984). It has been found that there are cell type-specific differences in the N-glycan moieties attached to the three sites of endogenous and recombinant tPA with differences in enzymatic activity between the different tPA glycoforms (Parekh et al., 1989a; Parekh et al., 1989b; Wittwer et al., 1989). For instance, occupancy of the third site hinders plasmin activation of tPA (Wittwer and Howard, 1990). Furthermore, studies have shown variation in cell culture conditions such as increased manganese or iron, reduced culture temperature and decreased growth rate all increase occupancy of the third site (Andersen et al., 2000; Gawlitzek et al., 2009).

Protein C is another protease that has exhibited differential N-glycosylation. It has three typical N-glycosylation sites, in addition to the atypical site mentioned earlier (Foster and Davie, 1984; Miletich and Broze, 1990). Plasma-derived protein C has between 70% and 80% occupancy of the atypical site (Miletich and Broze, 1990; Gil et al., 2009), with lower levels of occupancy for recombinant protein C generated in HepG2 cells (Miletich and Broze, 1990). In addition, there is also variation in the predominant N-glycan structures for each of the four N-glycosylation sites of recombinant protein C compared to plasma-derived protein C (Gil et al., 2009). Moreover, the four sites, either individually or collectively, affect secretion of protein C, glycosylation at the atypical site, catalytic efficiency, and activation by thrombin (Grinnell et al., 1991).

As glycosylation depends on a range of conditions it is possible that KLK14 and KLK4 zymogens may be glycosylated when expressed in the stable insect cell system but not in the transiently transfected mammalian Cos-7 cells. It has not been established whether KLK14 is glycosylated endogenously. However, as it is ubiquitously expressed in the human body, there is great potential for tissue-specific glycosylation which in turn may be a mode of modulating KLK14 activity. As shown in the KLK14 homology model in Figure 3.18, the N-glycosylation consensus site Asn184-Ile-Ser and the nonconsensus

sequons Asn182-Ile-Asn and Asn252-Leu-Cys are on the opposite side of the molecule to the active-site and substrate-binding pocket. N-glycosylation at one of these sites may alter the KLK14 active-site cleft configuration and change its catalytic efficiency.

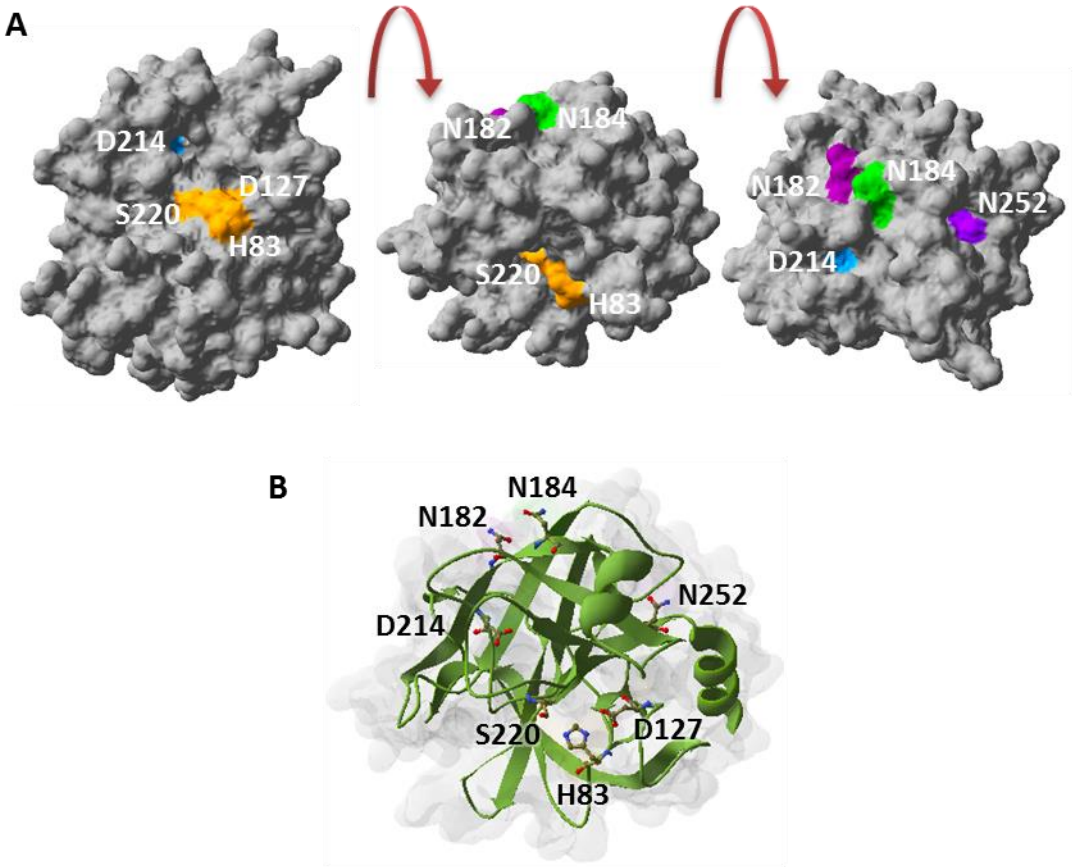

Figure 3.18 KLK14 homology model showing positions of potential N-glycosylation acceptor residues. A homology model of KLK14 based on the crystal structure of active KLK5 (PDB ID 2PSX) was generated using SWISS-MODEL. **A.** Incrementally rotated view of the molecular surface of the KLK14 homology model indicating the relative positions of the active site (orange), and the S1 residue in the substrate binding pocket (blue), the consensus N-glycosylation residue Asparagine (N184) (green) and the potential atypical N-glycosylation residues Asn182 and Asn252 (purple) on the opposite side to the active site cleft. **B.** KLK14 homology model shown as a ribbon plot, features indicated, shown as stick models, include the catalytic active-site residues histadine (H83), aspartate (D127) and serine (S220); the S1 residue aspartate (D214). The structure orientation of the centre image of (**A**) and the image in (**B**) are identical.

3.3.3 KLK14 activity

3.3.3.1 Catalytic efficiency of recombinant KLK14

In this study the catalytic efficiency (k_{cat}/K_M) of KLK14 for hydrolysis of the tripeptide substrate QAR-AMC was 4.66×10^4 $M^{-1}s^{-1}$. In contrast, Borgono and colleagues (2007c) obtained a value 3-fold higher at 14.19×10^4 $M^{-1}s^{-1}$ (8516.94 $mM^{-1}min^{-1}$) for the same substrate and kinetic assay parameters using recombinant KLK14 generated in *Pichia pastoris*.

The assay parameters used by Borgono and colleagues (2007c) were replicated in this project because of the sixteen tripeptide substrates analysed in kinetic assays, recombinant KLK14 had the greatest hydrolytic activity against QAR-AMC. Borgono and colleagues (2007c) also examined the activity of KLK14 in a Tris buffer compared to a phosphate buffer and found that pH 8.0 was optimal for KLK14 activity in these buffers. Moreover, KLK14 had 1.4-times greater activity in the phosphate buffer over the Tris buffer. Based on this, the tripeptide substrate QAR-AMC was used with a phosphate buffer at pH 8.0 to examine the hydrolytic activity of Sf9 cell-generated KLK14.

As mentioned earlier, N-glycosylation status has been shown to modulate catalytic efficiency of several serine proteases. Indeed, for KLK4 the lower catalytic efficiency of Sf9 cell- (Ramsay, 2008) and *Drosophila* cell-generated KLK14 (Matsumura et al., 2005) compared to that of *E. coli*-generated KLK4 (Debela et al., 2006a) was attributed to the N-glycosylation of insect cell-generated KLK4 (Ramsay, 2008). Similarly, as the kinetic parameters used by Borgono and colleagues (2007c) were replicated here in this study, the difference in the catalytic efficiency could be due to the N-glycosylation of Sf9 cell-generated KLK14, as the *Pichia pastoris*-generated KLK14 used by Borgono and colleagues (2007c) was not N-glycosylated (Borgono et al., 2003). Certainly, for Sf9 cell-generated KLK14, the impact of N-glycosylation on catalytic efficiency could be explored further by comparing wild-type KLK14 with KLK14 in which identified N-glycosylation acceptor residues have been mutated.

In another study examining KLK14 kinetic parameters, Brattsand and colleagues (2005) used recombinant KLK14 generated in the insect *Drosophila* Schneider 2 cells and tripeptide substrate PFR-pNA to obtained a k_{cat}/K_M of 1.2×10^4 $M^{-1}s^{-1}$. In contrast, Borgono and colleagues (2007c) obtained a 2-fold higher value of 2.5×10^4 $M^{-1}s^{-1}$ (1520.57 $mM^{-1}min^{-1}$) for *Pichia pastoris*-generated KLK14 using PFR-AMC, the same

substrate with a different cleavable reporter. The assay conditions, including the buffer, were different in the two studies, and the N-glycosylation status of *Drosophila* Schneider 2 cell-generated KLK14 was not reported by Brattsand and colleagues (2005). Therefore, it is a matter of speculation whether N-glycosylation or assay conditions modified the catalytic efficiency of *Drosophila* Schneider 2 cell-generated KLK14.

3.3.3.2 Pro-HGF activation by KLK14

This is the first study to show that KLK14 activates HGF in a dose-dependent manner. This study also confirms that the related protease KLK4 degrades rather than activates HGF, and that hepsin is a potent HGF activator. While these results show hepsin is a more efficient HGF activator compared to KLK14, a role for KLK14 in HGF activation should not be discounted. There appears to be a window where the molar ratio of KLK14 to HGF is optimal for HGF activation. In a physiological setting bimodal activity of KLK14 may have a role in regulation of HGF-dependent signalling with higher concentrations of KLK14 resulting in HGF degradation and lower concentrations resulting in activation.

Activation of HGF relies on proteolytic cleavage between Arg494↓Val495 (Gak et al., 1992; Naka et al., 1992; Naldini et al., 1992) and therefore, it is possible several serine proteases with specificity for an Arg P1 residue will activate HGF *in vivo*, including KLK14. As mentioned earlier, several *in vitro* HGF activators have been identified including HGFA (Shimomura et al., 1995; Itoh et al., 2004), matriptase (Lee et al., 2000; Owen et al., 2010), hepsin (Herter et al., 2005; Kirchhofer et al., 2005; Owen et al., 2010) and TMPRSS13 (Hashimoto et al., 2010). Likewise, several HGF-degrading proteases have been identified including uPA, tPA (Owen et al., 2010), KLK4 and KLK5 (Mukai et al., 2008).

Table 3.2 shows a summary of results from studies investigating KLK14, KLK4 and hepsin cleavage specificities beyond the P1 residue (Felber et al., 2005; Herter et al., 2005; Matsumura et al., 2005; Debela et al., 2006b; Borgono et al., 2007a; Beliveau et al., 2009; Swedberg et al., 2009; Owen et al., 2010; de Veer et al., 2011). These studies used a variety of techniques, including positional scanning synthetic combinatorial libraries (PS-SCL) (Schneider and Craik, 2009) and non-combinatorial sparse matrix libraries (NC-SML) (Swedberg et al., 2009; de Veer et al., 2011), to determine P4-P1 substrate

Table 3.2 Substrate cleavage specificities of KLK14, KLK4 and hepsin. Peptide substrate preferences of KLK14, KLK4 and hepsin as determined by phage-display library (PD), positional scanning synthetic combinatorial library (PS-SCL), non-combinatorial sparse matrix library (NC-SML), and internally quenched fluorescent peptide library (IQFP). The P4-P1 residues of HGF (KELR) are underlined.

Protease	Method	P4	P3	P2	P1	Reference
KLK14	PD	Gly	Ser Asn Leu	Leu Gln Gln	Arg	(Felber et al., 2005)
	PS-SCL	Tyr Trp	Lys Ala Ser Arg	Ala Pro Asn His Ser	Arg	(Borgono et al., 2007a)
	NC-SML	Tyr Trp	Ala	Val Ser	Arg	(de Veer et al., 2011)
KLK4	PS-SCL	Val Ile	Gln Val Ser	Gln Val Leu	Arg	(Matsumura et al., 2005)
	PS-SCL	Ile Val	Val Gln Gly	Gln Val Leu	Arg	(Debela et al., 2006b)
	PS-SCL	Val Ile	Gln Ser Ala Arg	Gln Leu	Arg	(Borgono et al., 2007a)
	NC-SML	Phe	Val	Gln	Arg	(Swedberg et al., 2009)
Hepsin	PS-SCL	Pro Lys	Glu Lys	Thr Leu Asp	Arg	(Herter et al., 2005)
	IQFP	Arg	Arg Ala Leu	Leu Arg Tyr	Arg	(Beliveau et al., 2009)
	PS-SCL	Lys Ile	Arg Gln Lys	Leu Thr Arg Asn	Arg	(Owen et al., 2010)

preferences. Differences in substrate specificities for proteases examined by different groups, using in some cases the same method, could be due to the different host cells used for recombinant protease generation. As discussed earlier, post-translational modifications imposed by different cell types such as N-glycosylation can alter the catalytic specificity of proteases. Interestingly, when compared to the P4-P1 residues of HGF (Lys-Glu-Leu-Arg) (Gak et al., 1992; Naka et al., 1992; Naldini et al., 1992), hepsin is the only protease in this group that has each of these residues as a preferred residue (Table 3.2, underlined residues). This reflects the potent and efficient HGF activation by hepsin.

Interestingly, KLK14 and KLK4 have Arg P1 and Leu P2 preferred substrate residues, however, KLK14 activates HGF but KLK4 does not. This highlights the phenomenon of subsite cooperativity (as reviewed by Ng and colleagues (2009)). Briefly, binding of a substrate residue to a protease subsite has a positive or negative effect on the binding of other residues at other sites. This extended cooperative effect plays a role in the substrate specificity of the protease. By the same token, the P4-P1 residues of HGF in addition to residues beyond this region including the P1'-P4' residues, as well as the co-operativity of the protease S1'-S4' subsites and beyond, influence the proteolytic activity of KLK14 and KLK4. This leads to the differential effects of KLK14 and KLK4 on HGF activation.

3.3.3.3 HAI-1 degradation by KLK14

In vitro studies have confirmed the Kunitz-type inhibitor HAI-1A or isoform HAI-1B are potent inhibitors of HGFA and matriptase as well as other HGF activators such as hepsin and TMPRSS13 (Kirchhofer et al., 2003; Herter et al., 2005; Kirchhofer et al., 2005; Hashimoto et al., 2010). While there are several serine proteases inhibited by the HAI-1 isoforms, several HGF activators such as factor XIa and factor XIIa (Shimomura et al., 1995; Peek et al., 2002) are not inhibited by HAI-1 isoforms (Kirchhofer et al., 2003). This suggests certain specificity to the inhibitory activity of HAI-1.

In this study, dose-dependent analysis indicated that the HGF-activator KLK14 was moderately inhibited by HAI-1A and HAI-1B. Limited access to recombinant HAI-1 meant that the IC50 of KLK14 inhibition could not be calculated. However, the results showed marginally greater inhibition for HAI-1A than HAI-1B as 50 nM of these

inhibited 5 nM KLK14 by 35% and 26%, respectively. Fan and colleagues (2005) also found that prostasin was moderately inhibited by HAI-1 isoforms. However, prostasin (3 nM) is marginally more inhibited by HAI-1B with IC50 values of 109 nM and 66 nM for HAI-1A and 1B, respectively (Fan et al., 2005). For comparison, HAI-1A potently inhibits hepsin (1 nM) with an IC50 of 12 nM (Herter et al., 2005). In contrast, HAI-1B has more moderate inhibition of hepsin (0.4 nM) and matriptase (0.5 nM) with IC50 values of 21 nM and 16 nM, respectively (Kirchhofer et al., 2003; Kirchhofer et al., 2005). HAI-1B has also been reported to weakly inhibit plasmin and plasma kallikrein with IC50 values of 399 nM for plasmin (4 nM) and 686 nM for plasma kallikrein (concentration not reported) (Kirchhofer et al., 2003).

As inhibition of serine proteases by HAI-1 isoforms is attributed to the P1 residues of the substrate-like reactive loops in KD1 and KD2 (Denda et al., 2002; Kirchhofer et al., 2003; Fan et al., 2005; Kirchhofer et al., 2005; Kojima et al., 2008), inhibition is based on the protease preference for either Arg or Lys, respectively, in their substrate binding pocket. Reflecting their substrate preferences, matriptase, prostasin, and hepsin are only inhibited by KD1 of HAI-1A and/or 1B (Kirchhofer et al., 2003; Fan et al., 2005; Kirchhofer et al., 2005; Oberst et al., 2005; Kojima et al., 2008). Likewise, KLK14, with a preference for Arg P1 residues, would probably be inhibited by KD1 with negligible to no inhibition afforded by KD2.

Interestingly, HAI-1 domain deletion studies for matriptase, prostasin, hepsin, plasma kallikrein, plasmin, TMPRSS13 and human airway trypsin-like protease (HAT), show the presence of KD2 attenuates HAI-1 inhibition, possibly by obstructing access to the reactive site of KD1 (Fan et al., 2005; Shia et al., 2005; Kojima et al., 2008; Hashimoto et al., 2010; Kato et al., 2011). In fact, full-length HAI-1A does not inhibit TMPRSS13 or HAT whereas as a truncated form lacking KD2 affords strong inhibition (Hashimoto et al., 2010; Kato et al., 2011). KLK4 and KLK5 are also inhibited by a truncated form of HAI-1A featuring KD1 (Mukai et al., 2008), however, the study did not show data for full-length HAI-1A.

There are some proteases that are inhibited by KD2. For instance, using domain deletion studies Denda and colleagues (2002) showed that trypsin is equally inhibited by KD1 and KD2 of HAI-1A. This is likely due to trypsin's preference for both Arg and Lys P1 residues. This group also showed that HGFA is also inhibited by KD2, though, to a lesser extent than KD1 (Denda et al., 2002).

While inhibition by HAI-1 isoforms is mediated by the Kunitz domains, the other HAI-1 domains play roles in either obstructing or enhancing the interaction (Kojima et al., 2008). The presence of a 16 amino acid insert in HAI-1B isoform between the two Kunitz domains has been speculated to create a relatively small structural change to HAI-1 and little change to the inhibition by KD1 (Kirchhofer et al., 2003). However, other than this project, the study of prostasin by Fan and colleagues (2005) is the only one to report direct comparison of inhibition by HAI-1A and 1B. In this study the IC50 for prostasin (3 nM) inhibition by HAI-1A (109 nM) was higher than for HAI-1B (66 nM), these are small changes and so far the significance is unknown.

The moderate inhibition of KLK14 by HAI-1 isoforms was examined further using SDS-PAGE as it has been reported that endogenous and recombinant HAI-1 form stable complexes with several proteases including matriptase, TMPRSS13, prostasin and HAT (Lin et al., 1999b; Benaud et al., 2001; Fan et al., 2005; Wang et al., 2009; Hashimoto et al., 2010; Kato et al., 2011). Interestingly, KLK14 does not form stable complexes with either HAI-1 isoform. Instead, there is a comprehensive degradation of both isoforms by KLK14 resulting in several HAI-1 fragments. This would indicate multiple hydrolysis points along HAI-1A and 1B amenable to KLK14 proteolysis. Likewise, hepsin does not form stable complexes with HAI-1B. Instead there are multiple HAI-1B degradation bands. In contrast, hepsin and HAI-1A form stable complexes, but there is also some dose-dependent degradation of HAI-1A. It is possible the extra 16 amino acid insert in HAI-1B alters the hepsin-HAI-1 interaction resulting in the increased HAI-1B cleavage and abrogation of complex formation. So far, a direct comparison of HAI-1A and HAI-1B inhibition of hepsin in an amidolytic assay has not been conducted. Such a comparison would further clarify the effect of the HAI-1B 16 amino acid insert on hepsin inhibition.

Fragmentation of transmembrane HAI-1 has previously been reported as shed forms of 58, 50, 48, 44, 40/39 and 25 kDa identified in conditioned media or bodily fluids such as milk (Shimomura et al., 1997; Lin et al., 1999b; Shimomura et al., 1999; Kataoka et al., 2000; Benaud et al., 2001; Kiyomiya et al., 2006; Wang et al., 2009). For instance, active matriptase has been isolated from human milk, urine and seminal plasma in SDS-stable complexes with 25 and 40 kDa HAI-1 (Lin et al., 1999b; Benaud et al., 2001; Wang et al., 2009), the 40 kDa fragment most likely containing KD1 (Lin et al., 1999b). Moreover, Kojima and colleagues (2008) suggested that matriptase interaction with

HAI-1A does not result in the degradation of HAI-1A. Instead, shedding of HAI-1 and subsequent fragmentation is thought to be mediated by metalloproteinase membrane-type-1 MMP (Domoto et al., 2012).

Fan and colleagues (2005) also reported formation of SDS- and reducing agent-stable prostasin-HAI-1B complexes as well as prostasin co-immunoprecipitation with cell-surface and shed HAI-1B from lysates and medium, respectively. Similarly, cell-surface HAI-1A has been co-immunoprecipitated with HAT (Kato et al., 2011). TMPRSS13 also forms SDS- and reducing agent-stable complexes with a truncated HAI-1A featuring KD1 but not with full-length HAI-1A consisting of both KD1 and KD2 (Hashimoto et al., 2010).

While stable complex formation with serine proteases is an inhibitory tactic of the Kunitz-type inhibitors (Laskowski and Qasim, 2000; Krowarsch et al., 2003), the purpose of HAI-1 fragmentation is unknown and the potential role of KLK14 (and hepsin) in this activity is intriguing. It is possible that as KD1 is a more potent inhibitor in isolation (Fan et al., 2005; Shia et al., 2005; Kojima et al., 2008; Hashimoto et al., 2010; Kato et al., 2011), KLK14 and hepsin may facilitate the inhibitory activity of HAI-1 through fragmentation to release this domain. In so doing this may lead to increased inhibition of HGF-activating proteases. Indeed, the degradation of HAI-1B by hepsin generates a predominant 40 kDa band, which is possibly the liberated KD1 fragment (Lin et al., 1999b) (Figure 3.14B). It is also possible that comprehensive degradation of HAI-1 isoforms by KLK14, or HAI-1B by hepsin modulates inhibition in the pericellular environment through reduction in HAI-1 availability.

Furthermore, this finding that HAI-1 is degraded by KLK14 is consistent with the apparent moderate inhibition of KLK14 in the amidolytic assays. As a competitive substrate HAI-1A would reduce the cleavage rate of the tri-peptide substrate QAR-AMC thereby feigning the role of KLK14 inhibitor.

3.3.4 Summary

In summary, this chapter reports the generation of KLK14 zymogen in an insect cell expression system, and purification and activation of the zymogen. While the catalytic efficiency for this Sf9 cell-generated KLK14 was lower than that generated by Borgono and colleagues (2007c) in a yeast cell expression system, these differences are likely

accounted for by the difference in glycosylation status. This is also the first report of KLK14 activation of HGF in a dose-dependent manner. Furthermore, this is the first report of Kunitz-type serine protease inhibitors HAI-1A and isoform 1B as KLK14 substrates. Through these experiments a potential role for KLK14 in the regulation of HGFR signalling by two pathways has been revealed, first, directly through KLK14 activation of HGF, and second, indirectly through degradation HAI-1, an inhibitor of a number of HGF-activating proteases.

This is also the first report of hepsin forming stable complexes with HAI-1A. Moreover, in a surprising result, it is also the first report of hepsin degrading HAI-1B. This suggests that HAI-1B is a hepsin substrate as opposed to inhibitor. However, this conclusion requires further experimental examination.

Chapter 4 Proteolytic and cell-surface interactions of KLK14 and other proteases

4.1 Introduction

The KLKs are generated as zymogens requiring activation by limited proteolysis (Borgono and Diamandis, 2004). As they have overlapping tissue distribution, KLKs are prime targets for intra-familial proteolytic cascade studies (Shaw and Diamandis, 2007). Studies of KLK proteolytic cascades have painted a complex picture of KLK inter-activation and regulation by proteolysis as well as participation in cascades with other proteases (Takayama et al., 2001b; Brattsand et al., 2005; Beaufort et al., 2006; Debela et al., 2006b; Borgono et al., 2007c; Yoon et al., 2007; Emami et al., 2008; Emami and Diamandis, 2008; Mukai et al., 2008; Yoon et al., 2008; Beaufort et al., 2010). The S1 residue of KLK4 and KLK14 (Figure 4.1) is an Asp, six residues before the catalytic Ser residue. These two KLKs were predicted to have trypsin-like specificity, cleaving substrates following an Arg or Lys residue (P1) (Nelson et al., 1999; Stephenson et al., 1999; Hooper et al., 2001a; Yousef et al., 2001). Studies have subsequently shown that KLK4 and KLK14 have a preference for cleaving after Arg residues (Takayama et al., 2001b; Brattsand et al., 2005; Felber et al., 2005; Matsumura et al., 2005; Debela et al., 2006a; Debela et al., 2006b; Obiezu et al., 2006; Oikonomopoulou et al., 2006a; Borgono et al., 2007a; Borgono et al., 2007b; Borgono et al., 2007c; Stefansson et al., 2008). Activation of KLK4 and KLK14 requires cleavage after Gln30 for KLK4 (Nelson et al., 1999; Stephenson et al., 1999; Hooper et al., 2001a; Yousef et al., 2001) and after Lys40 for KLK14 (Figure 4.1).

Results published by Yoon and colleagues (2007) showed that while KLK4 and KLK14 may have the potential to activate several members of the KLK family, KLK4 was one of the few KLKs able to proteolyse KLK14 at the pro- region cleavage site, and no KLKs were able to activate KLK4. In addition, they demonstrated that KLK14 had minimal self-activation capacity. In other studies by Brattsand and colleagues (2005) and Borgono and colleagues (2007c) it was found that recombinant KLK14 did not self-activate. However, Borgono and colleagues (2007c) showed that KLK14 readily auto-degraded. Beaufort and colleagues (2010) also found that none of the KLKs they tested was able to activate KLK4. Furthermore, several preferentially degraded KLK4 zymogen, including KLK4 itself. Taken together these results suggest that the proteases responsible for activation of KLK14 and KLK4 may not necessarily be members of the KLK family.

KLK4 and KLK14 are both highly expressed in prostate tissue and have been associated with progression of prostate cancer (Ramsay et al., 2008b). Other proteases that are similarly expressed in the prostate may have roles in activation or deactivation of these KLKs in this tissue. For instance, prostate-expressed transmembrane serine proteases hepsin and TMPRSS2 (TTSP family members) (Figure 4.1) are also associated with prostate cancer progression (Antalis et al., 2011). Furthermore, hepsin (unpublished data (Qiu et al., 2007)) and TMPRSS2 (Afar et al., 2001) autoactivate and so have the potential to be proteolytic cascade initiators (Bugge et al., 2009).

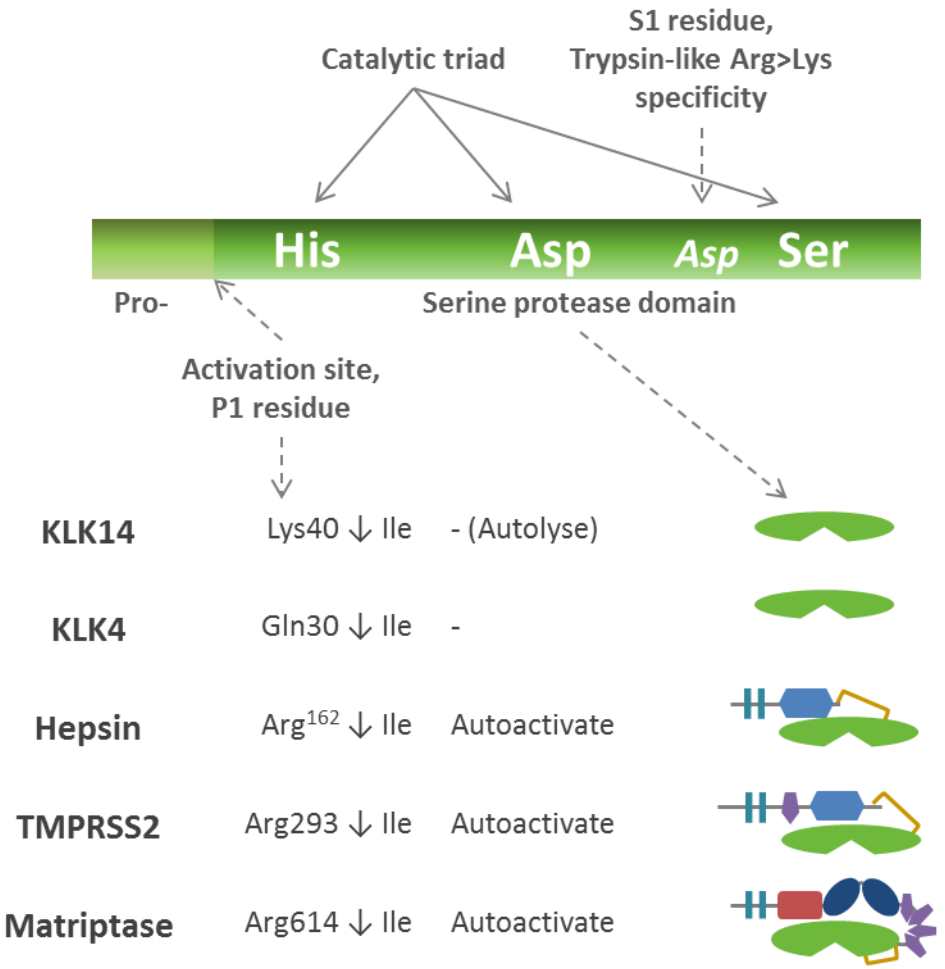

Figure 4.1 Pro-region cleavage site of the serine proteases KLK14, KLK4, hepsin, TMPRSS2 and matriptase. KLK14, KLK4, hepsin, TMPRSS2 and matriptase have an Asp S1 residue located six residues before the catalytic Ser. The P1 residues for activation of pro-KLK14 and pro-KLK4 are Lys and Gln, respectively. KLK14 and KLK4 do not autoactivate but active KLK14 auto-lyses. Hepsin, TMPRSS2 and matriptase each have an Arg P1. Hepsin, TMPRSS2 and matriptase autoactivate and the serine protease domains of these remain tethered to the stem region by an intramolecular disulphide bond.

Hepsin has trypsin-like specificity with a preference for cleaving substrates after an Arg residue (Herter et al., 2005; Beliveau et al., 2009; Owen et al., 2010), and to activate hepsin requires cleavage between Arg162 and Ile163 (Leytus et al., 1988; Somoza et al., 2003). The activation site of TMPRSS2 has been identified as between Arg292 and Ile293 (Afar et al., 2001). However, the preferred P1 substrate of TMPRSS2 is unknown. It is predicted to have trypsin-like specificity with a preference for cleaving substrates after Arg or Lys residues (Paoloni-Giacobino et al., 1997; Wilson et al., 2005).

There is also potential for secreted matrix metalloproteinases MMP3 and MMP9 (Figure 4.2) to participate in proteolytic cascades with the KLKs and TTSPs. These MMPs have also been associated with progression of prostate and other cancers (Deryugina and Quigley, 2006, 2010; Fanjul-Fernandez et al., 2010; Antalis et al., 2011; Gong et al., 2014). It has previously been determined that the autoactivating TTSP matriptase (Takeuchi et al., 2000; Lee et al., 2007) (Figure 4.1) activates MMP3 (Jin et al., 2006; Milner et al., 2010) and further, MMP3 activates KLK4 (Beaufort et al., 2010) and MMP9 (Ogata et al., 1992; Okada et al., 1992; Shapiro et al., 1995; Ramos-DeSimone et al., 1999; Toth et al., 2003).

MMP3 is activated in a stepwise manner (Nagase et al., 1990). Consistent with their specificity, proteases including chymotrypsin, plasma kallikrein and autoactivating matriptase first cleave within a stretch of amino acids (Phe51-Val-Arg-Arg-Lys-Asp56) near the middle of the MMP3 pro-region to yield an intermediate form (Nagase et al., 1990; Milner et al., 2010). This is followed by MMP3 self-activation by cleaving at His99-Phe100 to remove the remaining pro-region yielding a mature peptide (Nagase et al., 1990; Milner et al., 2010; Nagase, 2013) (Figure 4.2). MMP9 can also be activated in two steps. First, MMP3 cleaves between Glu59 and Met60 (Ogata et al., 1992), followed by a second cleavage at Arg106-Phe107 (Shapiro et al., 1995). However, MMP9 can also be activated directly by a single step cleavage between Arg106 and Phe107 by trypsin, KLK1 and other proteases (Desrivieres et al., 1993; Sang et al., 1995). As hepsin and TMPRSS2 have a preference for Arg P1 residues they may also activate these MMPs.

The aim in this chapter was to explore the proteolytic interactions of prostate cancer-associated secreted serine proteases KLK4 and KLK14, and transmembrane serine proteases hepsin and TMPRSS2. The proteolytic interactions between these proteases have not previously been published. Included to lesser extent in this study were secreted matrix metalloproteinases MMP3 and MMP9 and transmembrane serine proteases

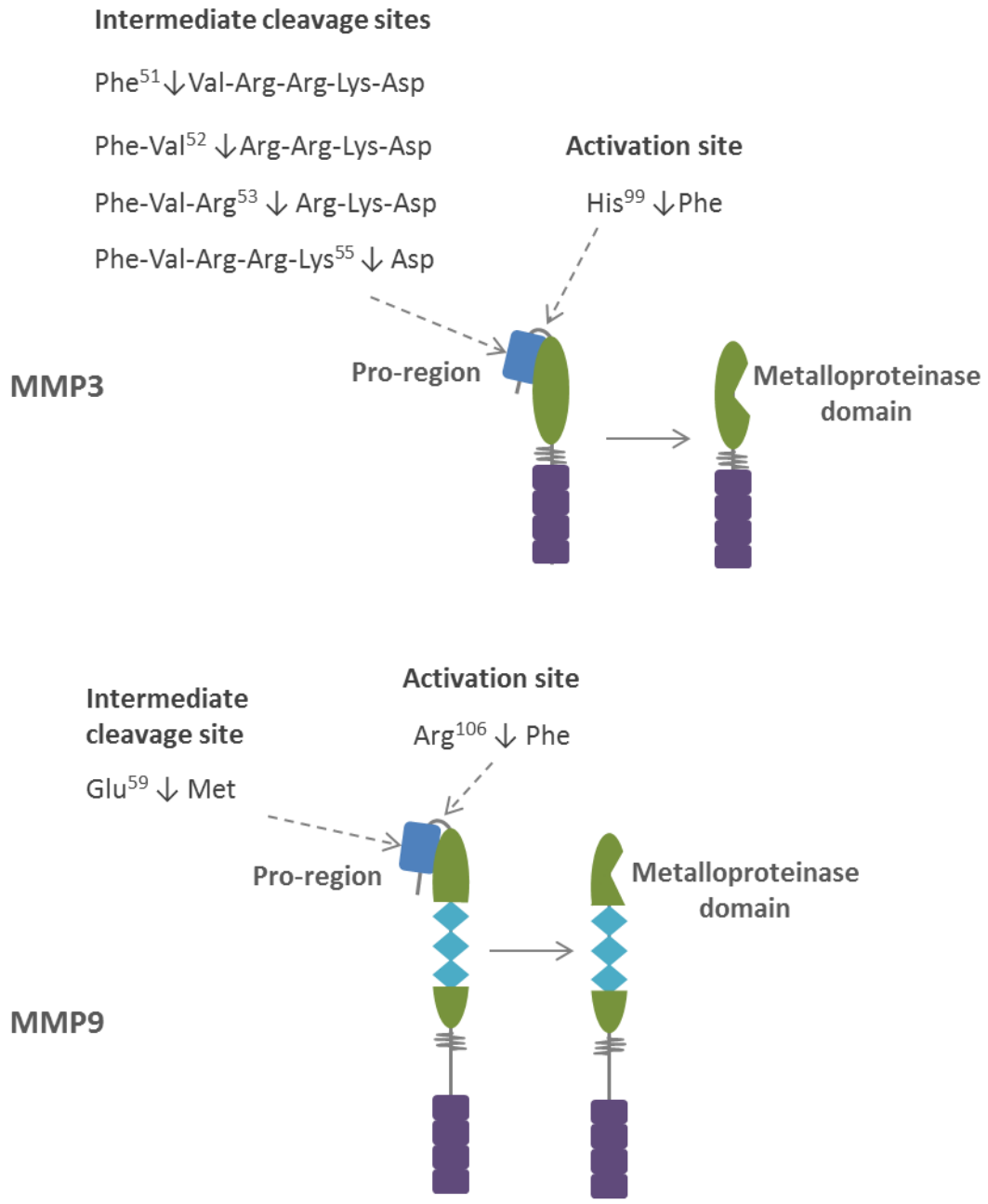

Figure 4.2 Pro-region cleavage sites and stepwise activation of the matrix metalloproteinases MMP3 and MMP9. A cysteine in the pro-region coordinates with zinc in the metalloproteinase domain to keep the protease inactive. Activation requires proteolytic removal of the pro-region or physical removal of the cysteine from coordination with the zinc. MMP3 is activated in a stepwise manner by protease cleavage at one of the intermediate sites followed by self-activation at the second site. MMP9 can also be activated in a stepwise manner by MMP3 which cleaves at the first site followed by the second site. Otherwise, MMP9 can be activated directly in a single step at the second site by several other proteases.

matriptase and enteropeptidase. Matriptase was included in this study as it is a known MMP3 activator. Enteropeptidase was included as it has a preference for Lys P1 residues (Zheng et al., 2009). Furthermore, while enteropeptidase has previously been used to activate KLK14 *in vitro* (Brattsand et al., 2005) it has not been investigated as an endogenous KLK14 activator. The techniques used in this chapter to examine the interactions between these proteases include co-expression models and recombinant protein assays as well as co-immunoprecipitation studies. As hepsin and TMPRSS2 are transmembrane proteases cell-surface expression analysis by cell-surface biotinylation was also included in the study.

4.2 Results

4.2.1 Proteolytic interactions of KLK14, KLK4, hepsin, TMPRSS2 and enteropeptidase

To investigate the proteolytic interactions between the secreted proteases KLK14 and KLK4 and the transmembrane serine proteases hepsin, TMPRSS2 and enteropeptidase, transient transfections and co-transfections into Cos-7 cells were conducted using constructs encoding each of the proteases, as well as constructs encoding active-site serine-to-alanine (SA) mutants of each protease. By using constructs encoding active-site mutants of the proteases, proteolysis of/by a protease can be attributed accordingly. For ease of detection of the proteases by Western blot analysis, all the constructs, except the one encoding enteropeptidase, were engineered to encode each protease with a C-terminal epitope tag, such as HA, Myc, Flag or V5. Purified recombinant proteases, when available, were also used in co-incubations to examine the proteolytic interactions further. Number of replicates are stated in figure legends, otherwise N=1.

4.2.1.1 Co-expression or co-incubation of KLK14 with KLK4 does not result in proteolysis

As mentioned in the introduction, results published by Yoon and colleagues (2007) showed the potential for KLK4 activation of KLK14, but not vice versa. Two approaches were taken to further investigate the potential for KLK14 and KLK4 cross-activation or proteolysis. First, analysis was performed on conditioned media from cells co-transfected with expression constructs encoding these proteases. Second, conditioned media from cells transfected with only one of these expression constructs

were incubated for between 0 and 24 hours with the conditioned media from cells transfected with the other expression construct. To analyse the status of KLK14 and KLK4 proteolysis, conditioned media from each approach were then examined by Western blot analysis using anti-Myc and anti-V5 antibodies.

These analyses revealed that KLK14 does not proteolyse KLK4 and KLK4 does not proteolyse KLK14 when co-expressed (Figure 4.3A) or when co-incubated (Figure 4.3B). The same result was obtained when the co-incubation assay was conducted using cells transfected and grown under serum-free-media conditions (data not shown). The minor variations in band intensity of mutant or wild-type KLK4 or KLK14 observed in these analyses were not attributed to proteolysis by KLK4 or KLK14 as they were not observed consistently in other analyses (data not shown) or did not correlate consistently with wild-type KLK4 or KLK14 co-expression. Instead these variations were attributed to gel loading or Western blot transfer inconsistencies.

4.2.1.2 Transfected hepsin self-activates in Cos-7 cells

Several TTSPs self-activate, including TMPRSS2 (Afar et al., 2001) and matriptase (Takeuchi et al., 2000; Lee et al., 2007). So in this section, to confirm results by Qiu and colleagues (2007), the potential for hepsin to self-activate was examined.

To determine whether hepsin will self-activate in transiently transfected Cos-7 cells, a construct encoding active-site mutant hepsin with a C-terminal Myc tag, hepsinSA-Myc, was co-transfected with constructs encoding wild-type or active-site mutant hepsin with a C-terminal Flag tag, hepsin-Flag or hepsinSA-Flag. As hepsin localizes to the plasma membrane (Tsuji et al., 1991; Kazama et al., 1995; Zacharski et al., 1998) cell lysates were examined by Western blot analysis using anti-Myc and anti-Flag antibodies. When hepsin is activated by limited proteolysis, the serine protease domain remains tethered to its stem region by a disulphide bond (Leytus et al., 1988; Somoza et al., 2003) (see Figure 4.1 for the domain structure schematic of hepsin). Therefore, when activated hepsin is examined under reducing conditions, the disulphide bond is reduced allowing the serine protease domain to run on the gel separated from the stem region. As the overexpressed hepsin has a C-terminal epitope tag, under reducing conditioned the anti-Myc and anti-Flag antibodies detect unactivated full-length hepsin, the separated serine protease domain, as well as any other forms that have the C-terminal and epitope tag.

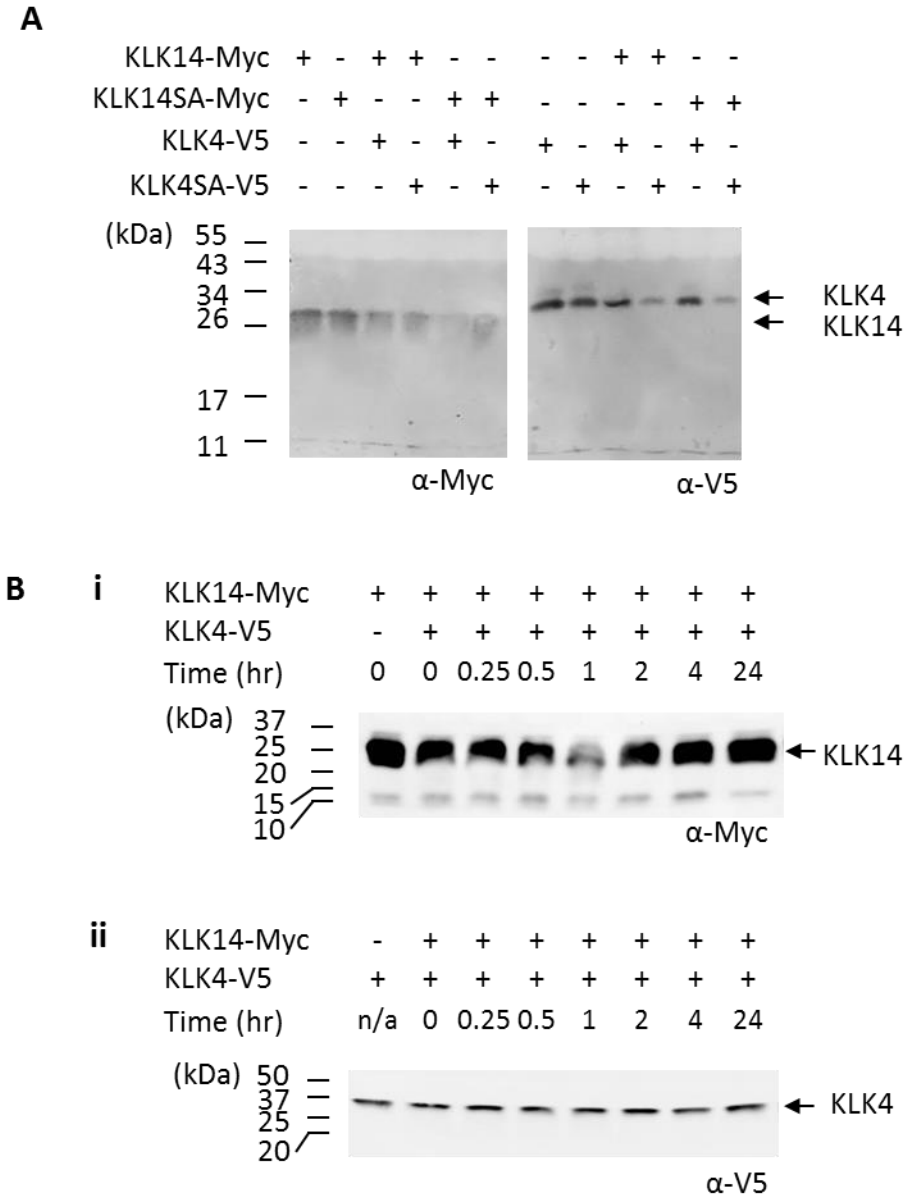

Figure 4.3 Co-expression or co-incubation of KLK14 with KLK4 does not result in proteolysis. A. Cos-7 cells were transiently transfected with constructs encoding wild-type or active-site mutant KLK14 (KLK14-Myc and KLK14SA-Myc) and co-transfected with constructs encoding wild-type or active-site mutant KLK4 (KLK4-V5 and KLK4-V5). After 24 hours, the conditioned media was subjected to SDS-PAGE under reducing conditions followed by analysis by Western blot using anti-Myc and anti-V5 antibodies, as indicated. Representative data from one of two experiments shown. **B**. Conditioned media from cells transiently transfected for 24 hours with constructs encoding either KLK14-Myc or KLK4-V5 were co-incubated for between 0 and 24 hours (as indicated). The co-incubated media was subjected to SDS-PAGE under reducing conditions followed by analysis by Western blot using anti-Myc and anti-V5 antibodies, as indicated. KLK4 was detected at 33 kDa. KLK14 was detected at 28 kDa.

As shown in Figure 4.4, hepsin-Myc, and hepsinSA-Myc, hepsin-Flag and hepsinSA-Flag each migrate to a position indicating a MW of 45 kDa, representing unactivated full-length hepsin. In addition, in assays in which cells were transfected with only a single expression construct, both hepsin-Myc and hepsin-Flag have a 26 kDa band that represents the serine protease domain of activated hepsin (Figure 4.4i, lane 1; Figure 4.4ii, lane 4 and 6). This serine protease domain band is absent from cells expressing active-site mutants hepsinSA-Myc or hepsinSA-Flag (Figure 4.4i, lane 2; Figure 4.4ii, lane 4 and 6) indicating that hepsin activation occurs via an autocatalytic mechanism. Consistent with this proposal, anti-Myc Western blot analysis of lysates from cells co-transfected with hepsin-Flag and active-site mutant hepsinSA-Myc revealed the hepsin-Myc serine protease domain migrating at 26 kDa (Figure 4.4i, lane 3). This 26 kDa band was not apparent from cells co-expressing catalytically inactive hepsinSA-Myc and active-site mutant hepsinSA-Flag (Figure 4.4ii, lane 4). These data indicate that hepsin is capable of undergoing autocatalytic activation.

These analyses also indicated further hepsin activity and self-proteolysis as there are also 30 kDa bands for hepsin-Myc and hepsin-Flag (Figure 4.4i, lane1 and Figure 4.4ii, lanes 3 and 5) that are absent for hepsinSA-Myc and hepsinSA-Flag (Figure 4.4i, lane 2; Figure 4.4ii, lane 4 and 6). However, the 30 kDa band is also generated when hepsinSA-Myc is co-expressed with hepsin-Flag (Figure 4.4i, lane3). Therefore, this 30 kDa band is also a product of hepsin proteolysis.

There are two further cleaved forms of hepsin detected by the anti-Flag and anti-Myc antibodies represented by 32 and 35 kDa bands. These forms are generated in part or completely by another protease as they are present for hepsin and hepsinSA alike. In addition, both hepsin and hepsin SA form SDS- and β-mercaptoethanol-stable complexes that can be seen at MWs above 90 kDa.

The significance of these alternate cleavage sites is unknown. They do not result in shedding of hepsin as it was not detected in the conditioned media (data not shown), nor was it detected in cell lysates under non-reducing conditions (data not shown), suggesting the cleaved forms remain attached to the stem via disulphide bonds. These forms will be discussed further in later sections.

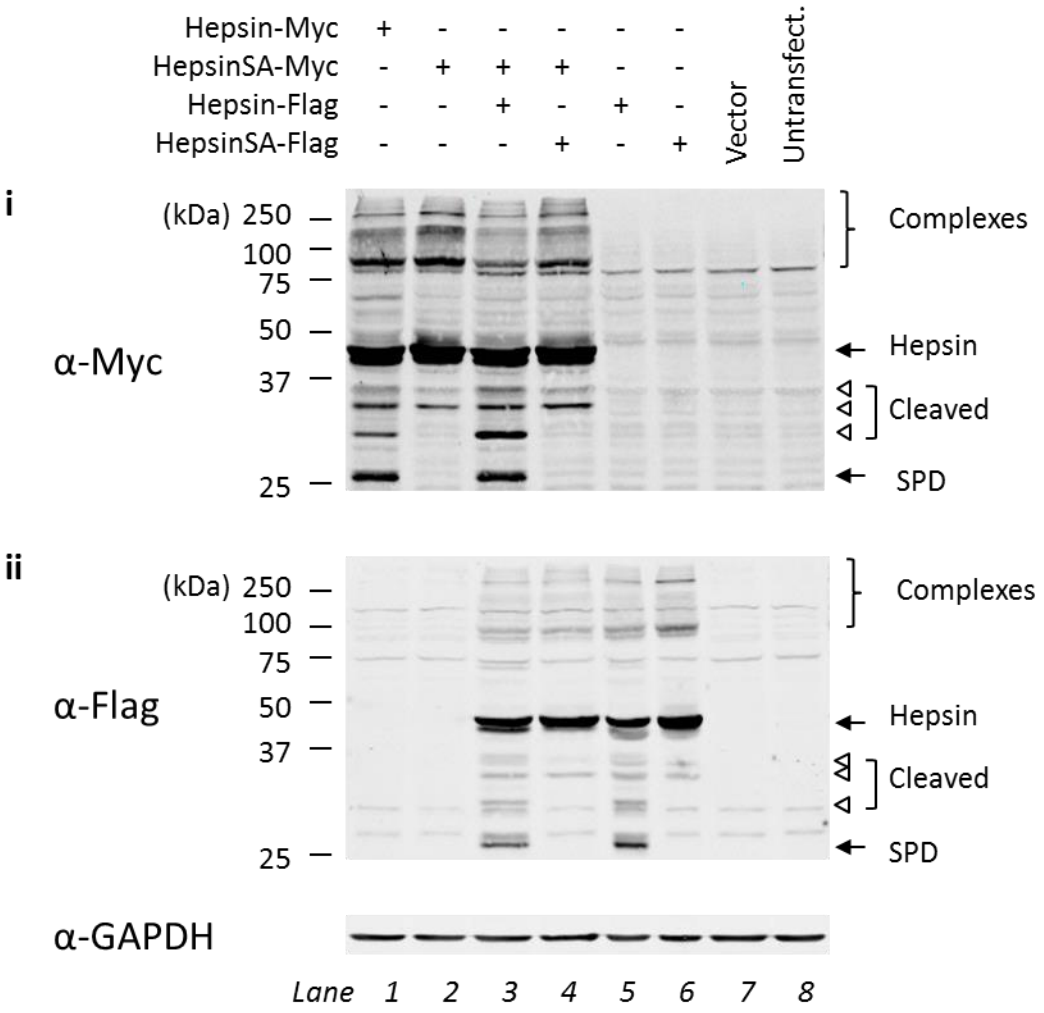

Figure 4.4 Hepsin self-activates in Cos-7 cells. Cells were transiently transfected with constructs encoding either wild-type or active-site mutated hepsin with C-terminal Myc tag (hepsin-Myc and hepsinSA-Myc) and co-transfected with constructs encoding wild-type or active-site mutated hepsin with C-terminal Flag tag (hepsin-Flag and hepsinSA-Flag) as indicated. Whole-cell lysate (WCL) was collected 24 hours post-transfection and subjected to SDS-PAGE under reducing conditions followed by analysis by Western blot using anti-Myc and anti-Flag antibodies as indicated. Anti-GAPDH probe of WCL blot was performed to examine protein loading. Full-length hepsin and hepsinSA were detected at 45 kDa. The hepsin serine protease domain (SPD) was detected at 26 kDa for hepsin-Myc (**i**, lane 1) and hepsin-Flag (**ii**, lanes 3 and *5*). HepsinSA-Myc SPD was detected at 26 kDa when co-expressed with hepsin-Flag (**i**, lane 3). Other forms of hepsin/hepsinSA detected include complexes >90 kDa (*braces*) and cleaved forms at 30, 35 and 36 kDa (*open arrowheads*).

4.2.1.3 Pericellular proteolysis of KLK14 by hepsin

As hepsin autoactivation in transiently transfected Cos-7 cells has been established, this knowledge can be used as a basis to examine the proteolysis of other proteases by hepsin. For this purpose hepsin-Myc and hepsinSA-Myc were co-expressed with KLK14HA or KLK14SA-HA and conditioned media and cell lysates were examined by Western blot analysis.

As shown in Figure 4.5, both KLK14 and KLK14SA migrated as 28 kDa in conditioned media without decrease in signal intensity indicating that they were unaffected by co-expression with either wild-type or catalytically inactive hepsin (Figure 4.5A, Media, lanes 3 and 5). However, surprisingly, analysis of cell lysates showed that cell-retained KLK14 and KLK14SA are cleaved by hepsin to 26 and 27 kDa, respectively (Figure 4.5A, WCL, lanes 3 and 5).

Consistent with the data shown in Figure 4.4, anti-Myc Western blot analysis for hepsin indicated that this protease autoactivates as evidenced by the presence of the 26 kDa serine protease domain (Figure 4.5B, WCL, lanes 1, 3 and 5). In addition, it is apparent from the analysis in Figure 4.5B that KLK14 did not proteolyse hepsin or hepsinSA. In data not shown, analysis of hepsin in conditioned media confirmed previous findings (Tsuji et al., 1991) that hepsin is not shed from the cell surface. Moreover, co-expression with KLK14 did not alter this.

4.2.1.4 Pericellular proteolysis of KLK14 by TMPRSS2

To examine the proteolytic relationship of autoactivating TMPRSS2 and KLK14, TMPRSS2-Myc and TMPRSS2SA-Myc were co-expressed with KLK14HA or KLK14SA-HA and conditioned media and cell lysates were examined by Western blot analysis. TMPRSS2 is similar to hepsin in that when activated, the serine protease domain remains tethered by a disulphide bond to its stem region (Paoloni-Giacobino et al., 1997) (See Figure 4.1 for TMPRSS2 domain structure schematic). Therefore, when examined under reducing conditions, the disulphide bond is reduced and the serine protease domain runs separately from the stem region of TMPRSS2. Like hepsin, TMPRSS2 is localized on the plasma membrane (Paoloni-Giacobino et al., 1997; Jacquinet et al., 2001; Chen et al., 2010b). However, in contrast with hepsin, studies have demonstrated that endogenous TMPRSS2 expressed by LNCaP cells is shed from

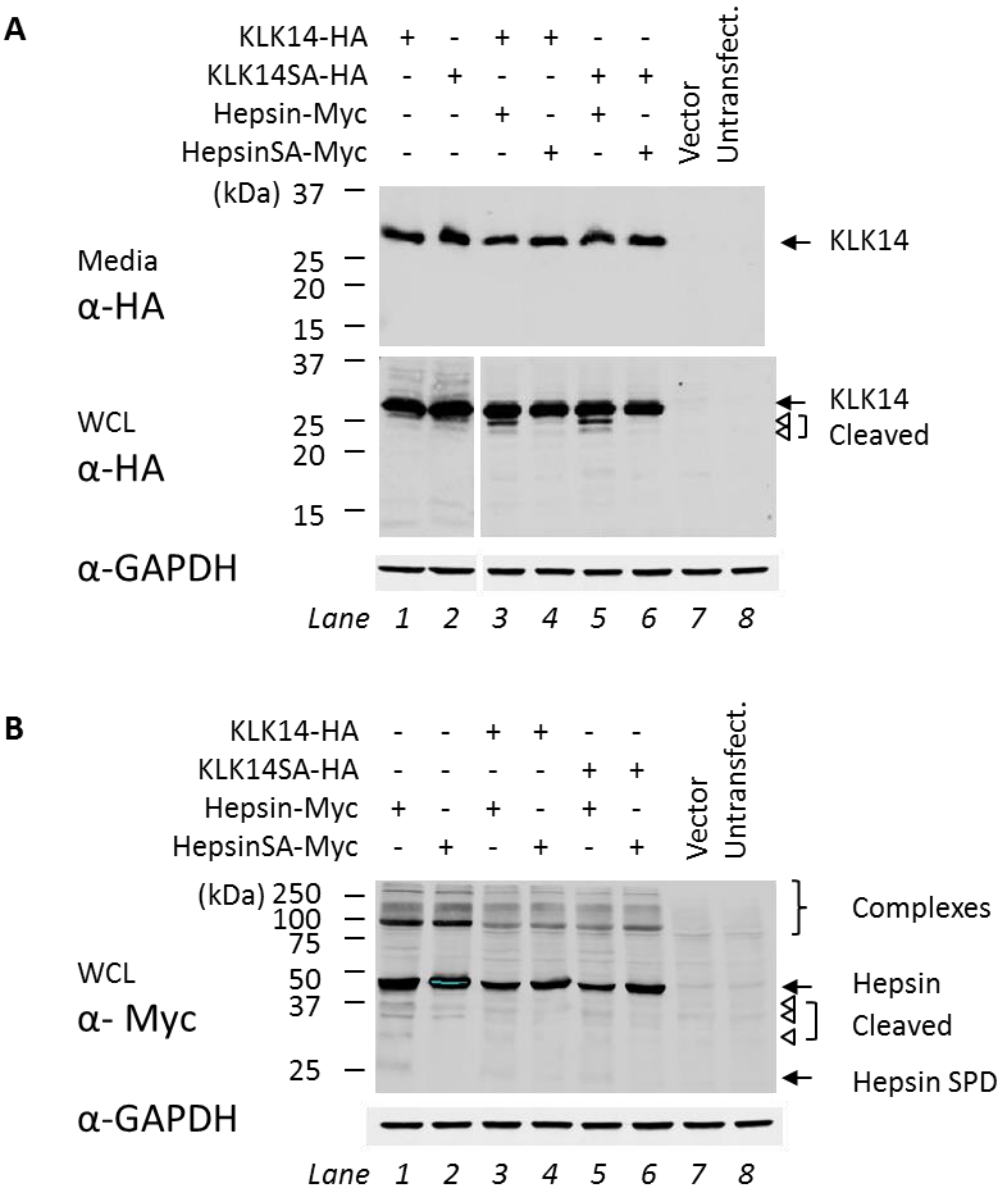

Figure 4.5 KLK14 is proteolysed when co-expressed with hepsin. Cos-7 cells were transiently transfected with constructs encoding either KLK14-HA or active-site mutated KLK14SA-HA and co-transfected with constructs encoding either hepsin-Myc or active-site mutated hepsinSA-Myc, as indicated. After 24 hours, media and whole-cell lysates (WCL) were subjected to reducing SDS-PAGE followed by Western blot analysis using anti-HA and anti-Myc antibodies, as indicated. Anti-GAPDH probe of WCL blots was performed to examine protein loading. **A.** KLK14-HA and KLK14SA-HA was detected in media at 28 kDa. When co-expressed with hepsin-Myc, cleaved KLK14-HA and KLK14SA-HA were detected in WCL at 24 and 26 kDa. (lanes 3 and 5). **B.** Hepsin-Myc and hepsinSA-Myc were not detected in the media. In the WCL, full-length hepsin-Myc and hepsinSA-Myc were detected at 45 kDa. Hepsin-Myc serine protease domain (SPD) was detected at 26 kDa (lanes 1, 3 and 5). Other hepsin/SA cleaved forms detected at 30, 35 and 36 kDa (*open arrowheads*) and complexes at >90 kDa (*brace*) are indicated. Representative data from one of two experiments shown.

the cell surface into the extracellular medium when the cells are treated with androgens but not in the absence of androgen treatment (Afar et al., 2001; Chen et al., 2010b).

As shown in Figure 4.6, 28 kDa KLK14 and KLK14SA are depleted from the media when co-expressed with TMPRSS2 (Figure 4.6A, Media, lanes 3 and 5) but not when co-expressed with active-site mutant TMPRSS2SA (Figure 4.6A, Media, lanes 4 and 6). Furthermore, examination of the cell lysate analysis (Figure 4.6A, WCL) shows that the 28 kDa KLK14 and KLK14SA are accompanied by a 27 kDa band which has a marginally increased signal intensity when co-expressed with TMPRSS2 (Figure 4.6A, WCL, lanes 3 and 5). These data suggest that similar to hepsin, TMPRSS2 is able to cleave cell-retained KLK14, albeit with less efficiency.

The analysis of TMPRSS2 expression in cell lysates in Figure 4.6B shows bands representing full-length TMPRSS2 at 53 kDa, and high MW complexes at >200 kDa. The analysis also conforms to a previous finding by Afar and colleagues (2001) that TMPRSS2 self-activates. This is evident from the 25 kDa band representing the serine protease domain of TMPRSS2 (Figure 4.6B, WCL, lanes 1, 3 and 5). The absence of this band for TMPRSS2SA demonstrates that integrity of the active-site is a requirement for TMPRSS2 activation (Figure 4.6B, WCL, lanes 2, 4 and 6). There are also cleaved forms of TMPRSS2 at 50, 40, 36, 35 and 30 kDa (Figure 4.6B, WCL, lanes 1, 3 and 4). With the exception of the 50 and 40 kDa bands, the low MW forms appear to be a result of self-proteolysis as they are absent for TMPRSS2SA (Figure 4.6B, lanes 2, 4 and 6). Interestingly, TMPRSS2SA (Figure 4.6B, WCL, lanes 2, 4 and 6) also has a band at around 54 kDa that is absent for TMPRSS2 (Figure 4.6B, WCL, lanes 1, 3 and 6) suggesting that this band was eliminated by TMPRSS2-dependent proteolysis. In data not shown, analysis of TMPRSS2 expression in conditioned media showed that it was not shed from the cell surface. Moreover, similar to the studies with KLK14 and hepsin, there is no indication in the analyses that KLK14 proteolysed TMPRSS2.

4.2.1.5 KLK14 proteolyses GAPDH

An unexpected finding was made during transient transfection assays to determine the proteolytic relationship between KLK14 and the transmembrane serine protease enteropeptidase. In these assays, Cos-7 cells were co-transfected with KLK14-HA and enteropeptidase, or the conditioned media from KLK14-HA transfected cells were applied to untransfected cells or cells transfected with enteropeptidase. Cell lysates were

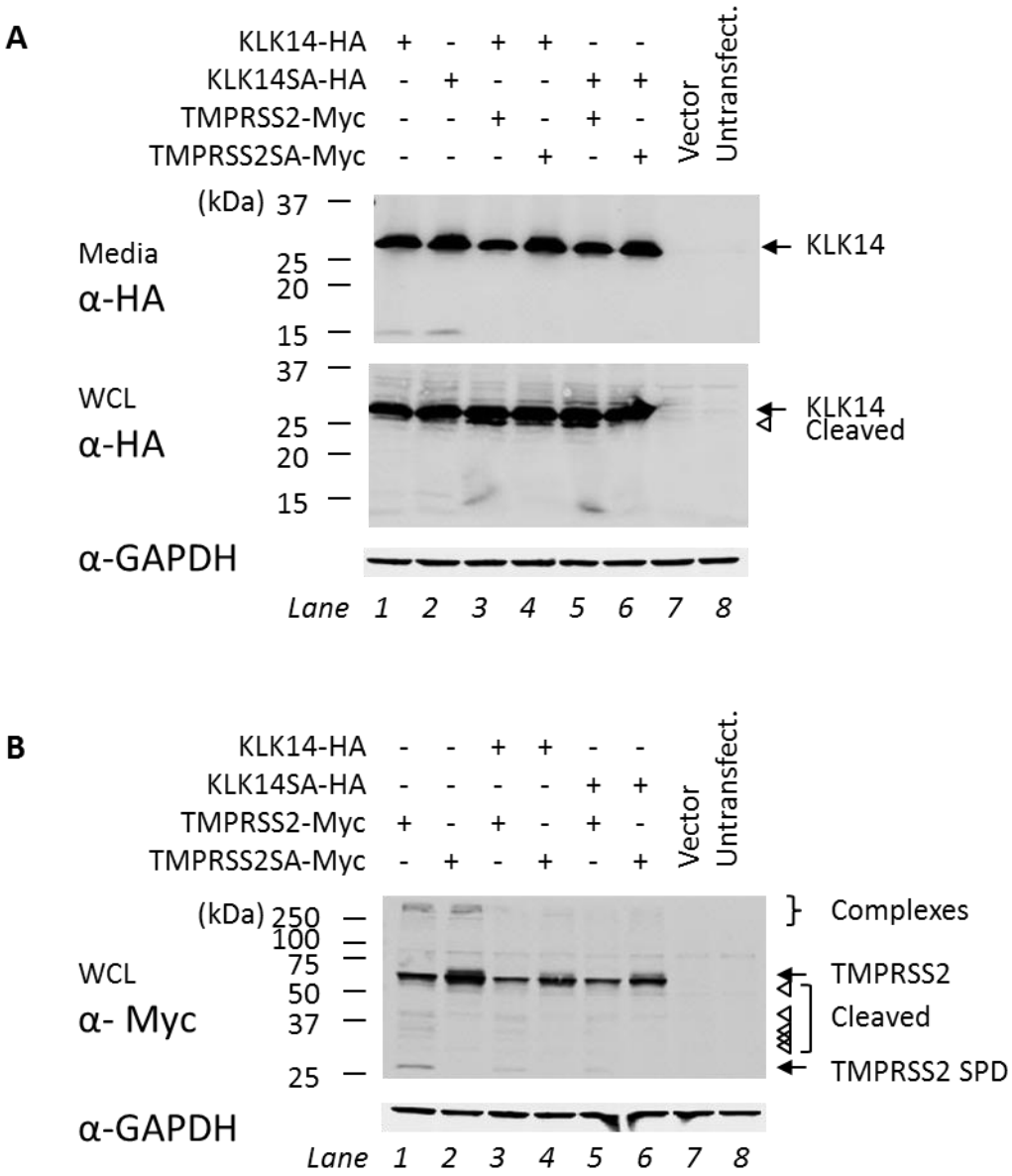

Figure 4.6 KLK14 is proteolysed when co-expressed with TMPRSS2. Cos-7 cells were transiently transfected with either KLK14-HA or active-site mutated KLK14SA-HA and co-transfected with constructs encoding either TMPRSS2-Myc or active-site mutated TMPRSS2SA-Myc, as indicated. After 24 hours media and whole-cell lysates (WCL) were subjected to reducing SDS-PAGE followed by Western blot analysis using anti-HA and anti-Myc antibodies, as indicated. Anti-GAPDH probe of WCL blots was performed to examine protein loading. **A.** KLK14 and KLK14SA was depleted from the media and cleaved to 27 kDa in the WCL when co-expressed with TMPRSS2 (lanes 3 and 5). **B.** TMPRSS2 and TMPRSS2SA were not detected in the media (data not shown). In the WCL full-length TMPRSS2 and TMPRSS2SA were detected at 53 kDa. TMPRSS2 serine protease domain (SPD) was detected at 25 kDa (lanes 1, 3 and 5). Other TMPRSS2/SA cleaved forms detected at 50, 40, 36, 35 and 30 kDa (*open arrowheads*) and complexes at >250 kDa (*brace*) are indicated. Representative data from one of two experiments shown.

then examined using anti-enteropeptidase, anti-KLK14 and anti-GAPDH antibodies. The anti-enteropeptidase antibody was not specific and so the data from this is not presented.

However, the anti-GAPDH Western blot analyses showed that KLK14 degraded GAPDH, independently of co-transfection with the enteropeptidase expression construct. As shown in the Western blot analysis when KLK14-HA is transfected, 37 kDa GAPDH is completely degraded (Figure 4.7A, lanes 2, 3, 6 and 7; Figure 4.7B, lanes 4-6). Similarly, when the conditioned media, from cells transfected with KLK-HA, are applied to untransfected cells, GAPDH is partially degraded into fragments ranging from 35 to <20 kDa (Figure 4.7B, lanes 1 and 2).

GAPDH is a ubiquitously expressed intracellular protein and is routinely used as a housekeeping protein in Western blot analysis (Sirover, 2012). As GAPDH is intracellular, degradation by exogenously applied KLK14-HA is likely to be due to the accidental omission of the protease inhibitor cocktail in the cell lysis buffer when preparing cell lysates. It remains undetermined whether release of intracellular proteases during cell lysis activated KLK14, or whether KLK14 was active prior to this. However, the intracellular proteases do not mediate GAPDH degradation as it only occurs in Cos-7 cells transfected with KLK14-HA or when it is exogenously applied. To be clear, this was an incidental finding and the degradation of GAPDH was not seen at any other time during the course of this project.

However, this observation may have significance because in addition to being an intracellular protein in eukaryotic cells, GAPDH is also cell-surface expressed by a number of pathogens including bacteria such as group A streptococci (*Streptococcus pyogenes*) and several mycoplasmas, and also fungal pathogens such as *Candida albicans* (Pancholi and Chhatwal, 2003). Cell-surface expressed GAPDH is thought to act as a virulence factor mediating pathogen activities including adhesion to tissues, invasion, and immune modulation and surveillance evasion (Seidler, 2013). For instance, bacterial GAPDH binds host plasminogen and plasmin, and facilitates plasminogen conversion to plasmin. This allows the bacteria to dysregulate plasmin activity, localizing activity leading to disruption of tissue barriers and facilitating invasion (Seidler, 2013). Furthermore, GAPDH is highly conserved, with pathogenic bacterial GAPDH having >40% sequence identity to human GAPDH (Seidler, 2013); therefore, KLK14 may also degrade extracellular bacterial GAPDH. This may be relevant to host defence as KLK14

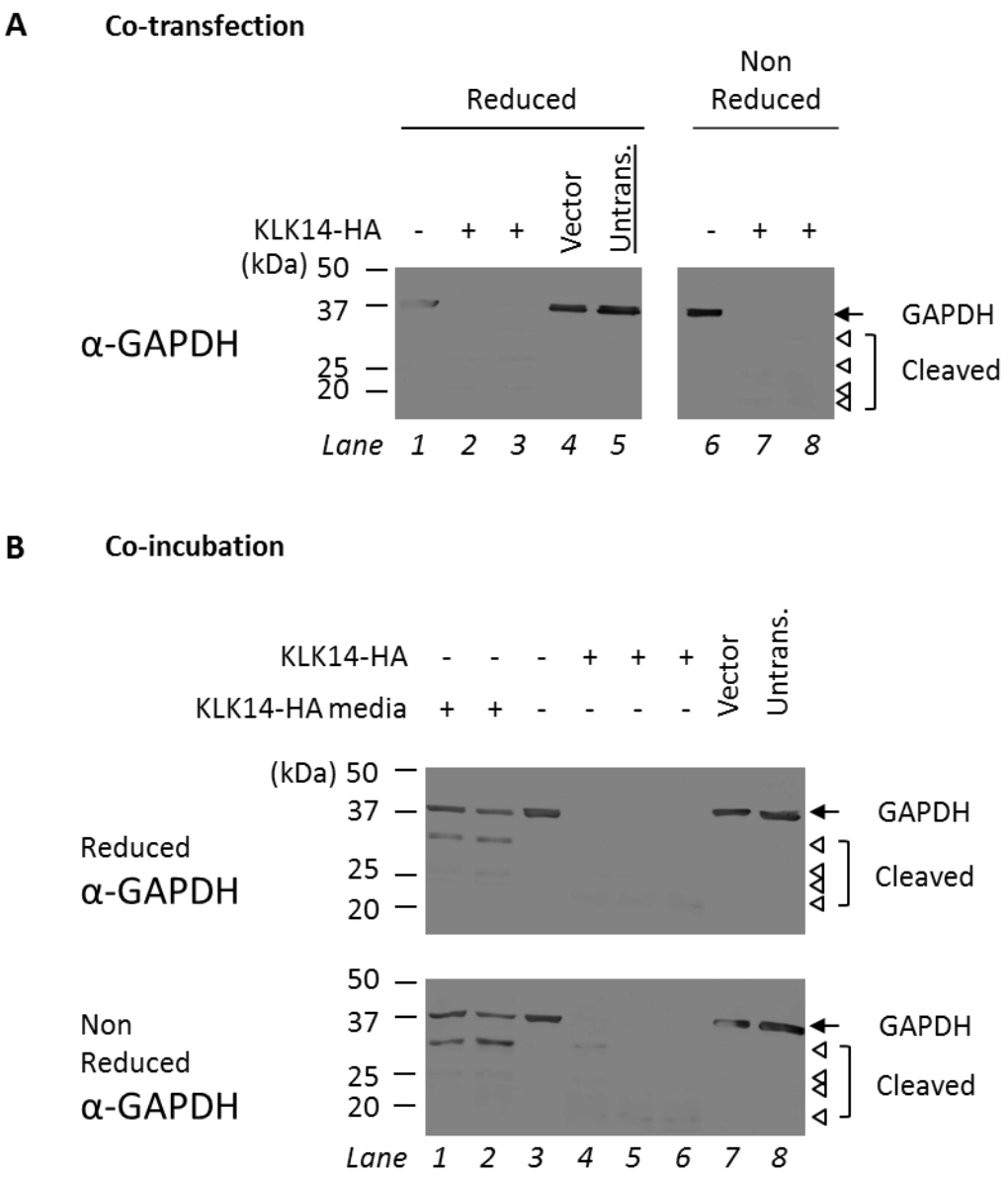

Figure 4.7 KLK14 proteolyses endogenous GAPDH. A. Cos-7 cells were transiently transfected with a construct encoding KLK14-HA. Conditioned media and whole-cell lysates (WCL) were collected 24 hours post-transfection and subjected to SDS-PAGE followed by Western blot analysis using anti-HA antibody. Anti-GAPDH probe of WCL blots was performed to examine protein loading. GAPDH was degraded when cells were transfected with KLK14 (lanes 2, 3, 7 and 8). **B.** Conditioned media was collected from Cos-7 cells transiently transfected for 24 hours with a construct encoding KLK14-HA. Untransfected cells were then co-incubated for 1 hour with conditioned media from KLK14-HA transfected cells. Whole-cell lysates (WCL) were collected and subjected to SDS-PAGE followed by Western blot analysis using anti-HA antibody as well as anti-GAPDH to examine protein loading. GAPDH was degraded when cells were co-incubated with conditioned media from KLK14-HA transfected cells (lane 1,2) or when cells were transfected with KLK14-HA (lanes 4-6).

is highly expressed in the skin as well as in a number of other tissues (Borgono et al., 2003; Komatsu et al., 2005; Borgono et al., 2007c; Shaw and Diamandis, 2007). Specifically, the highest expression in the skin is in the intra-epidermal and eccrine sweat glands (Borgono et al., 2003; Stefansson et al., 2006) and it is secreted in sweat (Komatsu et al., 2006). This specific, localized expression of KLK14 may decrease the incursion of pathogenic bacteria through the epidermal layers by way of the sweat glands.

Unfortunately, this hypothesis was not pursued further as the possible significance of the observation that KLK14 mediates GAPDH degradation was not noted until after the completion of laboratory work. Moreover, it is outside of the scope of this PhD investigation. However, the observation merits communication as it may lead to therapeutic strategies for managing bacterial and fungal pathogens.

4.2.1.6 Pericellular proteolysis of KLK4 by hepsin

To examine the proteolytic relationship of hepsin and KLK4, hepsin-Flag or active-site mutant hepsinSA-Flag were co-expressed with KLK4-V5 or active-site mutant KLK4SA-V5 and conditioned medium and cell lysate were examined by Western blot analysis under reducing conditions.

As shown in Figure 4.8, KLK4 and KLK4SA appear in the media at 33 kDa (Figure 4.8A, Media). When co-expressed with hepsin, KLK4 and KLK4SA levels appear diminished in the conditioned media (Figure 4.8A, Media, lanes 3 and 5) – but also diminished when co-expressed with hepsinSA. In the cell lysate analysis, hepsin proteolyses KLK4 and KLK4SA, increasing the signal intensity of a band at 17 kDa (Figure 4.8A, WCL, lanes 3 and 5).

Analysis of hepsin and hepsinSA in media (data not shown) and lysates (Figure 4.8B) shows a similar pattern of expression and cleavage to that previously shown in Figures 4.4 and 4.5. As noted earlier in Figure 4.4, there are 35 and 36 kDa forms of hepsin and hepsinSA that are partly generated by another protease as they are present independent of hepsin active-site integrity. However, interestingly, when hepsinSA is co-expressed with KLK4, the hepsinSA bands at 35 and 36 kDa increase in signal intensity (Figure 4.8B, WCL, lane 4) compared to when hepsin SA is transfected alone or with KLK4SA

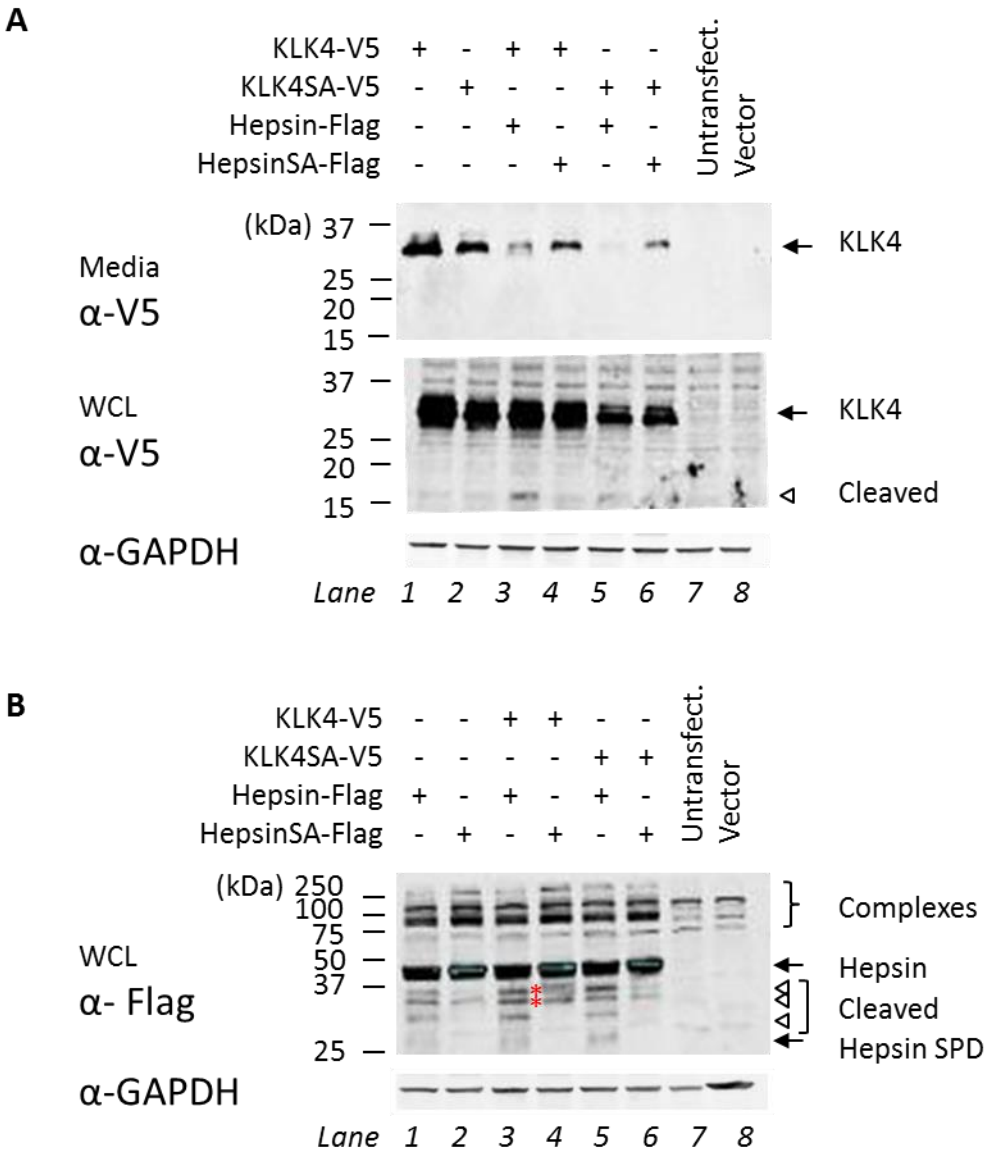

Figure 4.8 KLK4 is proteolysed when co-expressed with hepsin. Cos-7 cells were transiently transfected with constructs encoding either KLK4-V5 and or active-site mutated KLK4SA-V5 and co-transfected with constructs encoding either hepsin-Flag or active-site mutated hepsinSA-Flag, as indicated. After 24 hours, media and whole-cell lysates (WCL) were subjected to reducing SDS-PAGE followed by Western blot analysis using anti-V5 or anti-Flag antibodies, as indicated. Anti-GAPDH probe of WCL blots was performed to examine protein loading. **A.** In the media, 33 kDa KLK4 and KLK4SA (lanes 3 and 5) were depleted when co-expressed with hepsin. In WCL, cleaved KLK4 and KLK4SA 17 kDa were detected when co-expressed with hepsin (lanes 3 and 5). **B.** Hepsin and hepsinSA were not detected in the media (data not shown). In the WCL, full-length hepsin and hepsinSA were detected at 45 kDa. Hepsin serine protease domain (SPD) was detected at 26 kDa (lanes 1, 3 and 5). Other hepsin/SA cleaved forms detected at 30, 35 and 36 kDa (*open arrowheads, red asterisk indicate KLK4 generated forms*) and complexes >90 kDa (*brace*) are indicated. Representative data from one of three experiments shown.

(Figure 4.8B, WCL, lanes 2 and 6). Therefore, this indicates that KLK4 was active in the transient transfection and that it proteolysed hepsinSA.

4.2.1.7 Pericellular proteolysis of KLK4 by TMPRSS2

To examine the proteolytic relationship of TMPRSS2 and KLK4, TMPRSS2-Myc or active-site mutant TMPRSS2SA-Myc were co-expressed with KLK4-V5 or active-site mutant KLK4SA-V5 and conditioned medium and cell lysate were examined by Western blot analysis under reducing conditions.

These analyses showed that KLK4 and KLK4SA appear in media at 33 kDa (Figure 4.9A, Media). When co-expressed with TMPRSS2, KLK4 and KLK4SA (Figure 4.9A, Media, lanes 3 and 5) are converted to 31 kDa KLK4 and KLK4SA forms. This MW shift is representative of a proteolytic event at the N-terminal of KLK4 and KLK4SA as the forms were detected by antibodies to the C-terminal epitope tag. Analysis of cell lysates indicated that cell-retained KLK4 and KLK4SA are similarly converted to lower MW 31 kDa forms (Figure 4.9A, WCL, lane 3and 5). These data indicate that KLK4 is able to be cleaved by TMPRSS2.

Analysis for the presence of TMPRSS2 and TMPRSS2SA in media (data not shown) and lysates (Figure 4.9B) shows a very similar pattern to that previously shown in Figure 4.6. However, interestingly, when examining the multiple cleaved forms of TMPRSS2 and TMPRSS2SA, it is evident that when co-expressed with KLK4, the 30 kDa TMPRSS2 and TMPRSS2SA band increases in intensity (Figure 4.9B, WCL, lane 3 and 4). Therefore, these data indicate KLK4 was active and it proteolysed TMPRSS2 and TMPRSS2SA.

4.2.1.8 Recombinant hepsin proteolyses recombinant pro-KLK14 and pro-KLK4

KLK14 and KLK4 are cleaved as a result of hepsin expression at the cell surface and it appears that this transmembrane protease leads to reduced levels of KLK4 present in media (Figures 4.5A and 4.8A). The ability of hepsin to directly cleave KLK4 and KLK14 was examined using purified active recombinant hepsin and zymogens of KLK4 and KLK14 (pro-KLK14 and pro-KLK4). The hepsin used in these assays is a

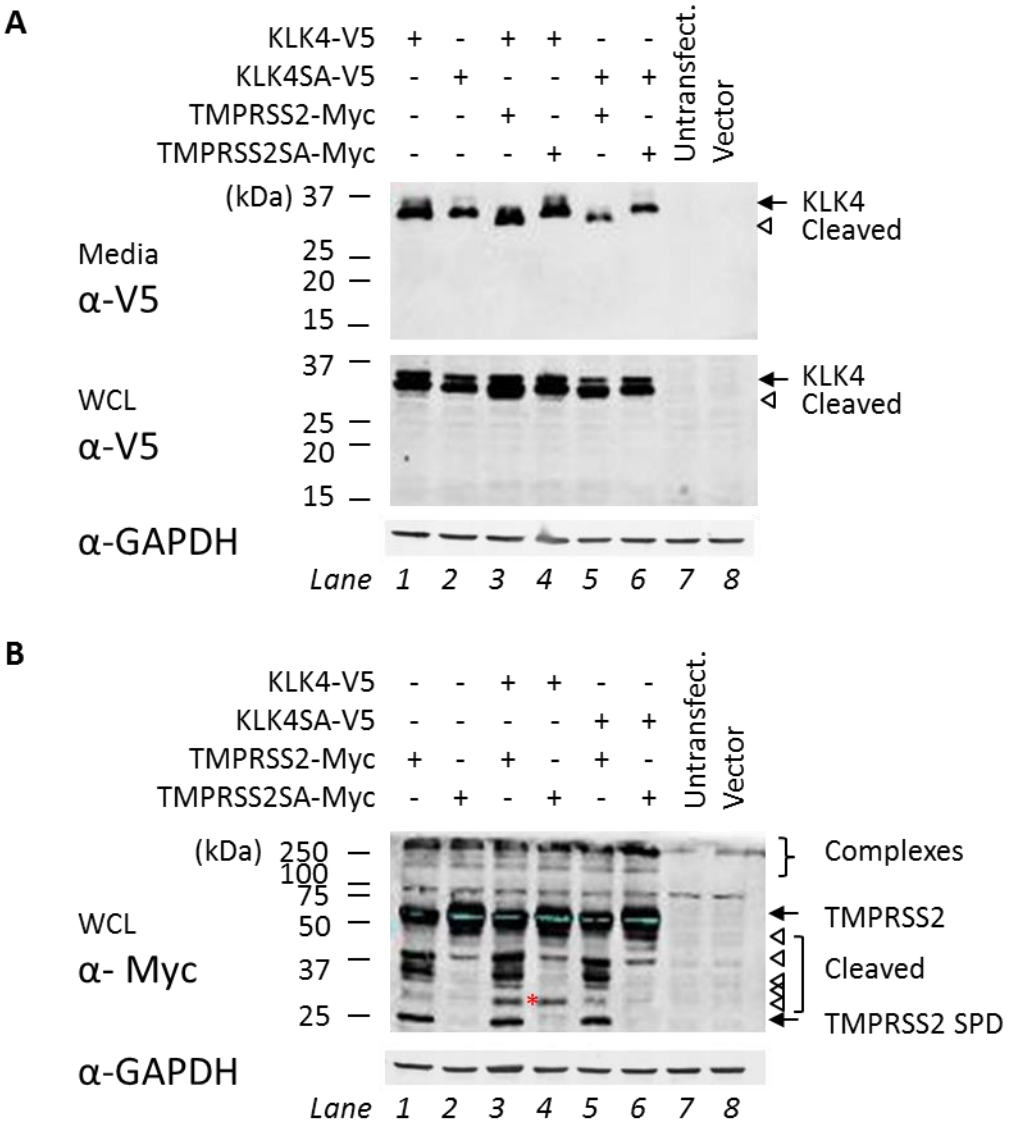

Figure 4.9 KLK4 is proteolysed when co-expressed with TMPRSS2. Cos-7 cells were transiently transfected with constructs encoding either KLK4-V5 or active-site mutated KLK4SA-V5 and co-transfected with constructs encoding either TMPRSS2-Myc or active-site mutated TMPRSS2SA-Myc, as indicated. After 24 hours, media and and whole-cell lysates (WCL) were subjected to reducing SDS-PAGE followed by Western blot analysis using anti-V5 and anti-Myc antibodies, as indicated. Anti-GAPDH probe of WCL blots was performed to examine protein loading. **A.** In the media, 33 kDa KLK4 and KLK4SA were depleted and 31 kDa forms generated (lanes 3 and 5) when co-expressed with TMPRSS2. In the WCL, when co-expressed with TMPRSS2, there is an increased amount of the 31 kDa KLK4 and KLK4SA forms (lanes 3 and 5). **B.** TMPRSS2 and TMPRSS2SA were not detected in the media. In the WCL full-length TMPRSS2 and TMPRSS2SA were detected at 53 kDa. TMPRSS2 serine protease domain (SPD) was detected at 25 kDa (lanes 1, 3 and 5) but not for TMPRSS2SA (lanes 2, 4 and 6). Other TMPRSS2/SA cleaved forms detected 50, 40, 36, 35 and 30 kDa (*open arrowheads, red asterisk indicate KLK4 generated forms*) and complexes >250 kDa (*brace*) are indicated. Representative data from one of three experiments shown.

spontaneously active soluble form with the complete sequence minus the transmembrane and intracellular regions (Kirchhofer et al., 2005).

Pro-KLK14-V5-His and pro-KLK4-V5-His, purified from Sf9 cells, were incubated with reducing molar ratios of recombinant hepsin. Western blot analysis was performed using anti-V5 antibody to detect all forms of KLK14 and KLK4 that have the C-terminal V5 tag attached. To detect any forms of KLK14 and KLK4 lacking the C-terminal epitope tags, an anti-KLK14 polyclonal antibody raised against a combination of N- and C-terminal KLK14 peptides, and two anti-KLK4 polyclonal antibodies raised against peptides from the mid and C-terminal of KLK4, were also used in the Western blot analyses.

As shown in the Western blot analyses in Figure 4.10, at the KLK14:hepsin molar ratio of 1:1 cleaved KLK14 (28 kDa) is apparent as a faint band just below intact KLK14 (29 kDa) (lane 2). This is consistent with the results shown previously (in Figure 4.5A) that co-expression with hepsin resulted in generation of a lower MW band of KLK14 in cell lysates. This may represent the removal of the pro-region of KLK14. However, as equimolar concentrations are required for the recombinant soluble domain hepsin to effect KLK14 cleavage, it is not an efficient reaction. In contrast, at ratios of KLK14:thermolysin of 1:0.08 and 1:0.008, KLK14 is cleaved to produce bands of 28, 26 and 25 kDa (lanes 8 and 9). This reflects the efficient proteolytic removal of the KLK14 pro- region or V5-His tag or both, by thermolysin, as discussed in Chapter 3.

KLK4, on the other hand, is degraded by hepsin as indicated by the diminished signal for KLK4 at ratios of 1:1, 1:0.1 and 1:0.01 (KLK4:hepsin) (Figure 4.10B, lanes 2-4). Furthermore, there is no lower MW band detected for KLK4. This is consistent with the observation made in Figures 4.8A that co-expression with hepsin results in KLK4 depletion. However, co-expression with hepsin had a more pronounced effect on KLK4 in the conditioned media than recombinant soluble hepsin has on recombinant KLK4 in this assay. In contrast, as shown previously by Ramsay (2008), thermolysin efficiently cleaves KLK4 to produce bands migrating at 31 and 32 kDa, reflecting removal of the pro-region or V5-His tag, or both (Figure 4.10B, lanes 8 and 9).

Taken together, these data indicate that soluble hepsin does not efficiently proteolyse KLK14 or KLK4, and that the activity of hepsin may be enhanced by cell-surface localization.

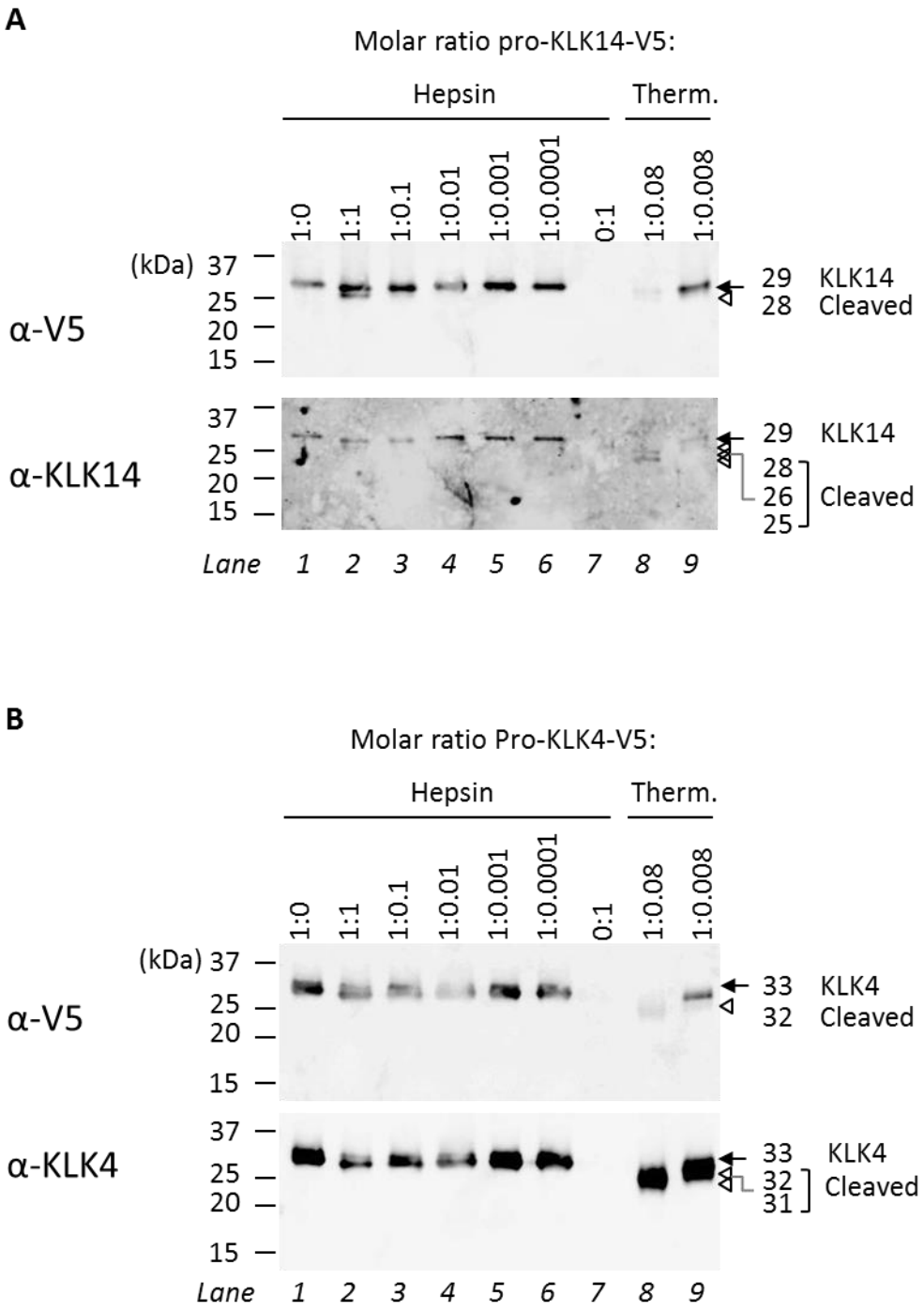

Figure 4.10 Recombinant hepsin proteolyses recombinant pro-KLK14 and pro-KLK4. Recombinant pro-KLK14-V5-His (**A**) and pro-KLK4-V5-His (**B**) (3 μM) were incubated with recombinant hepsin (0-3 μM) for 1 hour at 37°C, as indicated. Reactions stopped with reducing SDS-PAGE loading buffer were subjected to SDS-PAGE and then Western blot analysis using anti-V5, anti-KLK14 and anti-KLK4 antibodies, as indicated. Lanes 8 and 9 on each membrane represents activation controls; pro-KLK14–V5-His or pro-KLK4-V5-His incubated with thermolysin (Therm.) (0.24 or 0.024 μM).

4.2.1.9 KLK14 co-immunoprecipitates with hepsin and TMPRSS2

Having established that co-expression with hepsin or TMPRSS2 results in cleaved KLK14 in cell lysates, interactions between this secreted protease and the cell surface proteases were examined further using immunoprecipitation approaches.

To examine these interactions, KLK14-HA was transiently co-expressed in Cos-7 cells with hepsin-Flag, active-site mutant hepsinSA-Flag, TMPRSS2-Myc or active-site mutant TMPRSS2SA-Myc. Whole-cell lysates were subjected to immunoprecipitation using anti-Flag, anti-Myc or anti-HA antibodies and immunoprecipitates were examined by Western blot analysis under reducing conditions.

As shown in Figure 4.11A, anti-Flag immunoprecipitations of hepsin-Flag and hepsinSA-Flag co-immunopurified KLK14-HA (lanes 2 and 3). Interestingly, along with full-length KLK14-HA, several cleaved forms of this protease also co-immunoprecipitated with hepsin-Flag. On the other hand, only full-length KLK14-HA is co-immunoprecipitated with hepsinSA-Flag. These data suggest that cell associated hepsin cleaves KLK14.

Figure 4.11B shows anti-Flag antibody Western blot analysis of the reverse immunoprecipitation of KLK14-HA using the anti-HA antibody. Consistent with the data in Figure 4.11A, this analysis showed that hepsin-Flag and hepsinSA-Flag co-immunoprecipitate with KLK14-HA (Figure 4.11B, lanes 2 and 3). Interestingly, in addition to hepsin-flag and hepsinSA-Flag apparent at 45 kDa, complexes of >90 kDa were also co-immunoprecipitated with KLK14-HA. Also, as the 26 kDa serine protease domain of hepsin-Flag is apparent, a small amount of activated hepsin-Flag co-immunoprecipitated with KLK14-HA (Figure 4.11B, lane 2).

Similarly, Figure 4.12 shows that KLK14-HA co-immunopurified with anti-Myc immunoprecipitations of TMPRSS2-Myc and TMPRSS2SA-Myc (Figure 4.12A, lanes 2 and 3). Several cleaved forms of KLK14-HA also co-immunoprecipitated with TMPRSS2-Myc and TMPRSS2SA-Myc.

The anti-Myc Western blot analysis of the reverse immunoprecipitation is shown in Figure 4.12B and it can be seen that TMPRSS2-Myc and TMPRSS2SA-Myc co-immunoprecipitated with KLK14-HA (Figure 4.12B, lanes 2 and 3). In addition to full-length 53 kDa TMPRSS2-Myc and TMPRSS2SA-Myc, complexes of >250 kDa also co-immunoprecipitated KLK14-HA (Figure 4.12B, lanes 2 and 3). Furthermore, similar to

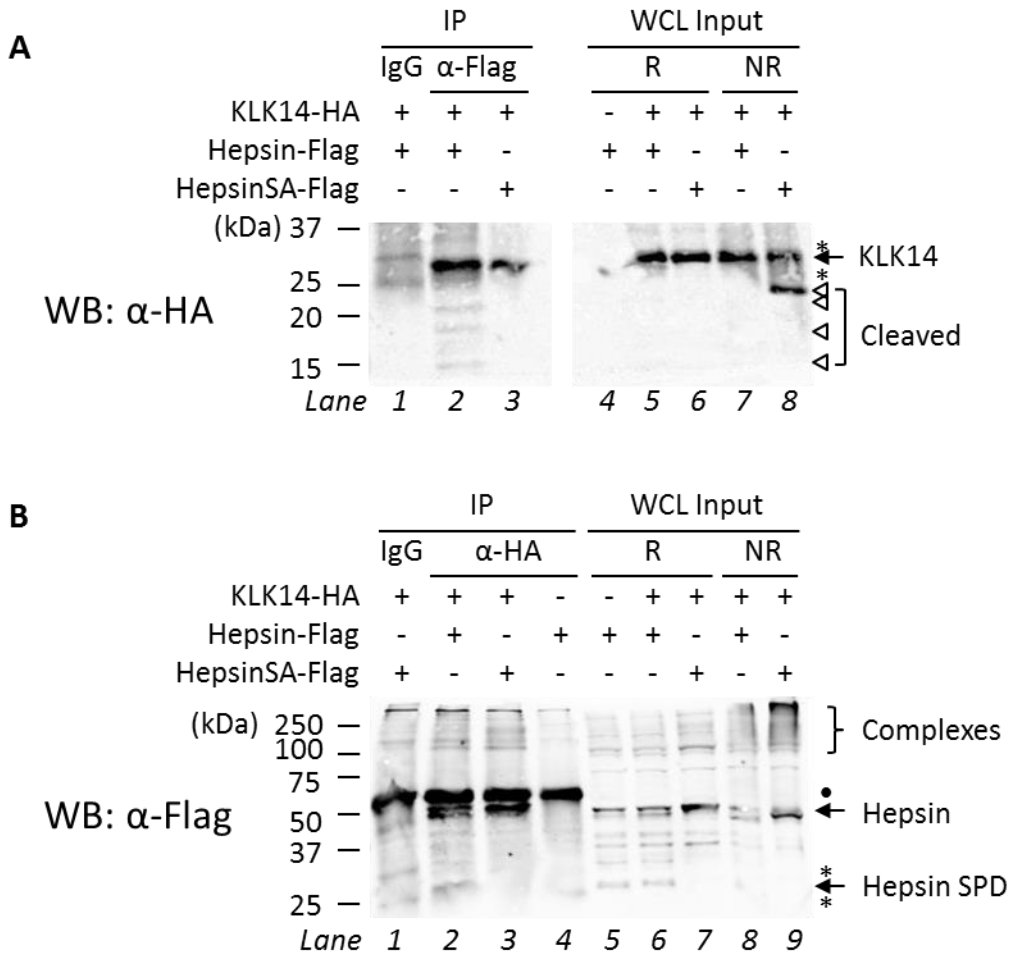

Figure 4.11 Co-immunoprecipitation of KLK14 with hepsin from transfected Cos-7 cells. Cells were transiently transfected with constructs encoding KLK14-HA and were co-transfected with constructs encoding hepsin-Flag or active-site mutated hepsinSA-Flag, as indicated. After 24 hours whole-cell lysates (WCL) were collected and subjected to immunoprecipitation (IP) and then SDS-PAGE under reducing conditions and Western blot (WB) analysis. Samples of the input WCL were also subjected to SDS-PAGE under reducing (R) and non-reducing (NR) conditions followed by Western blot analysis. **A**. Anti-HA Western blot analysis of anti-Flag immunoprecipitates and WCL input to detect KLK14-HA. **B**. Anti-Flag Western blot analysis of anti-HA immunoprecipitates and WCL input to detect hepsin–Flag and hepsinSA-Flag. •, IgG heavy chain; *, IgG light chain.

the co-immunoprecipitation of hepsin shown in Figure 4.11B, this analysis in Figure 4.12B shows that a small amount of activated TMPRSS2 co-immunoprecipitated with KLK14-HA as the 25 kDa TMPRSS2 serine protease domain is apparent in lane 2.

The last five lanes of the Western blot analyses in Figures 4.11 and 4.12 also show the WCL input resolved under reducing (R) and non-reducing (NR) conditions. Interestingly, when co-expressed with hepsinSA-Flag or TMPRSS2SA-Myc, a cleaved

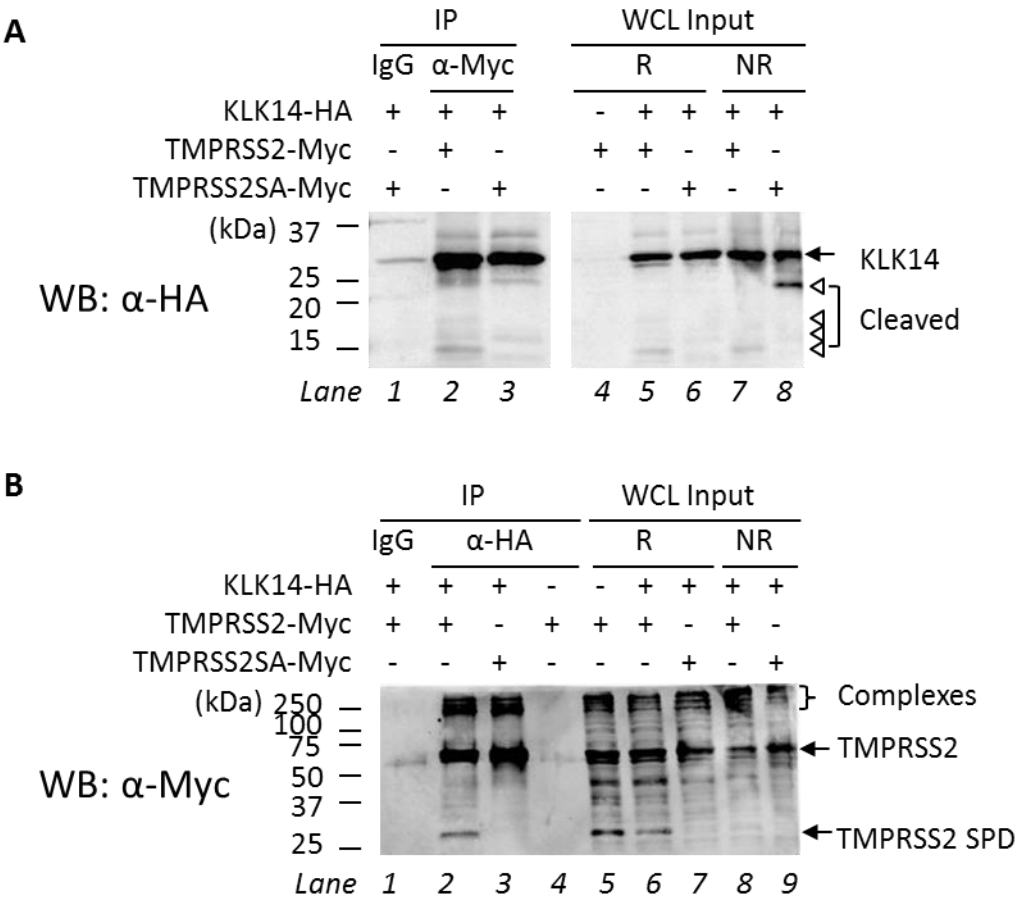

Figure 4.12 Co-immunoprecipitation of KLK14 with TMPRSS2 from transfected Cos-7 cells. Cells were transiently transfected with constructs encoding KLK14-HA and were co-transfected with constructs encoding TMPRSS2-Myc or active-site mutated TMPRSS2SA-Myc, as indicated. After 24 hours whole-cell lysates (WCL) were collected and subjected to immunoprecipitation (IP) and then SDS-PAGE under reducing conditions and Western blot (WB) analysis. Samples of the input WCL were also subjected to SDS-PAGE under reducing (R) and non-reducing (NR) conditions followed by Western blot analysis. **A**. Anti-HA Western blot analysis of anti-Myc immunoprecipitates and WCL input to detect KLK14-HA. **B**. Anti-Myc Western blot analysis of anti-HA immunoprecipitates and WCL inputs to detect TMPRSS2-Myc and TMPRSS2SA-Myc.

form of KLK14-HA is detected at 24 kDa under non-reducing conditions (Figures 4.11A and 4.12A, lanes 8). However, it is not detected under reducing conditions (Figures 4.11A and 4.12A, lanes 6). Furthermore, 24 kDa KLK14-HA is not detected when co-expressed with hepsin-Flag or TMPRSS2-Myc (Figures 4.11A and 4.12A, lanes 5 and 7). Taken together, this suggests that due to the lower MW and detection via the C-terminal HA epitope tag, N-terminal proteolysis occurred for a portion of KLK14-HA. Moreover, as the 24 kDa form is detected under non-reducing, but not reducing conditions, there is at least one other proteolysed site within KLK14-HA, with the

cleaved fragments remaining attached by intramolecular disulphide bond. Finally, TMPRSS2 and Hepsin were not the proteases responsible for the generation of 24 kDa KLK14-HA. However, as shown in Figures 4.11A and 4.12A, lanes 7, they proteolysed this form further, rendering it undetectable under non-reducing conditions.

The identity of the protease responsible for the generation of 24 kDa KLK14-HA is unknown. However, it is possible that it may be an auto-lytic event as active KLK14 has previously been shown to self-degrade by cleavage at multiple Arg residues (Borgono et al., 2007c). This speculation of course requires that in the transient transfections of Cos-7 cells, cell-retained or conditioned media-secreted KLK14-HA was active, a detail not established in this or previous assays.

4.2.1.10 KLK4 co-immunoprecipitates with hepsin and TMPRSS2

As cell-retained KLK4 is also cleaved by hepsin and TMPRSS2, interactions between the secreted protease and these membrane-anchored proteases were also examined further using immunoprecipitation approaches.

To examine these interactions KLK4-V5 was transiently co-expressed with hepsin-Flag, active-site mutant hepsinSA-Flag, TMPRSS2-Myc or active-site mutant TMPRSS2SA-Myc. As shown in the anti-V5 Western blot analysis in Figure 4.13A, KLK4-V5 co-immunoprecipitated with hepsin-Flag and hepsinSA-Flag from whole-cell lysates using the anti-Flag antibody (lanes 2 and 3). In addition, three other bands of cleaved KLK4-V5 at ~28, 22 and 17 kDa co-immunoprecipitated with hepsin-Flag (Figure 4.13A, lane 2), but not hepsinSA-Flag (Figure 4.13A, lane 3), suggesting that cell-retained KLK4 was proteolysed by hepsin.

Figure 4.13B is an anti-Flag Western blot analysis of the reverse immunoprecipitation of KLK4-V5 using the anti-V5 antibody. It shows that 45 kDa full-length hepsin-Flag and hepsinSA-Flag as well as hepsin complexes >90 kDa also co-immunoprecipitate with KLK4-V5 (lanes 2 and 3). Furthermore, similar to the co-immunoprecipitation of hepsin with KLK14-HA (Figure 4.11B), as the 26 kDa serine protease domain of hepsin-Flag is apparent, a small amount of activated hepsin-Flag co-immunoprecipitated with KLK4-V5 (Figure 4.13B, lane 2).

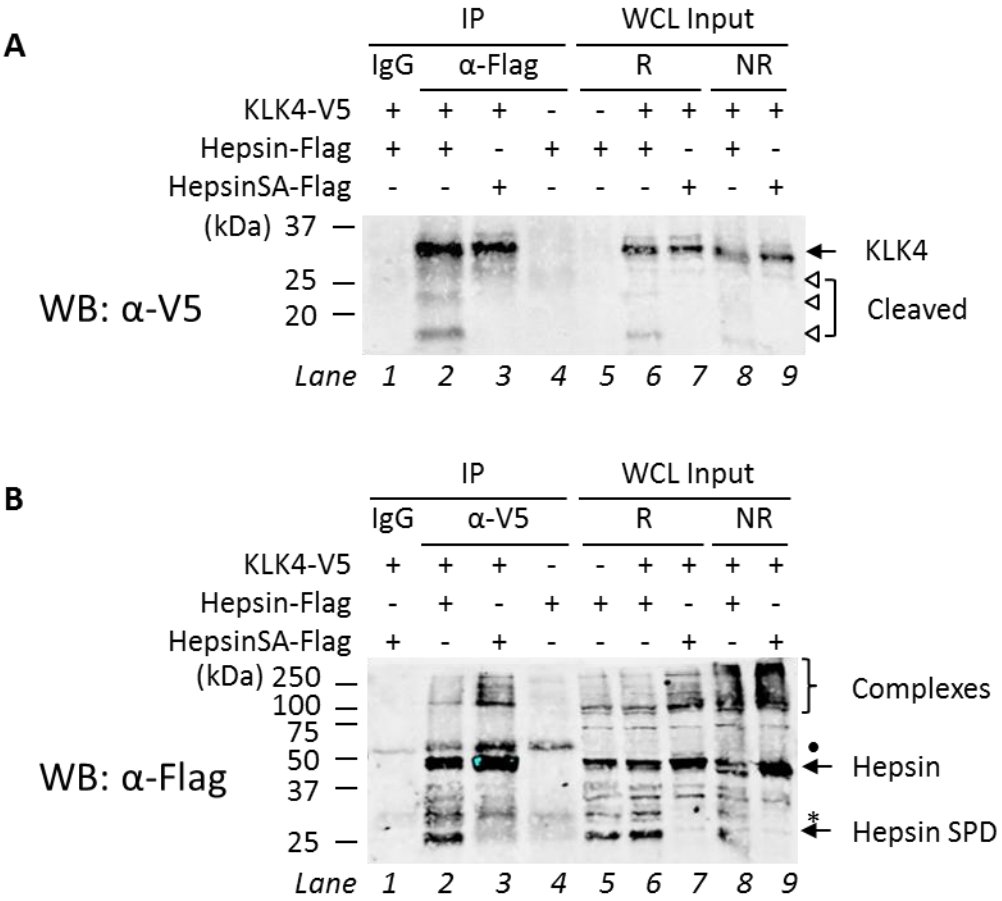

Figure 4.13 Co-immunoprecipitation of KLK4 with hepsin from transfected Cos-7 cells. Cells were transiently transfected with constructs encoding KLK4-V5 and were co-transfected with constructs encoding hepsin-Flag and active-site mutated hepsinSA-Flag, as indicated. After 24 hours whole-cell lysates (WCL) were collected and subjected to immunoprecipitation (IP) and then SDS-PAGE under reducing conditions followed by Western blot (WB) analysis. Samples of the input WCL were also subjected to Western blot analysis under reducing (R) and non-reducing (NR) conditions. **A**. Anti-V5 Western blot analysis of anti-Flag immunoprecipitates and WCL input to detect KLK4-V5. **B**. Anti-Flag Western blot analysis of anti-V5 immunoprecipitates and WCL input to detect hepsin–Flag and hepsinSA-Flag. Representative data from one of two experiments shown. •, IgG heavy chain; *, IgG light chain.

The anti-V5 Western blot analysis (Figure 4.14A) also shows that KLK4-V5 is co-immunoprecipitated with both TMPRSS2-Myc and TMPRSS2SA-Myc (lanes 2 and 3). In addition, this analysis shows that 17 kDa KLK4-V5 co-immunoprecipitated with TMPRSS2-Myc (Figure 4.14A, lane 2), but not TMPRSS2SA-Myc (Figure 4.14A, lane 3), indicating that KLK4 is proteolysed by TMPRSS2.

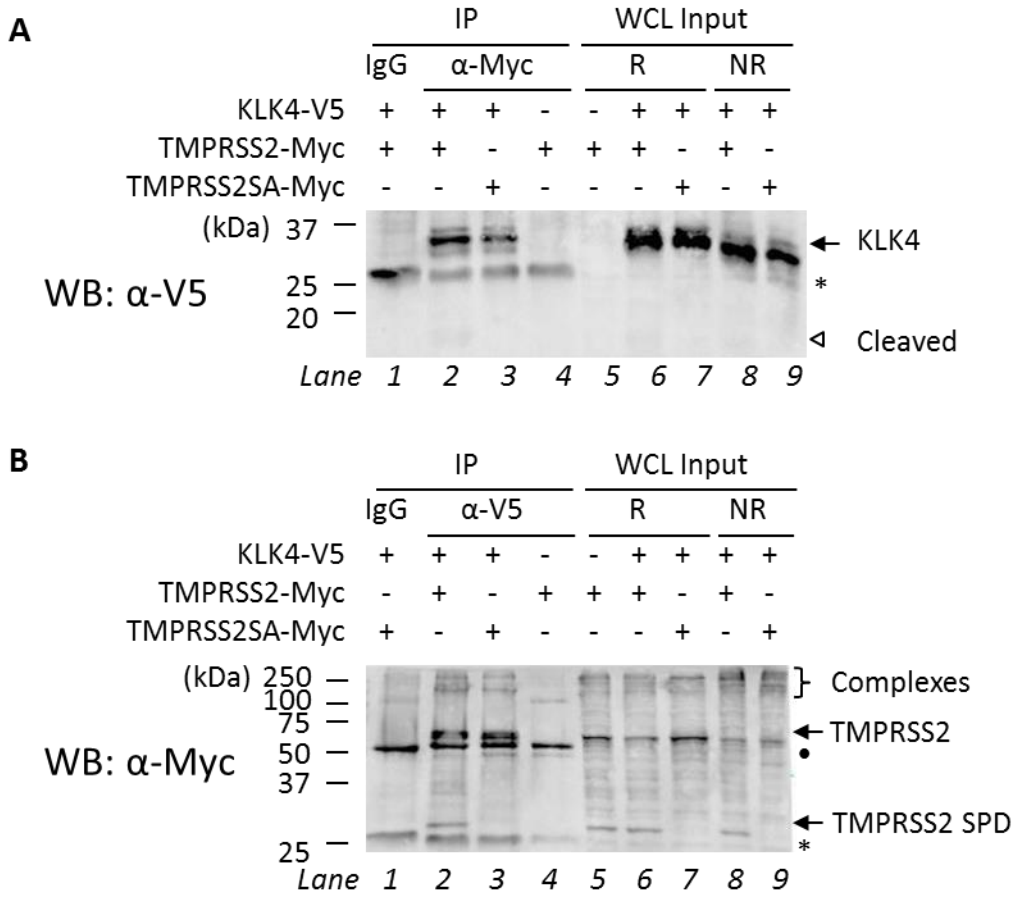

Figure 4.14 Co-immunoprecipitation of KLK4 with TMPRSS2 from transfected Cos-7 cells. Cells were transiently transfected with constructs encoding KLK4-V5 and were co-transfected with constructs encoding TMPRSS2-Myc or active-site mutated TMPRSS2SA-Myc as indicated. After 24 hours whole-cell lysates (WCL) were collected and subjected to immunoprecipitation (IP) and then SDS-PAGE under reducing conditions followed by Western blot (WB) analysis. Samples of the input WCL were also subjected to Western blot analysis under reducing (R) and non-reducing (NR) conditions. **A**. Anti-V5 Western blot analysis of anti-Myc immunoprecipitates and WCL input to detect KLK4-V5. **B**. Anti-Myc Western blot analysis of anti-V5 immunoprecipitates and WCL inputs to detect TMPRSS2-Myc and TMPRSS2SA-Myc. Representative data from one of two experiments shown. •, IgG heavy chain; *, IgG light chain.

In the anti-Myc Western blot analysis of the reverse immunoprecipitation (Figure 4.14B) it can be seen that TMPRSS2-Myc and TMPRSS2SA-Myc co-immunoprecipitated when KLK4-V5 was precipitated using the anti-V5 antibody (lanes 2 and 3). In addition, the figure shows that complexes >250 kDa containing TMPRSS2-Myc and TMPRSS2SA-Myc also co-immunoprecipitated with KLK4-V5. Furthermore, similar to the co-immunoprecipitation of TMPRSS2 with KLK14 shown previously in Figure 4.12B, as

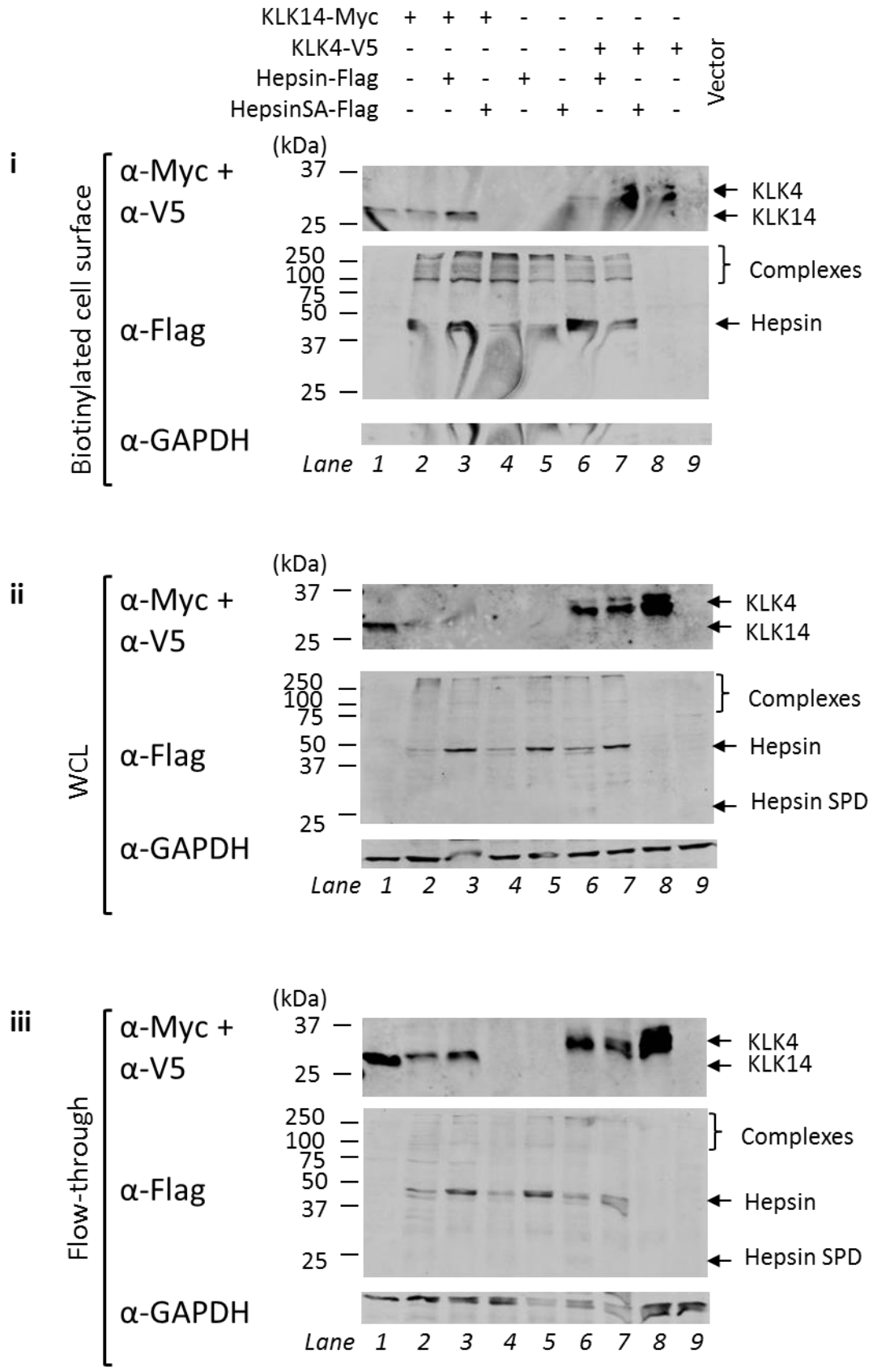
KLK14-Myc + + + - - - - -
KLK4-V5 - - - - - + + +
Hepsin-Flag - + - + - + - -
HepsinSA-Flag - - + - + - + -
Vector
i
Biotinylated cell surface
α-Myc + α-V5
α-Flag
α-GAPDH
(kDa)
37
25
250
100
75
50
37
25
KLK4
KLK14
Complexes
Hepsin
Lane 1 2 3 4 5 6 7 8 9
ii
WCL
α-Myc + α-V5
α-Flag
α-GAPDH
(kDa)
37
25
250
100
75
50
37
25
KLK4
KLK14
Complexes
Hepsin
Hepsin SPD
Lane 1 2 3 4 5 6 7 8 9
iii
Flow-through
α-Myc + α-V5
α-Flag
α-GAPDH
(kDa)
37
25
250
100
75
50
37
25
KLK4
KLK14
Complexes
Hepsin
Hepsin SPD
Lane 1 2 3 4 5 6 7 8 9

Figure 4.15

the 25 kDa TMPRSS2 serine protease domain is apparent (Figure 4.14B, lane 2) a small amount of activated TMPRSS2-Myc co-immunoprecipitated with KLK4-V5.

4.2.1.11 KLK14, KLK4 and hepsin are located on the cell surface of transfected Cos-7 cells

KLK14 and KLK4 are secreted proteases. However, the observation that these proteases co-immunoprecipitate from cell lysate with the membrane-anchored proteases hepsin and TMPRSS2 suggests that KLK4 and KLK14 may have roles in the pericellular environment. Alternatively, it is possible that interactions seen from cell lysates were anomalous due to disruption of normal cell structures allowing interactions between KLK4 and KLK14 and cell-surface localized hepsin and TMPRSS2 during transit to the cell surface. To address this issue further, cell-surface biotinylation was used to examine the localization of KLK4 and KLK14.

In these experiments KLK14-Myc and KLK4-V5 and were co-expressed with either hepsin-Flag or active-site mutant hepsinSA-Flag. Cell-surface proteins on intact cells were biotinylated, and labelled proteins then isolated from whole-cell lysates using streptavidin beads. Isolated proteins as well as cell lysates input and flow-through from the streptavidin capture were examined by Western blot analysis using anti-Flag, anti-Myc and anti-V5 antibodies. Anti-GAPDH Western blot analysis was used to examine protein loading across lanes as well as to assess whether biotinylated fractions contained intracellular proteins.

Interestingly, as shown in Figure 4.15i, KLK14 (lanes 1-3, upper image), KLK4 (lanes 6-8, upper image) and hepsin (lanes 2-7, middle image) were detected in the biotinylated

Figure 4.15 KLK14, KLK4 and hepsin are located on the cell surface of transfected Cos-7 cells. Cells were transiently transfected with constructs encoding either KLK14-Myc or KLK4-V5 and were co-transfected with constructs encoding either hepsin-Flag or active-site mutated hepsinSA-Flag, as indicated. Cell surface proteins were biotinylated 24 hours post-transfection. Whole-cell lysates (WCL) were collected and biotinylated proteins pulled-down with streptavidin agarose. Biotin isolated cell surface proteins (**i**), WCL input (**ii**) and flow-through **(iii)** were subjected to SDS-PAGE under reducing conditions followed by Western blot analysis using anti-Myc and anti-V5 antibodies to detect KLK14-Myc and KLK4-V5, respectively, and anti-Flag antibody to detect hepsin-Flag. Anti-GAPDH probe of the blots was also performed to demonstrate the absence of intracellular proteins in the biotinylated cell-surface fraction.

cell-surface fraction when expressed alone and also when co-expressed. The anti-GAPDH analysis (Figure 4.15i, lower image) demonstrates this biotinylated fraction was isolated free of intracellular proteins. In Figures 4.15ii and 4.15iii, KLK14, KLK4 and hepsin were detected in both cell lysate and the flow-through fractions from the biotinylation. Naturally, the anti-GAPDH analyses of these blots reflect the detection of intracellular proteins in both the whole-lysate and the flow-through of intracellular proteins not captured by cell-surface biotinylation-streptavidin isolation.

This result for hepsin is consistent with previous publications that have found it localized to the plasma membrane (Tsuji et al., 1991; Kazama et al., 1995; Zacharski et al., 1998). However, significantly, this is the first time KLK14 and KLK4 have been shown to be localized to the cell surface. Moreover, despite co-immunoprecipitation of KLK14 and KLK4 with hepsin, the cell surface localization is independent of hepsin or hepsin SA co-expression.

4.2.1.12 Activity-based probe pull-down of KLK4, hepsin and TMPRSS2 from the cell surface

As the previous results indicate that KLK4 is cell-surface localized as well as secreted, to examine whether it is active in either situation an approach was used that captures active serine proteases using biotin-tagged activity-based probes (ABPs). The probes used in the study, biotin-EGR-CMK and biotin-FPR-CMK, are designed to capture serine proteases with specificity for cleavage after Arg (Williams et al., 1989), such as KLK14, KLK4, hepsin and TMPRSS2. The presence of a biotin moiety allows subsequent isolation of bound proteases using resin-bound streptavidin (Williams et al., 1989).

In these experiments KLK4-V5 and active-site mutated KLK4SA-V5 were co-expressed with either hepsin-Flag or TMPRSS2-Myc. The ABPs were used to label active serine proteases on the surface of whole cells and in the conditioned media, and then they were isolated from whole-cell lysates and media using streptavidin beads. The isolated serine proteases were examined by Western blot analysis using anti-V5, anti-Flag and anti-Myc antibodies, as well as fluorescence probe-conjugated streptavidin (Streptavidin-680) to detect all the proteases pulled down.

As shown in the anti-V5 Western blot analyses in Figure 4.16, a small quantity of KLK4 was pulled-down from the cell surface by biotin-EGR-CMK and biotin-FPR-CMK

when expressed alone (lanes 1 and 14) and also when co-expressed with TMPRSS2 (lanes 5 and 18). However, KLK4 was not pulled-down from cells co-expressing hepsin (lanes 3 and 16).

Hepsin was also pulled down, as shown in the anti-Flag Western blot analyses in Figure 4.16. Full-length 45 kDa hepsin and 26 kDa hepsin serine protease domain were detected when co-expressed with KLK4 (lanes 3, 4, 16 and 17) and expressed alone (lane 20). Similarly, in the anti-Myc Western blot analyses in Figure 4.16, TMPRSS2 at 53 kDa (full-length) and 25 kDa (serine protease domain) were detected when co-expressed with KLK4 (lanes 5, 6, 18 and 19), and also when expressed alone (lanes 8 and 21). It is interesting that the full-length forms of hepsin and TMPRSS2 have been isolated because the proteases isolated by ABP-streptavidin were eluted from streptavidin resin using a combination of reducing SDS-PAGE buffer and heat (100°C) and, as discussed in previous sections, reduction of the disulphide bonds allows the serine protease domain of active hepsin and TMPRSS2 to separate from the stem region. It would be expected that under these conditions of isolation and elution only the active serine protease domain would be detected by the C-terminal tag antibodies. Therefore, detection of unactivated hepsin and TMPRSS2 suggests that these proteases have formed dimers or oligomers with active protease and are then concurrently pulled down by the ABPs.

To better detect KLK4, hepsin and TMPRSS2 by Western blot analysis, an increase in the number of cells subjected to the ABPs may be necessary. However, there is also marked variability in the detection of these proteases across the lanes. Consistent with this, the image of the Streptavidin-680 probed blot in Figure 4.16 shows that the variability is likely a product of the total amount of protease pulled down and loaded in each lane of the gel. In the Streptavidin blots, lanes 1 and 5 have considerably more protease detected by the Streptavidin-680 probe than any other lane. Likewise, lanes 17 and 18 have considerably more protease detected. So, it follows that these lanes correspond with the best detection of KLK4, hepsin and TMPRSS2 in the anti-V5, anti-Flag and anti-Myc analyses. As it stands, this protocol and these results cannot be used to assess the relative efficiency of KLK4, hepsin and TMPRSS2 pull-down by each ABP. However, from the pull-down of the control proteases (Figure 4.16), bovine trypsin, recombinant soluble hepsin and recombinant KLK4, it appears that trypsin may have a higher affinity for biotin-EGR-CMK (lane 11) than biotin-FPR-CMK (lane 24).

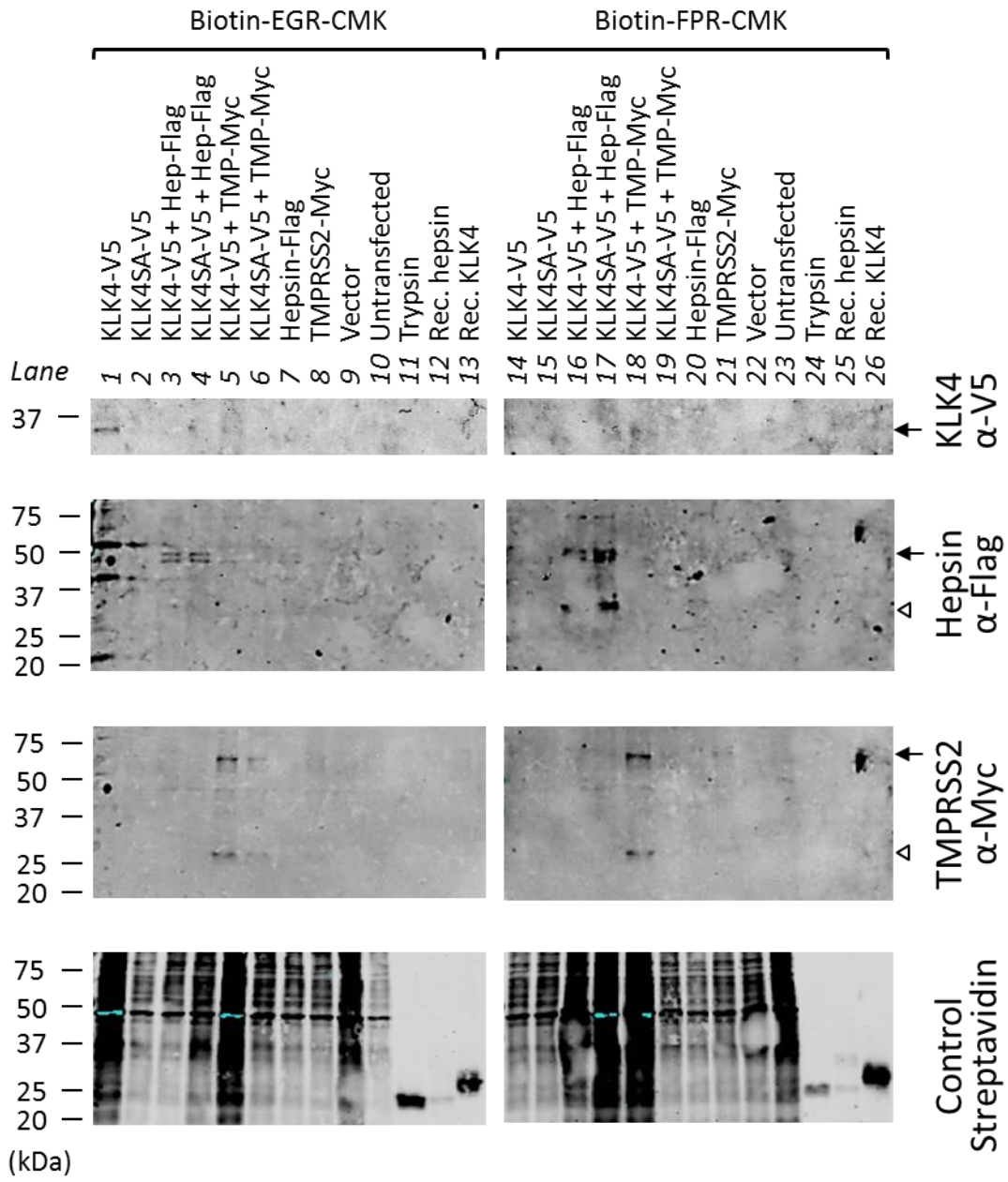

Figure 4.16 Activity-based probe pull-down of hepsin, TMPRSS2 and KLK4 from the cell surface of transfected Cos-7 cells. Cells were transiently transfected with constructs encoding either KLK4-V5 or active-site mutated KLK4SA-V5 and were co-transfected with constructs encoding either hepsin-Flag or TMPRSS2-Myc as indicated. Activity-based probes Biotin-EGR-CMK and Biotin-FPR-CMK were used to tag active serine proteases on the cell surface 24 hours post-transfection. Whole-cell lysates (WCL) were collected and biotin-tagged proteases pulled-down using streptavidin agarose. Precipitated proteases were subjected to SDS-PAGE under reducing conditions followed by Western blot analysis using anti-V5, anti-Flag and anti-Myc antibodies; and Streptavidin-680 probe as indicated. ABP controls include trypsin (~30 ng active), recombinant (rec.) hepsin (~15 ng active) and rec. KLK4 (~ 300 ng active). (*Arrows indicate KLK4, hepsin and TMPRSS2, open arrowheads indicate hepsin and TMPRSS2 serine protease domain*).

While in contrast, hepsin and KLK4 may have marginally more affinity for biotin-FPR-CMK (lanes 25 and 26) than biotin-EGR-CMK (lanes 12 and 13).

In contrast to the cell surface ABP pull-down, KLK4 was not isolated from conditioned media by either biotin-EGR-CMK or biotin-FPR-CMK (Figure 4.17A, anti-V5 blots). Multiple proteases were isolated from the conditioned media, as indicated by the blots probed with Streptavidin-680 (Figure 4.17A). Furthermore, the anti-V5 Western blot analysis of the input conditioned media (Figure 4.17B) shows that KLK4 and KLK4SA are expressed. Indeed, Figure 4.17B is consistent with data presented earlier (in Figures 4.8 and 4.9, respectively) that co-expression with hepsin causes a reduction in intensity of these bands (lanes 3 and 4), and co-expression with TMPRSS2 results in a reduction in MW of KLK4 and KLK4SA equivalent to ~1 kDa (lanes 10 and 11). It appears that processing of KLK4 by hepsin leads to degradation, while processing by TMPRSS2 results in truncation; however the ABP data suggests that at the time point analysed no active KLK4 was present in the medium.

ABP pull-down was also performed on cells co-expressing KLK14 and hepsin. Similar results were obtained as active KLK14 was not pulled down from the conditioned media (data not shown). Due to time-constraints further investigation of KLK14 was not undertaken.

Nonetheless, taken together, these data indicate that active KLK4, hepsin and TMPRSS2 can be isolated from the cell surface of transfected Cos-7 cells. Significantly, this is the first time active KLK4 has been demonstrated in cell-based assays.

4.2.2 Proteolytic interactions of hepsin, TMPRSS2 with MMP3 and MMP9

The above data indicate that hepsin and TMPRSS2 are able to mediate cleavage of KLK14 and KLK4 at the cell surface. It is possible that this pericellular activity extends to activation or degradation of other secreted proteases. It has previously been shown that the TTSP matriptase activates MMP3 (Jin et al., 2006) and that MMP3 activates MMP9 (Ogata et al., 1992; Shapiro et al., 1995) and KLK4 (Beaufort et al., 2010). So, MMP3 and MMP9 were chosen as there is potential for proteolytic cascades of activation and regulation between these MMPs as well as KLK14 and KLK4 and the TTSPs hepsin and TMPRSS2. The potential for hepsin and TMPRSS2 to interact with

secreted matrix metalloproteinases, MMP3 and MMP9, was examined in this section using approaches similar to the previous section. Matriptase was also included in some of the following assays as it has previously been shown to activate MMP3 (Jin et al., 2006; Milner et al., 2010).

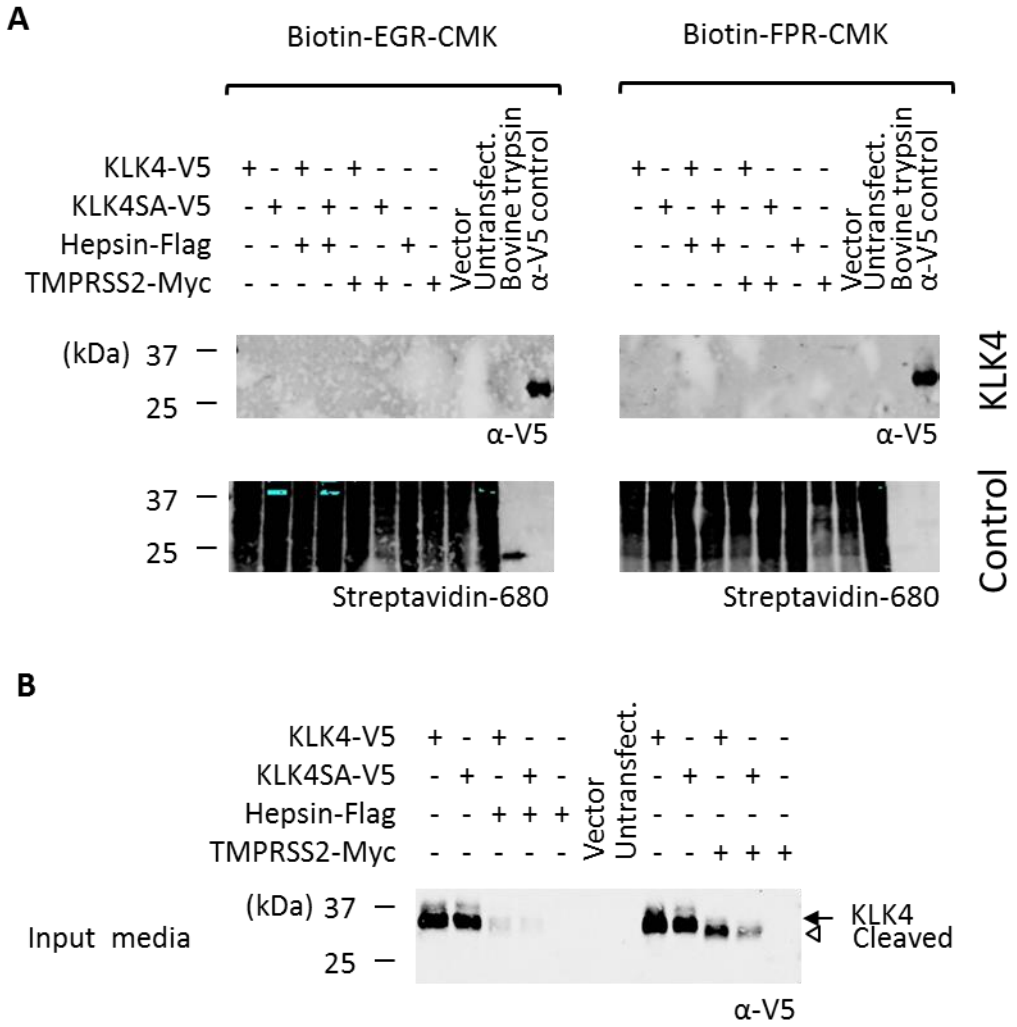

Figure 4.17 Activity-based probes do not pull down KLK4 from media of Cos-7 cells co-expressing hepsin or TMPRSS2. Cells were transiently transfected with constructs encoding either KLK4-V5 or active-site mutated KLK4SA-V5 and were co-transfected with constructs encoding either hepsin-Flag or TMPRSS2-Myc as indicated. **A**. After 24 hours transfection, activity-based probes (ABP) Biotin-EGR-CMK and Biotin-FPR-CMK were used to tag active serine proteases in the conditioned media. ABP tagged proteases were pulled-down with streptavidin agarose. Precipitated proteases were subjected to SDS-PAGE under reducing conditions followed by Western blot analysis using anti-V5 antibody (**i**) and streptavidin-680 (**ii**) as indicated. Bovine trypsin (~ 15 ng active) was used as an ABP control and a V5-tagged protein as an antibody control. **B**. Representative samples of input conditioned media were subjected to reducing SDS-PAGE followed by Western blot analysis using anti-V5 antibody.

4.2.2.1 Pericellular proteolysis of MMP3 and MMP9 by hepsin, TMPRSS2 and matriptase

To examine the interaction of hepsin with MMP3 and MMP9, hepsin-Flag, TMPRSS2-Myc and matriptase were co-expressed with MMP3 or MMP9, or both. Conditioned media and whole-cell lysates were examined by Western blot analysis using anti-MMP3 and anti-MMP9 antibodies under reducing and non-reducing (not shown) conditions.

As shown in Figures 4.18 to 4.20 of anti-MMP3 Western blot analyses, full-length MMP3 was detected at 57 kDa in cell lysate and conditioned medium. When MMP3 is co-expressed with hepsin, TMPRSS2 or matriptase, it is proteolysed to 46 and 45 kDa as well as several other cleaved forms including 53, 30 and 28 kDa. These cleaved forms were readily detected in cell lysate and to a lesser degree in conditioned media. Moreover, the co-expression of MMP9 does not alter the MMP3 cleavage products of hepsin, TMPRSS2 or matriptase.

Interestingly, as MMP3 has been shown to activate in a stepwise manner with proteases first cleaving MMP3 to an intermediate form followed by self-activation by cleaving the remaining part of the pro- region to yield a 45 kDa mature peptide (Okada et al., 1986; Okada et al., 1988; Nagase et al., 1990), it is possible hepsin, TMPRSS2 and matriptase activate MMP3 by generating the 53 kDa intermediate which then self-activates. However, the 53, 46 and 45 kDa bands are also present, to a lesser degree, when MMP3 is expressed alone. This may indicate the Cos-7 cells express a protease that is activating the expressed MMP3 as well.

In the anti-MMP9 Western blot analyses in Figures 4.18 to 4.20, full-length MMP9 was detected at 92 kDa in both cell lysates and conditioned media. When expressed alone, MMP9 also has an 86 kDa band that can only be seen in cell lysates. Interestingly, when MMP9 is co- expressed with hepsin, TMPRSS2 or matriptase there is almost complete conversion of the 92 kDa form to 86 and 82 kDa forms. Again these cleaved forms are only seen in cell lysates. Furthermore, the co-expression of MMP3 with hepsin or matriptase did not alter the bands generated. Like MMP3, MMP9 also activates in a stepwise manner with an ~86 kDa intermediate form generated first, followed by the ~82 kDa active form (Morodomi et al., 1992; Ogata et al., 1992). But MMP9 can also be activated by a single proteolysis step (Sorsa et al., 1997).

In summary, hepsin, TMPRSS2 and matriptase proteolysed MMP3 and MMP9 to produce putative active forms of 45 and 82 kDa, respectively.

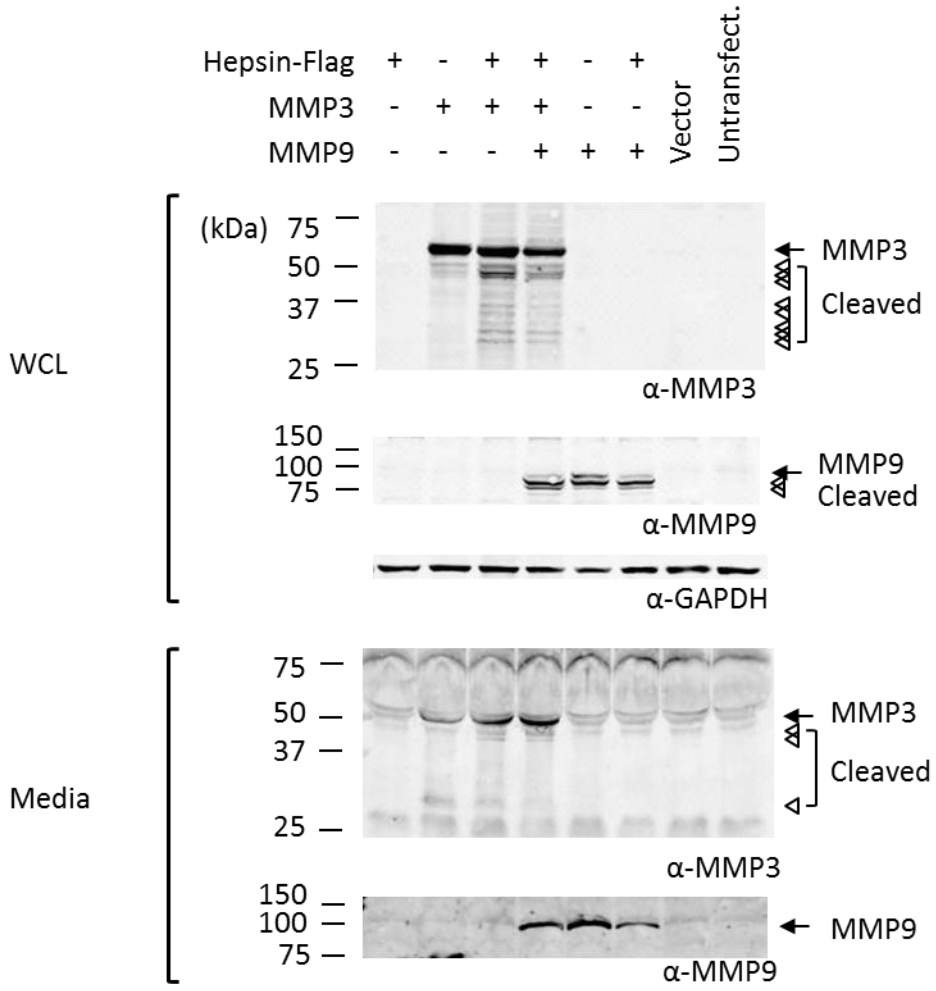

Figure 4.18 Pericellular proteolysis of MMP3 and MMP9 by hepsin. Cos-7 cells were transiently transfected with constructs encoding hepsin and were co-transfected with constructs encoding either MMP3 or MMP9, or both, as indicated. Conditioned media and whole-cell lysates (WCL) were collected 24 hours post-transfection and subjected to reducing SDS-PAGE followed by Western blot analysis using anti-MMP3 and anti-MMP9 antibodies. Anti-GAPDH probe of WCL blots was performed to examine protein loading. In the WCL, full-length MMP3 is detected at 57 kDa and bands of cleaved MMP3 detected include 53, 46, 45, 28 and 30 kDa. Full-length MMP9 is detected at 92 kDa and cleaved forms of MMP9 are detected at 86 and 82 kDa. In the media, full-length MMP3 is detected at 57 kDa with a cleaved form at and 53 kDa. MMP9 is detected at 92 kDa without any cleaved forms.

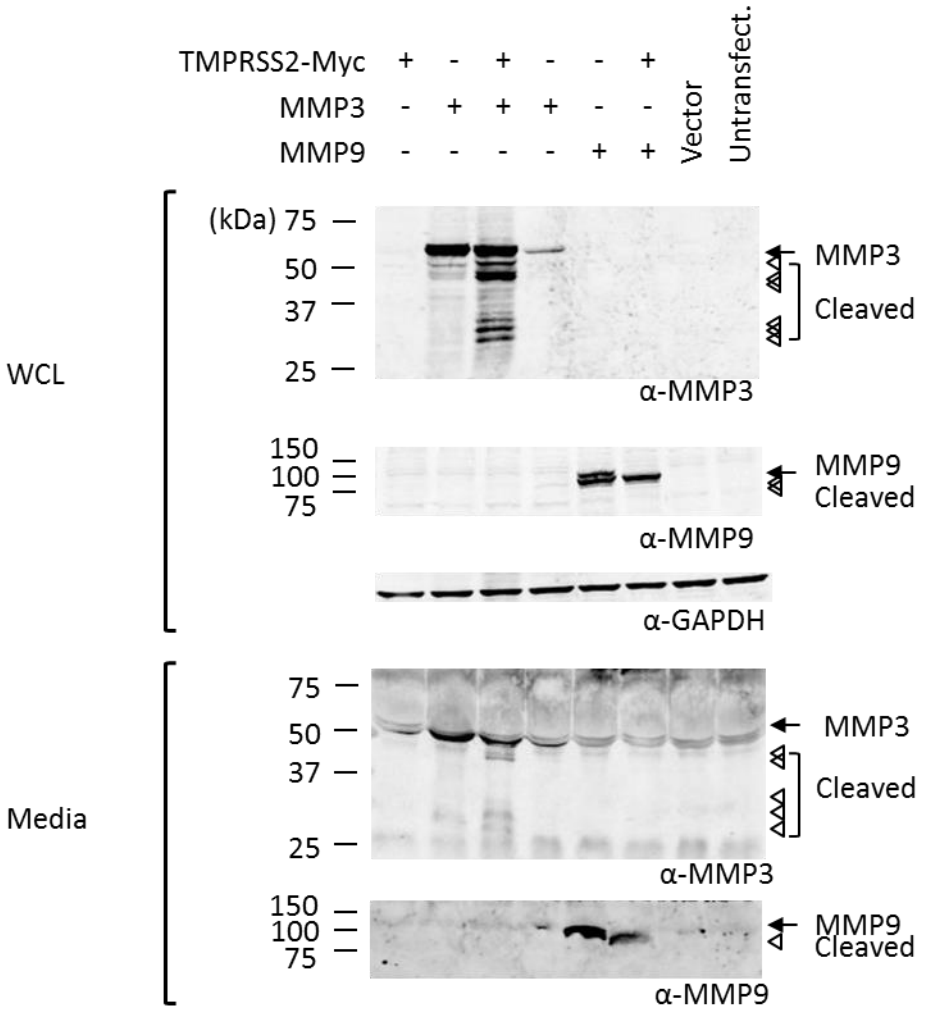

Figure 4.19 Pericellular proteolysis of MMP3 and MMP9 by TMPRSS2. Cos-7 cells were transiently transfected with constructs encoding TMPRSS2 and were co-transfected with constructs encoding either MMP3 or MMP9, or both, as indicated. Conditioned media and whole-cell lysates (WCL) were collected 24 hours post-transfection and subjected to reducing SDS-PAGE followed by Western blot analysis using anti-MMP3 and anti-MMP9 antibodies. Anti-GAPDH probe of WCL blots was performed to examine protein loading. In the WCL, full-length MMP3 is detected at 57 kDa and bands of cleaved MMP3 detected include 53, 46, 45, 28 and 30 kDa. Full-length MMP9 is detected at 92 kDa and cleaved forms of MMP9 are detected at 86 and 82 kDa. In the media, full-length MMP3 is detected at 57 kDa with a cleaved form at and 53 kDa. MMP9 is detected at 92 kDa without any cleaved forms.

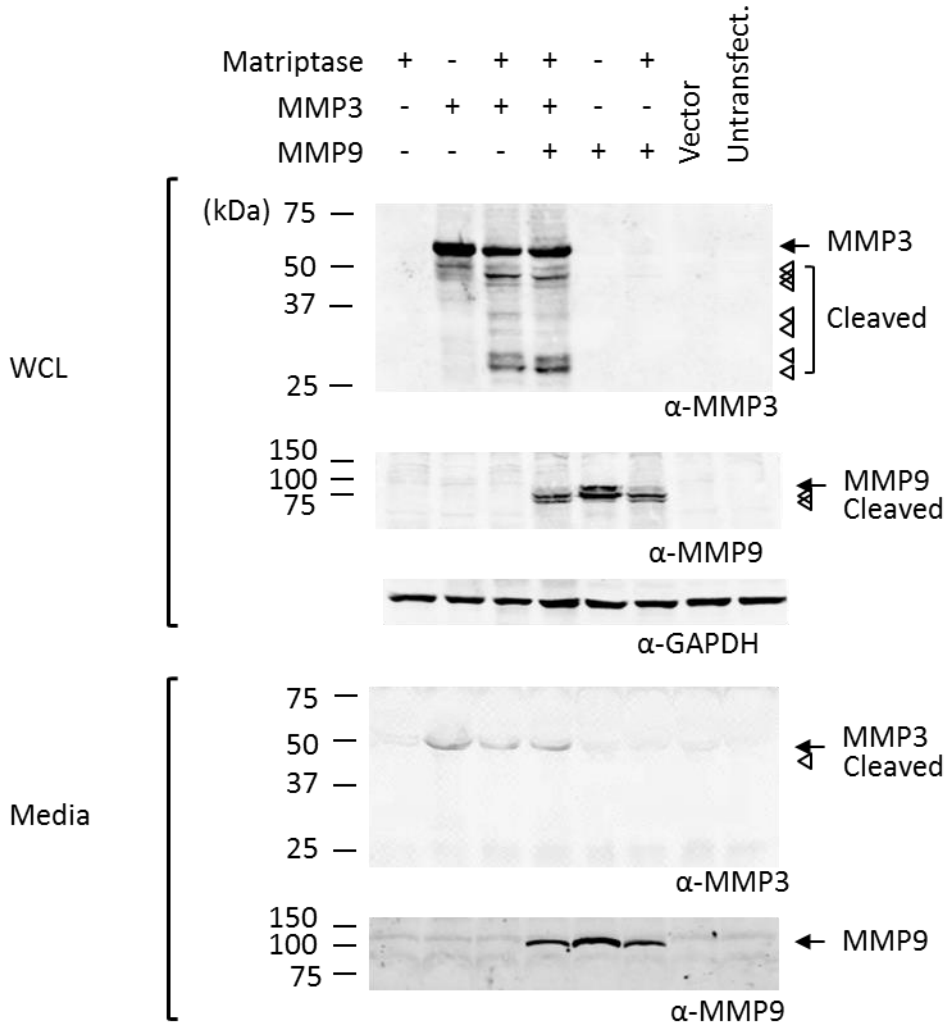

Figure 4.20 Pericellular proteolysis of MMP3 and MMP9 by matriptase. Cos-7 cells were transiently transfected with constructs encoding matriptase and were co-transfected with constructs encoding either MMP3 or MMP9, or both, as indicated. Conditioned media and whole-cell lysates (WCL) were collected 24 hours post-transfection and subjected to reducing SDS-PAGE followed by Western blot analysis using anti-MMP3 and anti-MMP9 antibodies. Anti-GAPDH probe of WCL blots was performed to examine protein loading. In the WCL, full-length MMP3 is detected at 57 kDa and bands of cleaved MMP3 detected include 53, 46, 45, 28 and 30 kDa. Full-length MMP9 is detected at 92 kDa and cleaved forms of MMP9 are detected at 86 and 82 kDa. In the media, full-length MMP3 is detected at 57 kDa with a cleaved form at and 53 kDa. MMP9 is detected at 92 kDa without any cleaved forms.

4.2.2.2 MMP3 and MMP9 co-immunoprecipitate with hepsin and TMPRSS2

As MMP3 and MMP9 are proteolysed by hepsin and TMPRSS2 at the cell surface, the interactions were examined further using immunoprecipitation of the transiently transfected proteases from cell lysates.

MMP3 and MMP9 were transiently co-expressed in Cos-7 cells with either hepsin-Myc or TMPRSS2-Myc. Cell lysates were subjected to immunoprecipitation using an anti-Myc antibody to precipitate hepsin-Myc and TMPRSS2-Myc, and anti-MMP3 or anti-MMP9 antibodies to precipitate MMP3 and MMP9, respectively. The precipitates were then examined by Western blot analysis under reducing conditions using anti-MMP3, anti-MMP9 and anti-Myc antibodies.

As shown in the anti-MMP3 Western blot analysis in Figure 4.21A, full-length MMP3 as well as 53, 45 and 46 kDa cleaved MMP3 were co-immunoprecipitated with hepsin and TMPRSS2. In contrast, in the anti-MMP9 Western blot analysis (Figure 4.21B), cleaved MMP9, at 86 and 82 kDa, were co-immunoprecipitated with hepsin and TMPRSS2 while full-length MMP9 at 92 kDa was not. This is consistent with results presented in Figures 4.18 and 4.19, where hepsin and TMPRSS2 co-expression resulted in the almost complete conversion of MMP9 to the 86 and 82 kDa forms. In addition, anti-MMP3 and anti-MMP9 Western blot analysis of the flow-through fractions from the immunoprecipitations shows the full-length MMP9 is only present in a substantial amount when MMP9 is expressed alone.

The reverse immunoprecipitation was used to confirm the interaction of MMP3 and MMP9 with hepsin and TMPRSS2. As shown in the anti-Myc Western blot analyses of the MMP3 and MMP9 immunoprecipitations in Figure 4.22, hepsin (Figure 4.22A) and TMPRSS2 (Figure 4.22B) are co-immunoprecipitated with MMP3 and MMP9. Furthermore, while hepsin and TMPRSS2 have multiple cleaved forms, full-length and the serine protease domain of hepsin/TMPRSS2 predominate in the co-immunoprecipitation.

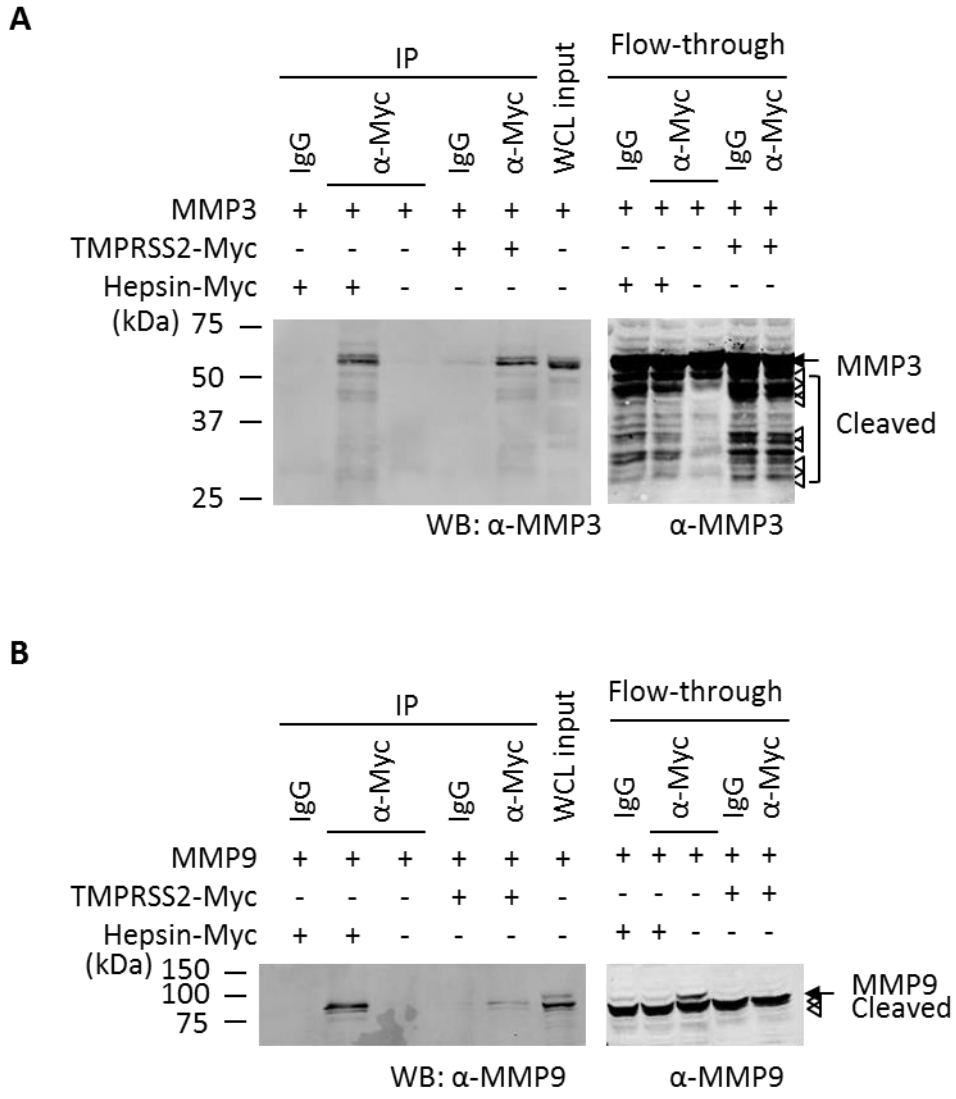

Figure 4.21 Co-immunoprecipitation of MMP3 and MMP9 with hepsin and TMPRSS2 from transfected Cos-7 cells. Cells were transiently transfected with constructs encoding either hepsin-Myc or TMPRSS2-Myc and were co-transfected with constructs encoding either MMP3 or MMP9 as indicated. Whole-cell lysates (WCL) were collected 24 hours post-transfection and subjected to immunoprecipitation (IP) followed by SDS-PAGE under reducing conditions and Western blot (WB) analysis. Samples of WCL input and IP flow-through were also subjected to SDS-PAGE under reducing conditions and Western blot analysis. **A**. Anti-MMP3 Western blot to detect MMP3 and **B**. Anti-MMP9 Western blot to detect MMP9 in hepsin and TMPRSS2 immunoprecipitates and in WCL and flow-through.

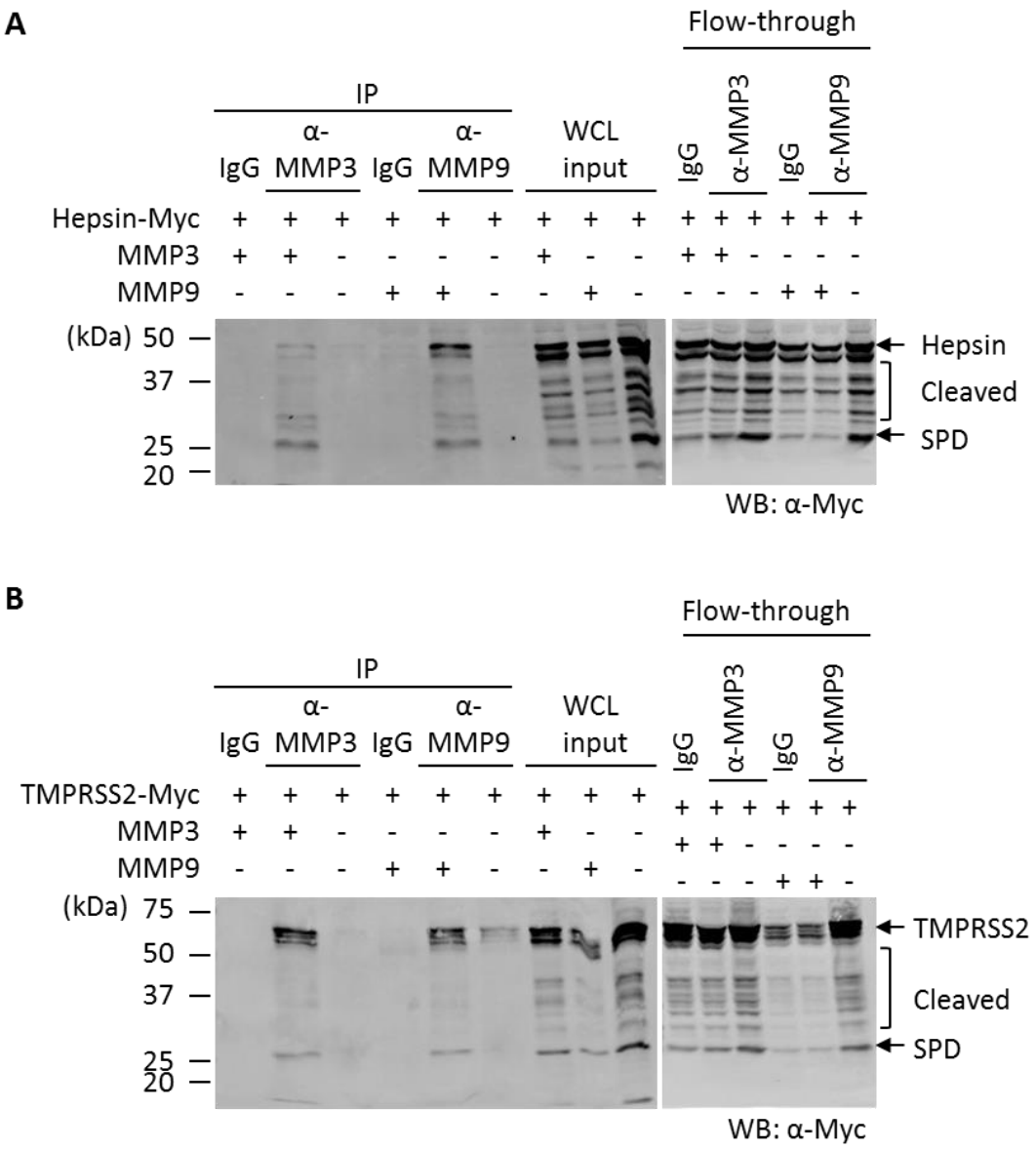

Figure 4.22 Co-immunoprecipitation of hepsin and TMPRSS2 with MMP3 and MMP9 from transfected Cos-7 cells. Cells were transiently transfected with constructs encoding either hepsin-Myc or TMPRSS2-Myc and were co-transfected with constructs encoding either MMP3 or MMP9 as indicated. Whole-cell lysates (WCL) were collected 24 hours post-transfection and subjected to immunoprecipitation (IP) followed by SDS-PAGE under reducing conditions and Western blot (WB) analysis. Samples of WCL input and IP flow-through were also subjected to SDS-PAGE under reducing conditions and Western blot analysis. Anti-Myc Western blots to detect **A**. hepsin-Myc and **B**. TMPRSS2-Myc in anti-MMP3 and anti-MMP9 immunoprecipitates and in WCL input and flow-through.

4.2.2.3 Gelatin zymography of MMP3 and MMP9 co-expressed with hepsin and TMPRSS2 in Cos-7 cells

As hepsin and TMPRSS2 mediate cleavage of MMP3 and MMP9 generating bands corresponding with the known MW for the active forms of these proteases, further experiments were performed to examine the proteolytic activity of the generated bands. Zymography was used as it is a method for visualising hydrolytic enzymes and has been used extensively for MMPs (Vandooren et al., 2013). Gelatin zymography relies on in-gel hydrolysis of gelatin by active protease followed by staining of the gel to show the areas of proteolytic activity. The hydrolysis in the gel is seen as a clear band, marking proteolytic activity. In the case of MMPs, the act of denaturing and renaturing the proteins, inherent in the zymography process, can activate pro- MMPs and intermediate forms by moving the inhibitory pro- region (Vandooren et al., 2013). So, these forms as well as MMPs that have been bound to inhibitors, and released by the denaturing process, will also be detected by zymography. Therefore, to distinguish which forms are intermediate and which forms have biologically relevant activity, a second assay should be used such as an activity based probe. However, due to time constraints, this investigation of MMP3 and MMP9 activity was not performed.

MMP3 and MMP9 were transiently co-expressed in Cos-7 cells with hepsin-Myc or TMPRSS2-Myc and the ×10 concentrated conditioned media subjected to SDS-PAGE using gelatin-infused gels which were resolved under non-reducing conditions to preserve the intramolecular disulphide bonds of the MMPs, followed by gelatin zymography.

As shown in Figure 4.23, there are bands on the gel representing pro-MMP3 (57 kDa) and the intermediate (53 kDa). However, the 45 kDa "active" MMP3 band is not present either when MMP3 is expressed alone or when co-expressed with hepsin or TMPRSS2. Moreover, no lower MW bands for MMP3 were detected on the gel. It is possible that the 45 kDa MMP3 band is obscured by a contaminant band that runs across all lanes at ~40 kDa – this contaminant band is not detected in the low intensity scan. On the other hand, it is possible the 45 kDa MMP3 is not in conditioned media; rather, it remains on the cell surface after activation. This is reflected by results shown previously in Figures 4.18 to 4.20 where very little cleaved MMP3 was detected in the media. From these results, however, it is unclear whether the 45 kDa MMP3 generated by hepsin and TMPRSS2 is active.

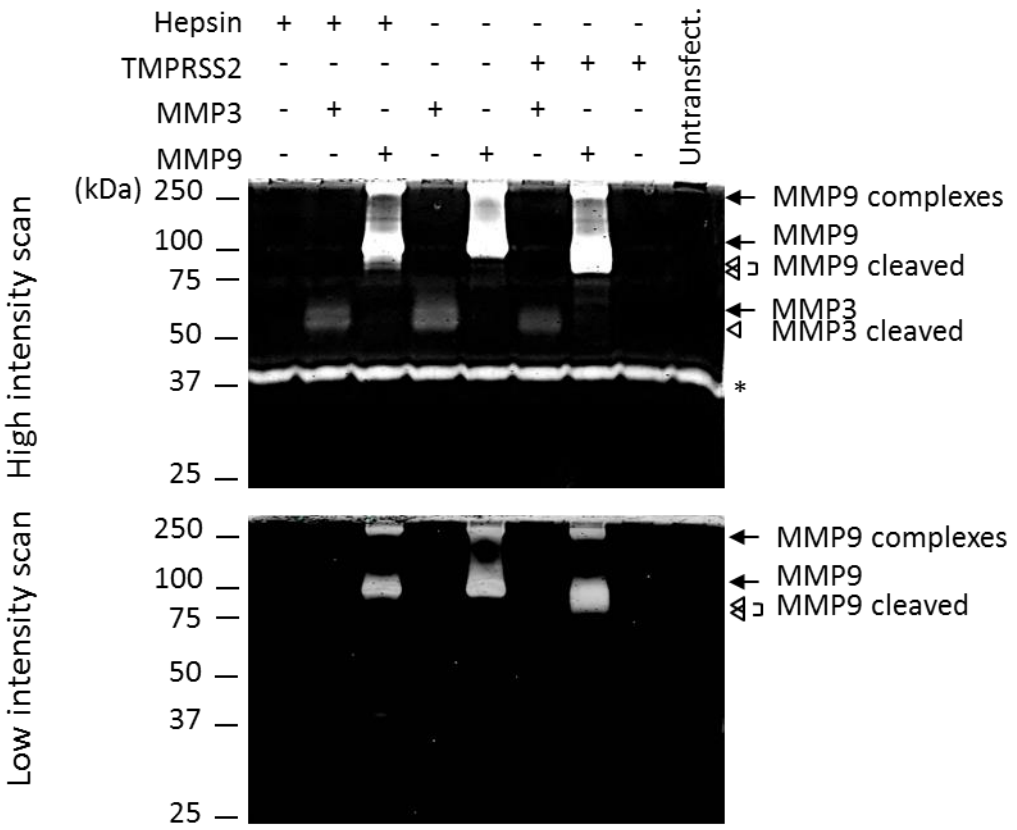

Figure 4.23 Gelatin zymography of MMP3 and MMP9 co-expressed with hepsin and TMPRSS2 in Cos-7 cells. Cells were transiently transfected with constructs encoding wild-type hepsin or TMPRSS2 and were co-transfected with constructs encoding either MMP3 or MMP9 as indicated. The conditioned media were collected 24 hours post-transfection, concentrated ×10 and subjected to gelatin zymography. The clear bands represent areas of gelatin digestion by proteases. *, non-specific gelatin digestion potentially caused by contaminating bacterial proteases.

Interestingly, in contrast, 86 and 82 kDa bands of MMP9 generated when co-expressed with hepsin or TMPRSS2 are detected in the zymogram. This result is interesting as the previous Western blot analyses, shown in Figures 4.18 and 4.19, cleaved MMP9 was not detected in conditioned media. However, in the ×10 concentrated media, these bands representing intermediate (86 kDa) and active MMP9 (82 kDa) as well as full-length 92 kDa MMP9 are detected on the zymogram.

MMP9 is also detected at >250 kDa, representing MMP9 that was in complex, possibly with an inhibitor such as α_2-macroglobulin. A large inhibitor (>180 kDa) such as this has a trapping mechanism which does not disable trapped the protease; rather it sterically hinders the protease active site to prevent substrate cleavage (Sottrup-Jensen,

1989; Rawlings et al., 2004). Therefore MMP9 released from this protease-inhibitor complex during the zymography denaturing-renaturing process may digest gelatin at this very high molecular weight.

4.2.2.4 Recombinant hepsin and matriptase and bovine trypsin proteolyse MMP3

Having established hepsin and matriptase cleave MMP3 and MMP9 in the pericellular environment, the interaction was examined further to see if soluble recombinant hepsin would activate the MMPs in conditioned media. Matriptase and bovine trypsin were assayed alongside because, as mentioned before, matriptase activates MMP3 (Jin et al., 2006) and trypsin activates MMP3 and MMP9 (Nagase et al., 1990; Okada et al., 1992; Sorsa et al., 1997). Conditioned media from Cos-7 cells transiently expressing MMP3 or MMP9 were incubated with active recombinant hepsin, matriptase and bovine trypsin and examined by Western blot analysis under reducing and non-reducing (not shown) conditions using anti-MMP3 and anti- MMP9 antibodies.

As shown in Figure 4.24, after 1 hour incubation MMP3 is proteolysed by hepsin, matriptase and trypsin to generate 53 kDa MMP3 (Figure 4.24A). Only hepsin generated potentially active 45 kDa and 46 kDa MMP3 within the first hour of incubation. However, all the serine proteases generated 45 and 46 kDa MMP3 within the 14 hours. Hepsin and matriptase also generated several lower MW forms of MMP3 in the 14 hours. These bands were also seen in the analyses of lysates and media from the co-expression assays (shown previously in Figures 4.18 to 4.20).

In contrast, after 14 hours incubation, hepsin proteolyses 92 kDa MMP9 to the 82 kDa band, but otherwise MMP9 is relatively untouched by hepsin, matriptase or trypsin (Figure 4.24B). This is interesting as several publications have noted that MMP9 activation is facilitated by the presence of cells or purified plasma membrane extract (Mazzieri et al., 1997; Fridman et al., 2003; Toth et al., 2003). Therefore, while MMP9 was proteolysed at the cell surface by hepsin, TMPRSS2 and matriptase, as evidenced by cell lysate analyses, (Figures 4.18 to 4.20), it may not be readily proteolysed in cell-free media.

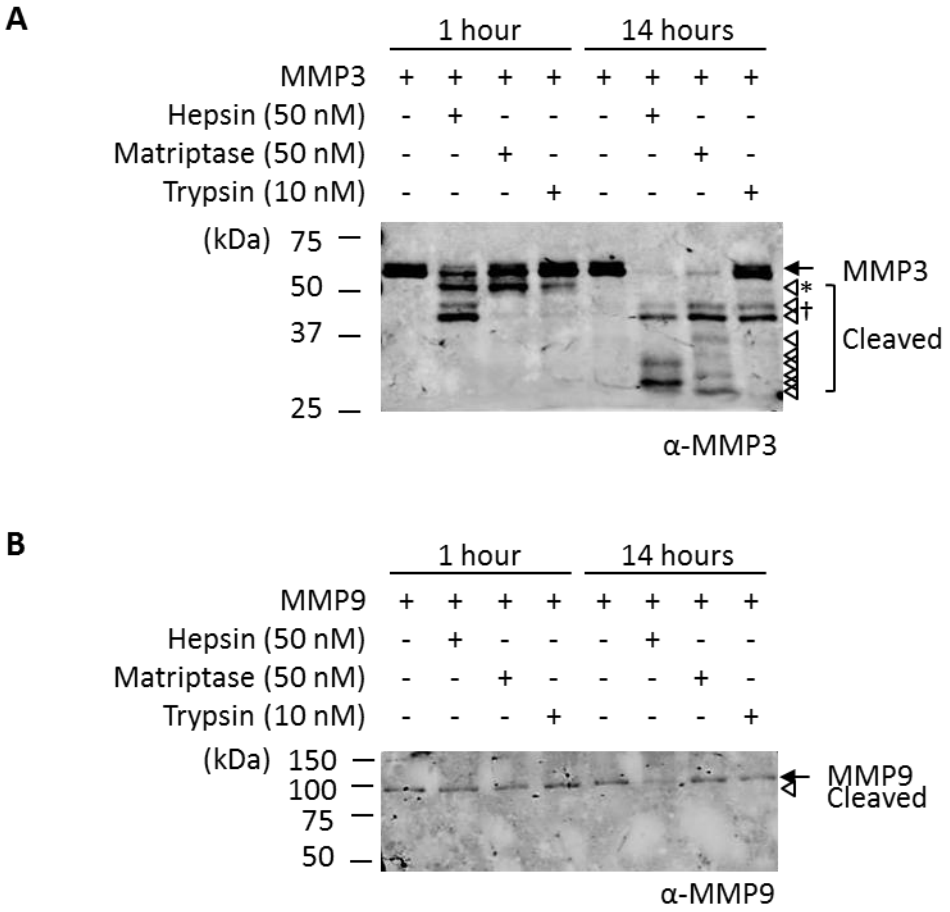

Figure 4.24 Co-incubation of recombinant hepsin, matriptase and bovine trypsin with MMP3 and MMP9 from transfected Cos-7 cells. Cells were transiently transfected with constructs encoding either MMP3 or MMP9. The conditioned media was collected 24 hours post-transfection and incubated at 37°C for 1 or 14 hours, as indicated, with either recombinant hepsin (50 nM), recombinant matriptase (50 nM) or bovine trypsin (10 nM). Reactions stopped with protease inhibitor cocktail and SDS-PAGE loading buffer were subjected to SDS-PAGE under reducing and non-reducing (not shown) conditions and analysis by Western blot using anti-MMP3 (**A**) and anti-MMP9 (**B**) antibodies.

4.3 Discussion

This chapter used a diverse range of approaches to explore the complexity of interactions occurring between secreted proteases KLK4 and KLK14, the transmembrane serine proteases hepsin and TMPRSS2, and to a lesser extent matriptase, and two matrix metalloproteinases MMP3 and MMP9. As summarized in Figure 4.25 the data suggest that:

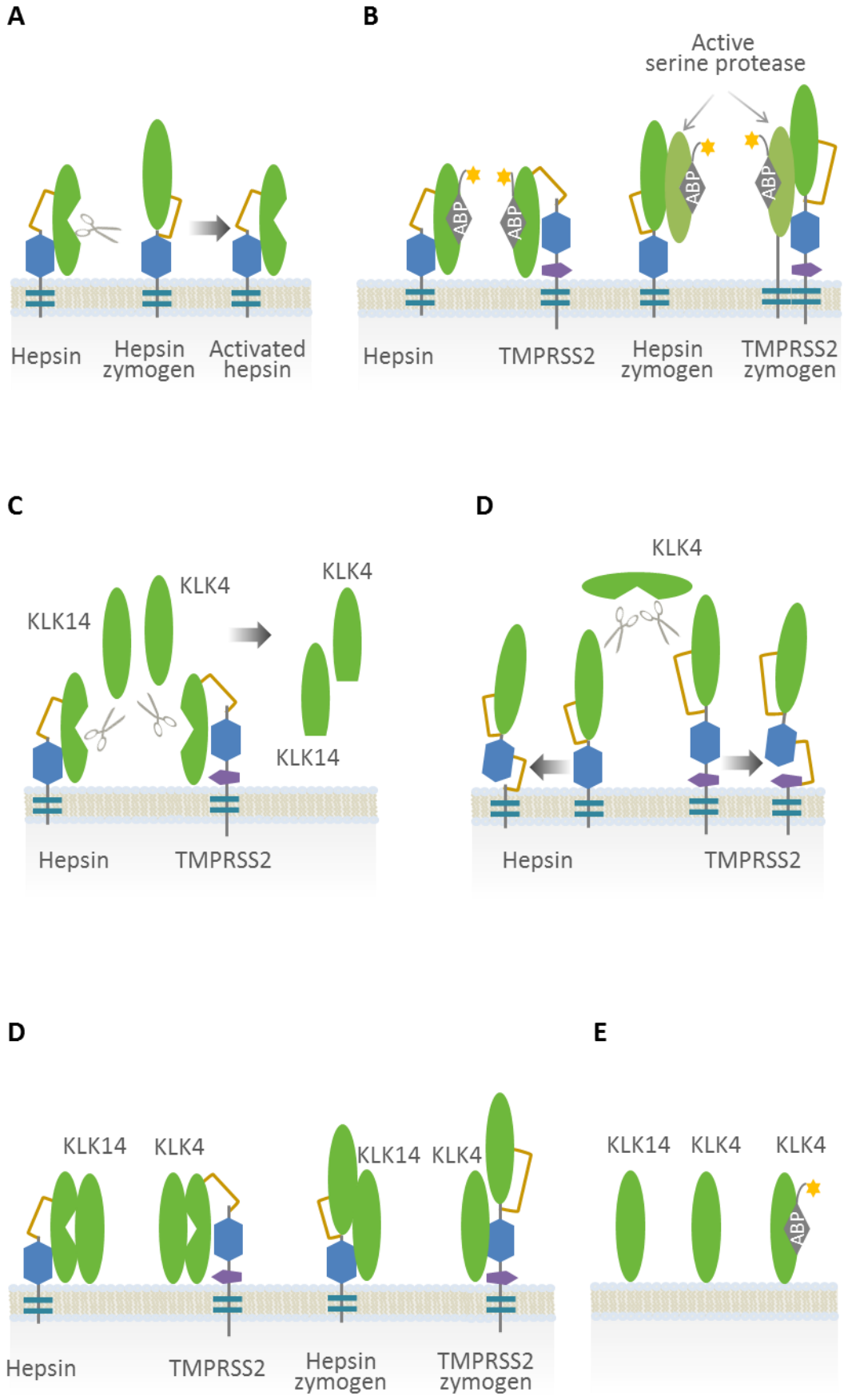
A
Hepsin
Hepsin zymogen
Activated hepsin
B
Active serine protease
ABP
Hepsin
TMPRSS2
Hepsin zymogen
TMPRSS2 zymogen
C
KLK14
KLK4
KLK4
KLK14
Hepsin
TMPRSS2
D
KLK4
Hepsin
TMPRSS2
D
KLK14
KLK4
KLK14
KLK4
Hepsin
TMPRSS2
Hepsin zymogen
TMPRSS2 zymogen
E
KLK14
KLK4
KLK4
ABP

Figure 4.25

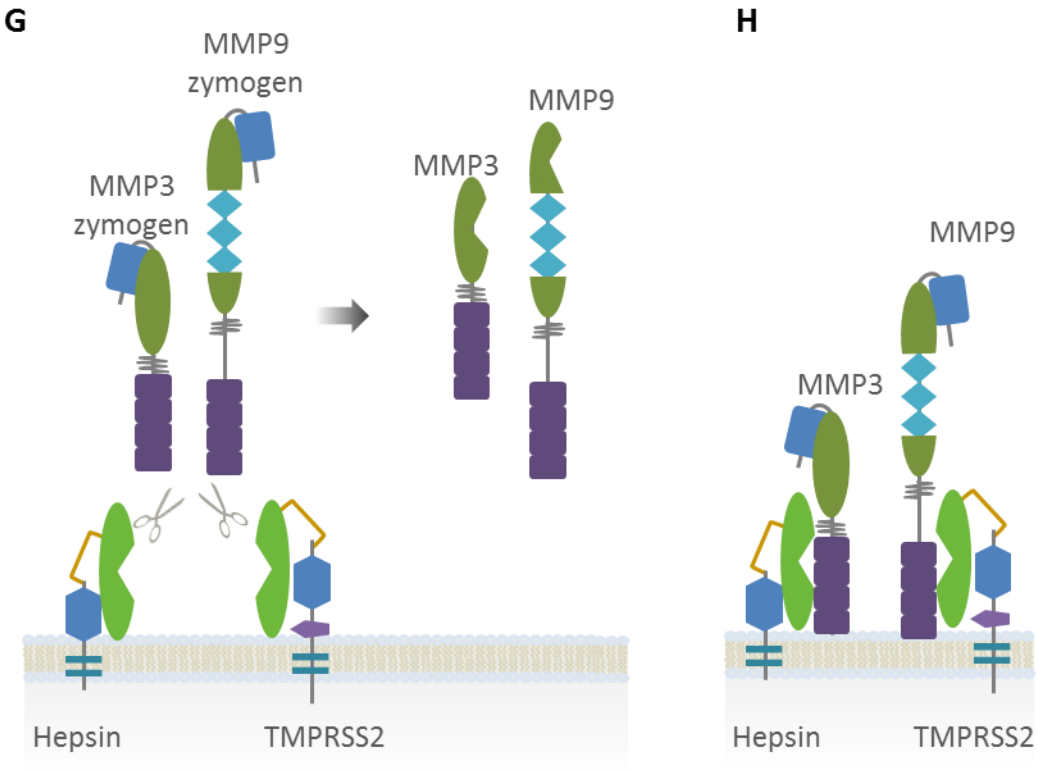

Figure 4.25 Pericellular activity of KLK4, KLK14, hepsin and TMPRSS2. A. Hepsin autoactivates. **B.** Active hepsin and TMPRSS2 localize to the cell surface, and zymogens of these form dimers or oligomers with active proteases. **C.** Hepsin and TMPRSS2 cleave KLK14 and KLK4. **D.** KLK4 cleaves hepsin and TMPRSS2. **E.** Hepsin and TMPRSS2 co-localize with KLK14 and KLK4 independently of hepsin and TMPRSS2 activation. **F.** KLK14 and KLK4 are located on the cell surface, and KLK4 is active on the cell surface. **G.** Hepsin and TMPRSS2 cleave MMP3 and MMP9. **H.** Hepsin and TMPRSS2 co-localize with MMP3 and MMP9. Abbreviation: ABP, activity-based probe.

- Hepsin autoactivates, and hepsin and TMPRSS2 form homo-dimers or oligomers with other proteases or proteins
- KLK4 and KLK14 are proteolysed by hepsin and TMPRSS2, and KLK4 proteolyses hepsin and TMPRSS2
- KLK4 and KLK14 co-localize with hepsin and TMPRSS2 independently of hepsin and TMPRSS2 activation
- KLK14 and KLK4 are located on the cell surface in addition to being secreted into the medium
- Active KLK4 is located on the cell surface
- MMP3 and MMP9 are proteolysed by hepsin and TMPRSS2 (and matriptase)
- MMP3 and MMP9 co-localize with hepsin and TMPRSS2 on the cell surface.

This is the first time cell-surface localization of KLK4 and KLK14 has been demonstrated. In addition, this is the first time active KLK4 has been isolated from the cell surface. The data in this chapter set up the premise for a proteolytic cascade at the plasma membrane involving TMPRSS2 or hepsin activating MMP3 and MMP9, with activated MMP3 in turn activating KLK4.

4.3.1 KLK4 and KLK14 are proteolysed by hepsin and TMPRSS2, and KLK4 proteolyses hepsin and TMPRSS2

As several members of the TTSP family autoactivate (Antalis et al., 2011), establishing the autoactivation status of hepsin was deemed a priority for the investigation of hepsin interactions with KLK14 and KLK4. The results presented in this Chapter are consistent with unpublished data by Qiu and colleagues (2007) and results from mouse hepsin studies by Vu and colleagues (1997) that human hepsin autoactivates. In addition, the results in this chapter indicate that TMPRSS2 autoactivates, consistent with a previous study by Afar and colleagues (2001).

The data also indicate that hepsin and TMPRSS2 form high MW complexes of >90 kDa and >200 kDa, respectively, which suggests that they form homo-dimers or oligomers with other proteins. Consistent with this, hepsin and TMPRSS2 zymogens were isolated by ABP pull-down, suggesting that the unactivated proteases formed oligomers with active protease in order for this to occur. It is possible that homo-dimer formation may be a mechanism by which hepsin and TMPRSS2 self-activate. Certainly, they each have an unpaired cysteine residue in their serine protease domain of unknown significance (Leytus et al., 1988; Kurachi et al., 1994; Paoloni-Giacobino et al., 1997; Jacquinet et al., 2001). It is possible these unpaired cysteines assist in dimerization and autoactivation through intermolecular disulphide bond formation. Investigation of autoactivation of matriptase has determined that a number of elements can induce and contribute to autoactivation including, reduced pH (Lee et al., 2007), serum sphingolipid sphingoine 1-phosphate and suramin (Lee et al., 2005), several regions of the matriptase stem domain (Oberst et al., 2003b; Lee et al., 2007; Inouye et al., 2013), and the serine protease prostasin as a co-factor (Szabo et al., 2012; Buzza et al., 2013). It is not yet known whether similar factors have a role in the autoactivation of hepsin or TMPRSS2.

As autoactivating proteases, hepsin and TMPRSS2 potentially have roles in initiating cellular processes. Hepsin has been ascribed roles in degradation of target proteins such

as laminin (Tripathi et al., 2008), and cascade participation through activation of several proteins including factor VII (Kazama et al., 1995; Halabian et al., 2009), matriptase (Camerer et al., 2010), HGF (Herter et al., 2005; Kirchhofer et al., 2005; Owen et al., 2010), uPA (Moran et al., 2006) and macrophage-stimulating protein (Ganesan et al., 2011). In contrast, there are few known substrates of TMPRSS2. To-date the only recognized proteolytic targets of TMPRSS2, other than itself, are PAR2 (Wilson et al., 2005), respiratory virus surface proteins associated with infectivity and spread (Bottcher et al., 2006; Shirogane et al., 2008; Chaipan et al., 2009; Bertram et al., 2010; Bottcher-Friebertshauser et al., 2010; Matsuyama et al., 2010; Glowacka et al., 2011; Shulla et al., 2011; Heurich et al., 2013; Shirato et al., 2013), and possibly the epithelial sodium channel (ENaC) (Donaldson et al., 2002).

The results in this chapter indicate that KLK14 and KLK4 may be substrates of hepsin and TMPRSS2. When co-expressed with hepsin or TMPRSS2, cleaved forms of KLK14 and KLK4 were generated, or the levels of KLK14 and KLK4 in the conditioned media were reduced. Furthermore, when recombinant KLK4 and KLK14 zymogens were co-incubated with the spontaneously active recombinant hepsin, KLK14 and KLK4 were proteolysed. However, the reaction was not efficient in this cell-free assay system as equimolar concentrations of hepsin were required to achieve KLK14 proteolysis, and little proteolysis was observed for either KLK14 or KLK4.

It was interesting that in the co-expression assays, hepsin- and TMPRSS2-cleaved forms of KLK14 remain either at the cell surface or are internalized as these forms were only detected in cell lysates and not in conditioned media. Furthermore, the reduced levels of KLK14 detected in the media when co-expressed with TMPRSS2 may be due to KLK14 being cleaved close to the C-terminal epitope tag rendering it undetectable by the antibody to the tag. Or it could be that KLK14 is cleaved and sequestered to the cell surface by TMPRSS2. Overall, however, the impact of hepsin or TMPRSS2 on the proteolysis of KLK14 appeared to be relatively minor. This may be a reflection of the short transfection time in the co-expression studies, or it may be that hepsin and TMPRSS2 have minor roles in the regulation of KLK14.

However, it is also likely that activation of KLK14 would be achieved by a protease with a preference for a Lys P1 residue. The transmembrane serine protease enteropeptidase is one such protease with a preference for Lys P1 (Zheng et al., 2009). Indeed, Brattsand and colleagues (2005) used enteropeptidase to activate recombinant KLK14. Due to

what was thought to be very restricted expression of enteropeptidase, it was not initially considered a candidate protease for endogenous activation. Enteropeptidase has been found repeatedly to be restricted in expression to the duodenum with expression rapidly tapering beyond this tissue (Zheng et al., 2009). Recently, however, enteropeptidase was detected in oral squamous cell carcinomas (Vilen et al., 2008), as well as during terminal differentiation of keratinocytes in the epidermis granular layer (Nakanishi et al., 2010). This is very interesting as KLK14 is located in the stratum corneum, in the outer most layer of the epidermis (Brattsand et al., 2005; Stefansson et al., 2006). Based on this information, preliminary experiments were performed to determine if co-expression of KLK14 and enteropeptidase resulted in KLK14 activation. Unfortunately, as anti-enteropeptidase antibody was not specific, the results were not able to be interpreted and further studies are required.

In comparison with KLK14, hepsin and TMPRSS2 co-expression had a greater impact on KLK4. In addition to detection of hepsin- and TMPRSS2-cleaved forms of KLK4 in cell lysates, TMPRSS2-cleaved KLK4 was also detected in media. Moreover, the levels of KLK4 in media were markedly reduced when co-expressed with hepsin. The interactions also differed from those with KLK14 in that KLK4 mediated cleavage in the stem regions of hepsin and TMPRSS2, the products of which were detected in the lysate. The activity of KLK4 was independent of hepsin and TMPRSS2 activity as KLK4 mediated hepsinSA and TMPRSS2SA cleavage as well. The significance of this for hepsin and TMPRSS2 function is not known but it does indicate that KLK4 was active in the transient transfections. This is interesting as KLK4 in conditioned media had no proteolytic impact on KLK14 in co-expression assays or co-incubation of conditioned media. This may have been because KLK4 was inactive, inhibited or had an alternative, preferred proteolysis target in the conditioned media. Certainly, activated KLK4 has been shown to form non-covalent oligomers consisting of stacked cyclic tetramers in solution (Debela et al., 2006a). Inactivity of KLK4 when in these conformations has been attributed to obstruction of the active site (Debela et al., 2006a). Taken together it was possible to speculate that active KLK4 was located at the cell surface but not in the media.

4.3.2 KLK4 and KLK14 co-immunoprecipitate with hepsin and TMPRSS2, and KLK14 and active KLK4 are located on the cell surface

As levels of KLK4 and KLK14, to a lesser extent, were reduced in conditioned media either through conversion to lower molecular weight forms or sequestration to the cell surface by hepsin and TMPRSS2, this led to investigation of the cell-surface interactions between KLK4 and KLK14 and the TTSPs. Immunoprecipitation was the first tool used to investigate these relationships and the results indicated that full-length KLK4 and KLK14, and hepsin- or TMPRSS2-generated cleaved forms, co-immunoprecipitated with hepsin and TMPRSS2. The co-immunoprecipitation of full-length KLK4 and KLK14 was independent of hepsin and TMPRSS2 active site integrity as they also co-immunoprecipitated with hepsinSA and TMPRSS2SA.

From these results, however, it is unclear whether the association between KLK14/KLK4 and hepsin/TMPRSS2 is direct or mediated by other proteins, and further, whether the interaction is at the cell surface or internal. Accordingly, cell-surface biotinylation was used to examine if KLK4 and KLK14 localized to the plasma membrane. These results showed that KLK14 and KLK4 were located on the cell surface of the transiently transfected cells, independent of hepsin or hepsinSA co-expression. Furthermore, active KLK4 and KLK14 were not isolated from the media by ABPs. However, when ABPs were used against cell-surface proteins, active KLK4 was detected in cell lysates. Again, active KLK4 was detected independent of hepsin and TMPRSS2 activity. As neither active KLK4 nor active KLK14 were detected in the media, as discussed earlier, it is possible that KLK4 and KLK14 are inactive (not activated). Or perhaps active forms are inhibited in the media by oligomerization, as previously observed for KLK4 (Debela et al., 2006a), or by secreted inhibitors. Other possibilities include that active KLK4 and KLK14 are rapidly degraded, or the transfection period was of insufficient length to allow accumulation of a detectable amount of activated protease in the media. Early experiments (data not shown) included transfections of up to 48 hours for co-expression of KLK4 and KLK14, as well as KLK4 and KLK14 with hepsin or TMPRSS2. The data in these experiments did not indicate any activity for KLK4 or KLK14 in the conditioned media. However, ABP assays were not performed in these instances.

Taken together, these data suggest a role for KLK14 and KLK4 in the pericellular environment. However, the mechanisms responsible for localizing secreted KLK14 and KLK4 at the surface are unknown. These proteases may be localized to the surface

upon secretion or sequestered from the medium by other cell-surface proteins. KLK14, KLK4, hepsin and TMPRSS2 may form part of a larger complex of proteins localized at the surface. Indeed, zymogen hepsin and TMPRSS2 were pulled-down in the ABP assays, possibly as a result of forming complexes with active proteases. It is possible the multi-protein complexes have a role in regulation of the activity of the individual components as cofactors, activators or regulation by degradation.

4.3.3 Interactions of MMP3, MMP9, hepsin and TMPRSS2

As mentioned earlier, KLK4 has a Gln as the P1 residue of its pro-region (Nelson et al., 1999; Stephenson et al., 1999). This is unique in the KLK family, as all the other KLKs have Arg or Lys as the P1 residue (Yousef and Diamandis, 2001). It also makes it unlikely a serine protease with trypsin-like specificity will activate KLK4 (Takayama et al., 2001a; Matsumura et al., 2005; Yoon et al., 2007). In searching for proteases that activate KLK4, studies have turned to proteases outside of the serine protease family. So far, two proteases have been shown to activate KLK4, dipeptidyl peptidase I (DPPI), also known as cathepsin C (Tye et al., 2009), and MMP3 (Beaufort et al., 2010). There is a potential activation cascade between an upstream protease activating MMP3 followed by MMP3 activating KLK4. MMP3 is able to be activated by a few serine proteases including matriptase and trypsin (Jin et al., 2006) and also plasmin (Ramos-DeSimone et al., 1999). In turn, MMP3 is able to activate MMP9 (Ogata et al., 1992; Shapiro et al., 1995). So, the possibility of an activation cascade was examined by first looking at the activation of MMP3 and MMP9 by hepsin and TMPRSS2 and also by matriptase.

The results of co-expression of MMP3 and MMP9 with hepsin, TMPRSS2 and matriptase were interesting. Similar to the results for KLK14 and KLK4 co-expression with hepsin and TMPRSS2, proteolysed MMP3 and MMP9 were detected in cell lysates. Moreover, bands of MWs corresponding to the active forms of MMP3 and MMP9 were among the cleaved forms detected in cell lysates. Interestingly, when compared to the double transfection of a TTSP with either MMP3 or MMP9, the triple co-transfection of a TTSP with both MMP3 and MMP9 conferred little to the proteolysis of MMP3 or MMP9. Very little cleaved MMP3 and no cleaved MMP9 were detected in the conditioned media. This could be because of the short transfection period of 24 hours. A longer transfection before processing the conditioned media may increase the detection of cleaved MMP9 and MMP3 in the media. However, the lack of cleaved

MMP3 and MMP9 in the media may also indicate a role for the activated MMPs in the pericellular environment.

Gelatin zymography was used to assess whether activated MMP3 and MMP9 could be detected in the media. Unfortunately, it is unclear whether the 45 kDa MMP3 generated by hepsin and TMPRSS2 was active as the zymography did not show a band at this MW in the media. However, the 82 kDa MMP9 generated by hepsin and TMPRSS2 was detected and was active in the media. To extend this work, two approaches can be taken. First, MMP3 and MMP9 should be isolated from cell lysates by antibody affinity chromatography and then gelatin zymography performed on the isolates. Second, another method should be used to validate the zymography of the media and cell lysates as zymography has an inherent weakness. As mentioned earlier, as well as biologically relevant active MMP, pro-MMP and intermediate forms are also detected in the zymography assay. So, to distinguish which forms are intermediate and which forms have biologically relevant activity, a second assay should be used to confirm the data such as an ABP-based approach. Due to time constraints, the additional investigation of MMP3 and MMP9 activity was not performed.

Co-immunoprecipitations of MMP3 and MMP9 with hepsin and TMPRSS2 from cell lysates reinforced the argument for a role for MMP3 and MMP9 in the pericellular environment through interaction with cell surface proteins. It is unknown if the interaction with the TTSPs is direct or mediated by a larger protein complex, as speculated earlier for KLK14 and KLK4. Indeed, several studies have shown MMP9 associated with the plasma membrane by a variety of interactions including endothelial cell focal contacts (Partridge et al., 1997), uPA and uPAR (Mazzieri et al., 1997), CD44 (Yu and Stamenkovic, 1999), and several integrins (Morini et al., 2000; Stefanidakis et al., 2004; Yang et al., 2008). It is possible that one or more of these interactions contributes to cell-surface association of MMP3 and MMP9 with the TTSPs.

Plasma membrane association is thought to favour activation of MMP9 (Toth et al., 2003). So it was interesting that MMP9 in conditioned media from transiently transfected cells was not proteolysed by recombinant matriptase or bovine trypsin. After 14 hours incubation, recombinant hepsin achieved minimal MMP9 cleavage. In contrast, MMP3 in conditioned media was efficiently proteolysed to generate the putative active 45 kDa form when incubated with recombinant hepsin. Matriptase and trypsin also generated this 45 kDa form of MMP3, however, not as rapidly as hepsin.

Together, these data suggest a role for hepsin and TMPRSS2 in the pericellular proteolysis and activation of MMP3 and MMP9. Furthermore, the proteolysis of MMP9 may be dependent on the plasma membrane.

4.3.4 Summary

In this chapter proteolytic interactions between the serine proteases KLK14, KLK4, hepsin and TMPRSS2 were examined as well as the interactions between hepsin and TMPRSS2 and the metalloproteinases MMP3 and MMP9. The results demonstrated that hepsin and TMPRSS2 interact with KLK14, KLK4, MMP3 and MMP9 in the pericellular environment resulting in proteolysis at the cell surface.

This work adds to the growing body of studies that have proposed proteolytic interactions between KLKs and members of other protease families. As summarized in the hypothetical zymogen cascade in Figure 4.26, TTSPs hepsin, TMPRSS2 and matriptase are all potentially capable of activating MMP3 which in turn activates KLK4. KLK14 on the other hand is potentially activated by other members of the KLK family such as KLK5, or by TTSP enteropeptidase. Both KLKs, however, interact with the plasminogen activation system: KLK4 through activation of uPA, which in turn activates plasminogen to plasmin; and KLK14 though activation by plasmin.

It is recognized that there are limitations to the overexpression approach used in this thesis to examining proteolytic interactions. These include that biologically irrelevant or non-preferred substrates may be cleaved because of the artificially high expression levels or because the proteases are not normally co-expressed (Overall and Blobel, 2007). It is therefore necessary to validate potential interactions using cells that endogenously express these proteins using methods such as co-immunoprecipitation to identify interacting partners. There are also knockout mouse models available for several of the proteases examined in this study, including KLK4 (Simmer et al., 2009), hepsin (Wu et al., 1998) and TMPRSS2 (Kim et al., 2006). These *in vivo* models can be used in approaches such as through global characterization of substrate processing by identifying amino-termini modification using methods such as terminal amine isotopic labelling of substrates (TAILS)(Kleifeld et al., 2011).

New proteolytic interactions in the pericellular environment are constantly emerging, however, there a numerous proteases whose proteolytic roles have not been determined.

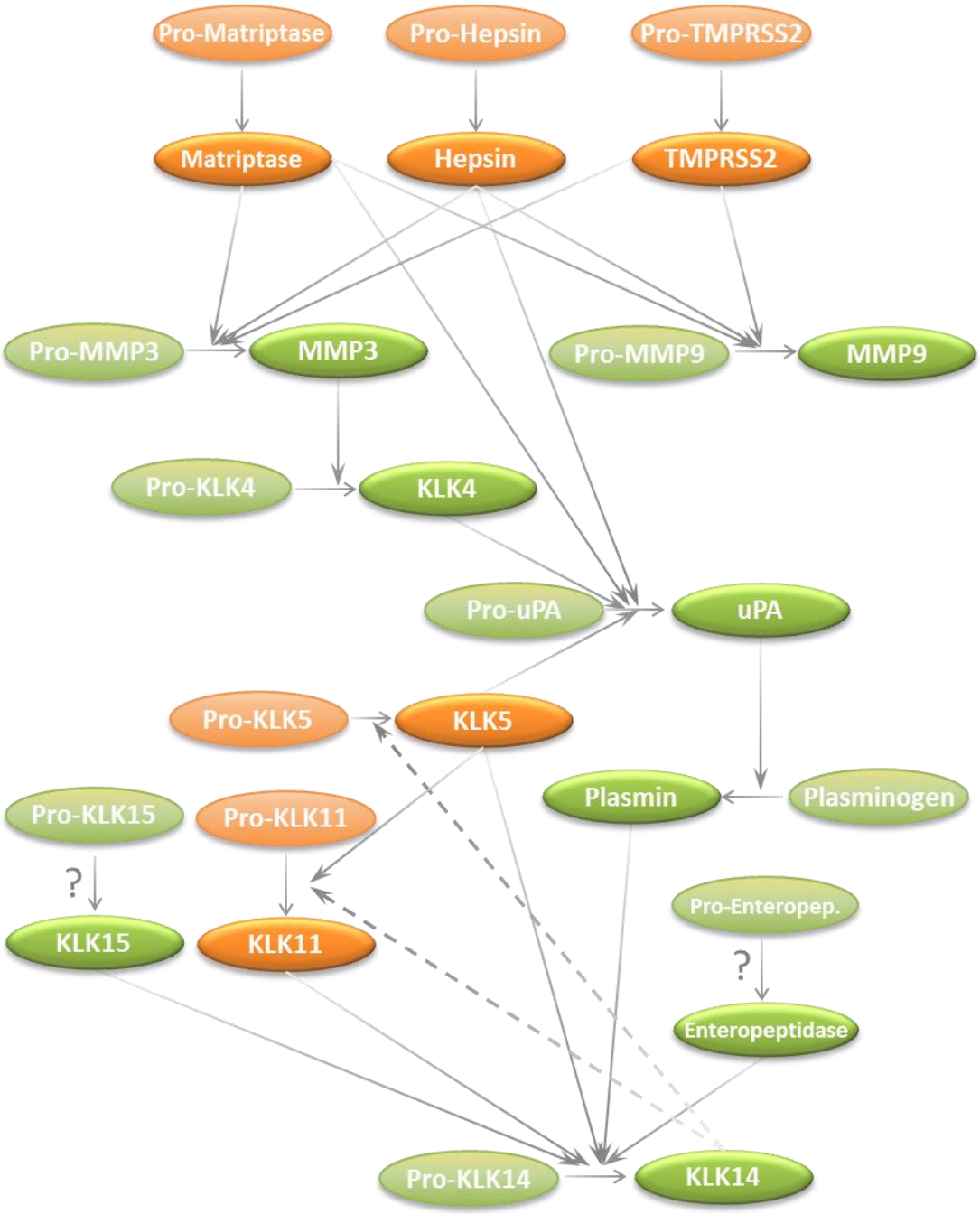

Figure 4.26 KLK4 and KLK14 in zymogen cascades. Serine proteases which KLK4 and KLK14 have been shown to activate, or be activated by. Matriptase, hepsin, TMPRSS2, KLK5 and KLK11 autoactivate (orange). The dashed lines indicate possible cascade amplification by KLK14 through activation of KLK5 and KLK11.

The serine proteases kallikrein 14 (KLK14) (2, 3), kallikrein 4 (KLK4) (4-8), hepsin (9-11) and TMPRSS2 (12, 13), are all overexpressed at the mRNA and/or protein level in prostate cancer tissues compared to normal prostate. Each of these serine proteases has the potential to interact in novel proteolytic cascade pathways in the dysregulated cancerous prostate environment and contribute to disease progression.

One of the results of proteolytic cascades can be initiation of cell signalling via cell surface receptors. A system that has gained recognition as a potential contributor to the progression of prostate cancer is the four member family of protease activated receptors (PARs) designated PAR-1 to PAR-4. Cleavage and signalling through the PARs, which constitute a sub-family of G protein-coupled receptors (GPCRs), is achieved by trypsin-like serine protease proteolysis of an activation peptide sequence from the extracellular N-terminal of the PAR. Activation of the PARs will be examined in more detail in the following chapter.

Chapter 5 Analysis of PAR activation by KLK4, KLK14 and hepsin

5.1 Introduction

PARs are members of the GPCR super-family, a family of structurally similar proteins that mediate outside-in cell signalling (Macfarlane et al., 2001; Oldham and Hamm, 2008). Intracellular signalling events initiated as a result of PAR activation are diverse and complex, and they contribute to myriad cellular events (as reviewed extensively in (Macfarlane et al., 2001; Ossovskaya and Bunnett, 2004; Coughlin, 2005; Steinhoff et al., 2005; Soh et al., 2010; Adams et al., 2011)). The role of PARs in tumours and the tumour microenvironment is of particular interest as there is a growing body of evidence that PAR-induced Ca^{2+} signalling can contribute to progression of some cancer characteristics such as inflammation, cell proliferation, migration and invasion (Ossovskaya and Bunnett, 2004; Steinhoff et al., 2005; Kaufmann and Hollenberg, 2012; Rothmeier and Ruf, 2012). Signalling via the PARs has been characterized in a number of cell lines and tumour cells including breast (Even-Ram et al., 1998; D'Andrea et al., 2001; Kamath et al., 2001; Matej et al., 2007; Su et al., 2009), non-melanoma skin cancer (Bocheva et al., 2009), colon (Darmoul et al., 2001; Darmoul et al., 2003; Darmoul et al., 2004a; Darmoul et al., 2004b; Gratio et al., 2009; Gratio et al., 2010; Gratio et al., 2011), renal (Kaufmann et al., 2002; Zhang et al., 2013) and prostate (Chay et al., 2002; Greenberg et al., 2003; Cottrell et al., 2004; Tantivejkul et al., 2005; Wilson et al., 2005; Kaushal et al., 2006; Black et al., 2007; Mize et al., 2008; Ramsay et al., 2008a; Zhang et al., 2009).

Activation of signalling via the PARs is one of the potential roles of serine proteases in the pericellular microenvironment. The serine proteases KLK4, KLK14, hepsin and matriptase are attractive targets for analysis of PAR activation due to their co-incident expression with PARs in several tissues. Of particular interest is that in prostate tissue and prostate cancer, KLK4 (Day et al., 2002; Obiezu et al., 2002; Xi et al., 2004; Dong et al., 2005; Obiezu et al., 2005; Klokk et al., 2007; Ramsay et al., 2008a; Seiz et al., 2010; Wang et al., 2010), KLK14 (Borgono et al., 2007c; Rabien et al., 2008), hepsin (Dhanasekaran et al., 2001; Xuan et al., 2006; Morrissey et al., 2008; Goel et al., 2011) and matriptase (Saleem et al., 2006) protein are expressed along with PAR1, PAR2 and PAR4 (D'Andrea et al., 1998; Myatt and Hill, 2005; Tantivejkul et al., 2005; Kaushal et al., 2006; Black et al., 2007; Ramsay et al., 2008a; Wang et al., 2008; Zhang et al., 2009; Mannowetz et al., 2010). Kidney is another tissue where expression of PAR1, PAR2 and PAR3 (Rondeau et al., 1996; D'Andrea et al., 1998; Grandaliano et al., 2000; Kaufmann et al., 2002; Grandaliano et al., 2003; Vesey et al., 2005; Vesey et al., 2007; Zhang et al.,

2013) and KLK4 (Shaw and Diamandis, 2007; Seiz et al., 2010) has been noted. In particular, overlapping protein expression of PAR2 and KLK4 has been reported in human kidney proximal tubule cells (PTC) by Vesey and colleagues (2007)(and personal communication). Furthermore, from the results in the previous chapter, KLK4 and KLK14 localization to the cell surface may be facilitated by multi-protein complexes involving TTSPs, such as hepsin and possibly matriptase, as well as MMPs. This cell surface localization of the KLKs may facilitate pericellular activity including activation of PARs.

As reviewed in Chapter 1, PARs can be activated by specific proteolysis of the extracellular N-terminal to reveal a new N-terminus known as the tethered ligand (Vu et al., 1991a; Ramachandran et al., 2012a). It is supposed that the PAR tethered ligand binds intra-molecularly to extracellular domains to effect PAR conformation change and intracellular C-terminal domain recruitment of G proteins and other signalling molecules (Vu et al., 1991a; Adams et al., 2011). One method used in this chapter for assessing PAR activation monitors intracellular mobilization of second messenger calcium (Ca^{2+}). This exploits elements of signalling cascades triggered by G_q-coupling to activated PAR (Macfarlane et al., 2001; Steinhoff et al., 2005; Kaufmann and Hollenberg, 2012) (Figure 5.1). Proteolysis at distinct sites in the N-terminal domain can also disarm PARs by rendering the tethered ligand unavailable for receptor activation (Renesto et al., 1997; Dulon et al., 2003; Nakayama et al., 2003; Adams et al., 2011).

As in other members of the GPCR super-family, PAR signalling is terminated by a range of mechanisms including phosphorylation of the intracellular C-terminal, recruitment of β-arrestins, subsequent uncoupling of the G-proteins and internalization of activated PARs (Soh et al., 2010; Adams et al., 2011). There is still a great deal to learn about PAR signal termination, especially for PAR3 and PAR4. However, as activation by proteolysis is irreversible, ultimately, the PARs are targeted for lysosomal degradation (Bohm et al., 1996a; Shapiro and Coughlin, 1998; Soh et al., 2010).

PAR1, PAR2 and PAR4 can also be selectively activated by short peptides, modelled on the tethered ligands, known as PAR agonist peptides (AP) (Vu et al., 1991a; Scarborough et al., 1992; Chen et al., 1994; Lerner et al., 1996). PAR APs are useful tools for interpreting the function of PARs (Hollenberg and Compton, 2002; Ramachandran et al., 2012b) and so are used for this purpose in this chapter. PAR3 can also be activated by proteolysis of the N-terminal (Ishihara et al., 1997). However, PAR3

signalling is complicated by its possible function as a cofactor for PAR4 activation (Nakanishi-Matsui et al., 2000; Bah et al., 2007) as well as regulator of PAR1 through receptor dimerization (McLaughlin et al., 2007). Moreover, a PAR AP capable of initiating signalling via PAR3 has not been identified (Ishihara et al., 1997; Nakanishi-Matsui et al., 2000). For these reasons PAR3 activation has not been included in this chapter.

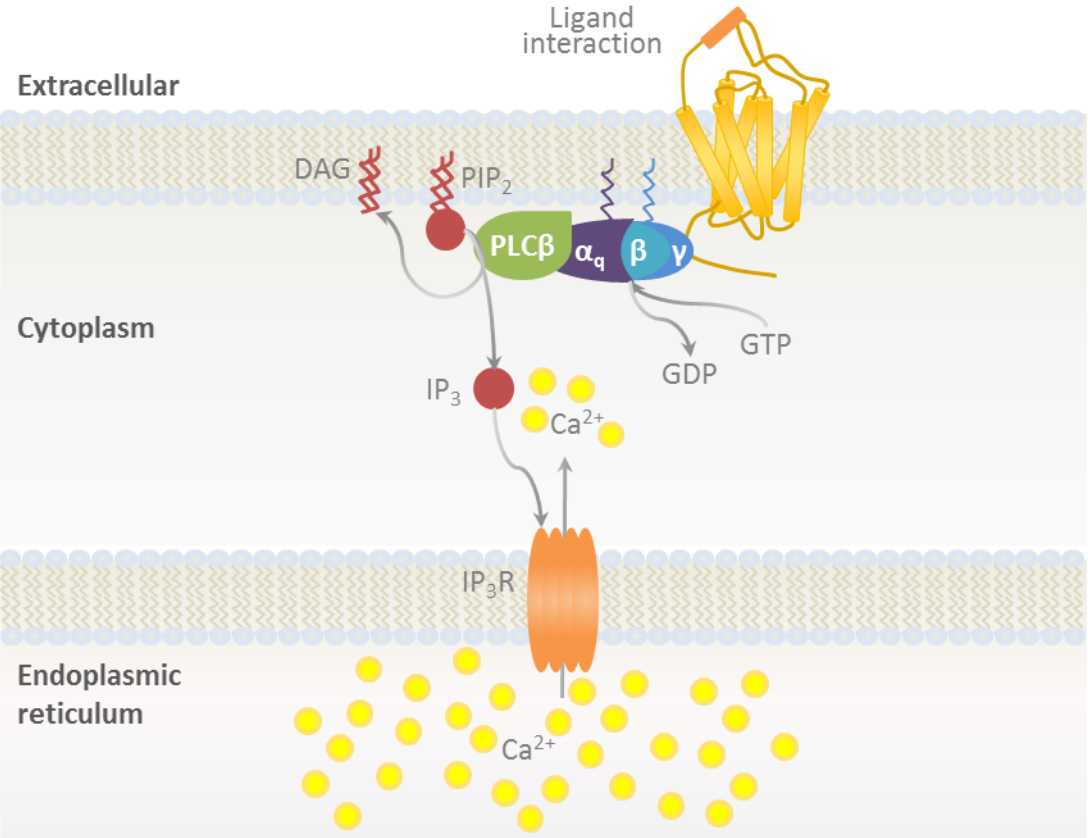

Figure 5.1 G_q-mediated calcium signalling. Calcium signalling mediated by GPCRs such as PARs is induced by coupling with heterotrimeric G protein subtype G_q. Ligand bound PAR induces activation of G_q through exchange of guanosine diphosphate (GDP) for guanosine triphosphate (GTP) on the Gα subunit. G_q α subunit activates phospholipase C-β (PLCβ). PLCβ cleaves membrane-bound phospholipid phosphatidylinositol 4,5-bisphosphate (PIP_2) into inositol-1,4,5-trisphosphate (IP_3) and diacylglycerol (DAG). Free IP_3 binds to inositol-1,4,5-trisphosphate receptor (IP_3R), a ligand gated calcium channel on the endoplasmic reticulum, which opens the ion channel to allow calcium to flow into the cytoplasm. Calcium is then able to activate a number of cytoplasmic and membrane bound molecules, enzymes, and reactions. *Adapted from* Clapham 2007 and Oldham 2008.

As the P1 residue of the activation site for the PARs is either an Arg (PAR1, PAR2 and PAR4) (Vu et al., 1991a; Nystedt et al., 1994; Nystedt et al., 1995a; Xu et al., 1998), or a Lys (PAR3) (Ishihara et al., 1997) residue, numerous trypsin-like serine proteases have been analysed for their ability to activate the PARs. The serine proteases used in this chapter, KLK4, KLK14 hepsin and matriptase, are ideal candidates to investigate the activation of PARs as they have a preference for cleaving after Arg residues (Lin et al., 1999c; Lee et al., 2000; Takeuchi et al., 2000; Takayama et al., 2001a; Friedrich et al., 2002; Brattsand et al., 2005; Felber et al., 2005; Herter et al., 2005; Matsumura et al., 2005; Debela et al., 2006a; Debela et al., 2006b; Obiezu et al., 2006; Oikonomopoulou et al., 2006a; Borgono et al., 2007a; Borgono et al., 2007b; Borgono et al., 2007c; Stefansson et al., 2008; Beliveau et al., 2009; Owen et al., 2010). They have previously been assessed for their ability to activate or disarm PARs by cleaving within the PAR N-terminal. It has been found that KLK4 activates PAR1 and PAR2 but not PAR4 (Mize et al., 2008; Ramsay et al., 2008a; Gratio et al., 2010); KLK14 activates PAR1, PAR2 and PAR4 and disarms PAR1 (Oikonomopoulou et al., 2006a; Stefansson et al., 2008; Gratio et al., 2011; Ramachandran et al., 2012a); and matriptase selectively activates PAR2 but not PAR1 or PAR4 (Takeuchi et al., 2000; Seitz et al., 2007; Camerer et al., 2010). Until recently it had not been established whether hepsin could activate members of the PAR family, but recently published work confirms the finding in this chapter that hepsin does not activate PAR1 or PAR2 (Camerer et al., 2010). Trypsin was also used in this chapter as a model PAR-activating protease. Trypsin was first recognized as a PAR2 activator by Nystedt and colleagues (1994). The presence of a trypsin cleavage site in the PAR2 N-terminal has allowed trypsin to be used extensively in PAR2 activation studies (Bohm et al., 1996b; Macfarlane et al., 2001). Trypsin also activates and disarms PAR1 (Vu et al., 1991a; Blackhart et al., 1996; Kawabata et al., 1999; Loew et al., 2000; Nakayama et al., 2003), and activates PAR4 (Kahn et al., 1998; Xu et al., 1998).

The aim of this chapter was to examine KLK4, KLK14, hepsin and matriptase activation of PARs. As an element of this, prostate cancer-derived LNCaP cells stably overexpressing hepsin were generated and characterized to examine proteolytic cascades resulting in activation of PARs.

5.2 Results

5.2.1 KLK14, matriptase and hepsin can affect signalling by either activating or disarming PARs

At the beginning of this project the ability of serine proteases KLK14 and hepsin to activate or disarm PARs had not previously been examined. The experiments described here use Ca^{2+} flux assays, assessing changes in free $[Ca^{2+}_i]$, to interrogate the activation of PAR1, PAR2 and PAR4 by active recombinant KLK14, hepsin, matriptase and bovine trypsin. As stated earlier in Chapter 2, the cell lines used in these experiments are derived from lung myofibroblasts immortalized from PAR1 -/- mice (Darrow et al., 1996). These cells, also lacking functional endogenous mouse PAR2 and PAR4, have been transfected to stably express one each of the human PARs, PAR1, PAR2 or PAR4 (Andrade-Gordon et al., 1999). Designated PAR1-LMF, PAR2-LMF and PAR4-LMF, these cell lines are useful *in vitro* tools for examining PAR activation as Ca^{2+} flux response is elicited from each line by the respective PAR AP. Consecutive treatments of serine protease followed by PAR AP provide information about the ability of the proteases to activate the PAR.

5.2.1.1 PAR1 activation

As shown in Figure 5.2A, PAR1AP (50 μM) elicited a robust change in free $[Ca^{2+}_i]$ in PAR1-LMF cells. Trypsin (10 nM) and KLK14 (150 nM) (Figure 5.2B and C) induced modest change in $[Ca^{2+}_i]$ while the follow up treatment with PAR1AP (50 μM), 180 seconds after KLK14 introduction, induced a small, brief change in $[Ca^{2+}_i]$. This indicates that 150 nM KLK14 activated a portion of the PAR1 on the LMF cell surface but a portion remained and was activated by PAR1AP.

In contrast, hepsin (50 nM) and matriptase (10 nM) elicited very little change in free $[Ca^{2+}_i]$ (Figures 5.2D and E). Moreover, the follow up treatment with PAR1AP (50 μM), 180 seconds after hepsin or matriptase, elicited a strong Ca^{2+} flux response of magnitude similar to that observed for the solo PAR1AP treatment shown in Figure 5.2A. This indicates that hepsin and matriptase neither activated nor disarmed PAR1 under these assay conditions.

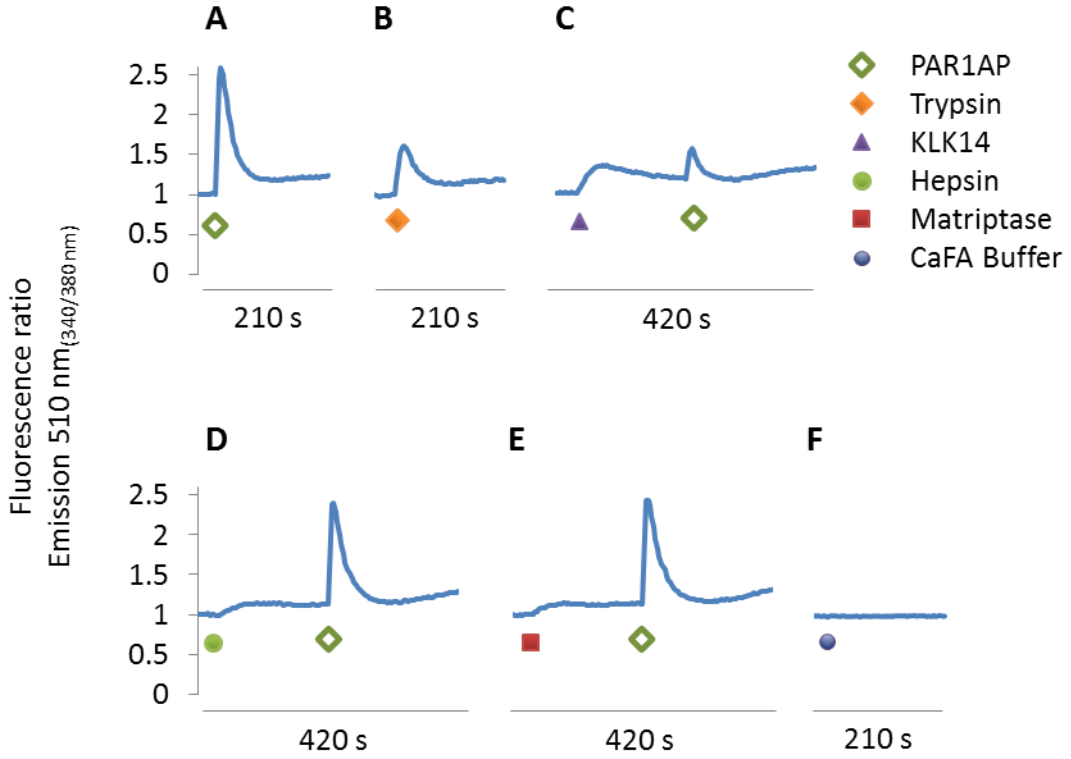

Figure 5.2 Serine protease-induced cytosolic calcium release in PAR1-LMF cells. PAR1-LMF cells were treated with (**A**) PAR1AP (50 µM) (◇) or (**B**) trypsin (10 nM) (◆), or treated with, (**C**) KLK14 (150 nM) (▲), (**D**) hepsin (50 nM) (●) or (**E**) matriptase (10 nM) (■) followed by PAR1AP (50 µM). Also included was (**F**) CaFA buffer (●) treatment. Changes in $[Ca^{2+}_i]$ were assayed by exciting ratiometric calcium indicator Fura-2 in the cells at alternating 340 and 380 nm. The emission at 510 nm was measured using a fluorescent plate reader. The ratio of emission 510 $nm_{(340/380\ nm)}$ is proportional to free $[Ca^{2+}_i]$. The symbols indicate treatment injection points at 30 seconds for single treatments, and 30 and 210 seconds for consecutive treatments. Data presented is the mean value of experiments performed in triplicate. Experiments were performed three times for trypsin (one representation shown) and performed once for all other serine proteases.

5.2.1.2 PAR2 activation

As shown in Figures 5.3, when compared to PAR2AP (50 µM), trypsin (10 nM) induced robust mobilization of free $[Ca^{2+}_i]$ in PAR2-LMF cells. The response to KLK14 (150 nM) was modest, and negligible response was induced by hepsin (50 nM) (Figure 5.3C and D). On the other hand, matriptase (10 nM) induced Ca^{2+} flux of a similar magnitude to that of trypsin (Figure 5.3E). The follow up treatment with PAR2AP (50 µM) after trypsin, KLK14 or matriptase, induced a small, brief change in $[Ca^{2+}_i]$. This indicates

that, at these protease concentrations a portion of the PAR2 remained on the LMF cell surface and was activated by PAR2AP (Figure 5.3B, C and E).

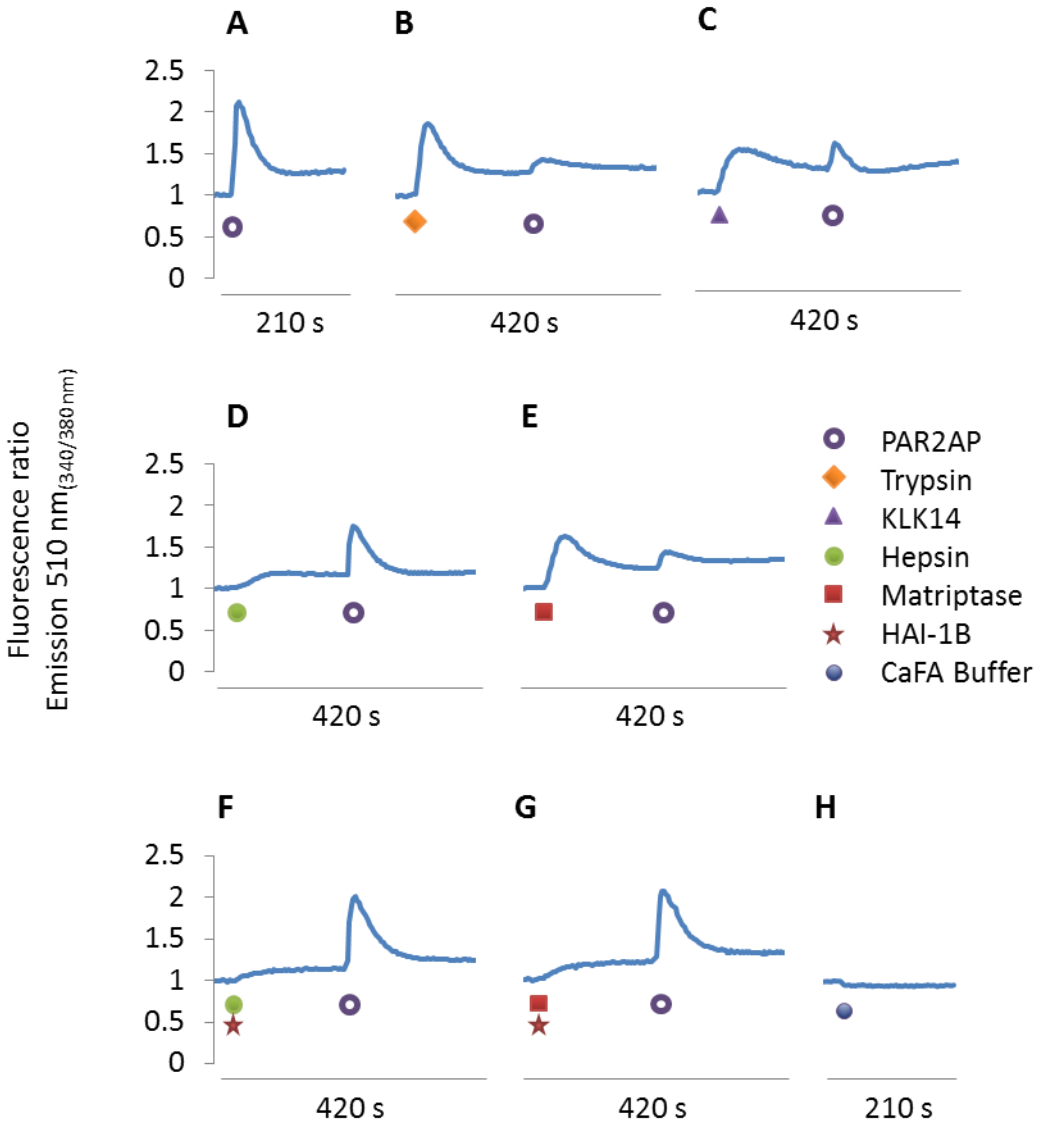

Figure 5.3 Serine protease-induced cytosolic calcium release in PAR2-LMF cells. PAR2-LMF cells were treated with (**A**) PAR2AP (50 µM) ( ), or treated with (**B**) trypsin (10 nM) ( ), (**C**) KLK14 (150 nM) ( ), (**D**) hepsin (50 nM) ( ), (**E**) matriptase (10 nM) ( ), (**F**) hepsin (50 nM) + HAI-1B (1 µM)( ), or (**G**) matriptase (10 nM) + HAI-1B (1 µM), followed by PAR2AP (50 µM). Also included was (**H**) CaFA buffer ( ) treatment. Changes in $[Ca^{2+}_i]$ were assayed by exciting ratiometric calcium indicator Fura-2 in the cells at alternating 340 and 380 nm. The emission at 510 nm was measured using a fluorescent plate reader. The ratio of emission 510 $nm_{(340/380\ nm)}$ is proportional to free Ca^{2+}_i. The symbols indicate treatment injection points at 30 seconds for single treatments, and 30 and 210 seconds for consecutive treatments. Data presented is the mean value of experiments performed in triplicate. Experiments were performed three times for trypsin (one representation shown) and performed once for all other serine proteases.

In contrast, the follow up treatment with PAR2AP (50 μM) after hepsin, elicited a strong Ca^{2+} flux response (Figure 5.3D). However, the magnitude of the post-hepsin PAR2AP response is lower than that observed for the solo PAR2AP treatment shown in Figure 5.3A. This indicates that while there is negligible hepsin-induced PAR2-mediated Ca^{2+} flux under these assay conditions, hepsin did render a portion of the PAR2 insensitive to activation by PAR2AP.

Further to this, when hepsin and matriptase were pre-incubated with the serine protease inhibitor HAI-1B (1 μM) (Figures 5.3F and G), the very small change in free $[Ca^{2+}_i]$ elicited by hepsin and the substantial response elicited by matriptase were largely abolished and the Ca^{2+} flux response to the PAR2AP follow-up treatment was near equal to that observed for the solo PAR2AP treatment (Figure 5.3A). This indicates HAI-1B prevented activation of PAR2 mediated Ca^{2+} flux by matriptase and also inactivation by hepsin.

5.2.1.3 PAR4 activation

PAR4 has been shown to be less sensitive than PAR1 or PAR2 to activation by AP, trypsin and other serine proteases (Vu et al., 1991a; Nystedt et al., 1994; Xu et al., 1998; Faruqi et al., 2000; de Garavilla et al., 2001; Al-Ani and Hollenberg, 2003). Therefore, to elicit robust Ca^{2+} mobilization PAR4AP was used at concentrations of 150-500 μM, and trypsin and matriptase were used at 50 nM in Ca^{2+} flux assays of PAR4-LMF cells, concentrations higher than used for the PAR1 and PAR2 assays. However, due to limited supply higher concentrations of KLK14 and hepsin were not feasible. KLK14 and hepsin were used at 150 and 50 nM, respectively, the same as used for the PAR1- and PAR2-LMF Ca^{2+} flux assays.

As shown in Figure 5.4A, PAR4AP (150 μM and 500 μM) induced robust Ca^{2+} flux response in the PAR4-LMF cells. PAR4AP at 500 μM was used in early Ca^{2+} flux assays, replicating methods published by Ramsay and colleagues (2008a). However, as shown in Figure 5.4A, 150 μM PAR4AP induced a higher Ca^{2+} mobilization response from the PAR4-LMF cells and so was used in subsequent assays.

Trypsin (50 nM) and KLK14 also activated PAR4 (Figures 5.4B and C). Subsequent application of PAR4AP (500 μM) after trypsin induced little change in free $[Ca^{2+}_i]$ indicating that trypsin activated most of the PAR4 on the LMF surface. In contrast, the

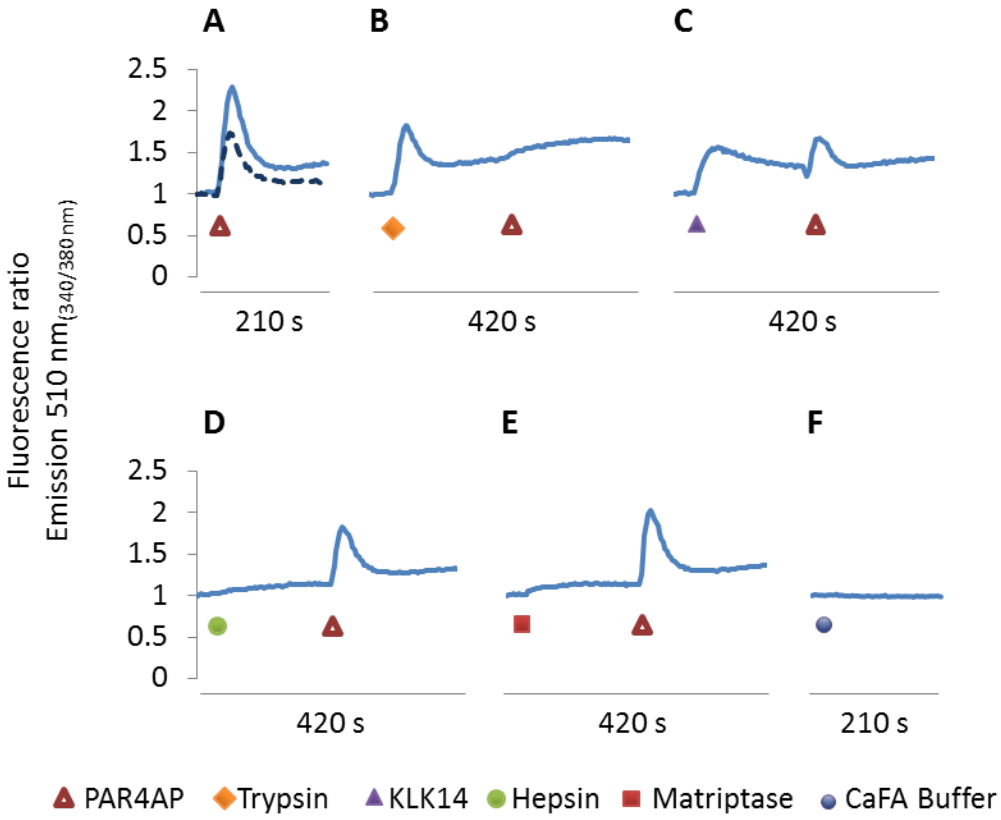

Figure 5.4 Serine protease-induced cytosolic calcium release in PAR4-LMF cells. PAR4-LMF cells were treated with (**A**) PAR4AP (150 µM, solid line; 500 µM, dashed line)(▲), or treated with (**B**) trypsin (10 nM) (◆), (**C**) KLK14 (150 nM) (▲), (**D**) hepsin (50 nM) (●) or (**E**) matriptase (10 nM) (■) followed by PAR4AP (150 µM for KLK14; 500 µM for trypsin, hepsin and matriptase). Also included was (**F**) CaFA buffer (●) treatment. Changes in $[Ca^{2+}_i]$ were assayed by exciting ratiometric calcium indicator Fura-2 in the cells at alternating 340 and 380 nm. The emission at 510 nm was measured using a fluorescent plate reader. The ratio of emission 510 $nm_{(340/380\ nm)}$ is proportional to free $[Ca^{2+}_i]$. The symbols indicate treatment injection points at 30 seconds for single treatments, and 30 and 210 seconds for consecutive treatments. Data presented is the mean value of experiments performed in triplicate. Experiments were performed three times for trypsin (one representation shown) and performed once for all other serine proteases.

KLK14 follow up PAR4AP (150 µM) treatment induced a brief change in $[Ca^{2+}_i]$ of similar magnitude to that induced by KLK14. This indicates that KLK14 activated a portion of the PAR4 on the LMF cell surface but a portion remained and was activated by PAR4AP. In contrast to trypsin and KLK14, hepsin (50 nM) and matriptase (50 nM) (Figures 5.4D and E) elicited no change in free $[Ca^{2+}_i]$. The follow up treatment of PAR4AP (500 µM) after hepsin and matriptase elicited strong Ca^{2+} flux responses of magnitude similar to that observed for 500 µM PAR4AP solo treatment. Therefore, hepsin and matriptase neither activated nor disarmed PAR4 under these conditions.

5.2.1.4 Dose response

A comparison was made between the Ca^{2+} flux response of PAR1-, PAR2- and PAR4-LMF cells to increasing concentrations of hepsin and trypsin, and of PAR2-LMF cells to increasing matriptase concentrations. As shown in Figures 5.5, with increasing concentrations of protease, maximal changes in free $[Ca^{2+}_i]$ were reached at concentrations of 50, 5 and 50 nM trypsin for the PAR1-, PAR2- and PAR4-LMF cells, respectively. Likewise, the maximum response was achieved with 6 nM matriptase for the PAR2-LMF cells. The half maximal response, EC_{50}, of trypsin was calculated to be ~3.6, 0.68 and 16 nM for PAR1-, PAR2- and PAR4-LMF cells, respectively.

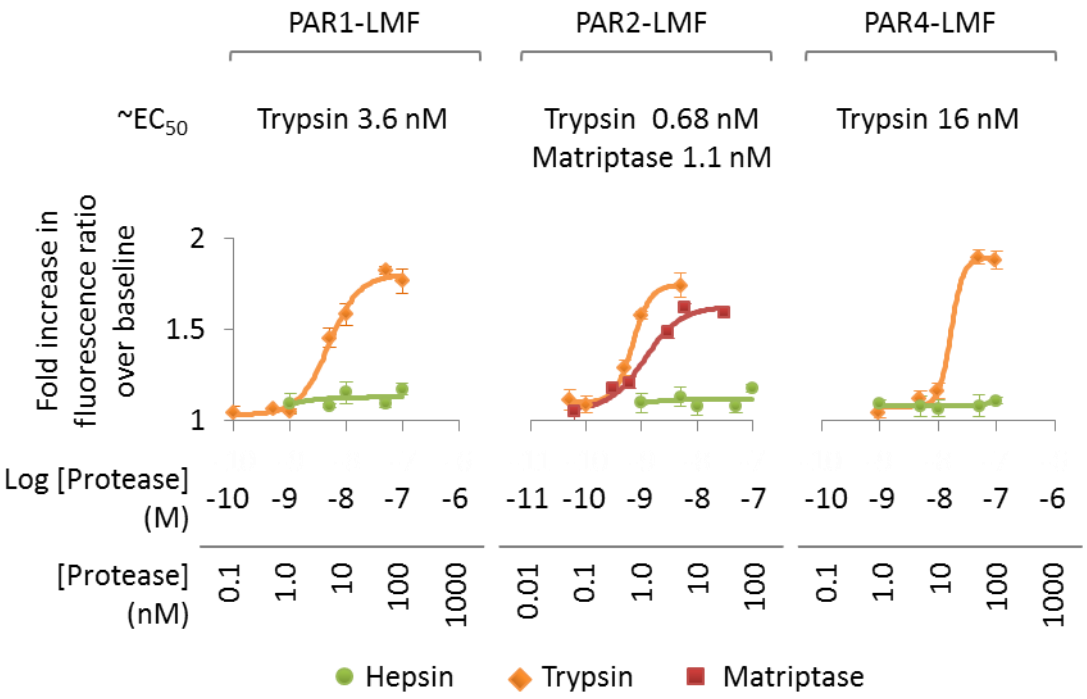

Figure 5.5 Dose-response curves for cytosolic calcium release in PAR-LMFs elicited by serine proteases. PAR1-LMF, PAR2-LMF and PAR4-LMF cells were incubated with hepsin (1 to 100 nM) (●) and trypsin (1 to 100 nM for PAR1- and PAR4-LMFs; 0.05 to 5 nM for PAR2-LMF) (◆). PAR2-LMF was also incubated with matriptase (0.06 to 30 nM) (■). Changes in $[Ca^{2+}_i]$ were assayed by exciting ratiometric calcium indicator Fura-2 in the cells at alternating 340 and 380 nm, the emission at 510 nm was measured using a fluorescent plate reader. The ratio of emission 510 $nm_{(340/380\ nm)}$ is proportional to free Ca^{2+}_i. Data presented is the mean value of experiments performed in triplicate, +/- SEM. Experiments were performed three times for trypsin (one representation shown) and performed once for matriptase and hepsin.

This is comparable to previously published trypsin EC_{50} results of 3.64 nM for PAR1, between 0.51 and 3 nM for PAR2, and 5 nM for PAR4 (Blackhart et al., 1996; Corvera

et al., 1997; Glusa et al., 1997; Xu et al., 1998; Knecht et al., 2007). The EC_{50} for matriptase was ~1.1 nM, comparable to previously published 0.3- >10 nM (Takeuchi et al., 2000; Camerer et al., 2010). In contrast, up to 100 nM hepsin failed to elicit substantial change in free $[Ca^{2+}_i]$ in the three PAR-LMF cell lines.

5.2.2 PAR2 activation by KLK4 in PAR2-LMF cell lines is inhibited by SFTI-FCQR

Recently an inhibitor, SFTI-FCQR, was engineered by modifying residues in SFTI, using substrate-guided design, to create a potent, KLK4-specific inhibitor (Swedberg et al., 2009). In addition, the ability of KLK4 to activate PAR2-induced Ca^{2+} flux has been previously published (Mize et al., 2008; Ramsay et al., 2008a). So, to assess the ability of SFTI-FCQR to inhibit KLK4 activation of PAR2, Ca^{2+} flux assays were used to monitor changes in free $[Ca^{2+}_i]$ in response to KLK4 treatment compared to SFTI-FCQR inhibited KLK4.

As shown in Figure 5.6, trypsin (10 nM), KLK4 (200 nM) and PAR2AP (50 μM) induced Ca^{2+} flux in the PAR2-LMF cells (Figure 5.6A-C). When applied alone, the inhibitor SFTI-FCQR did not induce Ca^{2+} flux (Figure 5.6D). Furthermore, pre-incubation of trypsin with SFTI-FCQR did not inhibit PAR2 activation by trypsin (Figure 5.6E). On the other hand, Ca^{2+} flux induced by KLK4 was completely abolished by pre-treatment with SFTI-FCQR (Figure 5.6F and G). Moreover, the PAR2 on the cell surface remains functional after treatment with KLK4/SFTI-FCQR as Ca^{2+} flux was induced by follow up treatment with either PAR2AP or trypsin. These results indicate that SFTI-FCQR inhibited KLK4 proteolytic activation of PAR2 and did not inhibit trypsin activation of PAR2.

5.2.3 Trypsin, but not KLK4, activates PAR2 in primary kidney PTC

Human kidney PTC have previously been shown to express both PAR2 and KLK4 protein (Vesey et al., 2007)(personal communication from Dr D. Vesey). Activation of PAR2 on these cells by trypsin and PAR2AP mediates a Ca^{2+} flux response (Vesey et al., 2007; Vesey et al., 2013). As KLK4 initiates Ca^{2+} flux via activation of PAR2 on PAR2-LMF and PC-3 cells (Ramsay et al., 2008a) (and Section 5.3.2), Ca^{2+} flux assays were used to assess the ability of KLK4 to activate PAR2 on human primary kidney PTC.

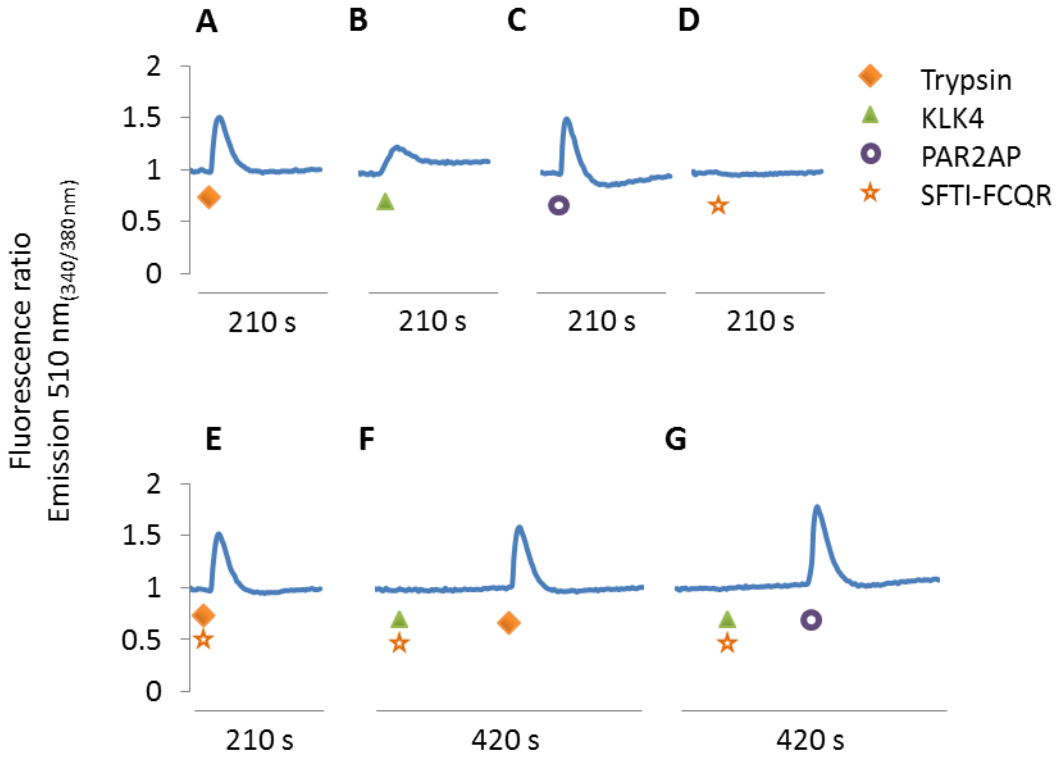

Figure 5.6 PAR2 activation by KLK4 in PAR2-LMF cell lines is inhibited by SFTI-FCQR. PAR2-LMF cells were treated with (**A**) trypsin (10 nM) (◆), (**B**) KLK4 (200 nM) (▲), (**C**) PAR2AP (50 µM) (◉), (**D**) SFTI-FCQR (1 µM) (★), (**E**) trypsin (10 nM) pre-incubated with SFTI-FCQR (1 µM), (**F**) KLK4 (200 nM) pre-incubated with SFTI-FCQR (1 µM), followed by a second treatment with trypsin (10 nM) (**G**) KLK4 (200 nM) pre-incubated with SFTI-FCQR (1 µM) followed by PAR2AP (50 µM). Changes in $[Ca^{2+}_i]$ were assayed by exciting ratiometric calcium indicator Fura-2 in the cells at alternating 340 and 380 nm. The emission at 510 nm was measured using a fluorescent plate reader. The ratio of emission 510 $nm_{(340/380\ nm)}$ is proportional to free Ca^{2+}_i. The symbols indicate treatment injection points at 30 seconds for single treatments, and 30 and 210 seconds for consecutive treatments. Data presented is the mean value of experiments performed in triplicate, performed three times.

As shown in Figure 5.7A, only a very gradual and slight response to 300 nM KLK4 was observed. This concentration of KLK4 was sufficient to cause a moderate Ca^{2+} flux response in both PC-3 and PAR2-LMF cells (Ramsay et al., 2008a). Indeed, 200 nM KLK4 was sufficient to induce Ca^{2+} flux in PAR2-LMF cells as shown in Figure 5.7B. Small increases in Ca^{2+} flux response to KLK4 were observed by increasing KLK4 treatments to 600 nM and 1.2 µM (Figures 5.7B and C). Treatment of the kidney PTC with PAR2AP (100 µM) induced a strong rapid response and also completely abolished the Ca^{2+} flux response to subsequent KLK4 (300 nM) treatment (Figure 5.7D).

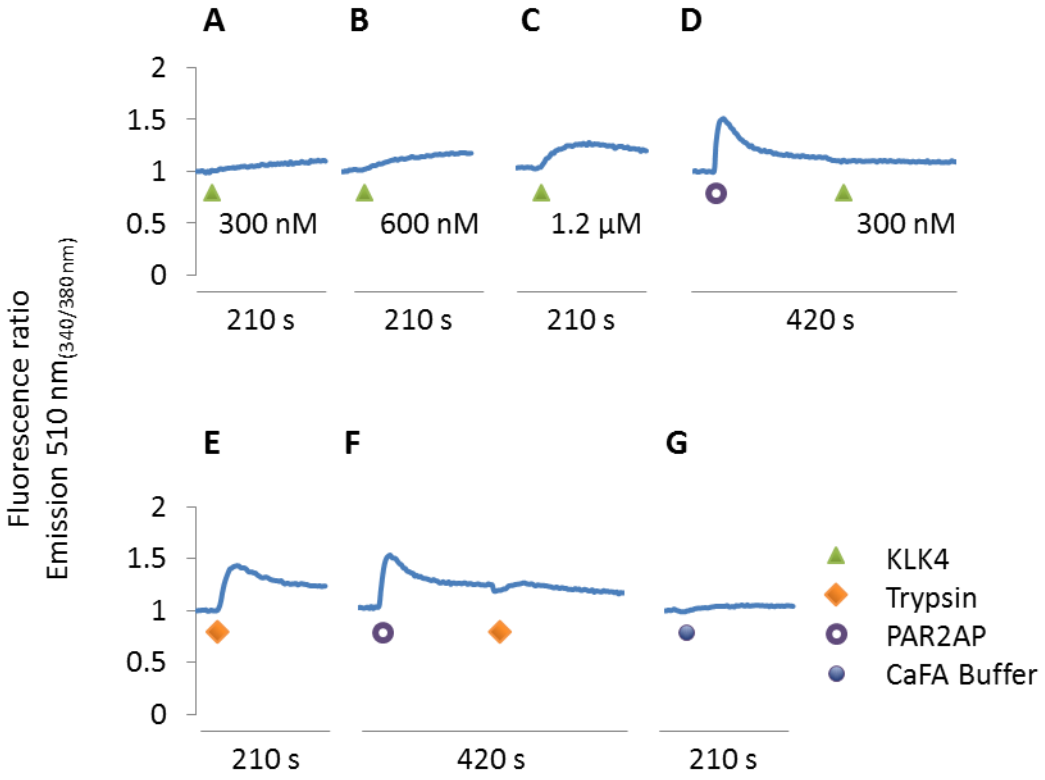

Figure 5.7 PAR2 activation in primary kidney proximal tubule cells. Human primary kidney proximal tubule cells were treated with (**A** - **C**) KLK4 (300 nM, 600 nM, 1.2 µM) (▲), (**D**) PAR2AP (100 µM) (◎) followed by KLK4 (300 nM), (**E**) trypsin (10 nM) (◆), (**F**) PAR2AP (100 µM) followed by trypsin (10 nM), and (**G**) CaFA Buffer (●). Changes in $[Ca^{2+}_i]$ were assayed by exciting ratiometric calcium indicator Fura-2 in the cells at alternating 340 and 380 nm. The emission at 510 nm was measured using a fluorescent plate reader. The ratio of emission $510\ nm_{(340/380\ nm)}$ is proportional to free Ca^{2+}_i. The symbols indicate treatment injection points at 30 seconds for single treatments, and 30 and 210 seconds for consecutive treatments.

This indicates that the slight response to KLK4 can be attributed to action through PAR2 on the kidney PTC. In contrast to KLK4, trypsin (10 nM) induced a prompt, robust Ca^{2+} flux (Figure 5.7E). Furthermore, treatment of the kidney PTC with PAR2AP (100 µM) almost completely abolished the response to a subsequent trypsin treatment (Figure 5.7F).

Taken together, this indicates that the PAR2 on the kidney PTC was functional, responding to both PAR2AP and trypsin. Moreover, the PTC response to trypsin and also the slight response to KLK4 can be attributed almost entirely to PAR2 activation. However, as KLK4 elicited very little Ca^{2+} flux response there may be some factor impeding KLK4, but not trypsin, activation of PAR2. And so, to further investigate the

KLK4 inhibition, active site titration using a MUGB assay was used to determine whether KLK4 was still active after exposure to the PTC in the Ca^{2+} flux assays. As the KLK4 was added to a cell suspension for the Ca^{2+} flux assay, the MUGB assay was conducted on the Ca^{2+} flux assay mix from the 300, 600 nM and 1.2 μM KLK4 treatments, with cells and also with cell-free medium after the cells had been removed by centrifugation. The MUGB assays showed that the activity of KLK4 was undiminished after the Ca^{2+} flux assay with the kidney PTC (data not shown). Neither the cell-free nor the cell-containing KLK4 from the Ca^{2+} flux assays showed any significant change in KLK4 activity under the MUGB assay conditions. Based on this result it is unlikely the limited PAR2 activation by KLK4 is due to an inhibitor either found on the surface of the kidney PTC or secreted into the extracellular medium. Further studies are required to examine this in greater detail.

5.2.4 Generation and characterization of prostate cancer LNCaP cells stably expressing the transmembrane serine protease hepsin

To examine the role of hepsin in proteolytic cascades resulting in activation of PAR2, LNCaP and PAR2-LMF cells were stably transfected with pcDNA3.1 and pEFIRES-p expression constructs, respectively, encoding hepsin-Flag or hepsinSA-Flag. LNCaP cells were chosen for this purpose because they express PAR2 (Chay et al., 2002; Greenberg et al., 2003; Ramsay et al., 2008a). Moreover, it has also been published that a change in $[Ca^{2+}_i]$ can be elicited in LNCaP cells upon application of the PAR agonists trypsin, TMPRSS2 and PAR2AP (Wilson et al., 2005). The PAR2-LMF cells were chosen to use in conjunction with the LNCaP cells because PAR2 is the only functional PAR they express (Andrade-Gordon et al., 1999). This allows for discrimination of the cellular response mediated by PAR2 activation in the PAR2-LMF cells.

5.2.4.1 Generation of LNCaP and PAR2-LMF cells stably expressing hepsin or catalytically inactive hepsin

LNCaP and PAR2-LMF stable transfectants were screened for cell-surface hepsin-Flag and hepsinSA-Flag by flow cytometry. As shown in Figure 5.8A and B, hepsinSA-Flag was expressed at high levels on the cell surface of both LNCaP and PAR2-LMF cells, as indicated by the high mean fluorescence intensity (MFI). In contrast, very little hepsin-Flag was detected; the MFI for the LNCaP-hepsin-Flag and PAR2-LMF-hepsin-Flag

were 15- and 35-fold lower than that of the LNCaP-hepsinSA-Flag and PAR2-LMF-hepsinSA-Flag cells, respectively. Moreover, there is little difference between the MFI of LNCaP-hepsin-Flag and PAR2-LMF-hepsin-Flag cells and either LNCaP-hepsin-Flag or PAR2-LMF cells stained with secondary antibody.

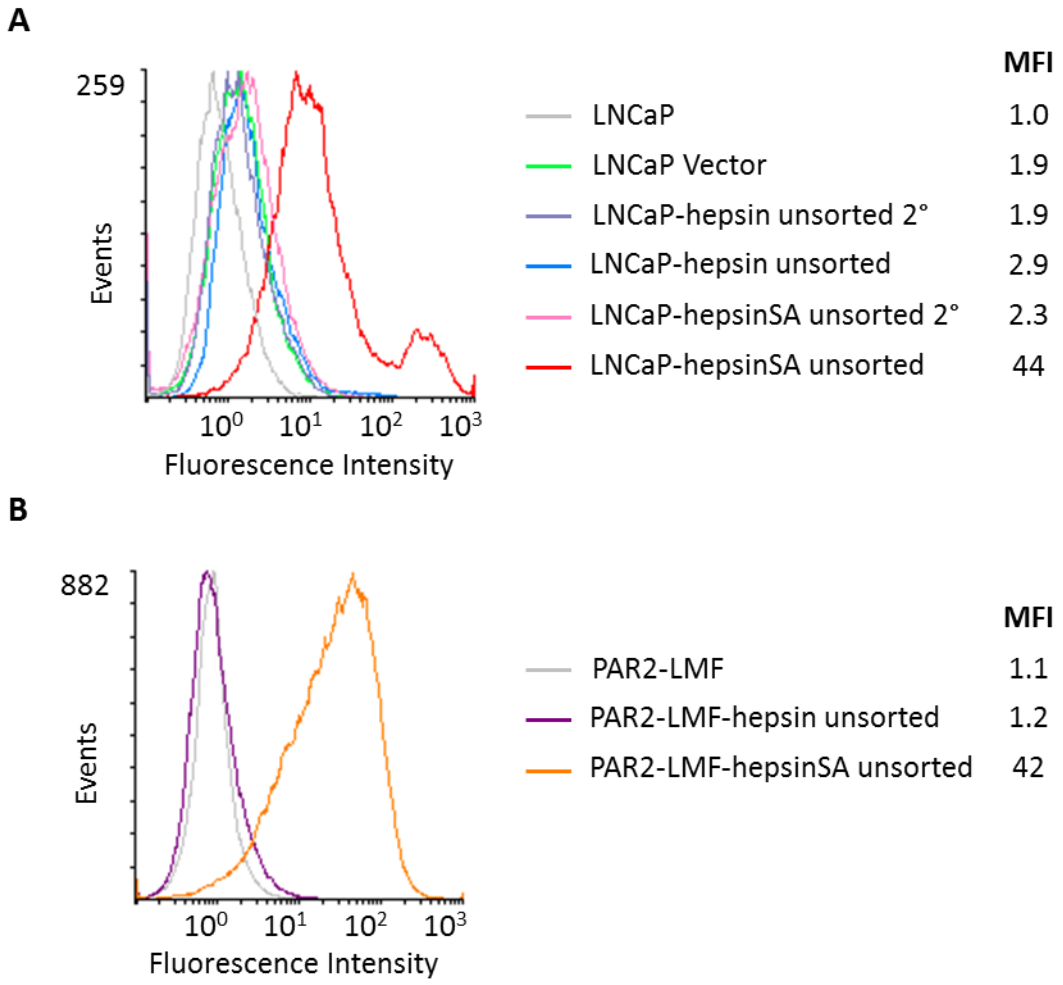

Figure 5.8 Cell-surface expression of hepsin-Flag and hepsinSA-Flag on stably transfected LNCaP and PAR2-LMF cells. Representative flow cytometry histograms of LNCaP (**A**) and PAR2-LMF (**B**) cells stably transfected with constructs encoding either hepsin-Flag or active-site mutated hepsinSA-Flag. Polyclonal populations were selected using G418-containing medium, expanded and maintained in G418-containing media. Flow cytometry screening of the polyclonal populations for cell-surface expression of hepsin-Flag and hepsinSA-Flag used a mouse anti-Flag primary antibody and goat anti-mouse Alexa Fluor® 488 secondary antibody. *MFI, Mean fluorescence intensity; 2°, secondary antibody only.*

As will be described in the following sections, propagation of LNCaP-hepsin-Flag cells expressing high consistent levels of hepsin-Flag on the cell surface proved to be

problematic. For this reason, generation of PAR2-LMF cells stably expressing plasma membrane localized wild-type and catalytically inactive hepsin was not pursued further.

5.2.4.2 Further attempts to generate LNCaP-hepsin and LNCaP-hepsinSA stable cell lines using FACS

To produce homogeneous populations of stably transfected LNCaP-hepsin-Flag and LNCaP–hepsinSA-Flag cells, FACS was performed a minimum of two weeks following transfection and antibiotic selection to isolate cells with high levels of plasma membrane expression of hepsin-Flag and hepsinSA-Flag.

In the first round of FACS, 480 single cells were selected for each of the LNCaP-hepsin and LNCaP-hepsinSA transfectants. After expansion as monoclonal populations, 40 LNCaP-hepsinSA-Flag clones survived (8.3% of cells isolated by FACS) and were reanalysed by flow cytometry for cell surface expression of hepsinSA-Flag. As shown in Figure 5.9A, six of these clones had uniform, high levels of hepsinSA-Flag expression. In contrast, only one LNCaP-hepsin-Flag clone survived (0.21%). However, as shown in Figure 5.9B, it was apparent from the flow cytometry analysis that this clone had little cell surface expression of hepsin-Flag.

A second round of FACs was performed using LNCaP-hepsin-Flag stable unsorted cells. In this FACs round, 960 single cells, as well as three collections of 8000 cells each, were collected into cell culture medium with increased FBS (20% v/v). Only five LNCaP-hepsin-Flag clones survived (0.52%) expansion as monoclonal populations. In contrast, all three polyclonal populations survived and were analysed by flow cytometry. However, as shown in Figure 5.10, the monoclonal and polyclonal LNCaP-hepsin-Flag populations had either very low or heterogeneous hepsin-Flag cell surface expression. This is indicated by the low MFIs and the broad or multiple peaks on the flow cytometry histograms.

In an attempt to obtain clonal populations with matched hepsin-Flag and hepsinSA-Flag expression levels, a third and final round of FACS was performed on the LNCaP-hepsin cells. To increase the probability of obtaining high expressing populations from this round of FACS, one polyclonal (poly 2) and two monoclonal (clones 3f10 and 9d4) populations were pooled from the second FACS round for a high-expressing hepsin-Flag enriched population for sorting. As there was success in expanding the polyclonal

populations from the second FACs round it was thought that paracrine effects might possibly induce higher survival for the LNCaP-hepsin-Flag cells. Therefore in the third FACS round in addition to 384 single cells collected, there were 288 collections of 3 cells/well for triclonal populations, and a further three collections of 30,000 high-expressing cells for polyclonal populations. The collection medium was of the same composition as the second round of FACS.

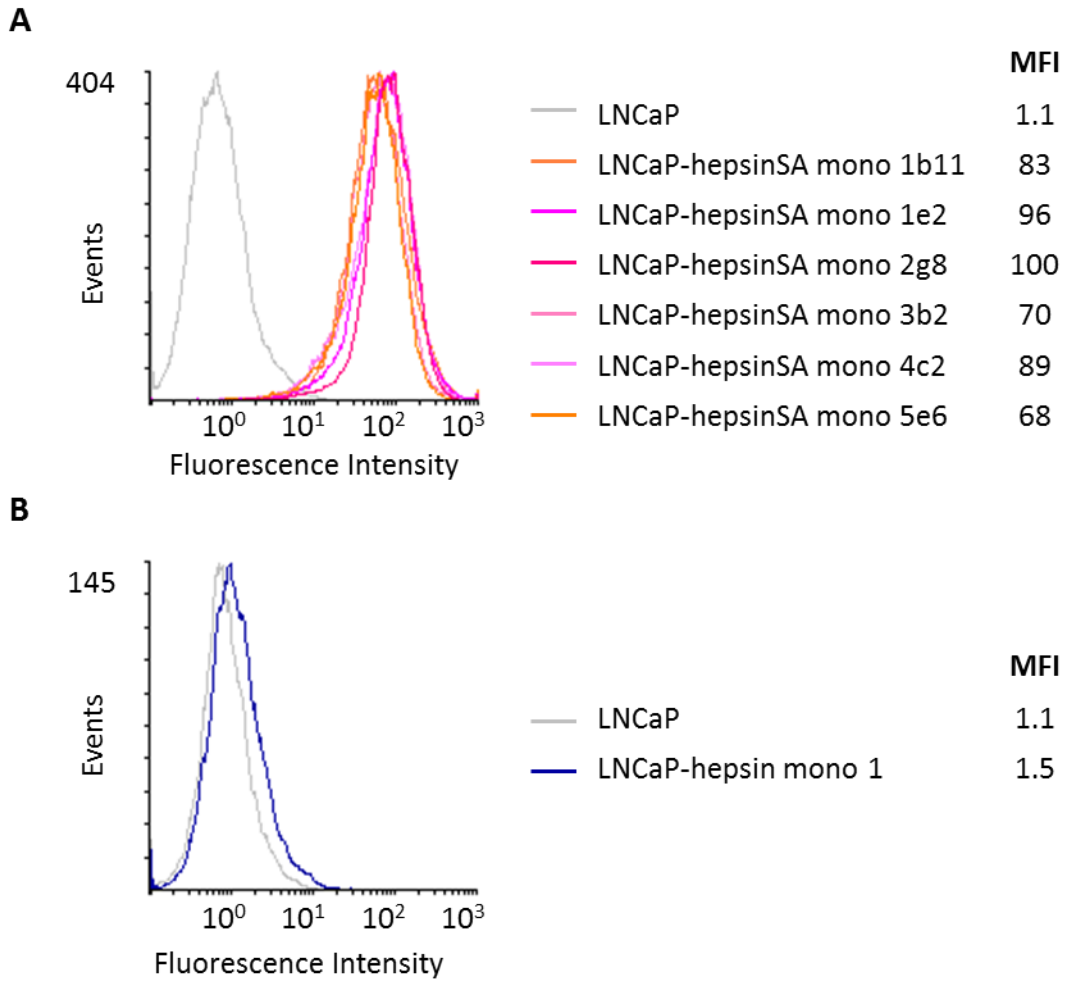

Figure 5.9 LNCaP-hepsinSA-Flag cell clones selected by FACS display a high, homogeneous level of hepsinSA-Flag. High expressing LNCaP-hepsin-Flag and hepsinSA-Flag clones were selected by FACS as 1 cell/well into 96 well plates. Clones that proliferated were screened by flow cytometry for hepsin-Flag and hepsinSA-Flag cell surface expression using a primary mouse anti-Flag antibody and goat anti-mouse Alexa Fluor® 488 secondary antibody. **A.** From 40 surviving LNCaP-hepsinSA-Flag clones screened, 6 clones were chosen with uniform, high levels of hepsinSA-Flag expression. **B.** One LNCaP-hepsin-Flag clone survived, which had very low levels of hepsin-Flag cell-surface expression. *MFI, Mean fluorescence intensity.*

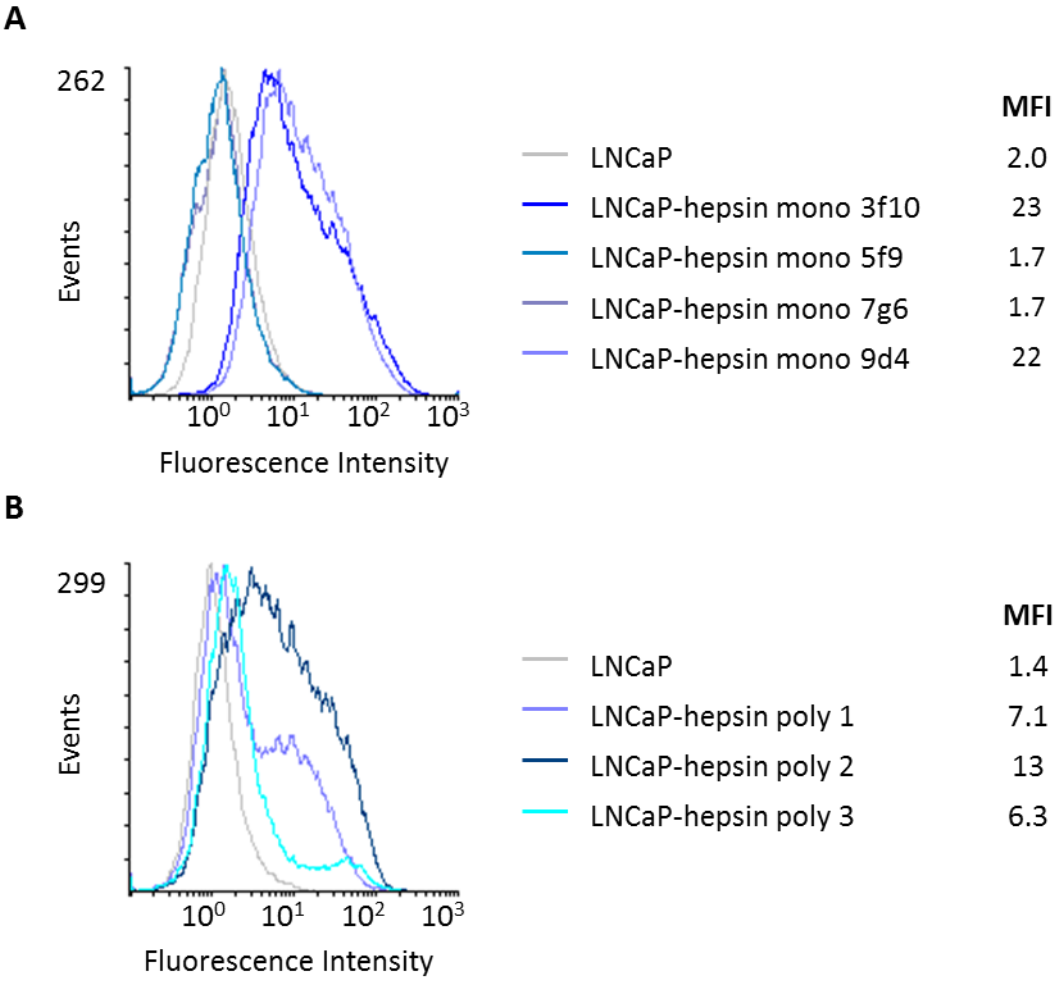

Figure 5.10 LNCaP-hepsin-Flag monoclonal and polyclonal populations selected by a second round of FACS yield populations with low, heterogeneous hepsin-Flag expression. Monoclonal population high expressing clones were selected by FACS as 1 cell/well into 96 well plates. Polyclonal populations were selected 8000 cells/well into a 24 well plate. Clones/populations that proliferated were screened by flow cytometry for hepsin-Flag cell surface expression using a primary mouse anti-Flag antibody and goat anti-mouse Alexa Fluor® 488 secondary antibody. **A**. Flow cytometry histograms of 4 of the 5 monoclonal populations that proliferated. **B**. Flow cytometry histograms of the three polyclonal populations generated. *MFI, Mean fluorescence intensity.*

The three polyclonal populations survived expansion. However, as with the previous cell sorting, there was poor survival of cells expanded from single cell collections as only five proliferated (1.3%). There was a slightly better result for cells expanded from 3 cells/well, as nine proliferated (3%). Figure 5.11 shows flow cytometry histogram analyses of hepsin-Flag cell surface expression for one of five monoclonal and two of the nine triclonal populations (Figure 5.11A), as well as the three polyclonal populations (Figure 5.11B). As with the populations of LNCaP-hepsin-Flag generated previously,

the new populations also had a either low or heterogeneous hepsin-Flag expression. Triclonal population LNCaP-hepsin 7b10 was the only population that showed homogeneous hepsin-Flag expression as demonstrated by the single peak on the histogram (Figure5.11A). However, the expression level of this population (MFI of 18) was still considerably lower than that of the LNCaP-hepsinSA-Flag (in Figure 5.10A).

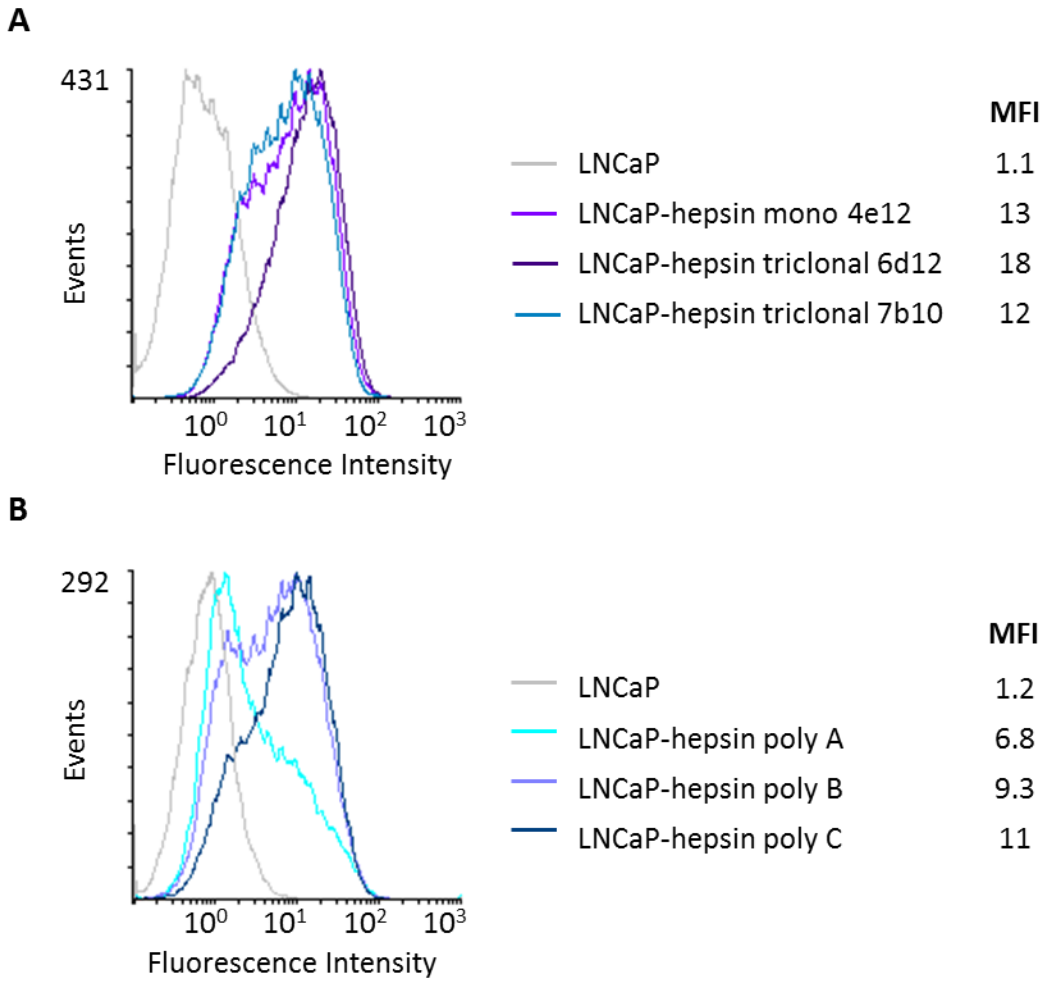

Figure 5.11 LNCaP-hepsin-Flag monoclonal and polyclonal populations selected by a third round of FACS yield populations with low, heterogeneous hepsin-Flag expression. LNCaP-hepsin-Flag populations with the highest levels of hepsin-Flag from the second round of FACS were pooled and subjected to a third round of FACS. Monoclonal population high expressing clones were selected by FACS as 1 cell/well into 96 well plates. The triclonal populations were collected as 3 cells/well into 96 well plates. The polyclonal populations were collected as 3×10^4 cells/well into a 6 well plate. Clones/populations that proliferated were screened for hepsin-Flag cell-surface expression by flow cytometry using a primary mouse anti-Flag antibody and goat anti-mouse Alexa Fluor® 488 secondary antibody. **A**. Flow cytometry histograms of 3 of the 5 monoclonal and 9 triclonal populations that survived and proliferated are shown. **B**. Flow cytometry histograms of all 3 polyclonal populations generated. *MFI, Mean fluorescence intensity.*

Table 5.1 provides a summary of the LNCaP-hepsin-Flag and LNCaP-hepsinSA-Flag clone screening. Six LNCaP-hepsinSA-Flag monoclones that showed high levels of hepsinSA-Flag surface expression were retained for further examination. Only low-medium level expressing LNCaP-hepsin-Flag clones were obtained and retained.

Table 5.1 Summary of LNCaP clones stably expressing hepsin-Flag and hepsinSA-Flag. A single round of FACS was used to obtain monoclonal populations for LNCaP-hepsinSA-Flag. Three FACS rounds were performed for LNCaP-hepsin-Flag to obtain monoclonal populations as well as several polyclonal and triclonal populations. *MFI, mean fluorescence intensity; -, clones not collected; ( ), clones saved and stored in liquid nitrogen (LN2).*

Population	Construct	Number of Clones			
		FACS sorted	Expanded	Hepsin low-medium expression (MFI >10<50)	Hepsin high expression (MFI >50)
Monoclonal	Hepsin	1824	11	5 (5)	0
	HepsinSA	480	40	13 (0)	17 (6)
Polyclonal	Hepsin	8	6	3 (3)	0
	HepsinSA	2	2	-	-
Triclonal	Hepsin	288	9	5 (3)	0
	HepsinSA	-	-	-	-

5.2.4.3 General observations of the growth characteristics of LNCaP-hepsin compared to LNCaP-hepsinSA cells

During expansion of the FACS-sorted cells, LNCaP-hepsin-Flag cells were observed (not qualitatively) to have reduced growth rate in comparison with the LNCaP-hepsinSA-Flag and LNCaP-vector cells. It was also observed that there was a very high level of senescence and cell death for the LNCaP-hepsin-Flag cells and this considerably reduced the number of clones that survived for screening by flow cytometry. Moreover, despite consistently selecting cells with high levels of expression of hepsin-Flag during FACS, only low to medium level expressors survived on each occasion.

5.2.4.4 Western blot analysis of cells stably expressing LNCaP-hepsin and LNCaP-hepsinSA

To further examine hepsin-Flag and hepsinSA-Flag levels in stably expressing LNCaP cells, lysates from a selection were examined by Western blot analysis using both anti-Flag and anti-hepsin antibodies. Anti-Hepsin A15 is a monoclonal antibody raised in hepsin -/- mice (Wu et al., 1998) to the complete extracellular region of human hepsin (Xuan et al., 2006).

As shown in Figure 5.12, Western blot analysis confirmed a consistently lower level of expression of hepsin-Flag (Figure 5.12, lanes 3-7) compared to hepsinSA-Flag (Figure 5.12, lanes 8-12). Full-length hepsin-Flag and hepsinSA-Flag were detected at 45 kDa. As the serine protease domain of activated hepsin is attached to the stem region of hepsin by a disulphide bond, it resolves separately from the stem region of hepsin when the lysates are resolved under reducing conditions. Consistent with this, very low levels the serine protease domain of activated hepsin-Flag were detected at 26 kDa under reducing conditions (Figure 5.12A, anti-Flag blot, lanes 3-7), while it was not detected for the catalytically inactive hepsinSA-Flag (Figure 5.12A, lanes 8-12).

Another form of hepsin-Flag and hepsinSA-Flag was also detected at ~30 kDa under both reducing and non-reducing conditions. This indicates that overexpressed hepsin-Flag and hepsinSA-Flag were proteolysed in the stem region by an alternative protease. It also indicates that as the 30 kDa forms of hepsin-Flag and hepsinSA-Flag were readily detected under non-reducing conditions, disulphide bonds were not the means by which the 30 kDa forms remain associated with the cell. There were also high MW complexes containing hepsin and hepsinSA >250 kDa detected under non-reducing conditions (Figure 5.12B). Interestingly, a greater proportion of hepsin-Flag than hepsinSA-Flag were detected in these complexes. It is possible that this is representative of activated hepsin in complex with other proteins such as protease inhibitors.

Another interesting observation was that while LNCaP cells have previously been shown to express hepsin (Srikantan et al., 2002; Owen et al., 2010), endogenous hepsin was not detected in either the untransfected or vector-transfected LNCaP whole-cell lysate probed with anti-Hepsin antibody. However, when a range of prostate cancer-derived cell lines were examined for endogenous hepsin expression, hepsin was detected in LNCaP and 22Rv1 cells, as well as to a lesser extent in DU145 and RWPE2 cells (Figure 5.13). In agreement with previously published results, hepsin was not detected in

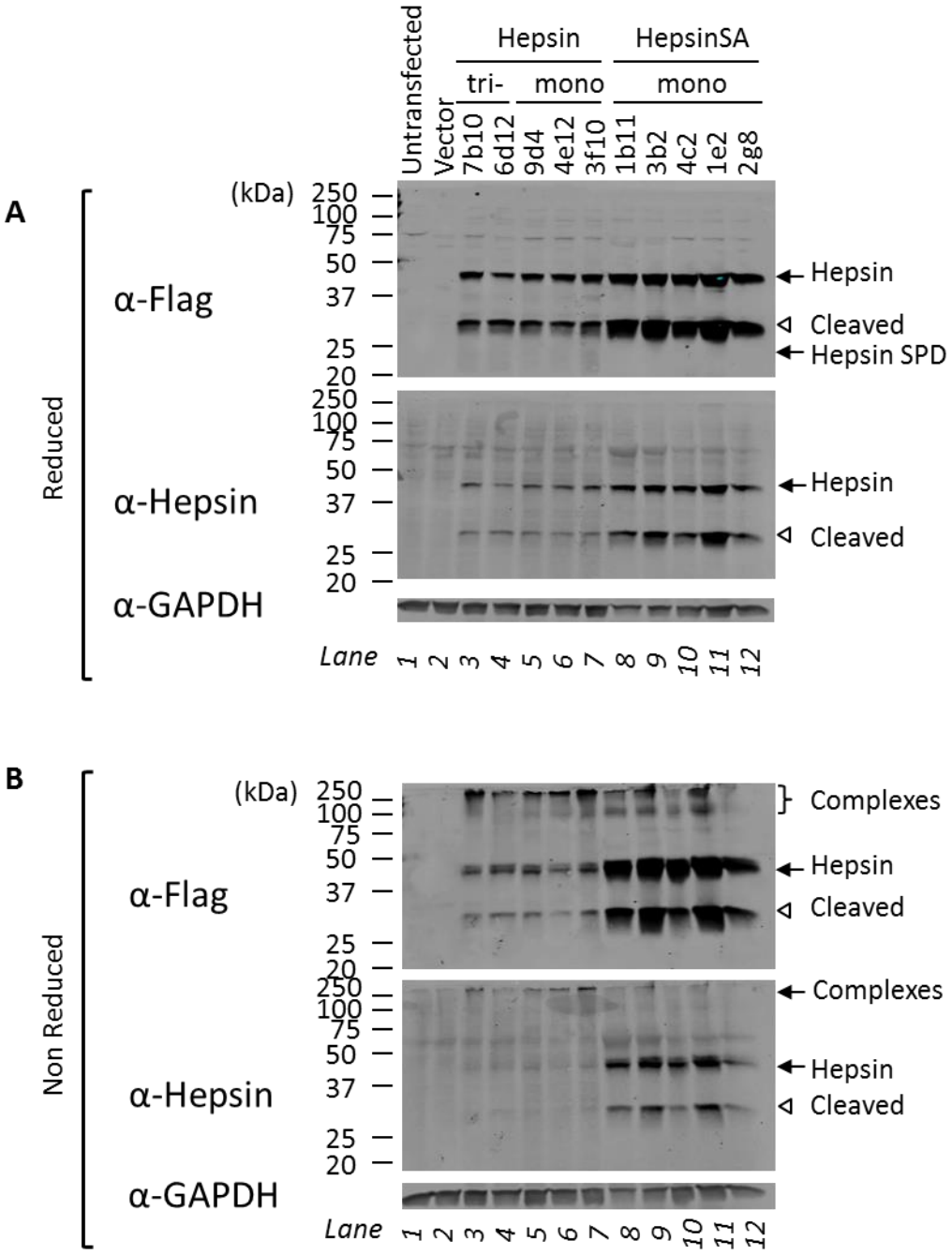

Figure 5.12 Expression analysis of LNCaP-hepsin and LNCaP-hepsinSA clones. WCL from a selection of LNCaP-hepsin-Flag and LNCaP-hepsinSA-Flag populations was subjected to SDS-PAGE under reducing (**A**) and non-reducing (**B**) conditions and Western blot analysis using anti-Flag and anti-hepsin A15 antibodies. Anti-GAPDH probe of the blot was performed to examine protein loading across lanes. *SPD, serine protease domain.*

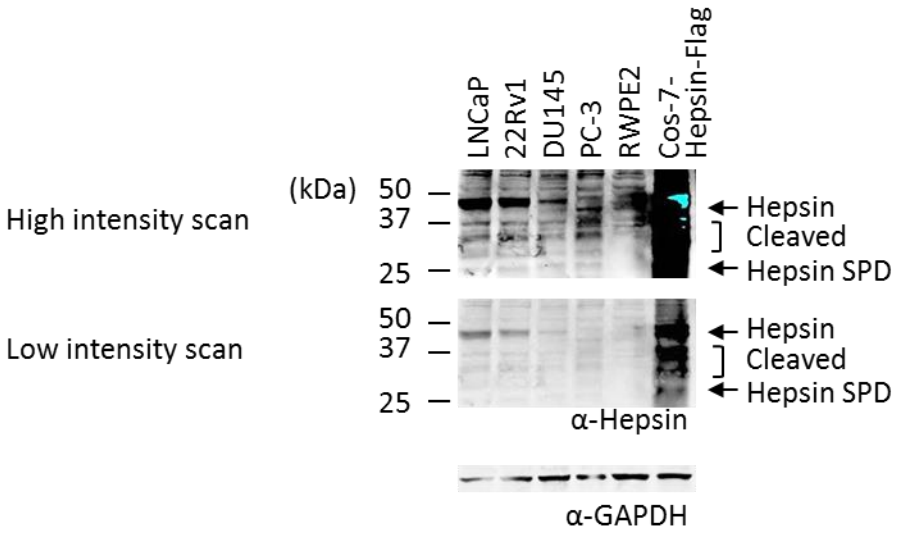

Figure 5.13 Endogenous expression of hepsin by prostate cancer cell lines. WCL from prostate cancer derived cell lines was subjected to SDS-PAGE under reducing conditions and Western blot analysis using the anti-hepsin A15 antibody. Anti-GAPDH probe of the blot was performed to examine protein loading across lanes. *SPD, serine protease domain.*

PC-3 cells (Srikantan et al., 2002; Owen et al., 2010). As a control, lysate from Cos-7 cells transiently transfected with hepsin-Flag gave a very robust signal. Moreover, the signal to detect hepsin in the prostate cancer lines is very low compared to the Cos-7-hepsin-Flag control. From these results it is possible to conclude that if the previous blots (Figure 5.12) were scanned at a higher intensity to detect the secondary antibody signal it might be possible to detect endogenous hepsin with the anti-hepsin A15 antibody.

5.2.4.5 Examination of plasma membrane expression of hepsin and hepsinSA by cell-surface biotinylation

To examine the relative proportion of hepsin-Flag and hepsinSA-Flag localized to the plasma membrane of stably expressing LNCaP cells, cell-surface biotinylation was conducted for one each of the LNCaP-hepsin-Flag and LNCaP-hepsinSA-Flag lines. In this, the proteins on the cell surface were biotinylated and then isolated from the whole-cell lysates. Untreated whole-cell lysate was then compared to the biotinylated and unbiotinylated (flow-through) fractions using Western blot analysis and anti-Flag, anti-Hepsin A15 and anti-GAPDH antibodies. The anti-GAPDH probe had a two-fold purpose on these analyses, to demonstrate relative protein loading in the lanes of the

whole-cell lysate and flow through blots, and also to demonstrate a lack of intercellular proteins in the cell-surface biotinylated fraction.

As shown in Figure 5.14, 45 kDa and 30 kDa cleaved hepsin-Flag and hepsinSA-Flag were detected in whole-cell lysates (Figure 5.14, whole-cell lysate, lanes 3 and 4). In addition, the serine protease domain of hepsin-Flag was detected at low levels at 26 kDa (Figure 5.14, whole-cell lysate, lane 3). Interestingly, endogenous hepsin was also detected at 45 kDa in the whole-cell-lysate of the LNCaP untransfected and LNCaP-vector cells by the anti-hepsin A15 antibody. The signal intensity is very low compared to overexpressed hepsin-Flag and hepsinSA-Flag. Nonetheless, it supports the results in the previous figure (Figure 5.13) that showed detection of endogenous hepsin in LNCaP cells.

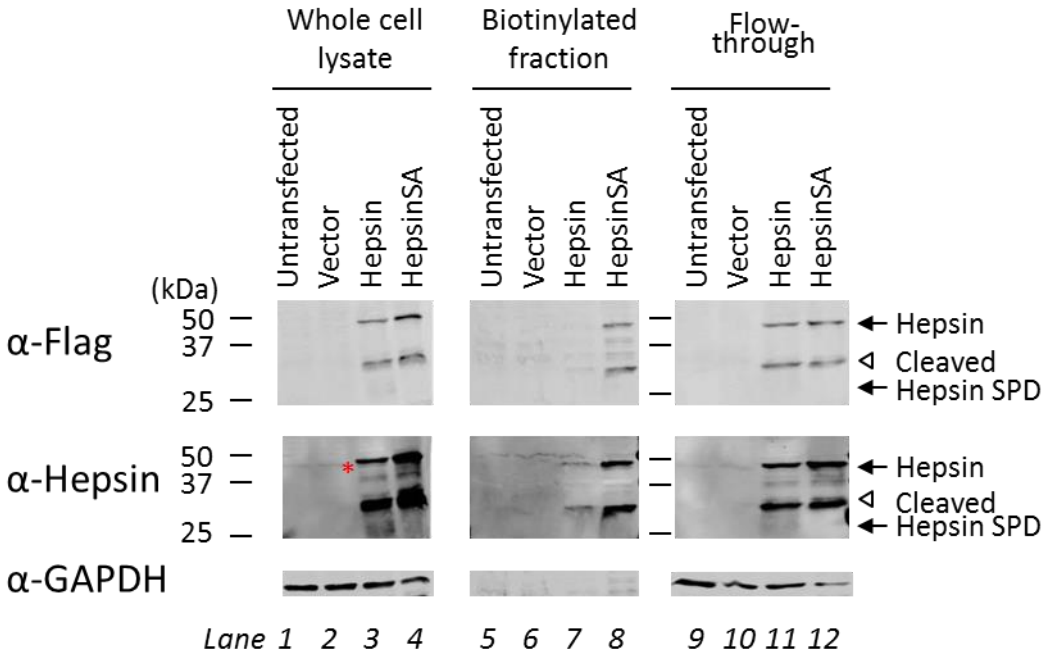

Figure 5.14 Examination of hepsin and hepsinSA cell-surface expression in LNCaP-hepsin and LNCaP-hepsinSA cells. Cell surface biotinylation of LNCaP-hepsin-Flag monoclone 4e12 and LNCaP-hepsinSA-Flag monoclone 2g8 was performed to establish the level of cell surface expression of hepsin and hepsinSA relative to total expression as represented by WCL. Biotinylated proteins, WCL input and flow-through were subjected to SDS-PAGE and Western blot analysis using anti-Flag and anti-hepsin A15 antibodies. Anti-GAPDH probe of the blots was also performed to demonstrate the absence of intercellular proteins in the biotinylated fraction and to examine protein loading across lanes. *SPD, serine protease domain. Red asterisk, endogenous hepsin in untransfected and vector transfected cells.*

Examination of biotinylated fractions shows that very little hepsin-Flag was present on the cell surface in comparison to hepsinSA-Flag (Figure 5.14, biotinylated fraction, lanes 3 and 4). Furthermore, as the signal intensity of the hepsin-Flag is very low, it was not possible to determine whether activated hepsin at 26 kDa represented a portion of the cell-surface hepsin-Flag. Interestingly, hepsin-Flag and hepsinSA-Flag were abundant in the flow-through fraction. Moreover, the serine protease domain of hepsin-Flag was detected in this fraction at 26 kDa. This raises the possibility that hepsin is either activated on the surface before internalization by an unknown mechanism, or hepsin is activated internally before presentation on the surface.

Overall, these results reflect the results previously shown from the flow cytometry where very little hepsin-Flag was detected on the cell surface whereas in contrast hepsinSA-Flag appears to be abundantly displayed on the surface of the LNCaP stable lines.

5.2.4.6 Examination of the interaction of recombinant pro-KLK4 and pro-KLK14 with LNCaP-hepsin and LNCaP-hepsinSA cells

It was previously shown in Chapter 4 that hepsin proteolyses KLK4, and to a lesser extent KLK14. It was also shown that KLK4 and KLK14 co-immunoprecipitate with hepsin, and furthermore, are cell-surface localized in addition to being secreted into the medium. As a preliminary step in the investigation of the role of hepsin in proteolytic cascades resulting in PAR activation, LNCaP-hepsin-Flag and LNCaP-hepsinSA-Flag cells were examined for their potential to interact with exogenous KLK4 and KLK14 zymogen. To do this the zymogens were applied to the LNCaP-hepsin-Flag and LNCaP-hepsinSA-Flag cells for 1 hour and 18 hour timepoints. Media and whole-cell lysates were subjected to Western blot analysis using anti-V5 and anti-Flag antibodies as shown in Figures 5.15 and 5.16.

From these analyses it can be seen that pro-KLK4-V5-His at 28 kDa is not proteolysed in the medium when applied to the LNCaP-hepsin-Flag, LNCaP-hepsinSA-Flag or LNCaP-vector cells as there is no apparent difference to the pro-KLK4-V5-His relative quantity or MW (Figure 5.15A). Examination of whole-cell lysates shows that a small amount of pro-KLK4-V5-His remained with the cells after they were washed (Figure 5.15B). However, there is no hepsin-Flag-mediated proteolysis of pro-KLK4-V5-His. Moreover, the association of pro-KLK4-V5-His is not exclusive to the LNCaP-hepsin-

Flag or LNCaP-hepsinSA-Flag cells as it is apparent from LNCaP-vector cells as well. Furthermore, the pro-KLK4-V5-His that remained with the cells was detected in high MW complexes on the non-reduced lysate analysis but again the interaction is independent of hepsin-Flag or hepsinSA-Flag overexpression.

The analysis of the LNCaP-hepsin-Flag and LNCaP-hepsinSA-Flag whole-cell lysate (Figure 5.15C) shows that pro-KLK4-V5-His had no apparent effect on the hepsin-Flag and hepsinSA-Flag forms detected. As was previously shown (Figure 5.12), hepsin-SA-Flag and hepsin-Flag were detected at 45 kDa and 30 kDa under reducing and non-reducing conditions. The serine protease domain of hepsin-Flag was also detected at 26 kDa.

In Figure 5.16 a similar result is shown for the association of pro-KLK14-V5-His with the LNCaP cells. Again, there was no apparent proteolysis of pro-KLK14-V5-His in the medium (Figure 5.16A) and there was also some proKLK14-V5-His that has remained stuck to the washed cells, independent of hepsin-Flag or hepsinSA-Flag expression (Figure 5.16B). The whole-cell lysate analysis of LNCaP-hepsin-Flag and LNCaP-hepsinSA-Flag in Figure 5.16C is very similar to that shown in Figure 5.15C with no apparent effect of pro-KLK14-V5-His on either hepsin-Flag or hepsinSA-Flag.

Overall, this result is consistent with results shown previously in Chapter 4 that recombinant hepsin had little proteolytic effect on recombinant KLK4-V5-His and KLK14-V5-His zymogens. The results in Chapter 4 showed that a near equal quantity of hepsin was required for proteolysis of these KLKs. So, as little hepsin-Flag localized on the plasma membrane of the LNCaP-hepsin-Flag cells, as shown in the cell-surface biotinylation in Figure 5.14, it is likely proteolysis of the exogenously applied KLKs would be minimal.

5.3 Discussion

In this chapter, activation of PAR1, PAR2 and PAR4, by the serine proteases KLK14, matriptase and hepsin was examined. Inhibition of KLK4 activation of PAR2 using the KLK4-specific inhibitor SFTI-FCQR was also examined in this chapter. This result was published as part of a body of work describing the design and efficacy of the SFTI-FCQR (Swedberg et al., 2009). KLK4 activation of PAR2 was investigated further using cultures of human primary kidney PTC. In the final section of this chapter, the prostate

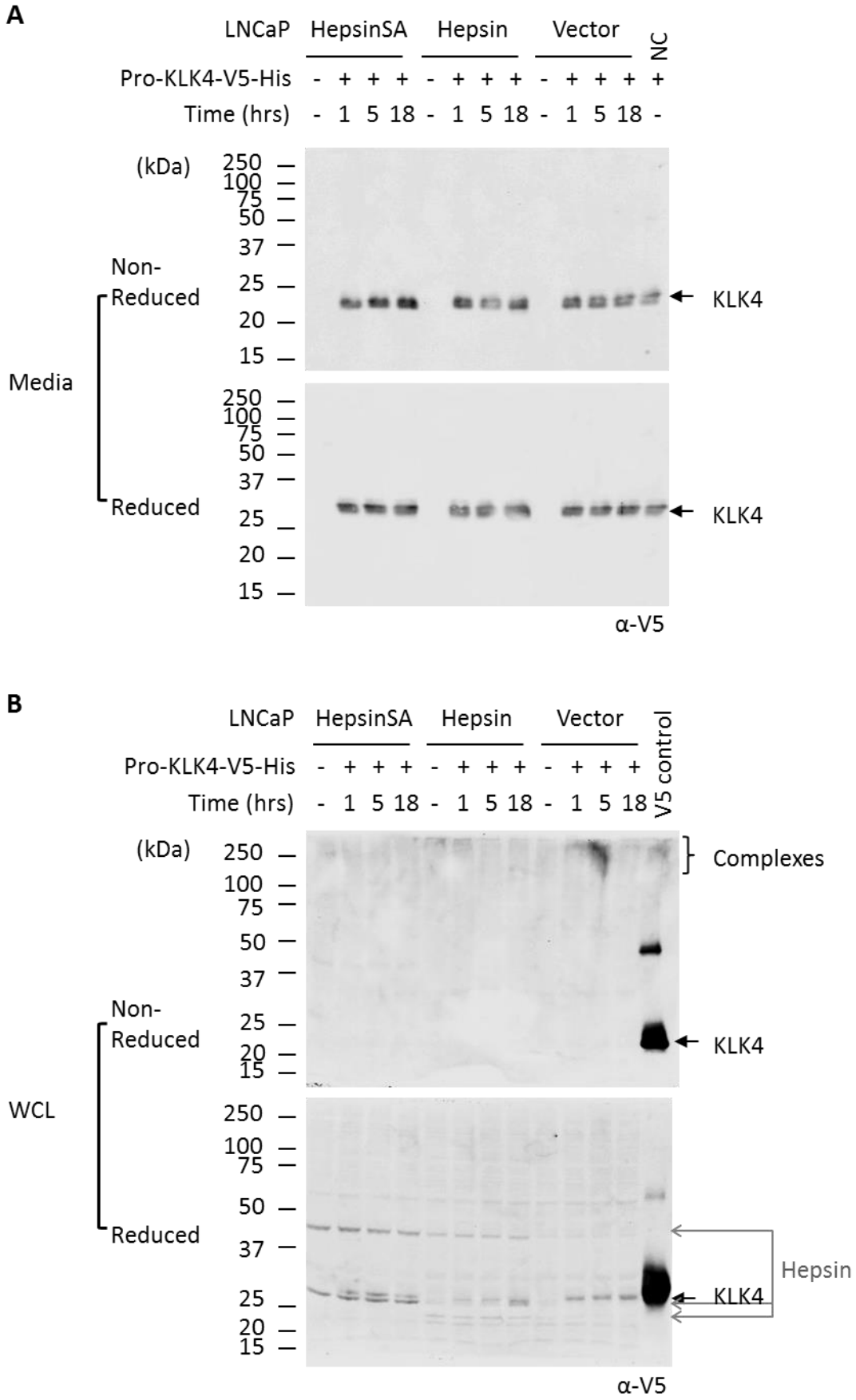
A
LNCaP
HepsinSA
Hepsin
Vector
NC
Pro-KLK4-V5-His
Time (hrs)
(kDa)
Non-Reduced
Media
Reduced
KLK4
α-V5
B
V5 control
Complexes
WCL
Hepsin

Figure 5.15

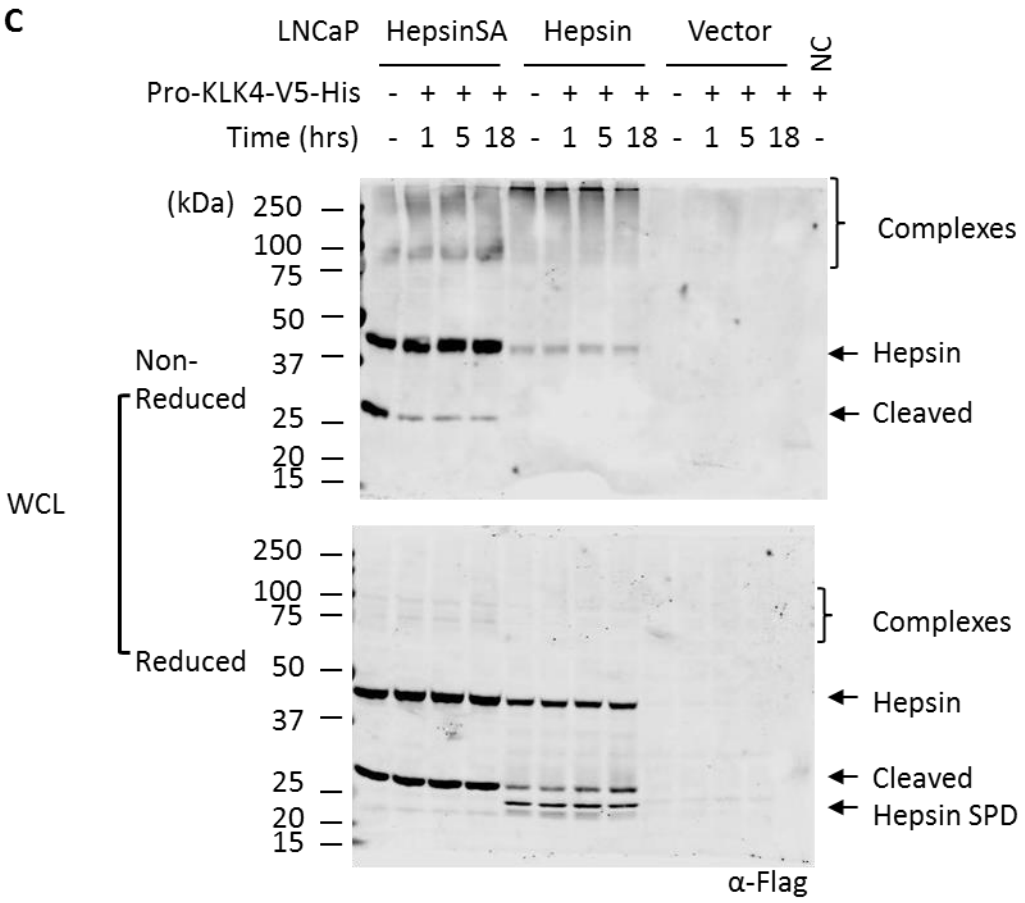

Figure 5.15 Recombinant pro-KLK4 is not proteolysed on LNCaP-hepsin cells. LNCaP-hepsin-Flag and LNCaP-hepsinSA-Flag as well as LNCaP-vector were incubated for 1, 5 or 18 hours, as indicated, with recombinant pro-KLK4-V5-His (80 μM) in RPMI-1640-L-Glutamine (without FBS), at 37°C under 5% CO_2. The whole-cell lysates (WCL) from washed cells, and the media, were subjected to SDS-PAGE under reducing and non-reducing conditions then Western blot analysis using anti-V5 (KLK4) (**A** and **B**) and anti-Flag (hepsin) (**C**) antibodies as indicated. **A**. KLK4 in the cell-conditioned media is not cleaved. **B**. KLK4 from the whole-cell lysate is not cleaved. **C**. The hepsin serine protease domain (SPD) is apparent on the reduced WCL analysis for the LNCaP-hepsin-Flag cells. *NC: no cells; SPD, serine protease domain.*

cancer cell line LNCaP was used to generate stable hepsin- and hepsinSA-overexpressing cell lines. The purpose of this was to produce a tool to investigate the participation of hepsin with other serine proteases in proteolytic cascades resulting in PAR activation. The key findings in this chapter were:

- KLK14 activated Ca^{2+} mobilization via PAR1, PAR2 and PAR4; matriptase activated PAR2 but not PAR1 or PAR4; and there was negligible activation of PAR1, PAR2 or PAR4 by hepsin

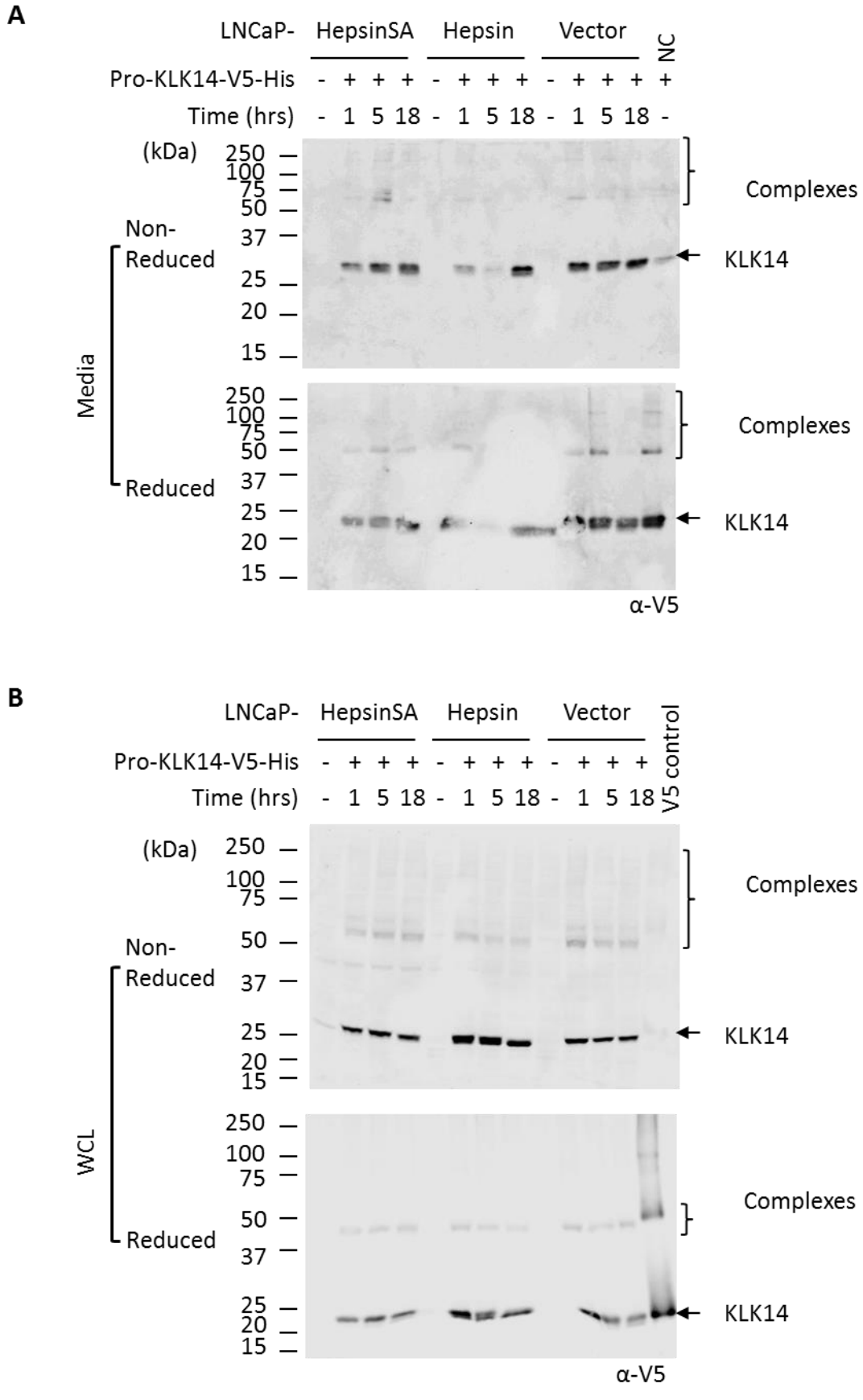
A
LNCaP-
HepsinSA
Hepsin
Vector
NC
Pro-KLK14-V5-His
Time (hrs)
(kDa)
Non-
Reduced
Media
Reduced
Complexes
KLK14
α-V5
B
LNCaP-
HepsinSA
Hepsin
Vector
V5 control
Pro-KLK14-V5-His
Time (hrs)
(kDa)
Non-
Reduced
WCL
Reduced
Complexes
KLK14
α-V5

Figure 5.16

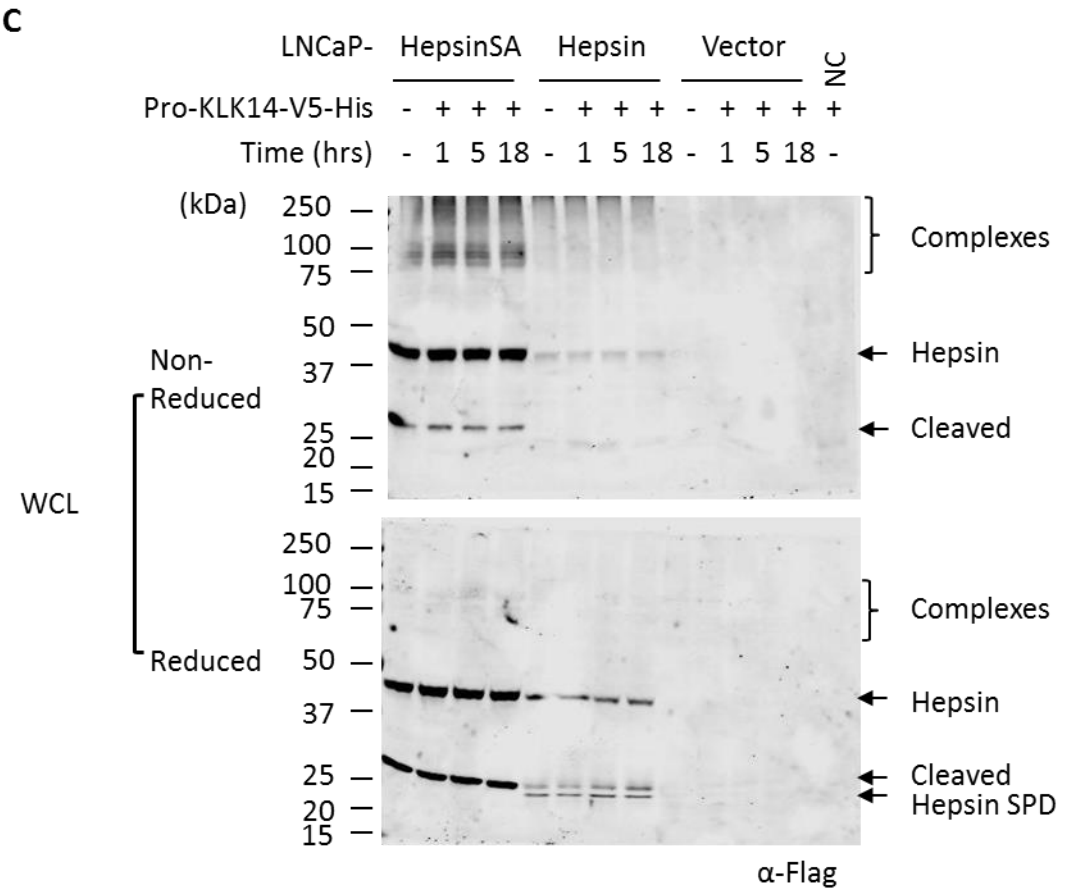

Figure 5.16 Recombinant pro-KLK14 is not proteolysed on LNCaP-hepsin cells. LNCaP-hepsin-Flag and LNCaP-hepsinSA-Flag as well as LNCaP-vector were incubated for 1, 5 or 18 hours, as indicated, with recombinant pro-KLK14-V5-His (80 μM) in RPMI-1640-L-Glutamine (without FBS), at 37°C under 5% CO_2. The whole-cell lysates (WCL) from washed cells, and the media, were subjected to SDS-PAGE under reducing and non-reducing conditions then Western blot analysis using anti-V5 (KLK14) (**A** and **B**) and anti-Flag (hepsin) (**C**) antibodies as indicated. **A**. KLK14 in the cell-conditioned media is not cleaved. **B**. KLK14 from the whole-cell lysate is not cleaved. **C**. The hepsin serine protease domain (SPD) is apparent on the reduced WCL analysis for the LNCaP-hepsin-Flag cells. *NC: no cells; SPD, serine protease domain.*

- KLK4 initiates robust Ca^{2+} mobilization via PAR2 which was inhibited by the KLK4-specific inhibitor SFTI-FCQR
- KLK4 elicited minimal PAR2 activation and Ca^{2+} mobilization in kidney PTC
- Overexpression of transmembrane protease hepsin in LNCaP cells did not support cell growth and resulted in minimal plasma membrane localization. In contrast, overexpression of catalytically inactive hepsin readily localized to the plasma membrane.

5.3.1 KLK14, matriptase and hepsin can affect signalling by either activating or disarming PARs

As mentioned in the Introduction, protease activation of PAR1, PAR2 and PAR4 to expose the tethered ligand requires limited proteolysis at an Arg residue. Furthermore, KLK14, matriptase and hepsin all have a preference for cleavage after an Arg P1 residue. So, while an Arg P1 residue is preferred for substrate proteolysis by these enzymes, the results in this chapter show that it is not sufficient to initiate PAR-mediated Ca^{2+} mobilization. This was exemplified by the variety of responses to the three proteases.

As summarized in Figure 5.17, it was found that KLK14 was equally adept at activating PAR1-, PAR2- and PAR4-mediated Ca^{2+} mobilization in LMF cells. In contrast, matriptase specifically activated PAR2. However, the potency of KLK14 was much lower than that of either trypsin or matriptase because 15-fold less trypsin or matriptase (10 nM) than KLK14 (150 nM) was required to induce a robust Ca^{2+} mobilization in the PAR2-LMF cells. Furthermore, 3-fold less trypsin (50nM) than KLK14 (150 nM) resulted in robust activation of PAR4.

As PAR activation is followed by rapid internalization of the activated receptor (Arora et al., 2007), follow up treatments of agonist peptide resulting in further Ca^{2+} mobilization can be attributed to unactivated PAR remaining on the cell surface. Consistent with this, KLK14 treatment didn't result in complete activation of PARs on the surface of the LMFs as subsequent agonist peptide treatment resulted in Ca^{2+} mobilization. Similarly, follow up agonist peptide treatment of trypsin- and matriptase-treated PAR2-LMF cells (10 nM) resulted in further Ca^{2+} mobilization. Moreover, the robust signal induced by agonist peptide post-matriptase treatment of PAR1- and PAR4-LMFs indicated that while matriptase treatment did not activate PAR1 or PAR4, they were able to be activated by synthetic agonist. In contrast, 50 nM trypsin resulted in complete activation of PAR4 as there was no further Ca^{2+} mobilization upon agonist peptide treatment.

However, it is also known that cleavage of PARs other than at the activation site can result in their inactivation or disarming (Hollenberg and Compton, 2002; Ramachandran et al., 2012b). Furthermore, PARs that have been disarmed in this manner can still be activated by synthetic agonist peptides (Kawabata et al., 1999; Kuliopulos et al., 1999;

Hollenberg and Compton, 2002; Dulon et al., 2003; Nakayama et al., 2003; Oikonomopoulou et al., 2006a; Ramachandran and Hollenberg, 2008). As KLK14 treatments did not result in complete internalization of the PARs, the remaining PARs were not cleaved or may have been proteolytically disarmed by KLK14. For example, it has previously been reported by Oikonomopoulou and colleagues (2006a) that PAR1 is preferentially disarmed by KLK14 through cleavage within the tethered ligand domain, rather than at the Arg residue immediately prior. They reasoned that this would render the tethered ligand unavailable for intramolecular docking and initiation of PAR1-activated Ca^{2+} mobilization. They also showed that in the human embryonic kidney-derived HEK293 cells, KLK14 activated PAR2 but induced negligible activation of PAR1. In addition, KLK14 prevented PAR1-mediated Ca^{2+} mobilization by rendering cells unresponsive to subsequent thrombin treatment (Oikonomopoulou et al., 2006a).

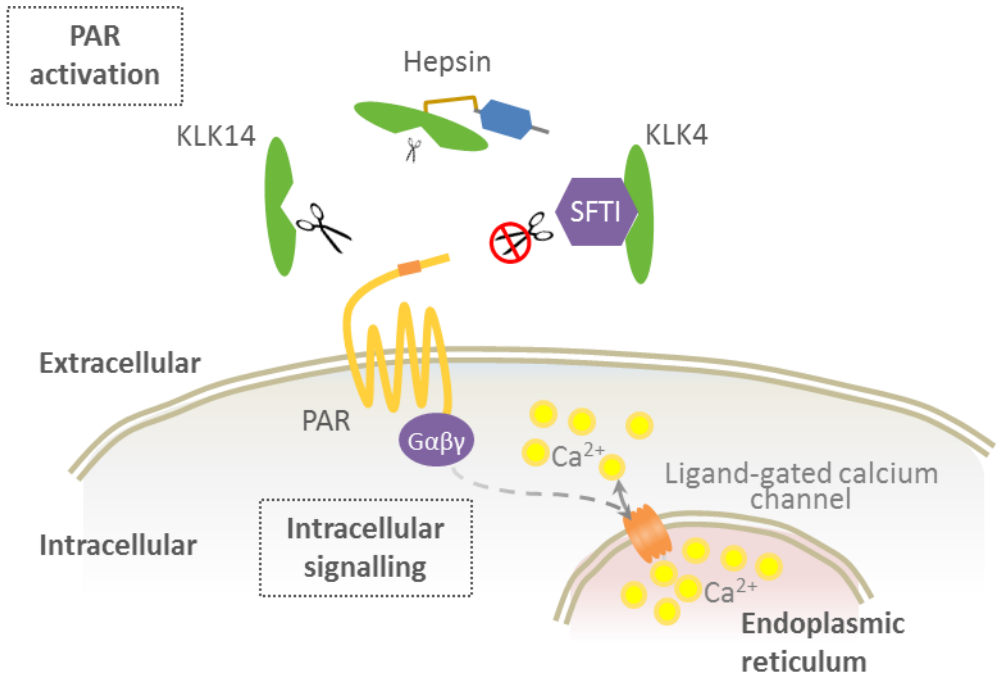

Figure 5.17 Intracellular calcium signalling is initiated by KLK14 via PARs. KLK14 activates PAR1, PAR2 and PAR4 to initiate intracellular calcium mobilization. Hepsin initiates minimal calcium mobilization via these PARs. KLK4-initiated calcium mobilization via PAR2 can be inhibited by KLK4-specific inhibitor SFTI-FCQR.

However, it is unresolved if this was the case in this chapter. To address this in the future, three consecutive treatments could be made, first KLK14, follow-up treatment

with trypsin followed by an AP treatment. This would assist with determination of the relative proportion of PARs activated/disarmed by KLK14, as disarmed PARs would not be activated by trypsin but would be activated by the subsequent AP treatment. Additionally, a dose-response assessment of PAR activation by KLK14 would assist in determining if there is predominantly receptor activation at certain concentrations and receptor deactivation at other concentrations of KLK14. However, as Ca^{2+} mobilization in the PAR1-LMF cells was achieved in this chapter using 150 nM KLK14, it is possible that under some circumstances KLK14 induces PAR-1 signalling by Ca^{2+} mobilization. Unfortunately, the concentration of KLK14 used in the experiments by Oikonomopoulou and colleagues (2006a) was reported as units of "trypsin-like equivalents of activity" as opposed to molar concentration. This makes comparison with the molar concentration used in this chapter difficult.

Interestingly, it appears that proteolytic disarming of PARs may also result in differential signalling, a process known as biased agonism. For instance, Ramachandran and colleagues (2011) have shown that neutrophil elastase, cathepsin-G and proteinase-3 disarm PAR2 by cleaving at distinct sites in the N-terminal to release the tethered ligand. Whereas it is apparent that these disarming events prevent signalling via G_q-coupled Ca^{2+} mobilization, neutrophil elastase, but not cathepsin-G or proteinase-3, activates PAR2 signalling via G_i or $G_{12/13}$-coupling and the ERK1/2 MAPK pathway (Ramachandran et al., 2011). Similarly, it would be interesting to examine whether disarming PAR1 with KLK14 selectively activates alternative intracellular signalling pathways such as the G_i or $G_{12/13}$-initiated ERK1/2 MAPK pathway. Certainly, Oikonomopoulou and colleagues (2006a) found that in addition to abrogating thrombin activation of PAR1, high KLK14 concentrations curtailed activation by PAR1AP (Oikonomopoulou et al., 2006a). So it is possible KLK14 is activating PAR1 resulting in receptor internalization and may represent a novel mechanism for modulation of PAR1 signalling by KLK14.

In contrast to KLK14, hepsin elicited negligible Ca^{2+} mobilization via PAR1, PAR2 and PAR4 (Figure 5.17). Due to limited hepsin availability, only up to 100 nM was tested for dose response on the LMF cells. However, hepsin (50 nM) did render a portion of PAR2 unresponsive to subsequent activation by agonist peptide. This was not seen for either PAR1 or PAR4. Furthermore, similar to matriptase, pre-treatment of hepsin with HAI-1B (1 μM) abolished the PAR2-mediated minimal Ca^{2+} mobilization response and

restored the complete response to agonist peptide. Therefore, as a portion of PAR2 was unresponsive to the follow up agonist peptide, it is possible that portion of PAR2 was activated by hepsin resulting in internalization. Moreover, as it caused minimal Ca^{2+} mobilization it is possible alternate signalling pathways were activated by G_i or $G_{12/13}$-coupling.

Interestingly, during the course of these experiments, research was published that showed that in the keratinocyte cell line HaCaT, low level hepsin activation of PAR2 could be attributed to indirect activation via a proteolytic cascade of hepsin activating endogenous matriptase which then activated PAR2 (Camerer et al., 2010). It is possible a similar cascade occurred in the PAR2-LMF cells, with hepsin activating endogenous matriptase, or another protease, which then activated PAR2. In this case, the low level of activation may reflect the relative amount of intermediate protease expressed by the PAR2-LMF cells. It may also reflect the rate-limited activation of the intermediate protease. Certainly, further work is required to determine if the role of hepsin in PAR activation is as an initiator of a proteolytic cascade, or if hepsin activates PARs directly resulting in initiation of alternate signalling pathways.

5.3.2 KLK4 activates PAR2 in PAR2-LMF cells but not in human primary kidney cells

Consistent with a previous report (Ramsay et al., 2008a), the results in this chapter showed that KLK4 activated Ca^{2+} mobilization via PAR2. In addition, it was shown that a small peptide inhibitor, SFTI-FCQR, re-engineered from SFTI using substrate-guided design (Swedberg et al., 2009), completely abolished KLK4 activation of PAR2 in LMF cells (Figure 5.17). Moreover, SFTI-FCQR did not elicit Ca^{2+} mobilization in the PAR2-LMF cells when applied alone nor did it inhibit trypsin (Swedberg et al., 2009), demonstrating the specificity of SFTI-FCQR for KLK4 inhibition in a cell based assay.

This specific inhibitor may have use in modulating pro-cancer effects of KLK4 activity. As well as inducing proliferation through PAR activation (Mize et al., 2008), these pro-cancer effects include inducing epithelial to mesenchymal cellular transformation and increasing migration (Veveris-Lowe et al., 2005), and increasing proliferation and colony formation (Klokk et al., 2007). Recently Dong and colleagues (2013) used SFTI-FCQR in an *in vitro* ovarian cancer ascites microenvironment model to mitigate the effects of KLK4. They showed that SFTI-FCQR reduced the resistance to the chemotherapy drug

paclitaxel in ovarian cancer cell line SKOV-3 as well as reducing the formation of multicellular spheroids induced by overexpressed or exogenous KLK4.

As mentioned in the Introduction and discussed in Chapter 1, KLK4 is expressed in a number of tissues apart from the prostate. For instance, it has also been detected at high levels in cancerous colon mucosa (Gratio et al., 2010) and breast cancer stroma (Mange et al., 2008) as well as normal liver and kidney tissue (Seiz et al., 2010). Moreover, KLK4 has specifically been determined to be highly expressed in kidney tubule cells of the kidney cortex (Seiz et al., 2010). Therefore, it was surprising to observe in this chapter that KLK4 elicited only minimal signalling via PAR2 expressed by human primary kidney PTC. In particular, the cells used in this chapter have previously been shown to express PAR1, PAR2 and PAR3 (Vesey et al., 2005; Vesey et al., 2007). Furthermore, Ca^{2+} is mobilized in these cells in a PAR1-dependent manner in response to thrombin and PAR1AP (Vesey et al., 2005); and in a PAR2-dependent manner in response to trypsin and PAR2AP (Vesey et al., 2007; Vesey et al., 2013). They showed that both trypsin and PAR2AP induce rapid and robust PAR2-dependent Ca^{2+} mobilization (Vesey et al., 2007). Consistent with this, in this chapter it was observed that trypsin elicited robust Ca^{2+} mobilization in the kidney PTC. In contrast, treatment of these cells with KLK4 (300 nM) elicited negligible response, with a marginally increased response upon increasing KLK4 concentration to 1 μM.

These results highlight contradictions that appear in the PAR activation/signalling field. For example, consistent with data in this chapter, Ramsay and colleagues (2008a) showed that KLK4 (300 nM) activates PAR2 as well as PAR1 expressed by LMF cells, as well as PAR2 in PC-3 cells. In contrast, recent work by Gratio and colleagues (2010) using the colon line HT-29, showed that Ca^{2+} mobilization induced by KLK4 (1 μM) could be attributed to PAR1 and not PAR2 activation. In addition, when examining KLK4 activation of ERK1/2 in prostate primary stromal cells, Wang and colleagues (2010) also concluded that KLK4 induced this signalling pathway by activating PAR1 and not PAR2.

The inconsistency in the Ca^{2+} mobilization results again raises the subject of biased agonism. The concept of biased agonism has expanded from the narrow definition of different ligands acting on the same GPCR to bring about different signalling responses as it has been found that the location of the GPCR in the plasma membrane (Zheng et al., 2008; Russo et al., 2009a) and formation of GPCR heterocomplexes (Gonzalez-

Maeso and Sealfon, 2012) can also cause different signalling responses. Also encompassed in this is the concept that each cell-type has a unique signalling tool-kit, that can lead to differences in cellular responses to agonism (Kenakin, 2011).

An example is the different intracellular signalling processes initiated via PAR1 depending on whether it is activated by thrombin or activated protein C (APC) in endothelial cells (Feistritzer and Riewald, 2005; Finigan et al., 2005; McLaughlin et al., 2005; Riewald and Ruf, 2005; Bae et al., 2007; Komarova et al., 2007; Mosnier et al., 2007; Russo et al., 2009a; Soh and Trejo, 2011; Mosnier et al., 2012). Whereas thrombin activation of PAR1 results in RhoA-mediated signalling (McLaughlin et al., 2005; Komarova et al., 2007), activation by APC results in Rac1-mediated signalling (Finigan et al., 2005; Russo et al., 2009a). Furthermore, to activate PAR1, APC requires compartmentalization of both PAR1 and an APC co-factor, endothelial protein C receptor, to cholesterol-rich caveolar microdomains in the plasma membrane (Bae et al., 2007; Russo et al., 2009a). This PAR1 caveolar-compartmentalization is not required for activation by thrombin (Russo et al., 2009a). The mode of signal transduction from APC-activated PAR1 to Rac-1 was also determined. Although PAR1 co-localizes with signal transduction partners β-arrestin and $G\alpha_i$ to the caveolar microdomains, induction of PAR1-Rac-1 (Russo et al., 2009a) signalling by APC is β-arrestin-dependent (Russo et al., 2009a) and not mediated by $G\alpha_i$ (Soh and Trejo, 2011). Other work investigating the biased agonism of thrombin- or APC-activated PAR1 suggests that N-terminal cleavage of PAR1 by APC reveals a novel tethered ligand differing from that revealed by thrombin. This novel tethered ligand elicits a different intracellular signalling response by PAR1 involving Akt/PI3K-mediated pathways (Mosnier et al., 2012).

Another example of biased agonism involves comparison of PAR4 activation by PAR4AP in hepatocellular carcinoma and colon cancer cell lines. In hepatocellular carcinoma cells, HEP-3B and SK-HEP1, PAR4-mediated Ca^{2+} mobilization responses were not elicited by PAR4AP (Kaufmann et al., 2007). However, in colon cancer HT-29 cells, PAR4AP treatment resulted in Ca^{2+} mobilization (Gratio et al., 2009).

Accordingly, the low level of KLK4-induced Ca^{2+} mobilization observed in this chapter in kidney PTC may be another example of biased agonism. This could be examined further by seeing if KLK4 treatment of the kidney PTC activates any PAR-dependent, Ca^{2+}-independent intracellular signalling pathways. The signalling toolkit of the kidney PTC may mean there are alternate pathways induced by KLK4 activation of PAR2. In

addition, it has not been established if cell surface compartmentalization of PAR2 or other signalling components are required for KLK4 activation of this receptor. Furthermore, as for epithelial cells, kidney PTC have apical basolateral polarity (Schluter and Margolis, 2012) and it has been shown recently that intestinal epithelial cells demonstrate differential signalling depending on whether PAR2 on the apical or the basolateral surface is activated (Lau et al., 2011). As the Ca^{2+}-flux assays in this chapter were conducted with the kidney PTC in suspension, cell polarity would have been lost and this may have altered the cells PAR2-mediated signalling response.

Biased agonism is one possible reason for the small Ca^{2+} mobilization induced in the kidney PTC by KLK4. However, there are other possibilities. For example, KLK4 may require a cell-surface cofactor to facilitate PAR2 activation. Indeed, the results shown in Chapter 4 suggest that hepsin and TMPRSS2 form cell-surface or intracellular complexes involving KLK4. The interaction of KLK4 with hepsin, TMPRSS2 or another surface protein may bring KLK4 into proximity with PAR2 to facilitate activation. There is also the possibility of an alternate or competitive substrate for KLK4 on the kidney PTC surface. Active-site titration of KLK4 immediately after exposure to the kidney PTC showed there was no irreversible inhibition of KLK4 activity. Moreover, when KLK4 concentrations were increased from 300 nM to 600 nM then 1.2 μM, there was a small increase in Ca^{2+} mobilization. This could indicate that the inhibitor-like effects of a competitive substrate on the kidney PTC were being overcome by an excess of KLK4. Increasing the PAR2 surface concentration could also overcome the putative competitive substrate by out-competing for the KLK4 active-site (Mathews et al., 2000).

Overall, the results for the kidney PTC raised some very interesting questions about the nature of the relationship between PAR2 (and PAR1) and KLK4. These results in context with other reports documenting PAR activation by KLK4 (Ramsay et al., 2008a; Gratio et al., 2010; Wang et al., 2010) suggest there is a complex relationship, possibly centred on cell-type differential signalling. The significance of this in normal or pathological states is unknown.

5.3.3 Generation and characterization of prostate cancer LNCaP cells stably expressing the transmembrane serine protease hepsin

Ca^{2+} mobilization, in response to PAR activation has been demonstrated in a number of prostate-derived cell lines. These include, PAR1 activation on primary prostate stromal cells (Wang et al., 2010), thrombin-activated PAR1 on primary prostate cancer cells derived from bone (Chay et al., 2002), and trypsin-activated PAR2 on primary BPH stromal cells (Myatt and Hill, 2005). Ca^{2+} mobilization has also been demonstrated in prostate cancer-derived cell lines. This includes, PAR2 activation by trypsin IV in PC-3 cells (Cottrell et al., 2004), TMPRSS2 in LNCaP cells (Wilson et al., 2005), trypsin in LNCaP cells (Mannowetz et al., 2010), and as mentioned earlier, KLK4 activation of PAR2 in PC-3 cells (Ramsay et al., 2008a).

In this chapter, LNCaP cells stably expressing hepsin and catalytically inactive hepsinSA were generated for the purpose of studying the contribution of hepsin to proteolytic cascades resulting in PAR activation. As hepsin self-activates (Chapter 4, Section 4.3.1) (Vu et al., 1997; Qiu et al., 2007), it is possible that it is an initiator of proteolytic cascades. Indeed, as discussed earlier, Camerer and colleagues (2010) showed that hepsin indirectly activates PAR2 by activating matriptase which activates PAR2.

However, generation of the LNCaP-hepsin stable cell lines proved to be challenging due to the high level of cell senescence, death associated with overexpression of this protein and the low and inconsistent levels of hepsin expression seen in stably transfected populations. In contrast, generation of the LNCaP-hepsinSA stable lines was comparatively straightforward. The LNCaP-hepsinSA cells had high, consistent hepsinSA expression levels as well as no discernible alteration to cell senescence or death when observed in comparison to LNCaP-vector transfected cells. From this, it was concluded that the difference in the ability to generate LNCaP-hepsin and LNCaP-hepsinSA cells was due to the catalytic activity of hepsin.

Interestingly, flow cytometry analysis indicated that very little hepsin localized to the surface of stably expressing LNCaP cells, in contrast with hepsinSA cells which showed high plasma membrane levels of the catalytically inactive version of this protease. This is interesting because it has been shown that in polarized epithelial cells matriptase activation at the basolateral surface is accompanied by rapid HAI-1 inhibition followed possibly by internalization and transcytosis to the apical surface for secretion (Wang et al., 2009). To avoid induction of cell senescence and death it may be possible that after

activation at the cell surface hepsin similarly requires rapid regulation by inhibitor binding and internalization.

Results reported in other studies may account for the difficulties encountered in generating LNCaP-hepsin stable cells in this project. For example, early results from Srikantan and colleagues (2002) showed that of three prostate cancer-derived cell lines, PC-3, LNCaP and DU145, neither PC-3 nor DU145 express hepsin. This study went on to show that hepsin overexpression in PC-3 and LNCaP cells led to reduced monolayer growth. Further examination of the hepsin overexpressing PC-3 cells showed there was ~75% inhibition of proliferation when compared to vector transfected cells. The hepsin overexpressing PC-3 cells also had reduced anchorage-independent growth as demonstrated by soft agar colony formation assays. The cell cycle distribution of the hepsin PC-3 cells compared to vector transfected cells showed that the hepsin PC-3 cells had increased levels of cells in cell-cycle arrest at G_2 (checkpoint) phase. This means fewer cells proceeding to M (mitosis) phase and as a consequence, reduced proliferation. In addition, the hepsin PC-3 cells had a higher proportion of apoptotic cells and decreased migration in Matrigel compared to the vector controls.

Another study also reported reduced monolayer proliferation and soft agar colony formation when hepsin was transfected into the liver adenocarcinoma cell line SK-HEP-1 (Chen et al., 2006). To confirm that hepsin was proteolytically active, expressing cells were assayed using factor VII as a substrate. This group further demonstrated that when active-site mutated hepsin was transfected, the growth and proliferation inhibition effects were abolished.

Reduced monolayer proliferation and soft agar colony formation has also been shown in ovarian cancer BG-1 (Nakamura et al., 2006) and endometrial adenocarcinoma Ishikawa cells (Nakamura et al., 2008) overexpressing hepsin. Further examination of the hepsin BG-1 cells showed hepsin-induced increased expression and activation of the p53 tumour suppressor protein and also p53-dependent apoptosis via activation of caspase-3, -6 and -7 (Nakamura et al., 2006). The hepsin Ishikawa cells were also shown to have increased p53 expression as well as increased expression of cell-cycle regulating protein 14-3-3σ, which is transcriptionally regulated by p53 (Nakamura et al., 2008). Cell cycle analysis showed increased numbers of cells in the G_2-M phase as well as increased apoptotic cells when compared to vector transfected cells. Increased apoptosis was also attributed to the p53-dependent activation of caspase-3. Additionally, these cells showed

reduced migration and invasion in Matrigel invasion assays. As a tumourigenesis model, when hepsin overexpressing BG-1 and Ishikawa cells were injected subcutaneously into nude mice, both showed reduced tumour growth when compared to untransfected cells (Nakamura et al., 2006; Nakamura et al., 2008).

Furthermore, in a recent study using doxycycline-inducible hepsin overexpression in PC-3 and HEK293 cells, Wittig-Blaich and colleagues (2011) demonstrated a doxycycline-dose-dependent loss of both cell viability and adhesion and also increased cell death in anchorage-dependent growth assays. This loss of viability was not seen in anchorage-independent growth. Moreover, viability and adhesion of the doxycycline-induced-hepsin PC-3 cells in anchorage-dependent growth could be recovered by plating cells on extracellular matrix (ECM) laid down by the immortalized non-malignant prostate cell line RWPE1 but not on ECM laid down by prostate cancer bone metastasis-derived PC-3 cells.

In contrast to the above studies, several others have shown that hepsin overexpression either has no effect on cell growth and invasive capability or, in fact, promotes growth and invasion either *in vitro* or *in vivo*. For example, in contrast to results shown by Srikantan and colleagues (2002), stable hepsin-expressing LNCaP cells, designated LNCaP-34, generated by Moran and colleagues (2006), showed no change to *in vitro* cell proliferation and invasion (Li et al., 2009). Serine protease activity of hepsin expressed by the LNCaP-34 cells was confirmed by proteolytic activation of pro-uPA, pro-HGF and pro-macrophage-stimulating protein, as was the abrogation of protease activity with inhibitor KD1 (Moran et al., 2006; Li et al., 2009; Ganesan et al., 2011; Ganesan et al., 2012). The cells also had increased migration on Laminin-332 (Tripathi et al., 2008). Moreover, when implanted orthotopically in the prostate of SCID/bg mice, LNCaP-34 cells showed increased tumour size, increased invasion in the mouse prostate as well as lymph node metastasis.(Li et al., 2009). These differences in the effects of hepsin expression in LNCaP cells between research laboratories could be due to differences culture conditions or passage number. Both of these factors have been shown to effect cell phenotype and performance in assays for a number of cell lines including LNCaP cells (Hughes et al., 2007).

In further work with LNCaP cells by Yemelyanov and colleagues (2007), they showed re-expression of glucocorticoid receptor (GR) in LNCaP cells that have lost endogenous expression and subsequent treatment of the cells with glucocorticoids inhibited

proliferation in monolayers and blocked anchorage-independent growth of the LNCaP cells. In an examination of changes to protein expression, induced by GR activation with glucocorticoids, it was shown that activation of the GR leads to, among other effects, normalized hepsin (decreased) and increased expression of the serine protease inhibitor maspin. In another example, in an ovarian cancer model, SKOV3 cells overexpressing hepsin injected subcutaneously in the left flank of nude mice showed increased tumour size compared to untransfected SKOV3 cells, this increase in size was ablated by the mutation of the hepsin catalytic site (Miao et al., 2008).

Suppression of endogenously expressed hepsin either by RNA silencing or with activity blocking antibodies has been another method used to examine the effects of hepsin on cancer progression. Indeed, down-regulation of endogenous hepsin by specific siRNA significantly reduced the *in vitro* proliferation and invasion of breast cancer MDA-MB-231 and HER18 cell lines compared to non-specific siRNA (Xing et al., 2011). This is consistent with earlier work by Torres-Rosado and colleagues (1993) which found that the hepatocellular carcinoma cell lines HepG2 and PLC/PRF/5 underwent growth arrest when hepsin antisense oligonucleotides or anti-hepsin antibodies were applied to the cells. In contrast, in work done by Xuan and colleagues (2006) they concluded that inhibiting hepsin proteolytic activity with hepsin neutralising antibodies had no effect on LNCaP, DU145 or CAOV-3 cell proliferation *in vitro*. However, in Matrigel invasion assays, they concluded that both DU145 and CAOV-3 were inhibited by the anti-hepsin antibodies. However, this study has an omission that may confound the results. They have not mentioned in the publication if they have tested for hepsin expression in the DU145 cells they used. DU145 cells used by two other groups have been shown to not express hepsin mRNA (Srikantan et al., 2002; Owen et al., 2010). Both LNCaP and CAOV-3, however, have been shown to express hepsin (Srikantan et al., 2002; Nakamura et al., 2006; Owen et al., 2010).

Hepsin overexpression and suppression are useful tools to examine hepsin contribution to cancer progression and cell function. However, these approaches are also exposing contradictions yet to be resolved. The increased cell senescence observed in this chapter in response to hepsin overexpression is not unique, and certainly, growth cycle arrest induced by hepsin is a possible mechanism facilitating this. However, there are contrasting reports indicating that hepsin overexpression does not alter cell growth.

Unfortunately due to the extended process undertaken to generate the LNCaP-hepsin cells, time constraints precluded PAR activation studies using these cells.

5.3.4 Summary

In conclusion, in this chapter KLK14 activated Ca^{2+} mobilization via PAR1, PAR2 and PAR4. However, it is not an efficient PAR activator in comparison to trypsin or matriptase as relatively high KLK14 concentrations induce modest activation. In contrast, hepsin elicited negligible Ca^{2+} mobilization via the PARs. However, it is possible hepsin induces alternate intracellular signalling pathways.

It was also shown that while KLK4 activates PAR2-mediated signalling in PAR2-LMFs and prostate cancer-derived PC-3 cells (Ramsay et al., 2008a), in this chapter KLK4 did not activate PAR2-mediated Ca^{2+} mobilization in human kidney PTC. It is possible this is due to biased agonism, with KLK4 activating alternative signalling pathways in these cells. Or it is possible KLK4 has an alternative proteolytic target in these cells. Each possibility is equally intriguing.

Also in this chapter, stable but rare populations of LNCaP hepsin cells were able to be generated. However, the data indicate that there are stark differences in cellular effects between overexpression of hepsin and catalytically inactive hepsinSA in LNCaP cells. The contrast between the achieved cell-surface expression level of hepsin and of catalytic mutant hepsinSA, as well as the contrast in the observed growth rates, cell death and senescence warrant further attention. There is also an avenue to explore hepsin cellular localization and possible internalization, as well as hepsin binding partners in this overexpression model. Furthermore, these generated cell lines can be used to examine whether hepsin expression facilitates or impedes PAR activation by different proteases including KLK4, KLK14 and matriptase.

Chapter 6 General Discussion

6.1 Key observations

This thesis has examined the proteolytic and cell-surface interactions of secreted serine proteases KLK4 and KLK14 with transmembrane serine proteases hepsin and TMPRSS2. This thesis also examined the interactions of hepsin, TMPRSS2 and matriptase with the secreted matrix metalloproteinases MMP3 and MMP9. A key observation in this thesis is that the KLKs and TTSPs interact at the cell surface, as do the TTSPs and MMPs, potentially forming multi-protein complexes. These cell-surface interactions potentially facilitate activation of the MMPs and KLK4. They also may facilitate activation of cell-surface signalling molecules such as PARs through the localization of the secreted proteases. Cell-surface localization of these proteases may also have direct and indirect effects on induction of HGFR signalling through KLK activation or degradation of the HGFR ligand HGF, and also through degradation of HAI-1 by KLK14. Figure 6.1 proposes a model for the interactions of these proteases in the pericellular environment, and this model will be discussed in greater detail in the following sections. This final Chapter highlights the implications of the findings and details strategies to develop further the results from this study.

A key aspect of this study was the generation of recombinant KLK14 zymogen in Sf9 cells. It was determined that it was an N-glycosylated protein when generated by these cells. However, KLK14 also demonstrated cell-type differential N-glycosylation as it was not N-glycosylated when generated in Cos-7 cells in this study or when generated in *Pichia pastoris* by another group (Borgono et al., 2003).

This study also examined the proteolytic interactions of KLK14 with pro-HGF, and with HAI-1A and HAI-1B. It was observed that KLK14 activates pro-HGF over a discrete concentration range, in contrast to KLK4 which primarily degrades this factor. It was also observed that KLK14 degrades HAI-1A and HAI-1B, while hepsin forms stable complexes with HAI-1A and degrades HAI-1B.

Proteolytic and cell-surface interactions of KLK14 and KLK4 with transmembrane proteases hepsin and TMPRSS2 were also examined. A critical finding was that human hepsin autoactivates, as previously determined for mouse hepsin (Vu et al., 1997) and suggested by unpublished data (Qiu et al., 2007). It was also determined that hepsin and autoactivating TMPRSS2 (Afar et al., 2001) proteolyse KLK14; however, there was a greater level of proteolysis of KLK4 by these proteases. Also, while these KLKs are secreted proteases, for the most part minimal evidence of their proteolysis by hepsin

and TMPRSS2 was detected in the conditioned media as the cleaved forms of KLK4 and KLK14 were primarily observed in cell lysates. Furthermore, while KLK4 and KLK14 were located on the cell surface, independently of hepsin and TMPRSS2, they also co-localized with these transmembrane proteases. In addition, active KLK4 and KLK14 were not isolated from conditioned media. However, active KLK4 was isolated from the cell surface, again, independently of hepsin and TMPRSS2.

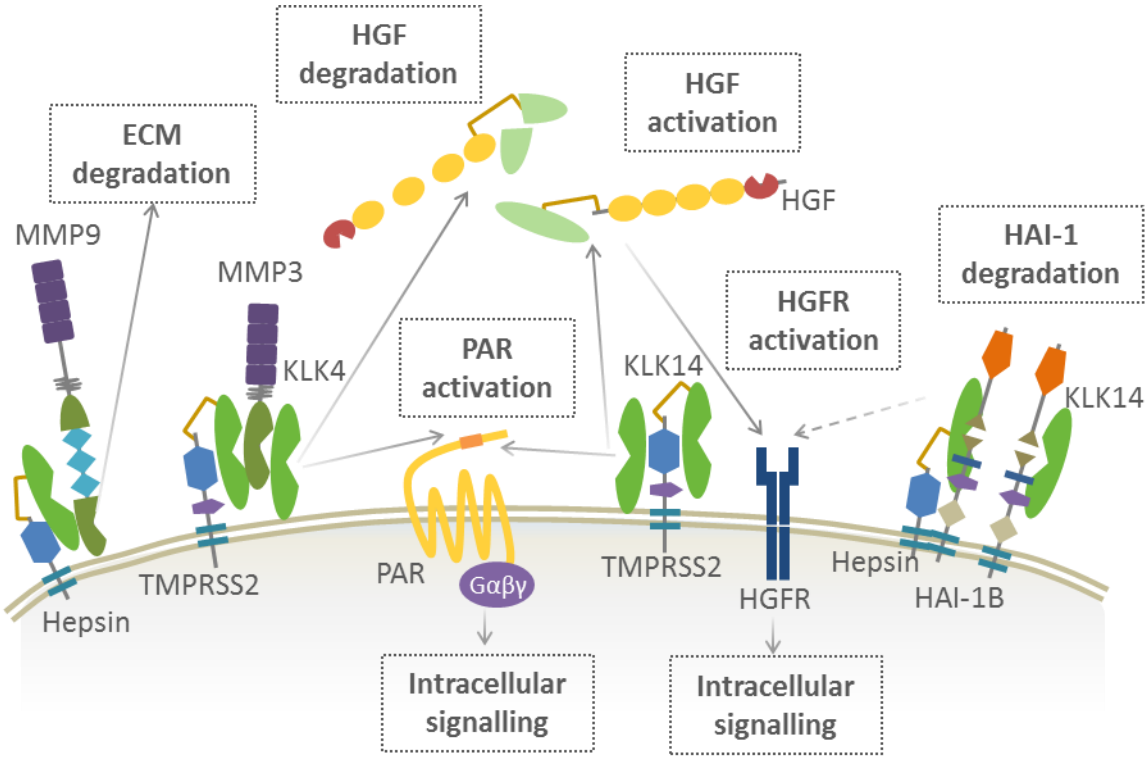

Figure 6.1 Model for the pericellular proteolytic activity of hepsin, TMPRSS2, KLK4, KLK14, MMP3 and MMP9. Hepsin and TMPRSS2 activate MMP3 and MMP9. MMP9 predominantly degrades extracellular matrix (ECM) components. MMP3 activates KLK4 which in turn activates PAR1 and PAR2, and deactivates HGF. KLK4 and KLK14 localize to the cell surface with hepsin and TMPRSS2. KLK14 activates PAR1, PAR2, PAR4 thereby initiating intracellular signalling. KLK14 activates HGF which in turn initiates HGFR-mediated intracellular signalling. KLK14 degrades HAI-1 isoforms HAI-1A and HAI-1B and hepsin degrades HAI-1B, in so doing may indirectly lead to HGFR signalling (broken line).

This study also examined the proteolytic and cell-surface interactions of hepsin and TMPRSS2 with the secreted proteases MMP3 and MMP9. Similar to the finding for KLK4 and KLK14, while MMP3 and MMP9 were proteolysed by hepsin and TMPRSS2, the cleaved products were observed primarily in cell lysates. Moreover, MMP3 and MMP9 co-localized with hepsin and TMPRSS2.

Focusing on the potential role of hepsin in facilitating cell-surface localization of KLK4 and KLK14 and other proteases, it was also determined in this study that stable overexpression of hepsin in LNCaP cells resulted in minimal plasma membrane localization. This was in contrast to catalytically inactive hepsin which readily localized to the plasma membrane.

KLK14- and hepsin-induced Ca^{2+} mobilization via PAR1, PAR2 and PAR4 were also examined in this study. It was determined that KLK14 activated Ca^{2+} mobilization via PAR1, PAR2 and PAR4 whereas hepsin elicited negligible Ca^{2+} mobilization via these receptors. In addition, following on from previous studies showing that KLK4 is able to activate PAR2 in several cell lines (Mize et al., 2008; Ramsay et al., 2008a), it was determined that Ca^{2+} mobilization elicited via this receptor could be abolished by the KLK4-specific inhibitor STFI-FCQR. Interestingly, this study also showed that KLK4 activation of Ca^{2+} mobilization via PAR2 is potentially cell type-dependent, as in human primary kidney cells it induced minimal Ca^{2+} mobilization via this receptor.

6.2 The potential contribution of KLK14 and KLK4 to the HGF-HGFR signalling cascade in prostate cancer

There are conflicting consequences of KLK14 overexpression in different pathologies which suggest tissue-specific tumour-suppressive or tumour-progressive roles (Borgono et al., 2007c; Lopez-Otin and Matrisian, 2007). For instance, KLK14 has increased serum levels in prostate cancer (Borgono et al., 2003; Borgono et al., 2007c) and there is a correlation between increased *KLK14* mRNA expression and late stage prostate cancer (Yousef et al., 2003b). Rabien and colleagues (2008) also demonstrated that increased KLK14 expression correlates with decreased progression-free survival. Similarly, KLK14 has increased expression in breast cancer (Fritzsche et al., 2006), with increased mRNA correlating with poor prognosis (Yousef et al., 2002). And recently, KLK14 was found present in colon cancer adenocarcinoma but not in normal epithelial cells (Gratio et al., 2011; Chung et al., 2012). Conversely, while KLK14 is also overexpressed in ovarian cancer (Borgono et al., 2003), increased *KLK14* expression in early stage ovarian cancer has been correlated with favourable prognosis (Yousef et al., 2003a).

The method by which KLK14 potentially facilitates these states is unknown. However, tumour suppression may be facilitated by KLK14 generation of angiostatic fragments

from degradation of plasminogen (Borgono et al., 2007c; Rajapakse and Takahashi, 2007). In contrast, tumour progression may be mediated by HGF activation and HAI-1 degradation.

Similar to KLK14, HGF and HGFR are overexpressed in prostate cancer (Kurimoto et al., 1998; Zhu and Humphrey, 2000) and there is increased activated HGF in the serum of patients with untreated prostate cancer compared to those with benign prostate disease (Hashem and Essam, 2005; Yasuda et al., 2009). HGF expression is also androgen-regulated (Yu et al., 2013). Furthermore, irregular receptor signalling due to HGFR and HGF overexpression has an established role in tumourigenesis (Trusolino et al., 2010; Gherardi et al., 2012) and has been associated with the progression of prostate cancer (Humphrey et al., 1995; Nakashiro et al., 2000; Knudsen et al., 2002; Nakashiro et al., 2003; Knudsen and Edlund, 2004; Hashem and Essam, 2005; Yasuda et al., 2009). However, activation of HGF is a rate limiting step in HGF-induced HGFR signalling (Kataoka and Kawaguchi, 2010). Therefore, as KLK14 activates HGF, increased KLK14 expression in prostate cancer may in turn lead to increased HGFR signalling (Figure 6.1).

In contrast to KLK14, KLK4 degrades HGF (Figure 6.1) and so potentially negatively regulates HGF-HGFR signalling. This is significant for prostate cancer progression as the abundant HGF expression in the tumour microenvironment is accompanied by an initial increase in KLK4 expression in the early stages of prostate cancer, followed by decreased KLK4 expression in the late stages (Seiz et al., 2010). So in this capacity, KLK4 may function as a tumour suppressor in the early stages of prostate cancer with this function lost progressively as KLK4 expression declines.

While HGF activation is potentially a direct method of KLK14 contributing to HGFR signalling, KLK14 may also contribute indirectly through degradation of HAI-1 (Figure 6.1). This degradation may increase the availability of HGF-activating proteases including HGFA, matriptase and hepsin. For instance, active, but not inactive, HGFA binds to HAI-1 on the cell surface (Kataoka et al., 2000). In so doing, HAI-1 acts as reservoir for active HGFA, as when the HAI-1 and HGFA complex is shed from the cell surface it dissociates, freeing proteolytically active HGFA (Kataoka et al., 2000). Similarly, matriptase activity in conditioned media is increased by membrane-type-1 matrix metalloproteinase (MT1-MMP)-mediated shedding of HAI-1 from the cell surface (Domoto et al., 2012). Furthermore, shed HAI-1 has been identified in several

MW forms suggesting that there are multiple points amenable to cleavage (Shimomura et al., 1999) and MT1-MMP is one protease able to generate multiple truncated forms of HAI-1 (Domoto et al., 2012). It is possible KLK14 also acts in this capacity, facilitating release of HAI-1 bound proteases through degradation. One step to explore this further would be to determine if KLK14 degrades HAI-1 when it is in complex with another protease such as hepsin or matriptase. As this study used soluble HAI-1, further analysis of KLK14 degradation of HAI-1 could be achieved by determining if it degrades cell-surface HAI-1.

It has been shown that suppression of HAI-1 leads to a more aggressive phenotype in prostate cancer-derived cells *in vitro* (Sanders et al., 2007). Similarly, HAI-1 suppression enhances the migratory, proliferative and invasive capabilities of breast cancer-derived cells (Parr and Jiang, 2006). It has also been shown in an *in vivo* model that when HAI-1 was suppressed in pancreatic cancer-derived cells injected into mouse tail veins, pulmonary metastasis was promoted (Fukushima et al., 2011). Moreover, in this study, co-injection of recombinant KD1 (the truncated form of HAI-1 featuring the first Kunitz domain) abrogated metastasis of these cells. Furthermore, HAI-1 expression is androgen-regulated in prostate cells with reduced androgen correlating with decreased HAI-1(Knudsen et al., 2005), and in patients with castration-resistant prostate cancer, PSA progression-free rate is worse for patients without HAI-1 expression than those positive for HAI-1 (Yasuda et al., 2013). Therefore, as increased KLK14 mRNA expression has been correlated with aggressive forms of prostate and breast cancer (Yousef et al., 2002; Yousef et al., 2003b; Fritzsche et al., 2006), it is possible that degradation of HAI-1 by KLK14 may lead the more aggressive *in vivo* phenotype.

Certainly, in pancreatic cancer and lung cancer-derived cells suppression of HAI-1 led to decreased E-cadherin expression and also induced EMT (Cheng et al., 2009; Fukushima et al., 2011), a change in cells that can facilitate migration and invasion (Lawrence et al., 2007). This EMT was mitigated by simultaneous knockdown of HAI-1 and matriptase or TMPRSS4, another member of the TTSP family. This suggests that the induction of E-cadherin expression and subsequent EMT was mediated in part by proteolytic activity (Cheng et al., 2009). The connection of HAI-1 to E-cadherin has also been noted by Oberst and colleagues (2001) who found that HAI-1 and matriptase expression in breast cancer-derived cells positively correlate with E-cadherin expression, and negatively correlate with invasive capability. Additionally, in endometrial cancer and pancreatic

cancer-derived cells, overexpression of HAI-1 induced increased E-cadherin expression (Cheng et al., 2009; Nakamura et al., 2011) and also restored epithelial cell morphology, a mesenchymal-epithelial transition (Cheng et al., 2009).

Interestingly, studies in our laboratory found that overexpression of KLK4 in prostate-cancer derived cells induced decreased E-cadherin expression as well as increased EMT and migration (Veveris-Lowe et al., 2005). The mechanism by which these changes were induced has not been established nor has the potential for KLK14 to induce similar phenotypic changes been examined. It is possible that involvement of KLK4 in the HGF-HGFR activation cascade through either HGF degradation or HGFA activation (Mukai et al., 2008) leads to modulation of E-cadherin expression. Certainly, truncated HGF, consisting of the amino terminus and the first kringle domain, also initiates signalling via the HGFR, decreasing E-cadherin expression and inducing EMT in prostate epithelium-derived cells (Pavone et al., 2011). While this truncated form of HGF is attributed to splice variation (Kataoka et al., 2003), it is possible that KLK4 proteolysis of HGF may generate similar fragments capable of initiating HGFR signalling pathways leading to decreased E-cadherin expression.

Study of the interaction of KLK14 and KLK4 with HGF, and KLK14 with HAI-1 isoforms, was conducted using N-glycosylated recombinant KLK14 and KLK4 generated in insect cells. As N-glycosylation can affect the catalytic activity of proteases (Skropeta, 2009), it is necessary to determine if these KLKs are endogenously N-glycosylated and whether it has an effect on inhibition by HAI-1 or activation of HGF (or PAR activation). Moreover, it would be interesting to determine if there are tissue- or disease-specific differences in KLK14 N-glycosylation potentially modulating specificity for proteolytic targets.

There are several experiments that could be used to address these issues. For example, after identifying the N-glycosylation acceptor residues in KLK14 and KLK4 using methods outline in the discussion of Chapter 3, recombinant proteases generated with the N-glycosylation sites mutated could be used to determine if N-glycosylation impacts KLK14 activation, or KLK4 degradation, of HGF. Similarly, KLK14 degradation of HAI-1 could be assessed plus or minus N-glycosylation. To address endogenous N-glycosylation, tissue-specific assessments could be made of KLK14 and KLK4 isolated from different tissue types. For instance, prostate-derived KLK14 could be compared to skin-derived forms using enzyme de-glycosylation and gel mobility shift assays.

Alternatively, N-glycosylation status could be assessed using lectin-antibody sandwich (enzyme-linked immunosorbent assay) ELISA.

6.3 Implications of cell-surface interactions of hepsin and TMPRSS2 with secreted proteases KLK4, KLK14, MMP3 and MMP9

One of the most interesting results in this thesis was that the secreted proteases KLK4 and KLK14 localized to, and active KLK4 was isolated from, the cell surface. In addition, it was interesting that these proteases co-localized with hepsin and TMPRSS2, and in turn that hepsin and TMPRSS2 co-localized with MMP3 and MMP9. As summarized in the model in Figure 6.1, these results set up the premise that these proteases co-localize in functional complexes facilitating activation of MMP3 and MMP9 and potentially KLK4 and KLK14.

These complexes may also facilitate activation of cell-surface receptors and other proteases, as well as degradative activity in the pericellular environment. For instance, as KLK4 was isolated from the cell surface but not from conditioned media it is possible these complexes may facilitate activation of KLK4 at the cell surface potentially through co-localization of MMP3. Furthermore, cell-surface localization of KLK4 may facilitate activation of PAR1 and PAR2. Similarly, pericellular activity of KLK14 may also be facilitated by cell-surface localization, enhancing activation of PAR family members as well as degradation of transmembrane HAI-1A and HAI-1B.

The results also showed that while KLK4 and KLK14 co-immunoprecipitate with hepsin and TMPRSS2, the KLKs also localize to the cell surface independently of the TTSPs. This suggests a pericellular role for the proteolytic activity of these KLKs. However, it is unknown if they localize to the surface directly upon secretion or if they are taken up from the extracellular environment post secretion by a cell-surface cofactor or receptor. It is also unknown if the activity of these KLKs is directed out into the pericellular environment, for example degradation or activation of proteins in the prostatic fluid in the prostate lumen, or if the activity of these proteases is directed at cell-surface proteolytic events.

Cell-surface localization has been determined to be a critical factor in the activity of a number of other secreted proteases. For instance, in the coagulation cascade, tissue

factor (TF) is crucial for the cell-surface localization, stabilization and enhanced activity of factor VIIa (FVIIa), and subsequent binding and activation of factor Xa (FXa) (Spronk et al., 2003) (Vadivel and Bajaj, 2012). Similarly, in the plasminogen activation system, uPA is localized to the cell surface by its cognate receptor uPAR (Ragno, 2006), and plasminogen is localized by several different types of cell-surface receptors (Godier and Hunt, 2013). However, in each instance in addition to C-terminal protease domains, the coagulation factors, plasminogen and the plasminogen activation proteases have non-proteolytic N-terminal domains that facilitate binding to their respective cell-surface receptors (Ragno, 2006; Godier and Hunt, 2013). In contrast, KLK4 and KLK14 have no such domains as they consist of a single serine protease domain. Binding of these KLKs to the cell surface is likely mediated by other surface localized proteins, however, apart from the protease active site there are no recognized motifs in the KLK protease domain that suggest possible binding partners or sites.

Interestingly, recent work by Rolland and colleagues (2014) to develop a protein-protein interactome map has revealed the cell-surface protein TYRO3 protein tyrosine kinase as a potential binding partner for KLK4. This receptor tyrosine kinase is from a family of three kinases whose expression is known to give cancer cells advantages through survival, chemoresistance and motility (Graham et al., 2014). TYRO3 and its cognate ligand growth arrest-specific 6 (GAS6) have also been linked to the proliferative state of prostate cancer cells in primary tumour (Taichman et al., 2013). Nonetheless, the nature of the interaction between KLK4 and TYRO has yet to be determined. To date it is the only KLK family member to have been associated with a transmembrane/cell-surface binding partner.

While this thesis is the first report of cell-surface localization of KLK4 and KLK14, MMP3 and MMP9 have previously been reported to be associated with the cell surface through interaction with a variety of binding partners (Murphy and Nagase, 2011). Mostly, the cell-surface binding of these MMPs has been attributed to interactions of their hemopexin domain. MMP9 in particular has been associated with a number of cell-surface proteins including, β1, β2 and β5 integrins (Stefanidakis et al., 2003; Bjorklund et al., 2004; Redondo-Munoz et al., 2010), CD44 (Yu and Stamenkovic, 1999; Desai et al., 2009), and low density lipoprotein-related protein (LRP) 1 and 2 (Van den Steen et al., 2006). In contrast, MMP3 has so far only been associated with cell-surface collagen I

(Murphy and Nagase, 2011). Certainly, one or more of these MMP binding partners may facilitate co-localization with the TTSPs hepsin, TMPRSS2 and matriptase.

The immediacy of the interactions between the proteases could also be assessed using methods such as bioluminescence resonance energy transfer (BRET). For instance, one protease generated as *Renilla*-tagged and another as yellow fluorescent protein (YFP)-tagged are co-transfected. BRET is then observed if the proteases are in close proximity and the resonant energy from the *Renilla* luciferase is transferred to YFP, exciting it and resulting in emission.

It is important to note that the over-expression of KLKs, TTSPs and the MMPs described in this thesis may create artificial interactions between the proteases due to alteration to cellular trafficking, cell-surface localization and protease activity. It is therefore necessary to corroborate the findings by examining the interactions of the endogenous proteins. It is also necessary to determine whether cell-surface localization of KLK14 and KLK4 is replicated by endogenous proteins.

In the first instance, methods used in this thesis, such as cell-surface biotinylation and activity-based probes, could be used on prostate cancer-derived cells to identify cell-surface-localized and active proteases. The interactions between these KLKs and the TTSPs on the cell surface could also be examined further using co-immunoprecipitation studies. Moreover, as KLK14 and KLK4 localized to the cell surface independently of hepsin or TMPRSS2, co-immunoprecipitation could also be used in conjunction with two-dimensional electrophoresis followed by MS/MS analysis to identify other proteins associated with the protease complexes.

As a feature of prostate cancer development from the prostate epithelium is loss of cell polarity, as the disease develops immunohistochemistry (IHC) of prostate tissue could also be used to examine if there are any global changes to localization of the TTSPs in relation to the KLKs.

6.4 The potential for cell-surface localization of KLKs to effect PAR activation

To date activation of PAR family members by KLK4 and KLK14 has been reported without consideration of potential cell-surface cofactors assisting with localization,

activation and activity of the KLKs. This is potentially an important aspect of KLK4 and KLK14 activation of PARs because when compared to trypsin activation of PAR1, PAR2 or PAR4, or matriptase activation of PAR2, 4- to 30-fold higher concentrations of these KLKs are require to effect significant Ca^{2+} mobilization via these receptors.

From the earliest days of PAR1 research, activation by thrombin has been acknowledged as facilitated by the hirudin-like domain of PAR1, facilitating thrombin binding and more potent thrombin action (Vu et al., 1991b; Nakanishi-Matsui et al., 2000). However, the hirudin-like domain is unnecessary for PAR1 activation by all proteases as an extensive number of proteases lacking hirudin domain-binding capacity activate PAR1 *in vitro* (Adams et al., 2011). Furthermore, PAR2 and PAR4 lack the hirudin-like domain, yet they are also activated by proteases with and without hirudin domain-binding capacity (Adams et al., 2011). For instance, in addition to activating PAR1, thrombin also activates PAR4 (Kahn et al., 1998; Xu et al., 1998). However, the potency of thrombin is 50-fold less than for PAR1, with higher concentrations required to elicit a Ca^{2+} mobilization response from PAR4 (Kahn et al., 1998; Xu et al., 1998). More potent PAR4 activation by thrombin is enabled through the formation of heterodimers with PAR1, with PAR1 acting as a co-factor to localize thrombin (Leger et al., 2006; Arachiche et al., 2013).

Similarly, it has been determined that cell-surface proteins can act as cofactors facilitating PAR activation. For instance, serine protease FVIIa alone will not activate PAR signalling, however, when in complex with TF, FVIIa activates PAR1 and PAR2 (Camerer et al., 2000). In addition, although FXa alone is a weak activator of PAR1, PAR2 and PAR4, when associated with the TF-FVIIa complex, FXa demonstrates potent activation of PAR1 and PAR2 (Camerer et al., 2000; Riewald and Ruf, 2001; Camerer et al., 2002). Another example of facilitated PAR activation is endothelial protein C receptor (EPCR) which binds protein C. This facilitates both protein C activation and activation of PAR1 and PAR2 by the bound activated protein C (Riewald et al., 2002; Kaneider et al., 2007; Julovi et al., 2011).

Therefore, it is possible that cell-surface proteins may facilitate KLK4 and KLK14 activation of PARs through localization of these KLKs to the surface (Figure 6.1). This is the first study to determine that KLK14 and active KLK4 localize to the cell surface. The generation of LNCaP cells overexpressing hepsin was an attempt to ascertain whether hepsin facilitates localization and activation of KLK4 and KLK14 and in turn

facilitating PAR activation by these KLKs. Indeed, matriptase activation of PAR2 has been shown to be facilitated by hepsin though activation of matriptase (Camerer et al., 2010). However, the transient co-transfection and cell-surface biotinylation experiments performed indicate that while KLK4 and KLK14 co-immunoprecipitate with hepsin, these KLKs localize to the cell surface independently of hepsin. Moreover, hepsin does not activate KLK4. Rather, it potentially degrades KLK4. However, it remains to be determined whether KLK14 is activated by hepsin (or TMPRSS2), for while activated KLK14 was not detected in the conditioned media of cells, the activity of cell-surface-retained KLK14 has not been examined yet.

One of the most interesting aspects of PAR activation examined in this chapter was that in human primary kidney-derived proximal tubule cells, KLK4 elicited minimal Ca^{2+} mobilization. This was in contrast to LMF cells in which KLK4 readily activated PAR2, as observed here and previously (Ramsay et al., 2008a), and prostate cancer-derived PC-3 cells in which KLK4 also activated PAR2 (Ramsay et al., 2008a). Certainly it is possible that KLK4 requires a cell-surface cofactor or binding partner to facilitate activation of PAR2 and that this factor is absent in these kidney-derived cells.

On the other hand, PAR2 may not be the primary substrate of KLK4 in the kidney. To explore this further, a comparative proteomics approach, such as stable isotope labelling by amino acids in cell culture (SILAC) (Ong et al., 2002), could be taken to identify KLK4 substrates. In this method, one population of kidney PTC would be grown in normal medium. The other population would be grown in culture medium lacking a standard amino acid, but supplemented with an isotopically labelled form of that amino acid. Incorporation of the labelled amino acid into newly synthesized proteins would allow the proteins from KLK4-treated kidney PTC to be distinguished from untreated cells in mass spectrometry analysis. This would allow identification of KLK4-cleaved proteins by increased abundance of the released portion in the extracellular medium. Similarly, this technique to identify KLK4-cleaved proteins could be applied to membrane and membrane-bound proteins (Liang et al., 2006).

However, it is also interesting to note that while KLK4 has been detected by immunohistochemistry in kidney tubular cells of the renal cortex (Seiz et al., 2010)(and personal communication from Dr D. Vesey), and by ELISA in kidney tissue (Shaw and Diamandis, 2007) and urine (Obiezu et al., 2005; Shaw and Diamandis, 2007), in contrast, mRNA expression studies have not detected KLK4 transcript in kidney tissue

(Nelson et al., 1999; Harvey et al., 2000; Shaw and Diamandis, 2007). The significance of this is unknown but this situation is not unique to the kidney as KLK4 has also been detected by ELISA in several other tissues, including the liver and heart, while the mRNA transcript has not been detected (Shaw and Diamandis, 2007).

One possible reason for this anomaly in the kidney tissue may be that these epithelial cells in the kidney proximal tubule may not be the primary source of KLK4. Rather, the presence of KLK4 in these cells may be accounted for by their function in protein resorption from the ultrafiltrate through endocytosis (Christensen et al., 2012). This is a process, mediated by LRP2 and other cell-surface proteins, to clear significant amounts of protein from the tubular fluid to prevent toxic effects in distal regions of the nephron, and also to recycle proteins through lysosomal degradation and basolateral secretion of recovered amino acids (Christensen et al., 2012). Indeed, endocytosis of a number of proteins including proteases uPA and plasminogen, and also the sex hormone carrier protein SHBG are mediated by LRP2 (Christensen et al., 2012). It is possible that the immunohistochemical and ELISA analyses (Shaw and Diamandis, 2007; Seiz et al., 2010) detected endocytosed KLK4 in the kidney proximal tubule cells. Certainly, this possibility could be examined further using two approaches. First, examine whether kidney PTC endocytoses KLK4 by applying green fluorescent protein (GFP)-tagged KLK4 and monitoring uptake by fluorescence microscopy. Second, uptake can also be examined by subcellular fractionation followed by Western blot analysis to determine which cellular compartments KLK4 is directed to.

Regardless, KLK4 interaction with kidney PTC requires further examination for four reasons. First, to determine if alternate signalling pathways are activated by biased agonism of PAR2 by KLK4. Second, to determine if there is an alternative competitive substrate for KLK4 in this tissue. Third, to determine if cell-surface cofactors or binding partners facilitate KLK4 activation of PAR2. Finally, to clarify the origin of KLK4 in these cells.

6.5 The autocrine and paracrine HGF and PAR activation by KLK14 in prostate cancer

Homeostasis in the adult prostate is marked by minimal proliferation and low cell death, and this state appears largely due to separation of the epithelial compartment from the

stromal compartment cells through maintenance of prostate architecture (Cunha et al., 2006). Changes in local interactions between nascent epithelial cancer cells and the stromal compartment cells potentially occur through a breach of the basal lamina (Barron and Rowley, 2012). This change promotes a form of damage response by the stroma termed the reactive stroma. It is typified by peri-tumoural stromal cells with fibroblastic and myofibroblastic phenotypes (Figure 6.2), increased capillary density, and increased expression of repair-associated growth factors (Cunha et al., 2006; Barron and Rowley, 2012). While the precise mechanisms of stromal activation are not clearly understood, it begins at the earliest stages of PIN, evolves as cancer progresses and stimulates the epithelial cancer cells (Cunha et al., 2006; Barron and Rowley, 2012).

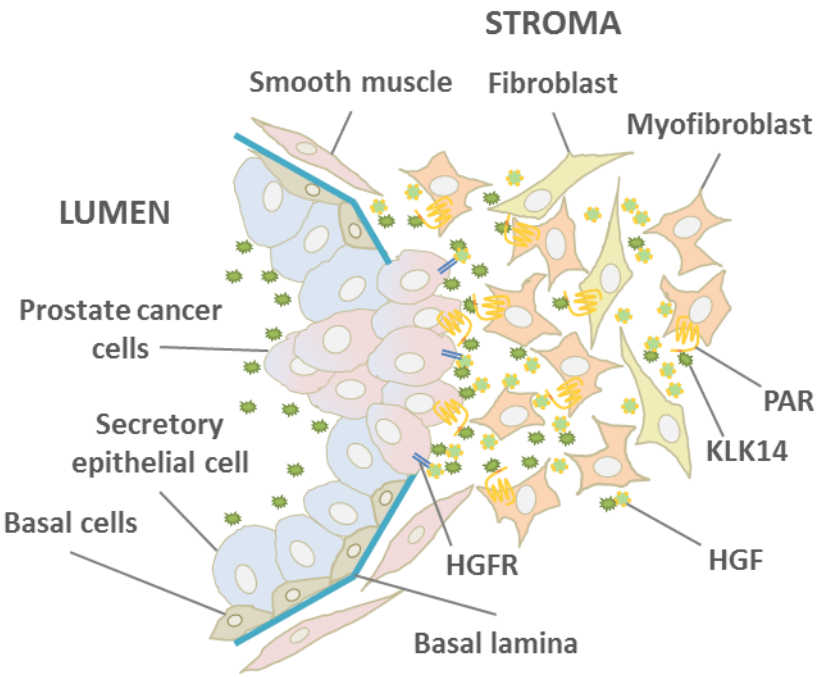

Figure 6.2 Interaction of epithelial cell-derived KLK14 with stromal cell-derived PARs and HGF in prostate cancer. As the basal lamina degrades and prostate cancer cells of epithelial origin lose cell polarity they secrete proteases into the stroma potentially including KLK14. KLK14 in turn may activate PARs on the surface of stromal myofibroblasts as well as on the cancer epithelial cells. KLK14 may also activate fibroblast- and myofibroblast-secreted HGF which in turn activates HGFR expressed by the epithelial cells. *Adapted from:* Barron and Rowley, 2012 and Kulasingam and Diamandis, 2008.

KLK14 may be a factor that participates in the cancer epithelial cell-reactive stroma cross-talk. The loss of normal prostate architecture and epithelial cell polarity in cancer may allow epithelial cell-secreted proteases such as KLK14 (Petraki et al., 2006; Rabien

et al., 2008) to enter the stromal compartment (Figure 6.2). In so doing, KLK14 may participate in a double paracrine loop through activation of smooth muscle- and myofibroblast-derived HGF (Humphrey et al., 1995; Nakashiro et al., 2003), and activated HGF in turn may stimulate the cancer epithelial cell-expressed HGFR (Nakashiro et al., 2000; Nakashiro et al., 2003) leading to the inherent mitogenic effects. Furthermore, there is potential for autocrine activation as both HGF and HGFR are expressed in some cancer foci (Nakashiro et al., 2003).

Similarly, KLK14 activation of PAR1 and PAR2 may have elements of autocrine and paracrine activation. In normal tissue these PARs are expressed by the prostate epithelial cells, with increased levels in primary cancer (Zhang et al., 2009; Mannowetz et al., 2010) which is opportune for activation by KLK14. Epithelial cell-derived KLK14 entering the stromal compartment may also activate PAR1, which has increased expression in the prostate cancer-associated myofibroblasts (Black et al., 2007; Zhang et al., 2009), and PAR2, which also has increased expression in stromal compartment cells (Mannowetz et al., 2010) (Figure 6.2).

6.6 KLK14 as a potential therapeutic target in prostate cancer

With aberrant expression in prostate cancer and association with aggressive disease (Yousef et al., 2003b; Borgono et al., 2007c; Rabien et al., 2008) KLK14 has potential to be a prognostic indicator for patients at higher risk of cancer recurrence after radical prostatectomy (Rabien et al., 2008). In addition, if endogenous KLK14 is differently N-glycosylated when expressed by prostate cancer cells it may also have clinical application in diagnosis of patients. For instance, KLK6 is differentially glycosylated when derived from ovarian cancer cells or the central nervous system (Kuzmanov et al., 2009). For this reason, serum level of this aberrantly glycosylated KLK has potential use as an early diagnosis biomarker for ovarian cancer.

In addition to the potential for KLK14 to be a diagnostic or prognostic marker, the association with aggressive disease suggests a significant role in prostate cancer. The results in this thesis suggest that the effects of KLK14 may be mediated by activation of HGF-HGFR signalling or degradation of inhibitors HAI-1A and HAI-1B. In clinical trials multi-target HGFR inhibitors have proven to be particularly effective against primary and metastatic tumours in patients with castration-resistant prostate cancer

(Gherardi et al., 2012). These inhibitors target the HGFR signalling pathway as well as associated pathways that may "rescue" signalling downstream of the primary HGFR inhibitor.

KLK14 may also mediate its effects in prostate cancer progression through activation of PAR1, PAR2 and PAR4. Similar to HGFR signalling, targeting PARs has therapeutic potential. Antagonists for PAR1, PAR2 and PAR4 have been developed, with development of PAR1 antagonists most advanced and some recent significant progress in PAR2 antagonists (Adams et al., 2011). However, the focus of the PAR1 antagonist clinical trials has been largely cardiovascular ailments.

An alternative approach is to target KLK14 with a selective protease inhibitor. For instance, as discussed earlier, the KLK4-selective inhibitor SFTI-FCQR was developed in our laboratory (Swedberg et al., 2009) and the results in this thesis show that it is an effective inhibitor of PAR2 activation by KLK4. SFTI-FCQR has potential as a cancer therapeutic as it was also recently shown to reverse KLK4-induced resistance in ovarian cancer cells to the chemotherapy drug paclitaxel (Dong et al., 2013). The precise mechanism of the reversal is unknown, it is likely that blocking KLK4 proteolytic activity with SFTI-FCQR prevented cleavage of a KLK4-specific substrate in the ovarian cancer cells as a similar, though lesser, effect was seen when the protease inhibitor aprotinin was used (Dong et al., 2013). While a KLK14-specific inhibitor has not been published yet, there have been preliminary developments in that area (Borgono et al., 2007c). If developed, it may also have clinical application when used in conjunction with multi-target HGFR inhibitors.

6.7 Summary

In summary, this thesis successfully identified novel proteolytic and cell-surface interactions between KLK4 and KLK14, and hepsin and TMPRSS2, as well as interactions between hepsin and TMPRSS2, and MMP3 and MMP9. These results provide a framework to further explore KLK4 and KLK14 activation of cell-surface proteins such as PARs in the context of cell-surface localization of these KLKs. The work in this thesis also proposes a novel method for KLK14 to promote prostate cancer progression through the activation of the mitogen HGF, and also through the degradation of a key inhibitor of HGF activating proteases, HAI-1. As HGFR signalling

is a key factor in progression of many types of cancer, this represents an interesting and exciting new avenue to examine the potential role of KLK14 in pathological processes.

References

Aalinkeel, R., B. B. Nair, J. L. Reynolds, D. E. Sykes, S. D. Mahajan, K. C. Chadha and S. A. Schwartz. 2011. "Overexpression of MMP-9 contributes to invasiveness of prostate cancer cell line LNCaP." *Immunol Invest* 40 (5): 447-64.

Abate-Shen, C. and M. M. Shen. 2000. "Molecular genetics of prostate cancer." *Genes Dev* 14 (19): 2410-34.

Abraham, G. N. and D. N. Podell. 1981. "Pyroglutamic acid. Non-metabolic formation, function in proteins and peptides, and characteristics of the enzymes effecting its removal." *Mol Cell Biochem* 38 Spec No (Pt 1): 181-90.

Adams, M. N., R. Ramachandran, M. K. Yau, J. Y. Suen, D. P. Fairlie, M. D. Hollenberg and J. D. Hooper. 2011. "Structure, function and pathophysiology of protease activated receptors." *Pharmacol Ther* 130 (3): 248-82.

Afar, D. E., I. Vivanco, R. S. Hubert, J. Kuo, E. Chen, D. C. Saffran, A. B. Raitano and A. Jakobovits. 2001. "Catalytic cleavage of the androgen-regulated TMPRSS2 protease results in its secretion by prostate and prostate cancer epithelia." *Cancer Res* 61 (4): 1686-92.

Affara, N. I., P. Andreu and L. M. Coussens. 2009. "Delineating protease functions during cancer development." *Methods Mol Biol* 539: 1-32.

AIHW&AACR. 2012. "Cancer in Australia: an overview 2012. ", edited by Australian Institute of Health and Welfare. Canberra.

Al-Ani, B. and M. D. Hollenberg. 2003. "Selective tryptic cleavage at the tethered ligand site of the amino terminal domain of proteinase-activated receptor-2 in intact cells." *J Pharmacol Exp Ther* 304 (3): 1120-8.

Altmann, F., E. Staudacher, I. B. Wilson and L. Marz. 1999. "Insect cells as hosts for the expression of recombinant glycoproteins." *Glycoconj J* 16 (2): 109-23.

Amour, A., M. Bird, L. Chaudry, J. Deadman, D. Hayes and C. Kay. 2004. "General considerations for proteolytic cascades." *Biochem Soc Trans* 32 (Pt 1): 15-6.

Andersen, D. C., T. Bridges, M. Gawlitzek and C. Hoy. 2000. "Multiple cell culture factors can affect the glycosylation of Asn-184 in CHO-produced tissue-type plasminogen activator." *Biotechnol Bioeng* 70 (1): 25-31.

Andrade-Gordon, P., B. E. Maryanoff, C. K. Derian, H. C. Zhang, M. F. Addo, A. L. Darrow, A. J. Eckardt, et al. 1999. "Design, synthesis, and biological characterization of a peptide-mimetic antagonist for a tethered-ligand receptor." *Proc Natl Acad Sci U S A* 96 (22): 12257-62.

Antalis, T. M., T. H. Bugge and Q. Wu. 2011. "Membrane-anchored serine proteases in health and disease." *Prog Mol Biol Transl Sci* 99: 1-50.

Apweiler, R., H. Hermjakob and N. Sharon. 1999. "On the frequency of protein glycosylation, as deduced from analysis of the SWISS-PROT database." *Biochim Biophys Acta* 1473 (1): 4-8.

Arachiche, A., M. M. Mumaw, M. de la Fuente and M. T. Nieman. 2013. "Protease-activated receptor 1 (PAR1) and PAR4 heterodimers are required for PAR1-enhanced cleavage of PAR4 by alpha-thrombin." *J Biol Chem* 288 (45): 32553-62.

Arnold, K., L. Bordoli, J. Kopp and T. Schwede. 2006. "The SWISS-MODEL workspace: a web-based environment for protein structure homology modelling." *Bioinformatics* 22 (2): 195-201.

Arora, P., T. K. Ricks and J. Trejo. 2007. "Protease-activated receptor signalling, endocytic sorting and dysregulation in cancer." *J Cell Sci* 120 (Pt 6): 921-8.

Aumuller, G. 1989. "Morphologic and regulatory aspects of prostatic function." *Anat Embryol (Berl)* 179 (6): 519-31.

Avgeris, M., K. Mavridis and A. Scorilas. 2012. "Kallikrein-related peptidases in prostate, breast, and ovarian cancers: from pathobiology to clinical relevance." *Biol Chem* 393 (5): 301-17.

Bacac, M., P. Provero, N. Mayran, J. C. Stehle, C. Fusco and I. Stamenkovic. 2006. "A mouse stromal response to tumor invasion predicts prostate and breast cancer patient survival." *PLoS One* 1: e32.

Bae, J. S., L. Yang and A. R. Rezaie. 2007. "Receptors of the protein C activation and activated protein C signaling pathways are colocalized in lipid rafts of endothelial cells." *Proc Natl Acad Sci U S A* 104 (8): 2867-72.

Bah, A., Z. Chen, L. A. Bush-Pelc, F. S. Mathews and E. Di Cera. 2007. "Crystal structures of murine thrombin in complex with the extracellular fragments of murine protease-activated receptors PAR3 and PAR4." *Proc Natl Acad Sci U S A* 104 (28): 11603-8.

Banacky, P. and B. Linder. 1981. "Model of serine proteases charge relay system -- PCILO study." *Biophys Chem* 13 (3): 223-31.

Barron, D. A. and D. R. Rowley. 2012. "The reactive stroma microenvironment and prostate cancer progression." *Endocr Relat Cancer* 19 (6): R187-204.

Bause, E. and G. Legler. 1981. "The role of the hydroxy amino acid in the triplet sequence Asn-Xaa-Thr(Ser) for the N-glycosylation step during glycoprotein biosynthesis." *Biochem J* 195 (3): 639-44.

Beaufort, N., M. Debela, S. Creutzburg, J. Kellermann, W. Bode, M. Schmitt, D. Pidard and V. Magdolen. 2006. "Interplay of human tissue kallikrein 4 (hK4) with the plasminogen activation system: hK4 regulates the structure and functions of the urokinase-type plasminogen activator receptor (uPAR)." *Biol Chem* 387 (2): 217-22.

Beaufort, N., K. Plaza, D. Utzschneider, A. Schwarz, J. M. Burkhart, S. Creutzburg, M. Debela, M. Schmitt, C. Ries and V. Magdolen. 2010. "Interdependence of kallikrein-related peptidases in proteolytic networks." *Biol Chem* 391 (5): 581-7.

Beck, A., M. C. Bussat, C. Klinguer-Hamour, L. Goetsch, J. P. Aubry, T. Champion, E. Julien, J. F. Haeuw, J. Y. Bonnefoy and N. Corvaia. 2001. "Stability and CTL activity of N-terminal glutamic acid containing peptides." *J Pept Res* 57 (6): 528-38.

Beliveau, F., A. Desilets and R. Leduc. 2009. "Probing the substrate specificities of matriptase, matriptase-2, hepsin and DESC1 with internally quenched fluorescent peptides." *Febs J* 276 (8): 2213-26.

Ben-Dor, S., N. Esterman, E. Rubin and N. Sharon. 2004. "Biases and complex patterns in the residues flanking protein N-glycosylation sites." *Glycobiology* 14 (2): 95-101.

Benaud, C., R. B. Dickson and C. Y. Lin. 2001. "Regulation of the activity of matriptase on epithelial cell surfaces by a blood-derived factor." *Eur J Biochem* 268 (5): 1439-47.

Benaud, C., M. Oberst, J. P. Hobson, S. Spiegel, R. B. Dickson and C. Y. Lin. 2002. "Sphingosine 1-phosphate, present in serum-derived lipoproteins, activates matriptase." *J Biol Chem* 277 (12): 10539-46.

Bertram, S., I. Glowacka, P. Blazejewska, E. Soilleux, P. Allen, S. Danisch, I. Steffen, et al. 2010. "TMPRSS2 and TMPRSS4 facilitate trypsin-independent spread of influenza virus in Caco-2 cells." *J Virol* 84 (19): 10016-25.

Bertram, S., A. Heurich, H. Lavender, S. Gierer, S. Danisch, P. Perin, J. M. Lucas, P. S. Nelson, S. Pohlmann and E. J. Soilleux. 2012. "Influenza and SARS-coronavirus activating proteases TMPRSS2 and HAT are expressed at multiple sites in human respiratory and gastrointestinal tracts." *PLoS One* 7 (4): e35876.

Bhatt, A. S., A. Welm, C. J. Farady, M. Vasquez, K. Wilson and C. S. Craik. 2007. "Coordinate expression and functional profiling identify an extracellular proteolytic signaling pathway." *Proc Natl Acad Sci U S A* 104 (14): 5771-6.

Bjorklund, M., P. Heikkila and E. Koivunen. 2004. "Peptide inhibition of catalytic and noncatalytic activities of matrix metalloproteinase-9 blocks tumor cell migration and invasion." *J Biol Chem* 279 (28): 29589-97.

Black, P. C., G. J. Mize, P. Karlin, D. L. Greenberg, S. J. Hawley, L. D. True, R. L. Vessella and T. K. Takayama. 2007. "Overexpression of protease-activated receptors-1,-2, and-4 (PAR-1, -2, and -4) in prostate cancer." *Prostate* 67 (7): 743-56.

Blackhart, B. D., K. Emilsson, D. Nguyen, W. Teng, A. J. Martelli, S. Nystedt, J. Sundelin and R. M. Scarborough. 1996. "Ligand cross-reactivity within the protease-activated receptor family." *J Biol Chem* 271 (28): 16466-71.

Blomback, B. 1967. "Derivatives of glutamine in peptides". In *Methods in Enzymology*, edited by C. H. W. Hirs.

Bocheva, G., A. Rattenholl, C. Kempkes, T. Goerge, C. Y. Lin, M. R. D'Andrea, S. Stander and M. Steinhoff. 2009. "Role of matriptase and proteinase-activated receptor-2 in nonmelanoma skin cancer." *J Invest Dermatol* 129 (7): 1816-23.

Bode, W., F. X. Gomis-Ruth and W. Stockler. 1993. "Astacins, serralysins, snake venom and matrix metalloproteinases exhibit identical zinc-binding environments (HEXXHXXGXXH and Met-turn) and topologies and should be grouped into a common family, the 'metzincins'." *FEBS Lett* 331 (1-2): 134-40.

Bodey, B., B. Bodey, Jr., S. E. Siegel and H. E. Kaiser. 2001. "Immunocytochemical detection of matrix metalloproteinase expression in prostate cancer." *In Vivo* 15 (1): 65-70.

Bohm, S. K., L. M. Khitin, E. F. Grady, G. Aponte, D. G. Payan and N. W. Bunnett. 1996a. "Mechanisms of desensitization and resensitization of proteinase-activated receptor-2." *J Biol Chem* 271 (36): 22003-16.

Bohm, S. K., W. Kong, D. Bromme, S. P. Smeekens, D. C. Anderson, A. Connolly, M. Kahn, et al. 1996b. "Molecular cloning, expression and potential functions of the human proteinase-activated receptor-2." *Biochem J* 314 (Pt 3): 1009-16.

Boire, A., L. Covic, A. Agarwal, S. Jacques, S. Sherifi and A. Kuliopulos. 2005. "PAR1 is a matrix metalloprotease-1 receptor that promotes invasion and tumorigenesis of breast cancer cells." *Cell* 120 (3): 303-13.

Borgono, C. A. and E. P. Diamandis. 2004. "The emerging roles of human tissue kallikreins in cancer." *Nat Rev Cancer* 4 (11): 876-90.

Borgono, C. A., J. A. Gavigan, J. Alves, B. Bowles, J. L. Harris, G. Sotiropoulou and E. P. Diamandis. 2007a. "Defining the extended substrate specificity of kallikrein 1-related peptidases." *Biol Chem* 388 (11): 1215-25.

Borgono, C. A., L. Grass, A. Soosaipillai, G. M. Yousef, C. D. Petraki, D. H. Howarth, S. Fracchioli, D. Katsaros and E. P. Diamandis. 2003. "Human kallikrein 14: a new potential biomarker for ovarian and breast cancer." *Cancer Res* 63 (24): 9032-41.

Borgono, C. A., I. P. Michael, N. Komatsu, A. Jayakumar, R. Kapadia, G. L. Clayman, G. Sotiropoulou and E. P. Diamandis. 2007b. "A potential role for multiple tissue kallikrein serine proteases in epidermal desquamation." *J Biol Chem* 282 (6): 3640-52.

Borgono, C. A., I. P. Michael, J. L. Shaw, L. Y. Luo, M. C. Ghosh, A. Soosaipillai, L. Grass, D. Katsaros and E. P. Diamandis. 2007c. "Expression and functional characterization of the cancer-related serine protease, human tissue kallikrein 14." *J Biol Chem* 282 (4): 2405-22.

Borisov, O. V., M. Field, V. T. Ling and R. J. Harris. 2009. "Characterization of oligosaccharides in recombinant tissue plasminogen activator produced in Chinese hamster ovary cells: two decades of analytical technology development." *Anal Chem* 81 (23): 9744-54.

Bottaro, D. P., J. S. Rubin, D. L. Faletto, A. M. Chan, T. E. Kmiecik, G. F. Vande Woude and S. A. Aaronson. 1991. "Identification of the hepatocyte growth factor receptor as the c-met proto-oncogene product." *Science* 251 (4995): 802-4.

Bottcher-Friebertshauser, E., C. Freuer, F. Sielaff, S. Schmidt, M. Eickmann, J. Uhlendorff, T. Steinmetzer, H. D. Klenk and W. Garten. 2010. "Cleavage of influenza virus hemagglutinin by airway proteases TMPRSS2 and HAT differs in subcellular localization and susceptibility to protease inhibitors." *J Virol* 84 (11): 5605-14.

Bottcher, E., T. Matrosovich, M. Beyerle, H. D. Klenk, W. Garten and M. Matrosovich. 2006. "Proteolytic activation of influenza viruses by serine proteases TMPRSS2 and HAT from human airway epithelium." *J Virol* 80 (19): 9896-8.

Boyd, L. K., X. Mao and Y. J. Lu. 2012. "The complexity of prostate cancer: genomic alterations and heterogeneity." *Nat Rev Urol* 9 (11): 652-64.

Brattsand, M. and T. Egelrud. 1999. "Purification, molecular cloning, and expression of a human stratum corneum trypsin-like serine protease with possible function in desquamation." *J Biol Chem* 274 (42): 30033-40.

Brattsand, M., K. Stefansson, C. Lundh, Y. Haasum and T. Egelrud. 2005. "A proteolytic cascade of kallikreins in the stratum corneum." *J Invest Dermatol* 124 (1): 198-203.

Brillard-Bourdet, M., T. Moreau and F. Gauthier. 1995. "Substrate specificity of tissue kallikreins: importance of an extended interaction site." *Biochim Biophys Acta* 1246 (1): 47-52.

Brondyk, W. H. 2009. "Selecting an appropriate method for expressing a recombinant protein." *Methods Enzymol* 463: 131-47.

Brown, T. A., T. M. Yang, T. Zaitsevskaia, Y. Xia, C. A. Dunn, R. O. Sigle, B. Knudsen and W. G. Carter. 2004. "Adhesion or plasmin regulates tyrosine phosphorylation of a novel membrane glycoprotein p80/gp140/CUB domain-containing protein 1 in epithelia." *J Biol Chem* 279 (15): 14772-83.

Bruni-Cardoso, A., L. C. Johnson, R. L. Vessella, T. E. Peterson and C. C. Lynch. 2010. "Osteoclast-derived matrix metalloproteinase-9 directly affects angiogenesis in the prostate tumor-bone microenvironment." *Mol Cancer Res* 8 (4): 459-70.

Bugge, T. H., T. M. Antalis and Q. Wu. 2009. "Type II transmembrane serine proteases." *J Biol Chem* 284 (35): 23177-81.

Buzza, M. S., E. W. Martin, K. H. Driesbaugh, A. Desilets, R. Leduc and T. M. Antalis. 2013. "Prostasin is required for matriptase activation in intestinal epithelial cells to regulate closure of the paracellular pathway." *J Biol Chem*.

Buzza, M. S., S. Netzel-Arnett, T. Shea-Donohue, A. Zhao, C. Y. Lin, K. List, R. Szabo, A. Fasano, T. H. Bugge and T. M. Antalis. 2010. "Membrane-anchored serine protease matriptase regulates epithelial barrier formation and permeability in the intestine." *Proc Natl Acad Sci U S A* 107 (9): 4200-5.

Camerer, E., A. Barker, D. N. Duong, R. Ganesan, H. Kataoka, I. Cornelissen, M. R. Darragh, et al. 2010. "Local protease signaling contributes to neural tube closure in the mouse embryo." *Dev Cell* 18 (1): 25-38.

Camerer, E., W. Huang and S. R. Coughlin. 2000. "Tissue factor- and factor X-dependent activation of protease-activated receptor 2 by factor VIIa." *Proc Natl Acad Sci U S A* 97 (10): 5255-60.

Camerer, E., H. Kataoka, M. Kahn, K. Lease and S. R. Coughlin. 2002. "Genetic evidence that protease-activated receptors mediate factor Xa signaling in endothelial cells." *J Biol Chem* 277 (18): 16081-7.

Casar, B., Y. He, M. Iconomou, J. D. Hooper, J. P. Quigley and E. I. Deryugina. 2012a. "Blocking of CDCP1 cleavage in vivo prevents Akt-dependent survival and inhibits metastatic colonization through PARP1-mediated apoptosis of cancer cells." *Oncogene* 31 (35): 3924-38.

Casar, B., I. Rimann, H. Kato, S. J. Shattil, J. P. Quigley and E. I. Deryugina. 2012b. "In vivo cleaved CDCP1 promotes early tumor dissemination via complexing with activated beta1 integrin and induction of FAK/PI3K/Akt motility signaling." *Oncogene*.

Castellino, F. J. and V. A. Ploplis. 2005. "Structure and function of the plasminogen/plasmin system." *Thromb Haemost* 93 (4): 647-54.

Cattley, S. and J. W. Arthur. 2007. "BioManager: the use of a bioinformatics web application as a teaching tool in undergraduate bioinformatics training." *Brief Bioinform* 8 (6): 457-65.

Caubet, C., N. Jonca, M. Brattsand, M. Guerrin, D. Bernard, R. Schmidt, T. Egelrud, M. Simon and G. Serre. 2004. "Degradation of corneodesmosome proteins by two serine proteases of the kallikrein family, SCTE/KLK5/hK5 and SCCE/KLK7/hK7." *J Invest Dermatol* 122 (5): 1235-44.

Chaipan, C., D. Kobasa, S. Bertram, I. Glowacka, I. Steffen, T. S. Tsegaye, M. Takeda, et al. 2009. "Proteolytic activation of the 1918 influenza virus hemagglutinin." *J Virol* 83 (7): 3200-11.

Chay, C. H., C. R. Cooper, J. D. Gendernalik, S. M. Dhanasekaran, A. M. Chinnaiyan, M. A. Rubin, A. H. Schmaier and K. J. Pienta. 2002. "A functional thrombin receptor (PAR1) is expressed on bone-derived prostate cancer cell lines." *Urology* 60 (5): 760-5.

Chelius, D., K. Jing, A. Lueras, D. S. Rehder, T. M. Dillon, A. Vizel, R. S. Rajan, T. Li, M. J. Treuheit and P. V. Bondarenko. 2006. "Formation of pyroglutamic acid from N-terminal glutamic acid in immunoglobulin gamma antibodies." *Anal Chem* 78 (7): 2370-6.

Chen, C. H., M. M. Paing and J. Trejo. 2004. "Termination of protease-activated receptor-1 signaling by beta-arrestins is independent of receptor phosphorylation." *J Biol Chem* 279 (11): 10020-31.

Chen, C. H., K. Y. Su, M. H. Tao, S. W. Lin, Y. H. Su, Y. C. Tsai, K. C. Cheng, Y. M. Jeng and J. C. Sheu. 2006. "Decreased expressions of hepsin in human hepatocellular carcinomas." *Liver Int* 26 (7): 774-80.

Chen, J., M. Ishii, L. Wang, K. Ishii and S. R. Coughlin. 1994. "Thrombin receptor activation. Confirmation of the intramolecular tethered liganding hypothesis and discovery of an alternative intermolecular liganding mode." *J Biol Chem* 269 (23): 16041-5.

Chen, M., L. M. Chen, C. Y. Lin and K. X. Chai. 2010a. "Hepsin activates prostasin and cleaves the extracellular domain of the epidermal growth factor receptor." *Mol Cell Biochem* 337 (1-2): 259-66.

Chen, Y. W., M. S. Lee, A. Lucht, F. P. Chou, W. Huang, T. C. Havighurst, K. Kim, et al. 2010b. "TMPRSS2, a serine protease expressed in the prostate on the apical surface of luminal epithelial cells and released into semen in prostasomes, is misregulated in prostate cancer cells." *Am J Pathol* 176 (6): 2986-96.

Chen, Z., Z. Fan, J. E. McNeal, R. Nolley, M. C. Caldwell, M. Mahadevappa, Z. Zhang, J. A. Warrington and T. A. Stamey. 2003. "Hepsin and maspin are inversely expressed in laser capture microdissectioned prostate cancer." *J Urol* 169 (4): 1316-9.

Cheng, H., T. Fukushima, N. Takahashi, H. Tanaka and H. Kataoka. 2009. "Hepatocyte growth factor activator inhibitor type 1 regulates epithelial to mesenchymal transition through membrane-bound serine proteinases." *Cancer Res* 69 (5): 1828-35.

Chi, Y. H., Y. D. Koo, S. Y. Dai, J. E. Ahn, D. J. Yun, S. Y. Lee and K. Zhu-Salzman. 2010. "N-glycosylation at non-canonical Asn-X-Cys sequence of an insect recombinant cathepsin B-like counter-defense protein." *Comp Biochem Physiol B Biochem Mol Biol* 156 (1): 40-7.

Christensen, E. I., H. Birn, T. Storm, K. Weyer and R. Nielsen. 2012. "Endocytic receptors in the renal proximal tubule." *Physiology (Bethesda)* 27 (4): 223-36.

Christofori, G. 2006. "New signals from the invasive front." *Nature* 441 (7092): 444-50.

Chung, H., M. Hamza, K. Oikonomopoulou, V. Gratio, M. Saifeddine, G. D. Virca, E. P. Diamandis, M. D. Hollenberg and D. Darmoul. 2012. "Kallikrein-related peptidase signaling in colon carcinoma cells: targeting proteinase-activated receptors." *Biol Chem* 393 (5): 413-20.

Clements, J. A., J. D. Hooper and Y. Dong. 2013. "The human tissue kallikrein and kallikrein-related peptidase family." In *Handbook of proteolytic enzymes,* edited by N. D. Rawlings and G. Salvesen. Amsterdam: Elsevier.

Clements, J., J. Hooper, Y. Dong and T. Harvey. 2001. "The expanded human kallikrein (KLK) gene family: genomic organisation, tissue-specific expression and potential functions." *Biol Chem* 382 (1): 5-14.

Corvera, C. U., O. Dery, K. McConalogue, S. K. Bohm, L. M. Khitin, G. H. Caughey, D. G. Payan and N. W. Bunnett. 1997. "Mast cell tryptase regulates rat colonic myocytes through proteinase-activated receptor 2." *J Clin Invest* 100 (6): 1383-93.

Costello, L. C., P. Feng, B. Milon, M. Tan and R. B. Franklin. 2004. "Role of zinc in the pathogenesis and treatment of prostate cancer: critical issues to resolve." *Prostate Cancer Prostatic Dis* 7 (2): 111-7.

Costello, L. C. and R. B. Franklin. 1998. "Novel role of zinc in the regulation of prostate citrate metabolism and its implications in prostate cancer." *Prostate* 35 (4): 285-96.

Cottrell, G. S., S. Amadesi, E. F. Grady and N. W. Bunnett. 2004. "Trypsin IV, a novel agonist of protease-activated receptors 2 and 4." *J Biol Chem* 279 (14): 13532-9.

Coughlin, S. R. 2005. "Protease-activated receptors in hemostasis, thrombosis and vascular biology." *J Thromb Haemost* 3 (8): 1800-14.

Cunha, A. C., B. Weigle, A. Kiessling, M. Bachmann and E. P. Rieber. 2006. "Tissue-specificity of prostate specific antigens: comparative analysis of transcript levels in prostate and non-prostatic tissues." *Cancer Lett* 236 (2): 229-38.

Cunningham, M. R., K. A. McIntosh, J. D. Pediani, J. Robben, A. E. Cooke, M. Nilsson, G. W. Gould, S. Mundell, G. Milligan and R. Plevin. 2012. "Novel role for proteinase-activated receptor 2 (PAR2) in membrane trafficking of proteinase-activated receptor 4 (PAR4)." *J Biol Chem* 287 (20): 16656-69.

D'Andrea, M. R., C. K. Derian, D. Leturcq, S. M. Baker, A. Brunmark, P. Ling, A. L. Darrow, R. J. Santulli, L. F. Brass and P. Andrade-Gordon. 1998. "Characterization of protease-activated receptor-2 immunoreactivity in normal human tissues." *J Histochem Cytochem* 46 (2): 157-64.

D'Andrea, M. R., C. K. Derian, R. J. Santulli and P. Andrade-Gordon. 2001. "Differential expression of protease-activated receptors-1 and -2 in stromal fibroblasts of normal, benign, and malignant human tissues." *Am J Pathol* 158 (6): 2031-41.

Darmoul, D., V. Gratio, H. Devaud and M. Laburthe. 2004a. "Protease-activated receptor 2 in colon cancer: trypsin-induced MAPK phosphorylation and cell proliferation are mediated by epidermal growth factor receptor transactivation." *J Biol Chem* 279 (20): 20927-34.

Darmoul, D., V. Gratio, H. Devaud, T. Lehy and M. Laburthe. 2003. "Aberrant expression and activation of the thrombin receptor protease-activated receptor-1 induces cell proliferation and motility in human colon cancer cells." *Am J Pathol* 162 (5): 1503-13.

Darmoul, D., V. Gratio, H. Devaud, F. Peiretti and M. Laburthe. 2004b. "Activation of proteinase-activated receptor 1 promotes human colon cancer cell proliferation through epidermal growth factor receptor transactivation." *Mol Cancer Res* 2 (9): 514-22.

Darmoul, D., J. C. Marie, H. Devaud, V. Gratio and M. Laburthe. 2001. "Initiation of human colon cancer cell proliferation by trypsin acting at protease-activated receptor-2." *Br J Cancer* 85 (5): 772-9.

Darrow, A. L., W. P. Fung-Leung, R. D. Ye, R. J. Santulli, W. M. Cheung, C. K. Derian, C. L. Burns, et al. 1996. "Biological consequences of thrombin receptor deficiency in mice." *Thromb Haemost* 76 (6): 860-6.

Day, C. H., G. R. Fanger, M. W. Retter, B. L. Hylander, R. B. Penetrante, R. L. Houghton, X. Zhang, et al. 2002. "Characterization of KLK4 expression and detection of KLK4-specific antibody in prostate cancer patient sera." *Oncogene* 21 (46): 7114-20.

de Garavilla, L., N. Vergnolle, S. H. Young, H. Ennes, M. Steinhoff, V. S. Ossovskaya, M. R. D'Andrea, et al. 2001. "Agonists of proteinase-activated receptor 1 induce plasma extravasation by a neurogenic mechanism." *Br J Pharmacol* 133 (7): 975-87.

de Veer, S. J., J. E. Swedberg, E. A. Parker and J. M. Harris. 2011. "Non-combinatorial library screening reveals subsite cooperativity and identifies new high efficiency substrates for kallikrein-related peptidase 14." *Biol Chem*.

Debela, M., N. Beaufort, V. Magdolen, N. M. Schechter, C. S. Craik, M. Schmitt, W. Bode and P. Goettig. 2008. "Structures and specificity of the human kallikrein-related peptidases KLK 4, 5, 6, and 7." *Biol Chem* 389 (6): 623-32.

Debela, M., P. Goettig, V. Magdolen, R. Huber, N. M. Schechter and W. Bode. 2007a. "Structural basis of the zinc inhibition of human tissue kallikrein 5." *J Mol Biol* 373 (4): 1017-31.

Debela, M., P. Hess, V. Magdolen, N. M. Schechter, T. Steiner, R. Huber, W. Bode and P. Goettig. 2007b. "Chymotryptic specificity determinants in the 1.0 A structure of the zinc-inhibited human tissue kallikrein 7." *Proc Natl Acad Sci U S A* 104 (41): 16086-91.

Debela, M., V. Magdolen, V. Grimminger, C. Sommerhoff, A. Messerschmidt, R. Huber, R. Friedrich, W. Bode and P. Goettig. 2006a. "Crystal structures of human tissue kallikrein 4: activity modulation by a specific zinc binding site." *J Mol Biol* 362 (5): 1094-107.

Debela, M., V. Magdolen, N. Schechter, M. Valachova, F. Lottspeich, C. S. Craik, Y. Choe, W. Bode and P. Goettig. 2006b. "Specificity profiling of seven human tissue kallikreins reveals individual subsite preferences." *J Biol Chem* 281 (35): 25678-88.

Defea, K. 2008. "Beta-arrestins and heterotrimeric G-proteins: collaborators and competitors in signal transduction." *Br J Pharmacol* 153 Suppl 1: S298-309.

DeFea, K. A., J. Zalevsky, M. S. Thoma, O. Dery, R. D. Mullins and N. W. Bunnett. 2000. "beta-arrestin-dependent endocytosis of proteinase-activated receptor 2 is required for intracellular targeting of activated ERK1/2." *J Cell Biol* 148 (6): 1267-81.

Denda, K., T. Shimomura, T. Kawaguchi, K. Miyazawa and N. Kitamura. 2002. "Functional characterization of Kunitz domains in hepatocyte growth factor activator inhibitor type 1." *J Biol Chem* 277 (16): 14053-9.

Denmeade, S. R., J. Lovgren, S. R. Khan, H. Lilja and J. T. Isaacs. 2001. "Activation of latent protease function of pro-hK2, but not pro-PSA, involves autoprocessing." *Prostate* 48 (2): 122-6.

Deraison, C., C. Bonnart, F. Lopez, C. Besson, R. Robinson, A. Jayakumar, F. Wagberg, et al. 2007. "LEKTI fragments specifically inhibit KLK5, KLK7, and KLK14 and control desquamation through a pH-dependent interaction." *Mol Biol Cell* 18 (9): 3607-19.

Dery, O., M. S. Thoma, H. Wong, E. F. Grady and N. W. Bunnett. 1999. "Trafficking of proteinase-activated receptor-2 and beta-arrestin-1 tagged with green fluorescent protein. beta-Arrestin-dependent endocytosis of a proteinase receptor." *J Biol Chem* 274 (26): 18524-35.

Deryugina, E. I. and J. P. Quigley. 2006. "Matrix metalloproteinases and tumor metastasis." *Cancer Metastasis Rev* 25 (1): 9-34.

Deryugina, E. I. and J. P. Quigley. 2010. "Pleiotropic roles of matrix metalloproteinases in tumor angiogenesis: contrasting, overlapping and compensatory functions." *Biochim Biophys Acta* 1803 (1): 103-20.

Deryugina, E. I. and J. P. Quigley. 2012. "Cell surface remodeling by plasmin: a new function for an old enzyme." *J Biomed Biotechnol* 2012: 564259.

Desai, B., T. Ma, J. Zhu and M. A. Chellaiah. 2009. "Characterization of the expression of variant and standard CD44 in prostate cancer cells: identification of the possible molecular mechanism of CD44/MMP9 complex formation on the cell surface." *J Cell Biochem* 108 (1): 272-84.

Desilets, A., F. Beliveau, G. Vandal, F. O. McDuff, P. Lavigne and R. Leduc. 2008. "Mutation G827R in matriptase causing autosomal recessive ichthyosis with hypotrichosis yields an inactive protease." *J Biol Chem* 283 (16): 10535-42.

Desrivieres, S., H. Lu, N. Peyri, C. Soria, Y. Legrand and S. Menashi. 1993. "Activation of the 92 kDa type IV collagenase by tissue kallikrein." *J Cell Physiol* 157 (3): 587-93.

Dhanasekaran, S. M., T. R. Barrette, D. Ghosh, R. Shah, S. Varambally, K. Kurachi, K. J. Pienta, M. A. Rubin and A. M. Chinnaiyan. 2001. "Delineation of prognostic biomarkers in prostate cancer." *Nature* 412 (6849): 822-6.

Djakiew, D., B. Pflug, R. Delsite, J. H. Lynch and M. Onoda. 1992. "Density dependent polarized secretion of a prostatic epithelial cell line." *Prostate* 20 (1): 15-27.

Domoto, T., T. Takino, L. Guo and H. Sato. 2012. "Cleavage of hepatocyte growth factor activator inhibitor-1 by membrane-type MMP-1 activates matriptase." *Cancer Sci* 103 (3): 448-54.

Donaldson, S. H., A. Hirsh, D. C. Li, G. Holloway, J. Chao, R. C. Boucher and S. E. Gabriel. 2002. "Regulation of the epithelial sodium channel by serine proteases in human airways." *J Biol Chem* 277 (10): 8338-45.

Donate, L. E., E. Gherardi, N. Srinivasan, R. Sowdhamini, S. Aparicio and T. L. Blundell. 1994. "Molecular evolution and domain structure of plasminogen-related growth factors (HGF/SF and HGF1/MSP)." *Protein Sci* 3 (12): 2378-94.

Dong, Y., L. T. Bui, D. M. Odorico, O. L. Tan, S. A. Myers, H. Samaratunga, R. A. Gardiner and J. A. Clements. 2005. "Compartmentalized expression of kallikrein 4 (KLK4/hK4) isoforms in prostate cancer: nuclear, cytoplasmic and secreted forms." *Endocr Relat Cancer* 12 (4): 875-89.

Dong, Y., C. Stephens, C. Walpole, J. E. Swedberg, G. M. Boyle, P. G. Parsons, M. A. McGuckin, J. M. Harris and J. A. Clements. 2013. "Paclitaxel resistance and multicellular spheroid formation are induced by kallikrein-related peptidase 4 in serous ovarian cancer cells in an ascites mimicking microenvironment." *PLoS One* 8 (2): e57056.

Dulon, S., C. Cande, N. W. Bunnett, M. D. Hollenberg, M. Chignard and D. Pidard. 2003. "Proteinase-activated receptor-2 and human lung epithelial cells: disarming by neutrophil serine proteinases." *Am J Respir Cell Mol Biol* 28 (3): 339-46.

Duncan, R. C., L. C. Wijeyewickrema and R. N. Pike. 2008. "The initiating proteases of the complement system: controlling the cleavage." *Biochimie* 90 (2): 387-95.

DuPont, B. R., C. C. Hu, X. Reveles and J. P. Simmer. 1999. "Assignment of serine protease 17 (PRSS17) to human chromosome bands 19q13.3-->q13.4 by in situ hybridization." *Cytogenet Cell Genet* 86 (3-4): 212-3.

Edlund, M., S. Y. Sung and L. W. Chung. 2004. "Modulation of prostate cancer growth in bone microenvironments." *J Cell Biochem* 91 (4): 686-705.

Egeblad, M. and Z. Werb. 2002. "New functions for the matrix metalloproteinases in cancer progression." *Nat Rev Cancer* 2 (3): 161-74.

Egelrud, T. 1993. "Purification and preliminary characterization of stratum corneum chymotryptic enzyme: a proteinase that may be involved in desquamation." *J Invest Dermatol* 101 (2): 200-4.

Eisen, A. Z., S. K. Sarkar, K. C. Neuman and G. I. Goldberg. 2013. "Matrix metalloproteinase 9/Gelatinase B." In *Handbook of proteolytic enzymes,* edited by N. D. Rawlings and G. Salvesen. Amsterdam: Elsevier.

Eisenthal, R., M. J. Danson and D. W. Hough. 2007. "Catalytic efficiency and kcat/KM: a useful comparator?" *Trends Biotechnol* 25 (6): 247-9.

Eissa, A., V. Amodeo, C. R. Smith and E. P. Diamandis. 2011. "Kallikrein-related peptidase-8 (KLK8) is an active serine protease in human epidermis and sweat and is involved in a skin barrier proteolytic cascade." *J Biol Chem* 286 (1): 687-706.

Ekholm, I. E., M. Brattsand and T. Egelrud. 2000. "Stratum corneum tryptic enzyme in normal epidermis: a missing link in the desquamation process?" *J Invest Dermatol* 114: 56-63.

Emami, N., D. Deperthes, J. Malm and E. P. Diamandis. 2008. "Major role of human KLK14 in seminal clot liquefaction." *J Biol Chem* 283 (28): 19561-9.

Emami, N. and E. P. Diamandis. 2008. "Human kallikrein-related peptidase 14 (KLK14) is a new activator component of the KLK proteolytic cascade. Possible function in seminal plasma and skin." *J Biol Chem* 283 (6): 3031-41.

Emami, N., A. Scorilas, A. Soosaipillai, T. Earle, B. Mullen and E. P. Diamandis. 2009. "Association between kallikrein-related peptidases (KLKs) and macroscopic indicators of semen analysis: their relation to sperm motility." *Biol Chem* 390 (9): 921-9.

Ernst, T., M. Hergenhahn, M. Kenzelmann, C. D. Cohen, M. Bonrouhi, A. Weninger, R. Klaren, et al. 2002. "Decrease and gain of gene expression are equally discriminatory markers for prostate carcinoma: a gene expression analysis on total and microdissected prostate tissue." *Am J Pathol* 160 (6): 2169-80.

Escaff, S., J. M. Fernandez, L. O. Gonzalez, A. Suarez, S. Gonzalez-Reyes, J. M. Gonzalez and F. J. Vizoso. 2010. "Study of matrix metalloproteinases and their inhibitors in prostate cancer." *Br J Cancer* 102 (5): 922-9.

Escaff, S., J. M. Fernandez, L. O. Gonzalez, A. Suarez, S. Gonzalez-Reyes, J. M. Gonzalez and F. J. Vizoso. 2011a. "Collagenase-3 expression by tumor cells and gelatinase B expression by stromal fibroblast-like cells are associated with biochemical recurrence after radical prostatectomy in patients with prostate cancer." *World J Urol* 29 (5): 657-63.

Escaff, S., J. M. Fernandez, L. O. Gonzalez, A. Suarez, S. Gonzalez-Reyes, J. M. Gonzalez and F. J. Vizoso. 2011b. "Comparative study of stromal metalloproteases expression in patients with benign hyperplasia and prostate cancer." *J Cancer Res Clin Oncol* 137 (3): 551-5.

Even-Ram, S., B. Uziely, P. Cohen, S. Grisaru-Granovsky, M. Maoz, Y. Ginzburg, R. Reich, I. Vlodavsky and R. Bar-Shavit. 1998. "Thrombin receptor overexpression in malignant and physiological invasion processes." *Nat Med* 4 (8): 909-14.

Fan, B., J. Brennan, D. Grant, F. Peale, L. Rangell and D. Kirchhofer. 2007. "Hepatocyte growth factor activator inhibitor-1 (HAI-1) is essential for the integrity of basement membranes in the developing placental labyrinth." *Dev Biol* 303 (1): 222-30.

Fan, B., T. D. Wu, W. Li and D. Kirchhofer. 2005. "Identification of hepatocyte growth factor activator inhibitor-1B as a potential physiological inhibitor of prostasin." *J Biol Chem* 280 (41): 34513-20.

Fanjul-Fernandez, M., A. R. Folgueras, S. Cabrera and C. Lopez-Otin. 2010. "Matrix metalloproteinases: evolution, gene regulation and functional analysis in mouse models." *Biochim Biophys Acta* 1803 (1): 3-19.

Faruqi, T. R., E. J. Weiss, M. J. Shapiro, W. Huang and S. R. Coughlin. 2000. "Structure-function analysis of protease-activated receptor 4 tethered ligand peptides. Determinants of specificity and utility in assays of receptor function." *J Biol Chem* 275 (26): 19728-34.

Feistritzer, C. and M. Riewald. 2005. "Endothelial barrier protection by activated protein C through PAR1-dependent sphingosine 1-phosphate receptor-1 crossactivation." *Blood* 105 (8): 3178-84.

Felber, L. M., C. A. Borgono, S. M. Cloutier, C. Kundig, T. Kishi, J. Ribeiro Chagas, P. Jichlinski, et al. 2005. "Enzymatic profiling of human kallikrein 14 using phage-display substrate technology." *Biol Chem* 386 (3): 291-8.

Ferreras, M., U. Felbor, T. Lenhard, B. R. Olsen and J. Delaisse. 2000. "Generation and degradation of human endostatin proteins by various proteinases." *FEBS Lett* 486 (3): 247-51.

Finigan, J. H., S. M. Dudek, P. A. Singleton, E. T. Chiang, J. R. Jacobson, S. M. Camp, S. Q. Ye and J. G. Garcia. 2005. "Activated protein C mediates novel lung endothelial barrier enhancement: role of sphingosine 1-phosphate receptor transactivation." *J Biol Chem* 280 (17): 17286-93.

Fischer, W. H. and J. Spiess. 1987. "Identification of a mammalian glutaminyl cyclase converting glutaminyl into pyroglutamyl peptides." *Proc Natl Acad Sci U S A* 84 (11): 3628-32.

Fonseca, P. and A. Light. 1983. "The purification and characterization of bovine enterokinase from membrane fragments in the duodenal mucosal fluid." *J Biol Chem* 258 (23): 14516-20.

Forbs, D., S. Thiel, M. C. Stella, A. Sturzebecher, A. Schweinitz, T. Steinmetzer, J. Sturzebecher and K. Uhland. 2005. "In vitro inhibition of matriptase prevents invasive growth of cell lines of prostate and colon carcinoma." *Int J Oncol* 27 (4): 1061-70.

Forneris, F., J. Wu and P. Gros. 2012. "The modular serine proteases of the complement cascade." *Curr Opin Struct Biol* 22 (3): 333-41.

Fortugno, P., A. Bresciani, C. Paolini, C. Pazzagli, M. El Hachem, M. D'Alessio and G. Zambruno. 2011. "Proteolytic Activation Cascade of the Netherton Syndrome-Defective

Protein, LEKTI, in the Epidermis: Implications for Skin Homeostasis." *J Invest Dermatol* 131 (11): 2223-32.

Foster, D. and E. W. Davie. 1984. "Characterization of a cDNA coding for human protein C." *Proc Natl Acad Sci U S A* 81 (15): 4766-70.

Fridman, R., M. Toth, I. Chvyrkova, S. O. Meroueh and S. Mobashery. 2003. "Cell surface association of matrix metalloproteinase-9 (gelatinase B)." *Cancer Metastasis Rev* 22 (2-3): 153-66.

Friedrich, R., P. Fuentes-Prior, E. Ong, G. Coombs, M. Hunter, R. Oehler, D. Pierson, et al. 2002. "Catalytic domain structures of MT-SP1/matriptase, a matrix-degrading transmembrane serine proteinase." *J Biol Chem* 277 (3): 2160-8.

Friis, S., S. Godiksen, J. Bornholdt, J. Selzer-Plon, H. B. Rasmussen, T. H. Bugge, C. Y. Lin and L. K. Vogel. 2011. "Transport via the transcytotic pathway makes prostasin available as a substrate for matriptase." *J Biol Chem* 286 (7): 5793-802.

Fritzsche, F., T. Gansukh, C. A. Borgono, M. Burkhardt, S. Pahl, E. Mayordomo, K. J. Winzer, et al. 2006. "Expression of human Kallikrein 14 (KLK14) in breast cancer is associated with higher tumour grades and positive nodal status." *Br J Cancer* 94 (4): 540-7.

Fromont, G., L. Chene, M. Vidaud, G. Vallancien, P. Mangin, G. Fournier, P. Validire, A. Latil and O. Cussenot. 2005. "Differential expression of 37 selected genes in hormone-refractory prostate cancer using quantitative taqman real-time RT-PCR." *Int J Cancer* 114 (2): 174-81.

Fukae, M., T. Tanabe, T. Uchida, S. K. Lee, O. H. Ryu, C. Murakami, K. Wakida, J. P. Simmer, Y. Yamada and J. D. Bartlett. 1998. "Enamelysin (matrix metalloproteinase-20): localization in the developing tooth and effects of pH and calcium on amelogenin hydrolysis." *J Dent Res* 77 (8): 1580-8.

Fukushima, T., M. Kawaguchi, M. Yamasaki, H. Tanaka, K. Yorita and H. Kataoka. 2011. "Hepatocyte growth factor activator inhibitor type 1 suppresses metastatic pulmonary colonization of pancreatic carcinoma cells." *Cancer Sci* 102 (2): 407-13.

Gak, E., W. G. Taylor, A. M. Chan and J. S. Rubin. 1992. "Processing of hepatocyte growth factor to the heterodimeric form is required for biological activity." *FEBS Lett* 311 (1): 17-21.

Galkin, A. V., L. Mullen, W. D. Fox, J. Brown, D. Duncan, O. Moreno, E. L. Madison and D. B. Agus. 2004. "CVS-3983, a selective matriptase inhibitor, suppresses the growth of androgen independent prostate tumor xenografts." *Prostate* 61 (3): 228-35.

Ganesan, R., G. A. Kolumam, S. J. Lin, M. H. Xie, L. Santell, T. D. Wu, R. A. Lazarus, A. Chaudhuri and D. Kirchhofer. 2011. "Proteolytic activation of pro-macrophage-stimulating protein by hepsin." *Mol Cancer Res* 9 (9): 1175-86.

Ganesan, R., Y. Zhang, K. E. Landgraf, S. J. Lin, P. Moran and D. Kirchhofer. 2012. "An allosteric anti-hepsin antibody derived from a constrained phage display library." *Protein Eng Des Sel* 25 (3): 127-33.

Gavel, Y. and G. von Heijne. 1990. "Sequence differences between glycosylated and non-glycosylated Asn-X-Thr/Ser acceptor sites: implications for protein engineering." *Protein Eng* 3 (5): 433-42.

Gawlitzek, M., M. Estacio, T. Furch and R. Kiss. 2009. "Identification of cell culture conditions to control N-glycosylation site-occupancy of recombinant glycoproteins expressed in CHO cells." *Biotechnol Bioeng* 103 (6): 1164-75.

Geiger, T. R. and D. S. Peeper. 2009. "Metastasis mechanisms." *Biochim Biophys Acta* 1796 (2): 293-308.

Gherardi, E., W. Birchmeier, C. Birchmeier and G. Vande Woude. 2012. "Targeting MET in cancer: rationale and progress." *Nat Rev Cancer* 12 (2): 89-103.

Gil, G. C., W. H. Velander and K. E. Van Cott. 2009. "N-glycosylation microheterogeneity and site occupancy of an Asn-X-Cys sequon in plasma-derived and recombinant protein C." *Proteomics* 9 (9): 2555-67.

Glowacka, I., S. Bertram, M. A. Muller, P. Allen, E. Soilleux, S. Pfefferle, I. Steffen, et al. 2011. "Evidence that TMPRSS2 activates the severe acute respiratory syndrome coronavirus spike protein for membrane fusion and reduces viral control by the humoral immune response." *J Virol* 85 (9): 4122-34.

Glusa, E., A. Saft, D. Prasa and J. Sturzebecher. 1997. "Trypsin- and SLIGRL-induced vascular relaxation and the inhibition by benzamidine derivatives." *Thromb Haemost* 78 (5): 1399-403.

Gmyrek, G. A., M. Walburg, C. P. Webb, H. M. Yu, X. You, E. D. Vaughan, G. F. Vande Woude and B. S. Knudsen. 2001. "Normal and malignant prostate epithelial cells differ in their response to hepatocyte growth factor/scatter factor." *Am J Pathol* 159 (2): 579-90.

Godier, A. and B. J. Hunt. 2013. "Plasminogen receptors and their role in the pathogenesis of inflammatory, autoimmune and malignant disease." *J Thromb Haemost* 11 (1): 26-34.

Goel, M. M., D. Agrawal, S. M. Natu and A. Goel. 2011. "Hepsin immunohistochemical expression in prostate cancer in relation to Gleason's grade and serum prostate specific antigen." *Indian J Pathol Microbiol* 54 (3): 476-81.

Goettig, P., V. Magdolen and H. Brandstetter. 2010. "Natural and synthetic inhibitors of kallikrein-related peptidases (KLKs)." *Biochimie* 92 (11): 1546-67.

Gomis-Ruth, F. X. 2009. "Catalytic domain architecture of metzincin metalloproteases." *J Biol Chem* 284 (23): 15353-7.

Gomis-Ruth, F. X., A. Bayes, G. Sotiropoulou, G. Pampalakis, T. Tsetsenis, V. Villegas, F. X. Aviles and M. Coll. 2002. "The structure of human prokallikrein 6 reveals a novel activation mechanism for the kallikrein family." *J Biol Chem* 277 (30): 27273-81.

Gong, Y., U. D. Chippada-Venkata and W. K. Oh. 2014. "Roles of matrix metalloproteinases and their natural inhibitors in prostate cancer progression." *Cancers (Basel)* 6 (3): 1298-327.

Gonzalez-Maeso, J. and S. C. Sealfon. 2012. "Functional selectivity in GPCR heterocomplexes." *Mini Rev Med Chem* 12 (9): 851-5.

Graham, D. K., D. DeRyckere, K. D. Davies and H. S. Earp. 2014. "The TAM family: phosphatidylserine-sensing receptor tyrosine kinases gone awry in cancer." *Nat Rev Cancer* 14 (12): 769-85.

Grandaliano, G., R. Monno, E. Ranieri, L. Gesualdo, F. P. Schena, C. Martino and M. Ursi. 2000. "Regenerative and proinflammatory effects of thrombin on human proximal tubular cells." *J Am Soc Nephrol* 11 (6): 1016-25.

Grandaliano, G., P. Pontrelli, G. Cerullo, R. Monno, E. Ranieri, M. Ursi, A. Loverre, L. Gesualdo and F. P. Schena. 2003. "Protease-activated receptor-2 expression in IgA

nephropathy: a potential role in the pathogenesis of interstitial fibrosis." *J Am Soc Nephrol* 14 (8): 2072-83.

Gratio, V., N. Beaufort, L. Seiz, J. Maier, G. D. Virca, M. Debela, N. Grebenchtchikov, V. Magdolen and D. Darmoul. 2010. "Kallikrein-related peptidase 4: a new activator of the aberrantly expressed protease-activated receptor 1 in colon cancer cells." *Am J Pathol* 176 (3): 1452-61.

Gratio, V., C. Loriot, G. D. Virca, K. Oikonomopoulou, F. Walker, E. P. Diamandis, M. D. Hollenberg and D. Darmoul. 2011. "Kallikrein-Related Peptidase 14 Acts on Proteinase-Activated Receptor 2 to Induce Signaling Pathway in Colon Cancer Cells." *Am J Pathol.*

Gratio, V., F. Walker, T. Lehy, M. Laburthe and D. Darmoul. 2009. "Aberrant expression of proteinase-activated receptor 4 promotes colon cancer cell proliferation through a persistent signaling that involves Src and ErbB-2 kinase." *Int J Cancer* 124 (7): 1517-25.

Greenberg, D. L., G. J. Mize and T. K. Takayama. 2003. "Protease-activated receptor mediated RhoA signaling and cytoskeletal reorganization in LNCaP cells." *Biochemistry* 42 (3): 702-9.

Grinnell, B. W., J. D. Walls and B. Gerlitz. 1991. "Glycosylation of human protein C affects its secretion, processing, functional activities, and activation by thrombin." *J Biol Chem* 266 (15): 9778-85.

Gross, Jürgen H. 2011. "Tandem Mass Spectrometry
Mass Spectrometry, 415-478: Springer Berlin Heidelberg.

Guex, N. and M. C. Peitsch. 1997. "SWISS-MODEL and the Swiss-PdbViewer: an environment for comparative protein modeling." *Electrophoresis* 18 (15): 2714-23.

Guipponi, M., J. Tan, P. Z. Cannon, L. Donley, P. Crewther, M. Clarke, Q. Wu, R. K. Shepherd and H. S. Scott. 2007. "Mice deficient for the type II transmembrane serine protease, TMPRSS1/hepsin, exhibit profound hearing loss." *Am J Pathol* 171 (2): 608-16.

Guipponi, M., M. Y. Toh, J. Tan, D. Park, K. Hanson, E. Ballana, D. Kwong, et al. 2008. "An integrated genetic and functional analysis of the role of type II transmembrane serine proteases (TMPRSSs) in hearing loss." *Hum Mutat* 29 (1): 130-41.

Guo, J., S. Chen, C. Huang, L. Chen, D. J. Studholme, S. Zhao and L. Yu. 2004. "MANSC: a seven-cysteine-containing domain present in animal membrane and extracellular proteins." *Trends Biochem Sci* 29 (4): 172-4.

Gupta, R. and S. Brunak. 2002. "Prediction of glycosylation across the human proteome and the correlation to protein function." *Pac Symp Biocomput*: 310-22.

Gupta, R., E. Jung and S. Brunak. 2004. *Prediction of N-glycosylation sites in human proteins.*: http://www.cbs.dtu.dk/services/NetNGlyc/.

Halabian, R., M. H. Roudkenar, N. S. Esmaeili, N. Masroori, A. M. Roushandeh and A. J. Najafabadi. 2009. "Establishment of a cell line expressing recombinant factor VII and its subsequent conversion to active form FVIIa through hepsin by genetic engineering method." *Vox Sang* 96 (4): 309-15.

Halvorsen, O. J., A. M. Oyan, T. H. Bo, S. Olsen, K. Rostad, S. A. Haukaas, A. M. Bakke, et al. 2005. "Gene expression profiles in prostate cancer: association with patient subgroups and tumour differentiation." *Int J Oncol* 26 (2): 329-36.

Hamano, Y., M. Zeisberg, H. Sugimoto, J. C. Lively, Y. Maeshima, C. Yang, R. O. Hynes, Z. Werb, A. Sudhakar and R. Kalluri. 2003. "Physiological levels of tumstatin, a fragment of collagen IV alpha3 chain, are generated by MMP-9 proteolysis and suppress angiogenesis via alphaV beta3 integrin." *Cancer Cell* 3 (6): 589-601.

Hanahan, D. and R. A. Weinberg. 2011. "Hallmarks of cancer: the next generation." *Cell* 144 (5): 646-74.

Hansen, K. K., M. Saifeddine and M. D. Hollenberg. 2004. "Tethered ligand-derived peptides of proteinase-activated receptor 3 (PAR3) activate PAR1 and PAR2 in Jurkat T cells." *Immunology* 112 (2): 183-90.

Hart, P. S., T. C. Hart, M. D. Michalec, O. H. Ryu, D. Simmons, S. Hong and J. T. Wright. 2004. "Mutation in kallikrein 4 causes autosomal recessive hypomaturation amelogenesis imperfecta." *J Med Genet* 41 (7): 545-9.

Harvey, T. J., Y. Dong, L. Bui, R. Jarrott, T. Walsh and J. A. Clements. 2003. "Production and characterization of antipeptide kallikrein 4 antibodies. Use of computer modeling to design peptides specific to Kallikrein 4." *Methods Mol Med* 81: 241-54.

Harvey, T. J., J. D. Hooper, S. A. Myers, S. A. Stephenson, L. K. Ashworth and J. A. Clements. 2000. "Tissue-specific expression patterns and fine mapping of the human kallikrein (KLK) locus on proximal 19q13.4." *J Biol Chem* 275 (48): 37397-406.

Hashem, M. and T. Essam. 2005. "Hepatocyte growth factor as a tumor marker in the serum of patients with prostate cancer." *J Egypt Natl Canc Inst* 17 (2): 114-20.

Hashimoto, T., M. Kato, T. Shimomura and N. Kitamura. 2010. "TMPRSS13, a type II transmembrane serine protease, is inhibited by hepatocyte growth factor activator inhibitor type 1 and activates pro-hepatocyte growth factor." *Febs J* 277 (23): 4888-900.

Hattori, M., A. Fujiyama, T. D. Taylor, H. Watanabe, T. Yada, H. S. Park, A. Toyoda, et al. 2000. "The DNA sequence of human chromosome 21." *Nature* 405 (6784): 311-9.

Hedstrom, L. 2002. "Serine protease mechanism and specificity." *Chem Rev* 102 (12): 4501-24.

Hein, L., K. Ishii, S. R. Coughlin and B. K. Kobilka. 1994. "Intracellular targeting and trafficking of thrombin receptors. A novel mechanism for resensitization of a G protein-coupled receptor." *J Biol Chem* 269 (44): 27719-26.

Heljasvaara, R., P. Nyberg, J. Luostarinen, M. Parikka, P. Heikkila, M. Rehn, T. Sorsa, T. Salo and T. Pihlajaniemi. 2005. "Generation of biologically active endostatin fragments from human collagen XVIII by distinct matrix metalloproteases." *Exp Cell Res* 307 (2): 292-304.

Herrala, A. M., K. S. Porvari, A. P. Kyllonen and P. T. Vihko. 2001. "Comparison of human prostate specific glandular kallikrein 2 and prostate specific antigen gene expression in prostate with gene amplification and overexpression of prostate specific glandular kallikrein 2 in tumor tissue." *Cancer* 92 (12): 2975-84.

Herter, S., D. E. Piper, W. Aaron, T. Gabriele, G. Cutler, P. Cao, A. S. Bhatt, et al. 2005. "Hepatocyte growth factor is a preferred in vitro substrate for human hepsin, a membrane-anchored serine protease implicated in prostate and ovarian cancers." *Biochem J* 390 (Pt 1): 125-36.

Heurich, A., H. Hofmann-Winkler, S. Gierer, T. Liepold, O. Jahn and S. Pohlmann. 2013. "TMPRSS2 and ADAM17 cleave ACE2 differentially and only proteolysis by TMPRSS2 augments entry driven by the SARS-coronavirus spike-protein." *J Virol.*

Hiss, J. A. and G. Schneider. 2009. "Architecture, function and prediction of long signal peptides." *Brief Bioinform* 10 (5): 569-78.

Hobbs, S., S. Jitrapakdee and J. C. Wallace. 1998. "Development of a bicistronic vector driven by the human polypeptide chain elongation factor 1alpha promoter for creation of stable mammalian cell lines that express very high levels of recombinant proteins." *Biochem Biophys Res Commun* 252 (2): 368-72.

Hollenberg, M. D. and S. J. Compton. 2002. "International Union of Pharmacology. XXVIII. Proteinase-activated receptors." *Pharmacol Rev* 54 (2): 203-17.

Hollenberg, M. D., M. Saifeddine, B. al-Ani and A. Kawabata. 1997. "Proteinase-activated receptors: structural requirements for activity, receptor cross-reactivity, and receptor selectivity of receptor-activating peptides." *Can J Physiol Pharmacol* 75 (7): 832-41.

Hooper, J. D., L. T. Bui, F. K. Rae, T. J. Harvey, S. A. Myers, L. K. Ashworth and J. A. Clements. 2001a. "Identification and characterization of KLK14, a novel kallikrein serine protease gene located on human chromosome 19q13.4 and expressed in prostate and skeletal muscle." *Genomics* 73 (1): 117-22.

Hooper, J. D., J. A. Clements, J. P. Quigley and T. M. Antalis. 2001b. "Type II transmembrane serine proteases. Insights into an emerging class of cell surface proteolytic enzymes." *J Biol Chem* 276 (2): 857-60.

Hughes, P., D. Marshall, Y. Reid, H. Parkes and C. Gelber. 2007. "The costs of using unauthenticated, over-passaged cell lines: how much more data do we need?" *Biotechniques* 43 (5): 575, 577-8, 581-2 passim.

Humphrey, P. A., X. Zhu, R. Zarnegar, P. E. Swanson, T. L. Ratliff, R. T. Vollmer and M. L. Day. 1995. "Hepatocyte growth factor and its receptor (c-MET) in prostatic carcinoma." *Am J Pathol* 147 (2): 386-96.

Hunkapiller, M. W., E. Lujan, F. Ostrander and L. E. Hood. 1983. "Isolation of microgram quantities of proteins from polyacrylamide gels for amino acid sequence analysis." *Methods Enzymol* 91: 227-36.

Ihara, S., E. Miyoshi, J. H. Ko, K. Murata, S. Nakahara, K. Honke, R. B. Dickson, C. Y. Lin and N. Taniguchi. 2002. "Prometastatic effect of N-acetylglucosaminyltransferase V is due to modification and stabilization of active matriptase by adding beta 1-6 GlcNAc branching." *J Biol Chem* 277 (19): 16960-7.

Ihara, S., E. Miyoshi, S. Nakahara, H. Sakiyama, H. Ihara, A. Akinaga, K. Honke, R. B. Dickson, C. Y. Lin and N. Taniguchi. 2004. "Addition of beta1-6 GlcNAc branching to the oligosaccharide attached to Asn 772 in the serine protease domain of matriptase plays a pivotal role in its stability and resistance against trypsin." *Glycobiology* 14 (2): 139-46.

Inouye, K., M. Tomoishi, M. Yasumoto, Y. Miyake, K. Kojima, S. Tsuzuki and T. Fushiki. 2013. "Roles of CUB and LDL receptor class A domain repeats of a transmembrane serine protease matriptase in its zymogen activation." *J Biochem* 153 (1): 51-61.

Ishida, E., M. Nakamura, K. Shimada, M. Kishi, S. Nakaoka and N. Konishi. 2003. "Distribution and secretory pathways of prostate specific antigen, alpha1-antichymotrypsin and prostate secretory granules in prostate cancers." *Pathol Int* 53 (7): 415-21.

Ishihara, H., A. J. Connolly, D. Zeng, M. L. Kahn, Y. W. Zheng, C. Timmons, T. Tram and S. R. Coughlin. 1997. "Protease-activated receptor 3 is a second thrombin receptor in humans." *Nature* 386 (6624): 502-6.

Ishii, K., J. Chen, M. Ishii, W. J. Koch, N. J. Freedman, R. J. Lefkowitz and S. R. Coughlin. 1994. "Inhibition of thrombin receptor signaling by a G-protein coupled receptor kinase. Functional specificity among G-protein coupled receptor kinases." *J Biol Chem* 269 (2): 1125-30.

Ishii, K., L. Hein, B. Kobilka and S. R. Coughlin. 1993. "Kinetics of thrombin receptor cleavage on intact cells. Relation to signaling." *J Biol Chem* 268 (13): 9780-6.

Ishikawa, Y., Y. Horii, H. Tamura and S. Shiosaka. 2008. "Neuropsin (KLK8)-dependent and -independent synaptic tagging in the Schaffer-collateral pathway of mouse hippocampus." *J Neurosci* 28 (4): 843-9.

Ito, Y., A. Akinaga, K. Yamanaka, T. Nakagawa, A. Kondo, R. B. Dickson, C. Y. Lin, A. Miyauchi, N. Taniguchi and E. Miyoshi. 2006. "Co-expression of matriptase and N-acetylglucosaminyltransferase V in thyroid cancer tissues--its possible role in prolonged stability in vivo by aberrant glycosylation." *Glycobiology* 16 (5): 368-74.

Itoh, H., H. Kataoka, M. Tomita, R. Hamasuna, Y. Nawa, N. Kitamura and M. Koono. 2000. "Upregulation of HGF activator inhibitor type 1 but not type 2 along with regeneration of intestinal mucosa." *Am J Physiol Gastrointest Liver Physiol* 278 (4): G635-43.

Itoh, H., S. Naganuma, N. Takeda, S. Miyata, S. Uchinokura, T. Fukushima, S. Uchiyama, et al. 2004. "Regeneration of injured intestinal mucosa is impaired in hepatocyte growth factor activator-deficient mice." *Gastroenterology* 127 (5): 1423-35.

Jacquinet, E., N. V. Rao, G. V. Rao, W. Zhengming, K. H. Albertine and J. R. Hoidal. 2001. "Cloning and characterization of the cDNA and gene for human epitheliasin." *Eur J Biochem* 268 (9): 2687-99.

Jaffre, F., A. E. Friedman, Z. Hu, N. Mackman and B. C. Blaxall. 2012. "beta-adrenergic receptor stimulation transactivates protease-activated receptor 1 via matrix metalloproteinase 13 in cardiac cells." *Circulation* 125 (24): 2993-3003.

Jameson, G. W., D. V. Roberts, R. W. Adams, W. S. Kyle and D. T. Elmore. 1973. "Determination of the operational molarity of solutions of bovine alpha-chymotrypsin, trypsin, thrombin and factor Xa by spectrofluorimetric titration." *Biochem J* 131 (1): 107-17.

Jequier, Anne M. 2008. "The Anatomy and Physiology of the Male Genital Tract." In *Male infertility : a guide for the clinician*. Oxford: Blackwell Science.

Jin, X., T. Hirosaki, C. Y. Lin, R. B. Dickson, S. Higashi, H. Kitamura and K. Miyazaki. 2005. "Production of soluble matriptase by human cancer cell lines and cell surface activation of its zymogen by trypsin." *J Cell Biochem* 95 (3): 632-47.

Jin, X., M. Yagi, N. Akiyama, T. Hirosaki, S. Higashi, C. Y. Lin, R. B. Dickson, H. Kitamura and K. Miyazaki. 2006. "Matriptase activates stromelysin (MMP-3) and promotes tumor growth and angiogenesis." *Cancer Sci* 97 (12): 1327-34.

Jin, Y., S. Qu, M. Tesikova, L. Wang, A. Kristian, G. M. Maelandsmo, H. Kong, et al. 2013. "Molecular circuit involving KLK4 integrates androgen and mTOR signaling in prostate cancer." *Proc Natl Acad Sci U S A* 110 (28): E2572-81.

Jones, G. H. 1974. "Cell-free synthesis of amino-terminal L-pyroglutamic acid." *Biochemistry* 13 (5): 855-60.

Jones, J., S. S. Krag and M. J. Betenbaugh. 2005. "Controlling N-linked glycan site occupancy." *Biochim Biophys Acta* 1726 (2): 121-37.

Julovi, S. M., M. Xue, S. Dervish, P. N. Sambrook, L. March and C. J. Jackson. 2011. "Protease activated receptor-2 mediates activated protein C-induced cutaneous wound healing via inhibition of p38." *Am J Pathol* 179 (5): 2233-42.

Jung, K., L. Nowak, M. Lein, F. Priem, D. Schnorr and S. A. Loening. 1997. "Matrix metalloproteinases 1 and 3, tissue inhibitor of metalloproteinase-1 and the complex of metalloproteinase-1/tissue inhibitor in plasma of patients with prostate cancer." *Int J Cancer* 74 (2): 220-3.

Kahn, M. L., Y. W. Zheng, W. Huang, V. Bigornia, D. Zeng, S. Moff, R. V. Farese, Jr., C. Tam and S. R. Coughlin. 1998. "A dual thrombin receptor system for platelet activation." *Nature* 394 (6694): 690-4.

Kall, L., A. Krogh and E. L. Sonnhammer. 2004. "A combined transmembrane topology and signal peptide prediction method." *J Mol Biol* 338 (5): 1027-36.

Kamath, L., A. Meydani, F. Foss and A. Kuliopulos. 2001. "Signaling from protease-activated receptor-1 inhibits migration and invasion of breast cancer cells." *Cancer Res* 61 (15): 5933-40.

Kaneider, N. C., A. J. Leger, A. Agarwal, N. Nguyen, G. Perides, C. Derian, L. Covic and A. Kuliopulos. 2007. "'Role reversal' for the receptor PAR1 in sepsis-induced vascular damage." *Nat Immunol* 8 (12): 1303-12.

Kasturi, L., H. Chen and S. H. Shakin-Eshleman. 1997. "Regulation of N-linked core glycosylation: use of a site-directed mutagenesis approach to identify Asn-Xaa-Ser/Thr sequons that are poor oligosaccharide acceptors." *Biochem J* 323 (Pt 2): 415-9.

Kataoka, H. and M. Kawaguchi. 2010. "Hepatocyte growth factor activator (HGFA): pathophysiological functions in vivo." *Febs J* 277 (10): 2230-7.

Kataoka, H., S. Miyata, S. Uchinokura and H. Itoh. 2003. "Roles of hepatocyte growth factor (HGF) activator and HGF activator inhibitor in the pericellular activation of HGF/scatter factor." *Cancer Metastasis Rev* 22 (2-3): 223-36.

Kataoka, H., T. Shimomura, T. Kawaguchi, R. Hamasuna, H. Itoh, N. Kitamura, K. Miyazawa and M. Koono. 2000. "Hepatocyte growth factor activator inhibitor type 1 is a specific cell surface binding protein of hepatocyte growth factor activator (HGFA) and regulates HGFA activity in the pericellular microenvironment." *J Biol Chem* 275 (51): 40453-62.

Kataoka, H., T. Suganuma, T. Shimomura, H. Itoh, N. Kitamura, K. Nabeshima and M. Koono. 1999. "Distribution of hepatocyte growth factor activator inhibitor type 1 (HAI-1) in human tissues. Cellular surface localization of HAI-1 in simple columnar epithelium and its modulated expression in injured and regenerative tissues." *J Histochem Cytochem* 47 (5): 673-82.

Kato, M., T. Hashimoto, T. Shimomura, H. Kataoka, H. Ohi and N. Kitamura. 2011. "Hepatocyte growth factor activator inhibitor type 1 inhibits protease activity and proteolytic activation of human airway trypsin-like protease." *J Biochem*.

Kaufmann, R. and M. D. Hollenberg. 2012. "Proteinase-activated receptors (PARs) and calcium signaling in cancer." *Adv Exp Med Biol* 740: 979-1000.

Kaufmann, R., U. Junker, K. Nuske, M. Westermann, P. Henklein, J. Scheele and K. Junker. 2002. "PAR-1- and PAR-3-type thrombin receptor expression in primary cultures of human renal cell carcinoma cells." *Int J Oncol* 20 (1): 177-80.

Kaufmann, R., S. Rahn, K. Pollrich, J. Hertel, Y. Dittmar, M. Hommann, P. Henklein, et al. 2007. "Thrombin-mediated hepatocellular carcinoma cell migration: cooperative action via proteinase-activated receptors 1 and 4." *J Cell Physiol* 211 (3): 699-707.

Kaufmann, R., B. Schulze, G. Krause, L. M. Mayr, U. Settmacher and P. Henklein. 2005. "Proteinase-activated receptors (PARs)--the PAR3 Neo-N-terminal peptide TFRGAP interacts with PAR1." *Regul Pept* 125 (1-3): 61-6.

Kaushal, V., M. Kohli, R. A. Dennis, E. R. Siegel, W. W. Chiles and P. Mukunyadzi. 2006. "Thrombin receptor expression is upregulated in prostate cancer." *Prostate* 66 (3): 273-82.

Kavanagh, J. P. 1985. "Sodium, potassium, calcium, magnesium, zinc, citrate and chloride content of human prostatic and seminal fluid." *J Reprod Fertil* 75 (1): 35-41.

Kawabata, A., M. Saifeddine, B. Al-Ani, L. Leblond and M. D. Hollenberg. 1999. "Evaluation of proteinase-activated receptor-1 (PAR1) agonists and antagonists using a cultured cell receptor desensitization assay: activation of PAR2 by PAR1-targeted ligands." *J Pharmacol Exp Ther* 288 (1): 358-70.

Kazama, Y., T. Hamamoto, D. C. Foster and W. Kisiel. 1995. "Hepsin, a putative membrane-associated serine protease, activates human factor VII and initiates a pathway of blood coagulation on the cell surface leading to thrombin formation." *J Biol Chem* 270 (1): 66-72.

Kellermann, J., F. Lottspeich, R. Geiger and R. Deutzmann. 1988. "Human urinary kallikrein--amino acid sequence and carbohydrate attachment sites." *Protein Seq Data Anal* 1 (3): 177-82.

Kenakin, T. 2007. "Functional selectivity through protean and biased agonism: who steers the ship?" *Mol Pharmacol* 72 (6): 1393-401.

Kenakin, T. 2011. "Functional selectivity and biased receptor signaling." *J Pharmacol Exp Ther* 336 (2): 296-302.

Khandke, K. M., T. Fairwell, B. T. Chait and B. N. Manjula. 1989. "Influence of ions on cyclization of the amino terminal glutamine residues of tryptic peptides of streptococcal PepM49 protein. Resolution of cyclized peptides by HPLC and characterization by mass spectrometry." *Int J Pept Protein Res* 34 (2): 118-23.

Kim, T. S., C. Heinlein, R. C. Hackman and P. S. Nelson. 2006. "Phenotypic analysis of mice lacking the Tmprss2-encoded protease." *Mol Cell Biol* 26 (3): 965-75.

Kirchhofer, D., M. Peek, W. Li, J. Stamos, C. Eigenbrot, S. Kadkhodayan, J. M. Elliott, R. T. Corpuz, R. A. Lazarus and P. Moran. 2003. "Tissue expression, protease specificity, and Kunitz domain functions of hepatocyte growth factor activator inhibitor-1B (HAI-1B), a new splice variant of HAI-1." *J Biol Chem* 278 (38): 36341-9.

Kirchhofer, D., M. Peek, M. T. Lipari, K. Billeci, B. Fan and P. Moran. 2005. "Hepsin activates pro-hepatocyte growth factor and is inhibited by hepatocyte growth factor activator inhibitor-1B (HAI-1B) and HAI-2." *FEBS Lett* 579 (9): 1945-50.

Kishibe, M., Y. Bando, R. Terayama, K. Namikawa, H. Takahashi, Y. Hashimoto, A. Ishida-Yamamoto, et al. 2007. "Kallikrein 8 is involved in skin desquamation in cooperation with other kallikreins." *J Biol Chem* 282 (8): 5834-41.

Kitagishi, K. and K. Hiromi. 1984. "Binding between thermolysin and its specific inhibitor, phosphoramidon." *J Biochem* 95 (2): 529-34.

Kitamoto, Y., R. A. Veile, H. Donis-Keller and J. E. Sadler. 1995. "cDNA sequence and chromosomal localization of human enterokinase, the proteolytic activator of trypsinogen." *Biochemistry* 34 (14): 4562-8.

Kiyomiya, K., M. S. Lee, I. C. Tseng, H. Zuo, R. J. Barndt, M. D. Johnson, R. B. Dickson and C. Y. Lin. 2006. "Matriptase activation and shedding with HAI-1 is induced by steroid sex hormones in human prostate cancer cells, but not in breast cancer cells." *Am J Physiol Cell Physiol* 291 (1): C40-9.

Kleifeld, O., A. Doucet, A. Prudova, U. auf dem Keller, M. Gioia, J. N. Kizhakkedathu and C. M. Overall. 2011. "Identifying and quantifying proteolytic events and the natural N terminome by terminal amine isotopic labeling of substrates." *Nat Protoc* 6 (10): 1578-611.

Klein, T. and R. Bischoff. 2011. "Physiology and pathophysiology of matrix metalloproteases." *Amino Acids* 41 (2): 271-90.

Klezovitch, O., J. Chevillet, J. Mirosevich, R. L. Roberts, R. J. Matusik and V. Vasioukhin. 2004. "Hepsin promotes prostate cancer progression and metastasis." *Cancer Cell* 6 (2): 185-95.

Klokk, T. I., A. Kilander, Z. Xi, H. Waehre, B. Risberg, H. E. Danielsen and F. Saatcioglu. 2007. "Kallikrein 4 is a proliferative factor that is overexpressed in prostate cancer." *Cancer Res* 67 (11): 5221-30.

Klos, A., A. J. Tenner, K. O. Johswich, R. R. Ager, E. S. Reis and J. Kohl. 2009. "The role of the anaphylatoxins in health and disease." *Mol Immunol* 46 (14): 2753-66.

Knecht, W., G. S. Cottrell, S. Amadesi, J. Mohlin, A. Skaregarde, K. Gedda, A. Peterson, et al. 2007. "Trypsin IV or mesotrypsin and p23 cleave protease-activated receptors 1 and 2 to induce inflammation and hyperalgesia." *J Biol Chem* 282 (36): 26089-100.

Knudsen, B. S. and M. Edlund. 2004. "Prostate cancer and the met hepatocyte growth factor receptor." *Adv Cancer Res* 91: 31-67.

Knudsen, B. S., G. A. Gmyrek, J. Inra, D. S. Scherr, E. D. Vaughan, D. M. Nanus, M. W. Kattan, W. L. Gerald and G. F. Vande Woude. 2002. "High expression of the Met receptor in prostate cancer metastasis to bone." *Urology* 60 (6): 1113-7.

Knudsen, B. S., J. M. Lucas, L. Fazli, S. Hawley, S. Falcon, I. M. Coleman, D. B. Martin, et al. 2005. "Regulation of hepatocyte activator inhibitor-1 expression by androgen and oncogenic transformation in the prostate." *Am J Pathol* 167 (1): 255-66.

Kojima, K., S. Tsuzuki, T. Fushiki and K. Inouye. 2008. "Roles of functional and structural domains of hepatocyte growth factor activator inhibitor type 1 in the inhibition of matriptase." *J Biol Chem* 283 (5): 2478-87.

Kojima, K., S. Tsuzuki, T. Fushiki and K. Inouye. 2009. "Role of the stem domain of matriptase in the interaction with its physiological inhibitor, hepatocyte growth factor activator inhibitor type I." *J Biochem* 145 (6): 783-90.

Komarova, Y. A., D. Mehta and A. B. Malik. 2007. "Dual regulation of endothelial junctional permeability." *Sci STKE* 2007 (412): re8.

Komatsu, N., K. Saijoh, C. Kuk, A. C. Liu, S. Khan, F. Shirasaki, K. Takehara and E. P. Diamandis. 2007a. "Human tissue kallikrein expression in the stratum corneum and serum of atopic dermatitis patients." *Exp Dermatol* 16 (6): 513-9.

Komatsu, N., K. Saijoh, C. Kuk, F. Shirasaki, K. Takehara and E. P. Diamandis. 2007b. "Aberrant human tissue kallikrein levels in the stratum corneum and serum of patients with psoriasis: dependence on phenotype, severity and therapy." *Br J Dermatol* 156 (5): 875-83.

Komatsu, N., K. Saijoh, M. Sidiropoulos, B. Tsai, K. Takehara and E. P. Diamandis. 2005. "Quantification of human tissue kallikreins in the stratum corneum: dependence on age and gender." *J Invest Dermatol* 125: 1182-1189.

Komatsu, Nahoko, Brian Tsai, Michael Sidiropoulos, Kiyofumi Saijoh, Michael A. Levesque, Kazuhiko Takehara and Eleftherios P. Diamandis. 2006. "Quantification of Eight Tissue Kallikreins in the Stratum Corneum and Sweat." *J Invest Dermatol* 126 (4): 927-931.

Kravets, F. G., J. Lee, B. Singh, A. Trocchia, S. N. Pentyala and S. A. Khan. 2000. "Prostasomes: current concepts." *Prostate* 43 (3): 169-74.

Krishna, R. G. and F. Wold. 1993. "Post-translational modification of proteins." *Adv Enzymol Relat Areas Mol Biol* 67: 265-98.

Krowarsch, D., T. Cierpicki, F. Jelen and J. Otlewski. 2003. "Canonical protein inhibitors of serine proteases." *Cell Mol Life Sci* 60 (11): 2427-44.

Kube, D. M., C. D. Savci-Heijink, A. F. Lamblin, F. Kosari, G. Vasmatzis, J. C. Cheville, D. P. Connelly and G. G. Klee. 2007. "Optimization of laser capture microdissection and RNA amplification for gene expression profiling of prostate cancer." *BMC Mol Biol* 8: 25.

Kulasingam, V. and E. P. Diamandis. 2008. "Strategies for discovering novel cancer biomarkers through utilization of emerging technologies." *Nat Clin Pract Oncol* 5 (10): 588-99.

Kuliopulos, A., L. Covic, S. K. Seeley, P. J. Sheridan, J. Helin and C. E. Costello. 1999. "Plasmin desensitization of the PAR1 thrombin receptor: kinetics, sites of truncation, and implications for thrombolytic therapy." *Biochemistry* 38 (14): 4572-85.

Kumar-Sinha, C., S. A. Tomlins and A. M. Chinnaiyan. 2008. "Recurrent gene fusions in prostate cancer." *Nat Rev Cancer* 8 (7): 497-511.

Kumar, A., S. D. Mikolajczyk, A. S. Goel, L. S. Millar and M. S. Saedi. 1997. "Expression of pro form of prostate-specific antigen by mammalian cells and its conversion to mature, active form by human kallikrein 2." *Cancer Res* 57 (15): 3111-4.

Kurachi, K., A. Torres-Rosado and A. Tsuji. 1994. "Hepsin." *Methods Enzymol* 244: 100-14.

Kurimoto, S., N. Moriyama, S. Horie, M. Sakai, S. Kameyama, Y. Akimoto, H. Hirano and K. Kawabe. 1998. "Co-expression of hepatocyte growth factor and its receptor in human prostate cancer." *Histochem J* 30 (1): 27-32.

Kuriyama, M., M. C. Wang, C. I. Lee, L. D. Papsidero, C. S. Killian, H. Inaji, N. H. Slack, T. Nishiura, G. P. Murphy and T. M. Chu. 1981. "Use of human prostate-specific antigen in monitoring prostate cancer." *Cancer Res* 41 (10): 3874-6.

Kuzmanov, U., N. Jiang, C. R. Smith, A. Soosaipillai and E. P. Diamandis. 2009. "Differential N-glycosylation of kallikrein 6 derived from ovarian cancer cells or the central nervous system." *Mol Cell Proteomics* 8 (4): 791-8.

Landers, K. A., M. J. Burger, M. A. Tebay, D. M. Purdie, B. Scells, H. Samaratunga, M. F. Lavin and R. A. Gardiner. 2005. "Use of multiple biomarkers for a molecular diagnosis of prostate cancer." *Int J Cancer* 114 (6): 950-6.

Larkin, M. A., G. Blackshields, N. P. Brown, R. Chenna, P. A. McGettigan, H. McWilliam, F. Valentin, et al. 2007. "Clustal W and Clustal X version 2.0." *Bioinformatics* 23 (21): 2947-8.

Laskowski, M. and M. A. Qasim. 2000. "What can the structures of enzyme-inhibitor complexes tell us about the structures of enzyme substrate complexes?" *Biochim Biophys Acta* 1477 (1-2): 324-37.

Lau, C., C. Lytle, D. S. Straus and K. A. DeFea. 2011. "Apical and basolateral pools of proteinase-activated receptor-2 direct distinct signaling events in the intestinal epithelium." *Am J Physiol Cell Physiol* 300 (1): C113-23.

Lawrence, M. G., J. Lai and J. A. Clements. 2010. "Kallikreins on steroids: structure, function, and hormonal regulation of prostate-specific antigen and the extended kallikrein locus." *Endocr Rev* 31 (4): 407-46.

Lawrence, M. G., T. L. Veveris-Lowe, A. K. Whitbread, D. L. Nicol and J. A. Clements. 2007. "Epithelial-mesenchymal transition in prostate cancer and the potential role of kallikrein serine proteases." *Cells Tissues Organs* 185 (1-3): 111-5.

Laxmikanthan, G., S. I. Blaber, M. J. Bernett, I. A. Scarisbrick, M. A. Juliano and M. Blaber. 2005. "1.70 A X-ray structure of human apo kallikrein 1: structural changes upon peptide inhibitor/substrate binding." *Proteins* 58 (4): 802-14.

Lee, M. S., K. Kiyomiya, C. Benaud, R. B. Dickson and C. Y. Lin. 2005. "Simultaneous activation and hepatocyte growth factor activator inhibitor 1-mediated inhibition of matriptase induced at activation foci in human mammary epithelial cells." *Am J Physiol Cell Physiol* 288 (4): C932-41.

Lee, M. S., I. C. Tseng, Y. Wang, K. Kiyomiya, M. D. Johnson, R. B. Dickson and C. Y. Lin. 2007. "Autoactivation of matriptase in vitro: requirement for biomembrane and LDL receptor domain." *Am J Physiol Cell Physiol* 293 (1): C95-105.

Lee, S. L., R. B. Dickson and C. Y. Lin. 2000. "Activation of hepatocyte growth factor and urokinase/plasminogen activator by matriptase, an epithelial membrane serine protease." *J Biol Chem* 275 (47): 36720-5.

Leger, A. J., S. L. Jacques, J. Badar, N. C. Kaneider, C. K. Derian, P. Andrade-Gordon, L. Covic and A. Kuliopulos. 2006. "Blocking the protease-activated receptor 1-4 heterodimer in platelet-mediated thrombosis." *Circulation* 113 (9): 1244-54.

Leone, J. W., B. Hampton, E. Fowler, M. Moyer, R. G. Krishna and C. C. Chin. 2011. "Removal of N-terminal blocking groups from proteins." *Curr Protoc Protein Sci* Chapter 11: Unit11 7.

Lerner, D. J., M. Chen, T. Tram and S. R. Coughlin. 1996. "Agonist recognition by proteinase-activated receptor 2 and thrombin receptor. Importance of extracellular loop interactions for receptor function." *J Biol Chem* 271 (24): 13943-7.

Leytus, S. P., K. R. Loeb, F. S. Hagen, K. Kurachi and E. W. Davie. 1988. "A novel trypsin-like serine protease (hepsin) with a putative transmembrane domain expressed by human liver and hepatoma cells." *Biochemistry* 27 (3): 1067-74.

Leyvraz, C., R. P. Charles, I. Rubera, M. Guitard, S. Rotman, B. Breiden, K. Sandhoff and E. Hummler. 2005. "The epidermal barrier function is dependent on the serine protease CAP1/Prss8." *J Cell Biol* 170 (3): 487-96.

Li, D., L. D'Angelo, M. Chavez and D. S. Woulfe. 2011. "Arrestin-2 differentially regulates PAR4 and ADP receptor signaling in platelets." *J Biol Chem* 286 (5): 3805-14.

Li, H. X., B. Y. Hwang, G. Laxmikanthan, S. I. Blaber, M. Blaber, P. A. Golubkov, P. Ren, B. L. Iverson and G. Georgiou. 2008. "Substrate specificity of human kallikreins 1 and 6 determined by phage display." *Protein Sci* 17 (4): 664-72.

Li, W., B. E. Wang, P. Moran, T. Lipari, R. Ganesan, R. Corpuz, M. J. Ludlam, et al. 2009. "Pegylated kunitz domain inhibitor suppresses hepsin-mediated invasive tumor growth and metastasis." *Cancer Res* 69 (21): 8395-402.

Li, Y. and P. J. Cozzi. 2007. "Targeting uPA/uPAR in prostate cancer." *Cancer Treat Rev* 33 (6): 521-7.

Li, Y., Z. Yu, X. Zhao and S. H. Shen. 2005. "Identification and characterization of hepsin/-TM, a non-transmembrane hepsin isoform." *Biochim Biophys Acta* 1681 (2-3): 157-65.

Liang, X., J. Zhao, M. Hajivandi, R. Wu, J. Tao, J. W. Amshey and R. M. Pope. 2006. "Quantification of membrane and membrane-bound proteins in normal and malignant breast cancer cells isolated from the same patient with primary breast carcinoma." *J Proteome Res* 5 (10): 2632-41.

Lilja, H., D. Ulmert and A. J. Vickers. 2008. "Prostate-specific antigen and prostate cancer: prediction, detection and monitoring." *Nat Rev Cancer* 8 (4): 268-78.

Lin, B., C. Ferguson, J. T. White, S. Wang, R. Vessella, L. D. True, L. Hood and P. S. Nelson. 1999a. "Prostate-localized and androgen-regulated expression of the membrane-bound serine protease TMPRSS2." *Cancer Res* 59 (17): 4180-4.

Lin, C. Y., J. Anders, M. Johnson and R. B. Dickson. 1999b. "Purification and characterization of a complex containing matriptase and a Kunitz-type serine protease inhibitor from human milk." *J Biol Chem* 274 (26): 18237-42.

Lin, C. Y., J. Anders, M. Johnson, Q. A. Sang and R. B. Dickson. 1999c. "Molecular cloning of cDNA for matriptase, a matrix-degrading serine protease with trypsin-like activity." *J Biol Chem* 274 (26): 18231-6.

List, K. 2009. "Matriptase: a culprit in cancer?" *Future Oncol* 5 (1): 97-104.

List, K., T. H. Bugge and R. Szabo. 2006a. "Matriptase: potent proteolysis on the cell surface." *Mol Med* 12 (1-3): 1-7.

List, K., B. Currie, T. C. Scharschmidt, R. Szabo, J. Shireman, A. Molinolo, B. F. Cravatt, J. Segre and T. H. Bugge. 2007. "Autosomal ichthyosis with hypotrichosis syndrome displays low

matriptase proteolytic activity and is phenocopied in ST14 hypomorphic mice." *J Biol Chem* 282 (50): 36714-23.

List, K., C. C. Haudenschild, R. Szabo, W. Chen, S. M. Wahl, W. Swaim, L. H. Engelholm, N. Behrendt and T. H. Bugge. 2002. "Matriptase/MT-SP1 is required for postnatal survival, epidermal barrier function, hair follicle development, and thymic homeostasis." *Oncogene* 21 (23): 3765-79.

List, K., P. Kosa, R. Szabo, A. L. Bey, C. B. Wang, A. Molinolo and T. H. Bugge. 2009. "Epithelial integrity is maintained by a matriptase-dependent proteolytic pathway." *Am J Pathol* 175 (4): 1453-63.

List, K., R. Szabo, A. Molinolo, B. S. Nielsen and T. H. Bugge. 2006b. "Delineation of matriptase protein expression by enzymatic gene trapping suggests diverging roles in barrier function, hair formation, and squamous cell carcinogenesis." *Am J Pathol* 168 (5): 1513-25.

List, K., R. Szabo, A. Molinolo, V. Sriuranpong, V. Redeye, T. Murdock, B. Burke, B. S. Nielsen, J. S. Gutkind and T. H. Bugge. 2005. "Deregulated matriptase causes ras-independent multistage carcinogenesis and promotes ras-mediated malignant transformation." *Genes Dev* 19 (16): 1934-50.

List, K., R. Szabo, P. W. Wertz, J. Segre, C. C. Haudenschild, S. Y. Kim and T. H. Bugge. 2003. "Loss of proteolytically processed filaggrin caused by epidermal deletion of Matriptase/MT-SP1." *J Cell Biol* 163 (4): 901-10.

Littlepage, L. E., M. D. Sternlicht, N. Rougier, J. Phillips, E. Gallo, Y. Yu, K. Williams, A. Brenot, J. I. Gordon and Z. Werb. 2010. "Matrix metalloproteinases contribute distinct roles in neuroendocrine prostate carcinogenesis, metastasis, and angiogenesis progression." *Cancer Res* 70 (6): 2224-34.

Liu, J., M. Bastian, P. Kohlschein, P. Schuff-Werner and M. Steiner. 2003. "Expression of functional protease-activated receptor 1 in human prostate cancer cell lines." *Urol Res* 31 (3): 163-8.

Loew, D., C. Perrault, M. Morales, S. Moog, C. Ravanat, S. Schuhler, R. Arcone, et al. 2000. "Proteolysis of the exodomain of recombinant protease-activated receptors: prediction of receptor activation or inactivation by MALDI mass spectrometry." *Biochemistry* 39 (35): 10812-22.

Lokker, N. A., M. R. Mark, E. A. Luis, G. L. Bennett, K. A. Robbins, J. B. Baker and P. J. Godowski. 1992. "Structure-function analysis of hepatocyte growth factor: identification of variants that lack mitogenic activity yet retain high affinity receptor binding." *Embo J* 11 (7): 2503-10.

London, C. A., H. S. Sekhon, V. Arora, D. A. Stein, P. L. Iversen and G. R. Devi. 2003. "A novel antisense inhibitor of MMP-9 attenuates angiogenesis, human prostate cancer cell invasion and tumorigenicity." *Cancer Gene Ther* 10 (11): 823-32.

Lopez-Otin, C. and J. S. Bond. 2008. "Proteases: multifunctional enzymes in life and disease." *J Biol Chem* 283 (45): 30433-7.

Lopez-Otin, C. and L. M. Matrisian. 2007. "Emerging roles of proteases in tumour suppression." *Nat Rev Cancer* 7 (10): 800-8.

Louvard, D., S. Maroux, J. Baratti and P. Desnuelle. 1973. "On the distribution of enterokinase in porcine intestine and on its subcellular localization." *Biochim Biophys Acta* 309 (1): 127-37.

Lovgren, J., K. Airas and H. Lilja. 1999. "Enzymatic action of human glandular kallikrein 2 (hK2). Substrate specificity and regulation by Zn2+ and extracellular protease inhibitors." *Eur J Biochem* 262 (3): 781-9.

Lovgren, J., K. Rajakoski, M. Karp, a Lundwall and H. Lilja. 1997. "Activation of the zymogen form of prostate-specific antigen by human glandular kallikrein 2." *Biochem Biophys Res Commun* 238 (2): 549-55.

Lu, Y., P. Papagerakis, Y. Yamakoshi, J. C. Hu, J. D. Bartlett and J. P. Simmer. 2008. "Functions of KLK4 and MMP-20 in dental enamel formation." *Biol Chem* 389 (6): 695-700.

Lucas, J. M., L. True, S. Hawley, M. Matsumura, C. Morrissey, R. Vessella and P. S. Nelson. 2008. "The androgen-regulated type II serine protease TMPRSS2 is differentially expressed and mislocalized in prostate adenocarcinoma." *J Pathol* 215 (2): 118-25.

Luckett, S., R. S. Garcia, J. J. Barker, A. V. Konarev, P. R. Shewry, A. R. Clarke and R. L. Brady. 1999. "High-resolution structure of a potent, cyclic proteinase inhibitor from sunflower seeds." *J Mol Biol* 290 (2): 525-33.

Lundstrom, A. and T. Egelrud. 1991. "Stratum corneum chymotryptic enzyme: a proteinase which may be generally present in the stratum corneum and with a possible involvement in desquamation." *Acta Derm Venereol* 71 (6): 471-4.

Lundwall, A., V. Band, M. Blaber, J. A. Clements, Y. Courty, E. P. Diamandis, H. Fritz, et al. 2006. "A comprehensive nomenclature for serine proteases with homology to tissue kallikreins." *Biol Chem* 387 (6): 637-41.

Lundwall, A. and M. Brattsand. 2008. "Kallikrein-related peptidases." *Cell Mol Life Sci* 65 (13): 2019-38.

Luo, J., D. J. Duggan, Y. Chen, J. Sauvageot, C. M. Ewing, M. L. Bittner, J. M. Trent and W. B. Isaacs. 2001. "Human prostate cancer and benign prostatic hyperplasia: molecular dissection by gene expression profiling." *Cancer Res* 61 (12): 4683-8.

Luo, L. Y. and W. Jiang. 2006. "Inhibition profiles of human tissue kallikreins by serine protease inhibitors." *Biol Chem* 387 (6): 813-6.

Luo, L. Y., S. J. Shan, M. B. Elliott, A. Soosaipillai and E. P. Diamandis. 2006. "Purification and characterization of human kallikrein 11, a candidate prostate and ovarian cancer biomarker, from seminal plasma." *Clin Cancer Res* 12 (3 Pt 1): 742-50.

Luo, W., Y. Wang and G. Reiser. 2007. "p24A, a type I transmembrane protein, controls ARF1-dependent resensitization of protease-activated receptor-2 by influence on receptor trafficking." *J Biol Chem* 282 (41): 30246-55.

Luttrell, L. M. 2008. "Reviews in molecular biology and biotechnology: transmembrane signaling by G protein-coupled receptors." *Mol Biotechnol* 39 (3): 239-64.

Lwaleed, B. A., R. Greenfield, A. Stewart, B. Birch and A. J. Cooper. 2004. "Seminal clotting and fibrinolytic balance: a possible physiological role in the male reproductive system." *Thromb Haemost* 92 (4): 752-66.

Macfarlane, S. R., M. J. Seatter, T. Kanke, G. D. Hunter and R. Plevin. 2001. "Proteinase-activated receptors." *Pharmacol Rev* 53 (2): 245-82.

Mackinnon, A. C., B. C. Yan, L. J. Joseph and H. A. Al-Ahmadie. 2009. "Molecular biology underlying the clinical heterogeneity of prostate cancer: an update." *Arch Pathol Lab Med* 133 (7): 1033-40.

Magee, J. A., T. Araki, S. Patil, T. Ehrig, L. True, P. A. Humphrey, W. J. Catalona, M. A. Watson and J. Milbrandt. 2001. "Expression profiling reveals hepsin overexpression in prostate cancer." *Cancer Res* 61 (15): 5692-6.

Magklara, A., A. A. Mellati, G. A. Wasney, S. P. Little, G. Sotiropoulou, G. W. Becker and E. P. Diamandis. 2003. "Characterization of the enzymatic activity of human kallikrein 6: Autoactivation, substrate specificity, and regulation by inhibitors." *Biochem Biophys Res Commun* 307 (4): 948-55.

Magklara, A., A. Scorilas, C. Stephan, G. O. Kristiansen, S. Hauptmann, K. Jung and E. P. Diamandis. 2000. "Decreased concentrations of prostate-specific antigen and human glandular kallikrein 2 in malignant versus nonmalignant prostatic tissue." *Urology* 56 (3): 527-32.

Malaquin, N., C. Vercamer, F. Bouali, S. Martien, E. Deruy, N. Wernert, M. Chwastyniak, F. Pinet, C. Abbadie and A. Pourtier. 2013. "Senescent fibroblasts enhance early skin carcinogenic events via a paracrine MMP-PAR-1 axis." *PLoS One* 8 (5): e63607.

Malm, J., J. Hellman, P. Hogg and H. Lilja. 2000. "Enzymatic action of prostate-specific antigen (PSA or hK3): substrate specificity and regulation by Zn(2+), a tight-binding inhibitor." *Prostate* 45 (2): 132-9.

Mange, A., C. Desmetz, M. L. Berthes, T. Maudelonde and J. Solassol. 2008. "Specific increase of human kallikrein 4 mRNA and protein levels in breast cancer stromal cells." *Biochem Biophys Res Commun* 375 (1): 107-12.

Mannowetz, N., R. Wurdinger, A. Zippel, G. Aumuller and G. Wennemuth. 2010. "Expression of proteinase-activated receptor-2 (PAR2) is androgen-dependent in stromal cell line (hPCPs) from benign prostatic hyperplasia." *Prostate* 70 (12): 1350-8.

Marshall, R. D. 1967." In *Seventh International Congress of Biochemistry, Tokyo*, edited by International Union of Biochemistry, 573-574: International Union of Biochemistry.

Matej, R., P. Mandakova, I. Netikova, P. Pouckova and T. Olejar. 2007. "Proteinase-activated receptor-2 expression in breast cancer and the role of trypsin on growth and metabolism of breast cancer cell line MDA MB-231." *Physiol Res* 56 (4): 475-84.

Mathews, Christopher K., K. E. Van Holde and Kevin G. Ahern. 2000. *Biochemistry*. 3rd ed. ed. San Francisco, Calif. ; Harlow: Benjamin Cummings.

Matsumura, M., A. S. Bhatt, D. Andress, N. Clegg, T. K. Takayama, C. S. Craik and P. S. Nelson. 2005. "Substrates of the prostate-specific serine protease prostase/KLK4 defined by positional-scanning peptide libraries." *Prostate* 62 (1): 1-13.

Matsuyama, S., N. Nagata, K. Shirato, M. Kawase, M. Takeda and F. Taguchi. 2010. "Efficient activation of the severe acute respiratory syndrome coronavirus spike protein by the transmembrane protease TMPRSS2." *J Virol* 84 (24): 12658-64.

Mazzieri, R., L. Masiero, L. Zanetta, S. Monea, M. Onisto, S. Garbisa and P. Mignatti. 1997. "Control of type IV collagenase activity by components of the urokinase-plasmin system: a regulatory mechanism with cell-bound reactants." *Embo J* 16 (9): 2319-32.

McCawley, L. J., H. C. Crawford, L. E. King, Jr., J. Mudgett and L. M. Matrisian. 2004. "A protective role for matrix metalloproteinase-3 in squamous cell carcinoma." *Cancer Res* 64 (19): 6965-72.

McCoy, K. L., S. F. Traynelis and J. R. Hepler. 2010. "PAR1 and PAR2 couple to overlapping and distinct sets of G proteins and linked signaling pathways to differentially regulate cell physiology." *Mol Pharmacol* 77 (6): 1005-15.

McLaughlin, J. N., M. M. Patterson and A. B. Malik. 2007. "Protease-activated receptor-3 (PAR3) regulates PAR1 signaling by receptor dimerization." *Proc Natl Acad Sci U S A* 104 (13): 5662-7.

McLaughlin, J. N., L. Shen, M. Holinstat, J. D. Brooks, E. Dibenedetto and H. E. Hamm. 2005. "Functional selectivity of G protein signaling by agonist peptides and thrombin for the protease-activated receptor-1." *J Biol Chem* 280 (26): 25048-59.

Mellquist, J. L., L. Kasturi, S. L. Spitalnik and S. H. Shakin-Eshleman. 1998. "The amino acid following an asn-X-Ser/Thr sequon is an important determinant of N-linked core glycosylation efficiency." *Biochemistry* 37 (19): 6833-7.

Menashi, S., R. Fridman, S. Desrivieres, H. Lu, Y. Legrand and C. Soria. 1994. "Regulation of 92-kDa gelatinase B activity in the extracellular matrix by tissue kallikrein." *Ann N Y Acad Sci* 732: 466-8.

Menez, R., S. Michel, B. H. Muller, M. Bossus, F. Ducancel, C. Jolivet-Reynaud and E. A. Stura. 2008. "Crystal structure of a ternary complex between human prostate-specific antigen, its substrate acyl intermediate and an activating antibody." *J Mol Biol* 376 (4): 1021-33.

Metaye, T., H. Gibelin, R. Perdrisot and J. L. Kraimps. 2005. "Pathophysiological roles of G-protein-coupled receptor kinases." *Cell Signal* 17 (8): 917-28.

Meyer-Hoffert, U., Z. Wu, T. Kantyka, J. Fischer, T. Latendorf, B. Hansmann, J. Bartels, Y. He, R. Glaser and J. M. Schroder. 2010. "Isolation of SPINK6 in human skin: selective inhibitor of kallikrein-related peptidases." *J Biol Chem* 285 (42): 32174-81.

Meyer, D., F. Sielaff, M. Hammami, E. Bottcher-Friebertshauser, W. Garten and T. Steinmetzer. 2013. "Identification of the first synthetic inhibitors of the type II transmembrane serine protease TMPRSS2 suitable for inhibition of influenza virus activation." *Biochem J* 452 (2): 331-43.

Miao, J., D. Mu, B. Ergel, R. Singavarapu, Z. Duan, S. Powers, E. Oliva and S. Orsulic. 2008. "Hepsin colocalizes with desmosomes and induces progression of ovarian cancer in a mouse model." *Int J Cancer* 123 (9): 2041-7.

Michael, I. P., G. Pampalakis, S. D. Mikolajczyk, J. Malm, G. Sotiropoulou and E. P. Diamandis. 2006. "Human tissue kallikrein 5 is a member of a proteolytic cascade pathway involved in seminal clot liquefaction and potentially in prostate cancer progression." *J Biol Chem* 281 (18): 12743-50.

Mikolajczyk, S. D., L. S. Millar, A. Kumar and M. S. Saedi. 1998. "Human glandular kallikrein, hK2, shows arginine-restricted specificity and forms complexes with plasma protease inhibitors." *Prostate* 34 (1): 44-50.

Miletich, J. P. and G. J. Broze, Jr. 1990. "Beta protein C is not glycosylated at asparagine 329. The rate of translation may influence the frequency of usage at asparagine-X-cysteine sites." *J Biol Chem* 265 (19): 11397-404.

Milner, J. M., A. Patel, R. K. Davidson, T. E. Swingler, A. Desilets, D. A. Young, E. B. Kelso, et al. 2010. "Matriptase is a novel initiator of cartilage matrix degradation in osteoarthritis." *Arthritis Rheum* 62 (7): 1955-66.

Miyake, Y., S. Tsuzuki, S. Mochida, T. Fushiki and K. Inouye. 2010. "The role of asparagine-linked glycosylation site on the catalytic domain of matriptase in its zymogen activation." *Biochim Biophys Acta* 1804 (1): 156-65.

Miyazawa, K., H. Tsubouchi, D. Naka, K. Takahashi, M. Okigaki, N. Arakaki, H. Nakayama, S. Hirono, O. Sakiyama and et al. 1989. "Molecular cloning and sequence analysis of cDNA for human hepatocyte growth factor." *Biochem Biophys Res Commun* 163 (2): 967-73.

Mize, G. J., W. Wang and T. K. Takayama. 2008. "Prostate-specific kallikreins-2 and -4 enhance the proliferation of DU-145 prostate cancer cells through protease-activated receptors-1 and -2." *Mol Cancer Res* 6 (6): 1043-51.

Moilanen, M., T. Sorsa, M. Stenman, P. Nyberg, O. Lindy, J. Vesterinen, A. Paju, Y. T. Konttinen, U. H. Stenman and T. Salo. 2003. "Tumor-associated trypsinogen-2 (trypsinogen-2) activates procollagenases (MMP-1, -8, -13) and stromelysin-1 (MMP-3) and degrades type I collagen." *Biochemistry* 42 (18): 5414-20.

Moran, P., W. Li, B. Fan, R. Vij, C. Eigenbrot and D. Kirchhofer. 2006. "Pro-urokinase-type plasminogen activator is a substrate for hepsin." *J Biol Chem* 281 (41): 30439-46.

Morgia, G., M. Falsaperla, G. Malaponte, M. Madonia, M. Indelicato, S. Travali and M. C. Mazzarino. 2005. "Matrix metalloproteinases as diagnostic (MMP-13) and prognostic (MMP-2, MMP-9) markers of prostate cancer." *Urol Res* 33 (1): 44-50.

Morihara, K. and H. Tsuzuki. 1966. "Proteolytic substrate specificity and some elastolytic properties of a thermostable bacterial proteinase." *Biochim Biophys Acta* 118 (1): 215-8.

Morini, M., M. Mottolese, N. Ferrari, F. Ghiorzo, S. Buglioni, R. Mortarini, D. M. Noonan, P. G. Natali and A. Albini. 2000. "The alpha 3 beta 1 integrin is associated with mammary carcinoma cell metastasis, invasion, and gelatinase B (MMP-9) activity." *Int J Cancer* 87 (3): 336-42.

Morodomi, T., Y. Ogata, Y. Sasaguri, M. Morimatsu and H. Nagase. 1992. "Purification and characterization of matrix metalloproteinase 9 from U937 monocytic leukaemia and HT1080 fibrosarcoma cells." *Biochem J* 285 (Pt 2): 603-11.

Morrissey, C., L. D. True, M. P. Roudier, I. M. Coleman, S. Hawley, P. S. Nelson, R. Coleman, et al. 2008. "Differential expression of angiogenesis associated genes in prostate cancer bone, liver and lymph node metastases." *Clin Exp Metastasis* 25 (4): 377-88.

Mosnier, L. O., R. K. Sinha, L. Burnier, E. A. Bouwens and J. H. Griffin. 2012. "Biased agonism of protease-activated receptor 1 by activated protein C caused by noncanonical cleavage at Arg46." *Blood* 120 (26): 5237-46.

Mosnier, L. O., B. V. Zlokovic and J. H. Griffin. 2007. "The cytoprotective protein C pathway." *Blood* 109 (8): 3161-72.

Mukai, S., T. Fukushima, D. Naka, H. Tanaka, Y. Osada and H. Kataoka. 2008. "Activation of hepatocyte growth factor activator zymogen (pro-HGFA) by human kallikrein 1-related peptidases." *Febs J* 275 (5): 1003-17.

Murphy, G. and H. Nagase. 2008. "Progress in matrix metalloproteinase research." *Mol Aspects Med* 29 (5): 290-308.

Murphy, G. and H. Nagase. 2011. "Localizing matrix metalloproteinase activities in the pericellular environment." *Febs J* 278 (1): 2-15.

Myatt, A. and S. J. Hill. 2005. "Trypsin stimulates the phosphorylation of p42,44 mitogen-activated protein kinases via the proteinase-activated receptor-2 and protein kinase C epsilon in human cultured prostate stromal cells." *Prostate* 64 (2): 175-85.

Nagakawa, O., T. Yamagishi, T. Akashi, K. Nagaike and H. Fuse. 2006. "Serum hepatocyte growth factor activator inhibitor type I (HAI-I) and type 2 (HAI-2) in prostate cancer." *Prostate* 66 (5): 447-52.

Nagase, H. 1998. "Stromelysins I and II." In *Matrix Metalloproteinases,* edited by W. C. Parks and R. P. Mecham, xii, 362. San Diego: Academic Press.

Nagase, H. 2013. "Matrix Metalloproteinase 3/Stromelysin 1." In *Handbook of proteolytic enzymes,* edited by N. D. Rawlings and G. Salvesen. Amsterdam: Elsevier.

Nagase, H., J. J. Enghild, K. Suzuki and G. Salvesen. 1990. "Stepwise activation mechanisms of the precursor of matrix metalloproteinase 3 (stromelysin) by proteinases and (4-aminophenyl)mercuric acetate." *Biochemistry* 29 (24): 5783-9.

Nagase, H., R. Visse and G. Murphy. 2006. "Structure and function of matrix metalloproteinases and TIMPs." *Cardiovasc Res* 69 (3): 562-73.

Naka, D., T. Ishii, Y. Yoshiyama, K. Miyazawa, H. Hara, T. Hishida and N. Kidamura. 1992. "Activation of hepatocyte growth factor by proteolytic conversion of a single chain form to a heterodimer." *J Biol Chem* 267 (28): 20114-9.

Nakamura, K., A. Hongo, J. Kodama and Y. Hiramatsu. 2011. "The role of hepatocyte growth factor activator inhibitor (HAI)-1 and HAI-2 in endometrial cancer." *Int J Cancer* 128 (11): 2613-24.

Nakamura, K., Y. Nasu, A. Hongo, T. Matsuo, J. Kodama, S. Ebara, A. Nagai, F. Abrzua, H. Kumon and Y. Hiramatsu. 2006. "Hepsin shows inhibitory effects through apoptotic pathway on ovarian cancer cell lines." *Int J Oncol* 28 (2): 393-8.

Nakamura, K., N. Takamoto, F. Abarzua, A. Hongo, J. Kodama, Y. Nasu, H. Kumon and Y. Hiramatsu. 2008. "Hepsin inhibits the cell growth of endometrial cancer." *Int J Mol Med* 22 (3): 389-97.

Nakamura, T. and S. Mizuno. 2010. "The discovery of hepatocyte growth factor (HGF) and its significance for cell biology, life sciences and clinical medicine." *Proc Jpn Acad Ser B Phys Biol Sci* 86 (6): 588-610.

Nakamura, T., T. Nishizawa, M. Hagiya, T. Seki, M. Shimonishi, A. Sugimura, K. Tashiro and S. Shimizu. 1989. "Molecular cloning and expression of human hepatocyte growth factor." *Nature* 342 (6248): 440-3.

Nakanishi-Matsui, M., Y. W. Zheng, D. J. Sulciner, E. J. Weiss, M. J. Ludeman and S. R. Coughlin. 2000. "PAR3 is a cofactor for PAR4 activation by thrombin." *Nature* 404 (6778): 609-13.

Nakanishi, J., M. Yamamoto, J. Koyama, J. Sato and T. Hibino. 2010. "Keratinocytes synthesize enteropeptidase and multiple forms of trypsinogen during terminal differentiation." *J Invest Dermatol* 130 (4): 944-52.

Nakashiro, K., Y. Hayashi and R. Oyasu. 2003. "Immunohistochemical expression of hepatocyte growth factor and c-Met/HGF receptor in benign and malignant human prostate tissue." *Oncol Rep* 10 (5): 1149-53.

Nakashiro, K., M. Okamoto, Y. Hayashi and R. Oyasu. 2000. "Hepatocyte growth factor secreted by prostate-derived stromal cells stimulates growth of androgen-independent human prostatic carcinoma cells." *Am J Pathol* 157 (3): 795-803.

Nakayama, T., K. Hirano, Y. Shintani, J. Nishimura, A. Nakatsuka, H. Kuga, S. Takahashi and H. Kanaide. 2003. "Unproductive cleavage and the inactivation of protease-activated receptor-1 by trypsin in vascular endothelial cells." *Br J Pharmacol* 138 (1): 121-30.

Naldini, L., L. Tamagnone, E. Vigna, M. Sachs, G. Hartmann, W. Birchmeier, Y. Daikuhara, H. Tsubouchi, F. Blasi and P. M. Comoglio. 1992. "Extracellular proteolytic cleavage by urokinase is required for activation of hepatocyte growth factor/scatter factor." *Embo J* 11 (13): 4825-33.

Nandana, S., K. Ellwood-Yen, C. Sawyers, M. Wills, B. Weidow, T. Case, V. Vasioukhin and R. Matusik. 2010. "Hepsin cooperates with MYC in the progression of adenocarcinoma in a prostate cancer mouse model." *Prostate* 70 (6): 591-600.

Nelson, P. S., L. Gan, C. Ferguson, P. Moss, R. Gelinas, L. Hood and K. Wang. 1999. "Molecular cloning and characterization of prostase, an androgen-regulated serine protease with prostate-restricted expression." *Proc Natl Acad Sci U S A* 96 (6): 3114-9.

Netzel-Arnett, S., B. M. Currie, R. Szabo, C. Y. Lin, L. M. Chen, K. X. Chai, T. M. Antalis, T. H. Bugge and K. List. 2006. "Evidence for a matriptase-prostasin proteolytic cascade regulating terminal epidermal differentiation." *J Biol Chem* 281 (44): 32941-5.

Neuberger, A. and R. D. Marshall. 1968. *Carbohydrates and their Roles*, edited by H. W. Schultz, R. F. Cain and R. W. Wrolstad. [S.l.]: The Avi Publising Co.

Ng, N. M., R. N. Pike and S. E. Boyd. 2009. "Subsite cooperativity in protease specificity." *Biol Chem* 390 (5-6): 401-7.

Noe, V., B. Fingleton, K. Jacobs, H. C. Crawford, S. Vermeulen, W. Steelant, E. Bruyneel, L. M. Matrisian and M. Mareel. 2001. "Release of an invasion promoter E-cadherin fragment by matrilysin and stromelysin-1." *J Cell Sci* 114 (Pt 1): 111-118.

Nystedt, S., K. Emilsson, A. K. Larsson, B. Strombeck and J. Sundelin. 1995a. "Molecular cloning and functional expression of the gene encoding the human proteinase-activated receptor 2." *Eur J Biochem* 232 (1): 84-9.

Nystedt, S., K. Emilsson, C. Wahlestedt and J. Sundelin. 1994. "Molecular cloning of a potential proteinase activated receptor." *Proc Natl Acad Sci U S A* 91 (20): 9208-12.

Nystedt, S., A. K. Larsson, H. Aberg and J. Sundelin. 1995b. "The mouse proteinase-activated receptor-2 cDNA and gene. Molecular cloning and functional expression." *J Biol Chem* 270 (11): 5950-55.

Oberst, M., J. Anders, B. Xie, B. Singh, M. Ossandon, M. Johnson, R. B. Dickson and C. Y. Lin. 2001. "Matriptase and HAI-1 are expressed by normal and malignant epithelial cells in vitro and in vivo." *Am J Pathol* 158 (4): 1301-11.

Oberst, M. D., L. Y. Chen, K. Kiyomiya, C. A. Williams, M. S. Lee, M. D. Johnson, R. B. Dickson and C. Y. Lin. 2005. "HAI-1 regulates activation and expression of matriptase, a membrane-bound serine protease." *Am J Physiol Cell Physiol* 289 (2): C462-70.

Oberst, M. D., B. Singh, M. Ozdemirli, R. B. Dickson, M. D. Johnson and C. Y. Lin. 2003a. "Characterization of matriptase expression in normal human tissues." *J Histochem Cytochem* 51 (8): 1017-25.

Oberst, M. D., C. A. Williams, R. B. Dickson, M. D. Johnson and C. Y. Lin. 2003b. "The activation of matriptase requires its noncatalytic domains, serine protease domain, and its cognate inhibitor." *J Biol Chem* 278 (29): 26773-9.

Obiezu, C. V., I. P. Michael, M. A. Levesque and E. P. Diamandis. 2006. "Human kallikrein 4: enzymatic activity, inhibition, and degradation of extracellular matrix proteins." *Biol Chem* 387 (6): 749-59.

Obiezu, C. V., S. J. Shan, A. Soosaipillai, L. Y. Luo, L. Grass, G. Sotiropoulou, C. D. Petraki, P. A. Papanastasiou, M. A. Levesque and E. P. Diamandis. 2005. "Human kallikrein 4: quantitative study in tissues and evidence for its secretion into biological fluids." *Clin Chem* 51 (8): 1432-42.

Obiezu, C. V., A. Soosaipillai, K. Jung, C. Stephan, A. Scorilas, D. H. Howarth and E. P. Diamandis. 2002. "Detection of human kallikrein 4 in healthy and cancerous prostatic tissues by immunofluorometry and immunohistochemistry." *Clin Chem* 48 (8): 1232-40.

Ogata, Y., J. J. Enghild and H. Nagase. 1992. "Matrix metalloproteinase 3 (stromelysin) activates the precursor for the human matrix metalloproteinase 9." *J Biol Chem* 267 (6): 3581-4.

Oikonomopoulou, K., R. A. Deangelis, H. Chen, E. P. Diamandis, M. D. Hollenberg, D. Ricklin and J. D. Lambris. 2013. "Induction of Complement C3a Receptor Responses by Kallikrein-Related Peptidase 14." *J Immunol.*

Oikonomopoulou, K., K. K. Hansen, M. Saifeddine, I. Tea, M. Blaber, S. I. Blaber, I. Scarisbrick, et al. 2006a. "Proteinase-activated receptors, targets for kallikrein signaling." *J Biol Chem* 281 (43): 32095-112.

Oikonomopoulou, K., K. K. Hansen, M. Saifeddine, N. Vergnolle, I. Tea, M. Blaber, S. I. Blaber, I. Scarisbrick, E. P. Diamandis and M. D. Hollenberg. 2006b. "Kallikrein-mediated cell signalling: targeting proteinase-activated receptors (PARs)." *Biol Chem* 387 (6): 817-24.

Oka, T., T. Hakoshima, M. Itakura, S. Yamamori, M. Takahashi, Y. Hashimoto, S. Shiosaka and K. Kato. 2002. "Role of loop structures of neuropsin in the activity of serine protease and regulated secretion." *J Biol Chem* 277 (17): 14724-30.

Okada, Y., Y. Gonoji, K. Naka, K. Tomita, I. Nakanishi, K. Iwata, K. Yamashita and T. Hayakawa. 1992. "Matrix metalloproteinase 9 (92-kDa gelatinase/type IV collagenase) from HT 1080 human fibrosarcoma cells. Purification and activation of the precursor and enzymic properties." *J Biol Chem* 267 (30): 21712-9.

Okada, Y., E. D. Harris, Jr. and H. Nagase. 1988. "The precursor of a metalloendopeptidase from human rheumatoid synovial fibroblasts. Purification and mechanisms of activation by endopeptidases and 4-aminophenylmercuric acetate." *Biochem J* 254 (3): 731-41.

Okada, Y., H. Nagase and E. D. Harris, Jr. 1986. "A metalloproteinase from human rheumatoid synovial fibroblasts that digests connective tissue matrix components. Purification and characterization." *J Biol Chem* 261 (30): 14245-55.

Oldham, W. M. and H. E. Hamm. 2008. "Heterotrimeric G protein activation by G-protein-coupled receptors." *Nat Rev Mol Cell Biol* 9 (1): 60-71.

Ong, S. E., B. Blagoev, I. Kratchmarova, D. B. Kristensen, H. Steen, A. Pandey and M. Mann. 2002. "Stable isotope labeling by amino acids in cell culture, SILAC, as a simple and accurate approach to expression proteomics." *Mol Cell Proteomics* 1 (5): 376-86.

Ossovskaya, V. S. and N. W. Bunnett. 2004. "Protease-activated receptors: contribution to physiology and disease." *Physiol Rev* 84 (2): 579-621.

Overall, C. M. and C. P. Blobel. 2007. "In search of partners: linking extracellular proteases to substrates." *Nat Rev Mol Cell Biol* 8 (3): 245-57.

Owen, K. A., D. Qiu, J. Alves, A. M. Schumacher, L. M. Kilpatrick, J. Li, J. L. Harris and V. Ellis. 2010. "Pericellular activation of hepatocyte growth factor by the transmembrane serine proteases matriptase and hepsin, but not by the membrane-associated protease uPA." *Biochem J* 426 (2): 219-28.

Page, M. J. and E. Di Cera. 2008. "Serine peptidases: classification, structure and function." *Cell Mol Life Sci* 65 (7-8): 1220-36.

Paing, M. M., C. A. Johnston, D. P. Siderovski and J. Trejo. 2006. "Clathrin adaptor AP2 regulates thrombin receptor constitutive internalization and endothelial cell resensitization." *Mol Cell Biol* 26 (8): 3231-42.

Paing, M. M., A. B. Stutts, T. A. Kohout, R. J. Lefkowitz and J. Trejo. 2002. "beta -Arrestins regulate protease-activated receptor-1 desensitization but not internalization or Down-regulation." *J Biol Chem* 277 (2): 1292-300.

Pampalakis, G. and G. Sotiropoulou. 2007. "Tissue kallikrein proteolytic cascade pathways in normal physiology and cancer." *Biochim Biophys Acta* 1776 (1): 22-31.

Pancholi, V. and G. S. Chhatwal. 2003. "Housekeeping enzymes as virulence factors for pathogens." *Int J Med Microbiol* 293 (6): 391-401.

Paoloni-Giacobino, A., H. Chen, M. C. Peitsch, C. Rossier and S. E. Antonarakis. 1997. "Cloning of the TMPRSS2 gene, which encodes a novel serine protease with transmembrane, LDLRA, and SRCR domains and maps to 21q22.3." *Genomics* 44 (3): 309-20.

Parekh, R. B., R. A. Dwek, P. M. Rudd, J. R. Thomas, T. W. Rademacher, T. Warren, T. C. Wun, et al. 1989a. "N-glycosylation and in vitro enzymatic activity of human recombinant tissue plasminogen activator expressed in Chinese hamster ovary cells and a murine cell line." *Biochemistry* 28 (19): 7670-9.

Parekh, R. B., R. A. Dwek, J. R. Thomas, G. Opdenakker, T. W. Rademacher, A. J. Wittwer, S. C. Howard, et al. 1989b. "Cell-type-specific and site-specific N-glycosylation of type I and type II human tissue plasminogen activator." *Biochemistry* 28 (19): 7644-62.

Parr, C. and W. G. Jiang. 2006. "Hepatocyte growth factor activation inhibitors (HAI-1 and HAI-2) regulate HGF-induced invasion of human breast cancer cells." *Int J Cancer* 119 (5): 1176-83.

Partanen, J. I., T. A. Tervonen, M. Myllynen, E. Lind, M. Imai, P. Katajisto, G. J. Dijkgraaf, et al. 2012. "Tumor suppressor function of Liver kinase B1 (Lkb1) is linked to regulation of epithelial integrity." *Proc Natl Acad Sci U S A* 109 (7): E388-97.

Partridge, C. A., P. G. Phillips, M. J. Niedbala and J. J. Jeffrey. 1997. "Localization and activation of type IV collagenase/gelatinase at endothelial focal contacts." *Am J Physiol* 272 (5 Pt 1): L813-22.

Pavone, L. M., F. Cattaneo, S. Rea, V. De Pasquale, A. Spina, E. Sauchelli, V. Mastellone and R. Ammendola. 2011. "Intracellular signaling cascades triggered by the NK1 fragment of hepatocyte growth factor in human prostate epithelial cell line PNT1A." *Cell Signal* 23 (12): 1961-71.

Payne, M. A., P. F. Neuenschwander, A. E. Johnson and J. H. Morrissey. 1996. "Effect of soluble tissue factor on the kinetic mechanism of factor VIIa: enhancement of p-guanidinobenzoate substrate hydrolysis." *Biochemistry* 35 (22): 7100-6.

Peek, M., P. Moran, N. Mendoza, D. Wickramasinghe and D. Kirchhofer. 2002. "Unusual proteolytic activation of pro-hepatocyte growth factor by plasma kallikrein and coagulation factor XIa." *J Biol Chem* 277 (49): 47804-9.

Perona, J. J. and C. S. Craik. 1995. "Structural basis of substrate specificity in the serine proteases." *Protein Sci* 4 (3): 337-60.

Perona, J. J. and C. S. Craik. 1997. "Evolutionary divergence of substrate specificity within the chymotrypsin-like serine protease fold." *J Biol Chem* 272 (48): 29987-90.

Petersen, B., T. N. Petersen, P. Andersen, M. Nielsen and C. Lundegaard. 2009. "A generic method for assignment of reliability scores applied to solvent accessibility predictions." *BMC Struct Biol* 9: 51.

Petersen, T. N., S. Brunak, G. von Heijne and H. Nielsen. 2011. "SignalP 4.0: discriminating signal peptides from transmembrane regions." *Nat Methods* 8 (10): 785-6.

Petraki, C. D., P. A. Papanastasiou, V. N. Karavana and E. P. Diamandis. 2006. "Cellular distribution of human tissue kallikreins: immunohistochemical localization." *Biol Chem* 387 (6): 653-63.

Petrescu, A. J., A. L. Milac, S. M. Petrescu, R. A. Dwek and M. R. Wormald. 2004. "Statistical analysis of the protein environment of N-glycosylation sites: implications for occupancy, structure, and folding." *Glycobiology* 14 (2): 103-14.

Picariello, G., P. Ferranti, G. Mamone, P. Roepstorff and F. Addeo. 2008. "Identification of N-linked glycoproteins in human milk by hydrophilic interaction liquid chromatography and mass spectrometry." *Proteomics* 8 (18): 3833-47.

Pinzani, P., K. Lind, F. Malentacchi, G. Nesi, F. Salvianti, D. Villari, M. Kubista, M. Pazzagli and C. Orlando. 2008. "Prostate-specific antigen mRNA and protein levels in laser microdissected cells of human prostate measured by real-time reverse transcriptase-quantitative polymerase chain reaction and immuno-quantitative polymerase chain reaction." *Hum Pathol* 39 (10): 1474-82.

Pohl, G., M. Kallstrom, N. Bergsdorf, P. Wallen and H. Jornvall. 1984. "Tissue plasminogen activator: peptide analyses confirm an indirectly derived amino acid sequence, identify the active site serine residue, establish glycosylation sites, and localize variant differences." *Biochemistry* 23 (16): 3701-7.

Poliakov, A., M. Spilman, T. Dokland, C. L. Amling and J. A. Mobley. 2009. "Structural heterogeneity and protein composition of exosome-like vesicles (prostasomes) in human semen." *Prostate* 69 (2): 159-67.

QIAGEN. 2003. *The QIAexpressionist: A handbook for high-level expression and purification of 6xHis-tagged proteins*, edited by QIAGEN. 5th Edition ed: QIAGEN.

Qiu, D., K. Owen, K. Gray, R. Bass and V. Ellis. 2007. "Roles and regulation of membrane-associated serine proteases." *Biochem Soc Trans* 35 (Pt 3): 583-7.

Qiu, S. D., C. Y. Young, D. L. Bilhartz, J. L. Prescott, G. M. Farrow, W. W. He and D. J. Tindall. 1990. "In situ hybridization of prostate-specific antigen mRNA in human prostate." *J Urol* 144 (6): 1550-6.

Quesada, V., G. R. Ordonez, L. M. Sanchez, X. S. Puente and C. Lopez-Otin. 2009. "The Degradome database: mammalian proteases and diseases of proteolysis." *Nucleic Acids Res* 37 (Database issue): D239-43.

Ra, H. J. and W. C. Parks. 2007. "Control of matrix metalloproteinase catalytic activity." *Matrix Biol* 26 (8): 587-96.

Rabien, A., F. Fritzsche, M. Jung, E. P. Diamandis, S. A. Loening, M. Dietel, K. Jung, C. Stephan and G. Kristiansen. 2008. "High expression of KLK14 in prostatic adenocarcinoma is associated with elevated risk of prostate-specific antigen relapse." *Tumour Biol* 29 (1): 1-8.

Ragno, P. 2006. "The urokinase receptor: a ligand or a receptor? Story of a sociable molecule." *Cell Mol Life Sci* 63 (9): 1028-37.

Rajapakse, S. and T. Takahashi. 2007. "Expression and enzymatic characterization of recombinant human kallikrein 14." *Zoolog Sci* 24 (8): 774-80.

Ramachandran, R., A. Eissa, K. Mihara, K. Oikonomopoulou, M. Saifeddine, B. Renaux, E. Diamandis and M. D. Hollenberg. 2012a. "Proteinase-activated receptors (PARs): differential signalling by kallikrein-related peptidases KLK8 and KLK14." *Biol Chem* 393 (5): 421-7.

Ramachandran, R. and M. D. Hollenberg. 2008. "Proteinases and signalling: pathophysiological and therapeutic implications via PARs and more." *Br J Pharmacol* 153 Suppl 1: S263-82.

Ramachandran, R., K. Mihara, H. Chung, B. Renaux, C. S. Lau, D. A. Muruve, K. A. DeFea, M. Bouvier and M. D. Hollenberg. 2011. "Neutrophil elastase acts as a biased agonist for proteinase-activated receptor-2 (PAR2)." *J Biol Chem* 286 (28): 24638-48.

Ramachandran, R., F. Noorbakhsh, K. Defea and M. D. Hollenberg. 2012b. "Targeting proteinase-activated receptors: therapeutic potential and challenges." *Nat Rev Drug Discov* 11 (1): 69-86.

Ramani, V. C. and R. S. Haun. 2008. "The extracellular matrix protein fibronectin is a substrate for kallikrein 7." *Biochem Biophys Res Commun* 369 (4): 1169-73.

Ramos-DeSimone, N., E. Hahn-Dantona, J. Sipley, H. Nagase, D. L. French and J. P. Quigley. 1999. "Activation of matrix metalloproteinase-9 (MMP-9) via a converging plasmin/stromelysin-1 cascade enhances tumor cell invasion." *J Biol Chem* 274 (19): 13066-76.

Ramsay, A. J. 2008. "Kallikrein-related peptidase 4 activation of protease-activated receptor family members and association with prostate cancer." PhD, Faculty of Science and Technology

and Institute of Health and Biomedical Innovation, Queensland University of Technology (29886).

Ramsay, A. J., Y. Dong, M. L. Hunt, M. Linn, H. Samaratunga, J. A. Clements and J. D. Hooper. 2008a. "Kallikrein-related peptidase 4 (KLK4) initiates intracellular signaling via protease-activated receptors (PARs). KLK4 and PAR-2 are co-expressed during prostate cancer progression." *J Biol Chem* 283 (18): 12293-304.

Ramsay, A. J., J. C. Reid, M. N. Adams, H. Samaratunga, Y. Dong, J. A. Clements and J. D. Hooper. 2008b. "Prostatic trypsin-like kallikrein-related peptidases (KLKs) and other prostate-expressed tryptic proteinases as regulators of signalling via proteinase-activated receptors (PARs)." *Biol Chem* 389 (6): 653-68.

Rawlings, N. D. and A. J. Barrett. 2013a. "Introduction: Metallopeptidases and their clans." In *Handbook of proteolytic enzymes,* edited by N. D. Rawlings and G. Salvesen. Amsterdam: Elsevier.

Rawlings, N. D. and A. J. Barrett. 2013b. "Introduction: Serine peptidases and their clans." In *Handbook of proteolytic enzymes,* edited by N. D. Rawlings and G. Salvesen. Amsterdam: Elsevier.

Rawlings, N. D., A. J. Barrett and A. Bateman. 2012. "MEROPS: the database of proteolytic enzymes, their substrates and inhibitors." *Nucleic Acids Res* 40 (Database issue): D343-50.

Rawlings, N. D. and G. Salvesen, eds. 2013. *Handbook of proteolytic enzymes*. Third edition. ed. Vol. 1. Amsterdam: Elsevier.

Rawlings, N. D., D. P. Tolle and A. J. Barrett. 2004. "Evolutionary families of peptidase inhibitors." *Biochem J* 378 (Pt 3): 705-16.

Reddy, V. B., S. G. Shimada, P. Sikand, R. H. Lamotte and E. A. Lerner. 2010. "Cathepsin S elicits itch and signals via protease-activated receptors." *J Invest Dermatol* 130 (5): 1468-70.

Redondo-Munoz, J., E. Ugarte-Berzal, M. J. Terol, P. E. Van den Steen, M. Hernandez del Cerro, M. Roderfeld, E. Roeb, G. Opdenakker, J. A. Garcia-Marco and A. Garcia-Pardo. 2010. "Matrix metalloproteinase-9 promotes chronic lymphocytic leukemia b cell survival through its hemopexin domain." *Cancer Cell* 17 (2): 160-72.

Rehder, D. S., T. M. Dillon, G. D. Pipes and P. V. Bondarenko. 2006. "Reversed-phase liquid chromatography/mass spectrometry analysis of reduced monoclonal antibodies in pharmaceutics." *J Chromatogr A* 1102 (1-2): 164-75.

Renesto, P., M. Si-Tahar, M. Moniatte, V. Balloy, A. Van Dorsselaer, D. Pidard and M. Chignard. 1997. "Specific inhibition of thrombin-induced cell activation by the neutrophil proteinases elastase, cathepsin G, and proteinase 3: evidence for distinct cleavage sites within the aminoterminal domain of the thrombin receptor." *Blood* 89 (6): 1944-53.

Rickles, F. R., S. Patierno and P. M. Fernandez. 2003. "Tissue factor, thrombin, and cancer." *Chest* 124 (3 Suppl): 58S-68S.

Ricks, T. K. and J. Trejo. 2009. "Phosphorylation of protease-activated receptor-2 differentially regulates desensitization and internalization." *J Biol Chem* 284 (49): 34444-57.

Riddick, A. C., C. J. Shukla, C. J. Pennington, R. Bass, R. K. Nuttall, A. Hogan, K. K. Sethia, et al. 2005. "Identification of degradome components associated with prostate cancer progression by expression analysis of human prostatic tissues." *Br J Cancer* 92 (12): 2171-80.

Riewald, M., R. J. Petrovan, A. Donner, B. M. Mueller and W. Ruf. 2002. "Activation of endothelial cell protease activated receptor 1 by the protein C pathway." *Science* 296 (5574): 1880-2.

Riewald, M. and W. Ruf. 2001. "Mechanistic coupling of protease signaling and initiation of coagulation by tissue factor." *Proc Natl Acad Sci U S A* 98 (14): 7742-7.

Riewald, M. and W. Ruf. 2005. "Protease-activated receptor-1 signaling by activated protein C in cytokine-perturbed endothelial cells is distinct from thrombin signaling." *J Biol Chem* 280 (20): 19808-14.

Rolland, T., M. Ta An, B. Charloteaux, S. J. Pevzner, Q. Zhong, N. Sahni, S. Yi, et al. 2014. "A proteome-scale map of the human interactome network." *Cell* 159 (5): 1212-26.

Rondeau, E., C. J. He, U. Zacharias and J. D. Sraer. 1996. "Thrombin stimulation of renal cells." *Semin Thromb Hemost* 22 (2): 135-8.

Roosterman, D., F. Schmidlin and N. W. Bunnett. 2003. "Rab5a and rab11a mediate agonist-induced trafficking of protease-activated receptor 2." *Am J Physiol Cell Physiol* 284 (5): C1319-29.

Rothmeier, A. S. and W. Ruf. 2012. "Protease-activated receptor 2 signaling in inflammation." *Semin Immunopathol* 34 (1): 133-49.

Russo, A., U. J. Soh, M. M. Paing, P. Arora and J. Trejo. 2009a. "Caveolae are required for protease-selective signaling by protease-activated receptor-1." *Proc Natl Acad Sci U S A* 106 (15): 6393-7.

Russo, A., U. J. Soh and J. Trejo. 2009b. "Proteases display biased agonism at protease-activated receptors: location matters!" *Mol Interv* 9 (2): 87-96.

Rutkowski, M. J., M. E. Sughrue, A. J. Kane, S. A. Mills and A. T. Parsa. 2010. "Cancer and the complement cascade." *Mol Cancer Res* 8 (11): 1453-65.

Ryu, O., J. C. Hu, Y. Yamakoshi, J. L. Villemain, X. Cao, C. Zhang, J. D. Bartlett and J. P. Simmer. 2002. "Porcine kallikrein-4 activation, glycosylation, activity, and expression in prokaryotic and eukaryotic hosts." *Eur J Oral Sci* 110 (5): 358-65.

Saleem, M., V. M. Adhami, W. Zhong, B. J. Longley, C. Y. Lin, R. B. Dickson, S. Reagan-Shaw, D. F. Jarrard and H. Mukhtar. 2006. "A novel biomarker for staging human prostate adenocarcinoma: overexpression of matriptase with concomitant loss of its inhibitor, hepatocyte growth factor activator inhibitor-1." *Cancer Epidemiol Biomarkers Prev* 15 (2): 217-27.

Sambrook, Joseph, Edward F. Fritsch and Thomas Maniatis. 1989. *Molecular cloning : a laboratory manual.* 2nd ed. ed. Cold Spring Harbor, N.Y.: Cold Spring Harbor Laboratory.

Sanchez, W. Y., S. J. de Veer, J. E. Swedberg, E. J. Hong, J. C. Reid, T. P. Walsh, J. D. Hooper, G. L. Hammond, J. A. Clements and J. M. Harris. 2012. "Selective cleavage of human sex hormone-binding globulin by kallikrein-related peptidases and effects on androgen action in LNCaP prostate cancer cells." *Endocrinology* 153 (7): 3179-89.

Sanders, A. J., C. Parr, G. Davies, T. A. Martin, J. Lane, M. D. Mason and W. G. Jiang. 2006. "Genetic reduction of matriptase-1 expression is associated with a reduction in the aggressive phenotype of prostate cancer cells in vitro and in vivo." *J Exp Ther Oncol* 6 (1): 39-48.

Sanders, A. J., C. Parr, M. D. Mason and W. G. Jiang. 2007. "Suppression of hepatocyte growth factor activator inhibitor-1 leads to a more aggressive phenotype of prostate cancer cells in vitro." *Int J Mol Med* 20 (4): 613-9.

Sang, Q. X., H. Birkedal-Hansen and H. E. Van Wart. 1995. "Proteolytic and non-proteolytic activation of human neutrophil progelatinase B." *Biochim Biophys Acta* 1251 (2): 99-108.

Scarborough, R. M., M. A. Naughton, W. Teng, D. T. Hung, J. Rose, T. K. Vu, V. I. Wheaton, C. W. Turck and S. R. Coughlin. 1992. "Tethered ligand agonist peptides. Structural requirements for thrombin receptor activation reveal mechanism of proteolytic unmasking of agonist function." *J Biol Chem* 267 (19): 13146-9.

Schechter, I. and A. Berger. 1967. "On the size of the active site in proteases. I. Papain." *Biochem Biophys Res Commun* 27 (2): 157-62.

Schluter, M. A. and B. Margolis. 2012. "Apicobasal polarity in the kidney." *Exp Cell Res* 318 (9): 1033-9.

Schmitt, M., V. Magdolen, F. Yang, M. Kiechle, J. Bayani, G. M. Yousef, A. Scorilas, E. P. Diamandis and J. Dorn. 2013. "Emerging clinical importance of the cancer biomarkers kallikrein-related peptidases (KLK) in female and male reproductive organ malignancies." *Radiol Oncol* 47 (4): 319-29.

Schneider, E. L. and C. S. Craik. 2009. "Positional scanning synthetic combinatorial libraries for substrate profiling." *Methods Mol Biol* 539: 59-78.

Schwede, T., J. Kopp, N. Guex and M. C. Peitsch. 2003. "SWISS-MODEL: An automated protein homology-modeling server." *Nucleic Acids Res* 31 (13): 3381-5.

Seidler, N. W. 2013. "GAPDH, as a virulence factor." *Adv Exp Med Biol* 985: 149-78.

Seitz, I., S. Hess, H. Schulz, R. Eckl, G. Busch, H. P. Montens, R. Brandl, S. Seidl, A. Schomig and I. Ott. 2007. "Membrane-type serine protease-1/matriptase induces interleukin-6 and -8 in endothelial cells by activation of protease-activated receptor-2: potential implications in atherosclerosis." *Arterioscler Thromb Vasc Biol* 27 (4): 769-75.

Seiz, L., M. Kotzsch, N. I. Grebenchtchikov, A. J. Geurts-Moespot, S. Fuessel, P. Goettig, A. Gkazepis, et al. 2010. "Polyclonal antibodies against kallikrein-related peptidase 4 (KLK4): immunohistochemical assessment of KLK4 expression in healthy tissues and prostate cancer." *Biol Chem* 391 (4): 391-401.

Shapiro, M. J. and S. R. Coughlin. 1998. "Separate signals for agonist-independent and agonist-triggered trafficking of protease-activated receptor 1." *J Biol Chem* 273 (44): 29009-14.

Shapiro, S. D., C. J. Fliszar, T. J. Broekelmann, R. P. Mecham, R. M. Senior and H. G. Welgus. 1995. "Activation of the 92-kDa gelatinase by stromelysin and 4-aminophenylmercuric acetate. Differential processing and stabilization of the carboxyl-terminal domain by tissue inhibitor of metalloproteinases (TIMP)." *J Biol Chem* 270 (11): 6351-6.

Shaw, J. L. and E. P. Diamandis. 2007. "Distribution of 15 human kallikreins in tissues and biological fluids." *Clin Chem* 53 (8): 1423-32.

Shi, Y. E., J. Torri, L. Yieh, A. Wellstein, M. E. Lippman and R. B. Dickson. 1993. "Identification and characterization of a novel matrix-degrading protease from hormone-dependent human breast cancer cells." *Cancer Res* 53 (6): 1409-15.

Shia, S., J. Stamos, D. Kirchhofer, B. Fan, J. Wu, R. T. Corpuz, L. Santell, R. A. Lazarus and C. Eigenbrot. 2005. "Conformational lability in serine protease active sites: structures of hepatocyte growth factor activator (HGFA) alone and with the inhibitory domain from HGFA inhibitor-1B." *J Mol Biol* 346 (5): 1335-49.

Shih, F. F. 1985. "Analysis of glutamine, glutamic acid and pyroglutamic acid in protein hydrolysates by high-performance liquid chromatography." *J Chromatogr* 322 (1): 248-56.

Shimomura, T., K. Denda, T. Kawaguchi, K. Matsumoto, K. Miyazawa and N. Kitamura. 1999. "Multiple sites of proteolytic cleavage to release soluble forms of hepatocyte growth factor activator inhibitor type 1 from a transmembrane form." *J Biochem* 126 (5): 821-8.

Shimomura, T., K. Denda, A. Kitamura, T. Kawaguchi, M. Kito, J. Kondo, S. Kagaya, et al. 1997. "Hepatocyte growth factor activator inhibitor, a novel Kunitz-type serine protease inhibitor." *J Biol Chem* 272 (10): 6370-6.

Shimomura, T., K. Miyazawa, Y. Komiyama, H. Hiraoka, D. Naka, Y. Morimoto and N. Kitamura. 1995. "Activation of hepatocyte growth factor by two homologous proteases, blood-coagulation factor XIIa and hepatocyte growth factor activator." *Eur J Biochem* 229 (1): 257-61.

Shirato, K., M. Kawase and S. Matsuyama. 2013. "Middle East Respiratory Syndrome Coronavirus (MERS-CoV) Infection Mediated by the Transmembrane Serine Protease TMPRSS2." *J Virol*.

Shirogane, Y., M. Takeda, M. Iwasaki, N. Ishiguro, H. Takeuchi, Y. Nakatsu, M. Tahara, H. Kikuta and Y. Yanagi. 2008. "Efficient multiplication of human metapneumovirus in Vero cells expressing the transmembrane serine protease TMPRSS2." *J Virol* 82 (17): 8942-6.

Shulla, A., T. Heald-Sargent, G. Subramanya, J. Zhao, S. Perlman and T. Gallagher. 2011. "A transmembrane serine protease is linked to the severe acute respiratory syndrome coronavirus receptor and activates virus entry." *J Virol* 85 (2): 873-82.

Sievers, F., A. Wilm, D. Dineen, T. J. Gibson, K. Karplus, W. Li, R. Lopez, et al. 2011. "Fast, scalable generation of high-quality protein multiple sequence alignments using Clustal Omega." *Mol Syst Biol* 7: 539.

Simmer, J. P., M. Fukae, T. Tanabe, Y. Yamakoshi, T. Uchida, J. Xue, H. C. Margolis, et al. 1998a. "Purification, characterization, and cloning of enamel matrix serine proteinase 1." *J Dent Res* 77 (2): 377-86.

Simmer, J. P., Y. Hu, R. Lertlam, Y. Yamakoshi and J. C. Hu. 2009. "Hypomaturation enamel defects in Klk4 knockout/LacZ knockin mice." *J Biol Chem* 284 (28): 19110-21.

Simmer, J. P., O. H. Ryu, Q. Qian, C. Zhang, X. Cao, X. Sun and C. C. Hu. 1998b. "Cloning and Characterisation of a cDNA encoding human EMSP1." In *Proceedings of the Sixth International Conference on the Chemistry and Biology of Mineralized Tissues, Vittel, France, 2000*, edited by M. Goldberg, A. Boskey and C. Robinson, 458: Rosemont, IL : American Academy of Orthopaedic Surgeons.

Sirover, M. A. 2012. "Subcellular dynamics of multifunctional protein regulation: mechanisms of GAPDH intracellular translocation." *J Cell Biochem* 113 (7): 2193-200.

Skropeta, D. 2009. "The effect of individual N-glycans on enzyme activity." *Bioorg Med Chem* 17 (7): 2645-53.

Smith, B. J., ed. 1997. *Protein Sequencing Protocols*. Vol. 64, *Methods in Molecular Biology*. Clifton, NJ: Humana Press Inc.

Smith, C. E., A. S. Richardson, Y. Hu, J. D. Bartlett, J. C. Hu and J. P. Simmer. 2011. "Effect of kallikrein 4 loss on enamel mineralization: comparison with mice lacking matrix metalloproteinase 20." *J Biol Chem* 286 (20): 18149-60.

Soh, U. J., M. R. Dores, B. Chen and J. Trejo. 2010. "Signal transduction by protease-activated receptors." *Br J Pharmacol* 160 (2): 191-203.

Soh, U. J. and J. Trejo. 2011. "Activated protein C promotes protease-activated receptor-1 cytoprotective signaling through beta-arrestin and dishevelled-2 scaffolds." *Proc Natl Acad Sci U S A* 108 (50): E1372-80.

Somoza, J. R., J. D. Ho, C. Luong, M. Ghate, P. A. Sprengeler, K. Mortara, W. D. Shrader, et al. 2003. "The structure of the extracellular region of human hepsin reveals a serine protease domain and a novel scavenger receptor cysteine-rich (SRCR) domain." *Structure* 11 (9): 1123-31.

Sorsa, T., T. Salo, E. Koivunen, J. Tyynela, Y. T. Konttinen, U. Bergmann, A. Tuuttila, et al. 1997. "Activation of type IV procollagenases by human tumor-associated trypsin-2." *J Biol Chem* 272 (34): 21067-74.

Sotiropoulou, G., G. Pampalakis and E. P. Diamandis. 2009. "Functional roles of human kallikrein-related peptidases." *J Biol Chem* 284 (48): 32989-94.

Sotiropoulou, G., V. Rogakos, T. Tsetsenis, G. Pampalakis, N. Zafiropoulos, G. Simillides, A. Yiotakis and E. P. Diamandis. 2003. "Emerging interest in the kallikrein gene family for understanding and diagnosing cancer." *Oncol Res* 13 (6-10): 381-91.

Sottrup-Jensen, L. 1989. "Alpha-macroglobulins: structure, shape, and mechanism of proteinase complex formation." *J Biol Chem* 264 (20): 11539-42.

Spronk, H. M., J. W. Govers-Riemslag and H. ten Cate. 2003. "The blood coagulation system as a molecular machine." *Bioessays* 25 (12): 1220-8.

Srikantan, V., M. Valladares, J. S. Rhim, J. W. Moul and S. Srivastava. 2002. "HEPSIN inhibits cell growth/invasion in prostate cancer cells." *Cancer Res* 62 (23): 6812-6.

Stamey, T. A., J. A. Warrington, M. C. Caldwell, Z. Chen, Z. Fan, M. Mahadevappa, J. E. McNeal, R. Nolley and Z. Zhang. 2001. "Molecular genetic profiling of Gleason grade 4/5 prostate cancers compared to benign prostatic hyperplasia." *J Urol* 166 (6): 2171-7.

Stearns, M. E. and M. Wang. 1993. "Type IV collagenase (M(r) 72,000) expression in human prostate: benign and malignant tissue." *Cancer Res* 53 (4): 878-83.

Stefanidakis, M., M. Bjorklund, E. Ihanus, C. G. Gahmberg and E. Koivunen. 2003. "Identification of a negatively charged peptide motif within the catalytic domain of progelatinases that mediates binding to leukocyte beta 2 integrins." *J Biol Chem* 278 (36): 34674-84.

Stefanidakis, M., T. Ruohtula, N. Borregaard, C. G. Gahmberg and E. Koivunen. 2004. "Intracellular and cell surface localization of a complex between alphaMbeta2 integrin and promatrix metalloproteinase-9 progelatinase in neutrophils." *J Immunol* 172 (11): 7060-8.

Stefansson, K., M. Brattsand, A. Ny, B. Glas and T. Egelrud. 2006. "Kallikrein-related peptidase 14 may be a major contributor to trypsin-like proteolytic activity in human stratum corneum." *Biol Chem* 387 (6): 761-8.

Stefansson, K., M. Brattsand, D. Roosterman, C. Kempkes, G. Bocheva, M. Steinhoff and T. Egelrud. 2008. "Activation of proteinase-activated receptor-2 by human kallikrein-related peptidases." *J Invest Dermatol* 128 (1): 18-25.

Steinhoff, M., J. Buddenkotte, V. Shpacovitch, A. Rattenholl, C. Moormann, N. Vergnolle, T. A. Luger and M. D. Hollenberg. 2005. "Proteinase-activated receptors: transducers of proteinase-mediated signaling in inflammation and immune response." *Endocr Rev* 26 (1): 1-43.

Stephan, C., G. M. Yousef, A. Scorilas, K. Jung, M. Jung, G. Kristiansen, S. Hauptmann, et al. 2004. "Hepsin is highly over expressed in and a new candidate for a prognostic indicator in prostate cancer." *J Urol* 171 (1): 187-91.

Stephenson, S. A., K. Verity, L. K. Ashworth and J. A. Clements. 1999. "Localization of a new prostate-specific antigen-related serine protease gene, KLK4, is evidence for an expanded human kallikrein gene family cluster on chromosome 19q13.3-13.4." *J Biol Chem* 274 (33): 23210-4.

Sternlicht, M. D., M. J. Bissell and Z. Werb. 2000. "The matrix metalloproteinase stromelysin-1 acts as a natural mammary tumor promoter." *Oncogene* 19 (8): 1102-13.

Sternlicht, M. D., A. Lochter, C. J. Sympson, B. Huey, J. P. Rougier, J. W. Gray, D. Pinkel, M. J. Bissell and Z. Werb. 1999. "The stromal proteinase MMP3/stromelysin-1 promotes mammary carcinogenesis." *Cell* 98 (2): 137-46.

Stief, T. W. 2007. "Thrombin and plasmin activity in semen." *Blood Coagul Fibrinolysis* 18 (4): 386-7.

Stott, D. I. and A. J. Munro. 1972. "The formation of pyrrolid-2-one-5-carboxylic acid at the N-terminus of immunoglobulin G heavy chain." *Biochem J* 128 (5): 1221-7.

Su, S., Y. Li, Y. Luo, Y. Sheng, Y. Su, R. N. Padia, Z. K. Pan, Z. Dong and S. Huang. 2009. "Proteinase-activated receptor 2 expression in breast cancer and its role in breast cancer cell migration." *Oncogene* 28 (34): 3047-57.

Swedberg, J. E., S. J. de Veer and J. M. Harris. 2010. "Natural and engineered kallikrein inhibitors: an emerging pharmacopoeia." *Biol Chem* 391 (4): 357-74.

Swedberg, J. E., L. V. Nigon, J. C. Reid, S. J. de Veer, C. M. Walpole, C. R. Stephens, T. P. Walsh, et al. 2009. "Substrate-guided design of a potent and selective kallikrein-related peptidase inhibitor for kallikrein 4." *Chem Biol* 16 (6): 633-43.

Szabo, R. and T. H. Bugge. 2008. "Type II transmembrane serine proteases in development and disease." *Int J Biochem Cell Biol* 40 (6-7): 1297-316.

Szabo, R., A. Molinolo, K. List and T. H. Bugge. 2007. "Matriptase inhibition by hepatocyte growth factor activator inhibitor-1 is essential for placental development." *Oncogene* 26 (11): 1546-56.

Szabo, R., K. Uzzun Sales, P. Kosa, N. A. Shylo, S. Godiksen, K. K. Hansen, S. Friis, et al. 2012. "Reduced prostasin (CAP1/PRSS8) activity eliminates HAI-1 and HAI-2 deficiency-associated developmental defects by preventing matriptase activation." *PLoS Genet* 8 (8): e1002937.

Taichman, R. S., L. R. Patel, R. Bedenis, J. Wang, S. Weidner, T. Schumann, K. Yumoto, J. E. Berry, Y. Shiozawa and K. J. Pienta. 2013. "GAS6 receptor status is associated with dormancy and bone metastatic tumor formation." *PLoS One* 8 (4): e61873.

Takada, Y., R. A. Skidgel and E. G. Erdos. 1985. "Purification of human urinary prokallikrein. Identification of the site of activation by the metalloproteinase thermolysin." *Biochem J* 232 (3): 851-8.

Takata, T., M. Zhao, T. Uchida, T. Wang, T. Aoki, J. D. Bartlett and H. Nikai. 2000. "Immunohistochemical detection and distribution of enamelysin (MMP-20) in human odontogenic tumors." *J Dent Res* 79 (8): 1608-13.

Takayama, T. K., C. A. Carter and T. Deng. 2001a. "Activation of prostate-specific antigen precursor (pro-PSA) by prostin, a novel human prostatic serine protease identified by degenerate PCR." *Biochemistry* 40 (6): 1679-87.

Takayama, T. K., K. Fujikawa and E. W. Davie. 1997. "Characterization of the precursor of prostate-specific antigen. Activation by trypsin and by human glandular kallikrein." *J Biol Chem* 272 (34): 21582-8.

Takayama, T. K., B. A. McMullen, P. S. Nelson, M. Matsumura and K. Fujikawa. 2001b. "Characterization of hK4 (prostase), a prostate-specific serine protease: activation of the precursor of prostate specific antigen (pro-PSA) and single-chain urokinase-type plasminogen activator and degradation of prostatic acid phosphatase." *Biochemistry* 40 (50): 15341-8.

Takeuchi, T., J. L. Harris, W. Huang, K. W. Yan, S. R. Coughlin and C. S. Craik. 2000. "Cellular localization of membrane-type serine protease 1 and identification of protease-activated receptor-2 and single-chain urokinase-type plasminogen activator as substrates." *J Biol Chem* 275 (34): 26333-42.

Takeuchi, T., M. A. Shuman and C. S. Craik. 1999. "Reverse biochemistry: use of macromolecular protease inhibitors to dissect complex biological processes and identify a membrane-type serine protease in epithelial cancer and normal tissue." *Proc Natl Acad Sci U S A* 96 (20): 11054-61.

Tallant, C., A. Marrero and F. X. Gomis-Ruth. 2010. "Matrix metalloproteinases: fold and function of their catalytic domains." *Biochim Biophys Acta* 1803 (1): 20-8.

Tanaka, H., T. Fukushima, K. Yorita, M. Kawaguchi and H. Kataoka. 2009. "Tissue injury alters the site of expression of hepatocyte growth factor activator inhibitor type 1 in bronchial epithelial cells." *Hum Cell* 22 (1): 11-7.

Tantivejkul, K., R. D. Loberg, S. C. Mawocha, L. L. Day, L. S. John, B. A. Pienta, M. A. Rubin and K. J. Pienta. 2005. "PAR1-mediated NFkappaB activation promotes survival of prostate cancer cells through a Bcl-xL-dependent mechanism." *J Cell Biochem* 96 (3): 641-52.

Terho, P. 2010. *Flowing Software* 1.6. Turku: Turku Centre for Biotechnology, University of Turku and Turku BioImaging.

Thiery, J. P. 2002. "Epithelial-mesenchymal transitions in tumour progression." *Nat Rev Cancer* 2 (6): 442-54.

Tiruppathi, C., W. Yan, R. Sandoval, T. Naqvi, A. N. Pronin, J. L. Benovic and A. B. Malik. 2000. "G protein-coupled receptor kinase-5 regulates thrombin-activated signaling in endothelial cells." *Proc Natl Acad Sci U S A* 97 (13): 7440-5.

Tomlins, S. A., D. R. Rhodes, S. Perner, S. M. Dhanasekaran, R. Mehra, X. W. Sun, S. Varambally, et al. 2005. "Recurrent fusion of TMPRSS2 and ETS transcription factor genes in prostate cancer." *Science* 310 (5748): 644-8.

Toriseva, M. and V. M. Kahari. 2009. "Proteinases in cutaneous wound healing." *Cell Mol Life Sci* 66 (2): 203-24.

Torres-Rosado, A., K. S. O'Shea, A. Tsuji, S. H. Chou and K. Kurachi. 1993. "Hepsin, a putative cell-surface serine protease, is required for mammalian cell growth." *Proc Natl Acad Sci U S A* 90 (15): 7181-5.

Toth, J., L. Gombos, Z. Simon, P. Medveczky, L. Szilagyi, L. Graf and A. Malnasi-Csizmadia. 2006. "Thermodynamic analysis reveals structural rearrangement during the acylation step in human trypsin 4 on 4-methylumbelliferyl 4-guanidinobenzoate substrate analogue." *J Biol Chem* 281 (18): 12596-602.

Toth, M., I. Chvyrkova, M. M. Bernardo, S. Hernandez-Barrantes and R. Fridman. 2003. "Pro-MMP-9 activation by the MT1-MMP/MMP-2 axis and MMP-3: role of TIMP-2 and plasma membranes." *Biochem Biophys Res Commun* 308 (2): 386-95.

Tripathi, M., S. Nandana, H. Yamashita, R. Ganesan, D. Kirchhofer and V. Quaranta. 2008. "Laminin-332 is a substrate for hepsin, a protease associated with prostate cancer progression." *J Biol Chem* 283 (45): 30576-84.

Trusolino, L., A. Bertotti and P. M. Comoglio. 2010. "MET signalling: principles and functions in development, organ regeneration and cancer." *Nat Rev Mol Cell Biol* 11 (12): 834-48.

Tsai, C. H., C. H. Teng, Y. T. Tu, T. S. Cheng, S. R. Wu, C. J. Ko, H. Y. Shyu, et al. 2013. "HAI-2 suppresses the invasive growth and metastasis of prostate cancer through regulation of matriptase." *Oncogene*.

Tschesche, H., J. Michaelis, U. Kohnert, J. Fedrowitz and R. Oberhoff. 1989. "Tissue kallikrein effectively activates latent matrix degrading metalloenzymes." *Adv Exp Med Biol* 247A: 545-8.

Tseng, I. C., H. Xu, F. P. Chou, G. Li, A. P. Vazzano, J. P. Kao, M. D. Johnson and C. Y. Lin. 2010. "Matriptase activation, an early cellular response to acidosis." *J Biol Chem* 285 (5): 3261-70.

Tsuji, A., A. Torres-Rosado, T. Arai, M. M. Le Beau, R. S. Lemons, S. H. Chou and K. Kurachi. 1991. "Hepsin, a cell membrane-associated protease. Characterization, tissue distribution, and gene localization." *J Biol Chem* 266 (25): 16948-53.

Twardzik, D. R. and A. Peterkofsky. 1972. "Glutamic acid as a precursor to N-terminal pyroglutamic acid in mouse plasmacytoma protein (protein synthesis-initiation-immunoglobulins-pyrrolidone carboxylic acid)." *Proc Natl Acad Sci U S A* 69 (1): 274-7.

Tye, C. E., C. T. Pham, J. P. Simmer and J. D. Bartlett. 2009. "DPPI may activate KLK4 during enamel formation." *J Dent Res* 88 (4): 323-7.

Urano, T., S. Urano and F. J. Castellino. 1988. "Reaction of tissue-type plasminogen activator with 4-methylumbelliferyl-p-guanidinobenzoate hydrochloride." *Biochem Biophys Res Commun* 150 (1): 45-51.

Urban, J. D., W. P. Clarke, M. von Zastrow, D. E. Nichols, B. Kobilka, H. Weinstein, J. A. Javitch, et al. 2007. "Functional selectivity and classical concepts of quantitative pharmacology." *J Pharmacol Exp Ther* 320 (1): 1-13.

Utleg, A. G., E. C. Yi, T. Xie, P. Shannon, J. T. White, D. R. Goodlett, L. Hood and B. Lin. 2003. "Proteomic analysis of human prostasomes." *Prostate* 56 (2): 150-61.

Vaananen, A., L. Tjaderhane, L. Eklund, R. Heljasvaara, T. Pihlajaniemi, R. Herva, Y. Ding, J. D. Bartlett and T. Salo. 2004. "Expression of collagen XVIII and MMP-20 in developing teeth and odontogenic tumors." *Matrix Biol* 23 (3): 153-61.

Vaarala, M. H., K. Porvari, A. Kyllonen, O. Lukkarinen and P. Vihko. 2001a. "The TMPRSS2 gene encoding transmembrane serine protease is overexpressed in a majority of prostate cancer patients: detection of mutated TMPRSS2 form in a case of aggressive disease." *Int J Cancer* 94 (5): 705-10.

Vaarala, M. H., K. S. Porvari, S. Kellokumpu, A. P. Kyllonen and P. T. Vihko. 2001b. "Expression of transmembrane serine protease TMPRSS2 in mouse and human tissues." *J Pathol* 193 (1): 134-40.

Vadivel, K. and S. P. Bajaj. 2012. "Structural biology of factor VIIa/tissue factor initiated coagulation." *Front Biosci (Landmark Ed)* 17: 2476-94.

Vaisanen, V., J. Lovgren, J. Hellman, T. Piironen, H. Lilja and K. Pettersson. 1999. "Characterization and processing of prostate specific antigen (hK3) and human glandular kallikrein (hK2) secreted by LNCaP cells." *Prostate Cancer Prostatic Dis* 2 (2): 91-97.

Valliere-Douglass, J. F., P. Kodama, M. Mujacic, L. J. Brady, W. Wang, A. Wallace, B. Yan, P. Reddy, M. J. Treuheit and A. Balland. 2009. "Asparagine-linked oligosaccharides present on a non-consensus amino acid sequence in the CH1 domain of human antibodies." *J Biol Chem* 284 (47): 32493-506.

van den Burg, B. and V. Eijsink. 2013. "Thermolysin and Related *Bacillus* Metallopeptidases." In *Handbook of proteolytic enzymes,* edited by N. D. Rawlings and G. Salvesen. Amsterdam: Elsevier.

Van den Steen, P. E., I. Van Aelst, V. Hvidberg, H. Piccard, P. Fiten, C. Jacobsen, S. K. Moestrup, et al. 2006. "The hemopexin and O-glycosylated domains tune gelatinase B/MMP-9 bioavailability via inhibition and binding to cargo receptors." *J Biol Chem* 281 (27): 18626-37.

Vandooren, J., N. Geurts, E. Martens, P. E. Van den Steen and G. Opdenakker. 2013. "Zymography methods for visualizing hydrolytic enzymes." *Nat Methods* 10 (3): 211-20.

Vasioukhin, V. 2004. "Hepsin paradox reveals unexpected complexity of metastatic process." *Cell Cycle* 3 (11): 1394-7.

Vesey, D. A., C. W. Cheung, W. A. Kruger, P. Poronnik, G. Gobe and D. W. Johnson. 2005. "Thrombin stimulates proinflammatory and proliferative responses in primary cultures of human proximal tubule cells." *Kidney Int* 67 (4): 1315-29.

Vesey, D. A., W. A. Kruger, P. Poronnik, G. C. Gobe and D. W. Johnson. 2007. "Proinflammatory and proliferative responses of human proximal tubule cells to PAR-2 activation." *Am J Physiol Renal Physiol* 293 (5): F1441-9.

Vesey, D. A., J. Y. Suen, V. Seow, R. J. Lohman, L. Liu, G. C. Gobe, D. W. Johnson and D. P. Fairlie. 2013. "PAR2-induced inflammatory responses in human kidney tubular epithelial cells." *Am J Physiol Renal Physiol* 304 (6): F737-50.

Veveris-Lowe, T. L., S. J. Kruger, T. Walsh, R. A. Gardiner and J. A. Clements. 2007. "Seminal fluid characterization for male fertility and prostate cancer: kallikrein-related serine proteases and whole proteome approaches." *Semin Thromb Hemost* 33 (1): 87-99.

Veveris-Lowe, T. L., M. G. Lawrence, R. L. Collard, L. Bui, A. C. Herington, D. L. Nicol and J. A. Clements. 2005. "Kallikrein 4 (hK4) and prostate-specific antigen (PSA) are associated with the loss of E-cadherin and an epithelial-mesenchymal transition (EMT)-like effect in prostate cancer cells." *Endocr Relat Cancer* 12 (3): 631-43.

Vilen, S. T., P. Nyberg, M. Hukkanen, M. Sutinen, M. Ylipalosaari, A. Bjartell, A. Paju, et al. 2008. "Intracellular co-localization of trypsin-2 and matrix metalloprotease-9: possible proteolytic cascade of trypsin-2, MMP-9 and enterokinase in carcinoma." *Exp Cell Res* 314 (4): 914-26.

Vu, T. K., D. T. Hung, V. I. Wheaton and S. R. Coughlin. 1991a. "Molecular cloning of a functional thrombin receptor reveals a novel proteolytic mechanism of receptor activation." *Cell* 64 (6): 1057-68.

Vu, T. K., R. W. Liu, C. J. Haaksma, J. J. Tomasek and E. W. Howard. 1997. "Identification and cloning of the membrane-associated serine protease, hepsin, from mouse preimplantation embryos." *J Biol Chem* 272 (50): 31315-20.

Vu, T. K., V. I. Wheaton, D. T. Hung, I. Charo and S. R. Coughlin. 1991b. "Domains specifying thrombin-receptor interaction." *Nature* 353 (6345): 674-7.

Walsh, M. J., J. McDougall and B. Wittmann-Liebold. 1988. "Extended N-terminal sequencing of proteins of archaebacterial ribosomes blotted from two-dimensional gels onto glass fiber and poly(vinylidene difluoride) membrane." *Biochemistry* 27 (18): 6867-76.

Wang, J. K., M. S. Lee, I. C. Tseng, F. P. Chou, Y. W. Chen, A. Fulton, H. S. Lee, C. J. Chen, M. D. Johnson and C. Y. Lin. 2009. "Polarized epithelial cells secrete matriptase as a consequence of zymogen activation and HAI-1-mediated inhibition." *Am J Physiol Cell Physiol* 297 (2): C459-70.

Wang, M. C., L. D. Papsidero, M. Kuriyama, L. A. Valenzuela, G. P. Murphy and T. M. Chu. 1981. "Prostate antigen: a new potential marker for prostatic cancer." *Prostate* 2 (1): 89-96.

Wang, W., G. J. Mize, X. Zhang and T. K. Takayama. 2010. "Kallikrein-related peptidase-4 initiates tumor-stroma interactions in prostate cancer through protease-activated receptor-1." *Int J Cancer* 126 (3): 599-610.

Wang, W., X. Zhang, G. J. Mize and T. K. Takayama. 2008. "Protease-activated receptor-1 upregulates fibroblast growth factor 7 in stroma of benign prostatic hyperplasia." *Prostate* 68 (10): 1064-75.

Warren, M., M. Twohig, T. Pier, J. Eickhoff, C. Y. Lin, D. Jarrard and W. Huang. 2009. "Protein expression of matriptase and its cognate inhibitor HAI-1 in human prostate cancer: a tissue microarray and automated quantitative analysis." *Appl Immunohistochem Mol Morphol* 17 (1): 23-30.

Webber, M. M., A. Waghray and D. Bello. 1995. "Prostate-specific antigen, a serine protease, facilitates human prostate cancer cell invasion." *Clin Cancer Res* 1 (10): 1089-94.

Welsh, J. B., L. M. Sapinoso, A. I. Su, S. G. Kern, J. Wang-Rodriguez, C. A. Moskaluk, H. F. Frierson, Jr. and G. M. Hampton. 2001. "Analysis of gene expression identifies candidate markers and pharmacological targets in prostate cancer." *Cancer Res* 61 (16): 5974-8.

Williams, E. B., S. Krishnaswamy and K. G. Mann. 1989. "Zymogen/enzyme discrimination using peptide chloromethyl ketones." *J Biol Chem* 264 (13): 7536-45.

Wilson, S., B. Greer, J. Hooper, A. Zijlstra, B. Walker, J. Quigley and S. Hawthorne. 2005. "The membrane-anchored serine protease, TMPRSS2, activates PAR-2 in prostate cancer cells." *Biochem J* 388 (Pt 3): 967-72.

Wittig-Blaich, S. M., L. A. Kacprzyk, T. Eismann, M. Bewerunge-Hudler, P. Kruse, E. Winkler, W. S. Strauss, et al. 2011. "Matrix-dependent regulation of AKT in Hepsin-overexpressing PC3 prostate cancer cells." *Neoplasia* 13 (7): 579-89.

Wittwer, A. J. and S. C. Howard. 1990. "Glycosylation at Asn-184 inhibits the conversion of single-chain to two-chain tissue-type plasminogen activator by plasmin." *Biochemistry* 29 (17): 4175-80.

Wittwer, A. J., S. C. Howard, L. S. Carr, N. K. Harakas, J. Feder, R. B. Parekh, P. M. Rudd, R. A. Dwek and T. W. Rademacher. 1989. "Effects of N-glycosylation on in vitro activity of Bowes melanoma and human colon fibroblast derived tissue plasminogen activator." *Biochemistry* 28 (19): 7662-9.

Wu, Q., D. Yu, J. Post, M. Halks-Miller, J. E. Sadler and J. Morser. 1998. "Generation and characterization of mice deficient in hepsin, a hepatic transmembrane serine protease." *J Clin Invest* 101 (2): 321-6.

Xi, Z., T. I. Klokk, K. Korkmaz, P. Kurys, C. Elbi, B. Risberg, H. Danielsen, M. Loda and F. Saatcioglu. 2004. "Kallikrein 4 is a predominantly nuclear protein and is overexpressed in prostate cancer." *Cancer Res* 64 (7): 2365-70.

Xing, P., J. G. Li, F. Jin, T. T. Zhao, Q. Liu, H. T. Dong and X. L. Wei. 2011. "Clinical and biological significance of hepsin overexpression in breast cancer." *J Investig Med* 59 (5): 803-10.

Xu, H., Z. Xu, I. C. Tseng, F. P. Chou, Y. W. Chen, J. K. Wang, M. D. Johnson, H. Kataoka and C. Y. Lin. 2011. "Mechanisms for the control of matriptase activity in the absence of sufficient HAI-1." *Am J Physiol Cell Physiol.*

Xu, W. F., H. Andersen, T. E. Whitmore, S. R. Presnell, D. P. Yee, A. Ching, T. Gilbert, E. W. Davie and D. C. Foster. 1998. "Cloning and characterization of human protease-activated receptor 4." *Proc Natl Acad Sci U S A* 95 (12): 6642-6.

Xuan, J. A., D. Schneider, P. Toy, R. Lin, A. Newton, Y. Zhu, S. Finster, et al. 2006. "Antibodies neutralizing hepsin protease activity do not impact cell growth but inhibit invasion of prostate and ovarian tumor cells in culture." *Cancer Res* 66 (7): 3611-9.

Yamakoshi, Y., J. C. Hu, M. Fukae, F. Yamakoshi and J. P. Simmer. 2006. "How do enamelysin and kallikrein 4 process the 32-kDa enamelin?" *Eur J Oral Sci* 114 Suppl 1: 45-51; discussion 93-5, 379-80.

Yamakoshi, Y., J. P. Simmer, J. D. Bartlett, T. Karakida and S. Oida. 2013. "MMP20 and KLK4 activation and inactivation interactions in vitro." *Arch Oral Biol* 58 (11): 1569-1577.

Yang, G. Y., K. S. Xu, Z. Q. Pan, Z. Y. Zhang, Y. T. Mi, J. S. Wang, R. Chen and J. Niu. 2008. "Integrin alpha v beta 6 mediates the potential for colon cancer cells to colonize in and metastasize to the liver." *Cancer Sci* 99 (5): 879-87.

Yasuda, K., A. Komiya, A. Watanabe, A. Morii, T. Oya, O. Nagakawa, Y. Fujiuchi and H. Fuse. 2013. "Expression of Hepatocyte Growth Factor Activator Inhibitor Type-1 (HAI-1) in Prostate Cancer." *Anticancer Res* 33 (2): 575-81.

Yasuda, K., O. Nagakawa, T. Akashi, Y. Fujiuchi, K. Koizumi, A. Komiya, I. Saiki and H. Fuse. 2009. "Serum active hepatocyte growth factor (AHGF) in benign prostatic disease and prostate cancer." *Prostate* 69 (4): 346-51.

Yemelyanov, A., J. Czwornog, D. Chebotaev, A. Karseladze, E. Kulevitch, X. Yang and I. Budunova. 2007. "Tumor suppressor activity of glucocorticoid receptor in the prostate." *Oncogene* 26 (13): 1885-96.

Yoon, H., S. I. Blaber, M. Debela, P. Goettig, I. A. Scarisbrick and M. Blaber. 2009. "A completed KLK activome profile: investigation of activation profiles of KLK9, 10, and 15." *Biol Chem* 390 (4): 373-7.

Yoon, H., S. I. Blaber, D. M. Evans, J. Trim, M. A. Juliano, I. A. Scarisbrick and M. Blaber. 2008. "Activation profiles of human kallikrein-related peptidases by proteases of the thrombostasis axis." *Protein Sci* 17 (11): 1998-2007.

Yoon, H., S. I. Blaber, W. Li, I. A. Scarisbrick and M. Blaber. 2013. "Activation profiles of human kallikrein-related peptidases by matrix metalloproteinases." *Biol Chem* 394 (1): 137-47.

Yoon, H., G. Laxmikanthan, J. Lee, S. I. Blaber, A. Rodriguez, J. M. Kogot, I. A. Scarisbrick and M. Blaber. 2007. "Activation profiles and regulatory cascades of the human kallikrein-related peptidases." *J Biol Chem* 282 (44): 31852-64.

Yousef, G. M., C. A. Borgono, A. Scorilas, R. Ponzone, N. Biglia, L. Iskander, M. E. Polymeris, R. Roagna, P. Sismondi and E. P. Diamandis. 2002. "Quantitative analysis of human kallikrein gene 14 expression in breast tumours indicates association with poor prognosis." *Br J Cancer* 87 (11): 1287-93.

Yousef, G. M. and E. P. Diamandis. 2001. "The new human tissue kallikrein gene family: structure, function, and association to disease." *Endocr Rev* 22: 184-204.

Yousef, G. M., S. Fracchioli, A. Scorilas, C. A. Borgono, L. Iskander, M. Puopolo, M. Massobrio, E. P. Diamandis and D. Katsaros. 2003a. "Steroid hormone regulation and prognostic value of the human kallikrein gene 14 in ovarian cancer." *Am J Clin Pathol* 119 (3): 346-55.

Yousef, G. M., A. Magklara, A. Chang, K. Jung, D. Katsaros and E. P. Diamandis. 2001. "Cloning of a new member of the human kallikrein gene family, KLK14, which is down-regulated in different malignancies." *Cancer Res* 61 (8): 3425-31.

Yousef, G. M., C. V. Obiezu, L. Y. Luo, M. H. Black and E. P. Diamandis. 1999. "Prostase/KLK-L1 is a new member of the human kallikrein gene family, is expressed in prostate and breast tissues, and is hormonally regulated." *Cancer Res* 59 (17): 4252-6.

Yousef, G. M., C. Stephan, A. Scorilas, M. A. Ellatif, K. Jung, G. Kristiansen, M. Jung, M. E. Polymeris and E. P. Diamandis. 2003b. "Differential expression of the human kallikrein gene 14 (KLK14) in normal and cancerous prostatic tissues." *Prostate* 56 (4): 287-92.

Yu, I. S., H. J. Chen, Y. S. Lee, P. H. Huang, S. R. Lin, T. W. Tsai and S. W. Lin. 2000. "Mice deficient in hepsin, a serine protease, exhibit normal embryogenesis and unchanged hepatocyte regeneration ability." *Thromb Haemost* 84 (5): 865-70.

Yu, Q. and I. Stamenkovic. 1999. "Localization of matrix metalloproteinase 9 to the cell surface provides a mechanism for CD44-mediated tumor invasion." *Genes Dev* 13 (1): 35-48.

Yu, S., S. Xia, D. Yang, K. Wang, S. Yeh, Z. Gao and C. Chang. 2013. "Androgen receptor in human prostate cancer-associated fibroblasts promotes prostate cancer epithelial cell growth and invasion." *Med Oncol* 30 (3): 674.

Zacharski, L. R., D. L. Ornstein, V. A. Memoli, S. M. Rousseau and W. Kisiel. 1998. "Expression of the factor VII activating protease, hepsin, in situ in renal cell carcinoma." *Thromb Haemost* 79 (4): 876-7.

Zain, J., Y. Q. Huang, X. Feng, M. L. Nierodzik, J. J. Li and S. Karpatkin. 2000. "Concentration-dependent dual effect of thrombin on impaired growth/apoptosis or mitogenesis in tumor cells." *Blood* 95 (10): 3133-8.

Zhang, X., W. Wang, G. J. Mize, T. K. Takayama, L. D. True and R. L. Vessella. 2013. "Protease-activated receptor 2 signaling upregulates angiogenic growth factors in renal cell carcinoma." *Exp Mol Pathol* 94 (1): 91-7.

Zhang, X., W. Wang, L. D. True, R. L. Vessella and T. K. Takayama. 2009. "Protease-activated receptor-1 is upregulated in reactive stroma of primary prostate cancer and bone metastasis." *Prostate* 69 (7): 727-36.

Zheng, H., J. Chu, Y. Qiu, H. H. Loh and P. Y. Law. 2008. "Agonist-selective signaling is determined by the receptor location within the membrane domains." *Proc Natl Acad Sci U S A* 105 (27): 9421-6.

Zheng, X. L., Y. Kitamoto and J. E. Sadler. 2009. "Enteropeptidase, a type II transmembrane serine protease." *Front Biosci (Elite Ed)* 1: 242-9.

Zhu, X. and P. A. Humphrey. 2000. "Overexpression and regulation of expression of scatter factor/hepatocyte growth factor in prostatic carcinoma." *Urology* 56 (6): 1071-4.